

Therapeutic potential of natural products in oxidative and metabolic diseases

Edited by

Ochuko Lucky Erukainure, Aliyu Muhammad,
Chika Ifeanyi Chukwuma and Md Shahidul Islam

Coordinated by

Olakunle Sanni and Veronica Folakemi Salau

Published in

Frontiers in Pharmacology



FRONTIERS EBOOK COPYRIGHT STATEMENT

The copyright in the text of individual articles in this ebook is the property of their respective authors or their respective institutions or funders. The copyright in graphics and images within each article may be subject to copyright of other parties. In both cases this is subject to a license granted to Frontiers.

The compilation of articles constituting this ebook is the property of Frontiers.

Each article within this ebook, and the ebook itself, are published under the most recent version of the Creative Commons CC-BY licence. The version current at the date of publication of this ebook is CC-BY 4.0. If the CC-BY licence is updated, the licence granted by Frontiers is automatically updated to the new version.

When exercising any right under the CC-BY licence, Frontiers must be attributed as the original publisher of the article or ebook, as applicable.

Authors have the responsibility of ensuring that any graphics or other materials which are the property of others may be included in the CC-BY licence, but this should be checked before relying on the CC-BY licence to reproduce those materials. Any copyright notices relating to those materials must be complied with.

Copyright and source acknowledgement notices may not be removed and must be displayed in any copy, derivative work or partial copy which includes the elements in question.

All copyright, and all rights therein, are protected by national and international copyright laws. The above represents a summary only. For further information please read Frontiers' Conditions for Website Use and Copyright Statement, and the applicable CC-BY licence.

ISSN 1664-8714
ISBN 978-2-8325-4556-0
DOI 10.3389/978-2-8325-4556-0

About Frontiers

Frontiers is more than just an open access publisher of scholarly articles: it is a pioneering approach to the world of academia, radically improving the way scholarly research is managed. The grand vision of Frontiers is a world where all people have an equal opportunity to seek, share and generate knowledge. Frontiers provides immediate and permanent online open access to all its publications, but this alone is not enough to realize our grand goals.

Frontiers journal series

The Frontiers journal series is a multi-tier and interdisciplinary set of open-access, online journals, promising a paradigm shift from the current review, selection and dissemination processes in academic publishing. All Frontiers journals are driven by researchers for researchers; therefore, they constitute a service to the scholarly community. At the same time, the *Frontiers journal series* operates on a revolutionary invention, the tiered publishing system, initially addressing specific communities of scholars, and gradually climbing up to broader public understanding, thus serving the interests of the lay society, too.

Dedication to quality

Each Frontiers article is a landmark of the highest quality, thanks to genuinely collaborative interactions between authors and review editors, who include some of the world's best academicians. Research must be certified by peers before entering a stream of knowledge that may eventually reach the public - and shape society; therefore, Frontiers only applies the most rigorous and unbiased reviews. Frontiers revolutionizes research publishing by freely delivering the most outstanding research, evaluated with no bias from both the academic and social point of view. By applying the most advanced information technologies, Frontiers is catapulting scholarly publishing into a new generation.

What are Frontiers Research Topics?

Frontiers Research Topics are very popular trademarks of the *Frontiers journals series*: they are collections of at least ten articles, all centered on a particular subject. With their unique mix of varied contributions from Original Research to Review Articles, Frontiers Research Topics unify the most influential researchers, the latest key findings and historical advances in a hot research area.

Find out more on how to host your own Frontiers Research Topic or contribute to one as an author by contacting the Frontiers editorial office: frontiersin.org/about/contact

Therapeutic potential of natural products in oxidative and metabolic diseases

Topic editors

Ochuko Lucky Erukainure — University of the Free State, South Africa

Aliyu Muhammad — Ahmadu Bello University, Nigeria

Chika Ifeanyi Chukwuma — Central University of Technology, South Africa

Md Shahidul Islam — University of KwaZulu, Natal, South Africa

Topic coordinators

Olakunle Sanni — Stellenbosch University, South Africa

Veronica Folakemi Salau — University of the Free State, South Africa

Citation

Erukainure, O. L., Muhammad, A., Chukwuma, C. I., Islam, M. S., Sanni, O., Salau, V. F., eds. (2024). *Therapeutic potential of natural products in oxidative and metabolic diseases*. Lausanne: Frontiers Media SA.
doi: 10.3389/978-2-8325-4556-0

Table of contents

- 05 **Editorial: Therapeutic potential of natural products in oxidative and metabolic diseases**
Aliyu Muhammad, Chika Ifeanyi Chukwuma, Ochuko Lucky Erukainure and Md. Shahidul Islam
- 07 ***Averrhoa carambola* leaves prevent dyslipidemia and oxidative stress in a rat model of poloxamer-407-induced acute hyperlipidemia**
Maisa Siddiq Abduh, Sultan A. M. Saghir, Amir M. Al Hroob, Albandari Bin-Ammar, Ayat H. Al-Tarawni, Vikneswaran Murugaiyah and Ayman M. Mahmoud
- 22 **Protective role of resveratrol against VCM-induced hepatotoxicity in male wistar rats**
Fahad S. Alshehri and Nasser M. Alorfi
- 31 **Pomegranate peel extract protects against the development of diabetic cardiomyopathy in rats by inhibiting pyroptosis and downregulating LncRNA-MALAT1**
Mariam Ali Abo-Saif, Amany E. Ragab, Amera O. Ibrahim, Othman F. Abdelzaher, Ahmed B. M. Mehanyd, Maha Saber-Ayad and Ola A. El-Feky
- 46 **Ginsenoside Rg1 can reverse fatigue behavior in CFS rats by regulating EGFR and affecting Taurine and Mannose 6-phosphate metabolism**
Chaofang Lei, Jiaxu Chen, Zhen Huang, Yinian Men, Yue Qian, Mingzhi Yu, Xinyi Xu, Lin Li, Xin Zhao, Youming Jiang and Yueyun Liu
- 63 ***Ageratina adenophora* (Spreng.) King & H. Rob. Standardized leaf extract as an antidiabetic agent for type 2 diabetes: An *in vitro* and *in vivo* evaluation**
Khaidem Devika Chanu, Nanaocha Sharma, Vimi Kshetrimayum, Sushil Kumar Chaudhary, Suparna Ghosh, Pallab Kanti Haldar and Pulok K. Mukherjee
- 80 **Pharmacological effects of baicalin in lung diseases**
Duoning Wang and Yi Li
- 91 **Zhilong Huoxue Tongyu capsule attenuates intracerebral hemorrhage induced redox imbalance by modulation of Nrf2 signaling pathway**
Maryam Mazhar, Guoqiang Yang, Houping Xu, Yulin Liu, Pan Liang, Luyin Yang, Roman Spáčil, Hongping Shen, Dechou Zhang, Wei Ren and Sijin Yang
- 105 **A flavonoid-rich fraction of *Euphorbia peplus* attenuates hyperglycemia, insulin resistance, and oxidative stress in a type 2 diabetes rat model**
Reem S. Alruhaimi, Gomaa Mostafa-Hedeab, Maisa Siddiq Abduh, Albandari Bin-Ammar, Emad H. M. Hassanein, Emadeldin M. Kamel and Ayman M. Mahmoud

- 123 **Natural products as novel anti-obesity agents: insights into mechanisms of action and potential for therapeutic management**
Ummul Fathima Shaik Mohamed Sayed, Said Moshawih, Hui Poh Goh, Nurolaini Kifli, Gaurav Gupta, Sachin Kumar Singh, Dinesh Kumar Chellappan, Kamal Dua, Andi Hermansyah, Hooi Leng Ser, Long Chiau Ming and Bey Hing Goh
- 153 ***In vitro* antiproliferative, anti-inflammatory effects and molecular docking studies of natural compounds isolated from *Sarcocephalus pobeguinii* (Hua ex Pobég)**
Emmanuel Mfotie Njoya, Brigitte Ndemangou, Jude Akinyelu, Aristide M. Munvera, Chika. I. Chukwuma, Pierre Mkounga, Samson S. Mashele, Tshepiso J. Makhafola and Lyndy J. McGaw
- 166 **Berberine enhances the function of db/db mice islet β cell through GLP-1/GLP-1R/PKA signaling pathway in intestinal L cell and islet α cell**
Wenbin Wu, Qingsong Xia, Yujin Guo, Hongzhan Wang, Hui Dong, Fuer Lu and Fen Yuan
- 178 **GC-MS chemical profiling, antioxidant, anti-diabetic, and anti-inflammatory activities of ethyl acetate fraction of *Spilanthes filicaulis* (Schumach. and Thonn.) C.D. Adams leaves: experimental and computational studies**
Oluwafemi Adeleke Ojo, Akingbolabo Daniel Ogunlakin, Gideon Ampoma Gyebi, Damilare IyinKristi Ayokunle, Adeshina Isaiah Odugbemi, Dare Ezekiel Babatunde, Omolola Adenike Ajayi-Odoko, Matthew Iyobhebhe, Samson Chukwuemeka Ezea, Christopher Oloruntoba Akintayo, Ademola Ayeleso, Adebola Busola Ojo and Omolara Olajumoke Ojo
- 198 ***Lippia javanica* (Burm. F.) Herbal Tea: Modulation of Hepatoprotective Effects in Chang Liver Cells via Mitigation of Redox Imbalance and Modulation of Perturbed Metabolic Activities**
Veronica F. Salau, Ochuko L. Erukainure, Kolawole A. Olofinisan, Recardia L. S. Schoeman and Motlalepula G. Matsabisa
- 212 **Attenuating effect of *Polygala tenuifolia* Willd. seed oil on progression of MAFLD**
Meiling Xin, Hanlin Wang, Meng Wang, Bendong Yang, Shufei Liang, Xiaoxue Xu, Ling Dong, Tianqi Cai, Yuhong Huang, Qing Wang, Chao Wang, Yuting Cui, Zhengbao Xu, Wenlong Sun, Xinhua Song and Jinyue Sun
- 222 **Reversal of mitochondrial permeability transition pore and pancreas degeneration by chloroform fraction of *Ocimum gratissimum* (L.) leaf extract in type 2 diabetic rat model**
A. J. Salemcity, John Oludele Olanlokun, A. O. Olowofolahan, F. O. Olojo, Ayodeji Mathias Adegoke and O. O. Olorunsogo



OPEN ACCESS

EDITED BY
Javier Echeverria,
University of Santiago, Chile

REVIEWED BY
Luca Rastrelli,
University of Salerno, Italy

*CORRESPONDENCE
Chika Ifeanyi Chukwuma,
✉ chykochi@yahoo.com,
✉ cchukwuma@cut.ac.za

RECEIVED 24 January 2024
ACCEPTED 12 February 2024
PUBLISHED 23 February 2024

CITATION
Muhammad A, Chukwuma CI, Erukainure OL
and Islam MS (2024), Editorial: Therapeutic
potential of natural products in oxidative and
metabolic diseases.
Front. Pharmacol. 15:1375788.
doi: 10.3389/fphar.2024.1375788

COPYRIGHT
© 2024 Muhammad, Chukwuma, Erukainure
and Islam. This is an open-access article
distributed under the terms of the [Creative
Commons Attribution License \(CC BY\)](#). The use,
distribution or reproduction in other forums is
permitted, provided the original author(s) and
the copyright owner(s) are credited and that the
original publication in this journal is cited, in
accordance with accepted academic practice.
No use, distribution or reproduction is
permitted which does not comply with
these terms.

Editorial: Therapeutic potential of natural products in oxidative and metabolic diseases

Aliyu Muhammad¹, Chika Ifeanyi Chukwuma ^{2*},
Ochuko Lucky Erukainure³ and Md. Shahidul Islam⁴

¹Department of Biochemistry, Faculty of Life Sciences, Ahmadu Bello University, Zaria, Kaduna, Nigeria, ²Centre for Quality of Health and Living (CQHL), Faculty of Health and Environmental Sciences, Central University of Technology, Bloemfontein, Free State, South Africa, ³Department of Microbiology, School of Life Sciences, University of KwaZulu-Natal, Durban, South Africa, ⁴Department of Biochemistry, School of Life Sciences, University of KwaZulu-Natal, Durban, South Africa

KEYWORDS

phytochemicals, functional foods, oxidative stress, diabetes, obesity, cardiovascular diseases

Editorial on the Research Topic

[Therapeutic potential of natural products in oxidative and metabolic diseases](#)

Introduction

Research on the therapeutic potential of natural products in oxidative and metabolic diseases has gained significant attention in the recent years. Oxidative stress and metabolic dysregulations have been implicated in various health conditions, including cardiovascular diseases, diabetes, neurodegenerative disorders, obesity and so on (Salau et al.). Natural products, derived from plants are rich in bioactive compounds with antioxidant and metabolic modulating properties (Chanu et al.). This thematic issue was conceived on the baseline information that oxidative and metabolic diseases represent a large proportion of global public health challenges and quality of life. These diseases are often characterised by the imbalance between the cellular prooxidant (products of metabolic processes) and the antioxidant molecules within the cells. The imbalance often leads to the underlying factors that exacerbate the pathogenesis of some life-threatening diseases such as cancer, obesity, diabetes, and cardiovascular diseases. On the other hand, natural products, including phytochemicals and functional foods are known for their ability to modulate metabolic processes such as ameliorating reactive oxygen species (ROS)-induced mitochondria dysfunction, mitigating inflammatory response, and other cellular functions that could ameliorate the disease developments (Alruhaimi et al.; Chanu et al.). Despite the relatively low toxicities of natural products as compared to synthetic medicines, further studies are still required to optimize their bioavailability, therapeutics, pharmaceuticals, at different experimental settings including pre-clinical and clinical trials in patients suffering from oxidative and metabolic diseases.

Over the years, the treatment and management of metabolic disorders and metabolic syndromes including diabetes, obesity and cardiovascular diseases have been challenging due to higher cost, lack of safety and several adverse effects of the synthetic drugs (Chanu et al.). As these disorders are exacerbated by oxidative and inflammatory stress, natural products including

phytochemicals, functional foods, and nutraceuticals with antioxidative and anti-inflammatory properties have now been increasingly utilized as an alternative therapeutics. Natural products are naturally embedded with pharmacological activities useful for the prevention and treatment of various diseases. They are often utilized as starting points for drug discovery research which can lead to the development of a new drug with improved efficacy and safety. Metabolic disorders are multifactorial diseases, thus the use of natural products as a supplement may also be effective in the treatment of these diseases.

The envisaged Research Topics are a collection of quality original research articles that provide both experimental and clinical data on the potential therapeutic relevance of natural products, including phytochemicals and functional foods in the management of oxidative and metabolic diseases. In addition to original research articles, we were able to accommodate some well-articulated review articles with original interpretations of existing knowledge to expose scientific gaps and to provide new insights into the therapeutic prospects of phytochemicals and functional food in oxidative and metabolic disorders. The thematic areas which were relevant to the therapeutic relevance of natural products in diabetes and obesity, cardiovascular diseases, and oxidative stress and inflammation were considered in the Research Topic. In this editorial, we attempted to highlight the findings and potential impacts of some of the notable articles published under the Research Topic as briefly described below.

As shown in some of the studies, the antidiabetic potentials of natural products comprise different mechanisms. [Chanu et al.](#)'s study provided scientific support for the utilization of *Ageratina adenophora* in treating type 2 diabetes in a the streptozotocin (STZ) and nicotinamide (NA)STZ-NA-induced diabetic rat model. The possible mechanisms include inhibiting carbohydrate digestion and improving insulin sensitivity. [Alruhaimi et al.](#) demonstrated that a flavonoid-rich fraction of *Euphorbia peplus* attenuates hyperglycaemia, insulin resistance, and oxidative stress in a type 2 diabetes rat model. Berberine's ability to enhance the function of the β -cells of pancreatic islets in db/db mice through the GLP-1/GLP-1R/PKA signalling pathway was reported by [Wu et al.](#) [Salemcity et al.](#) demonstrated the reversal of mitochondrial permeability transition pore and pancreas degeneration by the chloroform fraction of *Ocimum gratissimum* (L.) leaf extract in a type 2 diabetic rat model. All the above-mentioned studies highlighted the potentials of natural products and compounds for the management of type 2 diabetes.

Some other studies suggest that the anti-inflammatory and antioxidant potentials of natural products could mitigate the damage of key metabolic organs and improve associated disease conditions. [Alshehri and Alorfi](#) elucidated the protective efficacy of resveratrol against Vancomycin-induced hepatotoxicity in male Wistar rats through oral administration. The co-treatment of resveratrol with vancomycin demonstrated a pronounced hepatoprotective effect, averting the elevation of key markers such as AST, ALT, ALP, IL-6, and MDA. Additionally, it protected the liver from the depletion of NO and GSH. [Salau et al.](#) documented the hepatoprotective effects of *Lippia javanica*

(Burm. F.) Herbal Tea in Chang liver cells by mitigating redox imbalance and perturbed metabolic activities. This underscores its potential as a therapeutic agent for oxidative stress-related liver diseases.

[Abo-Saif et al.](#) reported the cardioprotective potential of pomegranate peel extract in diabetic rats, attributing its efficacy to unique antioxidant, anti-inflammatory, and antifibrotic properties. The inhibition of the NLRP3/caspase-1/IL-1 β signalling pathway and downregulation of lncRNA-MALAT1 were identified as key mechanisms in this study. The study of [Mazhar et al.](#) showed that Zhilong Huoxue Tongyu capsule could attenuate intracerebral haemorrhage-induced redox imbalance by modulating the Nrf2 signalling pathway.

The therapeutic potential of natural products on dyslipidaemia was also documented. [Abduh et al.](#) established that *Averrhoa carambola* leaves effectively prevent dyslipidaemia and oxidative stress in a rat model of acute hyperlipidaemia-induced by poloxamer-407. This protective effect was attributed to the modulation of factors related to lipoprotein lipase (LPL), phospholipids (PL), HMG-CoA reductase, and cholesterol synthesis. [Xin et al.](#) reported that *Polygala tenuifolia* Willd. seed oil (PWSO) treatment inactivated SREBP1 and SREBP2, inhibiting hepatic lipid accumulation and mitigating inflammation via the NF- κ B signalling pathway. This study suggested the potential use of PWSO as a dietary supplement to inhibit the occurrence and development of metabolism-associated fatty liver disease (MAFLD).

[Sayed et al.](#)'s comprehensive review provided insights into the mechanisms of action and therapeutic potential of natural products as novel anti-obesity agents. In another review, [Wang and Li](#) reported the therapeutic role of baicalin in various lung diseases, including chronic obstructive pulmonary disease, asthma, pulmonary fibrosis, pulmonary hypertension, pulmonary infections, acute lung injury/acute respiratory distress syndrome, and lung cancer, while elucidating the underlying mechanisms.

Overall, these insights encourage continued exploration of natural products for their valuable contributions to preventive and therapeutic strategies in human health, particularly for oxidative and metabolic disorders.

Author contributions

AM: Writing—original draft. CC: Writing—review and editing. OE: Writing—review and editing. MI: Writing—review and editing.

Conflict of interest

The authors declare that the research was conducted in the absence of any commercial or financial relationships that could be construed as a potential conflict of interest.



OPEN ACCESS

EDITED BY

Aliyu Muhammad,
Ahmadu Bello University, Nigeria

REVIEWED BY

Aminu Mohammed,
Ahmadu Bello University, Nigeria
Dharmani Devi Murugan,
University of Malaya, Malaysia

*CORRESPONDENCE

Maisa Siddiq Abduh,
✉ mabdoh@kau.edu.sa
Sultan A. M. Saghir,
✉ sultan_a1976@yahoo.com
Ayman M. Mahmoud,
✉ a.mahmoud@mmu.ac.uk

SPECIALTY SECTION

This article was submitted to
Ethnopharmacology,
a section of the journal
Frontiers in Pharmacology

RECEIVED 30 December 2022

ACCEPTED 23 January 2023

PUBLISHED 06 February 2023

CITATION

Abduh MS, Saghir SAM, Al Hroob AM,
Bin-Amman A, Al-Tarawni AH,
Murugaiyah V and Mahmoud AM (2023),
Averrhoa carambola leaves prevent
dyslipidemia and oxidative stress in a rat
model of poloxamer-407-induced
acute hyperlipidemia.
Front. Pharmacol. 14:1134812.
doi: 10.3389/fphar.2023.1134812

COPYRIGHT

© 2023 Abduh, Saghir, Al Hroob, Bin-Amman, Al-Tarawni, Murugaiyah and Mahmoud. This is an open-access article distributed under the terms of the [Creative Commons Attribution License \(CC BY\)](https://creativecommons.org/licenses/by/4.0/). The use, distribution or reproduction in other forums is permitted, provided the original author(s) and the copyright owner(s) are credited and that the original publication in this journal is cited, in accordance with accepted academic practice. No use, distribution or reproduction is permitted which does not comply with these terms.

Averrhoa carambola leaves prevent dyslipidemia and oxidative stress in a rat model of poloxamer-407-induced acute hyperlipidemia

Maisa Siddiq Abduh^{1,2*}, Sultan A. M. Saghir^{3,4*}, Amir M. Al Hroob³, Albandari Bin-Amman⁵, Ayat H. Al-Tarawni⁶, Vikneswaran Murugaiyah⁴ and Ayman M. Mahmoud^{7,8*}

¹Immune Responses in Different Diseases Research Group, Department of Medical Laboratory Sciences, Faculty of Applied Medical Sciences, King Abdulaziz University, Jeddah, Saudi Arabia, ²Center of Excellence in Genomic Medicine Research, King Abdulaziz University, Jeddah, Saudi Arabia, ³Department of Medical Analysis, Princess Aisha Bint Al-Hussein College of Nursing and Medical Sciences, Al-Hussein Bin Talal University, Ma'an, Jordan, ⁴Department of Pharmacology, School of Pharmaceutical Sciences, Universiti Sains Malaysia, Penang, Malaysia, ⁵Department of Clinical Nutrition, College of Applied Medical Sciences, University of Hail, Hail, Saudi Arabia, ⁶Department of Biological Sciences, Mutah University, Al-Karak, Jordan, ⁷Department of Life Sciences, Faculty of Science and Engineering, Manchester Metropolitan University, Manchester, United Kingdom, ⁸Physiology Division, Department of Zoology, Faculty of Science, Beni-Suef University, Beni-Suef, Egypt

Background: The star fruit [*Averrhoa carambola* L (Oxalidaceae)] is traditionally used in the treatment of many ailments in many countries. It possesses several pharmacological activities, including antioxidant and anti-inflammatory effects. However, it contains the neurotoxic caramboxin and its high content of oxalic acid limits its consumption by individuals with compromised kidney function. This study assessed the anti-hyperlipidemic and antioxidant activities of different fractions of the methanolic extract of *A. carambola* leaves (MEACL).

Methods: The antioxidant activity was investigated using FRAP, and ABTS and DPPH radical-scavenging assays and the inhibitory activity toward pancreatic lipase (PL) and HMG-CoA reductase was assayed *in vitro*. Acute hyperlipidemia was induced by poloxamer-407 (P-407) in rats and different fractions of MEACL (*n*-hexane, chloroform, *n*-butanol, ethyl acetate (EA), water, and chloroform) were orally administered. Cholesterol and triglycerides were determined at 0, 12, 24, and 48 h and LDL-C, vLDL-C, HDL-C, lipid peroxidation (LPO) and antioxidants were assayed after 48 h. The expression of ABCA1, ABCG5, ABCG8, LDL-R, SREBP-1, and SREBP-2 and the activity of HMG-CoA reductase were assayed in the liver of P-407-administered rats treated with the EA fraction.

Results: The *in vitro* data revealed potent radical-scavenging activities of MEACL fractions with the most potent effect showed by the EA fraction that also suppressed the activities of HMG-CoA reductase and PL. In P-407-induced hyperlipidemic rats, all fractions prevented dyslipidemia as shown by the decrease in total cholesterol, triglycerides, LDL-C, vLDL-C and atherogenic index. MEACL and its fractions prevented LPO and boosted GSH, superoxide dismutase, glutathione peroxidase, and catalase in P-407-administered rats. The EA fraction showed more effective anti-hyperlipidemic and antioxidant effects than other fractions and downregulated SREBP-2 while upregulated ABCA1 and LDL-R and ameliorated LPL and HMG-CoA reductase in hyperlipidemic rats.

Conclusion: MEACL showed *in vitro* and *in vivo* antioxidant activity and the EA fraction significantly ameliorated dyslipidemia in a rat model of P-407-induced acute hyperlipidemia by modulating LPL, PL, HMG-CoA reductase, and cholesterolgenesis-related factors. Therefore, the leaves of *A. carambola* represent a safe alternative for the star fruit particularly in kidney disease patients, and the EA is the most effective anti-hyperlipidemic and antioxidant fraction.

KEYWORDS

star fruit, dyslipidemia, oxidative stress, cholesterol, triglycerides

1 Introduction

Dyslipidemias are characterized by abnormal circulating levels of cholesterol (CHOL) and/or triglycerides (TG) and their related lipoprotein species (Berberich and Hegele, 2022). Dyslipidemia can increase the risk for cardiovascular disease (CVD) and increased atherosclerotic CVD risk is the common clinical consequence. High plasma CHOL is a characteristic feature of atherosclerosis which may lead to many serious diseases, including ischemic heart disease, stroke, and myocardial infarction (Berberich and Hegele, 2022). Hepatic synthesis and diet are the main sources of plasma CHOL and TG, and 3-hydroxy-3-methylglutaryl CoA (HMG-CoA) reductase is the rate limiting enzyme for hepatic cholesterol synthesis (Sato and Takano, 1995). Etiologically, many factors such as suboptimal diet, obesity, sedentary life style, genetic deviations, metabolism abnormalities, insulin resistance, defects in intestinal absorption of CHOL and lipids and mutations in cell surface receptors and enzymes could contribute to the development of the dyslipidemias (Su et al., 2022). The rising frequency of non-communicable diseases and its link to hyperlipidemias has reached epidemic statistical proportions, necessitating a greater focus on their influence on premature death, particularly among young adults. The number of years lost to cardiovascular illnesses with a metabolic base, such as coronary ischemia disease and ischemic stroke, climbed from fourth to first place between 1990 and 2017 (Afshin et al., 2019). Hyperlipidemia is associated with redox imbalance and oxidative stress (Yang et al., 2008; Singh et al., 2017). The accumulation of lipids within the cells increases reactive oxygen species (ROS) release, leading to oxidative stress which can negatively impact many organs (Furukawa et al., 2004). The oxidative modification of glucose, LDL-C, and proteins, along with activated NADPH oxidase and altered mitochondrial membrane properties leading to the leakage of ROS are the common contributors to hyperlipidemia-associated oxidative stress (Yang et al., 2008; Singh et al., 2017).

Lipid metabolism in mammals is tightly regulated through the controlling effect of the transcription factors sterol regulatory-element binding proteins (SREBPs) on the expression of genes involved in cholesterolgenesis, and synthesis of fatty acids and TG (Horton et al., 2002). SREBP-1 controls genes of many factors involved in TG biosynthesis and SREBP-2 controls important genes in the synthesis and uptake of CHOL such as HMG-CoA reductase and LDL receptor (LDL-R) (Horton et al., 2002). The CHOL efflux pathways are essential in inhibiting excessive CHOL accumulation within the cells and mediated *via* the ATP binding cassette (ABC) subfamily A member 1 (ABCA1), ABCG5 and ABCG8. ABCA1 is involved in maintaining CHOL homeostasis through the reverse CHOL transport pathway by facilitating CHOL transport to outside the cell where it being received by

apolipoprotein-A1 (Yang et al., 2016). ABCG5 and ABCG8 play a key role in the direct excretion of CHOL *via* the bile (Yu et al., 2002). Statins, bile acid sequestrants, fibrates, and lomitapide are among the lipid-lowering agents used for the management of dyslipidemias (Berberich and Hegele, 2022). Despite their beneficial lipid-lowering activities, the use of statins and other agents could be associated with adverse effects such as the development of muscle disorders and diabetes (He et al., 2018; Newman et al., 2019). Therefore, the search for new anti-hyperlipidemic agents with minimal or no side effects and high therapeutic efficacy would be valuable for the management of dyslipidemias.

Several plant species and their derived active constituents have shown beneficial lipid-lowering activities in preclinical models (Mahmoud, 2012; Mahmoud et al., 2012; Hozayen et al., 2016; Mahmoud et al., 2017; Aladaileh et al., 2019; Germoush et al., 2019; Elsayed et al., 2020). *Averrhoa carambola* L. (Oxalidaceae) is widely consumed in South American and Asian countries due to its rich content of vitamins and minerals. It is commonly known as star fruit and is traditionally used in the treatment of several ailments. The star fruit showed interesting pharmacological effects in different *in vitro* and *in vivo* studies (Luan et al., 2021). It ameliorated steatosis partly by suppressing lipogenesis in *db/db* mice (Pang et al., 2017), and attenuated adipocyte differentiation *in vitro* (Mohamed Rashid et al., 2016). The use of star fruit was associated with toxic effects, particularly seizures, confusion and even coma (Chang et al., 2000; Neto et al., 2003; Tsai et al., 2005). Neurological adverse effects mimicking a stroke have been recently reported to accompany acute intoxication with star fruit (Stumpf, 2020). The neurotoxicity of star fruit could be directly connected to the presence of the neurotoxin caramboxin (Yasawardene et al., 2020). The presence of large oxalate content renders the star fruit nephrotoxic (Chen et al., 2001). Therefore, the leaves of *A. carambola* could be a safe alternative to the use of the star fruit. The leaves of this plant species showed a topical anti-inflammatory effect in a murine model of ear edema by inhibiting myeloperoxidase activity (Cabrini et al., 2011). The hydro-ethanolic extract of the leaves protected rats against acidified ethanol-induced gastric ulcer (Goncalves, 2006) and showed potent hypoglycemic effect (Ferreira et al., 2008). Recently, we demonstrated that the methanolic extract of *A. carambola* leaves (MEACL) has no acute or chronic toxic effects in male and female rats using doses up to 5,000 mg/kg (Saghir et al., 2022). In addition, we have reported the lipid-lowering efficacy of MEACL in rats fed a high fat diet for 5 weeks (Aladaileh et al., 2019). The current study aimed to investigate the antioxidant and anti-dyslipidemia effects of different fractions of MEACL using *in vitro* assays and *in vivo* poloxamer-407 (P-407)-induced acute hyperlipidemic rat model.

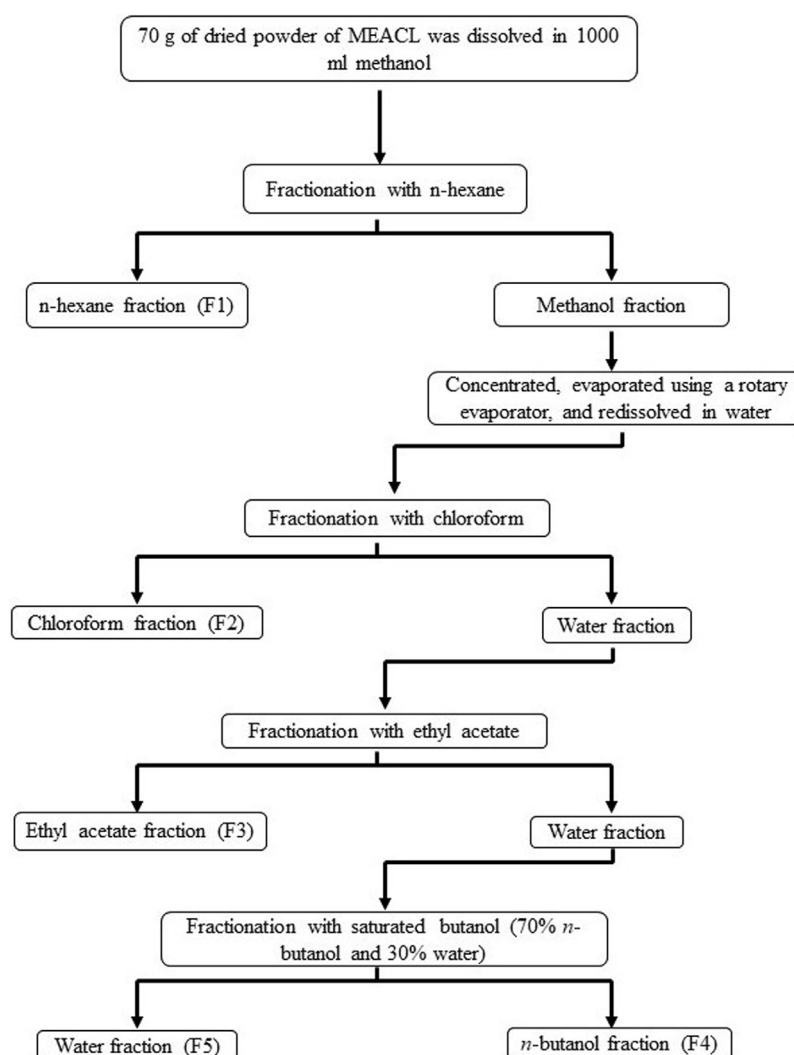


FIGURE 1

A flow chart showing the fractionation of MEACL.

2 Materials and methods

2.1 Chemicals and reagents

Ferrous sulfate heptahydrate, aluminum chloride (AlCl_3) and chloroform were purchased from R&M Chemicals (Malaysia). Ascorbic acid, 2,2'-diphenyl-1-picrylhydrazyl (DPPH), gallic acid, potassium acetate, Folin-Ciocalteu reagent, sodium carbonate, thiobarbituric acid (TBA), sodium nitrate, sodium hydroxide, carboxymethyl cellulose (CMC), 2,2-azino-bis (3-ethylbenzothiazoline-6-sulfonic acid) (ABTS), P-407, diammonium salt, ferric chloride (FeCl_3), 2,4,6-tri (2-pyridyl)-s-triazine (TPTZ), potassium chloride (KCl), hydrochloric acid (HCl) and potassium persulfate were purchased from Sigma-Aldrich (Germany). Total CHOL and TG assay kits were obtained from ThermoFisher Scientific (United States), and atorvastatin was purchased from Ranbaxy (Malaysia).

2.2 Collection and extraction of plant leaves, and fractionation of the methanolic extract

A. carambola leaves were collected from University Sains Malaysia (USM) main campus and authenticated under a voucher specimen No.11238. The leaves were cleaned, dried and ground in a mixer grinder. The powdered material was macerated in methanol at room temperature (RT) for 9 days at a ratio of 1:6 (w/v). The extract was decanted every 72 h and a new solvent was added. The extracts were pooled, filtered using cotton plug and Whatman No. 1 filter paper, concentrated with a rotary evaporator, and freeze-dried. The fractionation of MEACL was carried out using the liquid-liquid partition method, which involved utilizing several solvents in order of increasing polarity, from less polar to high polar (Ferreira et al., 2014). The used solvents were *n*-hexane, chloroform, ethyl acetate (EA) and *n*-butanol at a proportion of 1:1, repeated for 3 times each. Briefly, 70 g of MEACL was dissolved in 700 mL of methanol and fractionated

TABLE 1 Primers used for qRT-PCR.

Gene	Genbank accession number	Sequence (5'-3')	Amplicon size (bp)
<i>Abca1</i>	NM_178095.3	F: GCAGCGACCATGAAAGTGAC	185
		R: GAGGCGGTCATCAATCTCGT	
<i>Abcg5</i>	NM_053754.2	F: GGGAAGTGTTTGTGAACGGC	121
		R: GTGTATCTCAGCGTCTCCCG	
<i>Abcg8</i>	NM_130414.2	F: TTCTGATGACGTCTGGCACC	97
		R: TTGCTGTAGCGAGACAAGG	
<i>Srebp1</i>	NM_001276708.1	F: CGGAGCCATGGATTGCACATT	104
		R: CTGTCTCACCCCCAGCATAG	
<i>Srebp2</i>	NM_001033694.2	F: TCAAACATGGCGGCGGTTG	159
		R: AGCTCGCTGTTCTCATCCAT	
<i>Ldlr</i>	NM_175762.3	F: CATTTTCAGTGCCAAACGCC	127
		R: TGCCTCACACCAGTTTACCC	
<i>Actb</i>	NM_031144.3	F: AGGAGTACGATGAGTCCGGC	71
		R: CGCAGCTCAGTAACAGTCCG	

Abca1, ATP, binding cassette subfamily A member 1; *Abcg5*, ATP, binding cassette subfamily G member 5; *Abcg8*, ATP, binding cassette subfamily G member 8; *Srebp1*, sterol regulatory element binding protein 1; *Ldlr*, low density lipoprotein receptor; *Actb*, beta actin.

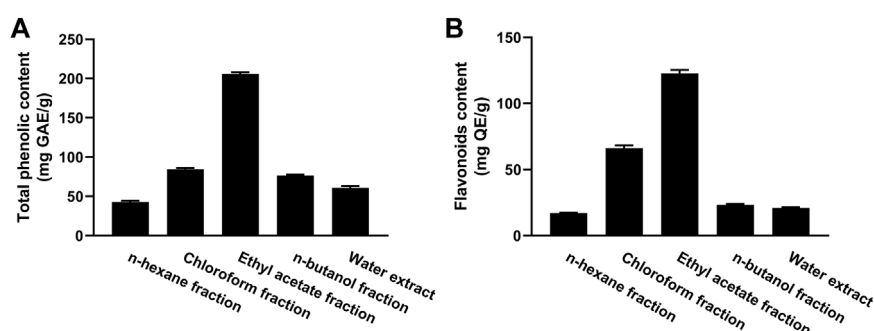


FIGURE 2

Total phenolic (A) and flavonoid (B) content of different fractions of MEACL. Data are Mean ± SEM (n = 3).

firstly with *n*-hexane to yield the *n*-hexane and methanol fractions. The latter was evaporated using rotary evaporator at 40°C and resubstituted in water, which was further fractionated with chloroform and EA to yield chloroform and EA fractions, respectively. Subsequently, fractionation was carried out with water saturated *n*-butanol to yield butanol and water fractions, respectively (Figure 1). All fractions were concentrated using rotary evaporator at 40°C except the water fraction which was concentrated using freeze drying. The yield was calculated based on the weight of crude methanol extract initially used for the partitioning.

2.3 Determination of total phenolic (TP) and flavonoid content

The TP of different fractions of MEACL was determined using Folin-Ciocalteu reagent and gallic acid (GA) as a standard (Singleton

and Rossi, 1965). The test samples (20 µL of extracts or GA) were mixed with distilled water (1.8 mL), 2 N Folin-Ciocalteu reagent (100 µL) and 20% sodium carbonate (300 µL). After incubation for 2 h at RT, the absorbance was measured at 765 nm. The flavonoid content was measured using AlCl₃ method with quercetin (QE) as a reference (Chang et al., 2002). Briefly, the sample (500 µL), 10% (w/v) AlCl₃ (100 µL), 1 M potassium acetate (100 µL), methanol (1,500 µL) and distilled water (2,800 µL) were mixed and incubated at RT for 30 min. The absorbance was measured at 415 nm and the flavonoid content was expressed as mg of quercetin equivalent/g extract.

2.4 Evaluation of *in vitro* antioxidant activity

Ferric Reducing Antioxidant Power (FRAP), DPPH radical scavenging and ABTS radical scavenging assays were employed to

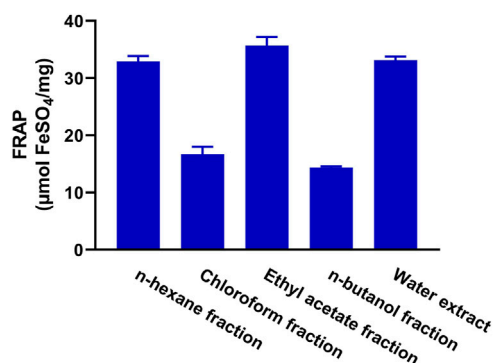


FIGURE 3
FRAP of the fractions of MEACL. Data are Mean \pm SEM ($n = 3$).

determine the antioxidant activity of MEACL fractions as described by Shahaboddin et al. (2011); Brand-Williams et al. (1995); Re et al. (1999), respectively. The FRAP reagent [10 mmol TPTZ in 40 mmol/L HCl, 20 mmol/L FeCl₃·6H₂O and 0.3 mmol/L acetate buffer (pH 3.6)]

was mixed with the samples and incubated for 4 min at 37°C. The absorbance was read at 593 nm against the blank (methanol) (Shahaboddin et al., 2011). In a 96-well plate, 100 μ L DPPH and 100 μ L sample were mixed and incubated for 30 min at RT in the dark. The absorbance of the mixture was measured at 517 nm (Brand-Williams et al., 1995). The ABTS radical cation (ABTS⁺) was prepared by mixing equal volumes of ABTS stock solution and 2.45 mM potassium persulfate. The mixture was left at RT for 12 h in dark prior to use. The concentrated ABTS⁺ solution was diluted to a final concentration that showed absorbance of 0.70 ± 0.02 at 734 nm. Each sample (50 μ L) was mixed with ABTS solution (150 μ L), vortexed for 15 s and the absorbance was recorded at 734 nm after 6 min.

2.5 Determination of HMG-CoA reductase and pancreatic lipase (PL) activities *in vitro*

The effect of the EA fraction on the activities of HMG-CoA reductase and PL was tested *in vitro*. The assay of the activity of HMG-CoA reductase is based on NADPH oxidation by the catalytic subunit of HMG reductase in the presence of HMG-CoA (Rao and Ramakrishnan, 1975) using pravastatin as a standard inhibitor. PL

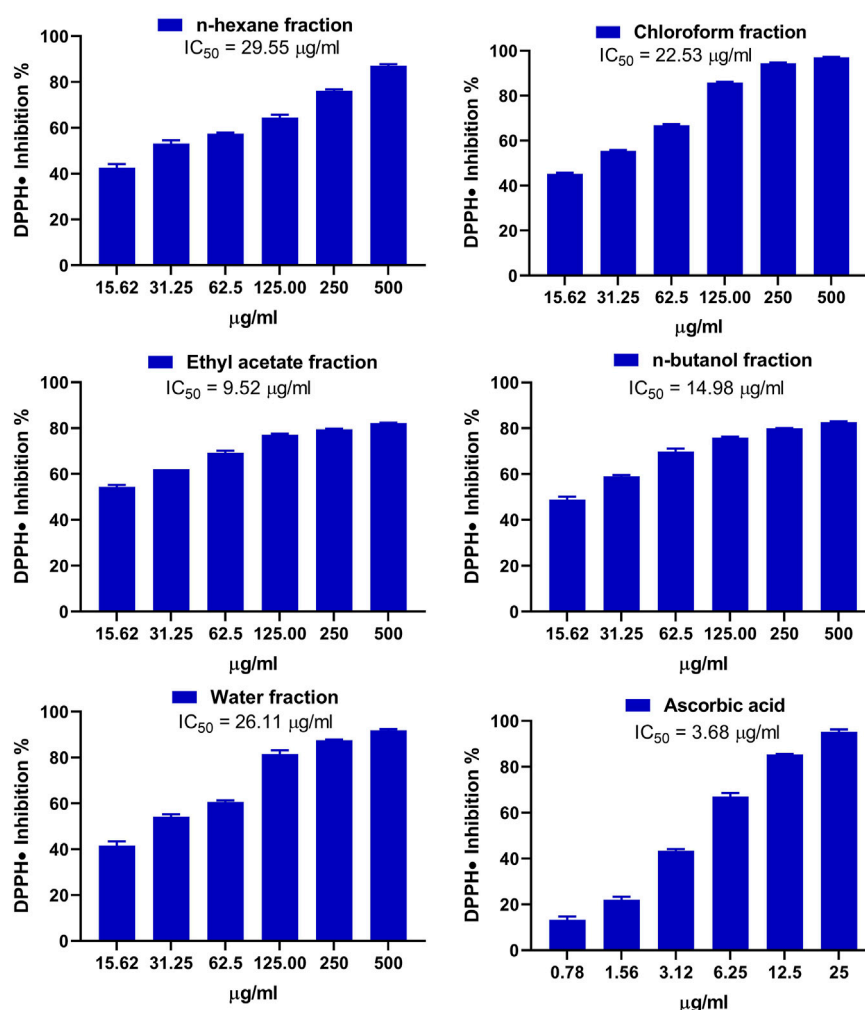


FIGURE 4
DPPH radical scavenging activity of the fractions of MEACL. Data are Mean \pm SEM ($n = 3$).

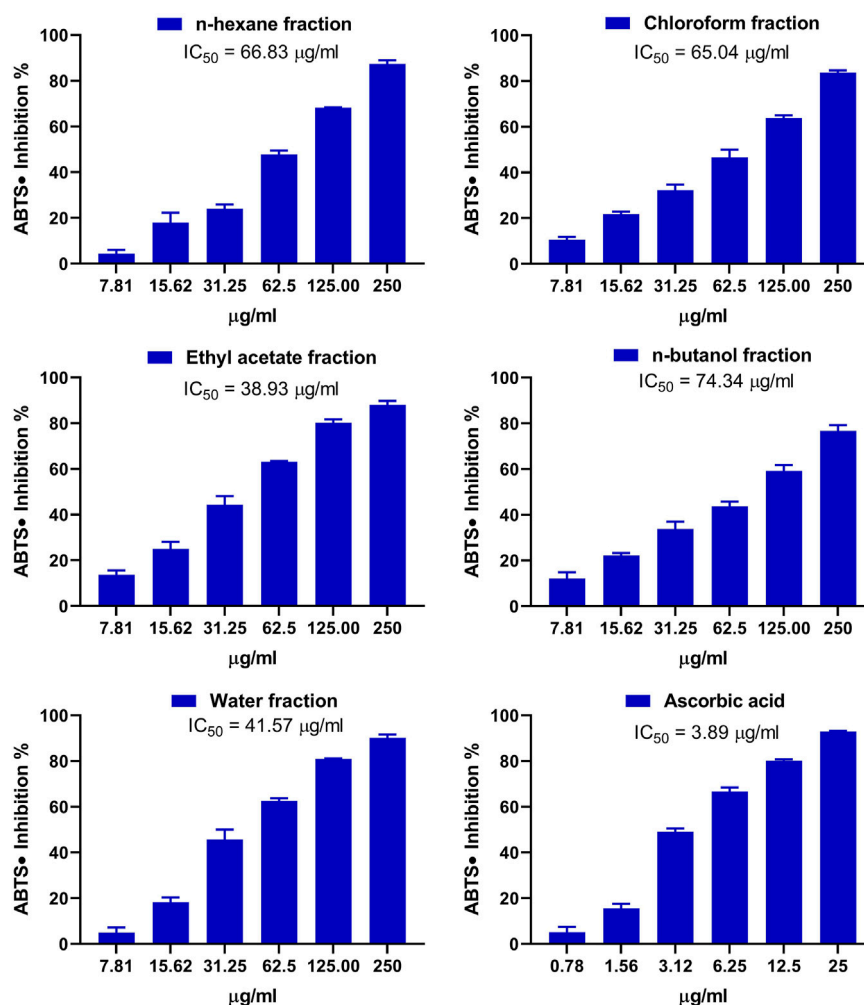


FIGURE 5
ABTS radical scavenging activity of the fractions of MEACL. Data are Mean \pm SEM ($n = 3$).

activity was measured using 4-methyl umbelliferone oleate (4 MUO) as a substrate. Using microplate reader at an excitation wavelength of 320 nm and an emission wavelength of 450 nm, the amount of 4-MUO liberated by lipase was measured.

2.6 *In vivo* anti-hyperlipidemic effect of MEACL fractions

2.6.1 Animals and treatments

Male Sprague Dawley (SD) rats (180–220 g) were obtained from the Animal Research and Service Centre (ARASC), University Sains Malaysia (USM). The rats were kept at standard temperature ($23^{\circ}\text{C} \pm 1^{\circ}\text{C}$) and humidity on a 12 h light/dark cycle with free access to food and tap water. The animals were maintained for 7 days to acclimate before the onset of experiment. The approval was obtained from Animal Ethics Committee, University Sains Malaysia, Penang, Malaysia [Approval number: USM/Animal Ethics Approval/2012/(77) (387)].

P-407-induced acute hyperlipidemia was developed to assess the antihyperlipidemic efficacy of MEACL fractions. P-407 was dissolved in physiological saline and refrigerated overnight to allow for cold

dissolution. Hyperlipidemia was produced by injecting a single dose (500 mg/kg) of P-407 intraperitoneally (i.p.) (Zanwar et al., 2014). A total of 48 SD rats were divided into eight groups ($n = 6$). Group I is control and groups II–VIII are hyperlipidemic rats as follows:

- Group I: Given i. p. injection of normal saline and 1% CMC.
- Group II: Received 1% CMC.
- Group III: Received 1,000 mg/kg *n*-hexane fraction dissolved in 1% CMC.
- Group IV: Received 1,000 mg/kg chloroform fraction dissolved in 1% CMC.
- Group V: Received 1,000 mg/kg EA fraction dissolved in 1% CMC.
- Group VI: Received 1,000 mg/kg *n*-butanol fraction dissolved in 1% CMC.
- Group VII: Received 1,000 mg/kg water fraction dissolved in 1% CMC.
- Group VIII: Received 60 mg/kg atorvastatin dissolved in 1% CMC.

CMC, atorvastatin, and the fractions were administered orally for 2 days (3 doses at 0, 24, and 48 h). To assay total CHOL (TC) and TG, about 150 μL of blood was taken from the tail vein at time 0 (pre), and

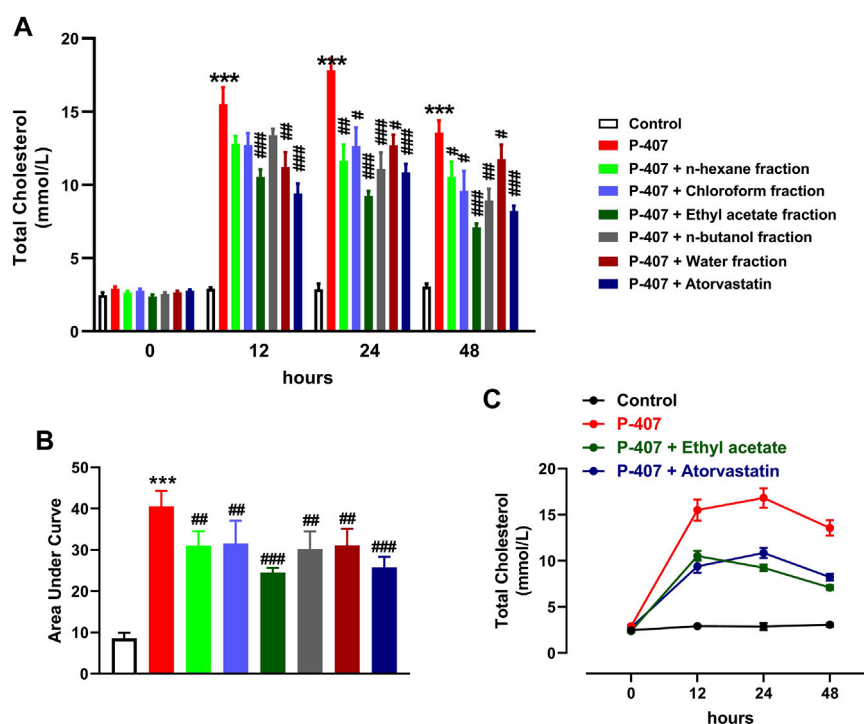


FIGURE 6

Effect of different fractions of MEACL on TC levels at 0, 12, 24, and 48 h (A, B). Changes in TC levels in control, hyperlipidemic and hyperlipidemic rats treated with ethyl acetate fraction or atorvastatin (C). Values are represented as mean \pm SEM ($n = 6$). *** $p < 0.001$ versus Control, and # $p < 0.05$, ## $p < 0.01$, and ### $p < 0.001$ versus P-407.

12 h and 24 h following the injection of P-407. Then, the terminal blood samples were obtained after 48 h *via* cardiac puncture under ketamine anesthesia to determine TC, TG, LDL-C, HDL-C, malondialdehyde (MDA), reduced glutathione (GSH), glutathione peroxidase (GPx), superoxide dismutase (SOD), and catalase (CAT). Blood samples were centrifuged for 10 min at 5,000 rpm to obtain serum, which was stored at -80°C prior to analysis. The rats were dissected and samples from the liver were collected on RNAlater for RNA isolation.

2.6.2 Biochemical assays

The levels of TC and TG were assayed using commercial kits according to the manufacturer's instructions. HDL-C and LDL-C were measured in serum using ARCHITECT C4000 Biochemistry Analyzer. Plasma Lipoprotein lipase (LPL) was measured as previously described (Hamilton et al., 1998; Mondragon et al., 2014). In this assay, the rats received 300 U/kg heparin intravenously and blood was collected after 15 min for the separation of plasma. LPL activity was calculated as total lipase minus the remaining activity after inhibition with 1 M NaCl. HMG-CoA reductase activity was determined in the liver as previously described (Rao and Ramakrishnan, 1975). The atherogenic index (AI) was calculated using the following equation (Wu et al., 2014).

$$AI = \frac{TC - HDL.C}{HDL.C}$$

MDA was assayed in serum samples according to Okhawa et al. (1979). This method uses the reaction of MDA with TBA and an MDA standard curve. GSH content was determined as previously reported (Ellman, 1959). SOD activity was determined depending

on its ability to inhibit superoxide radical formation in a reaction mixture containing xanthine and xanthine oxidase (XO). The activity of XO produces superoxide that reacts with hydroxylamine to form nitrite that could be detected by Griess reagent (Öyanagui, 1984). CAT activity was measured based on the enzyme-catalyzed decomposition of hydrogen peroxide (H_2O_2), whereby the residual H_2O_2 was determined (İşlekel et al., 1999). The assay of GPx activity was based on the decomposition of H_2O_2 to water and oxygen and the oxidation of GSH. The oxidized glutathione is reduced by glutathione reductase and the decrease in NADPH is monitored (Flohé and Günzler, 1984).

2.6.3 qRT-PCR

To assess the effect of the EA fraction on the expression of ABCA1, ABCG5, ABCG8, LDL-R, SREBP-1, and SREBP-2, RNA was isolated using Trizol reagent, treated with RNase-free DNase (Qiagen, Germany), quantified using a nanodrop, and sampled with A260/A280 ≥ 1.8 were used for cDNA synthesis using ThermoFisher (United States) kit. cDNA was amplified using SYBR Green master mix and the primers in Table 1 and B-actin as a control. The $2^{-\Delta\Delta\text{CT}}$ method (Livak and Schmittgen, 2001) was employed to analyze the data.

2.7 Statistical analysis

All results were expressed as mean \pm SEM. The statistical significance was determined by one-way ANOVA test followed by Tukey's *post hoc* test using GraphPad Prism 8. A $p < 0.05$ was considered significantly different.

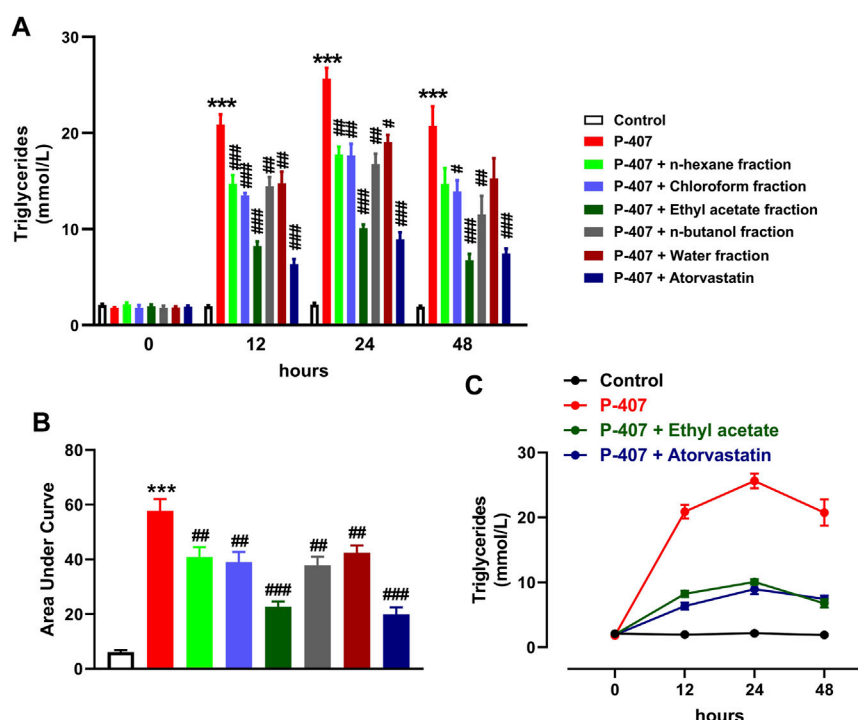


FIGURE 7

Effect of different fractions of MEACL on TG levels at 0, 12, 24, and 48 h (A, B). Changes in TG levels in control, hyperlipidemic and hyperlipidemic rats treated with ethyl acetate fraction or atorvastatin (C). Values are represented as mean \pm SEM ($n = 6$). *** $p < 0.001$ versus Control, and # $p < 0.05$, ## $p < 0.01$, and ### $p < 0.001$ versus P-407.

3 Results

3.1 Total phenolics (TP) and flavonoids

The TP content of the fractions of MEACL ranged from 42.75 to 205.65 mg GAE/g of dry extract (Figure 2A). The EA fraction exhibited the highest phenolic content (205.65 mg GAE/g) and the *n*-hexane fraction exhibited the lowest phenolic content (42.75 mg GAE/g). The flavonoid content ranged between 16.88 and 139.92 mg QE/g, with the highest content was recorded in the EA fraction followed by chloroform fraction (119.92 and 64.12 mg QE/g, respectively) as depicted in Figure 2B.

3.2 *In vitro* antioxidant activity

The antioxidant activity of the fractions of MEACL was assessed using FRAP (Figure 3), and DPPH (Figure 4) and ABTS (Figure 5) radical-scavenging assays. As shown in Figure 3, the highest activity was observed with the EA fraction (35.70 μ mol FeSO₄/mg) followed by water and *n*-hexane fractions (33.13 and 32.93 μ mol FeSO₄/mg, respectively), while the chloroform and *n*-butanol fractions showed the lowest FRAP (16.68 and 14.35 μ mol FeSO₄/mg, respectively). All fractions showed concentration-dependent scavenging activity toward DPPH and ABTS as shown in Figure 4 and Figure 5, respectively. The

EA fraction showed the lowest IC₅₀ values in both DPPH and ABTS radical-scavenging assays.

3.3 Anti-hyperlipidemic activity of different fractions of MEACL in P-407-administered rats

The data represented in Figures 6A–C and Figures 7A–C show the effect of various fractions of MEACL on TC and TG levels, respectively, in P-407-administered rats. Both TC and TG showed significant elevation after 12, 24, and 48 h in P-407-administered rats when compared with the control rats ($p < 0.001$). All fractions of MEACL as well as atorvastatin decreased blood TC and TG in P-407-administered rats at different time points. The effect of *n*-hexane, chloroform, and *n*-butanol fractions on TC levels at the 12 h time point was non-significant ($p > 0.05$), and *n*-hexane and water fractions decreased TG at 12 h and 24 h, but their effect after 48 h was non-significant. Among the MEACL fractions, the EA showed the most potent effect on blood TC and TG in P-407-administered rats at all time points. This anti-hyperlipidemic effect was further supported by the data represented in Figure 8. P-407 increased LDL-C (Figure 8A), vLDL (Figure 8B) and AI (Figure 8D) and decreased HDL-C (Figure 8C) significantly as compared to the control. The EA was the only effective fraction in decreasing serum LDL-C and increasing

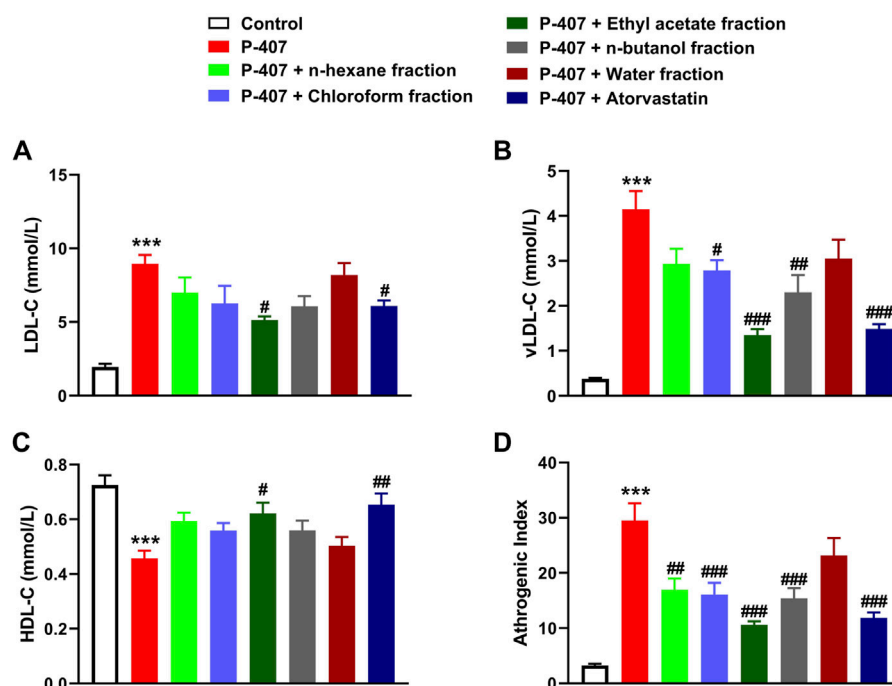


FIGURE 8

Effect of different fractions of MEACL on (A) LDL-C, (B) vLDL-C (C) HDL-C, and (D) atherogenic index after 48 h. Values are represented as mean \pm SEM ($n = 6$). *** $p < 0.001$ versus Control, and # $p < 0.05$, ## $p < 0.01$, and ### $p < 0.001$ versus P-407.

HDL-C in P-407-administered rats. The chloroform and *n*-butanol fractions decreased serum vLDL significantly and all fractions except the water fraction were effective in ameliorating the AI.

3.4 Different fractions of MEACL prevented oxidative stress in P-407-administered rats

MDA was significantly elevated in the blood of P-407-treated rats ($p < 0.001$) as represented in Figure 9A. The antioxidants GSH (Figure 9B), SOD (Figure 9C), CAT (Figure 9D), and GPx (Figure 9E) were decreased significantly in hyperlipidemic rats. All fractions of MEACL were effective in ameliorating MDA and enhancing GSH and antioxidant enzymes in hyperlipidemic rats. Of note, the EA fraction was more effective in decreasing MDA, and increasing GSH, CAT, and GPx.

3.5 Effect of the EA fraction on ABCA1, ABCG5, ABCG8, LDL-R, SREBP-1, and SREBP-2 in P-407-administered rats

Given that the EA fraction showed the most potent radical scavenging and anti-hyperlipidemic effects, we investigated its effect on the expression of ABCA1 (Figure 10A), ABCG5 (Figure 10B), ABCG8 (Figure 10C), LDL-R (Figure 10D), SREBP-1 (Figure 10E), and SREBP-2 (Figure 10F) in the liver of P-407-administered rats. The results showed decreased ABCA1 and LDL-R, and increased SREBP-2 in P-407-administered rats while ABCG5, ABCG8, and SREBP-1 were not changed. The EA fraction upregulated

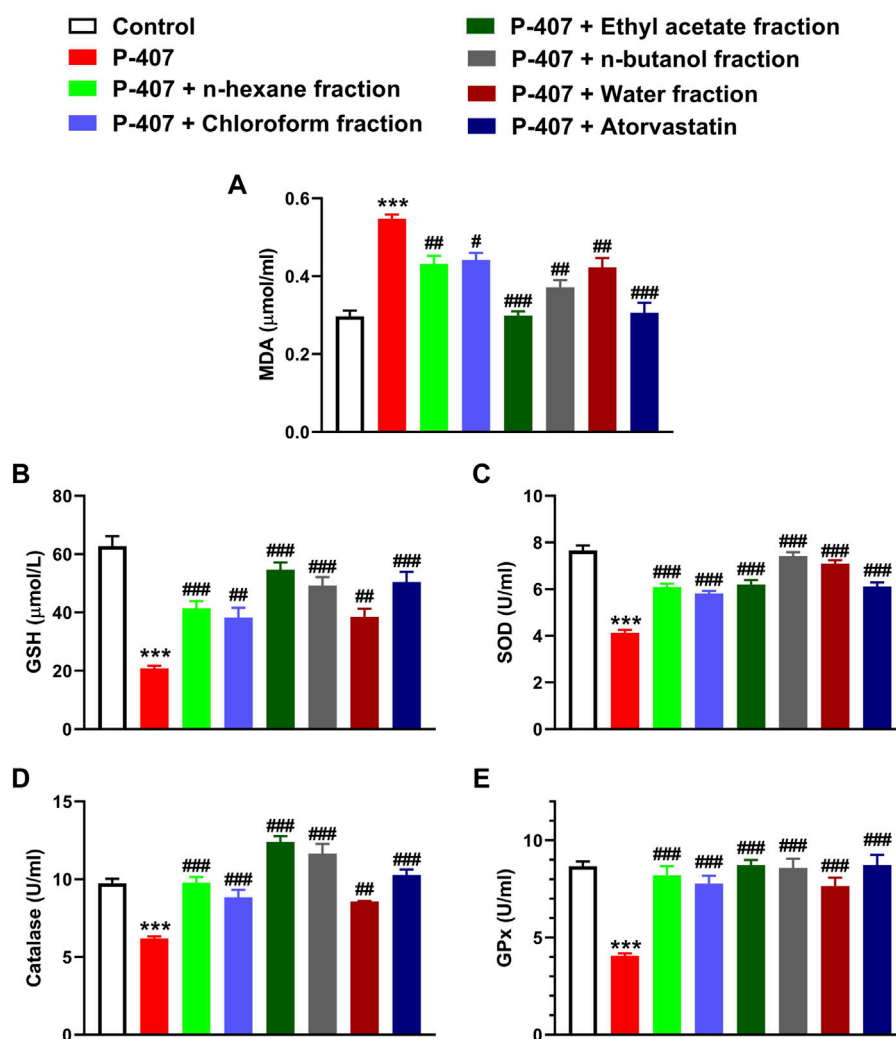
ABCA1 and LDL-R, and downregulated SREBP-2 in hyperlipidemic rats.

3.6 Effect of the EA fraction on HMG-CoA reductase, PL, and LPL

The administration of P-407 decreased plasma LPL (Figure 11A) and increased liver HMG-CoA reductase (Figure 11B) significantly in rats ($p < 0.001$). Treatment with the EA fraction increased LPL and decreased HMG-CoA reductase in P-407-administered rats. The EA fraction showed a concentration-dependent effect on the activity of HMG-CoA reductase *in vitro* when compared to the control as represented in Figure 11C. Similarly, the EA fraction exerted concentration-dependent inhibitory activity on PL (Figure 11D) *in vitro*.

4 Discussion

The star fruit (*A. carambola*) is traditionally used in many countries for the treatment of several ailments. Despite its beneficial effects, the use of the fruit could be associated with adverse effects such as neurotoxicity (Yasawardene et al., 2020). The leaves of *A. carambola* can represent a safe alternative and its methanolic extract (MEACL) has shown no acute or chronic toxicity up to 5,000 mg/kg (Saghir et al., 2022) and exhibited lipid-lowering efficacy in HFD-fed rats (Aladaileh et al., 2019). This study investigated the anti-hyperlipidemic and antioxidant efficacies of different fractions of MEACL in a rat model of acute

**FIGURE 9**

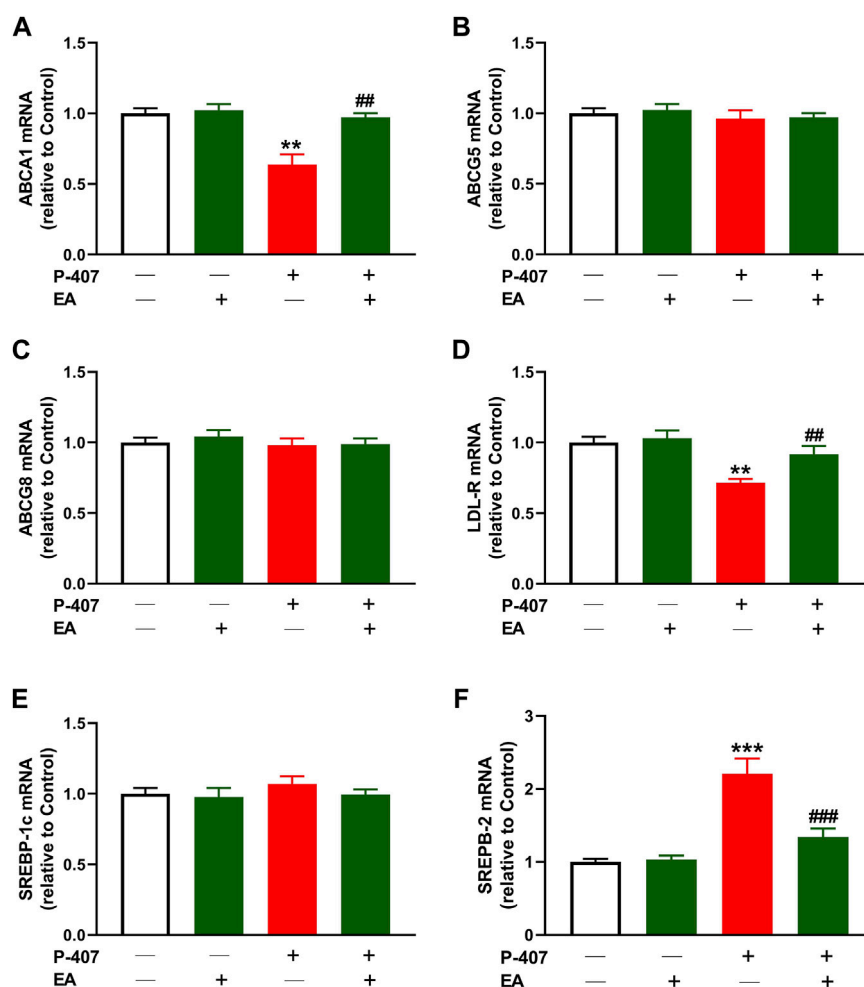
Effect of different fractions of MEACL (A) MDA, (B) GSH (C) SOD, (D) CAT, and (E) GPx in P-407-induced acute hyperlipidemic rats. Values are represented as mean \pm SEM ($n = 6$). *** $p < 0.001$ versus Control, and # $p < 0.05$, ## $p < 0.01$, and ### $p < 0.001$ versus P-407.

dyslipidemia, pointing to the changes in different factors related to lipid metabolism.

The phytochemical analysis of the fractions revealed that the TP and flavonoid content was the highest in the EA fraction followed by the chloroform fraction. In a prior investigation, MEACL demonstrated the highest levels of TP and flavonoid content among various extracts of *A. carambola* along with potent antioxidant activity (Saghir et al., 2016). The radical-scavenging and antioxidant power of polyphenolics, including flavonoids, through different mechanisms such as the hydrogen atom transfer and sequential proton loss electron transfer have been reported (Kamel et al., 2016; Elsayed et al., 2020). In accordance, the radical-scavenging activity (RSA) of different MEACL fractions have been demonstrated in this study. All fractions showed FRAP and scavenging properties against DPPH and ABST radicals, with the EA fraction was the most effective. This could be explained in terms of the higher content of TP and flavonoids. In accordance with our findings, Moresco et al. (2012) demonstrated that the EA fraction of the hydroalcoholic extract of *A. carambola* leaves had the highest TP

and flavonoids content and showed the highest DPPH RSA and FRAP when compared with other fractions. In our study, the superior RSA of the EA fraction was further supported by the ABTS assay that has been reported to be more reliable and accurate than DPPH in detecting the antioxidant capacity of natural products (Floegel et al., 2011).

The anti-hyperlipidemic effect of different MEACL fractions was studied in a rat model of hyperlipidemia induced by P-407. The administration of P-407 resulted in hypercholesterolemia and hypertriglyceridemia as previously reported in many studies (Johnston and Palmer, 1993; Leon et al., 2006; Chaudhary and Brocks, 2013; Park et al., 2016; Yeom et al., 2018). P-407 is a non-ionic copolymer surfactant that lacks toxicity and increases blood TC and TG significantly in different rodents mainly by suppressing LPL and TG hydrolysis, and inducing cholesterolgenesis (Johnston and Palmer, 1993; Leon et al., 2006; Chaudhary and Brocks, 2013). Treatment with different fractions of MEACL ameliorated serum TC and TG at 12, 24, and 48 h after the administration of P-407. Interestingly, the EA fraction showed the most potent ameliorative effect on serum TG and TC in P-407-treated rats, an effect that

**FIGURE 10**

Effect of the ethyl acetate fraction on (A) ABCA1, (B) ABCG5 (C) ABCG8, (D) LDL-R (E) SREBP-1, and (F) SREBP-2 in P-407-administered rats. Values are represented as mean \pm SEM ($n = 6$). ** $p < 0.01$ and *** $p < 0.001$ versus Control. ## $p < 0.01$, and ### $p < 0.001$ versus P-407.

coincided with the results of TP and flavonoid content and the *in vitro* RSA. In support of these findings, the EA was the only fraction that decreased serum LDL-C and increased HDL-C in P-407-administered rats. HDL-C is the good circulating CHOL that plays a role in decreasing blood CHOL levels and preventing the formation of atherosclerosis plaque (Stein and Stein, 1999). Thus, the increase in HDL-C following treatment with EA fraction pinpointed its protective effect against atherosclerosis and cardiovascular risk. Regarding the AI, all fractions except the water fraction were effective in decreasing its value.

Given that the EA fraction was the most effective in ameliorating hyperlipidemia in P-407-treated rats, we explored its effect on the expression of some genes involved in lipid metabolism in the liver. We assumed that the regulation of SREBPs and its regulated genes might be involved in the anti-hyperlipidemic effect of the EA fraction. In this study, P-407 injection did not alter SREBP-1 while increased hepatic SREBP-2 mRNA significantly, an effect that added support to previous studies showing similar findings (Leon et al., 2006; Park et al., 2016; Yeom et al., 2018). In conjunction with the upregulated SREBP-2, LDL-R mRNA was downregulated in P-407-treated rats. LDL-R is a

key receptor for the uptake and trafficking of CHOL and hence plays a role in its cellular and circulating homeostasis. As a target of SREBP-2, its transcription is regulated by intracellular sterol levels and is posttranscriptionally regulated by PCSK9 (Lambert et al., 2009). In the presence of high CHOL and its derivatives within the cells, SREBP-2 is complexed with SCAP and Insig in the endoplasmic reticulum and the transcription of LDL-R and genes necessary to lipogenesis are suppressed. When the cell sterols decrease, SREBP-2/SCAP dissociate from Insig and moves to Golgi apparatus where SREBP-2 is activated and subsequently promote the transcription of its target genes in the nucleus (Brown and Goldstein, 1999). In addition to SREBP-2 and LDL-R changes in P-407-treated rats, HMG-CoA reductase activity was upregulated in the liver of rats. HMG-CoA reductase is the rate-limiting enzyme in cholesterol synthesis and its transcription is regulated by SREBP-2. Inhibition of HMG-CoA reductase represents a main step in the treatment of hyperlipidemia through decreasing endogenous cholesterol synthesis. The EA fraction downregulated SREBP-2 and HMG-CoA reductase and upregulated LDL-R and hence increased cellular CHOL uptake and inhibited endogenous CHOL synthesis. The inhibitory effect of the

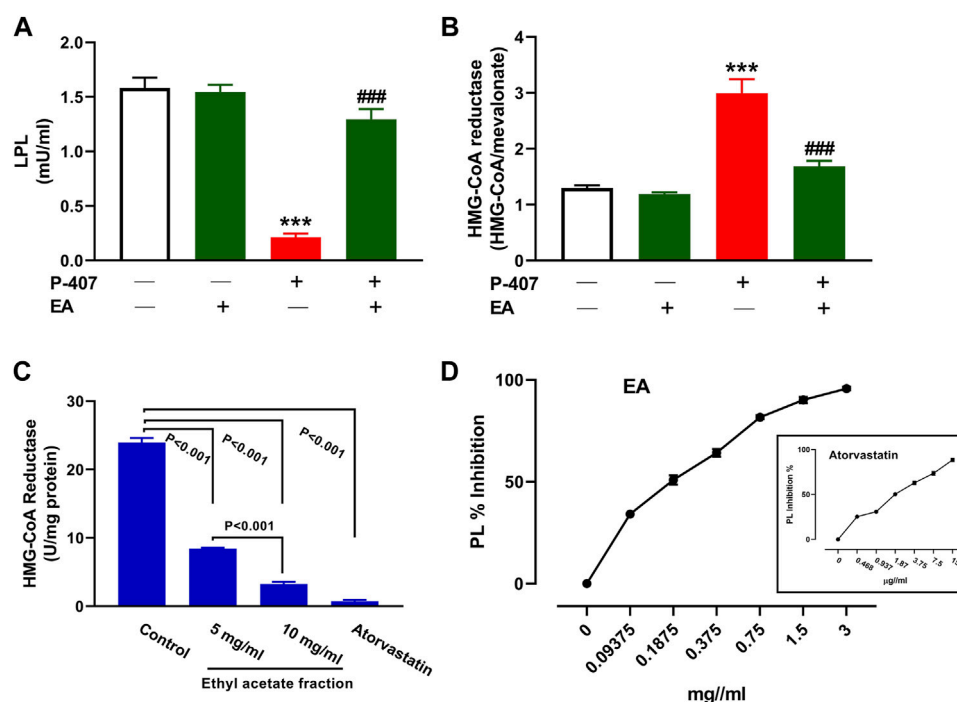


FIGURE 11

Effect of the EA fraction on plasma LPL (A) and hepatic HMG-CoA reductase (B) in P-407-administered rats. Values are represented as mean \pm SEM, ($n = 6$). *** $p < 0.001$ versus Control and ### $p < 0.001$ versus P-407. (C–D) Inhibitory activity of EA fraction on HMG-CoA reductase (C) and pancreatic lipase (D) *in vitro*. Data are Mean \pm SEM ($n = 3$).

EA fraction on hepatic HMG-CoA reductase in P-407-treated rats was supported by the *in vitro* assay that showed the concentration-dependent inhibitory activity of this fraction.

Besides studying the effect of the EA fraction on cholesterolgenesis-related factors, we evaluated its effect on the mRNA abundance of the genes involved in CHOL efflux, namely ABCA1, ABCG5 and ABCG8. The results showed that ABCA1 was downregulated whereas ABCG5 and ABCG8 mRNA levels were not affected in the liver of P-407-treated rats. In accordance with our findings, the expression of ABCG8 in the liver of P-407-administered mice was not changed as compared to the control mice as reported by Leon et al. (2006). The same study reported a trend decrease in the expression of hepatic ABCA1 in P-407-administered mice (Leon et al., 2006). The EA fraction ameliorated ABCA1 while had no effect on the expression of ABCG5 and ABCG8. These findings pinpointed that the anti-hypercholesterolemia effect of the EA is mediated *via* suppressing cholesterolgenesis and increasing CHOL and phospholipid efflux for the biosynthesis of HDL-C, but without affecting the biliary excretion of CHOL. Interestingly, these findings coincided with the decreased HDL-C levels in P-407-administered rats and its increase upon treatment with the EA fraction.

Hypertriglyceridemia caused by P-407 has mainly been attributed to the inhibition of LPL activity in rats and mice as previously reported (Johnston and Palmer, 1993). The findings of Johnston and Palmer study revealed that circulating TG increased following P-407 administration because of the reduced rate of TG hydrolysis (Johnston and Palmer, 1993). In addition to LPL, inhibition of hepatic lipase (HL) by P-407 in mice has been suggested to contribute to hypertriglyceridemia (Wasan et al., 2003). The current study showed a decrease in circulating LPL in P-407-

treated rats and its reversal in rats treated with the EA fraction. Furthermore, the EA fraction showed a concentration-dependent inhibition of PL *in vitro*. PL is a key enzyme responsible for TG hydrolysis and absorption in the small intestine and its inhibition can hence play a role in decreasing TG absorption and the increase in circulating TG level (Liu et al., 2013).

Given that the association between hyperlipidemia and redox imbalance was highlighted in different investigations (Yang et al., 2008; Singh et al., 2017) and the potent RSA of MEACL fractions, we evaluated changes in MDA and antioxidants in P-407-treated rats. The hyperlipidemic rats exhibited marked elevation in circulating MDA, and decreased GSH and antioxidant enzymes, demonstrating the development of oxidative stress. In accordance with the *in vitro* data, all fractions ameliorated MDA and enhanced antioxidant defenses. This could be directly attributed to the RSA of the fractions and to their anti-hyperlipidemic effect. MEACL has protected against oxidative stress in HFD-fed rats as we previously reported (Aladaileh et al., 2019).

The anti-hyperlipidemic and antioxidant effects of MEACL fractions are attributed to the contained phytochemicals, in particular phenolic compounds and flavonoids. Apigenin, GA, epicatechin, proanthocyanidines, carambolaflavone, and other active phytochemicals have been reported in *A. carambola* and shown to be responsible for its antioxidant activity (Aladaileh et al., 2019; Luan et al., 2021). We have previously reported that apigenin is the main constituent in MEACL (Aladaileh et al., 2019) and the study of Yunarto and Sulistyanningrum (2017) revealed that the EA fraction has the highest content of apigenin. The antioxidant activity and other beneficial effects of apigenin have been reported in several studies (reviewed in (Salehi et al., 2019)).

5 Conclusion

The current study revealed for the first time the antioxidant and anti-hyperlipidemic efficacy of MEACL fractions and the superior activity of the EA fraction in P-407-administered rats. All fractions showed *in vitro* RSA and *in vivo* antioxidant activity in P-407-treated rats. The anti-hyperlipidemic effects of the EA fraction included the modulation of LPL, PL, HMG-CoA reductase, and some cholesterolgenesis-related factors.

6 Limitations of the study

The lack of data showing the phytochemical constituents of MEACL fractions, and the protein expression levels of cholesterolgenesis-related factors are the main limitations of this study. However, this does not affect the quality of the study and further research and studies toward understanding the anti-hyperlipidemic activity of the leaves of *A. carambola* will be considered.

Data availability statement

The original contributions presented in the study are included in the article/supplementary material, further inquiries can be directed to the corresponding authors.

Ethics statement

The animal study was reviewed and approved by the Animal Ethics Committee, University Sains Malaysia, Penang, Malaysia (Approval number: USM/Animal Ethics Approval/2012/(77) (387)).

Author contributions

Conceptualization, MA, AM, VM, and SS; methodology, MA, SS, VM, AA, AB-A, and AM; software, MA, AM, and AB-A; validation,

MA, AM, VM, and SS; formal analysis, MA and AM; investigation, MA, SS, AB-A, AA, and AM; resources, MA, AA, AM, and VM; data curation, AM and MA; writing—original draft preparation, MA, SS, and AM; writing—review and editing, AM; visualization, MA, VM, and AM; supervision, VM and AM; project administration, MA, and VM; funding acquisition, MA, VM, and SS.

Funding

The Deanship of Scientific Research (DSR) at king Abdulaziz University (KAU), Jeddah, Saudi Arabia has funded this project, under grant no (RG-5-140-43). This research was also funded by a research grant from the University Sains Malaysia, under grant number (203/PFarmasi/6711190).

Acknowledgments

The authors gratefully acknowledge technical and financial support from the Deanship of Scientific Research (DSR) at king Abdulaziz University (KAU), Jeddah, Saudi Arabia. Also, Authors would like to thank University Sains Malaysia for providing facilities for performing this researching.

Conflict of interest

The authors declare that the research was conducted in the absence of any commercial or financial relationships that could be construed as a potential conflict of interest.

Publisher's note

All claims expressed in this article are solely those of the authors and do not necessarily represent those of their affiliated organizations, or those of the publisher, the editors and the reviewers. Any product that may be evaluated in this article, or claim that may be made by its manufacturer, is not guaranteed or endorsed by the publisher.

References

- Afshin, A., Sur, P. J., Fay, K. A., Cornaby, L., Ferrara, G., Salama, J. S., et al. (2019). Health effects of dietary risks in 195 countries, 1990–2017: A systematic analysis for the global burden of disease study 2017. *Lancet* 393, 1958–1972. doi:10.1016/S0140-6736(19)30041-8
- Aladaileh, S. H., Saghir, S. a. M., Murugesu, K., Sadikun, A., Ahmad, A., Kaur, G., et al. (2019). Antihyperlipidemic and antioxidant effects of avarrhoa carambola extract in high-fat diet-fed rats. *Biomedicines* 7, 72. doi:10.3390/biomedicines7030072
- Berberich, A. J., and Hegele, R. A. (2022). A modern approach to dyslipidemia. *Endocr. Rev.* 43, 611–653. doi:10.1210/edrv/bnab037
- Brand-Williams, W., Cuvelier, M. E., and Berset, C. (1995). Use of a free radical method to evaluate antioxidant activity. *LWT - Food Sci. Technol.* 28, 25–30. doi:10.1016/s0023-6438(95)80008-5
- Brown, M. S., and Goldstein, J. L. (1999). A proteolytic pathway that controls the cholesterol content of membranes, cells, and blood. *Proc. Natl. Acad. Sci. U. S. A.* 96, 11041–11048. doi:10.1073/pnas.96.20.11041
- Cabrini, D. A., Moresco, H. H., Imazu, P., Da Silva, C. D., Pietrowski, E. F., Mendes, D. A., et al. (2011). Analysis of the potential topical anti-inflammatory activity of avarrhoa carambola L. In mice. *Evid. Based Complement. Altern. Med.* 2011, 908059. doi:10.1093/ecam/neq026
- Chang, C. C., Yang, M. H., Wen, H. M., and Chern, J. C. (2002). Estimation of total flavonoid content in propolis by two complementary colorimetric methods. *J. Food Drug Anal.* 10, 178–182. doi:10.38212/2224-6614.2748
- Chang, J. M., Hwang, S. J., Kuo, H. T., Tsai, J. C., Guh, J. Y., Chen, H. C., et al. (2000). Fatal outcome after ingestion of star fruit (Avarrhoa carambola) in uremic patients. *Am. J. Kidney Dis.* 35, 189–193. doi:10.1016/s0272-6386(00)70325-8
- Chaudhary, H. R., and Brocks, D. R. (2013). The single dose poloxamer 407 model of hyperlipidemia; systemic effects on lipids assessed using pharmacokinetic methods, and its effects on adipokines. *J. Pharm. Pharm. Sci.* 16, 65–73. doi:10.18433/j37g7m
- Chen, C. L., Fang, H. C., Chou, K. J., Wang, J. S., and Chung, H. M. (2001). Acute oxalate nephropathy after ingestion of star fruit. *Am. J. Kidney Dis.* 37, 418–422. doi:10.1053/ajkd.2001.21333
- Ellman, G. L. (1959). Tissue sulphydryl groups. *Arch. Biochem. Biophys.* 82, 70–77. doi:10.1016/0003-9861(59)90090-6
- Elsayed, R. H., Kamel, E. M., Mahmoud, A. M., El-Bassuony, A. A., Bin-Jumah, M., Lamsabhi, A. M., et al. (2020). Rumex dentatus L. phenolics ameliorate hyperglycemia by modulating hepatic key enzymes of carbohydrate metabolism, oxidative stress and PPARγ in diabetic rats. *Food Chem. Toxicol.* 138, 111202. doi:10.1016/j.fct.2020.111202

- Ferreira, E. B., Fernandes, L. C., Galende, S. B., Cortez, D. a. G., and Bazotte, R. B. (2008). Hypoglycemic effect of the hydroalcoholic extract of leaves of *Averrhoa carambola* L. (Oxalidaceae). *Rev. Bras. Farmacogn.* 18, 339–343. doi:10.1590/s0102-695x2008000300005
- Ferreira, F. P., Morais, S. R., Bara, M. T., Conceição, E. C., Paula, J. R., Carvalho, T. C., et al. (2014). *Eugenia calycina* cambess extracts and their fractions: Their antimicrobial activity and the identification of major polar compounds using electrospray ionization FT-ICR mass spectrometry. *J. Pharm. Biomed. analysis* 99, 89–96. doi:10.1016/j.jpba.2014.07.003
- Floegel, A., Kim, D.-O., Chung, S.-J., Koo, S. I., and Chun, O. K. (2011). Comparison of ABTS/DPPH assays to measure antioxidant capacity in popular antioxidant-rich US foods. *J. food Compos. analysis* 24, 1043–1048. doi:10.1016/j.jfca.2011.01.008
- Flohé, L., and Günzler, W. A. (1984). Assays of glutathione peroxidase. *Methods Enzymol.* 105, 114–121. doi:10.1016/s0076-6879(84)05015-1
- Furukawa, S., Fujita, T., Shimabukuro, M., Iwaki, M., Yamada, Y., Nakajima, Y., et al. (2004). Increased oxidative stress in obesity and its impact on metabolic syndrome. *J. Clin. Invest.* 114, 1752–1761. doi:10.1172/JCI21625
- Germoush, M. O., Elgebaly, H. A., Hassan, S., Kamel, E. M., Bin-Jumah, M., and Mahmoud, A. M. (2019). Consumption of terpenoids-rich *padina pavonia* extract attenuates hyperglycemia, insulin resistance and oxidative stress, and upregulates PPAR γ in a rat model of type 2 diabetes. *Antioxidants (Basel)* 9, 22. doi:10.3390/antiox9010022
- Goncalves, S. T. B. S. B.-a. F. a. M. G. a. N. C. D. a. G. B.-a. C. a. C. R. K. (2006). Preliminary studies on gastric anti-ulcerogenic effects of *averrhoa carambola* in rats. *Acta farmaceutica bonaer. publicaci?n del Col. Farmac?uticos Prov. Buenos Aires Argent.* 25, 245–247.
- Hamilton, M. T., Etienne, J., McClure, W. C., Pavey, B. S., and Holloway, A. K. (1998). Role of local contractile activity and muscle fiber type on LPL regulation during exercise. *Am. J. Physiol.* 275, E1016–E1022. doi:10.1152/ajpendo.1998.275.6.E1016
- He, Y., Li, X., Gasevic, D., Brunt, E., McLachlan, F., Millenson, M., et al. (2018). Statins and multiple noncardiovascular outcomes: Umbrella review of meta-analyses of observational studies and randomized controlled trials. *Ann. Intern. Med.* 169, 543–553. doi:10.7326/M18-0808
- Horton, J. D., Goldstein, J. L., and Brown, M. S. (2002). SREBPs: Activators of the complete program of cholesterol and fatty acid synthesis in the liver. *J. Clin. Investigation* 109, 1125–1131. doi:10.1172/JCI15593
- Hozayen, W. G., Mahmoud, A. M., Soliman, H. A., and Mostafa, S. R. (2016). *Spirulina versicolor* improves insulin sensitivity and attenuates hyperglycemia-mediated oxidative stress in fructose-fed rats. *J. Intercult. Ethnopharmacol.* 5, 57–64. doi:10.5455/jice.20151230055930
- Işlekel, S., Işlekel, H., Güner, G., and Özdamar, N. (1999). Alterations in superoxide dismutase, glutathione peroxidase and catalase activities in experimental cerebral ischemia-reperfusion. *Res. Exp. Med.* 199, 167–176. doi:10.1007/s004330050121
- Johnston, T. P., and Palmer, W. K. (1993). Mechanism of poloxamer 407-induced hypertriglyceridemia in the rat. *Biochem. Pharmacol.* 46, 1037–1042. doi:10.1016/0006-2952(93)90668-m
- Kamel, E. M., Mahmoud, A. M., Ahmed, S. A., and Lamsabhi, A. M. (2016). A phytochemical and computational study on flavonoids isolated from *Trifolium resupinatum* L. and their novel hepatoprotective activity. *Food Funct.* 7, 2094–2106. doi:10.1039/c6fo00194g
- Lambert, G., Charlton, F., Rye, K. A., and Piper, D. E. (2009). Molecular basis of PCSK9 function. *Atherosclerosis* 203, 1–7. doi:10.1016/j.atherosclerosis.2008.06.010
- Leon, C., Wasan, K. M., Sachs-Barrable, K., and Johnston, T. P. (2006). Acute P-407 administration to mice causes hypercholesterolemia by inducing cholesterolgenesis and down-regulating low-density lipoprotein receptor expression. *Pharm. Res.* 23, 1597–1607. doi:10.1007/s10955-006-0276-8
- Liu, S., Li, D., Huang, B., Chen, Y., Lu, X., and Wang, Y. (2013). Inhibition of pancreatic lipase, α -glucosidase, α -amylase, and hypolipidemic effects of the total flavonoids from *Nelumbo nucifera* leaves. *J. Ethnopharmacol.* 149, 263–269. doi:10.1016/j.jep.2013.06.034
- Livak, K. J., and Schmittgen, T. D. (2001). Analysis of relative gene expression data using real-time quantitative PCR and the 2(-Delta Delta C(T)) Method. *Methods* 25, 402–408. doi:10.1006/meth.2001.1262
- Luan, F., Peng, L., Lei, Z., Jia, X., Zou, J., Yang, Y., et al. (2021). Traditional uses, phytochemical constituents and pharmacological properties of *averrhoa carambola* L.: A review. *Front. Pharmacol.* 12, 699899. doi:10.3389/fphar.2021.699899
- Mahmoud, A. M., Abd El-Twab, S. M., and Abdel-Reheim, E. S. (2017). Consumption of polyphenol-rich *morus alba* leaves extract attenuates early diabetic retinopathy: The underlying mechanism. *Eur. J. Nutr.* 56, 1671–1684. doi:10.1007/s00394-016-1214-0
- Mahmoud, A. M., Ashour, M. B., Abdel-Moneim, A., and Ahmed, O. M. (2012). Hesperidin and naringin attenuate hyperglycemia-mediated oxidative stress and proinflammatory cytokine production in high fat fed/streptozotocin-induced type 2 diabetic rats. *J. Diabetes Complicat.* 26, 483–490. doi:10.1016/j.jdiacomp.2012.06.001
- Mahmoud, A. M. (2012). Influence of rutin on biochemical alterations in hyperammonemia in rats. *Exp. Toxicol. Pathol.* 64, 783–789. doi:10.1016/j.etp.2011.01.016
- Mohamed Rashid, A., Lu, K., Yip, Y. M., and Zhang, D. (2016). *Averrhoa carambola* L. peel extract suppresses adipocyte differentiation in 3T3-L1 cells. *Food and Funct.* 7, 881–892. doi:10.1039/c5fo01208b
- Mondragon, A., Davidsson, D., Kyriakoudi, S., Bertling, A., Gomes-Faria, R., Cohen, P., et al. (2014). Divergent effects of liraglutide, exendin-4, and sitagliptin on beta-cell mass and indicators of pancreatitis in a mouse model of hyperglycaemia. *PLOS ONE* 9, e104873. doi:10.1371/journal.pone.0104873
- Moresco, H. H., Queiroz, G. S., Pizzolatti, M. G., and Brighente, I. (2012). Chemical constituents and evaluation of the toxic and antioxidant activities of *Averrhoa carambola* leaves. *Rev. Bras. Farmacogn.* 22, 319–324. doi:10.1590/s0102-695x2011005000217
- Neto, M. M., Da Costa, J. A., Garcia-Cairasco, N., Netto, J. C., Nakagawa, B., and Dantas, M. (2003). Intoxication by star fruit (*averrhoa carambola*) in 32 uraemic patients: Treatment and outcome. *Nephrol. Dial. Transpl.* 18, 120–125. doi:10.1093/ndt/18.1.120
- Newman, C. B., Preiss, D., Tobert, J. A., Jacobson, T. A., Page, R. L., 2nd, Goldstein, L. B., et al. (2019). Statin safety and associated adverse events: A scientific statement from the American heart association. *Arterioscler. Thromb. Vasc. Biol.* 39, e38–e81. doi:10.1161/ATV.0000000000000073
- Ohkawa, H., Ohishi, N., and Yagi, K. (1979). Assay for lipid peroxides in animal tissues by thiobarbituric acid reaction. *Anal. Biochem.* 95, 351–358. doi:10.1016/0003-2697(79)90738-3
- Oyanagui, Y. (1984). Reevaluation of assay methods and establishment of kit for superoxide dismutase activity. *Anal. Biochem.* 142, 290–296. doi:10.1016/0003-2697(84)90467-6
- Pang, D., You, L., Zhou, L., Li, T., Zheng, B., and Liu, R. H. (2017). *Averrhoa carambola* free phenolic extract ameliorates nonalcoholic hepatic steatosis by modulating microRNA-34a, microRNA-33 and AMPK pathways in leptin receptor-deficient db/db mice. *Food and Funct.* 8, 4496–4507. doi:10.1039/c7fo00833c
- Park, J., Yeom, M., and Hahm, D. H. (2016). Fucoidan improves serum lipid levels and atherosclerosis through hepatic SREBP-2-mediated regulation. *J. Pharmacol. Sci.* 131, 84–92. doi:10.1016/j.jphs.2016.03.007
- Rao, A. V., and Ramakrishnan, S. (1975). Indirect assessment of hydroxymethylglutaryl-CoA reductase (NADPH) activity in liver tissue. *Clin. Chem.* 21, 1523–1525. doi:10.1093/clinchem/21.10.1523
- Re, R., Pellegrini, N., Proteggente, A., Pannala, A., Yang, M., and Rice-Evans, C. (1999). Antioxidant activity applying an improved ABTS radical cation decolorization assay. *Free Radic. Biol. Med.* 26, 1231–1237. doi:10.1016/s0891-5849(98)00315-3
- Saghir, S. a. M., Abdulghani, M. a. M., Alruhaimi, R. S., Ahmeda, A. F., Al-Gabri, N. A., Alomaisi, S., et al. (2022). Acute and sub-chronic toxicological evaluation of *Averrhoa carambola* leaves in Sprague Dawley rats. *Environ. Sci. Pollut. Res. Int.* 29, 90058–90069. doi:10.1007/s11356-022-22019-7
- Saghir, S., Sadikun, A., Al-Suede, F. S., Msa Majid, A., and Murugaiyah, V. (2016). Antihyperlipidemic, antioxidant and cytotoxic activities of methanolic and aqueous extracts of different parts of star fruit. *Curr. Pharm. Biotechnol.* 17, 915–925. doi:10.2174/1389201017666160603013434
- Salehi, B., Venditti, A., Sharifi-Rad, M., Kęrgiel, D., Sharifi-Rad, J., Durazzo, A., et al. (2019). The therapeutic potential of apigenin. *Int. J. Mol. Sci.* 20, 1305. doi:10.3390/ijms20061305
- Sato, R., and Takano, T. (1995). Regulation of intracellular cholesterol metabolism. *Cell Struct. Funct.* 20, 421–427. doi:10.1247/csf.20.421
- Shahaboddin, M.-E., Pouramir, M., Moghadamnia, A.-A., Parsian, H., Lakzaei, M., and Mir, H. (2011). *Pyrus bioessieriana* Buhse leaf extract: An antioxidant, antihyperglycaemic and antihyperlipidemic agent. *Food Chem.* 126, 1730–1733. doi:10.1016/j.foodchem.2010.12.069
- Singh, U. N., Kumar, S., and Dhakal, S. (2017). Study of oxidative stress in hypercholesterolemia. *Int. J. Contemp. Med. Res.* 4, 1204–1207.
- Singleton, V. L., and Rossi, J. A. (1965). Colorimetry of total phenolics with phosphomolybdic-phosphotungstic acid reagents. *Am. J. Enol. Vitic.* 16, 144–158.
- Stein, O., and Stein, Y. (1999). Atheroprotective mechanisms of HDL. *Atherosclerosis* 144, 285–301. doi:10.1016/s0021-9150(99)00065-9
- Stumpf, M. S. a. B. G. R. M., Schuinski, A. F. M., Baroni, G., and Ramthun, M. (2020). Acute kidney injury with neurological features: Beware of the star fruit and its caramboxin. *Indian J. Nephrol.* 30, 42–46. doi:10.4103/ijn.IJN_53_19
- Su, X., Peng, H., Chen, X., Wu, X., and Wang, B. (2022). Hyperlipidemia and hypothyroidism. *Clin. Chim. Acta* 527, 61–70. doi:10.1016/j.cca.2022.01.006
- Tsai, M. H., Chang, W. N., Lui, C. C., Chung, K. J., Hsu, K. T., Huang, C. R., et al. (2005). Status epilepticus induced by star fruit intoxication in patients with chronic renal disease. *Seizure* 14, 521–525. doi:10.1016/j.seizure.2005.08.004
- Wasan, K. M., Subramanian, R., Kwong, M., Goldberg, I. J., Wright, T., and Johnston, T. P. (2003). Poloxamer 407-mediated alterations in the activities of enzymes regulating lipid metabolism in rats. *J. Pharm. Pharm. Sci.* 6, 189–197.
- Wu, Q., Zhang, H., Dong, X., Chen, X.-F., Zhu, Z.-Y., Hong, Z.-Y., et al. (2014). UPLC-Q-TOF/MS based metabolomic profiling of serum and urine of hyperlipidemic rats induced by high fat diet. *J. Pharm. analysis* 4, 360–367. doi:10.1016/j.jpba.2014.04.002

- Yang, R.-L., Shi, Y.-H., Hao, G., Li, W., and Le, G.-W. (2008). Increasing oxidative stress with progressive hyperlipidemia in human: Relation between malondialdehyde and atherogenic index. *J. Clin. Biochem. Nutr.* 43, 154–158. doi:10.3164/jcbs.2008044
- Yang, S. T., Kreutzberger, A. J. B., Lee, J., Kiessling, V., and Tamm, L. K. (2016). The role of cholesterol in membrane fusion. *Chem. Phys. Lipids* 199, 136–143. doi:10.1016/j.chemphyslip.2016.05.003
- Yasawardene, P., Jayarajah, U., De Zoysa, I., and Seneviratne, S. L. (2020). Mechanisms of star fruit (*Averrhoa carambola*) toxicity: A mini-review. *Toxicon* 187, 198–202. doi:10.1016/j.toxicon.2020.09.010
- Yeom, M., Park, J., Lee, B., Lee, H. S., Park, H.-J., Won, R., et al. (2018). Electroacupuncture ameliorates poloxamer 407-induced hyperlipidemia through suppressing hepatic SREBP-2 expression in rats. *Life Sci.* 203, 20–26. doi:10.1016/j.lfs.2018.04.016
- Yu, L., Li-Hawkins, J., Hammer, R. E., Berge, K. E., Horton, J. D., Cohen, J. C., et al. (2002). Overexpression of ABCG5 and ABCG8 promotes biliary cholesterol secretion and reduces fractional absorption of dietary cholesterol. *J. Clin. Invest.* 110, 671–680. doi:10.1172/JCI16001
- Yunarto, N., and Sulistyningrum, S. (2017). Quantitative analysis of bioactive compounds in extract and fraction of star fruit (*Averrhoa carambola* L.) leaves using high performance liquid chromatography. *Indonesian Pharm. J.* 7, 26–33.
- Zanwar, A. A., Hegde, M. V., Rojatk, S. R., and Bodhankar, S. L. (2014). Antihyperlipidemic activity of concomitant administration of methanolic fraction of flax lignan concentrate and omega-3-fatty acid in poloxamer-407 induced experimental hyperlipidemia. *Industrial Crops Prod.* 52, 656–663. doi:10.1016/j.indcrop.2013.11.041



OPEN ACCESS

EDITED BY

Ochuko Lucky Erukainure,
University of the Free State, South Africa

REVIEWED BY

Rebecca Reddy,
Durban University of Technology, South Africa
Fils Armand Ella,
University of the Free State, South Africa
Babangida Sanusi,
Ahmadu Bello University, Nigeria

*CORRESPONDENCE

Fahad S. Alshehri,
✉ fsshehri@uqu.edu.sa

SPECIALTY SECTION

This article was submitted to
Ethnopharmacology,
a section of the journal
Frontiers in Pharmacology

RECEIVED 23 December 2022

ACCEPTED 30 January 2023

PUBLISHED 07 February 2023

CITATION

Alshehri FS and Alorfi NM (2023),
Protective role of resveratrol against VCM-
induced hepatotoxicity in male wistar rats.
Front. Pharmacol. 14:1130670.
doi: 10.3389/fphar.2023.1130670

COPYRIGHT

© 2023 Alshehri and Alorfi. This is an open-access article distributed under the terms of the [Creative Commons Attribution License \(CC BY\)](https://creativecommons.org/licenses/by/4.0/). The use, distribution or reproduction in other forums is permitted, provided the original author(s) and the copyright owner(s) are credited and that the original publication in this journal is cited, in accordance with accepted academic practice. No use, distribution or reproduction is permitted which does not comply with these terms.

Protective role of resveratrol against VCM-induced hepatotoxicity in male wistar rats

Fahad S. Alshehri* and Nasser M. Alorfi

Department of Pharmacology and Toxicology, College of Pharmacy, Umm Al-Qura University, Makkah, Saudi Arabia

Background: Vancomycin is a glycopeptide antibiotic with a high risk of acute liver injury. Resveratrol is believed to protect the liver against toxicity.

Aim: To investigate the ability of resveratrol to attenuate vancomycin-induced liver toxicity in rats injected with vancomycin.

Method: Twenty-four adult male Wistar rats were distributed into three groups. The control group received only a vehicle, while the treated group received either vancomycin 200 (mg/kg, i. p.) only or vancomycin (200 mg/kg, i. p.) with resveratrol (20 mg/kg, oral gavage). All groups received their dose once daily for 7 days. Hepatic damage was assessed by measuring biochemical parameter levels in serum, aspartate transaminase (AST), alanine transaminase (ALT), alkaline phosphatase (ALP), and lactate dehydrogenase (LDH). Also, antioxidants and inflammation biomarkers such as Interleukin-6 (IL-6), malondialdehyde (MDA), nitric oxide (NO), and glutathione (GSH) were measured. Furthermore, the vancomycin-induced pathological changes in the liver were evaluated by histopathological studies.

Results: In the vancomycin-treated group, hepatic serum biomarkers such as AST, ALT, ALP, IL-6, and MDA were elevated, while NO and GSH were depleted. However, resveratrol co-treatment with vancomycin prevented the elevation of AST, ALT, ALP, IL-6, and MDA and it protected the liver from NO and GSH depletion. Also, regarding vancomycin-induced degeneration of hepatocytes, resveratrol co-treatment with vancomycin prevented such degeneration and improved mononuclear cells in the liver.

Conclusion: The results showed that oral administration of resveratrol has a significant hepatoprotective effect against vancomycin-induced hepatotoxicity.

KEYWORDS

vancomycin, resveratrol, hepatotoxicity, hepatoprotection, glycopeptide

Introduction

Many drugs are known to produce liver injury, and these adverse hepatic events usually result in severe liver injury if not treated properly (Bissell et al., 2001). It has been estimated that drug-induced liver failure represents half of the cases of all forms of acute and chronic liver disease (Kaplowitz, 2001). Approximately 10% of chronic hepatitis cases occur due to drug use, and 5% from hospital admissions, while 50% of acute liver failure cases occur due to drug use (Pandit et al., 2012). Hepatotoxicity associated with antibiotics is asymptomatic and usually presents mild hepatic injury (Thiim and Friedman, 2003). Vancomycin is a glycopeptide antibiotic with known bactericidal activity, and it is considered the drug of choice for treating methicillin-resistant *Staphylococcus aureus* infections (David and Daum, 2010; Steinmetz et al.,

2015). However, several side effects have been reported with vancomycin, such as hypotension, phlebitis, nephrotoxicity, and hepatotoxicity (Badran et al., 2011; Bamgbola, 2016).

Moreover, a few reports have shown that chronic use of glycopeptide antibiotics has the potential to elevate liver enzymes and induce hepatotoxicity (Cadle et al., 2006; Chen et al., 2011; Brunetti et al., 2020). However, data to support the influence of vancomycin on liver dysfunction are limited, and the mechanism of vancomycin-induced hepatotoxicity has not been studied effectively. Many risk factors contribute to vancomycin-induced hepatotoxicities, such as long-term treatments, high doses, obesity, patient age, and overall health (Larrey, 2002; Breedt et al., 2005; Kohno et al., 2007; Florescu et al., 2008). Moreover, the hepatic injury associated with vancomycin could also be due to sepsis, bacterial endotoxins, fever, or hemolysis (Sibai, 2004; Shah et al., 2010; Kouijzer et al., 2021). While different strategies have been suggested to reduce any potential risk of hepatotoxicity associated with vancomycin treatment (Aldaz et al., 2000; Hwang et al., 2015; Regal et al., 2019; Tsutsuura et al., 2021), the exact mechanism for this injury is not fully understood. Several studies have suggested that vancomycin-induced toxicity could be due to several factors, including the generation of free radicals, oxidative stress, and inflammation, which cause liver injury in animal studies (Sahin et al., 2006; El Bohi et al., 2021). In addition, reactive oxygen species (ROS) are usually generated within cells, leading to the initiation of oxidative stress-related intermediates, which contribute to chronic inflammation and liver fibrogenesis (Bataller and Brenner, 2005; Friedman, 2008; Novo and Parola, 2008). Therefore, herbal compounds with antioxidant and anti-inflammatory properties have been considered.

Indeed, cumulative reports have suggested that herbal compounds have a great potential to attenuate drug-induced liver toxicity due to their antioxidant and anti-inflammatory properties (Abou Seif, 2016; Parthasarathy and Evan Prince, 2021). Hence, many herbal compounds have been used as traditional medicines for liver disorders (Ali et al., 2008; Zhang et al., 2018; Philips et al., 2020; Das et al., 2022). In addition, these are potential sources of new therapeutic agents that could be used to prevent hepatic injuries. For example, resveratrol has long been known to have antioxidant and anti-inflammatory effects. Moreover, researchers have recently become more interested in resveratrol, from its ability to extend human lifespans to its effect on chemoprevention, cardiovascular diseases, and neurodegenerative disorders, as reported in several studies (Gescher and Steward, 2003; Srivastava et al., 2013; Pourhanifeh et al., 2019; Banez et al., 2020; Labban et al., 2021a; Labban et al., 2021b). The antioxidant properties of resveratrol have been demonstrated in several *in vitro* studies. The antioxidant property of resveratrol has been demonstrated by inhibiting nicotinamide adenine dinucleotide phosphate oxidases, which inhibit the production of reactive oxygen species (ROS) (Halliwell, 2007; Yousefian et al., 2019). As well as protecting cells from oxidative stress, resveratrol also promotes the expression of antioxidative enzymes and their substrates (Miguel et al., 2021; Santos et al., 2021). Recently, it has been suggested that resveratrol has hepatoprotection properties through its anti-inflammatory and antioxidant effects (Chupradit et al., 2022; Ma et al., 2022; Tong et al., 2022). It has also been reported that resveratrol attenuates acetaminophen toxic metabolite N-acetyl-p-

benzoquinone-imine and facilitates liver regeneration by modulating the silent mating type information regulation two homolog (SIRT1), tumor protein P53, and Tumor Necrosis Factor- α (TNF- α) (Sener et al., 2006; Wang et al., 2015). Moreover, resveratrol has been shown to improve glutathione (GSH) levels and antioxidant enzyme activities, and to decrease ROS production in liver tissues (Bujanda et al., 2008; Rivera et al., 2008; Rubiolo and Vega, 2008; Sebai et al., 2010). Also, one study reported that the thioacetamide-induced hepatotoxic effect associated with TNF- α and iNOS elevation was inhibited by resveratrol (Ebrahim et al., 2022).

This study investigates the effect of high doses of vancomycin administered to induce liver toxicity. A few studies have investigated similar regimens and found that high doses of vancomycin were associated with elevated levels of liver enzymes, the tissue activities of catalase, superoxide dismutase activities, lipid peroxidation, and malondialdehyde (MDA) (Ahmida, 2012; Çağlayan et al., 2019; El Bohi et al., 2021). Moreover, this research investigates the ability of resveratrol to attenuate vancomycin-induced liver toxicity through several biomarkers, such as liver tissues, inflammatory mediators, liver enzymes, and antioxidant property markers.

Materials and methods

Drugs

Resveratrol (ProHealth, United States) and vancomycin (Medis, Tunisia) were used in the study. All other chemicals and reagents used were of analytical grade. Resveratrol and vancomycin were dissolved in a saline solution (0.9% NaCl) as a vehicle for both drugs.

Dose selection

The vancomycin dose was based on several recent studies using 200 mg/kg, i. p. to induce hepatotoxicity (Kucukler et al., 2020) and nephrotoxicity (Ahmida, 2012) once daily for seven consecutive days. The resveratrol dose was based on several studies using the same dose against several compounds, such as dimethylnitrosamine (Lee et al., 2010) and concanavalin (Zhou et al., 2015).

Animals

Twenty-four male adult Wistar rats (weighing 170–207 g) were used. The animals were housed in plastic cages (4 rats per cage) under a 12 h light/12 h dark schedule in a humidity-controlled room and were fed a normal diet. They had access to food and water *ad libitum* and were monitored daily to ensure proper animal welfare. The rats were acclimatized for 1 week before starting the experiment. Then, the rats were distributed into three groups (n = 8 in each group). The rats received only a vehicle in the first group (control). In the second group, vancomycin, the rats received vancomycin (200 mg/kg, i. p.) once daily for seven consecutive days. In the last group, vancomycin + resveratrol, the rats received vancomycin (200 mg/kg, i. p.) and resveratrol (20 mg/kg, oral gavage) once daily for seven consecutive days. All the treatments were carried out within 7 days, and the animals were euthanized using CO₂ and sacrificed on the eighth day. The tissue and serum samples were collected, homogenized, centrifuged, for analysis.

Measurement of biochemical parameters

The serum samples were used for the measurement of all biochemical parameters. The usage of serum samples was based on several reports that have used similar methods to assess hepatic function. Aspartate transaminase (AST), Alanine transferase (ALT) as reported in (Yin et al., 2019), Alkaline phosphatase (ALP) (Ibrahim et al., 2020), Interleukin-6 (IL-6) (Xia et al., 2019), nitric oxide (NO) (Fathy et al., 2019), GSH (Ibrahim et al., 2020) and MDA (Omara et al., 2021).

Markers of liver tissue damage

The serum samples were analyzed using assay kits and ELISA for liver functions. Aspartate transaminase (AST), Alanine transferase (ALT) and Alkaline phosphatase (ALP) were assessed using ELISA kits (MyBioSource kits catalog: MBS269614, MBS264975, MBS011598, MBS726781; MyBioSource, Inc.) A centrifuge was then performed at approximately 1000× g for 15 min. Serum was collected, and the assay was immediately performed according to the manufacturer's recommendations (MyBioSource, Inc.). A standard curve was established using a series diluent. A Microplate reader (450 nm detection wavelength filter, 570 nm or 630 nm correction wavelength filters) was used to perform all the tests.

Markers of inflammation

Interleukin-6 (IL-6) and nitric oxide (NO) levels in the serum were measured with the fully automatic ELISA DSX best 2000[®] microtiter plate and the ELISA kits. A centrifuge was then performed at approximately 1000× g for 15 min. Serum was collected, and the assay was immediately performed according to the manufacturer's recommendations (MyBioSource, Inc.).

Markers of antioxidant and prooxidant

GSH and MDA levels in the serum were measured using an ELISA DSX best 2000[®] microtiter plate and the ELISA kits. In a serum separator tube, the serum was clotted for 2 hours at room temperature and overnight at 2°C–8°C. A centrifuge was then performed at approximately 1000× g for 15 min. Serum was collected, and the assay was immediately performed according to the manufacturer's recommendations (MyBioSource, Inc.). A Microplate reader (450 nm detection wavelength filter) was used to perform all the tests.

Histopathology

The liver tissues were used for the histopathological assessment and prepared in 10% formalin solution for 2 days. In addition, the tissue was embedded in paraffin blocks following routine tissue tracking procedures. Finally, Hematoxylin and eosin stains were used to stain the slides. Masson's Trichrome method was employed, which involves deparaffinizing and rehydrating the liver in descending series of alcohols before staining them with Biebrich scarlet-acid fuchsin solution. A solution of phosphomolybdic-phosphotungstic acid was then used to differentiate the sections.

Statistical analysis

Statistical analyses were performed using GraphPad Prism[™] (v9.3.1). Data were expressed as mean ± standard error of the mean. A one-way ANOVA, followed by Tukey's post hoc test, was

used for comparisons. A *p*-value of <0.05 was considered statistically significant.

Results

Measured levels of AST, ALT, ALP, and LDH

The effect of vancomycin on AST, ALT, ALP and LDH was observed in the rats' serum. The one-way ANOVA test revealed a significant main effect on the AST serum levels [F (2, 21) = 216.0, *p* < 0.0001, Figure 1A]. Further analysis using Tukey's multiple comparisons test revealed that rats injected with only vancomycin had significantly increased levels of AST compared to the control group (*p* < 0.0001). Interestingly, the rats injected with resveratrol and vancomycin were protected against vancomycin-induced toxicity. In addition, the vancomycin + resveratrol group of rats showed a significant increase in AST levels, *p* = 0.0083, compared to the control group.

Moreover, vancomycin had a significant main effect on the ALT serum levels in the groups [F (2, 21) = 124.0, *p* < 0.0001, Figure 1B]. Further analysis using Tukey's multiple comparisons test revealed that the control group rats displayed no change in ALT, *p* = 0.1949. However, the rats injected with only vancomycin displayed a significant increase in ALT compared to the control group (*p* < 0.0001). Interestingly, the rats injected with resveratrol and vancomycin were protected against vancomycin-induced toxicity.

Another significant main effect on ALP serum levels in the groups [F (2, 21) = 209.3, *p* < 0.0001, Figure 1C]. Further analysis using Tukey's multiple comparisons test revealed that the control rats displayed no change in ALP, *p* = 0.5888. The rats injected with vancomycin showed a significant increase in ALP compared to the control group (*p* < 0.0001), and the rats injected with resveratrol and vancomycin were protected against vancomycin-induced toxicity.

Moreover, significant main effect on LDH serum levels in the groups [F (2, 21) = 130.9, *p* < 0.0001, Figure 1D]. Additional analysis using Tukey's multiple comparisons tests indicated that the control group rats had no change in LDH, *p* = 0.8200. However, the rats injected with only vancomycin displayed a significant increase in LDH compared to the control group (*p* < 0.0001). Remarkably, resveratrol demonstrated a protective role against vancomycin-induced toxicity.

Measured levels of IL-6 and NO

The effect of vancomycin on IL-6 and NO levels was observed in the rats' serum. The one-way ANOVA test revealed that vancomycin had a significant main effect on the IL-6 serum levels in the groups F (2, 21) = 141.8, *p* < 0.0001, Figure 2A. Further analysis using Tukey's multiple comparisons test revealed that the control rats displayed no change in IL-6, *p* = 0.9185. However, the rats injected with only vancomycin had a significant increase in IL-6 compared to the control group (*p* < 0.0001). Interestingly, the rats injected with resveratrol and vancomycin were protected against vancomycin-induced toxicity.

The significant main effect on NO serum levels in the groups [F (2, 21) = 118.3, *p* < 0.0001, Figure 2B]. Tukey's multiple comparisons test revealed that the control group rats displayed no change in NO serum levels, *p* = 0.6613. However, the rats injected with only vancomycin

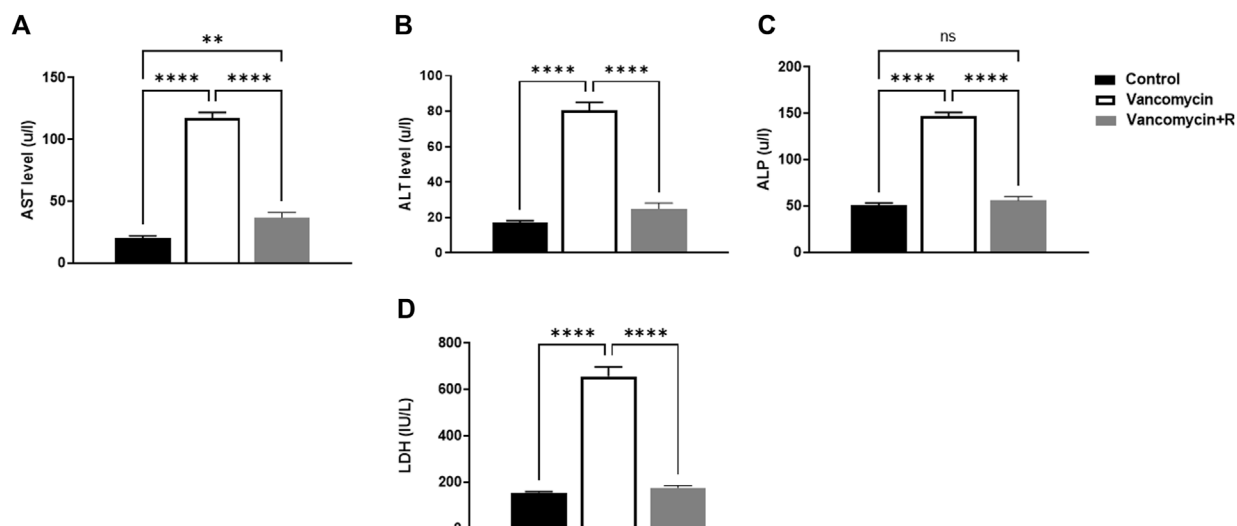


FIGURE 1

(A) Aspartate transaminase (AST) levels in u/l, (B) Alanine aminotransferase (ALT) in u/l, (C) Alkaline phosphatase (ALP) in unit/liter (u/l), and (D) lactate dehydrogenase (LDH) (IU/L), were measured in the control rats, rats injected with vancomycin only, and rats injected with vancomycin and resveratrol. Significant difference: ns = non-significant, ** $p < 0.001$ **** $p < 0.0001$.

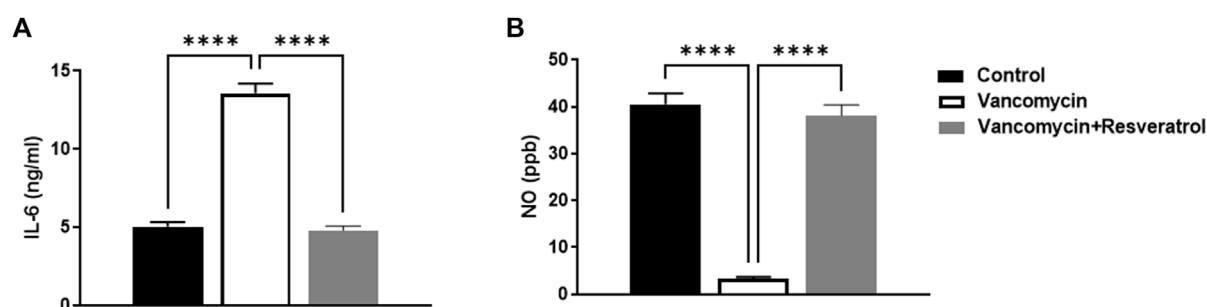


FIGURE 2

Interleukin-6 (IL-6) levels in ng/ml and (B) nitric oxide (NO) levels in parts per million (ppb) were measured in the control rats, rats injected with vancomycin only, and rats injected with vancomycin and resveratrol. Significant difference: **** $p < 0.0001$.

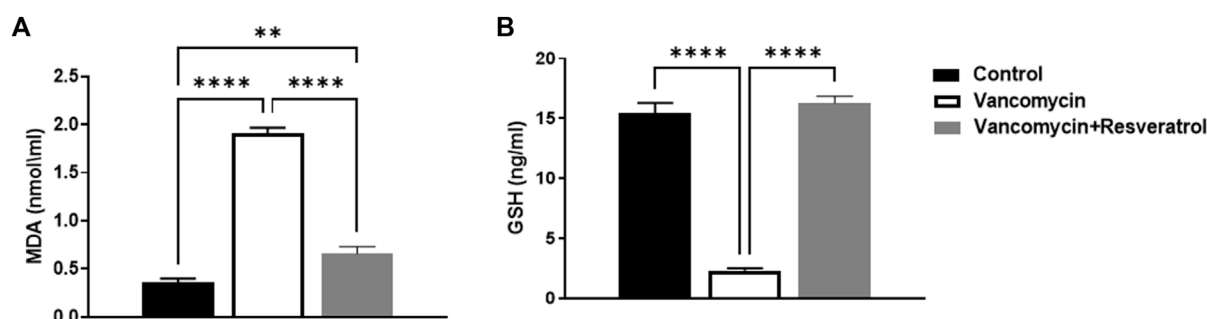


FIGURE 3

(A) Malondialdehyde (MDA) (nmol/ml) and (B) Glutathione (GSH) levels in ng/ml were measured in the control rats, rats injected with vancomycin only, and rats injected with vancomycin and resveratrol. Significant difference: ** $p < 0.001$; **** $p < 0.0001$.

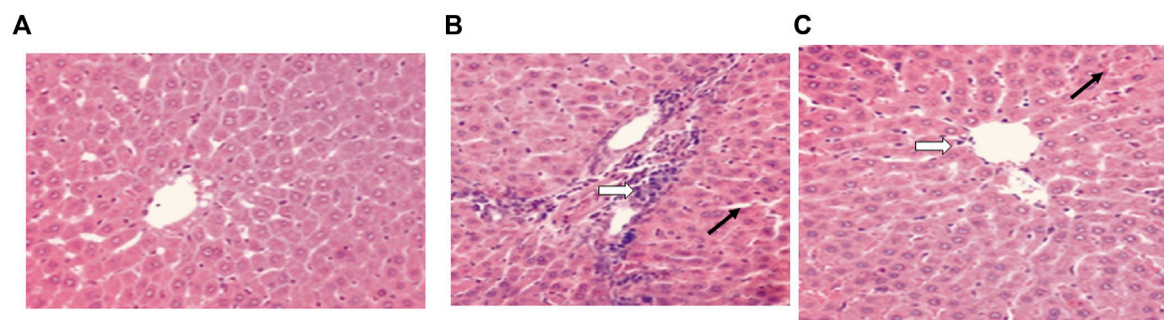


FIGURE 4

Histopathological liver evaluation in (A) control rats, (B) rats injected with vancomycin only, liver-Intralobular mononuclear inflammatory infiltrations (white arrow), and Mallory bodies (black arrow) due to degeneration of hepatocytes and increased vacuolation in the cytoplasm of hepatocytes appeared as indistinct clear vacuoles (black arrow) indicate glycogen infiltration and (C) rats injected with vancomycin and resveratrol, liver-showed marked improved on a mononuclear cell, and decrease number of mononuclear inflammatory infiltrates (white arrow) and decrease of Mallory bodies (black arrow).

showed a significant NO increase compared to the control group ($p < 0.0001$). Remarkably, the rats injected with resveratrol and vancomycin were protected against vancomycin-induced toxicity.

Measured levels of MDA and GSH

The effect of vancomycin on MDA was observed in the rats' serum. A further one-way ANOVA test showed that vancomycin had a significant main effect on the MDA serum levels in the groups [$F(2, 21) = 190.2, p < 0.0001$, Figure 3A]. Also, Tukey's multiple comparisons test revealed that the control group rats displayed a significant change in MDA serum levels, $p < 0.0057$. Again, the rats injected with only vancomycin displayed a significant increase in LDH compared to the control group ($p < 0.0001$), while the rats injected with resveratrol and vancomycin were protected against vancomycin-induced toxicity.

The effect of vancomycin on GSH levels was observed in rats' serum. The test revealed a significant main effect on GSH serum levels in the groups [$F(2, 21) = 167.3 < 0.0001$, Figure 3B]. Further analysis using Tukey's multiple comparisons test revealed that the control group rats displayed no change in GSH, $p = 0.5894$. However, rats injected with only vancomycin displayed a significant decrease in GSH compared to the control group ($p < 0.0001$). Interestingly, the rats injected with resveratrol and vancomycin were protected against vancomycin-induced toxicity.

Histopathological results

For the control group, a microscopic examination of the liver revealed a normal appearance, as shown in Figure 4A. For the control + vancomycin group, liver-intralobular mononuclear inflammatory infiltrations and Mallory bodies were evident due to the degeneration of hepatocytes, as shown in Figure 4B. For the vancomycin + resveratrol group, the liver showed a marked improvement in the mononuclear cells, as shown in Figure 4C.

Discussion

Biological systems depend on the liver to detoxify xenobiotics (Apte and Krishnamurthy, 2011). Several studies have shown that

hepatic damage disrupts the body's regular metabolism (Fabbrini and Magkos, 2015; Kurland et al., 2015). There are several causes of acute liver failure, including viral hepatitis, toxic liver damage caused by poisons and drugs, and ischemia (Jalan et al., 2012; Bernal and Wendon, 2013). The liver metabolises xenobiotics as the body's first line of defense against ingested toxins and drugs, which often cause necrosis and apoptosis (Tsochatzis et al., 2014). A growing body of research focuses on the potential toxicity of antibiotics in the liver (Acevedo, 2015; Fernández et al., 2016; Zoratti et al., 2022). Vancomycin tends to cause adverse events after prolonged use, and large doses may be toxic to the liver (Kucukler et al., 2020). This study aimed to determine whether resveratrol plays a beneficial protective role against vancomycin-induced toxicity in the livers of male Wistar rats.

This study's findings align with several other research studies that present vancomycin's potential toxicity (Kucukler et al., 2020). However, to our knowledge, no previous study has investigated the protective role of resveratrol. This study revealed an elevation in serum biomarkers such as AST, ALT, and ALP levels in the groups given only vancomycin or vancomycin with resveratrol, compared to the control group. The serum level of ALT is the most widely used clinical biomarker of hepatic function (Senior, 2012). Furthermore, GSH, an antioxidant, was restored to the normal level in the rats injected with vancomycin and resveratrol, indicating the antioxidant activity of the latter.

Moreover, the rats injected with vancomycin only had significantly reduced GSH levels, confirming the previous findings. Several parameters were affected by the administration of vancomycin. The levels of IL-6, LDH, MDA, and NO were highly increased in the rats injected with vancomycin. Vancomycin administration caused hepatocyte damage, leading to liver enzyme elevation. Hepatotoxic studies commonly measure liver enzyme levels such as ALT, AST, and ALP as serum hepatic biomarkers for determining liver lesions (Deshpande et al., 1998; Sadeghi et al., 2008; Mehrzadi et al., 2018). In this study, vancomycin caused a significant elevation in the serum hepatic biomarkers ALT, AST, and ALP. The concentration of ALT and AST enzymes in serum reflects the severity of liver damage as these enzymes are present in high concentrations in the liver (Adeyemi and Akanji, 2011; Adeyemi and Adewumi, 2014; Yilmaz et al.,

2017). In addition, many tissues in the body contain ALP; therefore, it can be considered a non-specific enzyme (López-Posadas et al., 2011). Furthermore, hepatobiliary duct dysfunction or the destruction of hepatic cell membranes can cause a rise in serum ALP, which could indicate a problem with the excretory function (Lowe et al., 2017; Kashima et al., 2018). On the other hand, co-treatment of vancomycin with resveratrol protected against vancomycin-induced hepatic damage, evidenced by the significantly decreased levels of the hepatic serums AST, ALT, and ALP.

It is well known that vancomycin is almost completely eliminated from the body by the kidneys; however, the mechanism by which nephrotoxicity occurs is still unclear. It has been demonstrated in experimental animals that the drug may cause tubular ischemia and acute tubulointerstitial injury by inducing oxidative stress in the proximal renal tubule cells (King and Smith, 2004; Gupta et al., 2011a). Here, vancomycin increased the serum levels of IL-6 (a pro-inflammatory cytokine). The cell surface receptors of the IL-6 family of cytokines regulate cell function (Taga and Kishimoto, 1997). IL-6 consists of two structural subunits: a ligand-binding subunit called the IL-6 receptor and a signal-transducing glycoprotein called Gp130 (Yamauchi-Takahara and Kishimoto, 2000). The liver synthesizes several acute phase proteins in response to IL-6 as it is involved in the pathogenesis of many fibrogenic diseases (Choi et al., 1994). In recent studies, IL-6 has been linked to acute and chronic liver damage (Cao et al., 1998; Gewiese-Rabsch et al., 2010; Bergmann et al., 2017; Shao et al., 2020). In addition, many xenobiotics drugs can injure the liver and trigger the release of pro-inflammatory cytokines like TNF- α and IL6 into the bloodstream (Takai et al., 2016; Olaniyan et al., 2018; Wu et al., 2018). By demonstrating the changes in cytokines that occur in hepatic cells, rodent models can illustrate the molecular changes associated with human hepatic cell death. In this study, we also tested the serum level of MDA, an oxidative stress biomarker that serves as an index of oxidative damage in the liver (Bakan et al., 2002). MDA has been reported to induce collagen production by hepatic stellate cells, resulting in fibrosis (Hadizadeh et al., 2017). Also, it has been reported that vancomycin could initiate an intracellular production of peroxides that triggers the production of MDA (Oktem et al., 2005). Thus, in this study, the vancomycin-induced high serum levels of MDA could be due to vancomycin's free radical trapping activity and oxidative stress.

GSH has several functions, including serving as an antioxidant, and playing a role in redox and cell signaling (Franco and Cidowski, 2009; Mari et al., 2009). It acts by reducing hydrogen peroxide, scavenging ROS, and reactive nitrogen species (RNS); therefore, it protects cells against oxidative damage (Day and Suzuki, 2005; Winter et al., 2017). The build-up of an oxidized form of GSH, glutathione disulfide (GSSG), and the depletion of GSH are closely related to ROS and RNS effects on the liver and cells (Yuan and Kaplowitz, 2009; Eskandari et al., 2012). Hepatic NO and its derivatives are essential in liver physiology and pathophysiology (Laskin et al., 2001; Chen et al., 2003; Diesen and Kuo, 2010). It is also a second messenger that acts in several pathways and plays a crucial role in regulating blood pressure by relaxing the endothelium, attacking tumor cells, and stimulating the

brain (Gupta et al., 2011b; Korde Choudhari et al., 2013; Picon-Pages et al., 2019). Although NO has multiple and complex roles, it has been suggested that it affects the pathogenesis and progression of liver diseases (Iwakiri and Kim, 2015; Ekhlasi et al., 2017; Wang et al., 2018). On the other hand, LDH (a non-specific tissue damage biomarker) was elevated in vancomycin-treated animals. Numerous tissues and organs in the body produce LDH, including the muscles, liver, heart, pancreas, kidneys, brain, and blood. Body tissue damage can be detected by using the LDH test, determining its location and severity (Farhana and Lappin, 2022). In this study, vancomycin administration causes liver damage, contributing to LDH elevation in the serum. This elevation could arise from vancomycin, causing damage to the kidneys. It has been reported that vancomycin can cause kidney damage (Naghbi et al., 2007), making this test a non-specific marker for liver damage.

Resveratrol is a natural compound extensively studied in preclinical studies as a nutraceutical and therapeutic agent. In addition, the antioxidant properties of resveratrol have been demonstrated in a wide range of hepatic disorders (Pan et al., 2017; Bircan et al., 2018). The antioxidant effect functions mainly by reducing ROS and eliminating direct free radicals, while improving the activity of endogenous antioxidant enzymes superoxide dismutase, catalase, and GSH (Carrizzo et al., 2013; de Oliveira et al., 2018). Furthermore, it has been reported that resveratrol is involved in several vital pathways regulating *de novo* fibrogenesis deposition in the liver (Hessin et al., 2017). For example, resveratrol (10 and 20 mg/kg/day) was administered to cirrhotic rats, where it reduced portal pressure, improved vasodilatory acetylcholine responsiveness, and reduced the production of thromboxane A₂, resulting in liver tissue regeneration (Di Pascoli et al., 2013; Zhang et al., 2016).

Globally, liver illnesses continue to be a severe health burden. For the treatment of this category of disorders, new and secure therapeutic options are required. This study shows that resveratrol is a good alternative in this area. This approach could significantly improve potential resveratrol therapeutic applications. Understanding how resveratrol improves many liver disease conditions may lead to novel treatment possibilities. For example, resveratrol produces beneficial effects and reduces possible toxic effects when combined with other medications and substances. As a result, there is still future work to be done because there are still significant gaps in our knowledge about this chemical.

Data availability statement

The raw data supporting the conclusions of this article will be made available by the authors, without undue reservation.

Ethics statement

The study was conducted according to the guidelines for ethical scientific research at Umm Alqura University. The Biomedical Committee of Research Ethics at the faculty of medicine at Umm Al-Qura University approved the study (Approval No. HAPO-02-K-012-2022-06-1127).

Author contributions

FA, NA participated protocol design, data collection and in conducting the study. FA wrote the manuscript. NA analyzed the data. All authors reviewed the approved the final manuscript.

Funding

This project was funded by the Deanship for Research and Innovation, Ministry of Education in Saudi Arabia through project number: IFP22UQU4310453DSR244.

Acknowledgments

The authors extend their appreciation to the Deanship for Research and Innovation, Ministry of Education in Saudi Arabia

References

- Abou Seif, H. S. (2016). Physiological changes due to hepatotoxicity and the protective role of some medicinal plants. *Beni-suef Univ. J. basic Appl. Sci.* 5 (2), 134–146. doi:10.1016/j.bjbas.2016.03.004
- Acevedo, J. (2015). Multiresistant bacterial infections in liver cirrhosis: Clinical impact and new empirical antibiotic treatment policies. *World J. hepatology* 7 (7), 916–921. doi:10.4254/wjh.v7.i7.916
- Adeyemi, O. S., and Adewumi, I. (2014). Biochemical evaluation of silver nanoparticles in wistar rats. *Int. Sch. Res. Not.* 2014, 196091. doi:10.1155/2014/196091
- Adeyemi, O. S., and Akanji, M. A. (2011). Biochemical changes in the kidney and liver of rats following administration of ethanolic extract of Psidium guajava leaves. *Hum. Exp. Toxicol.* 30 (9), 1266–1274. doi:10.1177/0960327110388534
- Ahmida, M. H. (2012). Protective role of curcumin in nephrotoxic oxidative damage induced by vancomycin in rats. *Exp. Toxicol. Pathol.* 64 (3), 149–153. doi:10.1016/j.etp.2010.07.010
- Aldaz, A., Ortega, A., Idoate, A., Giraldez, J., Brugarolas, A., and Brugarolas, A. (2000). Effects of hepatic function on vancomycin pharmacokinetics in patients with cancer. *Ther. Drug Monit.* 22 (3), 250–257. doi:10.1097/00007691-200006000-00004
- Ali, S. S., Kasoju, N., Luthra, A., Singh, A., Sharanabasava, H., Sahu, A., et al. (2008). Indian medicinal herbs as sources of antioxidants. *Food Res. Int.* 41 (1), 1–15. doi:10.1016/j.foodres.2007.10.001
- Apte, U., and Krishnamurthy, P. (2011). *Detoxification Functions of the Liver. Molecular pathology of liver diseases*. Springer, 147–163.
- Badran, E., Shamayleh, A., and Irshaid, Y. (2011). Pharmacokinetics of vancomycin in neonates admitted to the neonatology unit at the Jordan University Hospital. *Int. J. Clin. Pharmacol. Ther.* 49 (4), 252–257. doi:10.5414/CP201456
- Bakan, E., Taysi, S., Polat, M. F., Dalga, S., Umudum, Z., Bakan, N., et al. (2002). Nitric oxide levels and lipid peroxidation in plasma of patients with gastric cancer. *Jpn. J. Clin. Oncol.* 32 (5), 162–166. doi:10.1093/jjco/hyf035
- Bamgbola, O. (2016). Review of vancomycin-induced renal toxicity: An update. *Ther. Adv. Endocrinol. Metab.* 7 (3), 136–147. doi:10.1177/2042018816638223
- Banez, M. J., Geluz, M. I., Chandra, A., Hamdan, T., Biswas, O. S., Bryan, N. S., et al. (2020). A systemic review on the antioxidant and anti-inflammatory effects of resveratrol, curcumin, and dietary nitric oxide supplementation on human cardiovascular health. *Nutr. Res.* 78, 11–26. doi:10.1016/j.nutres.2020.03.002
- Battaller, R., and Brenner, D. A. (2005). Liver fibrosis. *J. Clin. investigation* 115 (2), 209–218. doi:10.1172/JCI24282
- Bergmann, J., Müller, M., Baumann, N., Reichert, M., Heneweer, C., Bolik, J., et al. (2017). IL-6 trans-signaling is essential for the development of hepatocellular carcinoma in mice. *Hepatology* 65 (1), 89–103. doi:10.1002/hep.28874
- Bernal, W., and Wendon, J. (2013). Acute liver failure. *N. Engl. J. Med.* 369 (26), 2525–2534. doi:10.1056/NEJMra1208937
- Bircan, F., Pasaoglu, O., and Turkozkan, N. (2018). The effects of resveratrol on hepatic oxidative stress in metabolic syndrome model induced by high fructose diet. *Bratisl. Lek. listy* 119 (1), 36–40. doi:10.4149/BLL_2018_008
- Bissell, D. M., Gores, G. J., Laskin, D. L., and Hoofnagle, J. H. (2001). Drug-induced liver injury: Mechanisms and test systems. *Hepatology* 33 (4), 1009–1013. doi:10.1053/jhep.2001.23505

for funding this research work through project number: IFP22UQU4310453DSR244.

Conflict of interest

The authors declare that the research was conducted in the absence of any commercial or financial relationships that could be construed as a potential conflict of interest.

Publisher's note

All claims expressed in this article are solely those of the authors and do not necessarily represent those of their affiliated organizations, or those of the publisher, the editors and the reviewers. Any product that may be evaluated in this article, or claim that may be made by its manufacturer, is not guaranteed or endorsed by the publisher.

- Breedit, J., Teras, J., Gardovskis, J., Maritz, F. J., Vaasna, T., Ross, D. P., et al. (2005). Safety and efficacy of tigecycline in treatment of skin and skin structure infections: Results of a double-blind phase 3 comparison study with vancomycin-aztreonam. *Antimicrob. Agents Chemother.* 49 (11), 4658–4666. doi:10.1128/AAC.49.11.4658-4666.2005
- Brunetti, L., Song, J. H., Suh, D., Kim, H. J., Seong, Y. H., Lee, D. S., et al. (2020). The risk of vancomycin toxicity in patients with liver impairment. *Ann. Clin. Microbiol. Antimicrob.* 19 (1), 13. doi:10.1186/s12941-020-00354-2
- Bujanda, L., Hijona, E., Larzabal, M., Beraza, M., Aldazabal, P., Garcia-Urkia, N., et al. (2008). Resveratrol inhibits nonalcoholic fatty liver disease in rats. *BMC Gastroenterol.* 8 (1), 40. doi:10.1186/1471-230X-8-40
- Cadle, R. M., Mansouri, M. D., and Darouiche, R. O. (2006). Vancomycin-induced elevation of liver enzyme levels. *Ann. Pharmacother.* 40 (6), 1186–1189. doi:10.1345/aph.1G668
- Çağlayan, C., Taslimi, P., Demir, Y., Küçükler, S., Kandemir, F. M., and Gulcin, I. (2019). The effects of zingerone against vancomycin-induced lung, liver, kidney and testis toxicity in rats: The behavior of some metabolic enzymes. *J. Biochem. Mol. Toxicol.* 33 (10), e22381. doi:10.1002/jbt.22381
- Cao, Q., Batey, R., Pang, G., Russell, A., and Clancy, R. (1998). IL-6, IFN-gamma and TNF-alpha production by liver-associated T cells and acute liver injury in rats administered concanavalin A. *Immunol. Cell Biol.* 76 (6), 542–549. doi:10.1046/j.1440-1711.1998.00779.x
- Carrizzo, A., Forte, M., Damato, A., Trimarco, V., Salzano, F., Bartolo, M., et al. (2013). Antioxidant effects of resveratrol in cardiovascular, cerebral and metabolic diseases. *Food Chem. Toxicol.* 61, 215–226. doi:10.1016/j.fct.2013.07.021
- Chen, T., Zamora, R., Zuckerbraun, B., and Billiar, T. R. (2003). Role of nitric oxide in liver injury. *Curr. Mol. Med.* 3 (6), 519–526. doi:10.2174/1566524033479582
- Chen, Y., Yang, X. Y., Zeckel, M., Killian, C., Hornbuckle, K., Regev, A., et al. (2011). Risk of hepatic events in patients treated with vancomycin in clinical studies: A systematic review and meta-analysis. *Drug Saf.* 34 (1), 73–82. doi:10.2165/11539560-000000000-00000
- Choi, I., Kang, H. S., Yang, Y., and Pyun, K. H. (1994). IL-6 induces hepatic inflammation and collagen synthesis *in vivo*. *Clin. Exp. Immunol.* 95 (3), 530–535. doi:10.1111/j.1365-2249.1994.tb07031.x
- Chupradit, S., Bokov, D., Zamanian, M. Y., Heidari, M., and Hakimzadeh, E. (2022). Hepatoprotective and therapeutic effects of resveratrol: A focus on anti-inflammatory and antioxidative activities. *Fundam. Clin. Pharmacol.* 36 (3), 468–485. doi:10.1111/fcp.12746
- Das, R., Mitra, S., Tareq, A. M., Emran, T. B., Hossain, M. J., Alqahtani, A. M., et al. (2022). Medicinal plants used against hepatic disorders in Bangladesh: A comprehensive review. *J. Ethnopharmacol.* 282, 114588. doi:10.1016/j.jep.2021.114588
- David, M. Z., and Daum, R. S. (2010). Community-associated methicillin-resistant *Staphylococcus aureus*: Epidemiology and clinical consequences of an emerging epidemic. *Clin. Microbiol. Rev.* 23 (3), 616–687. doi:10.1128/CMR.00081-09
- Day, R. M., and Suzuki, Y. J. (2005). Cell proliferation, reactive oxygen and cellular glutathione. *Dose-response* 3 (3), 425–442. doi:10.2203/dose-response.003.03.010
- de Oliveira, M. R., Chenet, A. L., Duarte, A. R., Scaini, G., and Quevedo, J. (2018). Molecular mechanisms underlying the anti-depressant effects of resveratrol: A review. *Mol. Neurobiol.* 55 (6), 4543–4559. doi:10.1007/s12035-017-0680-6

- Deshpande, U. R., Gadre, S. G., Raste, A. S., Pillai, D., Bhide, S. V., and Samuel, A. M. (1998). Protective effect of turmeric (*Curcuma longa* L.) extract on carbon tetrachloride-induced liver damage in rats. *Indian J. Exp. Biol.* 36 (6), 573–577.
- Di Pascoli, M., Divi, M., Rodriguez-Vilarrupla, A., Rosado, E., Gracia-Sancho, J., Vilaseca, M., et al. (2013). Resveratrol improves intrahepatic endothelial dysfunction and reduces hepatic fibrosis and portal pressure in cirrhotic rats. *J. Hepatol.* 58 (5), 904–910. doi:10.1016/j.jhep.2012.12.012
- Diesen, D. L., and Kuo, P. C. (2010). Nitric oxide and redox regulation in the liver: Part I. General considerations and redox biology in hepatitis. *J. Surg. Res.* 162 (1), 95–109. doi:10.1016/j.jss.2009.09.019
- Ebrahim, H. A., Kamar, S. S., Haidara, M. A., Latif, N. S. A., Ellatif, M. A., ShamsEldeen, A. M., et al. (2022). Association of resveratrol with the suppression of TNF- α /NF- κ B/iNOS/HIF-1 α axis-mediated fibrosis and systemic hypertension in thioacetamide-induced liver injury. *Naunyn Schmiedeb. Arch. Pharmacol.* 395 (9), 1087–1095. doi:10.1007/s00210-022-02264-w
- Ekhlesi, G., Zarrati, M., Agah, S., Hosseini, A. F., Hosseini, S., Shidfar, S., et al. (2017). Effects of symbiotic and vitamin E supplementation on blood pressure, nitric oxide and inflammatory factors in non-alcoholic fatty liver disease. *EXCLI J.* 16, 278–290. doi:10.17179/excli2016-846
- El Bohi, K. M., Abdel-Motal, S. M., Khalil, S. R., Abd-Elal, M. M., Metwally, M. M. M., and Wm, E. L. (2021). The efficiency of pomegranate (*Punica granatum*) peel ethanolic extract in attenuating the vancomycin-triggered liver and kidney tissues injury in rats. *Environ. Sci. Pollut. Res. Int.* 28 (6), 7134–7150. doi:10.1007/s11356-020-10999-3
- Eskandari, M. R., Fard, J. K., Hosseini, M. J., and Pourahmad, J. (2012). Glutathione mediated reductive activation and mitochondrial dysfunction play key roles in lithium induced oxidative stress and cytotoxicity in liver. *Biometals* 25 (5), 863–873. doi:10.1007/s10534-012-9552-8
- Fabbri, E., and Magkos, F. (2015). Hepatic steatosis as a marker of metabolic dysfunction. *Nutrients* 7 (6), 4995–5019. doi:10.3390/nu7064995
- Farhana, A., and Lappin, S. L. (2022). *Biochemistry, lactate dehydrogenase. StatPearls. Treasure island (FL)*. StatPearls Publishing.
- Fathy, M., Khalifa, E. M., and Fawzy, M. A. (2019). Modulation of inducible nitric oxide synthase pathway by eugenol and telmisartan in carbon tetrachloride-induced liver injury in rats. *Life Sci.* 216, 207–214. doi:10.1016/j.lfs.2018.11.031
- Fernández, J., Tandon, P., Mensa, J., and Garcia Tsao, G. (2016). Antibiotic prophylaxis in cirrhosis: Good and bad. *Hepatology* 63 (6), 2019–2031. doi:10.1002/hep.28330
- Florescu, I., Beuran, M., Dimov, R., Razbadauskas, A., Bochan, M., Fichev, G., et al. (2008). Efficacy and safety of tigecycline compared with vancomycin or linezolid for treatment of serious infections with methicillin-resistant *Staphylococcus aureus* or vancomycin-resistant enterococci: A phase 3, multicentre, double-blind, randomized study. *J. Antimicrob. Chemother.* 62 (1), i17–i28. doi:10.1093/jac/dkn250
- Franco, R., and Cidlowski, J. A. (2009). Apoptosis and glutathione: Beyond an antioxidant. *Cell Death Differ.* 16 (10), 1303–1314. doi:10.1038/cdd.2009.107
- Friedman, S. L. (2008). Mechanisms of hepatic fibrogenesis. *Gastroenterology* 134 (6), 1655–1669. doi:10.1053/j.gastro.2008.03.003
- Gescher, A. J., and Steward, W. P. (2003). Relationship between mechanisms, bioavailability, and preclinical chemopreventive efficacy of resveratrol: A conundrum. *Cancer Epidemiol. Prev. Biomarkers* 12 (10), 953–957.
- Gewiese-Rabsch, J., Drucker, C., Malchow, S., Scheller, J., and Rose-John, S. (2010). Role of IL-6 trans-signaling in CCl₄-induced liver damage. *Biochimica Biophysica Acta (BBA)-Molecular Basis Dis.* 1802 (11), 1054–1061. doi:10.1016/j.bbdis.2010.07.023
- Gupta, A., Biyani, M., Khaira, A., and KhAirA, A. (2011). Vancomycin nephrotoxicity: Myths and facts. *Neth J. Med.* 69 (9), 379–383.
- Gupta, K. J., Fernie, A. R., Kaiser, W. M., and van Dongen, J. T. (2011). On the origins of nitric oxide. *Trends Plant Sci.* 16 (3), 160–168. doi:10.1016/j.tplants.2010.11.007
- Hadizadeh, F., Faghihmani, E., and Adibi, P. (2017). Nonalcoholic fatty liver disease: Diagnostic biomarkers. *World J. Gastrointest. Pathophysiol.* 8 (2), 11–26. doi:10.4291/wjgp.v8.i2.11
- Halliwel, B. (2007). Dietary polyphenols: Good, bad, or indifferent for your health? *Cardiovasc. Res.* 73 (2), 341–347. doi:10.1016/j.cardiores.2006.10.004
- Hessin, A. F., Hegazy, R. R., Hassan, A. A., Yassin, N. Z., and Kenawy, S. A. (2017). Resveratrol prevents liver fibrosis via two possible pathways: Modulation of alpha fetoprotein transcriptional levels and normalization of protein kinase C responses. *Indian J. Pharmacol.* 49 (4), 282–289. doi:10.4103/ijp.IJP_299_16
- Hwang, J. H., Lee, J. H., Hwang, J. H., Chung, K. M., Lee, E. J., Yoon, Y. J., et al. (2015). Comparison of arbutin and hepatoprotective potentials of curcuminoid isolates from turmeric (*Curcuma longa*) rhizome on CCl₄-induced hepatic damage in Wistar rats. *J. Taibah Univ. Sci.* 14 (1), 908–915. doi:10.1080/16583655.2020.1790928
- Iwakiri, Y., and Kim, M. Y. (2015). Nitric oxide in liver diseases. *Trends Pharmacol. Sci.* 36 (8), 524–536. doi:10.1016/j.tips.2015.05.001
- Jalan, R., Gines, P., Olson, J. C., Mookerjee, R. P., Moreau, R., Garcia-Tsao, G., et al. (2012). Acute-on chronic liver failure. *J. hepatology* 57 (6), 1336–1348. doi:10.1016/j.jhep.2012.06.026
- Kaplowitz, N. (2001). Drug-induced liver disorders: Implications for drug development and regulation. *Drug Saf.* 24 (7), 483–490. doi:10.2165/00002018-200124070-00001
- Kashima, J., Okuma, Y., Shimizuguchi, R., and Chiba, K. (2018). Bile duct obstruction in a patient treated with nivolumab as second-line chemotherapy for advanced non-small-cell lung cancer: A case report. *Cancer Immunol. Immunother.* 67 (1), 61–65. doi:10.1007/s00262-017-2062-3
- King, D. W., and Smith, M. A. (2004). Proliferative responses observed following vancomycin treatment in renal proximal tubule epithelial cells. *Toxicol Vitro* 18 (6), 797–803. doi:10.1016/j.tiv.2004.03.013
- Kohno, S., Yamaguchi, K., Aikawa, N., Sumiyama, Y., Odagiri, S., Aoki, N., et al. (2007). Linezolid versus vancomycin for the treatment of infections caused by methicillin-resistant *Staphylococcus aureus* in Japan. *J. Antimicrob. Chemother.* 60 (6), 1361–1369. doi:10.1093/jac/dkm369
- Korde Choudhary, S., Chaudhary, M., Bagde, S., Gadgil, A. R., and Joshi, V. (2013). Nitric oxide and cancer: A review. *World J. Surg. Oncol.* 11 (1), 118–211. doi:10.1186/1477-7819-11-118
- Kouijzer, I. J., van Leerdam, E. J., Gompelman, M., Tuinte, R. A., Aarntzen, E. H., Berrevoets, M. A., et al. (2021). Intravenous to oral switch in complicated *Staphylococcus aureus* bacteremia without endovascular infection: A retrospective single-center cohort study. *Clin. Infect. Dis.* 73 (5), 895–898. doi:10.1093/cid/ciab156
- Kucukler, S., Darendelioglu, E., Caglayan, C., Ayna, A., Yildirim, S., and Kandemir, F. M. (2020). Zingerone attenuates vancomycin-induced hepatotoxicity in rats through regulation of oxidative stress, inflammation and apoptosis. *Life Sci.* 259, 118382. doi:10.1016/j.lfs.2020.118382
- Kurland, I. J., Broin, P. O., Golden, A., Su, G., Meng, F., Liu, L., et al. (2015). Integrative metabolic signatures for hepatic radiation injury. *PLoS One* 10 (6), e0124795. doi:10.1371/journal.pone.0124795
- Labban, S., Alghamdi, B. S., Alshehri, F. S., and Kurdi, M. (2021). Effects of melatonin and resveratrol on recognition memory and passive avoidance performance in a mouse model of Alzheimer's disease. *Behav. Brain Res.* 402, 113100. doi:10.1016/j.bbr.2020.113100
- Labban, S., Alshehri, F. S., Kurdi, M., Alatawi, Y., and Alghamdi, B. S. (2021). Melatonin improves short-term spatial memory in a mouse model of Alzheimer's disease. *Degener. Neurol. Neuromuscul. Dis.* 11, 15–27. doi:10.2147/DNND.S291172
- D. Larrey (Editor) (2002). "Epidemiology and individual susceptibility to adverse drug reactions affecting the liver," *Seminars in liver disease* (Medical Publishers, Inc.). Copyright© 2002 by Thieme333 Seventh Avenue, New.
- Laskin, J. D., Heck, D. E., Gardner, C. R., and Laskin, D. L. (2001). Prooxidant and antioxidant functions of nitric oxide in liver toxicity. *Antioxid. Redox Signal* 3 (2), 261–271. doi:10.1089/152308601300185214
- Lee, E. S., Shin, M. O., Yoon, S., and Moon, J. O. (2010). Resveratrol inhibits dimethylnitrosamine-induced hepatic fibrosis in rats. *Arch. Pharm. Res.* 33 (6), 925–932. doi:10.1007/s12272-010-0616-4
- López-Posadas, R., Gonzalez, R., Ballester, I., Martínez-Moya, P., Romero-Calvo, I., Suárez, M. D., et al. (2011). Tissue-nonspecific alkaline phosphatase is activated in enterocytes by oxidative stress via changes in glycosylation. *Inflamm. bowel Dis.* 17 (2), 543–556. doi:10.1002/ibd.21381
- Lowe, D., Sanvictores, T., and John, S. (2017). *Alkaline phosphatase*.
- Ma, Z., Sheng, L., Li, J., Qian, J., Wu, G., Wang, Z., et al. (2022). Resveratrol alleviates hepatic fibrosis in associated with decreased endoplasmic reticulum stress-mediated apoptosis and inflammation. *Inflammation* 45 (2), 812–823. doi:10.1007/s10753-021-01586-w
- Mari, M., Morales, A., Colell, A., Garcia-Ruiz, C., and Fernandez-Checa, J. C. (2009). Mitochondrial glutathione, a key survival antioxidant. *Antioxid. Redox Signal* 11 (11), 2685–2700. doi:10.1089/ARS.2009.2695
- Mehrzadi, S., Fatemi, I., Esmailizadeh, M., Ghaznavi, H., Kalantar, H., and Goudarzi, M. (2018). Hepatoprotective effect of berberine against methotrexate induced liver toxicity in rats. *Biomed. Pharmacother.* 97, 233–239. doi:10.1016/j.biopha.2017.10.113
- Miguel, C., Noya-Riobó, M., Mazzone, G., Villar, M., and Coronel, M. (2021). Antioxidant, anti-inflammatory and neuroprotective actions of resveratrol after experimental nervous system insults. Special focus on the molecular mechanisms involved. *Neurochem. Int.* 150, 105188. doi:10.1016/j.neuint.2021.105188
- Naghbi, B., Ghafghazi, T., Hajhashemi, V., and Talebi, A. (2007). Vancomycin-induced nephrotoxicity in rats: Is enzyme elevation a consistent finding in tubular injury? *J. Nephrol.* 20 (4), 482–488.
- Novo, E., and Parola, M. (2008). Redox mechanisms in hepatic chronic wound healing and fibrogenesis. *Fibrogenes. Tissue Repair* 1, 5–58. doi:10.1186/1755-1536-1-5
- Oktem, F., Arslan, M. K., Ozguner, F., Candir, O., Yilmaz, H. R., Ciris, M., et al. (2005). *In vivo* evidences suggesting the role of oxidative stress in pathogenesis of vancomycin-induced nephrotoxicity: Protection by erdostein. *Toxicology* 215 (3), 227–233. doi:10.1016/j.tox.2005.07.009
- Olaniyan, M. F., Atibor, R. A., and Afolabi, T. (2018). Evaluation of tumor necrosis factor alpha (TNF α), interleukin 4, interleukin 6, aspartate aminotransferase, and alanine

- aminotransferase in rabbits overdosed with ibuprofen and supplemented with guava leaf (Psidium guajava) extract. *Biomed. Biotechnol. Res. J. (BBRJ)* 2 (4), 254. doi:10.4103/bbrj.bbrj_121_18
- Omara, F., Aziz, S., El-Sheikh, S., and Said, M. (2021). Ascorbic acid attenuated the hepatic parenchymal necrosis induced by azithromycin-eticorixib interaction in rats. *J. Anim. Health Prod.* 9 (1), 42–48. doi:10.17582/journal.jahp/2021/9.s1.42.48
- Pan, Y., Zhang, H., Zheng, Y., Zhou, J., Yuan, J., Yu, Y., et al. (2017). Resveratrol exerts antioxidant effects by activating SIRT2 to deacetylate Prx1. *Biochemistry* 56 (48), 6325–6328. doi:10.1021/acs.biochem.7b00859
- Pandit, A., Sachdeva, T., and Bafna, P. (2012). Drug-induced hepatotoxicity: A review. *J. Appl. Pharm. Sci.* 2 (5), 233–243.
- Parthasarathy, M., and Evan Prince, S. (2021). The potential effect of phytochemicals and herbal plant remedies for treating drug-induced hepatotoxicity: A review. *Mol. Biol. Rep.* 48 (5), 4767–4788. doi:10.1007/s11033-021-06444-4
- Philips, C. A., Ahamed, R., Rajesh, S., George, T., Mohanan, M., and Augustine, P. (2020). Comprehensive review of hepatotoxicity associated with traditional Indian Ayurvedic herbs. *World J. Hepatol.* 12 (9), 574–595. doi:10.4254/wjh.v12.i9.574
- Picon-Pages, P., Garcia-Buendia, J., and Munoz, F. J. (2019). Functions and dysfunctions of nitric oxide in brain. *Biochim. Biophys. Acta Mol. Basis Dis.* 1865 (8), 1949–1967. doi:10.1016/j.bbdis.2018.11.007
- Pourhanifeh, M. H., Shafabakhsh, R., Reiter, R. J., and Asemi, Z. (2019). The effect of resveratrol on neurodegenerative disorders: Possible protective actions against autophagy, apoptosis, inflammation and oxidative stress. *Curr. Pharm. Des.* 25 (19), 2178–2191. doi:10.2174/1381612825666190717110932
- Regal, R. E., Ren, S. P., Paige, G., and Alaniz, C. (2019). Evaluation of vancomycin dosing in patients with cirrhosis: Beginning de-liver-ations about a new nomogram. *Hosp. Pharm.* 54 (2), 125–129. doi:10.1177/0018578718772266
- Rivera, H., Shibayama, M., Tsutsumi, V., Perez-Alvarez, V., and Muriel, P. (2008). Resveratrol and trimethylated resveratrol protect from acute liver damage induced by CCl4 in the rat. *J. Appl. Toxicol.* 28 (2), 147–155. doi:10.1002/jat.1260
- Rubiolo, J. A., and Vega, F. V. (2008). Resveratrol protects primary rat hepatocytes against necrosis induced by reactive oxygen species. *Biomed. Pharmacother.* 62 (9), 606–612. doi:10.1016/j.biopha.2008.06.034
- Sadeghi, H., Nikbakht, M. R., Izadpanah, G., and Sabzali, S. (2008). Hepatoprotective effect of Cichorium intybus on CCl4-induced liver damage in rats. *Afr. J. Biochem. Res.* 2 (6), 141–144.
- Sahin, M., Cam, H., Olgar, S., Tunc, S. E., Arslan, C., Uz, E., et al. (2006). Protective role of erdosteine on vancomycin-induced oxidative stress in rat liver. *Mol. Cell Biochem.* 291 (1–2), 155–160. doi:10.1007/s11010-006-9209-4
- Santos, M. A., Franco, F. N., Caldeira, C. A., de Araújo, G. R., Vieira, A., Chaves, M. M., et al. (2021). Antioxidant effect of Resveratrol: Change in MAPK cell signaling pathway during the aging process. *Archives Gerontology Geriatrics* 92, 104266. doi:10.1016/j.archger.2020.104266
- Sebai, H., Sani, M., Yacoubi, M. T., Aouani, E., Ghanem-Boughanmi, N., and Ben-Attia, M. (2010). Resveratrol, a red wine polyphenol, attenuates lipopolysaccharide-induced oxidative stress in rat liver. *Ecotoxicol. Environ. Saf.* 73 (5), 1078–1083. doi:10.1016/j.ecoenv.2009.12.031
- Sener, G., Toklu, H. Z., Sehirli, A. O., Velioglu-Ogunc, A., Cetinel, S., and Gedik, N. (2006). Protective effects of resveratrol against acetaminophen-induced toxicity in mice. *Hepatol. Res.* 35 (1), 62–68. doi:10.1016/j.hepres.2006.02.005
- Senior, J. R. (2012). Alanine aminotransferase: A clinical and regulatory tool for detecting liver injury-past, present, and future. *Clin. Pharmacol. Ther.* 92 (3), 332–339. doi:10.1038/clpt.2012.108
- Shah, A. A., Patton, M., Chishty, W. H., and Hussain, A. (2010). Analysis of elevated liver enzymes in an acute medical setting: Jaundice may indicate increased survival in elderly patients with bacterial sepsis. *Saudi J. Gastroenterol.* 16 (4), 260–263. doi:10.4103/1319-3767.70609
- Shao, M., Xu, Q., Wu, Z., Chen, Y., Shu, Y., Cao, X., et al. (2020). Exosomes derived from human umbilical cord mesenchymal stem cells ameliorate IL-6-induced acute liver injury through miR-455-3p. *Stem Cell Res. Ther.* 11 (1), 37–13. doi:10.1186/s13287-020-1550-0
- Sibai, B. M. (2004). Diagnosis, controversies, and management of the syndrome of hemolysis, elevated liver enzymes, and low platelet count. *Obstet. Gynecol.* 103 (5), 981–991. doi:10.1097/01.AOG.0000126245.35811.2a
- Srivastava, P., Prabhu, V. V., Yadav, N., Gogada, R., and Chandra, D. (2013). *Effect of dietary resveratrol in the treatment of cancer. Cancer chemoprevention and treatment by diet therapy.* Springer, 1–22.
- Steinmetz, T., Eliakim-Raz, N., Goldberg, E., Leibovici, L., and Yahav, D. (2015). Association of vancomycin serum concentrations with efficacy in patients with MRSA infections: A systematic review and meta-analysis. *Clin. Microbiol. Infect.* 21 (7), 665–673. doi:10.1016/j.cmi.2015.04.003
- Taga, T., and Kishimoto, T. (1997). Gp130 and the interleukin-6 family of cytokines. *Annu. Rev. Immunol.* 15, 797–819. doi:10.1146/annurev.immunol.15.1.797
- Takai, S., Oda, S., Tsuneyama, K., Fukami, T., Nakajima, M., and Yokoi, T. (2016). Establishment of a mouse model for amiodarone-induced liver injury and analyses of its hepatotoxic mechanism. *J. Appl. Toxicol.* 36 (1), 35–47. doi:10.1002/jat.3141
- Thiim, M., and Friedman, L. S. (2003). Hepatotoxicity of antibiotics and antifungals. *Clin. Liver Dis.* 7 (2), 381–399. vi-vii. doi:10.1016/s1089-3261(03)00021-7
- Tong, Y., Yu, X., Huang, Y., Zhang, Z., Mi, L., and Bao, Z. (2022). Hepatic-targeted nano-enzyme with resveratrol loading for precise relief of nonalcoholic steatohepatitis. *ChemMedChem.* doi:10.1002/cmdc.202200468
- Tsochatzis, E. A., Bosch, J., and Burroughs, A. K. (2014). Liver cirrhosis. *Lancet* 383 (9930), 1749–1761. doi:10.1016/S0140-6736(14)60121-5
- Tsutsuura, M., Moriyama, H., Kojima, N., Mizukami, Y., Tashiro, S., Osa, S., et al. (2021). The monitoring of vancomycin: A systematic review and meta-analyses of area under the concentration-time curve-guided dosing and trough-guided dosing. *BMC Infect. Dis.* 21 (1), 153. doi:10.1186/s12879-021-05858-6
- Wang, Y., Jiang, Y., Fan, X., Tan, H., Zeng, H., Wang, Y., et al. (2015). Hepato-protective effect of resveratrol against acetaminophen-induced liver injury is associated with inhibition of CYP-mediated bioactivation and regulation of SIRT1-p53 signaling pathways. *Toxicol. Lett.* 236 (2), 82–89. doi:10.1016/j.toxlet.2015.05.001
- Wang, Y. Y., Chen, M. T., Hong, H. M., Wang, Y., Li, Q., Liu, H., et al. (2018). Role of reduced nitric oxide in liver cell apoptosis inhibition during liver damage. *Arch. Med. Res.* 49 (4), 219–225. doi:10.1016/j.arcmed.2018.09.001
- Winter, A. N., Ross, E. K., Daliparthi, V., Sumner, W. A., Kirchhof, D. M., Manning, E., et al. (2017). A cystine-rich whey supplement (Immunocal®) provides neuroprotection from diverse oxidative stress-inducing agents *in vitro* by preserving cellular glutathione. *Oxid. Med. Cell Longev.* 2017, 3103272. doi:10.1155/2017/3103272
- Wu, K., Fan, J., Huang, X., Wu, X., and Guo, C. (2018). Hepatoprotective effects exerted by Poria Cocos polysaccharides against acetaminophen-induced liver injury in mice. *Int. J. Biol. Macromol.* 114, 137–142. doi:10.1016/j.ijbiomac.2018.03.107
- Xia, H. M., Wang, J., Xie, X. J., Xu, L. J., and Tang, S. Q. (2019). Green tea polyphenols attenuate hepatic steatosis, and reduce insulin resistance and inflammation in high-fat diet-induced rats. *Int. J. Mol. Med.* 44 (4), 1523–1530. doi:10.3892/ijmm.2019.4285
- Yamauchi-Takahara, K., and Kishimoto, T. (2000). Cytokines and their receptors in cardiovascular diseases—Role of gp130 signalling pathway in cardiac myocyte growth and maintenance. *Int. J. Exp. pathology* 81 (1), 1–16. doi:10.1046/j.1365-2613.2000.00139.x
- Yilmaz, S., Kaya, E., and Comakli, S. (2017). Vitamin E (alpha tocopherol) attenuates toxicity and oxidative stress induced by aflatoxin in rats. *Adv. Clin. Exp. Med.* 26 (6), 907–917. doi:10.17219/acem/66347
- Yin, Y., Liu, H., Zheng, Z., Lu, R., and Jiang, Z. (2019). Genistein can ameliorate hepatic inflammatory reaction in nonalcoholic steatohepatitis rats. *Biomed. Pharmacother.* 111, 1290–1296. doi:10.1016/j.biopha.2019.01.004
- Yousefian, M., Shakour, N., Hosseinzadeh, H., Hayes, A. W., Hadizadeh, F., and Karimi, G. (2019). The natural phenolic compounds as modulators of NADPH oxidases in hypertension. *Phytomedicine* 55, 200–213. doi:10.1016/j.phymed.2018.08.002
- Yuan, L., and Kaplowitz, N. (2009). Glutathione in liver diseases and hepatotoxicity. *Mol. Asp. Med.* 30 (1–2), 29–41. doi:10.1016/j.mam.2008.08.003
- Zhang, C., Wang, N., Xu, Y., Tan, H. Y., Li, S., and Feng, Y. (2018). Molecular mechanisms involved in oxidative stress-associated liver injury induced by Chinese herbal medicine: An experimental evidence-based literature review and network Pharmacology study. *Int. J. Mol. Sci.* 19 (9), 2745. doi:10.3390/ijms19092745
- Zhang, D. Q., Sun, P., Jin, Q., Li, X., Zhang, Y., Zhang, Y. J., et al. (2016). Resveratrol regulates activated hepatic stellate cells by modulating NF-κB and the PI3K/akt signaling pathway. *J. Food Sci.* 81 (1), H240–H245. doi:10.1111/1750-3841.13157
- Zhou, Y., Chen, K., He, L., Xia, Y., Dai, W., Wang, F., et al. (2015). The protective effect of resveratrol on concanavalin-A-induced acute hepatic injury in mice. *Gastroenterol. Res. Pract.* 2015, 506390. doi:10.1155/2015/506390
- Zoratti, C., Moretti, R., Rebuzzi, L., Alberghini, I. V., Di Somma, A., Decorti, G., et al. (2022). Antibiotics and liver cirrhosis: What the physicians need to know. *Antibiotics* 11 (1), 31. doi:10.3390/antibiotics11010031



OPEN ACCESS

EDITED BY

Chika Ifeanyi Chukwuma,
Central University of Technology, South
Africa

REVIEWED BY

Sushil Kumar Chaudhary,
Institute of Bio-Resources and
Sustainable Development (IBSD), India
Ntethelelo Sibiya,
Rhodes University, South Africa
Jude Akinyelu,
Federal University Oye-Ekiti, Nigeria

*CORRESPONDENCE

Amany E. Ragab,
✉ amany.ragab@pharm.tanta.edu.eg
Maha Saber-Ayad,
✉ msaber@sharjah.ac.ae

[†]These authors have contributed equally
to this work

SPECIALTY SECTION

This article was submitted to
Ethnopharmacology,
a section of the journal
Frontiers in Pharmacology

RECEIVED 15 February 2023

ACCEPTED 13 March 2023

PUBLISHED 28 March 2023

CITATION

Abo-Saif MA, Ragab AE, Ibrahim AO,
Abdelzaher OF, Mehanyd ABM,
Saber-Ayad M and El-Feky OA (2023),
Pomegranate peel extract protects
against the development of diabetic
cardiomyopathy in rats by inhibiting
pyroptosis and downregulating LncRNA-
MALAT1.
Front. Pharmacol. 14:1166653.
doi: 10.3389/fphar.2023.1166653

COPYRIGHT

© 2023 Abo-Saif, Ragab, Ibrahim,
Abdelzaher, Mehanyd, Saber-Ayad and
El-Feky. This is an open-access article
distributed under the terms of the
Creative Commons Attribution License
(CC BY). The use, distribution or
reproduction in other forums is
permitted, provided the original author(s)
and the copyright owner(s) are credited
and that the original publication in this
journal is cited, in accordance with
accepted academic practice. No use,
distribution or reproduction is permitted
which does not comply with these terms.

Pomegranate peel extract protects against the development of diabetic cardiomyopathy in rats by inhibiting pyroptosis and downregulating LncRNA-MALAT1

Mariam Ali Abo-Saif^{1†}, Amany E. Ragab^{2*†}, Amera O. Ibrahim¹,
Othman F. Abdelzaher³, Ahmed B. M. Mehanyd³,
Maha Saber-Ayad^{4,5*} and Ola A. El-Feky¹

¹Department of Biochemistry, Faculty of Pharmacy, Tanta University, Tanta, Egypt, ²Department of Pharmacognosy, Faculty of Pharmacy, Tanta University, Tanta, Egypt, ³Zoology Department, Faculty of Science, Al-Azhar University, Cairo, Egypt, ⁴Department of Clinical Sciences, College of Medicine and Research Institute for Medical and Health Sciences, University of Sharjah, Sharjah, United Arab Emirates, ⁵Department of Pharmacology, College of Medicine, Cairo University, Giza, Egypt

Background: Pyroptosis is an inflammatory programmed cell death accompanied by activation of inflammasomes and maturation of pro-inflammatory cytokines interleukin-1 β (IL-1 β) and IL-18. Pyroptosis is closely linked to the development of diabetic cardiomyopathy (DC). Pomegranate peel extract (PPE) exhibits a cardioprotective effect due to its antioxidant and anti-inflammatory properties. This study aimed to investigate the underlying mechanisms of the protective effect of PPE on the myocardium in a rat model of DC and determine the underlying molecular mechanism.

Methods: Type 1 diabetes (T1DM) was induced in rats by intraperitoneal injection of streptozotocin. The rats in the treated groups received (150 mg/kg) PPE orally and daily for 8 weeks. The effects on the survival rate, lipid profile, serum cardiac troponin-1, lipid peroxidation, and tissue fibrosis were assessed. Additionally, the expression of pyroptosis-related genes (NLRP3 and caspase-1) and LncRNA-MALAT1 in the heart tissue was determined. The PPE was analyzed using UPLC-MS/MS and NMR for characterizing the phytochemical content.

Results: Prophylactic treatment with PPE significantly ameliorated cardiac hypertrophy in the diabetic rats and increased the survival rate. Moreover, prophylactic treatment with PPE in the diabetic rats significantly improved the lipid profile, decreased serum cardiac troponin-1, and decreased lipid peroxidation in the myocardial tissue. Histopathological examination of the cardiac tissues showed a marked reduction in fibrosis (decrease in collagen volume and number of TGF- β -positive cells) and preservation of normal myocardial structures in the diabetic rats treated with PPE. There was a significant decrease in the expression of pyroptosis-related genes (NLRP3 and caspase-1) and LncRNA-MALAT1 in the heart tissue of the diabetic rats treated with PPE. In addition, the concentration of IL-1 β and caspase-1 significantly decreased in the heart tissue of the same group. The protective effect of PPE on diabetic cardiomyopathy could be due to the inhibition of pyroptosis and downregulation of LncRNA-MALAT1. The phytochemical analysis of the PPE indicated that the

major compounds were hexahydroxydiphenic acid glucoside, caffeoylquinic acid, gluconic acid, citric acid, gallic acid, and punicalagin.

Conclusion: PPE exhibited a cardioprotective potential in diabetic rats due to its unique antioxidant, anti-inflammatory, and antifibrotic properties and its ability to improve the lipid profile. The protective effect of PPE on DC could be due to the inhibition of the NLRP3/caspase-1/IL-1 β signaling pathway and downregulation of lncRNA-MALAT1. PPE could be a promising therapy to protect against the development of DC, but further clinical studies are recommended.

KEYWORDS

long non-coding RNA-metastasis-associated lung adenocarcinoma transcript-1, NLRP3, caspase-1, IL1 β , TGF- β , pomegranate peel extract

1 Introduction

Diabetic patients with poor glycemic control have a high probability of developing diabetic cardiomyopathy (DC) and heart failure. The pathophysiology of DC is linked to impaired glucose metabolism in diabetic myocardium caused by reduced insulin signaling and the heart's dependence on fatty acid oxidation for energy (Yan et al., 2020). Altered glucose and lipid metabolism in diabetic cardiomyocytes increases mitochondrial production of nitric oxide radicals and stimulates multiple inflammatory pathways. Prominent oxidative stress, chronic inflammation, and increased production of advanced glycation end-products (AGEs) lead to myocardial tissue damage with pathological remodeling of the cardiac tissue and fibrosis (Prandi et al., 2022).

Pyroptosis is an inflammatory programmed cell death activated in response to microbial infection, cellular damage, or metabolic imbalances (Xue et al., 2019). Pyroptosis is characterized by the formation of the nucleotide-binding domain (NOD)-like receptor protein 3 (NLRP3) inflammasome complex that is composed of NLRP3, apoptosis-associated speck-like protein (ASC), and pro-caspase-1. Oligomerization of NLRP3 inflammasome mediates the activation of caspase-1 and the release of pro-inflammatory cytokines IL-1 β and IL-18 (Zheng and Li, 2020).

Previous studies have shown that pyroptosis activation is associated with the development of DC. Reactive oxygen species (ROS) and hyperglycemia activate NLRP3 oligomerization and the associated inflammatory programmed cell death, which can progress to DC (Lu et al., 2022). Moreover, Meng et al. (2022) reported that the downregulation of NLRP3 inflammasome restores myocardial function in DC models.

Long non-coding RNAs (lncRNAs) are a group of RNA transcripts that comprise more than 200 nucleotides, but they do not have the ability to encode protein. lncRNAs are involved in different pathological mechanisms in various diseases (Khorkova et al., 2015). Metastasis-associated lung adenocarcinoma transcript-1 (MALAT1) is an lncRNA which is essential in the regulation of different biological pathways and has been reported to be involved in the pathogenesis of DC (Zhang et al., 2016; Abdulle et al., 2019). Recently, Shi et al. (2021) reported that lncRNA-MALAT1 is upregulated in DC and that knockdown of MALAT1 protects against the development of DC by affecting the NLRP3 formation.

So far, there has been no specific treatment addressing the pathogenesis of DC. The cardioprotective strategies for DC

prevention include the use of antioxidants, antifibrotic agents, and anti-inflammatory agents (Lorenzo-Almorós et al., 2022). Botanicals from plants are an invaluable source of biological effects. They include many classes of compounds, of which polyphenolic compounds, triterpenes, saponins, alkaloids, and glycosides are common. Polyphenolic compounds are strong antioxidants common in fruits and vegetables. Pomegranate fruit (*Punica granatum* L., family Lythraceae) is rich in polyphenolic compounds with strong antioxidative and anti-inflammatory properties (Ismail et al., 2012). Moreover, punicalagin (an active constituent extracted from pomegranate peel) can induce pyroptosis in a collagen-induced arthritis model (El-Mansi and Al-Kahtani, 2019; Ge et al., 2022).

Regeneration of pancreatic β cells may be enhanced by the pomegranate peel aqueous extract (Punasiya et al., 2010). Previous studies showed that pomegranate peel extract (PPE) has antidiabetic and cardiovascular protection properties *in vitro* (Arun et al., 2017), and it also has a cardioprotective effect in a diabetic rat model (Albarakti, 2016). In addition, the study by El-Mansi and Al-Kahtani (2019) demonstrated that PPE showed a cardioprotective effect on diabetic mother rats and their neonates, and the study recommended the use of PPE as a promising treatment, which protects against the secondary myocardial complications of diabetes. Moreover, a recent study by Dab et al. (2022) reported that PPE improves the cardiac extracellular matrix remodeling and decreases fibrosis in diabetic rats. Interestingly, PPE may exhibit a liver protective effect and reduce histological and functional changes in a rat model of diabetes (Faddladdeen and Ojaimi, 2019).

This study aimed to investigate the underlying mechanisms of the potential protective effect of PPE against DC. Intriguingly, we demonstrated, for the first time that PPE interferes with pyroptosis by inhibiting the NLRP3/caspase-1/IL1 β signaling pathway through downregulating lncRNA-MALAT1.

2 Materials and methods

2.1 Plant material

Pomegranate (*Punica granatum* L. var. Edkawy) fruits were obtained from a private farm in Edku city, Al-Beheira Governorate, and verified by the Agricultural Research Center in Cairo. The peel of the fruits was washed with water and air dried. A voucher sample (PD-201-AR) was kept at the Department of Pharmacognosy,

Faculty of Pharmacy, Tanta University. After complete drying, the peel was kept in an oven at 40°C for 10 h to ensure the removal of all water content, and then it was ground into fine powder. The powdered material (800 g) was extracted by 70% methanol (25 mL solvent per 1 g powder) using a magnetic stirrer overnight. The extract was filtered, and the process was repeated for 3 days to ensure exhaustion. The combined solvent filtrates were evaporated under vacuum to leave a reddish-brown residue (yield, 15% w/w).

2.2 Phytochemical characterization of the extract

The PPE was analyzed using UPLC-PDA-MS/MS following a previously reported methodology (Ragab et al., 2022; Assar et al., 2021a; Assar et al., 2021b). A Nexera-i LC-2040 (Shimadzu, Kyoto, Japan) system connected to a UPLC C₁₈ column (Shim-pack Velox, 2.1 × 50 mm; 2.7 μm particle) was used. The mobile-phase gradient and the preparation of the sample were as reported (Assar et al., 2021a; Assar et al., 2021b; Ragab et al., 2022). The mobile phase gradient (solvent A: water containing 0.1% formic acid; solvent B: acetonitrile) at a flow rate of 0.2 mL/min: 0–2 min: 10% B; 2–5: linear gradient to 30% B; 5–15 min: linear gradient to 70% B; 15–22 min: linear gradient to 90% B; 22–25 min: linear gradient to 95% B; 25–26 min: linear gradient to 100% B; 26–29 min: isocratic 100% B; 29–30 min: linear gradient to 10% B was used. A PDA detector (LC-2030/2040) and a triple quadrupole mass spectrometer (LC-MS 8045) equipped with an electrospray ionization (ESI) source in a negative mode (Shimadzu, Kyoto, Japan) were used for detecting the compounds using the reported settings (Assar et al., 2021a; Assar et al., 2021b; Ragab et al., 2022).

A Bruker Avance 400 spectrophotometer at 400 MHz was used for the ¹H NMR analysis of the PPE. DMSO-*d*₆ was used as a solvent. The method development parameters were the same as those published in our recent work on pomegranate extract from the Manfaloty variety (Ragab et al., 2022).

2.3 Biological evaluation

2.3.1 Animal model and experimental design

This study was carried out based on the Guidelines for the Care and Use of Laboratory Animals and approved by the Research Ethical Committee, Faculty of Pharmacy, Tanta University, Egypt (ethical approval code: TP/RE/06/22P-0016). Forty-eight male Wistar rats, aged 6 weeks, and weighing about 120–150 g, were purchased from the National Research Center (Cairo, Egypt). The rats were fed pellet chow (El-Nasr Chemical®, Egypt) and allowed free access to diet and water. The animals were housed under identical environmental conditions and maintained for 2 weeks for acclimatization (Torika et al., 2018).

After the acclimatization, the animals were randomly divided into four groups (*n* = 15): negative control group (normal rat), positive control group (diabetic rats), diabetic treated group (diabetes rats treated with PPE), and normal treated group (normal rats treated with PPE). Type 1 diabetes mellitus (T1DM) was induced by a single ip dose of 60 mg/kg streptozotocin (Sigma

Aldrich, St. Louis, United States) dissolved in 0.1 M sodium citrate buffer. Type 1 diabetes developed 72 h after streptozotocin injection. Rats in the negative control group received a single ip dose of the vehicle (0.1 M sodium citrate buffer 0.25 mL/kg).

Only those rats with blood glucose concentrations greater than 16.7 mmol/L (300 mg/dL) were considered diabetic and were chosen to complete the study. Blood glucose was determined using a blood glucose meter Accu-Chek Performa (Roche Diagnostics, Indianapolis, United States) by tail vein puncture (Babu and Srinivasan, 1997; Riazi et al., 2006).

Rats in the diabetic treated group and non-diabetic treated group were given 1 mL of the PPE at a dose of 150 mg/kg orally and daily for eight consecutive weeks, while rats in the negative and positive control groups were given 1 mL of the vehicle orally and daily for eight consecutive weeks model (El-Mansi and Al-Kahtani, 2019; Mayyas et al., 2021).

At the end of our experiment, the total body weight of the rats was measured, and random blood glucose levels were determined using a blood glucose meter. The rats were fasted for 16 h and sacrificed. Blood was collected by cardiac puncture, and the serum was separated for determination of lipid profile and serum cardiac troponin I (cTnI). The heart was removed and washed with cold saline (pH = 7.4), and the weight of the heart was determined. The heart was cut into two portions; one portion was fixed in 10% formaldehyde for histopathological evaluation and immunohistochemical staining of transforming growth factor beta (TGF-β), while the other portion was kept at −80°C for biochemical estimations of malondialdehyde (MDA), enzyme-linked immunosorbent assay (ELISA) of interleukin 1 beta (IL-1β) and caspase-1, and quantitative reverse transcriptase-polymerase chain reaction (qRT-PCR) for gene expression of pyroptosis markers (NLRP3 and caspase-1) and lncRNA-MALAT1.

2.3.2 Determination of fasting serum lipid profile

A cholesterol assay kit—HDL and LDL/VLDL (Abcam, Cambridge, United Kingdom)—was used to determine total cholesterol (T-Chol), high-density lipoprotein cholesterol (HDLc), and low-density lipoprotein cholesterol/very-low-density lipoprotein cholesterol (LDLc/VLDLc) in the serum of the studied rat groups according to the manufacturer's instructions. The kit quantifies T-Chol by an enzymatic colorimetric method and includes a simple technique to separate HDLc and LDLc/VLDLc for their determination. The color intensity of the reaction product is measured at 570 nm, and it is directly proportional to cholesterol levels.

A low-density lipoprotein cholesterol colorimetric assay kit (Elabscience, Wuhan, China) was used to determine LDLc in the serum of the rat groups according to the manufacturer's instructions. The kit quantifies LDLc using an enzymatic colorimetric method, and the color intensity of the reaction product is measured at 546 nm using a microplate reader (Thermo Fisher Scientific, Waltham, MA, United States). The determined value of LDLc was used to obtain the VLDLc level by subtracting the LDLc value from the non-HDLc (LDLc/VLDLc) value.

A triglyceride (TG) colorimetric assay kit (Elabscience, Wuhan, China) was used to determine TG in the serum of the rat groups according to the manufacturer's instructions. The color intensity of

the generated quinones is directly proportional to the TG content. The absorbance was measured at 240 nm using a spectrophotometer (Analytik Jena, Jena, Germany) (Konda et al., 2017).

2.3.3 ELISA for the determination of cardiac troponin I, IL1- β , and caspase-1

A rat cardiac troponin I ELISA kit (Abcam, Cambridge, United Kingdom) was used for the determination of cardiac troponin I (a marker of myocardial injury) in the serum of the rat groups according to the manufacturer's protocol (Jin et al., 2021). In addition, a rat IL1- β ELISA kit (Abcam, Cambridge, United Kingdom) and a rat caspase-1 ELISA kit (MyBioSource, California, United States) were used for the determination of IL1- β (pro-inflammatory cytokine released as a result of NLRP3 activation) and caspase-1 (IL-1 converting enzyme), respectively, in the heart tissues, according to the manufacturer's protocol. The colored intensity of the final product was measured at 450 nm using a microplate reader (Thermo Fisher Scientific, Waltham, MA, United States).

2.3.4 Determination of oxidative stress in myocardial tissue

The degree of myocardial lipid peroxidation was determined by measuring the level of MDA using an MDA assay kit (Biodiagnostic, Cairo, Egypt). According to the manufacturer's protocol, a pink color is produced by the reaction of thiobarbituric acid with MDA. The absorbance was measured at 534 nm using a spectrophotometer (Analytik Jena®, Jena, Germany) (Ohkawa et al., 1979).

2.3.5 RNA extraction and qRT-PCR for lncRNA-MALAT1, NLRP3, and caspase-1

Total RNA from the cardiac tissue was extracted using an miRNeasy® Mini Kit (Qiagen Co., Hilden, Germany) and reverse-transcribed to the cDNA with the two-step RT-PCR kit (Qiagen Co., Hilden, Germany). The PCR was performed with QuantiTect SYBR Green I PCR (Qiagen Co., Hilden, Germany) by denaturing at 95°C for 10 s, annealing at 60°C for 15 s and extending at 72°C for 25 s. The primers were obtained from Willowfort Co. (Birmingham, England), and the primer sequences were as follows: MALAT1 (NR_144568.1) forward (5'-AAAGCAAGGTCTCCCCACAAG-3') and reverse: (5'-GGTCTGTGCTAGATCAAAAGGCA-3') (Wu et al., 2020), NLRP3 (NM_001191642.1) forward (5'-AGC CTCAGGGCACCAAA-3') and reverse (5'-GGTATGGCGTGG CAAGAGTC-3'), caspase-1 (NM_012762.3) forward (5'-ATG GATTGCTGGATGAAC T-3') and reverse (5'-GATAACCTT GGGCTTGTCTT- 3'), and GAPDH (NM_017008.4) forward (5'-TCCATGACAACCTTTGGCATC-3') and reverse (5'-CATGTC AGATCCACCACGGA-3') (Du et al., 2018). The gene expression was calculated using the $2^{-\Delta\Delta CT}$ method (Heid et al., 1996).

2.3.6 Histopathological examination

At the end of our experiment, the heart sections of four rats were selected randomly from each group. The heart tissues were fixed in 10% neutral formalin for 12 h. Each sample was then soaked in paraffin, and sections (5- μ m thick) were cut and stained with hematoxylin-eosin (H&E). The sections were evaluated using an optical microscope (CX43; Olympus, Tokyo, Japan) for the detection of histopathological abnormality (Saber et al., 2020).

2.3.7 Immunohistochemical staining of TGF- β as a marker for fibrosis

Immunohistochemical demonstration of TGF- β in paraffin-embedded heart sections was performed using the TGF- β kit (Sigma Aldrich, St. Louis, United States). Cardiac tissues were fixed with 10% neutral formaldehyde. Tissue sections were cut (5- μ m thick) and deparaffinized. The endogenous peroxidase was quenched with two drops of 3% H₂O₂ for 5 min. Then, the sections were treated with a blocking reagent for 10 min. The primary antibody (rabbit anti-cyclooxygenase-2 in buffered saline) or the negative control was added and incubated for 1 hour. Then, the secondary biotinylated antibody (goat anti-rabbit IgG in buffered saline) was added and incubated for 20 min. Peroxidase was applied and incubated for another 20 min. A substrate reagent and aminoethylcarbazole in *N*, *N*-dimethylformamide chromogen were applied and incubated for 10 min. Mayer's hematoxylin was used for immunohistochemistry (IHC) counterstain. Six typical fields were selected randomly from each slice for observation under an optical microscope (CX43; Olympus, Tokyo, Japan). The cytoplasm of the positive cells was red-rose to brownish-red (Kuo et al., 2005).

2.3.8 Masson's trichrome stain for determination of collagen in the rat myocardium

For determining the collagen content of the rat myocardium, Masson's trichrome staining kit (Beijing Solarbio Science & Technology, Beijing, China) was used to stain the rat myocardium. The method of staining was modified from the method used by Ukong et al. (2008). The slides stained with Masson's trichrome stain were examined using a polarized light microscope (Leica, Wetzlar, Germany), and the intensity of the blue color was determined (representing the collagen density) using a software image analyzer.

2.4 Statistical analysis

The data are expressed as the mean \pm SD, and SPSS version 22 software was used for the statistical analysis. The statistical comparison between groups was analyzed by one-way analysis of variance (ANOVA), followed by *post-hoc* Fisher's least significant difference (LSD). $p < 0.05$ was considered statistically significant.

3 Results

3.1 Phytochemical analysis of the PPE

In a negative ion mode, the UPLC-PDA-MS/MS analysis of the PPE detected 28 peaks (Figure 1). The compounds were identified (Table 1) by comparing the retention times, mass, and MS/MS data to the published literature for pomegranate (Abid et al., 2017; Yisimayili et al., 2019; García et al., 2021; Ragab et al., 2022). According to the area under the peaks, the major compounds identified are gluconic acid (18.39%), caffeoylquinic acid (14.0%), citric acid (19.53%), punicalagin (7.84%), delphinidin-3-*O*-glucoside (1.80%), ellagic acid-*O*-pentoside

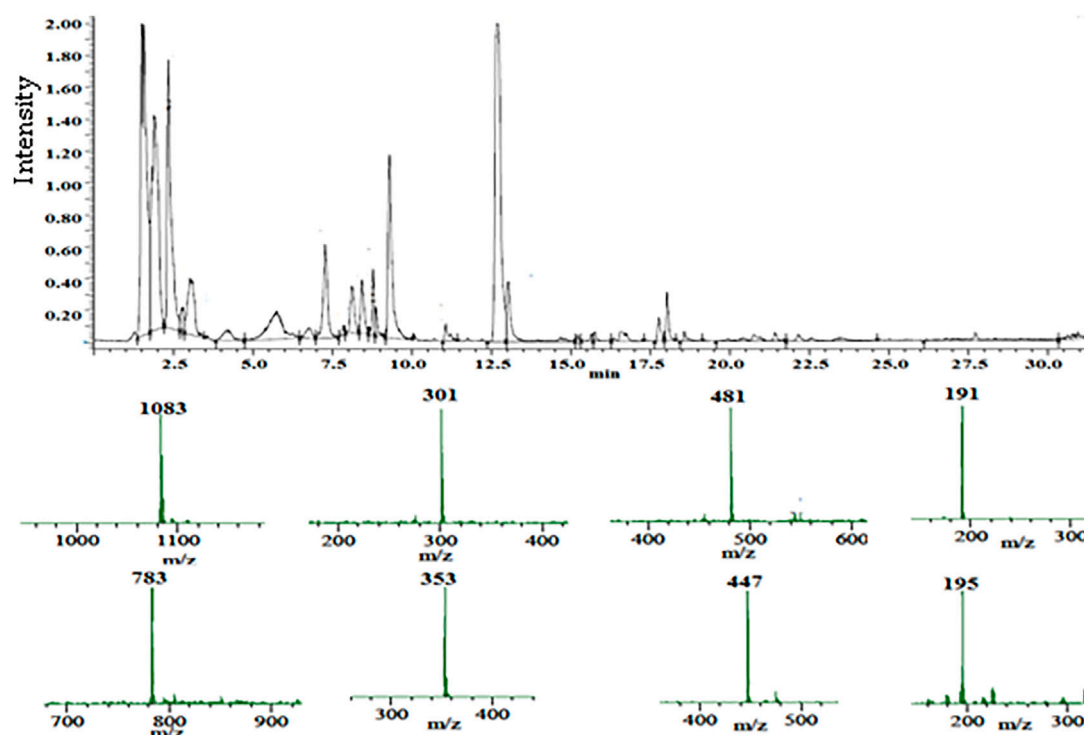


FIGURE 1

Total ion chromatogram of the UPLC-PDA-MS/MS analysis of the pomegranate peel extract PPE (top), and the mass spectra of the major constituents (bottom).

(0.68%), ellagic acid (18.26%), and hexahydroxydiphenoyl glucoside (HHDPG, 21.54%). The latter compound is the prevalent phenolic compound in the extract (21.54%) based on the area under the peak.

The ^1H NMR analysis of the PPE (Figure 2) indicated that the characteristic signals for HHDPG, ellagic acid, gluconic acid, and citric acid were predominant compared to the published literature (Guy, 1998; Bajko et al., 2016; Wan et al., 2017; Ahmed et al., 2019; Gabr et al., 2019; Tian et al., 2019; Hammoud Mahdi et al., 2020; Hasanpour et al., 2020). The signals at δ_{H} 6.51 and 6.52 were assigned to H-6' and H-6'' in HHDP moiety (Gabr et al., 2019), respectively, while the signals at δ_{H} 7.42 and 7.46 were assigned to H-5 and H-5' in ellagic acid derivatives (Ahmed et al., 2019), respectively. The signals at δ_{H} 2.64 and 2.73 were ascribed to the symmetrical methylene diastereotopic protons of citric acid (Guy, 1998). The signals at δ_{H} 3.40–3.75 were ascribed to the protons of gluconic acid (Hammoud Mahdi et al., 2020). The signals at δ_{H} 6.30, 6.77, 6.92, 7.04, 7.53, 9.43, and 9.53 are characteristic of caffeoylquinic acids (Bajko et al., 2016; Wan et al., 2017). Signals for cyanidin-3-O-glucoside appeared at δ_{H} 6.44, 6.93, 8.21, 8.26, and 9.25, which are consistent with the literature (Tian et al., 2019). Signals at δ_{H} 6.72, 6.88, 6.90, 6.97, 7.05, 7.12, 7.21, and 7.26 were attributed to the aromatic protons of α and β punicalagin as compared to the literature (Hasanpour et al., 2020). Signals at δ_{H} 6.30, 6.31, 6.50, 6.54, 6.59, 6.60, 6.63, and 6.64 were consistent with pedunculagin (Khanbabaee and Großer, 2003). Other compounds detected by

UPLC-PDA-MS were below the detection limit by NMR under the used concentration and conditions.

3.2 Biological evaluation

3.2.1 Effect on cardiac hypertrophy in the diabetic rats and the survival rate

The overall survival rate of rats was 76.66% (46/60). In the negative control group, positive control group, diabetic treated group, and only treated group, the numbers of survival were 14, 8, 11, and 13, respectively, and the survival rates of the rats were 93.33%, 53.33%, 73.33%, and 86.67%, respectively.

At the end of our experiment, the total body weight of the rats was determined. The weight of the heart was determined after animal sacrifice, and the relative heart weight was calculated. The present study showed that the relative heart weight of the diabetic rats in the positive control group (0.488 ± 0.030 g) was significantly higher than the relative heart weight of the normal rats in the negative control group (0.2851 ± 0.033 g) ($p < 0.001$). Prophylactic treatment with the PPE in the diabetic rats significantly decreased the relative heart weight (0.391 ± 0.043 g) compared to the untreated diabetic rats in the positive control group ($p < 0.001$). In addition, the relative heart weight of the non-diabetic normal rats treated with the PPE showed no significant difference from the relative heart weight of the untreated normal rats in the negative control group (Figures 3A–C).

TABLE 1 UPLC-PDA-MS/MS analysis results of pomegranate peel extract (PPE).

No.	Rt min	[M-H] ⁻ (<i>m/z</i>)	MS ² ions (<i>m/z</i>)	Identification
1	1.50	195	177, 159, 129, 99, and 75	Gluconic acid
2	1.89	353	261, 219, 191, 173, 149, and 113	Caffeoylquinic acid
3	2.34	191	173 and 111	Citric acid
4	2.80	205	205	Unknown
5	3.02	205	205	Unknown
6	4.23	783	481, 301, and 275	Pedunculagin I
7	5.72	541*	541 and 302	Punicalagin
	7.71	1083	1083, 781, 603, 601, 575, 541, and 302	
8	6.73	783	765, 481, 301, and 275	Pedunculagin II
9	7.84	801	649, 348, 347, and 301	Puniguconin
10	8.13	463	302	Delphinidin-3- <i>O</i> -glucoside
11	8.42	469	425, 301, 169, and 125	Valoneic acid dilactone
12	8.86	447	345, 259, 219, 160, and 113	Cyanidin-3- <i>O</i> -glucoside
14	9.28	301	301, 229, and 185	Ellagic acid
15	12.50–13.50	481	301	HHDPG
16	15.21	213	ND	Unknown
17	15.64	499	455 and 437	Carboxy ursolic acid
18	15.75	485	455, 422, and 365	Methoxy ursolic acid
19	16.56	487	455, 469, 467, 421, 392, and 375	Dihydroxy ursolic acid
21	17.76	485	455, 422, and 365	Methoxy ursolic acid isomer
22	18.02	487	455, 469, 467, 421, 392, and 375	Dihydroxy ursolic acid isomer
24	21.41	471	423, 407, 405, and 393	Maslinic acid
27	27.71	339	339	Behenic acid
28	31.38	487	487	Asiatic acid

ND, not detected; *, [M-2H]⁻; Rt, retention time.

3.2.2 Effect on fasting serum lipid profile and random blood glucose concentration

Fasting serum profile and random blood glucose of the studied rat groups were determined at the end of our experiment (Figure 3D). Prophylactic treatment with the PPE significantly decreased ($p < 0.001$) total cholesterol (188.50 ± 13.16 mg/dL), low-density lipoprotein cholesterol (122.75 ± 11.79 mg/dL), very-low-density lipoprotein cholesterol (23.88 ± 2.03 mg/dL), non-high-density lipoprotein cholesterol (146.75 ± 11.61 mg/dL), triglycerides (186.43 ± 20.55 mg/dL), and the total cholesterol/HDLc risk ratio (4.38 ± 0.56) levels in the serum of the diabetic rats compared to their levels in the serum of the untreated diabetic rats in the positive control group (248.50 ± 28.69 mg/dL, 175.88 ± 7.93 mg/dL, 39.63 ± 3.07 mg/dL, 215.50 ± 7.65 mg/dL, 265.00 ± 28.02 mg/dL, and 7.64 ± 0.56 , respectively). Moreover, the HDLc levels increased significantly in the serum of the diabetic rats treated with the PPE (43.75 ± 4.77 mg/dL) compared to the untreated diabetic rats in the positive control group (32.00 ± 3.07 mg/dL) ($p < 0.001$). The random blood glucose concentrations were significantly

higher in the diabetic rats in the positive control group (472.38 ± 72.18 mg/dL) than in the normal rats in the negative control group (123.43 ± 15.98 mg/dL) ($p < 0.001$), but the blood glucose concentrations of the diabetic rats treated with the PPE showed no significant difference from blood glucose concentrations of the untreated diabetic rats in the positive control group.

3.2.3 Effect on serum cardiac troponin 1

Cardiac troponin I concentration in the serum of the studied rat groups was determined as a marker of myocardial injury. The concentration of serum cTnI was significantly higher in the diabetic rats of the positive control group (294.13 ± 16.09 pg/mL) than in the non-diabetic rats in the negative control group (85.00 ± 14.64 pg/mL) ($p < 0.001$). Moreover, the prophylactic treatment of the diabetic rats with the PPE significantly decreased serum cTnI levels (203.63 ± 20.98 pg/mL) compared to the cTnI concentration in the serum of the untreated diabetic rats in the positive control group ($p < 0.001$). The concentration of cTnI in the serum of the normal rats treated with the PPE ($88.43 \pm$

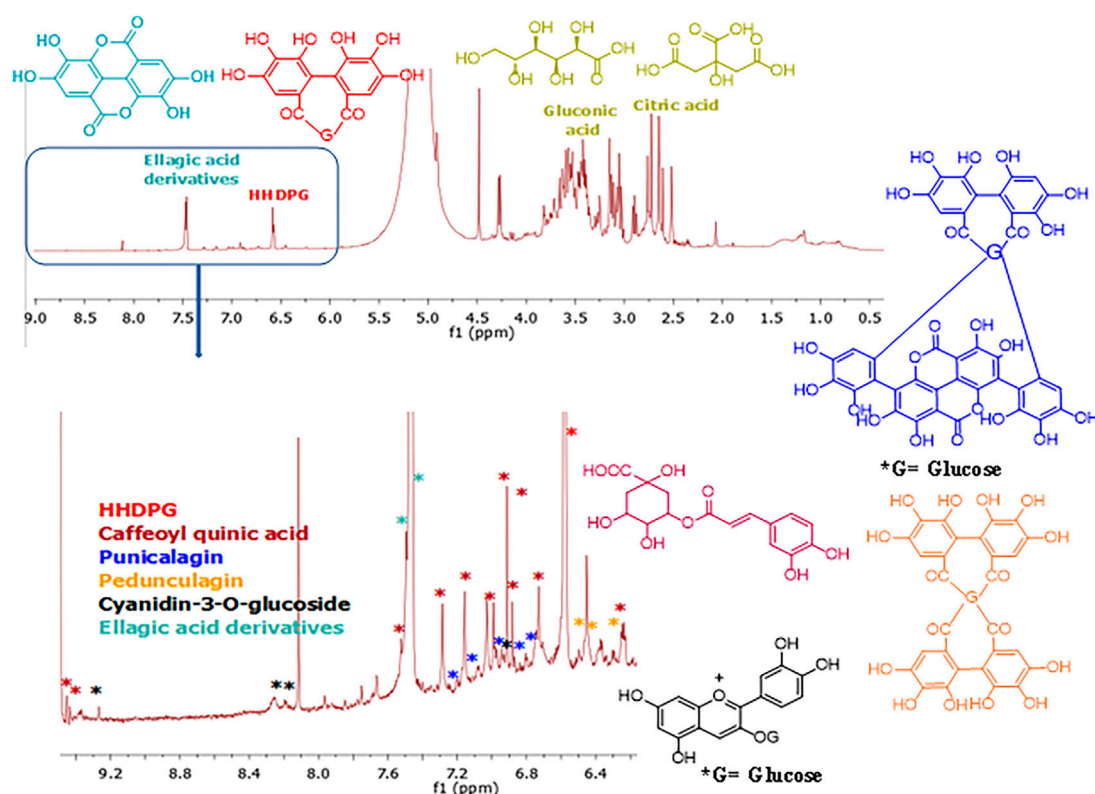


FIGURE 2

¹H NMR fingerprint of the pomegranate peel extract PPE (Top) and expanded aromatic protons region (6.30–9.50 ppm) (bottom). The structures of the detected compounds are shown. Red: HHDPG, dark red: caffeoyl quinic acid, dark blue: punicalagin, orange: pedunculagin, black: cyanidin-3-O-glucoside, light blue: ellagic acid derivatives.

18.42 pg/mL) showed no significant difference from the concentration of cTnI in the serum of rats in the negative control group (Figure 3E).

3.2.4 Effect on oxidative stress marker in the myocardial tissue

Malondialdehyde (MDA) concentration was determined in the cardiac tissue as a marker of myocardial lipid peroxidation. The concentration of MDA was significantly higher in the cardiac tissue of the diabetic rats in the positive control group (470.05 ± 32.21 nmol/g tissue) than in non-diabetic rats in the negative control group (253.13 ± 34.92 nmol/g tissue) ($p < 0.001$). More interestingly, prophylactic treatment of the diabetic rats with the PPE significantly decreased MDA levels in the myocardium tissue (322.11 ± 24.31 nmol/g tissue) compared to the untreated diabetic rats in the positive control group ($p < 0.001$). MDA concentration in the heart of the normal rats treated with the PPE (244.27 ± 27.83 nmol/g tissue) showed no significant difference from MDA concentration in the heart of the rats in the negative control group (Figure 4A).

3.2.5 Effect on the level of IL-1 β and caspase-1 in the myocardial tissue

The concentrations of the pro-inflammatory cytokine (IL-1 β), which was released as a result of the NLRP3 activation, and caspase-

1 (IL-1-converting enzyme) were determined in the cardiac tissues of the studied rat groups as a marker of pyroptosis. The concentrations of IL-1 β and caspase-1 were significantly higher in the cardiac tissue of the diabetic rats in the positive control group (13.11 ± 0.88 pg/mg and 43.49 ± 2.12 pg/mg, respectively) than in the non-diabetic rats in the negative control group (7.67 ± 0.46 pg/mg and 25.28 ± 2.23 , respectively) ($p < 0.001$). Prophylactic treatment of the diabetic rats with the PPE significantly decreased IL-1 β and caspase-1 concentrations in the myocardium tissue (10.44 ± 0.76 pg/mg and 33.55 ± 2.52 pg/mg, respectively) compared to the untreated diabetic rats in the positive control group ($p < 0.001$). Moreover, the concentrations of IL-1 β and caspase-1 in the heart of the normal rats treated with the PPE (6.96 ± 0.75 pg/mg and 24.44 ± 1.923 , respectively) showed no significant difference from their concentrations in the heart of the normal rats in the negative control group (Figures 4B, C).

3.2.6 Effect on lncRNA-MALAT1 and pyroptosis in the cardiac tissue

Our RT-PCR data showed that the gene expressions of lncRNA-MALAT1 and the pyroptosis markers (NLRP3 and caspase-1) in the cardiac tissue of the diabetic rats in the positive control group (5.374 ± 0.715 , 6.079 ± 0.742 , and 5.248 ± 0.584 folds, respectively) were significantly higher than their gene expressions in the cardiac

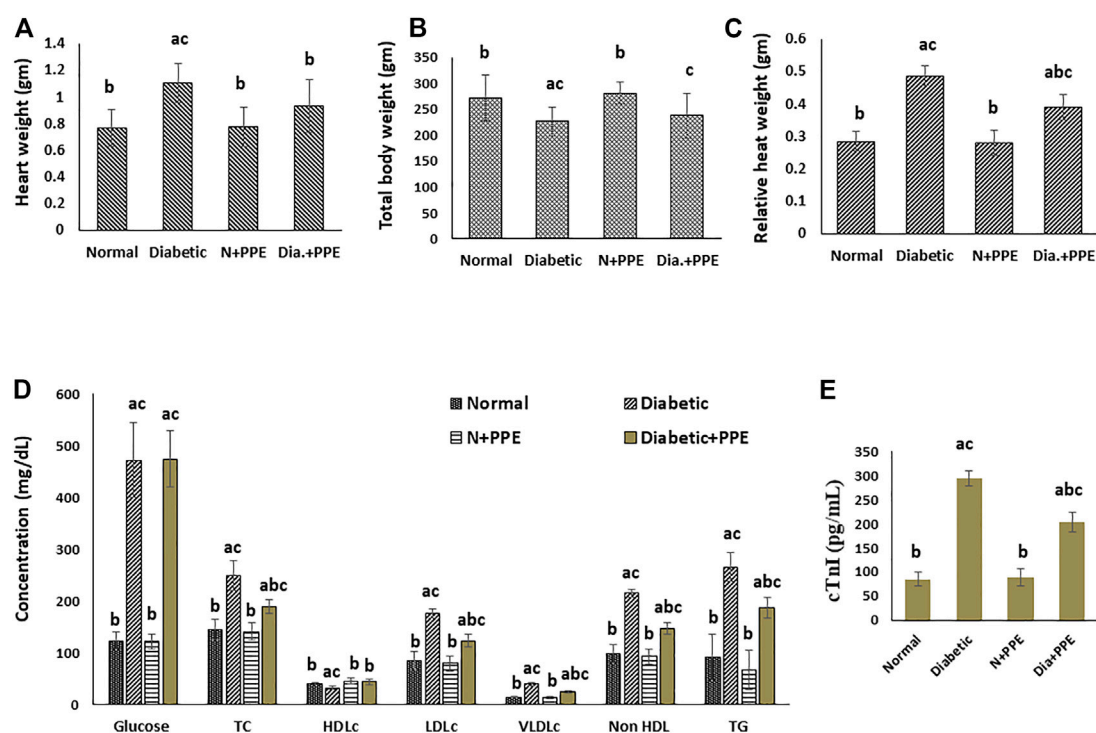


FIGURE 3

Effect of the pomegranate peel extract treatment on the studied rat groups (A) heart weight, (B) total body weight, (C) relative heart weight, (D) random blood glucose and fasting serum lipids, and (E) serum cardiac troponin-I concentration. Data are presented as mean \pm SD; $n = 7$. cTnI: cardiac troponin I, Normal: normal rats (negative control group), Diabetic: non-treated diabetic rats (positive control group), N+PPE: normal rats treated with the pomegranate peel extract, Dia+PPE: diabetic rats treated with the pomegranate peel extract. HDLc: high density lipoprotein cholesterol, LDLc: low density lipoprotein cholesterol, Non HDL: non high density lipoprotein, TC: total cholesterol, TG: triglyceride, VLDLc: very low density lipoprotein cholesterol.

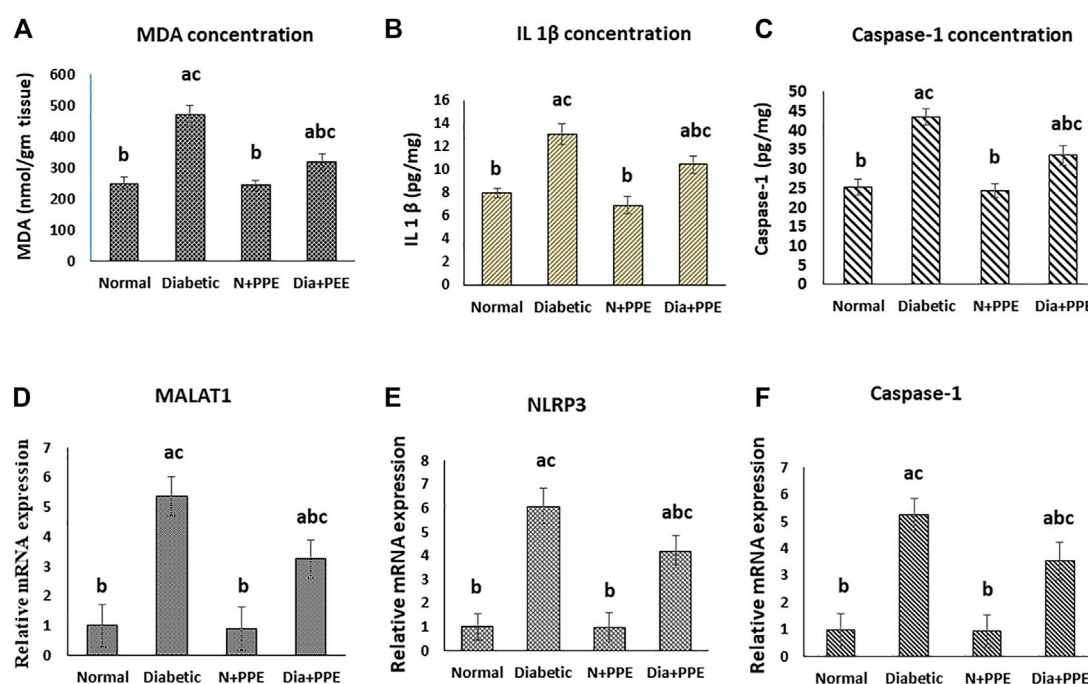
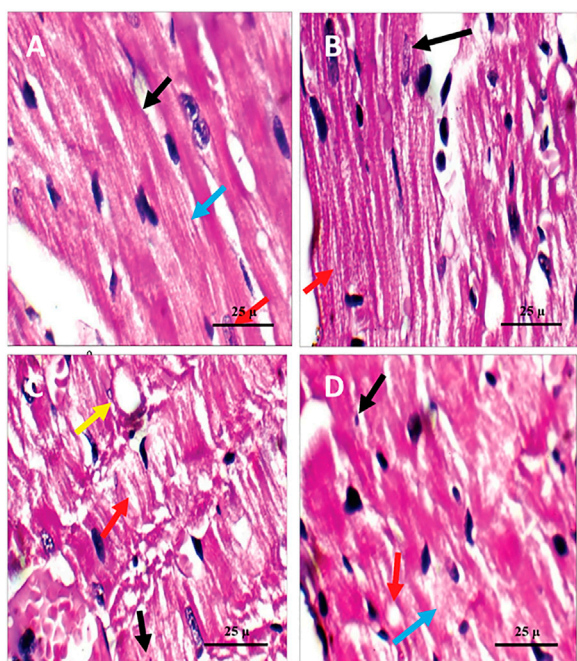


FIGURE 4

Effect of the pomegranate peel extract treatment on heart tissue of the studied rat groups. (A): MDA level as marker of lipid peroxidation, (B): IL-1 β content detected by ELISA. (C–E): gene expression analysis of lncRNA-MALAT1, NLRP3, and caspase-1 respectively. The gene expression was measured (Continued)

FIGURE 4 (Continued)

using quantitative RT-PCR. Data are expressed as the mean \pm SD. $n = 7$ for MDA and IL-1 β concentration while for gene expression analysis $n = 3$. IL-1 β : interleukin 1 beta; MALAT1: Metastasis associated lung adenocarcinoma transcript 1; MDA: malondialdehyde; NLRP3: nucleotide-binding domain (NOD)-like receptor protein 3, Normal: normal rats (negative control group), Diabetic: non-treated diabetic rats (positive control group), N+PPE: normal rats treated with the pomegranate peel extract, Dia+PPE: diabetic rats treated with the pomegranate peel extract.

**FIGURE 5**

Microscopic pictures of the cardiac tissue of the studied rat groups stained with H&E. (A) Cardiac wall of the non-diabetic rats in the negative control group showing viable cardiac muscle fibers with distinct cell borders (black arrow), preserved cross striations (blue arrow), and central oval/elongated nuclei (red arrow). (B) Cardiac wall of the non-diabetic rats treated with the pomegranate peel extract showing cardiac muscle fibers with centrally located nuclei (black arrow) and preserved cross striations (red arrow). (C) Cardiac wall of the diabetic rats in the positive control group showing scattered cardiac muscle fibers with small pyknotic nuclei (black arrow), partial loss of cross striations (red arrow), mildly congested intervening blood capillaries (blue arrow), and scattered cytoplasmic vacuoles (yellow arrow). (D) Cardiac wall of the diabetic rats treated with the pomegranate peel extract showing mildly scattered cardiac muscle fibers with small pyknotic nuclei (black arrow), few scattered cytoplasmic vacuoles (blue arrow), and partial loss of cross striations (red arrow).

tissue of the non-diabetic rats in the negative control group (1-fold, $p < 0.001$). Meanwhile, prophylactic administration of the PPE induced significant a decrease in the gene expressions of lncRNA-MALAT1 and pyroptosis markers (NLRP3 and caspase-1) in the cardiac tissue of the diabetic rats (3.252 ± 0.643 , 4.162 ± 0.668 , and 3.534 ± 0.745 fold, respectively, $p < 0.05$). Our results showed that the gene expressions of lncRNA-MALAT1 and the pyroptosis markers (NLRP3 and caspase-1) in the cardiac tissue of the non-diabetic rats treated with the PPE (0.913 ± 0.742 , 0.974 ± 0.632 , and 0.941 ± 0.553 fold, respectively) showed no significant difference

from their gene expressions in the cardiac tissue of the non-diabetic rats in the negative control group (1-fold) (Figures 4D–F).

3.2.7 Histopathological examinations

Histopathological examination revealed that the cardiac wall of the non-diabetic rats in the negative control group showed normal viable cardiac muscle fibers with distinct cell borders, preserved cross striations, and central oval/elongated nuclei (Figure 5A). The cardiac wall of the non-diabetic rats treated with the PPE showed an appearance similar to that of the normal control group as the cardiac muscle fibers showed centrally located nuclei and preserved cross striations (Figure 5B). Meanwhile, the cardiac wall from the diabetic rats in the positive control group showed scattered cardiac muscle fibers with small pyknotic nuclei, partial loss of cross striations, mildly congested intervening blood capillaries, and scattered cytoplasmic vacuoles (Figure 5C). More interestingly, the cardiac wall of the diabetic rats treated with the PPE showed mildly scattered cardiac muscle fibers with small pyknotic nuclei, few scattered cytoplasmic vacuoles, and partial loss of cross striations (Table 2; Figure 5D).

3.2.8 Effect on TGF- β as a marker for fibrosis

To confirm fibrosis in the cardiac tissue, immunostaining of TGF- β was performed. Immunostained cardiac myofibrils against TGF- β showed a cardiac wall with negative cell membrane reactivity in the non-diabetic rats in the negative control group and the non-diabetic rats treated with the PPE (Figures 6A, B). Meanwhile, cardiac myofibrils from the diabetic rats in the positive control group showed marked cell membrane reactivity in the cardiac wall (Figure 6C). More interestingly, the cardiac myofibrils from diabetic rats treated with the PPE showed a cardiac wall with weak cell membrane reactivity (Figure 6D). Figure 6E illustrates that the number of reactive cells against TGF- β in cardiac myofibrils from diabetic rats treated with PPE was significantly lower than their number in diabetic untreated rats ($p < 0.001$).

3.2.9 Determination of the amount of collagen in the cardiac tissue of diabetic rats

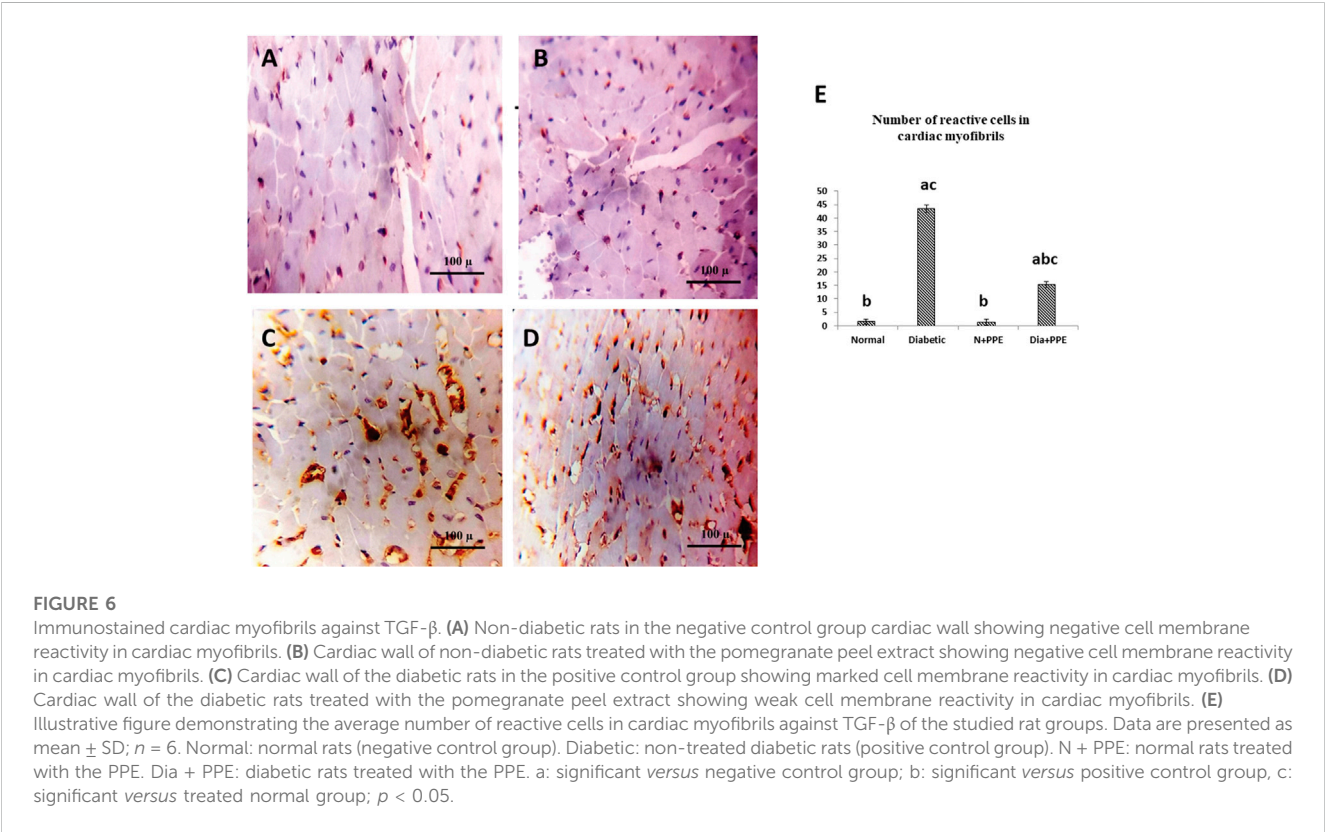
For collagen amount determination in the rat myocardium, Masson staining was used. Microscopic pictures of Masson's trichrome staining of the cardiac tissues of the non-diabetic rats in the negative control group and non-diabetic rats treated with the PPE showed normal delicate fibrous strands (Figures 7A, B). Meanwhile, the cardiac tissues of the diabetic rats in the positive control group showed thick fibrous bands (Figure 7C). In addition, the cardiac tissues of the diabetic rats treated with the PPE illustrated a mild amount of collagen fibers (Figure 7D).

Figure 7E illustrates the quantitative measurements of the optical density of collagen fibers in the heart of the studied rat

TABLE 2 Effect of pomegranate peel extract (PPE) on histopathological scoring of alterations caused by diabetes in rats' cardiac tissues of the studied groups.

Group	Normal	Diabetic	N + PPE	Dia + PPE
Scattered cardiac muscle fibers	–	++	–	+
Pyknotic nuclei	–	+	–	+
Edema	–	++	–	–
Cytoplasmic vacuoles	–	++	–	+
Congestive blood vessel	–	+	–	–

Normal: normal rats (negative control group); diabetic: non-treated diabetic rats (positive control group); N + PPE: normal rats treated with the PPE; Dia + PPE: diabetic rats treated with the PPE.



groups using the Masson trichrome technique. The amount of collagen fiber per unit area in cardiac myofibrils from diabetic rats was significantly higher than its amount in the non-diabetic rats in negative control group ($p < 0.001$). Moreover, prophylactic treatment of the diabetic rats with PPE significantly decreased the amount of collagen fiber in cardiac myofibrils per unit area ($p < 0.001$).

4 Discussion

Diabetic cardiomyopathy is a recognized complication of diabetes mellitus, with a prevalence of 1.1% (Dandamudi et al., 2014). Oxidative stress and lipid peroxidation are core factors in the pathophysiology of diabetes-induced cardiac injury (El-Missiry

et al., 2015). These factors are a consequence of higher reactive oxygen species generation produced by metabolic disturbances. The disease is characterized by myocardial hypertrophy, myocardial fibrosis, and an elevated level of cTn-I. Currently, there is no specific treatment for DC, and the cardioprotective strategies for DC prevention include the use of antioxidants, antifibrotic agents, and anti-inflammatory agents (Lorenzo-Almorós et al., 2022). Our findings showed, for the first time, that PPE ameliorates the impact of diabetes on the myocardium and revealed the likely mechanisms of its favorable effects, which are downregulation of lncRNA-MALAT1, with subsequent downregulation of the pyroptosis-related genes (NLRP3 and caspase-1), and reduction of IL-1β. This study revealed that PPE treatment increased the survival rate and protected against the development of cardiac hypertrophy in diabetic rats. Our results showed that the survival

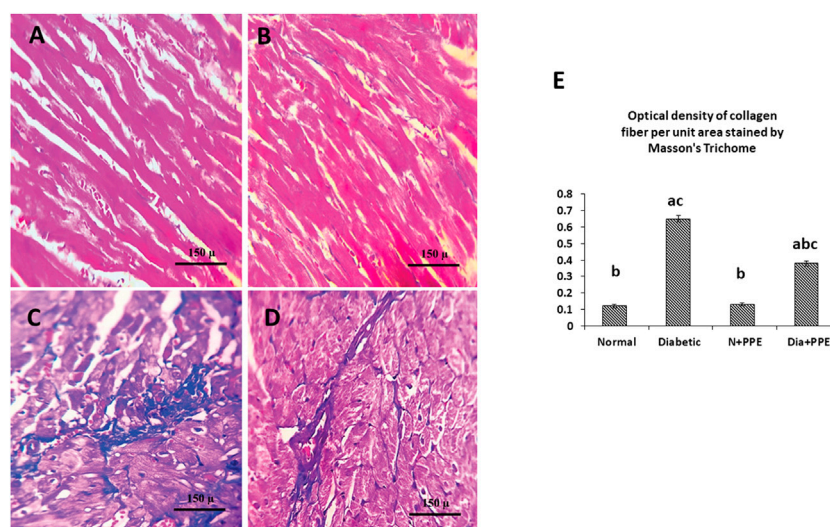


FIGURE 7

Masson's trichome staining of the cardiac tissues of the studied rat groups. (A) Cardiac tissue from the non-diabetic rats in the negative control group showing normal delicate fibrous strand. (B) Cardiac tissue from the non-diabetic rats treated with the pomegranate peel extract showing an appearance similar to that of interstitial collagen as the negative control group. (C) Cardiac tissue from the diabetic rats in the positive control group showing thick fibrous bands. (D) Cardiac tissue from the diabetic rats treated with pomegranate peel extract group illustrating a mild amount of collagen fibers. (E) Illustrative figure demonstrating the quantitative measurement of the optical density of collagen fiber per unit area stained by Masson's trichome. Data are presented as mean \pm SD; $n = 6$. Normal: normal rats (negative control group). Diabetic: non-treated diabetic rats (positive control group). N + PPE: normal rats treated with the PPE. Dia + PPE: diabetic rats treated with the PPE. a: significant versus negative control group; b: significant versus positive control group, c: significant versus treated normal group; $p < 0.05$.

rate of the rats in the positive control group was 53.33%, while the survival rate of the rats in the diabetic treated group was 73.33%. Moreover, prophylactic treatment of the diabetic rats with PPE significantly decreased the relative heart weight compared to the untreated diabetic rats in the positive control group ($p < 0.001$).

Diabetes mellitus notoriously leads to a myriad of complications, such as DC that may be eventually complicated by the occurrence of heart failure and arrhythmia. Metabolic derangement, mitochondrial dysfunction, autophagy, and inflammatory cell death are all implicated in initial myocardial hypertrophy and, eventually, fibrosis (Yan et al., 2020; Prandi et al., 2022).

The animal model used in this study is of type 1 diabetes mellitus. In patients with T1DM, the disease is characterized by hyperglycemia and dyslipidemia as frequently occurring metabolic abnormalities. Both are associated with an increased cardiovascular risk (Zabeen et al., 2018; Jebrailei et al., 2021). Our results showed that prophylactic treatment of the diabetic rats with PPE significantly improved the serum lipid profile ($p < 0.05$), with no significant effect on the blood glucose concentration.

Our results were in agreement with those of Hou et al. (2019), who reported that pomegranate extract regulates lipid metabolism and improves lipid profile in metabolic-disorder-associated diseases such as non-alcoholic fatty liver disease and type 2 diabetes. On the other hand, our findings showed that PPE could improve the pathological effect of diabetes on the lipid profile of rats, but it did not significantly affect the normal lipid profile in the non-diabetic rats.

Serum cTnI is a common marker of myocardial injury (El-Mansi and Al-Kahtani, 2019; Jin et al., 2021). This study showed that

prophylactic treatment of the diabetic rats with PPE significantly decreased the serum cTnI concentration compared to the untreated diabetic rats in the positive control group ($p < 0.001$). Our results were in line with those of Jin et al. (2021), who found that increased serum cTnI in diabetic mother rats was decreased by prophylactic treatment with PPE.

In diabetes, superoxide anion radicals are overproduced in the mitochondria, subsequently inducing an increased polyol pathway flux and activation of the receptor for AGE and protein kinase C isoforms. It is of note that such pathways not only directly cause diabetic cardiomyopathy but are also leading sources of ROS (Prandi et al., 2022). The ROS and oxidative stress lead to cellular malfunction injury through several mechanisms, including protein oxidation, lipid peroxidation, DNA damage, and oxidative changes in microRNAs (Pizzino et al., 2017).

In this study, we determined MDA in the cardiac tissue as a marker of lipid peroxidation. MDA is an end product of the oxidation of polyunsaturated fatty acids containing more than two double bonds and its increased level reflects high levels of ROS and oxidative stress. Our data showed that the prophylactic treatment of the diabetic rats with PPE significantly decreased the MDA levels in the myocardium tissue compared to the untreated diabetic rats in the positive control group ($p < 0.001$). Our findings agreed with those of Jin et al. (2021), who found that the increased MDA in the myocardium of diabetic mother rats was decreased by prophylactic treatment with allisartan isoproxil. In the current study, the PPE could decrease the elevated pathological level of MDA due to hyperglycemia in diabetic rats, but it did not significantly affect the normal MDA level in non-diabetic rats.

This effect could be attributed to the antioxidant and ameliorative action of pomegranate polyphenolic constituents, which scavenge the free radicals through the AMPK-Nrf2 signaling pathway and thus decrease lipid peroxidation (Aboonabi et al., 2014; Sun et al., 2016; Akuru et al., 2022).

Pyroptosis is an inflammatory programmed cell death which is strongly associated with the development of DC. ROS and hyperglycemia associated with diabetes activate NLRP3 oligomerization which triggers the activation of caspase-1. Active caspase-1 converts the inactive pro-inflammatory cytokine IL-1 β into its active form and facilitates the release of active IL-1 β out of the cell (Xue et al., 2019; Zheng and Li, 2020). Our real-time PCR data showed that the prophylactic treatment with PPE significantly decreased the gene expression of pyroptosis markers (NLRP3 and caspase-1) in the cardiac tissue of the diabetic rats compared to those of rats in the positive control group ($p < 0.05$). This effect could be explained by the antioxidant effect of PPE, thus deactivating NLRP3 and its related processes.

In the present study, the ELISA technique was performed for further confirmation of our real-time PCR findings. The concentrations of caspase-1 and IL-1 β in the cardiac tissues of the studied rat groups were determined by ELISA. The prophylactic treatment of the diabetic rats with PPE significantly decreased the concentration of caspase-1 and IL-1 β in the myocardium tissue compared to the untreated diabetic rats in the positive control group ($p < 0.001$). In the present study, the PPE could inhibit the diabetes-activated pyroptosis pathway in diabetic rats, but it did not significantly affect the pyroptosis in non-diabetic rats as it is un-activated and has normal glucose level and no or low level of ROS.

The lncRNA-MALAT1 is involved in several pathophysiological mechanisms in multiple diseases, including DC (Zhang et al., 2016; Abdulle et al., 2019). lncRNA-MALAT1 is upregulated in DC, and the knockdown of MALAT1 protects against the development of DC. Intriguingly, MALAT1 could be a novel therapeutic target for DC (Shi et al., 2021). Gene expression analysis in this study showed that prophylactic treatment with PPE significantly decreased the gene expression of lncRNA-MALAT1 in the cardiac tissue of the diabetic rats compared to those of rats in the positive control group ($p < 0.05$). On the other hand, PPE had no significant effect on the normal level of lncRNA-MALAT1 in non-diabetic rats.

Our findings revealed, for the first time, that the protective effect of PPE on DC could be due to the inhibition of pyroptosis, specifically by downregulating lncRNA-MALAT1. Our findings were supported by Wu et al. (2021), who found that lncRNA-MALAT1 promotes pyroptosis induced by high glucose concentration in the H9C2 cardiomyocyte via downregulating miR-141-3p.

Transforming growth factor- β is the master cytokine that mediates fibrosis in various tissues as a consequence of tissue injury and inflammation (Khalil et al., 2017). In the current study, immunostaining of TGF- β was performed to confirm fibrosis in the cardiac tissue. Moreover, Masson staining was used for the determination of the collagen amount. The microscopic examination of the cardiac tissues of the studied rat groups revealed that prophylactic treatment with PPE significantly decreased the number of TGF- β -positive cells and the amount of collagen in the cardiac tissue of the diabetic rats. The current data

were in line with the findings of Dab et al. (2022), who reported that PPE modulates the cardiac extracellular matrix and decreases the content of hydroxyproline and total collagen in a rat diabetic model.

Metabolic derangement, mitochondrial dysfunction, and inflammatory cell death are all implicated in myocardial hypertrophy and, eventually, fibrosis (Yan et al., 2020; Prandi et al., 2022). Fibrosis is a key feature of DC, leading to increased stiffness and loss of contractile function in diastolic and systolic DC types, respectively. Such pathological processes lead to complications, including heart failure and arrhythmias (Russo and Frangogiannis, 2016; Youssef et al., 2022).

Our histopathologic and immunohistochemistry findings were in agreement with our biochemical data. The histopathologic and immunohistochemistry staining showed that prophylactic treatment with PPE prevented deleterious histopathological alterations in the cardiac myocytes and ameliorated the tissue damage caused by diabetes. The favorable changes were indicated by the attenuated collagen accumulation and the decreased number of TGF- β -positive cells.

Our current findings have impactful translational meaning in clinical practice. Applied to all types of diabetes mellitus, DC may be diagnosed in patients with diabetes as any cardiac systolic, or at least, moderate diastolic dysfunction, with no history of other cardiac diseases including hypertension, coronary, and significant valvular or congenital heart disease (Dandamudi et al., 2014). A prevalence study by Dandamudi et al., 2014 revealed that DC occurs in 1.1% of the general population. About 17% of diabetic patients included in their study had DC (54.4% with diastolic dysfunction). Out of the studied diabetic patients, 22% developed heart failure within the 9-year follow-up period (Dandamudi et al., 2014).

The prevalence of diabetes mellitus type 2 is more than 20-fold higher than that of type 1; therefore, diabetic cardiomyopathy is mainly observed in type 2 diabetic patients. However, our model represents the two main pathological derangements linking DM, in all its types, to DC, which are hyperglycemia and dyslipidemia.

The PPE is rich in ellagitannins and anthocyanins, which are strong antioxidant agents. In our study, punicalagin, pedunculagin, valoneic acid dilactone, HHDPG, and ellagic acid are the ellagitannins detected, whereas cyanidin-3-*O*-glucoside and delphinidin-3-*O*-glucoside were the major anthocyanins. Ellagitannins are metabolized to ellagic acid and then to urolithin compounds, which are considered responsible for the biological activities of ellagitannins (Villalba et al., 2019). Punicalagin demonstrated a cardioprotective effect in diabetic conditions where it significantly decreased elevated cTn-I to normal levels, attenuated IL-1 β , IL-6, and TNF- α , and ameliorated the lipid profile in a streptozotocin-induced diabetic model (El-Missiry et al., 2015). Urolithin compounds A and B prevent the development of diabetic cardiomyopathy (Savi et al., 2017; Chen et al., 2022; Selma et al., 2021) by increasing the expression of sarco(endo)plasmic reticulum calcium ATPase 2 (SERCA2) and the activation of SIRT1; consequently, glycolysis is increased *via* a positive modulation of pyruvate dehydrogenase activity and ameliorated cardiac function. The anti-inflammatory effect of urolithin B was evidenced by a decrease in some inflammatory cytokines, including interleukin-6 (IL-6), interferon- γ (IFN- γ), tumor necrosis factor- α (TNF- α), interleukin-4 (IL-4), and IL-1 β through the inhibition of nuclear factor- κ -gene binding (NF- κ B) activation and mitogen-activated protein kinase (MAPK). In addition, urolithin B exhibits antioxidant activity mediated by decreasing the

production of ROS and the expression of NADPH oxidase subunit in addition to upregulating heme oxygenase-1 expression via the Nrf2/ARE signaling pathway (Lee et al., 2019).

It was reported that ellagic acid stimulates cardiac silent information regulator 1 signaling, thus protecting against DC in rats (Altamimi et al., 2020). Ellagic acid lowers triglyceride content, malondialdehyde level, (IL)-beta, IL-6, and TNF-alpha in the cardiac tissues (Chao et al., 2009). Additionally, ellagic acid upregulates cardiac mRNA expression of glutathione peroxidase, superoxide dismutase, and catalase, which accounts for its antioxidant effect (Chao et al., 2009).

Anthocyanins were reported to have a cardioprotective effect against streptozotocin-associated DC (Chen et al., 2016). Anthocyanins upregulate Nrf2, thus inducing the production of endogenous antioxidants (Sapian et al., 2022). Moreover, anthocyanins are evidently effective against increased cytokine production, lipid peroxidation, and inflammation. Cyanidin-3-O-glucoside and delphinidin-3-O-glucoside, detected in our study, are among the anthocyanins that have positive effects on diabetes-associated complications (Chen et al., 2016). Cyanidin-3-O-glucoside and delphinidin-3-O-glucoside showed cardioprotective action in DC due to their antioxidant properties (Liobikas et al., 2016; Li et al., 2018).

Nutritional intervention has become an essential component of the management plans for chronic diseases. Thus, initiatives and campaigns planned to increase vegetable and fruit intake are required and justified. The promotion of vegetable and fruit consumption by health policies can be a promising strategy to help prevent and improve the outcome of diabetes mellitus, among other chronic illnesses (Boeing et al., 2012). Guidance may include specific research-based advice, e.g., promoting PPE intake in diabetic patients to hopefully prevent and improve the outcome of DC.

5 Conclusion

The current study demonstrated that pomegranate peel extract showed a cardioprotective effect in diabetic rats, most likely due to its unique antioxidant, anti-inflammatory, and antifibrotic properties and its ability to improve the lipid profile. The protective effect of PPE could be due to the inhibition of the NLRP3/caspase-1/IL1 β signaling pathway and downregulation of lncRNA-MALAT1. Thus, PPE could be a promising protective remedy against the development of DC. Clinical studies are recommended to evaluate the effect of PPE as a cardioprotective supplement in DC.

References

- Abdulle, L. E., Hao, J., Pant, O. P., Liu, X., Zhou, D., Gao, Y., et al. (2019). MALAT1 as a diagnostic and therapeutic target in diabetes-related complications: A promising long-noncoding RNA. *Int. J. Med. Sci.* 16 (4), 548–555. doi:10.7150/ijms.30097
- Abid, M., Yaich, H., Cheikhrouhou, S., Khemakhem, I., Bouaziz, M., Attia, H., et al. (2017). Antioxidant properties and phenolic profile characterization by LC-MS/MS of selected Tunisian pomegranate peels. *J. Food Sci. Technol.* 54 (9), 2890–2901. doi:10.1007/s13197-017-2727-0
- Aboonabi, A., Rahmat, A., and Othman, F. (2014). Antioxidant effect of pomegranate against streptozotocin-nicotinamide generated oxidative stress induced diabetic rats. *Toxicol. Rep.* 1, 915–922. doi:10.1016/j.toxrep.2014.10.022
- Ahmed, S. R., El-Sherei, M. M., El-Dine, R. S., and El-Toumy, S. A. (2019). Phytoconstituents, hepatoprotective, and antioxidant activities of *Euphorbia cooperi* N. E. Br. Egypt. J. Chem. 62, 831–840.
- Akuru, E. A., Chukwuma, C. I., Oyeagu, C. E., Erukainure, O. L., Mashile, B., Setlhodi, R., et al. (2022). Nutritional and phytochemical profile of pomegranate ("Wonderful variety") peel and its effects on hepatic oxidative stress and metabolic alterations. *J. Food Biochem.* 46 (4), e13913. doi:10.1111/jfbc.13913
- Albarakati, A. Y. (2016). Protective effects of pomegranate peel extract on cardiac muscle in streptozotocin-induced diabetes in rats. *Int. J. Toxicol. Pharmacol. Res.* 8 (5), 379–383.

Data availability statement

The original contributions presented in the study are included in the article/Supplementary Material; further inquiries can be directed to the corresponding authors.

Ethics statement

The animal study was reviewed and approved by the Research Ethical Committee, Faculty of Pharmacy, Tanta University, Egypt (ethical approval code: TP/RE/06/22P-0016).

Author contributions

Conceptualization and methodology: MS, AR, AI, and OF; software and formal analysis: MS, AR, AI, OA, AM, and OF; validation: MS, AR, AI, and OF; investigation: MS, AR, AI, and OF; data curation: MS, AR, AI, OA, AM, and OF; writing—original draft preparation: MS, AR, AI, OA, AM, OF, and MA; writing—review and editing: AR, MS, and MA. All authors have read and agreed to the published version of the manuscript.

Funding

MA is funded by the University of Sharjah competitive grant (#22010902104) and collaborative grant (#2001090279).

Conflict of interest

The authors declare that the research was conducted in the absence of any commercial or financial relationships that could be construed as a potential conflict of interest.

Publisher's note

All claims expressed in this article are solely those of the authors and do not necessarily represent those of their affiliated organizations, or those of the publisher, the editors, and the reviewers. Any product that may be evaluated in this article, or claim that may be made by its manufacturer, is not guaranteed or endorsed by the publisher.

- Altamimi, J. Z., Alfari, N. A., Alshammari, G. M., Alagal, R. I., Aljabryn, D. H., Aldera, H., et al. (2020). Ellagic acid protects against diabetic cardiomyopathy in rats by stimulating cardiac silent information regulator 1 signaling. *J. Physiol. Pharmacol.* 71 (10). doi:10.26402/jpp.2020.6.12
- Arun, K. B., Jayamurthy, P., Anusha, C. V., Mahesh, S. K., and Nisha, P. (2017). Studies on activity guided fractionation of pomegranate peel extracts and its effect on antidiabetic and cardiovascular protection properties. *J. Food Process. Preserv.* 41 (1), e13108. doi:10.1111/jfpp.13108
- Assar, D. H., Elhabashi, N., Mokhatly, A. A. A., Ragab, A. E., Elbaly, Z. I., Rizk, S. A., et al. (2021b). Wound healing potential of licorice extract in rat model: Antioxidants, histopathological, immunohistochemical and gene expression evidences. *Biomed. Pharmacother.* 143, 112151. doi:10.1016/j.biopha.2021.112151
- Assar, D. H., Mokhatly, A. A. A., Ghazy, E. W., Ragab, A. E., Abou Asa, S., Abdo, W., et al. (2021a). Ameliorative effects of *Aspergillus awamori* against the initiation of hepatocarcinogenesis induced by diethylnitrosamine in a rat model: Regulation of Cyp19 and p53 gene expression. *Antioxidants* 10 (6), 922. doi:10.3390/antiox10060922
- Babu, P. S., and Srinivasan, K. (1997). Influence of dietary capsaicin and onion on the metabolic abnormalities associated with streptozotocin induced diabetes mellitus. *Mol. Cell. Biochem.* 175 (1–2), 49–57. doi:10.1023/a:1006881027166
- Bajko, E., Kalinowska, M., Borowski, P., Siergiejczyk, L., and Lewandowski, W. (2016). 5-O-Caffeoylquinic acid: A spectroscopic study and biological screening for antimicrobial activity. *LWT-Food Sci. Technol.* 65, 471–479. doi:10.1016/j.lwt.2015.08.024
- Boeing, H., Bechthold, A., Bub, A., Ellinger, S., Haller, D., Kroke, A., et al. (2012). Critical review: Vegetables and fruit in the prevention of chronic diseases. *Eur. J. Nutr.* 51 (6), 637–663. doi:10.1007/s00394-012-0380-y
- Chao, P. C., Hsu, C. C., and Yin, M. C. (2009). Anti-inflammatory and anti-coagulatory activities of caffeic acid and ellagic acid in cardiac tissue of diabetic mice. *Nutr. Metabol.* 6 (1), 33–38. doi:10.1186/1743-7075-6-33
- Chen, P., Guo, Z., Chen, F., Wu, Y., and Zhou, B. (2022). Recent advances and perspectives on the health benefits of urolithin B, A bioactive natural product derived from ellagitannins. *Front. Pharmacol.* 13, 917266. doi:10.3389/fphar.2022.917266
- Chen, Y. F., Shibu, M. A., Fan, M. J., Chen, M. C., Viswanadha, V. P., Lin, Y. L., et al. (2016). Purple rice anthocyanin extract protects cardiac function in STZ-induced diabetes rat hearts by inhibiting cardiac hypertrophy and fibrosis. *J. Nutr. Biochem.* 98–105. doi:10.1016/j.jnutbio.2015.12.020
- Dab, H., Chehidi, A., Tlili, M., Ben Saad, A., Khabir, A., and Zourgui, L. (2022). Cardiac extracellular matrix modulation in a rat-diabetic model: Biochemical and antioxidant beneficial effect of pomegranate (*Punica granatum*) peel extract. *Biomarkers* 27 (1), 50–59. doi:10.1080/1354750X.2021.2006312
- Dandamudi, S., Slusser, J., Mahoney, D. W., Redfield, M. M., Rodeheffer, R. J., and Chen, H. H. (2014). The prevalence of diabetic cardiomyopathy: A population-based study in olmsted county, Minnesota. *J. Card. Fail.* 20 (5), 304–309. doi:10.1016/j.cardfail.2014.02.007
- Du, S., Wang, X., Zhu, W., Ye, Y., Yang, J., Ma, S., et al. (2018). Acupuncture inhibits TXNIP-associated oxidative stress and inflammation to attenuate cognitive impairment in vascular dementia rats. *CNS Neurosci. Ther.* 24 (1), 39–46. doi:10.1111/cns.12773
- El-Mansi, A. A., and Al-Kahtani, M. A. (2019). Calcitriol and *Punica granatum* extract concomitantly attenuate cardiomyopathy of diabetic mother rats and their neonates via activation of Raf/MEK/ERK signalling and mitigation of apoptotic pathways. *Folia Biol.* 65 (2), 70–87.
- El-Missiry, M. A., Amer, M. A., Hemieda, F. A., Othman, A. I., Sakr, D. A., and Abdulhadi, H. L. (2015). Cardioameliorative effect of punicalagin against streptozotocin-induced apoptosis, redox imbalance, metabolic changes and inflammation. *Egypt. J. Basic Appl. Sci.* 2 (4), 247–260. doi:10.1016/j.ejbas.2015.09.004
- Faddladdeen, K. A., and Ojaimi, A. A. (2019). Protective effect of pomegranate (*Punica granatum*) extract against diabetic changes in adult male rat liver: Histological study. *J. Microsc. Ultrastruct.* 7 (4), 165–170. . Epub 2019 Nov 18. PMID: 31803570; PMCID: PMC6880321. doi:10.4103/JMAU.JMAU_6_19
- Gabr, S. K., Bakr, R. O., Mostafa, E. S., El-Fishawy, A. M., and El-Alfy, T. S. (2019). Antioxidant activity and molecular docking study of *Erythrina×neillii* polyphenolics. *S. Afr. J. Bot.* 121, 470–477. doi:10.1016/j.sajb.2018.12.011
- García, P., Fredes, C., Cea, I., Lozano-Sánchez, J., Leyva-Jiménez, F. J., Robert, P., et al. (2021). Recovery of bioactive compounds from pomegranate (*Punica granatum* L.) peel using pressurized liquid extraction. *Foods* 10 (2), 203. doi:10.3390/foods10020203
- Ge, G., Bai, J., Wang, Q., Liang, X., Tao, H., Chen, H., et al. (2022). Punicalagin ameliorates collagen-induced arthritis by downregulating M1 macrophage and pyroptosis via NF- κ B signaling pathway. *Sci. China Life Sci.* 65 (3), 588–603. doi:10.1007/s11427-020-1939-1
- Guy, A. (1998). Identification and chromatographic separation of antimony species with α -hydroxy acids. *Analyst* 123 (7), 1513–1518. doi:10.1039/a708574e
- Hammoud Mahdi, D., Hubert, J., Renault, J.-H., Martinez, A., Schubert, A., Engel, K. M., et al. (2020). Chemical profile and antimicrobial activity of the fungus-growing termite strain *Macrotermes bellicosus* used in traditional medicine in the Republic of Benin. *Molecules* 25, 5015. doi:10.3390/molecules25215015
- Hasanpour, M., Saberi, S., and Iranshahi, M. (2020). Metabolic profiling and untargeted ¹H-NMR -based metabolomics study of different Iranian pomegranate (*Punica granatum*) ecotypes. *Planta Med.* 86, 212–219. doi:10.1055/a-1038-6592
- Heid, C. A., Stevens, J., Livak, K. J., and Williams, P. M. (1996). Real time quantitative PCR. *Genome Res.* 6 (10), 986–994. doi:10.1101/gr.6.10.986
- Hou, C., Zhang, W., Li, J., Du, L., Lv, O., Zhao, S., et al. (2019). Beneficial effects of pomegranate on lipid metabolism in metabolic disorders. *Mol. Nutr. Food Res.* 63 (16), 1800773. doi:10.1002/mnfr.201800773
- Ismail, T., Sestili, P., and Akhtar, S. (2012). Pomegranate peel and fruit extracts: A review of potential anti-inflammatory and anti-infective effects. *J. Ethnopharmacol.* 143 (2), 397–405. doi:10.1016/j.jep.2012.07.004
- Jebraeli, H., Shabbidar, S., Sajjadpour, Z., Aghdam, S. D., Qorbani, M., Rajab, A., et al. (2021). The association between carbohydrate quality index and anthropometry, blood glucose, lipid profile and blood pressure in people with type 1 diabetes mellitus: A cross-sectional study in Iran. *J. Diabetes Metab. Disord.* 20 (2), 1349–1358. doi:10.1007/s40200-021-00864-6
- Jin, Q., Zhu, Q., Wang, K., Chen, M., and Li, X. (2021). Allisartan isoproxil attenuates oxidative stress and inflammation through the SIRT1/Nrf2/NF- κ B signalling pathway in diabetic cardiomyopathy rats. *Mol. Med. Rep.* 23 (3), 215. doi:10.3892/mmr.2021.11854
- Khalil, H., Kanisicak, O., Prasad, V., Correll, R. N., Fu, X., Schips, T., et al. (2017). Fibroblast-specific TGF- β -Smad2/3 signaling underlies cardiac fibrosis. *J. Clin. Investig.* 127 (10), 3770–3783. doi:10.1172/JCI94753
- Khanbabaee, K., and Großer, M. (2003). An efficient total synthesis of pedunculagin by using a twofold intramolecular double esterification strategy. *Eur. J. Org. Chem.* 2003, 2128–2131. doi:10.1002/ejoc.200300006
- Khorkova, O., Hsiao, J., and Wahlestedt, C. (2015). Basic biology and therapeutic implications of lncRNA. *Adv. Drug Deliv. Rev.* 87, 15–24. doi:10.1016/j.addr.2015.05.012
- Konda, V. R., Eerike, M., Chary, R. P., Arunachalam, R., Yeddula, V. R., Meti, V., et al. (2017). Effect of aluminum chloride on blood glucose level and lipid profile in normal, diabetic and treated diabetic rats. *Indian J. Pharmacol.* 49 (5), 357–365. doi:10.4103/ijp.ijp_786_16
- Kuo, Y., Wu, W., Jeng, S., Wang, F., Huang, H., Lin, C., et al. (2005). Suppressed TGF- β 1 expression is correlated with up-regulation of matrix metalloproteinase-13 in keloid regression after flashlamp pulsed-dye laser treatment. *Lasers Surg. Med.* 36 (1), 38–42. doi:10.1002/lsm.20104
- Lee, G., Park, J. S., Lee, E. J., Ahn, J. H., and Kim, H. S. (2019). Anti-inflammatory and antioxidant mechanisms of urolithin B in activated microglia. *Phytomedicine* 55, 50–57. doi:10.1016/j.phymed.2018.06.032
- Li, W., Chen, S., Zhou, G., Li, H., Zhong, L., and Liu, S. (2018). Potential role of cyanidin 3-glucoside (C3G) in diabetic cardiomyopathy in diabetic rats: An *in vivo* approach. *Saudi J. Biol. Sci.* 25 (3), 500–506. doi:10.1016/j.sjbs.2016.11.007
- Liobikas, J., Skemiene, K., Trumbeckaitė, S., and Borutaite, V. (2016). Anthocyanins in cardioprotection: A path through mitochondria. *Pharmacol. Res.* 113, 808–815. doi:10.1016/j.phrs.2016.03.036
- Lorenzo-Almorós, A., Cepeda-Rodrigo, J. M., and Lorenzo, Ó. (2022). Diabetic cardiomyopathy. *Rev. Clin. Esp.* 222 (2), 100–111. doi:10.1016/j.rceng.2019.10.012
- Lu, Y., Lu, Y., Meng, J., and Wang, Z. (2022). Pyroptosis and its regulation in diabetic cardiomyopathy. *Front. Physiol.* 2436. doi:10.3389/fphys.2021.791848
- Mayyas, A., Abu-Sini, M., Amr, R., Akasheh, R. T., Zalloum, W., Khair, A., et al. (2021). Novel *in vitro* and *in vivo* anti-*Helicobacter pylori* effects of pomegranate peel ethanol extract. *Vet. World* 14 (1), 120–128. doi:10.14202/vetworld.2021.120-128
- Meng, L., Lin, H., Huang, X., Weng, J., Peng, F., and Wu, S. (2022). METTL14 suppresses pyroptosis and diabetic cardiomyopathy by downregulating TINCR lncRNA. *Cell Death Dis.* 13 (1), 38–13. doi:10.1038/s41419-021-04484-z
- Ohkawa, H., Ohishi, N., and Yagi, K. (1979). Assay for lipid peroxides in animal tissues by thiobarbituric acid reaction. *Anal. Biochem.* 95 (2), 351–358. doi:10.1016/0003-2697(79)90738-3
- Pizzino, G., Irrera, N., Cucinotta, M., Pallio, G., Mannino, F., Arcoraci, V., et al. (2017). Oxidative stress: Harms and benefits for human health. *Oxid. Med. Cell Longev.* 2017, 8416763. doi:10.1155/2017/8416763
- Prandi, F. R., Evangelista, I., Sergi, D., Palazzuoli, A., and Romeo, F. (2022). Mechanisms of cardiac dysfunction in diabetic cardiomyopathy: Molecular abnormalities and phenotypical variants. *Heart fail. Rev.* 1–10. doi:10.1007/s10741-021-10200-y
- Punasiya, R., Joshi, A., and Patidar, K. (2010). Antidiabetic effect of an aqueous extract of pomegranate (*Punica granatum* L.) peels in normal and alloxan diabetic rats. *Res. J. Pharm. Tech.* 3 (1), 272–274.
- Ragab, A. E., Al-Madbolly, L. A., Al-Ashmawy, G. M., Saber-Ayad, M., and Abo-Saif, M. A. (2022). Unravelling the *in vitro* and *in vivo* anti-*Helicobacter pylori* effect of delphinidin-3-O-glucoside rich extract from pomegranate exocarp: Enhancing autophagy and downregulating TNF- α and COX2. *Antioxidants* 11, 1752. doi:10.3390/antiox11091752

- Riazi, S., Maric, C., and Ecelbarger, C. A. (2006). 17- β Estradiol attenuates streptozotocin-induced diabetes and regulates the expression of renal sodium transporters. *Kidney Int.* 69 (3), 471–480. doi:10.1038/sj.ki.5000140
- Russo, I., and Frangogiannis, N. G. (2016). Diabetes-associated cardiac fibrosis: Cellular effectors, molecular mechanisms and therapeutic opportunities. *J. Mol. Cell Cardiol.* 90, 84–93. doi:10.1016/j.yjmcc.2015.12.011
- Saber, S., Abd El-Kader, E. M., Sharaf, H., El-Shamy, R., El-Saeed, B., Mostafa, A., et al. (2020). Celastrol augments sensitivity of NLRP3 to CP-456773 by modulating HSP-90 and inducing autophagy in dextran sodium sulphate-induced colitis in rats. *Toxicol. Appl. Pharmacol.* 400, 115075. doi:10.1016/j.taap.2020.115075
- Sapian, S., Taib, I. S., Katas, H., Latip, J., Zainalabidin, S., Hamid, Z. A., et al. (2022). The Role of anthocyanin in modulating diabetic cardiovascular disease and its potential to be developed as a nutraceutical. *Pharmaceuticals* 15 (11), 1344. doi:10.3390/ph15111344
- Savi, M., Bocchi, L., Mena, P., Dall'Asta, M., Crozier, A., Brighenti, F., et al. (2017). *In vivo* administration of urolithin A and B prevents the occurrence of cardiac dysfunction in streptozotocin-induced diabetic rats. *Cardiovasc. Diabetol.* 16 (1), 80–13. doi:10.1186/s12933-017-0561-3
- Shi, C., Wu, L., and Li, L. (2021). LncRNA-MALAT 1 regulates cardiomyocyte scorching in diabetic cardiomyopathy by targeting NLRP3. *Cell. Mol. Biol.* 67 (6), 213–219. doi:10.14715/cmb/2021.67.6.28
- Sun, W., Yan, C., Frost, B., Wang, X., Hou, C., Zeng, M., et al. (2016). Pomegranate extract decreases oxidative stress and alleviates mitochondrial impairment by activating AMPK-Nrf2 in hypothalamic paraventricular nucleus of spontaneously hypertensive rats. *Sci. Rep.* 6 (1). doi:10.1038/srep34246
- Tian, J. L., Liao, X. J., Wang, Y. H., Si, X., Shu, C., Gong, E. S., et al. (2019). Identification of cyanidin-3-arabinoside extracted from blueberry as a selective protein tyrosine phosphatase 1B inhibitor. *J. Agric. Food Chem.* 67, 13624–13634. doi:10.1021/acs.jafc.9b06155
- Torika, N., Asraf, K., Apte, R. N., and Fleisher-Berkovich, S. (2018). Candesartan ameliorates brain inflammation associated with Alzheimer's disease. *CNS Neurosci. Ther.* 24 (3), 231–242. doi:10.1111/cns.12802
- Ukong, S., Ampawong, S., and Kengkoom, K. (2008). Collagen measurement and staining pattern of wound healing comparison with fixation and stain. *J. Microsc. Soc. Thail.* 22, 37–41.
- Villalba, K. J. O., Barka, F. V., Pasos, C. V., and Rodríguez, P. E. (2019). Food ellagitannins: Structure, metabolomic fate, and biological properties. *Tannins-structural Prop. Biol. Prop. Curr. Knowl.*, 26–46.
- Wan, C., Li, S., Liu, L., Chen, C., and Fan, S. (2017). Caffeoylquinic acids from the aerial parts of *Chrysanthemum coronarium* L. *Plants* 6, 10. doi:10.3390/plants6010010
- Wu, A., Sun, W., and Mou, F. (2021). LncRNA-MALAT1 promotes high glucose-induced H9C2 cardiomyocyte pyroptosis by downregulating miR-141-3p expression. *Mol. Med. Rep.* 23 (4), 259. doi:10.3892/mmr.2021.11898
- Wu, J., Wang, C., and Ding, H. (2020). LncRNA MALAT1 promotes neuropathic pain progression through the miR-154-5p/AQP9 axis in CCI rat models. *Mol. Med. Rep.* 21 (1), 291–303. doi:10.3892/mmr.2019.10829
- Xue, Y., Tuipulotu, D. E., Tan, W. H., Kay, C., and Man, S. M. (2019). Emerging activators and regulators of inflammasomes and pyroptosis. *Trends Immunol.* 40 (11), 1035–1052. doi:10.1016/j.it.2019.09.005
- Yan, D., Cai, Y., Luo, J., Liu, J., Li, X., Ying, F., et al. (2020). FOXO1 contributes to diabetic cardiomyopathy via inducing imbalanced oxidative metabolism in type 1 diabetes. *J. Cell. Mol. Med.* 24 (14), 7850–7861. doi:10.1111/jcmm.15418
- Yisimayili, Z., Abdulla, R., Tian, Q., Wang, Y., Chen, M., Sun, Z., et al. (2019). A comprehensive study of pomegranate flowers polyphenols and metabolites in rat biological samples by high-performance liquid chromatography quadrupole time-of-flight mass spectrometry. *J. Chromatogr. A* 1604, 460472. doi:10.1016/j.chroma.2019.460472
- Youssef, M. E., El-Azab, M. F., Abdel-Dayem, M. A., Yahya, G., Alanazi, I. S., and Saber, S. (2022). Electrocardiographic and histopathological characterizations of diabetic cardiomyopathy in rats. *Environ. Sci. Pollut. Res.* 29 (17), 25723–25732. doi:10.1007/s11356-021-17831-6
- Zabeen, B., Balsa, A. M., Islam, N., Parveen, M., Nahar, J., and Azad, K. (2018). Lipid profile in relation to glycemic control in type 1 diabetes children and adolescents in Bangladesh. *Indian J. Endocrinol. Metab.* 22 (1), 89–92. doi:10.4103/ijem.IJEM_217_17
- Zhang, M., Gu, H., Chen, J., and Zhou, X. (2016). Involvement of long noncoding RNA MALAT1 in the pathogenesis of diabetic cardiomyopathy. *Int. J. Cardiol.* 202, 753–755. doi:10.1016/j.ijcard.2015.10.019
- Zheng, Z., and Li, G. (2020). Mechanisms and therapeutic regulation of pyroptosis in inflammatory diseases and cancer. *Int. J. Mol. Sci.* 21 (4), 1456. doi:10.3390/ijms21041456



OPEN ACCESS

EDITED BY

Ochuko Lucky Erukainure,
University of the Free State, South Africa

REVIEWED BY

Rebecca Reddy,
Durban University of Technology, South Africa
Viola Anuli Nicholas-Okpara,
Federal Institute of Industrial Research
Oshodi, Nigeria

*CORRESPONDENCE

Yueyun Liu,
✉ chloelou@126.com

[†]These authors share first authorship

SPECIALTY SECTION

This article was submitted to
Ethnopharmacology, a section of the
journal Frontiers in Pharmacology

RECEIVED 11 February 2023

ACCEPTED 30 March 2023

PUBLISHED 10 April 2023

CITATION

Lei C, Chen J, Huang Z, Men Y, Qian Y,
Yu M, Xu X, Li L, Zhao X, Jiang Y and Liu Y
(2023), Ginsenoside Rg1 can reverse
fatigue behavior in CFS rats by regulating
EGFR and affecting Taurine and Mannose
6-phosphate metabolism.
Front. Pharmacol. 14:1163638.
doi: 10.3389/fphar.2023.1163638

COPYRIGHT

© 2023 Lei, Chen, Huang, Men, Qian, Yu,
Xu, Li, Zhao, Jiang and Liu. This is an
open-access article distributed under the
terms of the [Creative Commons
Attribution License \(CC BY\)](#). The use,
distribution or reproduction in other
forums is permitted, provided the original
author(s) and the copyright owner(s) are
credited and that the original publication
in this journal is cited, in accordance with
accepted academic practice. No use,
distribution or reproduction is permitted
which does not comply with these terms.

Ginsenoside Rg1 can reverse fatigue behavior in CFS rats by regulating EGFR and affecting Taurine and Mannose 6-phosphate metabolism

Chaofang Lei¹, Jiayu Chen^{1,2†}, Zhen Huang¹, Yinian Men¹,
Yue Qian¹, Mingzhi Yu¹, Xinyi Xu¹, Lin Li³, Xin Zhao¹,
Youming Jiang³ and Yueyun Liu^{1*}

¹School of Traditional Chinese Medicine, Beijing University of Chinese Medicine, Beijing, China,

²Guangzhou Key Laboratory of Formula-Pattern of Traditional Chinese Medicine, School of Traditional Chinese Medicine, Jinan University, Guangzhou, China, ³School of Life Sciences, Beijing University of Chinese Medicine, Beijing, China

Background: Chronic fatigue syndrome (CFS) is characterized by significant and persistent fatigue. Ginseng is a traditional anti-fatigue Chinese medicine with a long history in Asia, as demonstrated by clinical and experimental studies. Ginsenoside Rg1 is mainly derived from ginseng, and its anti-fatigue metabolic mechanism has not been thoroughly explored.

Methods: We performed non-targeted metabolomics of rat serum using LC-MS and multivariate data analysis to identify potential biomarkers and metabolic pathways. In addition, we implemented network pharmacological analysis to reveal the potential target of ginsenoside Rg1 in CFS rats. The expression levels of target proteins were measured by PCR and Western blotting.

Results: Metabolomics analysis confirmed metabolic disorders in the serum of CFS rats. Ginsenoside Rg1 can regulate metabolic pathways to reverse metabolic biases in CFS rats. We found a total of 34 biomarkers, including key markers Taurine and Mannose 6-phosphate. AKT1, VEGFA and EGFR were identified as anti-fatigue targets of ginsenoside Rg1 using network pharmacological analysis. Finally, biological analysis showed that ginsenoside Rg1 was able to down-regulate the expression of EGFR.

Conclusion: Our results suggest ginsenoside Rg1 has an anti-fatigue effect, impacting the metabolism of Taurine and Mannose 6-phosphate through EGFR regulation. This demonstrates ginsenoside Rg1 is a promising alternative treatment for patients presenting with chronic fatigue syndrome.

KEYWORDS

ginsenoside Rg1, metabolomics, network pharmacology, EGFR, AKT1, VEGFA, taurine, Mannose 6-phosphate

1 Introduction

Chronic fatigue syndrome (CFS) is a common (0.006%–3%), severely disabling disorder characterized by long-term extreme fatigue that persists even after resting (Nguyen et al., 2019; Moore et al., 2021). CFS is accompanied by depression, concentration difficulty and memory loss (Cvejic et al., 2016; Chaves-Filho et al., 2019). An estimated 1–5 million people present with CFS in Europe every year, with an estimated annual cost of approximately €40 billion in health expenses (Nacul et al., 2021); while in the United States CFS affects 1–2.5 million people yearly and costs between \$1.7~\$24 billion (Bested and Marshall, 2015), compared to 44.71 ± 6.10 cases/100,000 people in South Korea (Lim et al., 2021). In China, a previous cross-sectional study found CFS is prevalent among adolescents (Shi et al., 2018).

At present, CFS's etiology remains unknown, and there are no effective treatments available (Sandler and Lloyd, 2020), with deficient and unspecific diagnostic criteria further preventing appropriate approaches. This makes it imperative to increase the efforts for discovering biomarkers to aid diagnosis and include Chinese medicine has as a potential area for therapy.

Spleen deficiency represents the core pathogenesis of CFS (Geng and Wang, 2012) and can be treated with ginseng, a classic herbal prescription (Ma et al., 2021) that contains ginsenosides as main active components, of which Rg1, a triterpenoid saponin, is the most abundant (Mohan et al., 2018; Yousuf et al., 2022). In addition, Rg1 presents anti-fatigue effects, as demonstrated by an increase in swimming, fight, and rest times in CFS model rats, which are associated with an increase in serum IgA, IgG, IgM, IFN- β , IFN- γ , T-AOC and Ache (He et al., 2020). Li et al. (2022) found that Panax notoginseng saponin R1 can be efficiently transformed into ginsenoside Rg1 to enhance anti-fatigue effects. CFS is also associated with several metabolic disorders, including energy, amino acids, nucleotides, nitrogen, hormones, lipids and neurotransmitter-related pathways (Armstrong et al., 2014; Nagy-Szakal et al., 2018). However, it remains unclear whether ginsenoside Rg1 can regulate these metabolic disorders in CFS rats.

Traditional Chinese medicine has played an important role in health protection and disease treatment for thousands of years, and is becoming gradually recognized by the international community, as shown by the development of metabolomics, an emerging systems biology technology whose core idea is similar to the holistic approach of traditional Chinese medicine (Wang et al., 2015). Moreover, network analysis explores the associations between drugs, targets, and diseases through network information, whereby combining it with metabolomics can provide insights into the complex interrelationships between biomarkers and disease.

2 Materials and methods

2.1 Animals, drug administration and sample collection

We purchased 32 male Sprague-Dawley rats from the Beijing Vital River Laboratory Animal Technology Co., Ltd. [animal license No. SCXK (Beijing) 2016–0006]. The rats were kept under controlled environmental conditions (room temperature 22°C ± 2°C, 12-h light/dark cycle) with free access to standard food and water. All

experiments were performed according to the EU (Directive 2010/63/EU) ethical guidelines and were approved by the Animal Care and Therapy Ethics Committee of the Beijing University of Chinese Medicine (BUCM-4-2019030402–1036).

After 1 week of adaptive feeding, all rats were randomly divided into four groups (n = 8 per group), including the normal Control group (Control), the model group (CFS), the model + positive control group (CFS+ Oryzanol&VB1), and the model + ginsenoside Rg1 group (CFS + Rg1). Starting from week 3, all groups were given intragastric administration 30 min before modeling every day.

The rats in each group were given continuous gavage for 2 weeks, once a day, and received the following treatments: 1) Control: intragastric administration of double distilled water (10 ml/kg body weight); 2) CFS: intragastric administration of double distilled water (10 ml/kg body weight); 3) CFS+ Oryzanol&VB1 group: gavage glutamine and vitamin B1, (3.15 mg/kg/d, 10 ml/kg body weight) (Xu et al., 2019); 4) CFS + Rg1 group: intragastric administration of ginsenoside Rg1 (50 mg/kg/d, 10 ml/kg body weight) (Feng et al., 2010; Heinrich et al., 2020).

After performing behavioral tests, we anesthetized the animals using isoflurane. The hippocampus and prefrontal cortex were stripped and quickly preserved in liquid nitrogen. Blood was collected through the abdominal aorta and serum was separated by centrifugation (3500 rpm, 10 min, 4°C). Serum and brain tissue were stored at -80°C until analyzed.

2.2 Chemicals and reagents

Ginsenoside Rg1 was purchased from Chengdu DeSiTe Bio-Technology Co., Ltd. with the following specifications: 5 g/bottle (HPLC ≥ 98%, CAS No.22427-39-0). Guweisu tablets were purchased from Beijing Zhongxin Pharmaceutical Co., Ltd. with the following specifications: 10mg/tablet (No.H13020683). Vitamin B1 tablets were purchased from Tianjin Feiying Yuchuan Pharmaceutical Co., Ltd. with the following specifications: 10 mg/tablet (No.12020592). D-xylose was purchased from BioRuler.

UPLC Methanol, Acetonitrile, and ultra-pure water were purchased from Fisher Chemical (Fair Lawn, United States). Uplc-grade FormicAcid was purchased from CNW (Shanghai, China). UPLC Grade 2-Propanol was purchased from Merck (Darmstadt, Germany). 2-Chloro-L-Phenylalanine (≥98%) was obtained from Adamas-beta (Shanghai, China).

Bicinchoninic acid (BCA) protein quantitative detection Kit, SDS-PAGE Gel Preparation Kit, Radio-Immunoprecipitation Assay (RIPA) Lysate, and enhanced chemiluminescence (ECL) were purchased from Servicebio (Wuhan, China). GAPDH (GB15002) was purchased from Servicebio (Wuhan, China). AKT1 (ab81283), VEGFA (ab214424), and EGFR (ab52894) were purchased from Abcam (Shanghai, China).

2.3 Chronic fatigue syndrome model establishment

A multi-factor modeling method was used to simulate CFS pathogenesis (Shao et al., 2017): 1) Load-weighted forced swimming;

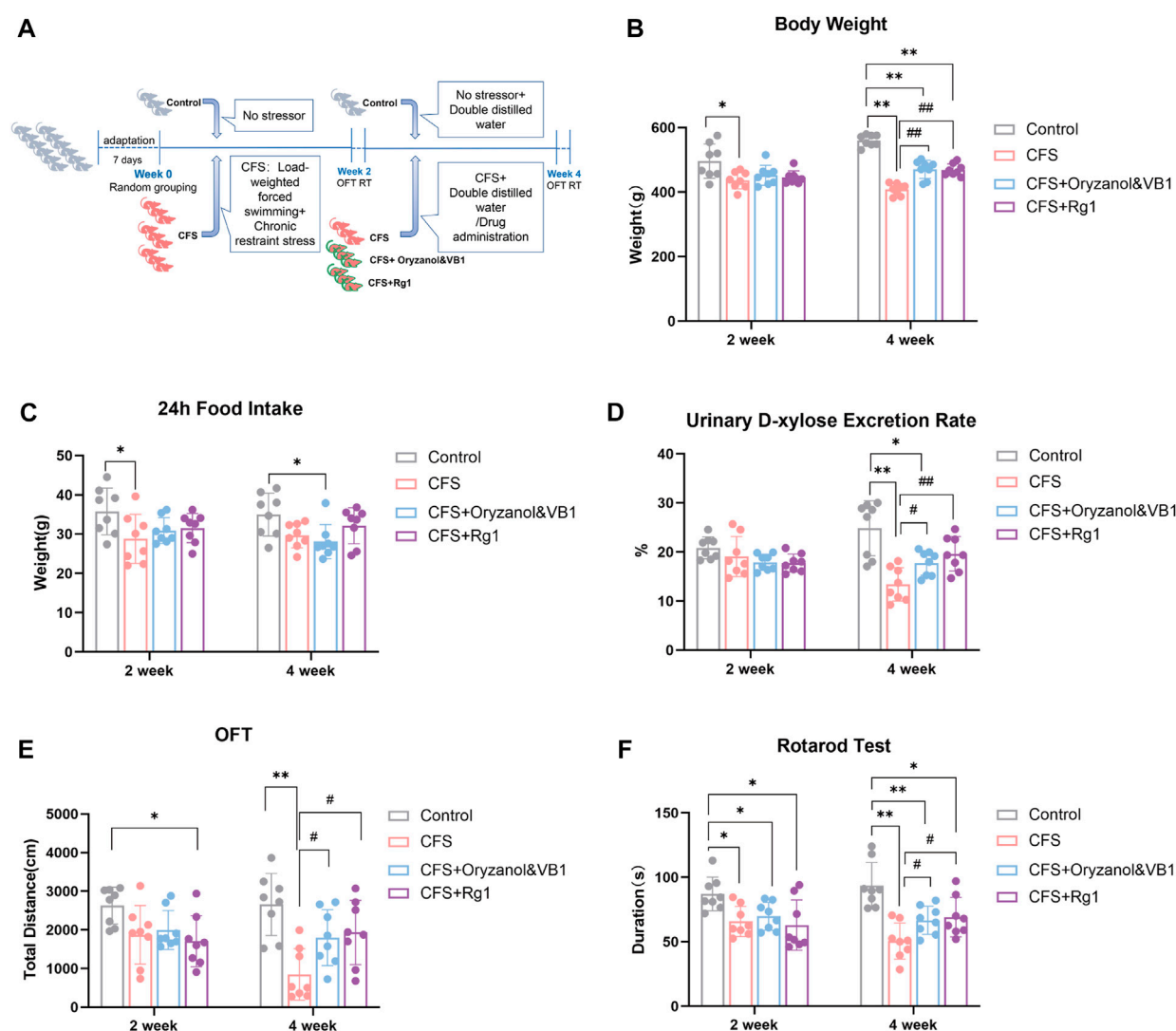


FIGURE 1

(A) Experimental procedure implemented for a CFS rat model. (B) Body weight changes in the four rat groups. (C) 24-h food intake of the four rat groups. (D) 24-h urinary D-xylose excretion rate in the four rat groups. (E) Total travel distance of the four rat groups in the Open Field Test. (F) Time spent on the rod in the four rat groups (Rotarod Test). Data are shown as the mean \pm standard deviation, $n = 8$. * $p < 0.05$, ** $p < 0.01$ versus control group; # $p < 0.05$, ## $p < 0.01$ versus CFS group.

Rats in the modeling group swam in a transparent toughened plastic bucket (diameter 20 \times height 50 cm) for 10 min every day for 28 days. The water temperature of the swimming pool was controlled at $23^{\circ}\text{C} \pm 2^{\circ}\text{C}$. A small artery clip was attached to the lead wire about 5% of the body weight of the rat, and then the weight was placed on the back hair of each rat. 2) Restriction: The rats in the model group were bound to the wooden restriction frame (22 \times 10 \times 2 cm in length and 10 \times 2 cm in thickness) for 3 h every day, respectively, and subjected to chronic restriction stress for 4 weeks. The Control group did not participate in the above two modeling methods and was fed normally. The experimental procedure is shown in Figure 1A.

2.4 Evaluation of the CFS model

Body weight, 24-h food intake, urine D-xylose and behavioral tests (including the open field and rotarod tests) were performed 2 and 4 weeks after modeling for evaluation. In the open field test, the EthoVision 3.0 behavioral device of the Noldus Company (Netherlands) was used to analyze videos and calculate the 5-min total distance of spontaneous movement of each rat group. A rat rotating rod fatigue instrument (Anhui Zhenghua Biological Instrument Equipment Co., Ltd. ZH-300B) was used to measure the time during which rats were able to sustain a constant 30rpm speed. The upper limit of the recording time was set to 5 min.

2.5 LC-MS-based serum metabolomics

2.5.1 Sample preparation

100 μ L of serum samples were collected in a 2 ml centrifuge tube. The metabolites were extracted from 400 μ L of extract solution (methanol: water = 4:1 (v:v)) containing 0.02 mg/ml internal standard (L-2-chlorophenyl alanine). The sample preparation process is described in a previous study (Lei et al., 2022). Equal amounts of the mixture were extracted from all samples and used as QC samples for LC-MS.

2.5.2 Untargeted LC-MS analysis

We used Thermo's ultra-high-performance liquid chromatography-tandem time-of-flight mass spectrometry UHPLC-Q Exactive HF-X system as the instrument platform. A total of 2 μ L samples were separated using an HSS T3 chromatographic column (100 mm \times 2.1 mm i. d. 1.8 μ m) and then detected by mass spectrometry. The mobile phase A consisted of 95% water and 5% acetonitrile (containing 0.1% formic acid). The mobile phase B consisted of 47.5% acetonitrile, 47.5% isopropyl alcohol, and 5% water (containing 0.1% formic acid). The column temperature was set to 40 $^{\circ}$ C. The positive and negative ion scanning modes were used for mass spectrum signal acquisition.

2.5.3 Data processing

LC-MS raw data was imported into Progenesis QI (Waters Corporation, Milford, United States) for baseline filtering, peak identification, integration, retention time correction, and peak alignment. This allowed us to obtain a data matrix of the retention time, mass/charge ratio, and peak intensity. We normalized the data matrix for subsequent analysis. The metabolite information was obtained by matching MS and MS/MS mass spectrometry information with the metabolic public databases HMDB (<https://hmdb.ca/>) and Metlin (<https://metlin.scripps.edu/>).

2.5.4 Metabolomic data analysis

The pre-processed data was uploaded to the Majorbio Cloud Platform (<http://www.majorbio.com/>) for data analysis. The R software package ropls (Version 1.6.2) was used for performing principal component analysis (PCA) and orthogonal least partial square discriminant analysis (OPLS-DA). The stability of the model was evaluated using seven cyclic interaction validations. We also performed a Student's t-test analysis. The selection of differential metabolites was determined based on the variable weight value (VIP) obtained by the OPLS-DA model and the *p*-value of the student's t-test. Metabolites with VIP > 1.0 and *p* < 0.05 were selected as metabolic markers. We use the KEGG database (<https://www.kegg.jp/kegg/pathway.html>) for uncovering metabolic pathways and identify differences in associated metabolites, with *p* < 0.05 used as the standard. The Python software package scipy.stats was used for pathway enrichment analysis, and the most relevant biological pathways were extracted using Fisher's exact test.

2.6 Network analysis

2.6.1 Target prediction

The BATMAN-TCM (<http://bionet.ncpsb.org/batman-tcm/>) and SwissTargetPrediction (<http://www.swisstargetprediction.ch/>) databases were used to obtain information on the targets of ginsenoside Rg1.

We identified potential targets by searching CFS keywords on public databases, including Genecards (<http://www.genecards.org/>), OMIM (<https://www.omim.org/>), and DRUGBANK (<https://go.drugbank.com/>).

Differential metabolites were entered into the MetScape database to identify target proteins interacting with these metabolites.

The targets associated with CFS were standardized through the UniProt knowledge Base (<http://www.uniprot.org/>), converting all retrieved targets into official genetic symbols to facilitate downstream data analysis.

A Venn diagram was drawn using DeepVenn (<http://www.deepvenn.com/>) to show the common targets of ginsenoside Rg1, the differential metabolites, and CFS-related targets. These genes were considered as potential targets of ginsenoside Rg1 for the treatment of CFS.

2.6.2 Network construction and enrichment analysis

A large number of studies showed proteins exert biological activity through protein-protein interactions. We submitted potential target genes to the Interaction Gene Retrieval Tool (<http://string-db.org/>) and performed Protein-Protein Interaction Network (PPI) analysis. PPI networks were used to analyze core targets of ginsenoside Rg1 in the CFS-treatment using Cytoscape 3.7.1.

We used OmicShare Tools (<https://www.omicshare.com/tools/>) for GO and KEGG enrichment analyses to obtain the biological functions and related pathways of ginsenoside Rg1 as potential targets for CFS treatment. The correlation pathways with *p* < 0.05 were considered as statistically significant.

2.7 Experimental validation

2.7.1 Quantitative real-time PCR

Total RNA in the hippocampus (Hip) and prefrontal cortex (PFC) was extracted with an RNA extraction solution (Servicebio, China). Reverse transcription was performed with a first-strand cDNA synthesis kit (Servicebio, China) following manufacturer's guidelines. The expression levels were determined using real-time PCR with SYBR Green Mix (Servicebio, China). Relative mRNA expression was calculated using the $2^{-\Delta\Delta CT}$ method. GAPDH was used as a normalization control for mRNA levels. The primer sequences are shown in Table 1.

2.7.2 Western blot

RIPA lysate was added to the tissues, crushed by ultrasound, and centrifuged at room temperature for 10 min (12,000 rpm, 4 $^{\circ}$ C). After

TABLE 1 List of PCR primers.

Primers	Forward	Reverse	Gene accession no.
AKT1	CGACGTAGCCATTGTGAAGGAG	ATTGTGCCACTGAGAAGTTGTTG	NM_033230.2
VEGFA	GCAATGATGAAGCCCTGGAGT	GGCTTTGTTCTATCTTTCTTTGGTC	NM_031836.3
EGFR	AGAACAAACACCTGGTCTGGAA	CCACCACTACTATGAAGAGGAGGC	NM_031507.1
GAPDH	CTGGAGAAACCTGCCAAGTATG	GGTGAAGAATGGGAGTTGCT	NM_017008.4

this, we collected the supernatant, which was considered as the total protein solution. The BCA kit was used to measure the concentration of the protein solution. We added 5× protein loading buffer and denatured the protein in a boiling water bath for 5 min. The same amount of protein solution was subjected to sodium dodecyl sulfate-polyacrylamide gel electrophoresis (SDS-PAGE), after which the gel was transferred to the polyvinylidene fluoride (PVDF) membrane. A 5% skim milk solution containing TBS + Tween (TBST) was kept at room temperature for 30 min and added to the primary antibody at 4°C for overnight incubation in a shak (GAPDH (1:2000), AKT1 (1:1000), VEGFA (1:1000), EGFR (1:1000)). After rinsing with phosphate buffered solution tween (PBST) for 3 × 5 min, the membrane was placed in an horseradish peroxidase (HRP) labeled secondary antibody (1:5000) and incubated at room temperature for 1 h. After rinsing with PBST for 3 × 5 min, the gel imaging system was used for image acquisition. The Alpha Innotech software was used to calculate and analyze the gray scale of protein bands.

2.8 Statistical analysis

Statistical analysis was performed using SPSS (version 20.0) and GraphPad Prism (version 9.0). All data are expressed as the mean ± standard deviation ($\bar{x} \pm SD$). Based on data normality and homogeneity of variance, a one-way ANOVA or a non-parametric test were used for comparison. $p < 0.05$ was considered as statistically significant and $p < 0.01$ was considered highly significant.

3 Results

3.1 Effects of CFS modeling on body weight, food intake, and urinary D-xylose excretion rate in rats

3.1.1 Weight

The body weight of rats in each group is shown in Figure 1B. After 2 weeks of modeling, the rats in the CFS group had lower weight compared to the Control group ($p = 0.0443$). There were no significant differences among model groups. After 4 weeks of modeling, the body weight of the three modeling groups decreased significantly compared with the Control group ($p < 0.0001$). Finally, rat weight in both Oryzanol&VB1 and Rg1 groups recovered significantly compared to the CFS group ($p = 0.0005$, $p < 0.0001$).

3.1.2 Food intake

The 24-h food intake of each group is shown in Figure 1C. After 2 weeks, the food intake of rats in the CFS group was lower than in the Control group ($p = 0.0237$). We found no significant differences among the model groups. After 4 weeks, food intake decreased in the Oryzanol&VB1 group compared to Control ($p = 0.0240$). No significant differences were found between the CFS, the Oryzanol&VB-1 and the Rg1 groups.

3.1.3 Urinary D-xylose excretion rate

The 24-h urinary D-xylose excretion rate of rats in each group is shown in Figure 1D. We found no differences between groups after 2 weeks. However, after 4 weeks of modelling, the urinary D-xylose-excretion rate in the CFS and Oryzanol&VB-1 groups was significantly decreased compared to the Control group ($p = 0.0011$, $p = 0.0228$), and a significant recovery occurred in the Oryzanol&VB1 and Rg1 groups compared to CFS ($p = 0.0230$, $p = 0.0054$).

These results show that CFS modeling produces significant effects on body weight and the urinary D-xylose excretion rate of rats, but no significant differences in food intake. We also note that body weight and urinary D-xylose excretion rate were further decreased in the CFS group over the course of the last 2 weeks of treatment. Crucially, ginsenoside Rg1 intervention could significantly reverse this course, suggesting it is able to improve gastrointestinal absorption.

3.2 CFS modeling, spontaneous activity and rotarod test

3.2.1 Open field test

The 5-min total movement distance of each group is shown in Figure 1E. Rats in the Rg1 group moved less than those in the Control group after 2 weeks ($p = 0.0187$), but there were no significant differences among model groups. After 4 weeks, the total movement distance of rats in the CFS group was significantly decreased compared to the Control group ($p = 0.0007$), with a recovery observed in the Oryzanol&VB1 and Rg1 groups ($p = 0.0296$, $p = 0.0229$).

3.2.2 Rotarod test

The time spent on the rod is shown in Figure 1F. Duration decreased in all model groups after 2 weeks ($p = 0.0105$, $p = 0.0306$, $p = 0.0323$), with no significant differences among them. These differences to the Control group became significant after 4 weeks ($p = 0.0004$, $p = 0.0097$, $p = 0.0286$), with both Oryzanol&VB1 and Rg1 groups recovering ($p = 0.0421$, $p = 0.0440$).

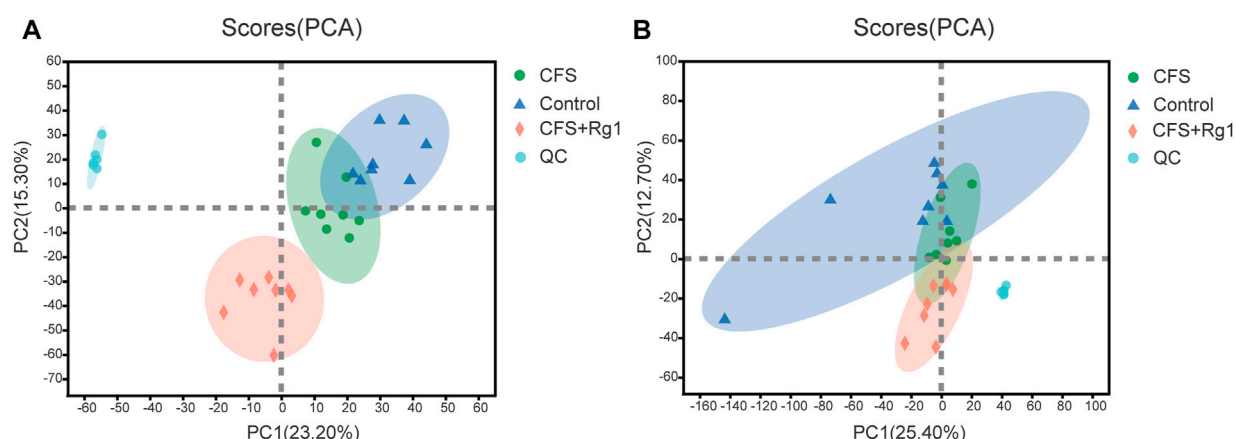


FIGURE 2
PCA scores for Control (blue), CFS (green) and CFS + Rg1 (pink) groups in positive and negative ion modes (A, B), $n = 8$.

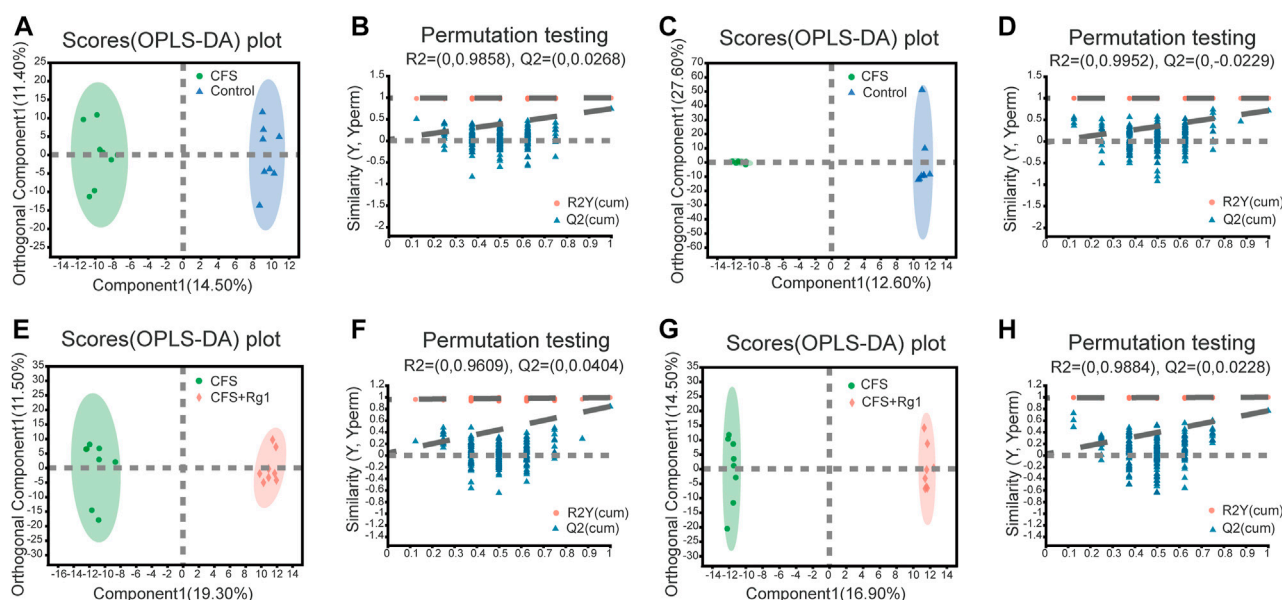


FIGURE 3
OPLS-DA and permutation tests in the positive (A, B) and negative (C, D) ion modes of Control and CFS groups, $n = 8$. OPLS-DA and permutation tests in positive (E, F) and negative (G, H) ion modes in CFS and CFS + Rg1 groups, $n = 8$.

These results show CFS modeling had a significant effect on rat spontaneous activity and muscle fatigue. Over the course of the last 2 weeks of modeling, the groups treated with ginsenoside Rg1 recovered significantly, showing its significant anti-fatigue effect.

3.3 Metabolomics analysis of serum samples

In order to study changes in endogenous serum metabolites in CFS rats and reveal the mechanisms of ginsenoside Rg1-mediated treatment, we comprehensively scanned serum metabolites of Control, CFS and CFS + Rg1 groups using the UHPLC-

QExactiveHF-X system. Principal component analysis (PCA) showed significant differences between these groups. QC analysis showed obvious sample clustering, indicating the analytical method is stable and repeatable. These results are illustrated in Figure 2.

OPLS-DA was further used to screen for potential biomarkers. As shown in Figures 3A–D, samples from the Control and the CFS groups were significantly different. The R^2_X , R^2_Y and Q^2 values of permutation tests applied in the positive ion mode were 0.259, 0.99 and 0.739, respectively; and 0.567, 0.998 and 0.709, respectively, in the negative ion mode. The CFS and the CFS + Rg1 groups were also clearly different. In these groups, the R^2_X , R^2_Y and Q^2 of permutation tests in the positive ion mode were 0.308, 0.993 and

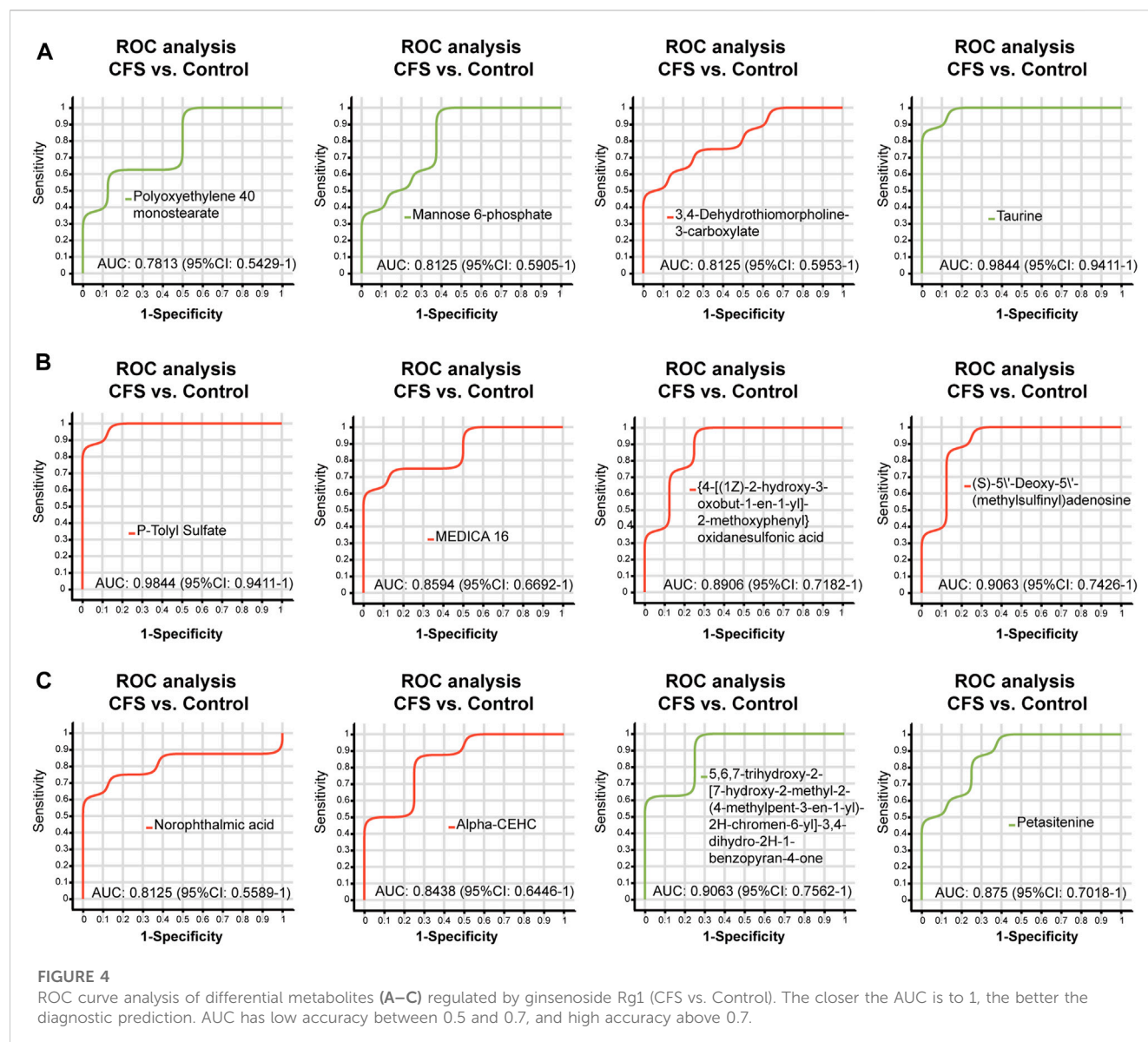
TABLE 2 Differential metabolites associated with ginsenoside Rg1 in serum.

NO.	Metabolite	M/Z	Formula	Trend CFS/Control	Trend CFS + Rg1/CFS
1	PC(18:0/0:0)	524.3705732	C26H54NO7P	↓**	↓##
2	3-Pyridinebutanoic acid	331.1647303	C9H11NO2	↓**	↓ [#]
3	PC(17:0/0:0)	510.3549983	C25H52NO7P	↓**	↓##
4	N6-Methyl-2'-deoxyadenosine	266.1231266	C11H15N5O3	↓**	↓ [#]
5	Blepharin	310.0951397	C14H17NO8	↓*	↓ [#]
6	N-Succinyl-2-amino-6-ketopimelate	353.0929004	C11H15NO8	↓**	↓ [#]
7	5-Methoxytryptophan	217.0970874	C12H14N2O3	↑*	↑##
8	Polyoxyethylene 40 monostearate	346.3312399	C20H40O3	↓*	↑ [#]
9	Azaspiracid	443.7371548	C47H71NO12	↑**	↑##
10	Palmitoyl-L-carnitine	400.3418928	C23H45NO4	↓*	↓##
11	S-(PG)2-glutathione	624.2952782	C30H47N3O10S	↑**	↑ [#]
12	PC(20:4/0:0)	566.3210231	C28H50NO7P	↓*	↓##
13	Methyl cellulose	487.2790688	C20H38O11	↓**	↓##
14	Octadecenylcarnitine	426.3574449	C25H47NO4	↓**	↓##
15	Tanacetol B	314.2321816	C17H28O4	↓**	↓ [#]
16	Tyrosyl-Serine	233.0919633	C12H16N2O5	↑*	↑##
17	Arginyl-Proline	316.1363843	C11H21N5O3	↓*	↓ [#]
18	Mannose 6-phosphate	261.0393069	C6H13O9P	↓*	↑ [#]
19	Maysin 3'-methyl ether	307.082906	C28H30O14	↓*	↓##
20	3,4-Dehydrothiomorpholine-3-carboxylate	146.0269537	C5H7NO2S	↑*	↓##
21	Taurine	126.0220252	C2H7NO3S	↓**	↑##
22	Norophthalmic acid	274.1044428	C10H17N3O6	↑*	↓ [#]
23	L-Aspartic Acid	132.0293516	C4H7NO4	↓**	↓ [#]
24	3-Hydroxy-L-proline	307.1145828	C5H9NO3	↓**	↓ [#]
25	Acetyl-DL-Leucine	172.0972364	C8H15NO3	↓**	↓##
26	P-Tolyl Sulfate	187.0064671	C7H8O4S	↑**	↓##
27	Alpha-CEHC	313.1194597	C16H22O4	↑*	↓ [#]
28	MEDICA 16	341.2695802	C20H38O4	↑*	↓##
29	5,6,7-trihydroxy-2-[7-hydroxy-2-methyl-2-(4-methylpent-3-en-1-yl)-2H-chromen-6-yl]-3,4-dihydro-2H-1-benzopyran-4-one	419.1530259	C25H26O7	↓**	↑ [#]
30	Petasitenine	402.1502652	C19H27NO7	↓**	↑##
31	Furanogermenone	267.1137544	C15H20O2	↑**	↑ [#]
32	{4-[(1Z)-2-hydroxy-3-oxobut-1-en-1-yl]-2-methoxyphenyl}oxidanesulfonic acid	269.0126903	C11H12O7S	↑**	↓ [#]
33	(S)-5'-Deoxy-5'-(methylsulfinyl)adenosine	294.0653396	C11H15N5O4S	↑**	↓##
34	LysoPC(18:0)	558.3330623	C26H54NO7P	↓**	↓##

↑ represents upregulation and ↓ represents downregulation.

***p* < 0.01, **p* < 0.05 as CFS group versus control group.

##*p* < 0.01, #*p* < 0.05 as CFS + Rg1 group versus CFS group.



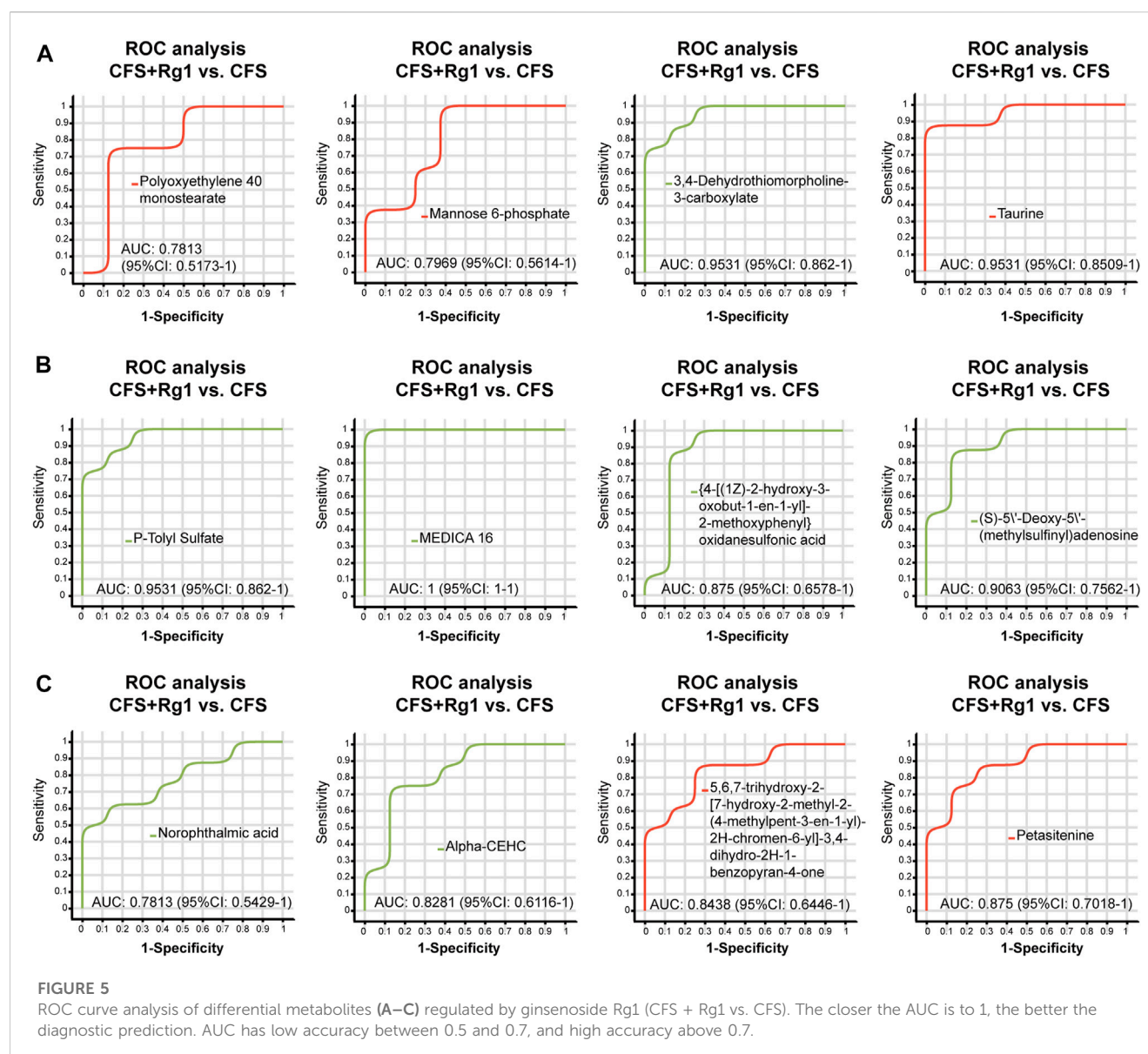
0.84, respectively; and 0.383, 0.999 and 0.766, respectively, in the negative ion mode. These results are shown in Figures 3E–H and indicate the model has good explanatory and predictive abilities, with no overfitting present.

We found a total of 34 differential metabolites that are potential biomarkers using the screening conditions $VIP > 1.0$ and $p < 0.05$ (Table 2). Of these, 12 and 22 metabolites were increased and decreased, respectively, in the CFS group compared to Control. Ginsenoside Rg1 treatment could restore Polyoxyethylene 40 monostearate, Mannose 6-phosphate, Taurine, Petasitenine and 5,6,7-trihydroxy-2-[7-hydroxy-2-methyl-2-(4-methylpent-3-en-1-yl)-2H-chromen-6-yl]-3,4-dihydro-2H-1-benzopyran-4-one levels in CFS rats, while lowering 3,4-Dehydrothiomorpholine-3-carboxylate, P-Tolyl Sulfate, MEDICA 16, {4-[(1Z)-2-hydroxy-3-oxobut-1-en-1-yl]-2-methoxyphenyl}oxidanesulfonic acid, (S)-5'-Deoxy-5'-(methylsulfinyl)adenosine, Norphthalamic acid, and Alpha-CEHC. ROC curve analysis showed good diagnostic effect for these metabolites (AUC > 0.7; Figure 4, Figure 5).

3.4 Potential biomarker identification and metabolic pathway analysis

KEGG pathway enrichment analysis of differential metabolites was performed using the Majorbio Cloud Platform. We identified nine pathways using $p < 0.05$ (Figure 6A) associated with the metabolites L-Aspartic Acid, Taurine, Mannose 6-phosphate, LysoPC(18:0), PC(17:0/0:0), and PC(18:0/0:0). Five of these pathways are particularly associated with ginsenoside Rg1 treatment of CFS, including *Taurine and hypotaurine metabolism*; *Arginine biosynthesis*; *Ether lipid metabolism*; *Alanine, aspartate and glutamate metabolism*; and *Pantothenate and CoA biosynthesis*. The Lipid metabolism category included the highest number of differential metabolites (Figure 6B).

The differential metabolites were imported into the MetScape database to construct a “Compound Gene” network (Figure 6C) consisting of 64 target proteins. The related differential metabolites included were L-Aspartic Acid, Taurine, Mannose 6-phosphate,



LysoPC(18:0) (1-Ornanyl-2-lyso-sn-glycero-3-phosphocholine), PC(17:0/0:0) (1-Acyl-sn-glycero-3-phosphocholine), and Palmitoyl-L-carnitine. Our results demonstrate that Taurine and Mannose 6-phosphate are key metabolic markers of ginsenoside Rg1 treatment of CFS.

3.5 Network analysis

3.5.1 Ginsenoside Rg1 acts on potential CFS targets

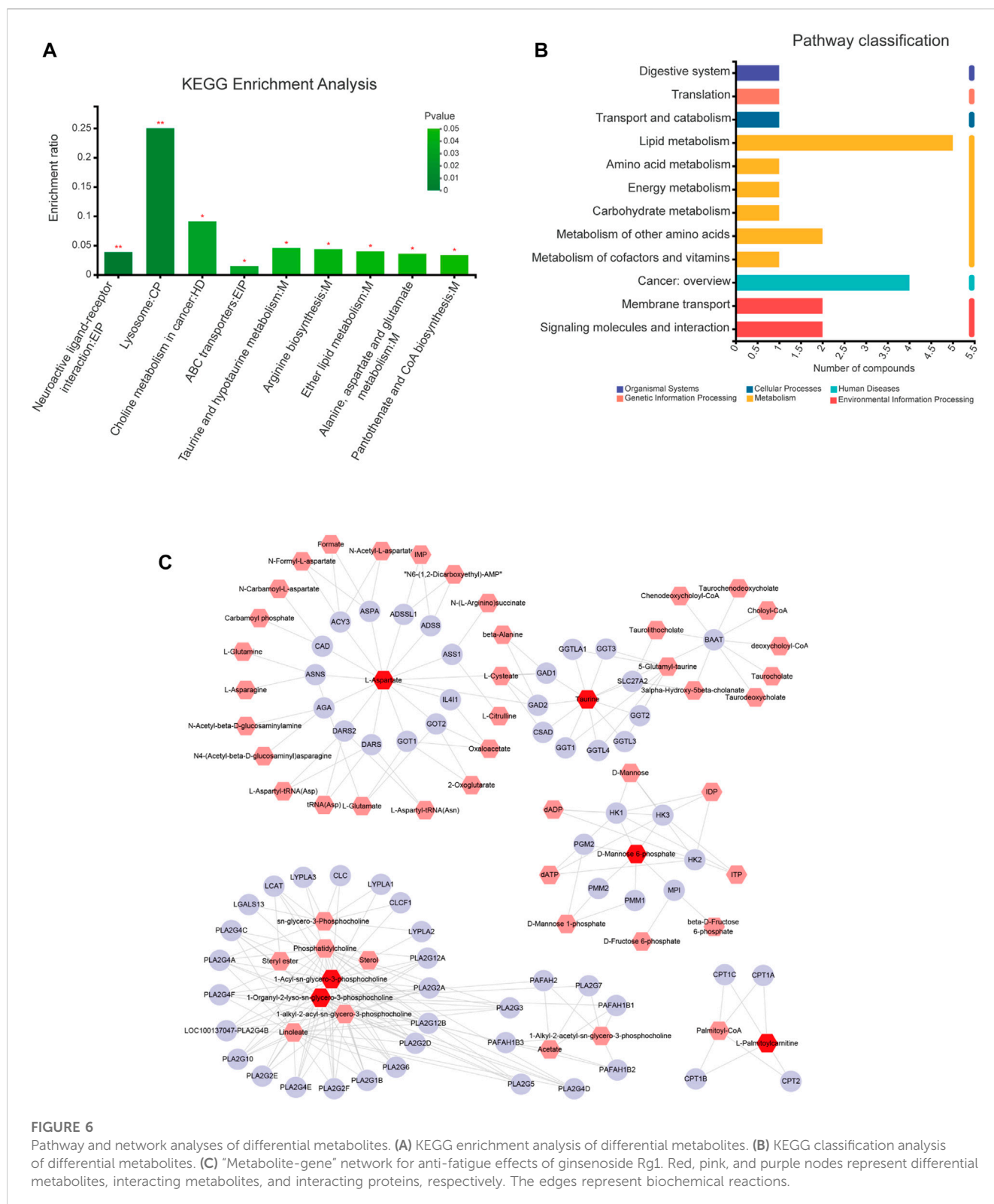
A total of 107 ginsenoside Rg1 targets were obtained through the BATMAN-TCM and SwissTargetPrediction databases. In addition, a total of 3796 disease targets of CFS were obtained from the Genecards, OMIM, and DRUGBANK databases. The differential metabolites were imported into the MetScape database to construct a “Compound-Gene” network, allowing us to identify a total of 64 target proteins (Figure 6C).

There were 72 identical targets of CFS and ginsenoside Rg1, and 15 identical targets of CFS and differential metabolites,

totaling 87 potential ginsenoside Rg1 targets for CFS treatment (Figure 7A).

3.5.2 Ginsenoside Rg1 pathways of action

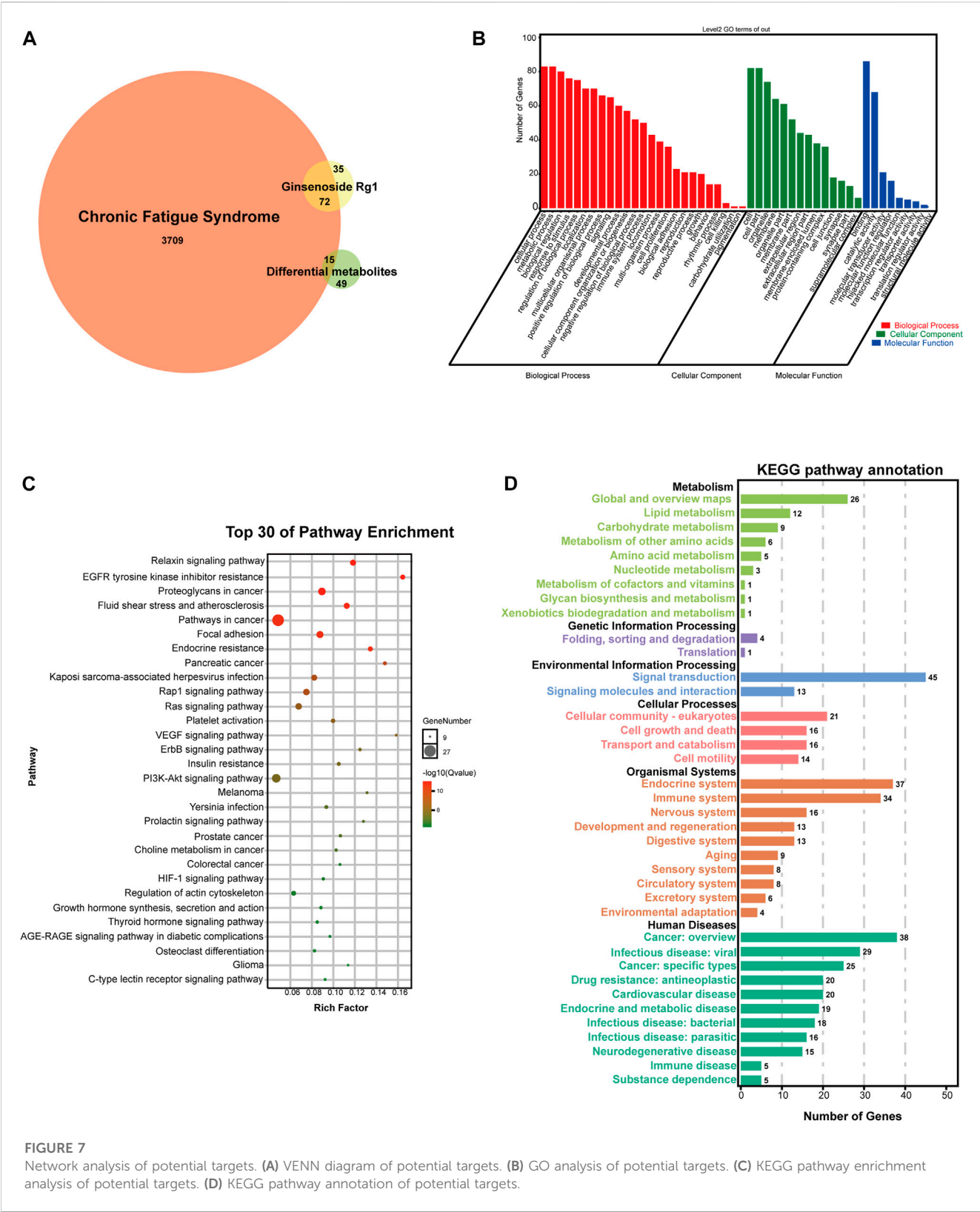
We used the OmicShare cloud platform to perform GO enrichment analysis and elucidate the biological associations of potential targets. We identified a total of 48 GO terms for ginsenoside Rg1, 25 for biological processes (BP), 14 for molecular functions (MF), and nine for cellular components (CC) (Figure 7B). BP results predicted the involvement of a high number of genes in cellular process, metabolic process, biological regulation, response to stimulus, localization, multicellular organismal process, positive developmental process, negative regulation of biological process, immune system process, locomotion, multi-organism process, cell proliferation, and biological adhesion. In addition, CC and MF results revealed that the anti-fatigue effects of ginsenoside Rg1 were mainly associated with cell, organelle, membrane, extracellular region, membrane-enclosed lumen, protein-containing complex, cell junction, synapse, supramolecular complex, catalytic



activity, molecular transducer activity, molecular function regulator, hijacked molecular function, transcription regulator activity.

We also performed KEGG analysis to evaluate the functional pathways associated with ginsenoside Rg1 treatment of CFS.

Figure 7C shows the top 30 signaling pathways obtained from the KEGG enrichment, while Figure 7D shows KEGG pathway annotation. The main therapeutic pathways associated with ginsenoside Rg1 treatment are EGFR tyrosine kinase inhibitor



resistance, Relaxin signaling pathway, Endocrine resistance, Rap1 signaling pathway, Ras signaling pathway, VEGF signaling pathway, ErbB signaling pathway, PI3K-Akt signaling pathway,

Prolactin signaling pathway, HIF-1 signaling pathway. An annotated statistical diagram of these pathways revealed ginsenoside Rg1 anti-fatigue effect impacts the Immune system,

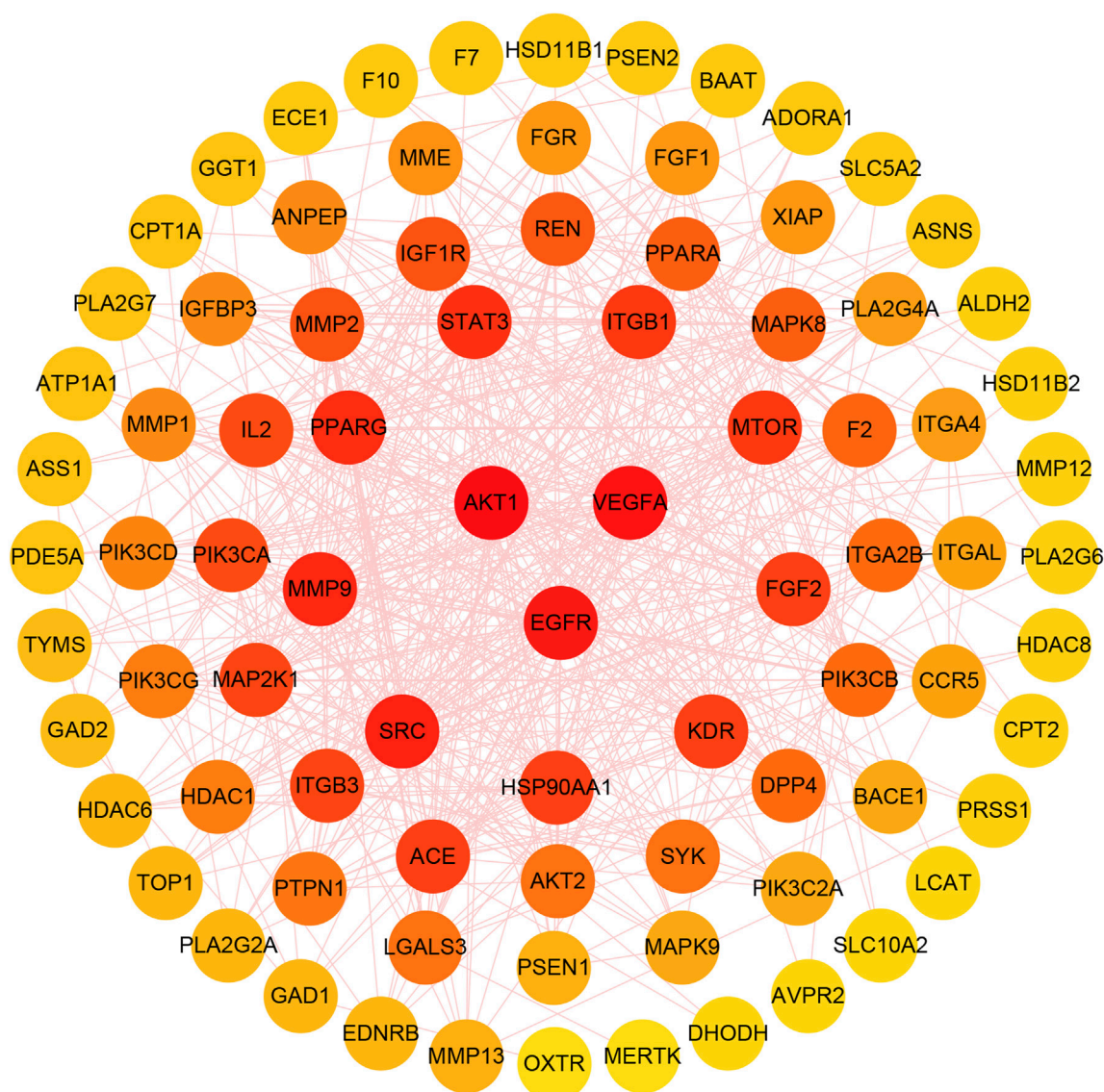


FIGURE 8

The gradual change of circle colors from red to yellow represents the change in Degree values, from large to small. The three targets in the center of the figure have the highest Degree values.

Nervous system, Endocrine system, Lipid metabolism, Amino acid metabolism, Metabolism of cofactors and vitamins.

3.5.3 PPI network analysis of ginsenoside Rg1's anti-fatigue effects

The protein-protein interaction relationship of potential targets was obtained through the STRING database and consisted of a PPI network containing 87 nodes and 587 edges. This information was imported into Cytoscape3.7.1 software to visualize network relationships. The CytoHubba function was used to calculate the Degree. The results show that the top three targets were AKT1, VEGFA and EGFR, with degrees of 49, 44 and 43, respectively. These targets were therefore considered as key anti-fatigue targets of ginsenoside Rg1 (Figure 8).

3.6 Effects of ginsenoside Rg1 treatment on mRNA expression of AKT1, VEGFA and EGFR

The mRNA expressions of AKT1, VEGFA and EGFR in the rat hippocampus and prefrontal cortex are shown in Figures 9A,B. In the hippocampus, VEGFA expression was increased in the CFS + Rg1 group compared to the Control group ($p = 0.043$), while the CFS + Rg1 showed increased expressions of AKT1 and VEGFA compared to CFS ($p = 0.001$, $p = 0.015$). The expression of EGFR remained relatively constant. As for the prefrontal cortex, VEGFA expression was significantly decreased in CFS + Rg1 compared to Control ($p = 0.005$), and EGFR expression was significantly increased in CFS ($p = 0.002$). In addition, VEGFA and EGFR levels were significantly lower in the CFS+ Rg1 group

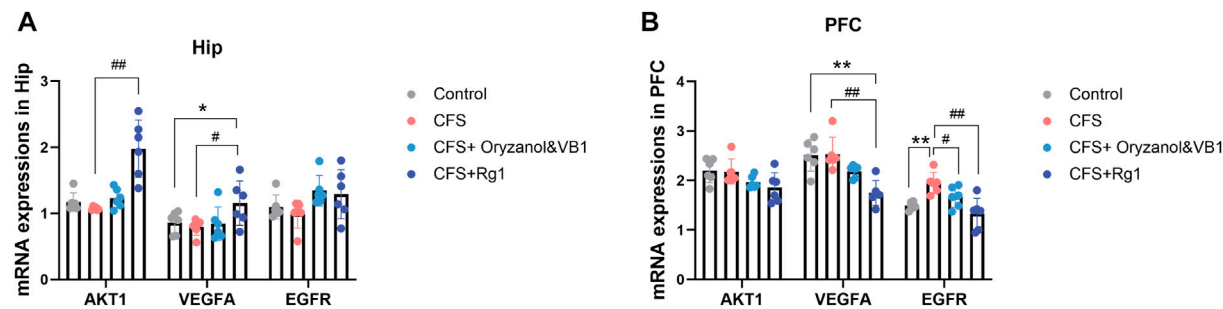


FIGURE 9
(A) Relative mRNA expression of AKT1, VEGFA and EGFR in the hippocampus (Hip) after 2 weeks of treatment. (B) Relative mRNA expression of AKT1, VEGFA and EGFR in the prefrontal cortex (PFC) after 2 weeks of treatment. Data are mean \pm standard deviation, $n = 6$. * $p < 0.05$, ** $p < 0.01$ versus Control group; # $p < 0.05$, ## $p < 0.01$ versus CFS group.

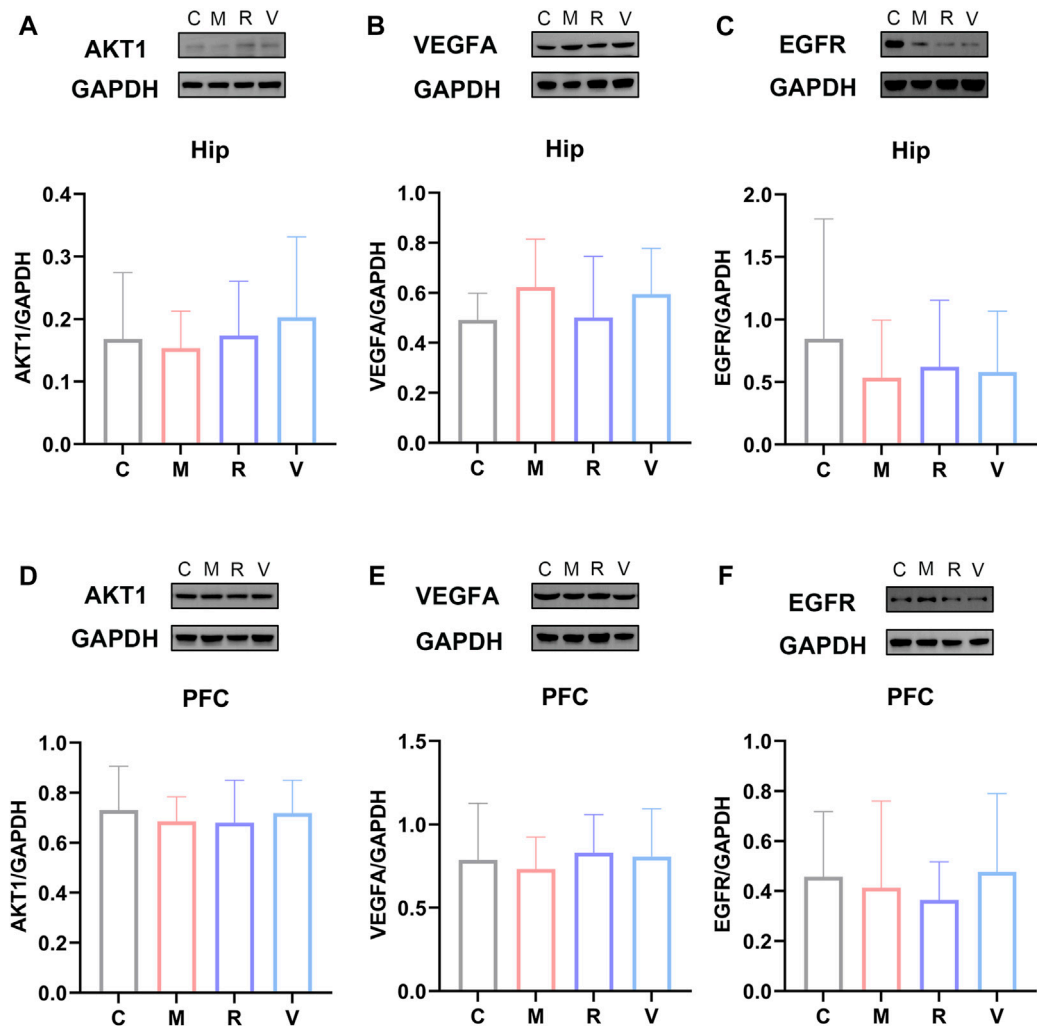


FIGURE 10
Relative protein expression of AKT1 (A), VEGFA (B), and EGFR (C) in the hippocampus. Relative protein abundance of AKT1 (D), VEGFA (E) and EGFR (F) in the prefrontal cortex. C: Control group, M: CFS group, R: CFS + Rg1 group, and V: CFS+ Oryzanol&VB1 group. Data are mean \pm standard deviation, $n = 6$. * $p < 0.05$, ** $p < 0.01$ versus Control group; # $p < 0.05$, ## $p < 0.01$ versus CFS group.

compared with the CFS group ($p = 0.006$, $p < 0.001$) and EGFR levels were lower in the CFS+ Oryzanol&VB1 group ($p = 0.038$). These results show ginsenoside Rg1 regulates EGFR in the prefrontal cortex of CFS rats.

3.7 Protein expression levels of AKT1, VEGFA and EGFR

We performed western blot analysis to confirm the effect of ginsenoside Rg1 on the protein levels of AKT1, VEGFA and EGFR in the hippocampus and prefrontal cortex. As shown in Figure 10 (A, B, C), ginsenoside Rg1 up-regulates AKT1, EGFR and down-regulates VEGFA protein expression in the hippocampus, despite no statistical significance ($p > 0.05$). In the prefrontal cortex, ginsenoside Rg1 up-regulates VEGFA and down-regulates EGFR protein expression, with no statistical significance ($p > 0.05$) (Figures 10 D, E, F). EGFR protein and mRNA levels were similar in the prefrontal cortex. These results show ginsenoside Rg1 produces anti-fatigue effects by down-regulating EGFR expression.

4 Discussion

Chronic fatigue syndrome, also known as myalgic encephalomyelitis, is an underappreciated debilitating disease with a significant impact on patient quality of life (Bornstein et al., 2022). CFS is characterized by chronic, disabling and multi-system disease with no effective treatment methods or diagnostic markers available at present (König et al., 2021; Wirth et al., 2021). CFS is associated with a variety of diseases, such as brucellosis, coronavirus infection, depression, and cancer. Recent studies found that patients recovering from COVID-19 may have persistent debilitating symptoms, and CFS remains the most dominant and common trait in these patients (Bansal et al., 2022). Current treatment guidelines for CFS mainly include cognitive behavioral therapy, graded exercise program and symptomatic therapy (Sapra and Bhandari, 2022), with limited clinical efficacy (Fang et al., 2022). In China, herbal medicine is widely used to treat CFS (Joung et al., 2019; Shin et al., 2021), with a previous meta-analysis showing TCM is safe and effective for CFS treatment (Zhang et al., 2022), which has sparked interest in its application (Wang et al., 2014; Dai et al., 2019; Zhang et al., 2020; Yang et al., 2022).

In this study, we explored the metabolic fingerprints and potential mechanisms of action of ginsenoside Rg1 in CFS treatment. We used multi-factor modeling (load-weighted forced swimming and restriction) to verify the anti-fatigue effects of ginsenoside Rg1 in CFS rats. The forced swimming animal model presents the core symptoms of CFS, such as fatigue and behavioral and cognitive abnormalities, but also pathological changes that have been found in CFS clinical studies (Sarma et al., 2015; Li and Han, 2022). Similarly, chronic restriction is simple to implement and can significantly induce fatigue symptoms (Li and Han, 2022). The rotarod test is widely used to assess athletic endurance with high reproducibility. In fact, the improvement of exercise tolerance is the strongest evidence for the existence of anti-fatigue effects (Kwon et al., 2021). In this study, CFS rats showed a decline in exercise

tolerance that could be reversed by ginsenoside Rg1. The Open field test is a classic experimental method that reflects the spontaneous activity behavior of rats in an unfamiliar environment and is used to evaluate the locomotor ability of rats (Ferreira et al., 2022). We showed that the total movement distance in the CFS group was significantly reduced, as illustrated by decreased exercise ability that is also observed in clinical CFS patients (Aerenhouts et al., 2015). D-xylose is a common symptom of spleen deficiency and often used to evaluate intestinal absorption (Zeyue et al., 2022). We found that the D-xylose-excretion rate of CFS rats was statistically different from that of the Control group, indicating that a spleen deficiency syndrome model was successfully established. Accordingly, under similar feeding conditions, CFS mainly affects the gastrointestinal absorption function of rats to induce weight loss. These results demonstrated that the anti-fatigue effect of ginsenoside Rg1 was related to exercise tolerance, spontaneous activity and intestinal absorption function in CFS rats.

We identified 34 differential metabolites in the LC-MS analysis of non-targeted serum metabolites. These metabolites are involved in Taurine and hypotaurine metabolism, Arginine biosynthesis, Ether lipid metabolism, Alanine, aspartate and glutamate metabolism, and Pantothenate and CoA biosynthesis. In addition, we have found that Taurine and Mannose 6-phosphate are key metabolic markers of ginsenoside Rg1 in the treatment of CFS. Previous results showed that the differential metabolites identified here were also associated with CFS in different contexts and animal models, which attests the validity of our work. Among these metabolites, Taurine plays a specifically important role (Germain et al., 2017; Glass et al., 2023). Germain et al. found that CFS patients had low Taurine content, which was mainly affected by lipid metabolism and amino acids (Germain et al., 2017). Taurine is an internal metabolite that acts as an antioxidant and anti-fatigue agent (Schaffer and Kim, 2018), and represents the second most abundant amino acid in human muscle after glutamic acid (Ripps and Shen, 2012). Corsetti et al. suggested that Taurine content is a useful indicator of muscle injury and possible long-term fatigue (Corsetti et al., 2016), as documented by other studies (Luckose et al., 2015; Khalil et al., 2018; Thirupathi et al., 2018; Vidot et al., 2018). Yatabe et al. found that the use of Taurine significantly increased the duration of running time to exhaustion in rats (Yatabe et al., 2009). Moreover, a systematic review showed low-dose Taurine (0.05 g) can reduce muscle fatigue, which suggests it may be an effective drug, especially in high-intensity activities (Chen et al., 2021). Interestingly, Taurine used as a nutritional supplement promotes recovery from muscle injury caused by vigorous exercise (Wei et al., 2021). In addition, Liu et al. found that the therapeutic effect of ginseng on spleen deficiency rats may be realized by regulating Taurine and hypotaurine metabolism, and its metabolites can be used as potential biomarkers for the diagnosis and monitoring of spleen deficiency (Liu et al., 2022). Armstrong et al. analyzed the metabolic profile of the blood and urine of CFS patients and found that CFS patients had abnormal metabolism of alanine, aspartate, glutamate and other energy (Armstrong et al., 2015). These findings confirm the reliability of our results.

Network analysis showed that AKT1, VEGFA and EGFR were the key targets of ginsenoside Rg1 for enabling anti-fatigue effects. AKT1 encodes serine/threonine kinases that play an important role in several normal and pathological cell processes (Millischer et al.,

2020), and a deficiency in AKT1 increases energy consumption (Wan et al., 2012). A randomized controlled trial found that AKT1 is an important core target for the treatment of cancer-induced fatigue (Cui et al., 2022). Furthermore, Liu et al. found that ginsenosides could enhance mice body ability and play an anti-fatigue role by upregulating the expression of AKT1 (Liu et al., 2019). We present similar results here and showed ginsenoside Rg1 up-regulates AKT1 protein expression despite not significantly. VEGFA is a key regulator of vascular growth. Angiogenesis in skeletal muscle can maintain oxygen and nutrient supply and clear metabolic byproducts that may lead to fatigue (Mohamad Shalan et al., 2016), which is associated with decreased levels of VEGFA (Wågström et al., 2021). A study on metabolic gene polymorphisms conducted progressive fatigue tests on athletes and identified VEGFA rs2010963C as an “endurance allele” of elite athletes (Ahmetov et al., 2009). We showed that CFS rats have decreased VEGFA levels in the prefrontal cortex, similar to patients with chronic fatigue (Landi et al., 2016).

The pathogenesis of CFS is closely related to the central nervous system (Mohamad Shalan et al., 2016; Sapra and Bhandari, 2022), with this syndrome being included in the neurology category (8E49) in ICD-11 (Gandasegui et al., 2021). In fatigue tests, reduced hippocampus activation is associated with HPA axis dysfunction and higher fatigue ratings (Klaassen et al., 2013). Saury JM et al. believes that the hippocampus plays an important role in the pathogenesis of CFS, and the trigger factors of CFS will also affect the hippocampus, leading to neurocognitive defects and disorders in the regulation of the pressure system and pain perception, which will further affect the hippocampus and trigger a vicious cycle of increased disability (Saury, 2016). There is a negative correlation between fatigue and hippocampus volume in CFS patients (Thapaliya et al., 2022). In addition, the prefrontal cortex has been identified as critical to fatigue (Ifuku et al., 2014). Bilateral prefrontal cortex volume was reduced in CFS patients, and the level of volume reduction in the right prefrontal cortex was correlated with the severity of fatigue (Nakatomi et al., 2014). An fMRI study found abnormal signals of functional activity in the prefrontal cortex of CFS patients (Caseras et al., 2006). These findings all support a strong link between the hippocampus, the prefrontal cortex, and CFS. We further performed PCR and Western Blot analyses on three key targets on the hippocampus and prefrontal cortex of CFS rats. Our results suggest that ginsenoside Rg1 can down-regulate the EGFR protein and mRNA expression. These observations have far-reaching significance for exploring the anti-fatigue mechanism of ginsenoside Rg1 at the molecular level. EGFR is an epidermal growth factor receptor and membrane surface receptor with tyrosine kinase activity (Cheng et al., 2022). Elevated levels of circulating ligands of EGFR, such as epidermal growth factor (EGF) and transforming growth factor α (TGF- α), can inhibit neural signals that drive normal behavior (Rich et al., 2017). Moreover, EGFR activation can stimulate the production of reactive oxygen species (ROS) by stimulating the PI3K pathway (Mansour et al., 2021). Previous studies showed ROS-induced mitochondrial function decline is related to fatigue (Nicolson, 2007; Pieczenik and Neustadt, 2007), and long-term oxidative stress can trigger CFS (Morris et al., 2017). At the same time, the level of oxidative stress in CFS patients is increased and correlated with clinical symptoms (Kennedy et al., 2005). Excessive ROS triggers oxidative stress, which

is positively correlated with the severity of CFS symptoms (Gupta et al., 2010). Recent studies showed serum samples from CFS patients induce the production of ROS and nitric oxide in human HMC3 microglia (Gottschalk et al., 2022). A randomized controlled trial found that ginseng can reduce ROS levels in chronic fatigue patients and play an anti-fatigue role (Kim et al., 2013), which corroborates our observations.

5 Conclusion

This study explored for the first time the pharmacological mechanisms of ginsenoside Rg1 in CFS treatment using a comprehensive metabolomic model, network analysis and biological methods. We systematically elucidated the multi-target and multi-mechanisms behind ginsenoside Rg1 anti-fatigue effects. Ginsenoside Rg1 can effectively treat CFS by regulating expression levels of AKT1, VEGFA and EGFR, and interfering with the metabolism of Taurine and Mannose 6-phosphate. We experimentally confirmed that EGFR is the most critical target. These findings provide a theoretical basis for the clinical application of ginsenoside Rg1 for CFS treatment.

Data availability statement

The raw data supporting the conclusions of this article will be made available by the authors, without undue reservation.

Ethics statement

The animal study was reviewed and approved by Animal Care and Therapy Ethics Committee of the Beijing University of Chinese Medicine.

Author contributions

CL wrote the manuscript. YL and JC designed the experiments. ZH, YM, YQ, MY, XX and LL performed the experiments. XZ and YJ assisted on dealing with the statistical data. YL and JC revised and proof-read the manuscript. All the authors have read and approved the final version of the manuscript.

Funding

This work was supported by Beijing Natural Science Foundation (No. 7212182), National Natural Science Foundation of China (No. 81603514).

Conflict of interest

The authors declare that the research was conducted in the absence of any commercial or financial relationships that could be construed as a potential conflict of interest.

Publisher's note

All claims expressed in this article are solely those of the authors and do not necessarily represent those of their affiliated

References

- Aerenhouts, D., Ickmans, K., Clarys, P., Zinzen, E., Meersdom, G., Lambrecht, L., et al. (2015). 'Sleep characteristics, exercise capacity and physical activity in patients with chronic fatigue syndrome. *Disabil. Rehabil.* 37, 2044–2050. doi:10.3109/09638288.2014.993093
- AhmetovII, Williams, A. G., Popov, D. V., Lyubaeva, E. V., Hakimullina, A. M., Fedotovskaya, O. N., et al. (2009). 'The combined impact of metabolic gene polymorphisms on elite endurance athlete status and related phenotypes. *Hum. Genet.* 126, 751–761. doi:10.1007/s00439-009-0728-4
- Armstrong, C. W., McGregor, N. R., Butt, H. L., and Gooley, P. R. (2014). 'Metabolism in chronic fatigue syndrome. *Adv. Clin. Chem.* 66, 121–172. doi:10.1016/b978-0-12-801401-1.00005-0
- Armstrong, C. W., McGregor, N. R., Lewis, D. P., Butt, H. L., and Gooley, P. R. (2015). 'Metabolic profiling reveals anomalous energy metabolism and oxidative stress pathways in chronic fatigue syndrome patients. *Metabolomics* 11, 1626–1639. doi:10.1007/s11306-015-0816-5
- Bansal, R., Gubbi, S., and Koch, C. A. (2022). 'COVID-19 and chronic fatigue syndrome: An endocrine perspective. *J. Clin. Transl. Endocrinol.* 27, 100284. doi:10.1016/j.jcte.2021.100284
- Bested, A. C., and Marshall, L. M. (2015). Review of myalgic encephalomyelitis/chronic fatigue syndrome: An evidence-based approach to diagnosis and management by clinicians. *Rev. Environ. Health* 30, 223–249. doi:10.1515/revheh-2015-0026
- Bornstein, S. R., Voit-Bak, K., Donate, T., Rodionov, R. N., Gainetdinov, R. R., Tselmin, S., et al. (2022). Chronic post-COVID-19 syndrome and chronic fatigue syndrome: Is there a role for extracorporeal apheresis? *Mol. Psychiatry* 27, 34–37. doi:10.1038/s41380-021-01148-4
- Caseras, X., Mataix-Cols, D., Giampietro, V., Rimes, K. A., Brammer, M., Zelaya, F., et al. (2006). 'Probing the working memory system in chronic fatigue syndrome: A functional magnetic resonance imaging study using the n-back task. *Psychosom. Med.* 68, 947–955. doi:10.1097/01.psy.0000242770.50979.5f
- Chaves-Filho, A. J. M., Macedo, D. S., de Lucena, D. F., and Maes, M. (2019). 'Shared microglial mechanisms underpinning depression and chronic fatigue syndrome and their comorbidities. *Behav. Brain Res.* 372, 111975. doi:10.1016/j.bbr.2019.111975
- Chen, Q., Li, Z., Pinho, R. A., Gupta, R. C., Ugbole, U. C., Thirupathi, A., et al. (2021). 'The dose response of taurine on aerobic and strength exercises: A systematic review. *Front. Physiol.* 12, 700352. doi:10.3389/fphys.2021.700352
- Cheng, L., Wang, F., Li, Z. H., Wen, C., Ding, L., Zhang, S. B., et al. (2022). 'Study on the active components and mechanism of Suanzaoren decoction in improving cognitive impairment caused by sleep deprivation. *J. Ethnopharmacol.* 296, 115502. doi:10.1016/j.jep.2022.115502
- Corsetti, R., Barassi, A., Perego, S., Sansoni, V., Rossi, A., Damele, C. A., et al. (2016). 'Changes in urinary amino acids excretion in relationship with muscle activity markers over a professional cycling stage race: In search of fatigue markers. *Amino Acids* 48, 183–192. doi:10.1007/s00726-015-2077-z
- Cui, Y., Mi, J., Feng, Y., Li, L., Wang, Y., Hu, J., et al. (2022). '[Huangqi sijunzi decoction for treating cancer-related fatigue in breast cancer patients: A randomized trial and network pharmacology study]. *Nan Fang. Yi Ke Da Xue Xue Bao* 42, 649–657. doi:10.12122/j.issn.1673-4254.2022.05.04
- Cvejic, E., Birch, R. C., and Vollmer-Conna, U. (2016). 'Cognitive dysfunction in chronic fatigue syndrome: A review of recent evidence. *Curr. Rheumatol. Rep.* 18, 24. doi:10.1007/s11926-016-0577-9
- Dai, L., Zhou, W. J., Wang, M., Zhou, S. G., and Ji, G. (2019). 'Efficacy and safety of sijunzi decoction for chronic fatigue syndrome with spleen deficiency pattern: Study protocol for a randomized, double-blind, placebo-controlled trial. *Ann. Transl. Med.* 7, 587. doi:10.21037/atm.2019.09.136
- Fang, Y., Yue, B. W., Ma, H. B., and Yuan, Y. P. (2022). *Acupuncture and moxibustion for chronic fatigue syndrome: A systematic review and network meta-analysis*, 101, e29310. doi:10.1097/md.00000000000029310Med. Baltim.
- Feng, Yichong, Xu, Zhiwei, Pan, Huashan., and Zhao, Ziming. (2010). 'Effects of ginsenoside Rg1 on structure and function of rat skeletal muscle with exercise-induced fatigue. *J. Guangzhou Univ. Traditional Chin. Med.* 27, 40–44. doi:10.13359/j.cnki.gzxbtcm.2010.01.018
- Ferreira, J. S., Leite Junior, J. B., de Mello Bastos, J. M., Samuels, R. I., Carey, R. J., and Carrera, M. P. (2022). 'A new method to study learning and memory using spontaneous locomotor activity in an open-field arena. *J. Neurosci. Methods* 366, 109429. doi:10.1016/j.jneumeth.2021.109429
- Gandasegui, I. M., Laka, L. A., Gargiulo, P. Á., Gómez-Esteban, J. C., and Sánchez, J. L. (2021). Myalgic encephalomyelitis/chronic fatigue syndrome: A neurological entity? *Med. Kaunas*. 57, 1030. doi:10.3390/medicina57101030
- Geng, L., and Wang, Y. (2012). Spleen deficiency is the core pathogenesis of chronic fatigue syndrome. *J. Heilongjiang Traditional Chin. Med.* 41, 8–9. doi:10.3969/j.issn.1000-9906.2012.04.003
- Germain, A., Ruppert, D., Levine, S. M., and Hanson, M. R. (2017). 'Metabolic profiling of a myalgic encephalomyelitis/chronic fatigue syndrome discovery cohort reveals disturbances in fatty acid and lipid metabolism. *Mol. Biosyst.* 13, 371–379. doi:10.1039/c6mb00600k
- Glass, K. A., Germain, A., Huang, Y. V., and Hanson, M. R. (2023). 'Urine metabolomics exposes anomalous recovery after maximal exertion in female ME/CFS patients. *Int. J. Mol. Sci.* 24, 3685. doi:10.3390/ijms24043685
- Gottschalk, G., Peterson, D., Knox, K., Maynard, M., Whelan, R. J., and Roy, A. (2022). 'Elevated ATG13 in serum of patients with ME/CFS stimulates oxidative stress response in microglial cells via activation of receptor for advanced glycation end products (RAGE). *Mol. Cell. Neurosci.* 120, 103731. doi:10.1016/j.mcn.2022.103731
- Gupta, A., Vij, G., and Chopra, K. (2010). 'Possible role of oxidative stress and immunological activation in mouse model of chronic fatigue syndrome and its attenuation by olive extract. *J. Neuroimmunol.* 226, 3–7. doi:10.1016/j.jneuroim.2010.05.021
- He, J., Yu, Q., Wu, C., Sun, Z., Wu, X., Liu, R., et al. (2020). 'Acupuncture of the Beishu acupoint participates in regulatory effects of ginsenoside Rg1 on T cell subsets of rats with chronic fatigue syndrome. *Ann. Palliat. Med.* 9, 3436–3446. doi:10.21037/apm-20-1714
- Heinrich, M., Appendino, G., Efferth, T., Fürst, R., Izzo, A. A., Kayser, O., et al. (2020). 'Best practice in research - overcoming common challenges in phytopharmacological research. *J. Ethnopharmacol.* 246, 112230. doi:10.1016/j.jep.2019.112230
- Ifuku, M., Hossain, S. M., Noda, M., and Katafuchi, T. (2014). 'Induction of interleukin-1 β by activated microglia is a prerequisite for immunologically induced fatigue. *Eur. J. Neurosci.* 40, 3253–3263. doi:10.1111/ejn.12668
- Joung, J. Y., Lee, J. S., Cho, J. H., Lee, D. S., Ahn, Y. C., and Son, C. G. (2019). 'The efficacy and safety of myelophil, an ethanol extract mixture of astragali radix and salviae radix, for chronic fatigue syndrome: A randomized clinical trial. *Front. Pharmacol.* 10, 991. doi:10.3389/fphar.2019.00991
- Kennedy, G., Spence, V. A., McLaren, M., Hill, A., Underwood, C., and Belch, J. J. (2005). 'Oxidative stress levels are raised in chronic fatigue syndrome and are associated with clinical symptoms. *Free Radic. Biol. Med.* 39, 584–589. doi:10.1016/j.freeradbiomed.2005.04.020
- Khalil, R. M., Abdo, W. S., Saad, A., and Khedr, E. G. (2018). 'Muscle proteolytic system modulation through the effect of taurine on mice bearing muscular atrophy. *Mol. Cell. Biochem.* 444, 161–168. doi:10.1007/s11010-017-3240-5
- Kim, H. G., Cho, J. H., Yoo, S. R., Lee, J. S., Han, J. M., Lee, N. H., et al. (2013). 'Antifatigue effects of Panax ginseng C.A. Meyer: A randomized, double-blind, placebo-controlled trial. *PLoS One* 8, e61271. doi:10.1371/journal.pone.0061271
- Klaassen, E. B., de Groot, R. H., Evers, E. A., Nicolson, N. A., Veltman, D. J., and Jolles, J. (2013). 'Cortisol and induced cognitive fatigue: Effects on memory activation in healthy males. *Biol. Psychol.* 94, 167–174. doi:10.1016/j.biopsycho.2013.05.015
- König, R. S., Albrich, W. C., Kahlert, C. R., Bahr, L. S., Löber, U., Vernazza, P., et al. (2021). The gut microbiome in myalgic encephalomyelitis (ME)/Chronic fatigue syndrome (CFS). *Front. Immunol.* 12, 628741. doi:10.3389/fimmu.2021.628741
- Kwon, D. A., Kim, Y. S., Kim, S. K., Baek, S. H., Kim, H. K., and Lee, H. S. (2021). 'Antioxidant and antifatigue effect of a standardized fraction (HemoHIM) from Angelica gigas, Cnidium officinale, and Paeonia lactiflora. *Pharm. Biol.* 59, 391–400. doi:10.1080/13880209.2021.1900878
- Landi, A., Broadhurst, D., Vernon, S. D., Tyrrell, D. L., and Houghton, M. (2016). 'Reductions in circulating levels of IL-16, IL-7 and VEGF-A in myalgic encephalomyelitis/chronic fatigue syndrome. *Cytokine* 78, 27–36. doi:10.1016/j.cyto.2015.11.018
- Lei, C., Chen, Z., Fan, L., Xue, Z., Chen, J., Wang, X., et al. (2022). 'Integrating metabolomics and network analysis for exploring the mechanism underlying the antidepressant activity of paeoniflorin in rats with CUMS-induced depression. *Front. Pharmacol.* 13, 904190. doi:10.3389/fphar.2022.904190
- Li, Y., and Han, X. (2022). 'Construction and evaluation of animal models of chronic fatigue syndrome. *Chin. J. Exp. Traditional Med. Formulae* 29, 234–242. doi:10.13422/j.cnki.syfjx.20230999

- Li, Q., Wang, L., Fang, X., and Zhao, L. (2022). 'Highly efficient biotransformation of notoginsenoside R1 into ginsenoside Rg1 by dictyoglomus thermophilum β -xylosidase xln-DT. *J. Microbiol. Biotechnol.* 32, 447–457. doi:10.4014/jmb.2111.11020
- Lim, E. J., Lee, J. S., Lee, E. J., Jeong, S. J., Park, H. Y., Ahn, Y. C., et al. (2021). 'Nationwide epidemiological characteristics of chronic fatigue syndrome in South Korea. *J. Transl. Med.* 19, 502. doi:10.1186/s12967-021-03170-0
- Liu, F. X., Lin, Z. X., Zhang, H. L., Zhang, Z. Q., Yang, K. Q., Fan, X. F., et al. (2019). '[Analysis of anti-fatigue mechanism and potential targets of ginseng]. *Zhongguo Zhong Yao Za Zhi* 44, 5479–5487. doi:10.19540/j.cnki.cjcm.20190805.401
- Liu, M., Li, F., Cai, Y., Xie, D., Wu, Y., Zhang, M., et al. (2022). 'Intervention effects of ginseng on spleen-qi deficiency in rats revealed by GC-MS-based metabonomic approach. *J. Pharm. Biomed. Anal.* 217, 114834. doi:10.1016/j.jpba.2022.114834
- Luckose, F., Pandey, M. C., and Radhakrishna, K. (2015). 'Effects of amino acid derivatives on physical, mental, and physiological activities. *Crit. Rev. Food Sci. Nutr.* 55, 1793–1807. doi:10.1080/10408398.2012.708368
- Ma, P., Peng, Y., Zhao, L., Liu, F., and Li, X. (2021). Differential effect of polysaccharide and nonpolysaccharide components in Sijunzi decoction on spleen deficiency syndrome and their mechanisms. *Phytomedicine* 93, 153790. doi:10.1016/j.phymed.2021.153790
- Mansour, H. M., Fawzy, H. M., El-Khatib, A. S., and Khatib, M. M. (2021). 'Potential repositioning of anti-cancer EGFR inhibitors in alzheimer's disease: Current perspectives and challenging prospects. *Neuroscience* 469, 191–196. doi:10.1016/j.neuroscience.2021.06.013
- Millischer, V., Matheson, G. J., Martinsson, L., Römer, I. E., Schalling, M., Lavebratt, C., et al. (2020). 'AKT1 and genetic vulnerability to bipolar disorder. *Psychiatry Res.* 284, 112677. doi:10.1016/j.psychres.2019.112677
- Mohamad Shalan, N. A., Mustapha, N. M., and Mohamed, S. (2016). 'Morinda citrifolia leaf enhanced performance by improving angiogenesis, mitochondrial biogenesis, antioxidant, anti-inflammatory & stress responses. *Food Chem.* 212, 443–452. doi:10.1016/j.foodchem.2016.05.179
- Mohanan, P., Subramaniyam, S., Mathiyalagan, R., and Yang, D. C. (2018). 'Molecular signaling of ginsenosides Rb1, Rg1, and Rg3 and their mode of actions. *J. Ginseng Res.* 42, 123–132. doi:10.1016/j.jgr.2017.01.008
- Moore, Y., Serafimova, T., Anderson, N., King, H., Richards, A., Brigden, A., et al. (2021). 'Recovery from chronic fatigue syndrome: A systematic review-heterogeneity of definition limits study comparison. *Arch. Dis. Child.* 106, 1087–1094. doi:10.1136/archdischild-2020-320196
- Morris, G., Berk, M., Klein, H., Walder, K., Galecki, P., and Maes, M. (2017). 'Nitrosative stress, hypernitrosylation, and autoimmune responses to nitrosylated proteins: New pathways in neuroprogressive disorders including depression and chronic fatigue syndrome. *Mol. Neurobiol.* 54, 4271–4291. doi:10.1007/s12035-016-9975-2
- Nacul, L., Authier, F. J., Scheibenbogen, C., Lorusso, L., Helland, I. B., Martin, J. A., et al. (2021). 'European network on myalgic encephalomyelitis/chronic fatigue syndrome (EUROMENE): Expert consensus on the diagnosis, service provision, and Care of people with ME/CFS in Europe. *Med. Kaunas.* 57, 510. doi:10.3390/medicina57050510
- Nagy-Szakal, D., Barupal, D. K., Lee, B., Che, X., Williams, B. L., Kahn, E. J. R., et al. (2018). 'Insights into myalgic encephalomyelitis/chronic fatigue syndrome phenotypes through comprehensive metabolomics. *Sci. Rep.* 8, 10056. doi:10.1038/s41598-018-28477-9
- Nakatomi, Y., Mizuno, K., Ishii, A., Wada, Y., Tanaka, M., Tazawa, S., et al. (2014). 'Neuroinflammation in patients with chronic fatigue syndrome/myalgic encephalomyelitis: An ^{11}C -(R)-PK11195 PET study. *J. Nucl. Med.* 55, 945–950. doi:10.2967/jnumed.113.131045
- Nguyen, C. B., Kumar, S., Zucknick, M., Kristensen, V. N., Gjerstad, J., Nilsen, H., et al. (2019). 'Associations between clinical symptoms, plasma norepinephrine and deregulated immune gene networks in subgroups of adolescent with Chronic Fatigue Syndrome. *Brain Behav. Immun.* 76, 82–96. doi:10.1016/j.bbi.2018.11.008
- Nicolson, G. L. (2007). 'Metabolic syndrome and mitochondrial function: Molecular replacement and antioxidant supplements to prevent membrane peroxidation and restore mitochondrial function. *J. Cell. Biochem.* 100, 1352–1369. doi:10.1002/jcb.21247
- Piecznik, S. R., and Neustadt, J. (2007). 'Mitochondrial dysfunction and molecular pathways of disease. *Exp. Mol. Pathol.* 83, 84–92. doi:10.1016/j.yexmp.2006.09.008
- Rich, T., Zhao, F., Cruciani, R. A., Cella, D., Manola, J., and Fisch, M. J. (2017). 'Association of fatigue and depression with circulating levels of proinflammatory cytokines and epidermal growth factor receptor ligands: A correlative study of a placebo-controlled fatigue trial. *Cancer Manag. Res.* 9, 1–10. doi:10.2147/cmar.S115835
- Ripps, H., and Shen, W. (2012). Review: Taurine: A "very essential" amino acid. *Mol. Vis.* 18, 2673–2686.
- Sandler, C. X., and Lloyd, A. R. (2020). 'Chronic fatigue syndrome: Progress and possibilities. *Med. J. Aust.* 212, 428–433. doi:10.5694/mja2.50553
- Sapra, A., and Bhandari, P. (2022). "Chronic fatigue syndrome," in *StatPearls* (Treasure Island (FL): StatPearls Publishing Copyright © 2022, StatPearls Publishing LLC).
- Sarma, P., Borah, M., and Das, S. (2015). 'Evaluation of the effect of ethanolic extract of fruit pulp of *Cassia fistula* Linn. on forced swimming induced chronic fatigue syndrome in mice. *Res. Pharm. Sci.* 10, 206–213. doi:10.1016/0016-6480(84)90098-4
- Saury, J. M. (2016). The role of the hippocampus in the pathogenesis of myalgic encephalomyelitis/chronic fatigue syndrome (ME/CFS). *Med. Hypotheses* 86, 30–38. doi:10.1016/j.mehy.2015.11.024
- Schaffer, S., and Kim, H. W. (2018). 'Effects and mechanisms of taurine as a therapeutic agent. *Biomol. Ther. Seoul.* 26, 225–241. doi:10.4062/biomolther.2017.251
- Shao, C., Ren, Y., Wang, Z., Kang, C., Jiang, H., and Chi, A. (2017). Detection of urine metabolites in a rat model of chronic fatigue syndrome before and after exercise. *Biomed. Res. Int.* 2017, 8182020. doi:10.1155/2017/8182020
- Shi, J., Shen, J., Xie, J., Zhi, J., and Xu, Y. (2018). Chronic fatigue syndrome in Chinese middle-school students. *Med. Baltim.* 97, e9716. doi:10.1097/md.00000000000009716
- Shin, S., Park, S. J., and Hwang, M. (2021). 'Effectiveness a herbal medicine (Sipjeondaebotang) on adults with chronic fatigue syndrome: A randomized, double-blind, placebo-controlled trial. *Integr. Med. Res.* 10, 100664. doi:10.1016/j.imr.2020.100664
- Thapaliya, K., Staines, D., Marshall-Gradinsnik, S., Su, J., and Barnden, L. (2022). 'Volumetric differences in hippocampal subfields and associations with clinical measures in myalgic encephalomyelitis/chronic fatigue syndrome. *J. Neurosci. Res.* 100, 1476–1486. doi:10.1002/jnr.25048
- Thirupathi, A., Freitas, S., Sorato, H. R., Pedrosa, G. S., Effting, P. S., Damiani, A. P., et al. (2018). 'Modulatory effects of taurine on metabolic and oxidative stress parameters in a mice model of muscle overuse. *Nutrition* 54, 158–164. doi:10.1016/j.nut.2018.03.058
- Vidot, H., Cvejic, E., Carey, S., Strasser, S. I., McCaughan, G. W., Allman-Farinelli, M., et al. (2018). 'Randomised clinical trial: Oral taurine supplementation versus placebo reduces muscle cramps in patients with chronic liver disease. *Aliment. Pharmacol. Ther.* 48, 704–712. doi:10.1111/apt.14950
- Wågström, P., Nilsdotter-Augustinsson, Å., Nilsson, M., Björkander, J., Dahle, C., and Nyström, S. (2021). 'Fatigue is common in immunoglobulin G subclass deficiency and correlates with inflammatory response and need for immunoglobulin replacement therapy. *Front. Immunol.* 12, 797336. doi:10.3389/fimmu.2021.797336
- Wan, M., Easton, R. M., Gleason, C. E., Monks, B. R., Ueki, K., Kahn, C. R., et al. (2012). 'Loss of Akt1 in mice increases energy expenditure and protects against diet-induced obesity. *Mol. Cell. Biol.* 32, 96–106. doi:10.1128/mcb.05806-11
- Wang, Y. Y., Li, X. X., Liu, J. P., Luo, H., Ma, L. X., and Alraek, T. (2014). 'Traditional Chinese medicine for chronic fatigue syndrome: A systematic review of randomized clinical trials. *Complement. Ther. Med.* 22, 826–833. doi:10.1016/j.ctim.2014.06.004
- Wang, P., Wang, Q., Yang, B., Zhao, S., and Kuang, H. (2015). 'The progress of metabolomics study in traditional Chinese medicine research. *Am. J. Chin. Med.* 43, 1281–1310. doi:10.1142/s0192415x15500731
- Wei, C., Zhao, S., Zhang, Y., Gu, W., Kumar Sarker, S., Liu, S., et al. (2021). 'Effect of multiple-nutrient supplement on muscle damage, liver, and kidney function after exercising under heat: Based on a pilot study and a randomised controlled trial. *Front. Nutr.* 8, 740741. doi:10.3389/fnut.2021.740741
- Wirth, K. J., Scheibenbogen, C., and Paul, F. (2021). 'An attempt to explain the neurological symptoms of Myalgic Encephalomyelitis/Chronic Fatigue Syndrome. *J. Transl. Med.* 19, 471. doi:10.1186/s12967-021-03143-3
- Xu, Y. X., Luo, H. S., Sun, D., Wang, R., and Cai, J. (2019). '[Acupuncture in the treatment of chronic fatigue syndrome based on "interaction of brain and kidney" in TCM: A randomized controlled trial]. *Zhongguo Zhen Jiu* 39, 123–127. doi:10.13703/j.0255-2930.2019.02.003
- Yang, J., Shin, K. M., Abu Dabrh, A. M., Bierle, D. M., Zhou, X., Bauer, B. A., et al. (2022). 'Ginseng for the treatment of chronic fatigue syndrome: A systematic review of clinical studies. *Glob. Adv. Health Med.* 11, 2164957x221079790. doi:10.1177/2164957x221079790
- Yatabe, Y., Miyakawa, S., Ohmori, H., Mishima, H., and Adachi, T. (2009). 'Effects of taurine administration on exercise. *Adv. Exp. Med. Biol.* 643, 245–252. doi:10.1007/978-0-387-75681-3_25
- Yousuf, S., Liu, H., Yingshu, Z., Zahid, D., Ghayas, H., Li, M., et al. (2022). 'Ginsenoside Rg1 modulates intestinal microbiota and supports re-generation of immune cells in dexamethasone-treated mice. *Acta Microbiol. Immunol. Hung* 69, 259–269. doi:10.1556/030.2022.01881
- Zeyue, Y. U., Liyu, H., Zongyuan, L. I., Jianhui, S., Hongying, C., Hairu, H., et al. (2022). 'Correlation between slow transit constipation and spleen deficiency, and gut microbiota: A pilot study. *J. Tradit. Chin. Med.* 42, 353–363. doi:10.19852/j.cnki.jtcm.20220408.002
- Zhang, X., Wang, M., and Zhou, S. (2020). Advances in clinical research on traditional Chinese medicine treatment of chronic fatigue syndrome. *Evid. Based Complement. Altern. Med.* 2020, 4715679. doi:10.1155/2020/4715679
- Zhang, Y., Jin, F., Wei, X., Jin, Q., Xie, J., Pan, Y., et al. (2022). 'Chinese herbal medicine for the treatment of chronic fatigue syndrome: A systematic review and meta-analysis. *Front. Pharmacol.* 13, 958005. doi:10.3389/fphar.2022.958005



OPEN ACCESS

EDITED BY

Chika Ifeanyi Chukwuma,
Central University of Technology, South
Africa

REVIEWED BY

Rinku Baishya,
North East Institute of Science and
Technology (CSIR), India
Ugochukwu Offor,
University of the Witwatersrand, South
Africa
Neeraj Kumar Sethiya,
DIT University, India

*CORRESPONDENCE

Nanaocha Sharma,
✉ sharma.nanaocha@gmail.com

RECEIVED 03 March 2023

ACCEPTED 04 April 2023

PUBLISHED 17 April 2023

CITATION

Chanu KD, Sharma N, Kshetrimayum V,
Chaudhary SK, Ghosh S, Haldar PK and
Mukherjee PK (2023), *Ageratina*
adenophora (Spreng.) King & H. Rob.
Standardized leaf extract as an
antidiabetic agent for type 2 diabetes: An
in vitro and *in vivo* evaluation.
Front. Pharmacol. 14:1178904.
doi: 10.3389/fphar.2023.1178904

COPYRIGHT

© 2023 Chanu, Sharma, Kshetrimayum,
Chaudhary, Ghosh, Haldar and
Mukherjee. This is an open-access article
distributed under the terms of the
[Creative Commons Attribution License](#)
(CC BY). The use, distribution or
reproduction in other forums is
permitted, provided the original author(s)
and the copyright owner(s) are credited
and that the original publication in this
journal is cited, in accordance with
accepted academic practice. No use,
distribution or reproduction is permitted
which does not comply with these terms.

Ageratina adenophora (Spreng.) King & H. Rob. Standardized leaf extract as an antidiabetic agent for type 2 diabetes: An *in vitro* and *in* *vivo* evaluation

Khaidem Devika Chanu^{1,2}, Nanaocha Sharma^{1*},
Vimi Kshetrimayum^{1,2}, Sushil Kumar Chaudhary¹, Suparna Ghosh³,
Pallab Kanti Haldar³ and Pulok K. Mukherjee¹

¹Institute of Bio-resources and Sustainable Development (IBSD), Imphal, Manipur, India, ²School of
Biotechnology, Kalinga Institute of Industrial Technology (KIIT), Deemed to Be University, Bhubaneswar,
Odisha, India, ³School of Natural Product Studies, Department of Pharmaceutical Technology, Jadavpur
University (JU), Kolkata, West Bengal, India

Type 2 diabetes has become one of the major health concerns of the 21st century, marked by hyperglycemia or glycosuria, and is associated with the development of several secondary health complications. Due to the fact that chemically synthesized drugs lead to several inevitable side effects, new antidiabetic medications from plants have gained substantial attention. Thus, the current study aims to evaluate the antidiabetic capacity of the *Ageratina adenophora* hydroalcoholic (AAHY) extract in streptozotocin–nicotinamide (STZ–NA)-induced diabetic Wistar albino rats. The rats were segregated randomly into five groups with six rats each. Group I was normal control, and the other four groups were STZ–NA-induced. Group II was designated diabetic control, and group III, IV, and V received metformin (150 mg/kg b.w.) and AAHY extract (200 and 400 mg/kg b.w.) for 28 days. Fasting blood glucose, serum biochemicals, liver and kidney antioxidant parameters, and pancreatic histopathology were observed after the experimental design. The study concludes that the AAHY extract has a significant blood glucose lowering capacity on normoglycemic (87.01 ± 0.54 to 57.21 ± 0.31), diabetic (324 ± 2.94 to 93 ± 2.04), and oral glucose-loaded (117.75 ± 3.35 to 92.75 ± 2.09) Wistar albino rats. The *in vitro* studies show that the AAHY extract has α -glucosidase and α -amylase inhibitory activities which can restore the altered blood glucose level, glycated hemoglobin, body weight, and serum enzymes such as serum glutamic pyruvic transaminase, serum glutamic oxaloacetic transaminase, serum alkaline phosphatase, total protein, urea, and creatinine levels close to the normal range in the treated STZ–NA-induced diabetic rats. The evaluation of these serum biochemicals is crucial for monitoring the diabetic condition. The AAHY extract has significantly enhanced tissue antioxidant parameters, such as superoxide dismutase, glutathione, and lipid peroxidation, close to normal levels. The presence of high-quantity chlorogenic (6.47% w/w) and caffeic (3.28% w/w) acids as some of the major phytoconstituents may contribute to the improvement of insulin resistance and oxidative stress. The study provides scientific support for the utilization of *A. adenophora* to treat type 2 diabetes in the STZ–NA-induced diabetic rat model. Although the preventive role of the AAHY extract in treating Wistar albino rat models against type 2 diabetes

mellitus is undeniable, further elaborative research is required for efficacy and safety assessment in human beings.

KEYWORDS

antidiabetic activity, *Ageratina adenophora*, streptozotocin–nicotinamide, type 2 diabetes, chlorogenic acid, caffeic acid

1 Introduction

A significant global health concern of the 21st century is the incidence of type 2 diabetes mellitus (T2DM) or diabetes mellitus (DM), which has reached an epidemic level (Chan et al., 2005). Hyperglycemia, hyperlipidemia or dyslipidemia, and glycosuria are the hallmarks of diabetes mellitus. It is a complex and multifactorial metabolic condition typically brought on by faulty protein, carbohydrate and fat metabolism, damaged pancreatic beta cells, insulin resistance, or insulin insufficiency (Oguntibeju, 2019). This metabolic condition led to increased blood glucose levels (BGLs) and develops into chronic, life-threatening microvascular, macrovascular, and neuropathic consequences over time. Nephropathy, retinopathy, cataract, neuropathy, cardiovascular, stroke, coronary artery diseases, and food-related diseases are among the many consequences linked to DM (Khurshed et al., 2019; Padhi et al., 2020). In 2017, it was projected that 415 million people have diabetes globally. By 2025, there will be 300 million adult cases, which are still expected to upsurge till 693 million by 2045. According to the predicted diabetic population, more than half (49.7%) are undiagnosed (Liu et al., 2013; Cho et al., 2018). In surge of the increasing incidence of DM, it becomes a necessity to curb this metabolic disorder. Several marketed antidiabetic drugs are in use with a goal to suppress the disease progression on a global scale. However, due to affordability and safety concerns, many researchers are inclined toward naturally occurring antidiabetic bioactive compounds from plant sources.

Biological-derived or chemical drugs such as sulfonylureas, thiazolidinediones, biguanides, meglitinides, α -glucosidase inhibitors, dipeptidyl peptidase-4 (DPP-4) inhibitors, glucagon-like peptide-1 (GLP1) receptor agonists, and dopamine D2-receptor agonists are currently the principal antidiabetic medications for diabetes mellitus (Blonde, 2009; Tahrani et al., 2011; He et al., 2019). Sulfonylureas thiazolidinediones, biguanides, and meglitinides act by stimulating insulin production; α -glucosidase inhibitors halt carbohydrate breakdown, thereby enhancing glycemic index; DPP-4 inhibitors and GLP1 receptor agonists enhance insulin production, while inhibiting glucagon secretion from pancreatic islets of Langerhans; and dopamine D2-receptor agonists enhance the glycemic index via activation of hypothalamic dopamine D2-receptors (Dahlén et al., 2022). The recovery of diabetic patients is, however, significantly hampered by several unfavorable side effects and poor efficacy of these hypoglycemic medications. For instance, trodusquemine, which is a protein tyrosine phosphatase 1B (PTP-1B) inhibitor drug, has been disapproved by the Food and Drug Administration (FDA) for lower selectivity and adverse effects. Sodium-glucose co-transporter 2 (SGLT2) inhibitor drugs such as dapagliflozin, canagliflozin, and empagliflozin possess several side effects such as dehydration, diabetic ketoacidosis, vaginal yeast

infections, urinary tract infections, joint ache, Fournier's gangrene, and low blood pressure (Dowarah and Singh, 2020). Sulfonylureas, thiazolidinediones, α -glucosidase inhibitors, and biguanides can lead to hypoglycemic risk, weight gain, hepatotoxicity, gastrointestinal disorders, and lactic acidosis (Feldman, 1985; Lebovitz and Banerji, 2001; Carles et al., 2008; Chaudhury et al., 2017). DPP-4 inhibitors can also result in nausea, nasopharyngitis, headache, and hypersensitivity. Despite the fact that incretin-based medications have many advantages, they are nonetheless accompanied by significant gastrointestinal issues such as nausea, sour stomach, indigestion, belching, vomiting, and diarrhea (Drucker, 2006). There are several synthesized FDA-approved drugs which have made substantial improvement with time and has helped millions of T2DM patients as well as manage secondary complications. However, the dynamic nature of drug approval and withdrawal occurs as many drugs are more or less accompanied by certain deleterious effect in the long run (Dahlén et al., 2022). Therefore, the development of safer and more effective treatment medications is still critically needed.

Fortunately, many naturally occurring antidiabetic bioactive agents have never lost their effectiveness and continue to be a key component in the treatment as well as anti-T2DM drug discovery (Xu et al., 2018). Due to their affordability and safety concerns, almost 80% of people use plant-based traditional medicines (Ekor, 2014). A survey found that over a thousand plant species are utilized as a traditional folk treatment for diabetic mellitus (Osadebe et al., 2014). The primary medication on the market for the management of type 2 diabetes, metformin, is likewise made from guanidines that are extracted from the *Galegine officinalis* plant. For over 60 years, several new therapeutic antidiabetic drugs have been introduced; however, metformin is prioritized for T2DM patients, considering its safety profile and also affordability compared to other newer alternatives such as SGLT2 inhibitors as well as GLP1 receptor agonists (Bailey and Day, 2004; Triggler et al., 2022).

Ageratina adenophora (Spreng.) R. King & H. Robinson, also known as *Eupatorium adenophorum* Spreng., originated in Mexico and Costa Rica, belongs to the Asteraceae family and is widely distributed in Southeast Asian countries such as India, Pakistan, China, Nepal, Singapore, Thailand, Malaysia and the Philippines, New Zealand, eastern Australia, Northern America, and South Africa (Wan et al., 2010). The plant is commonly referred to as Crofton weed, eupatory, sticky snakeroot, Mexican devil, and Banmara (Muniappan et al., 2009), and in Manipur, India, the plant is locally called Naga mana or Japanpu (Ringmichon and Gopalkrishnan, 2017). It has been observed that the plant is an herbaceous perennial invasive weed and possesses several secondary metabolites that are pharmacologically intriguing, including terpenoids, alkaloids, polyphenols, saponins, flavonoids, coumarins, phenylpropanoids, steroids, and phenolic acids (Liu

et al., 2015). Several pharmacological studies showed that *A. adenophora* extract has various biological therapeutic properties such as antiviral, antiinflammatory, wound-healing, antioxidant, antibacterial, antipyretic, wound-healing, and analgesic properties (André et al., 2019; Poudel et al., 2020). The leaves and tender parts of the plant have abundant chlorogenic acid or 5-O-caffeoylquinic acid (C₁₆H₁₈O₉, 354.31 g/mol) (Liu et al., 2016). The chlorogenic acid is an ester of caffeic acid (C₉H₈O₄, 180.16 g/mol) and quinic acid, which has attracted substantial attention due to its antioxidant, antiinflammatory, antimicrobial, antilipidemic, antihypertensive, and antitumor properties (Santana-Gálvez et al., 2017; Naveed et al., 2018). There are several antidiabetic reports of chlorogenic (Cho et al., 2010; Meng et al., 2013) and caffeic acids (Zhao et al., 2022) used as novel insulin sensitizers; they improve glucose tolerance, insulin resistance, and cellular oxidative stress and manage obesity. It has been reported that caffeic acid shows prophylactic activity against diabetic kidney disease by suppressing autophagy regulatory miRNAs (miR-133b, miR-342, and miR-30a) in high-fat diet streptozotocin-induced diabetic rats (Matboli et al., 2017). Caffeic acid and a majority of its derivatives reduce oxidative stress, manage hyperglycemic condition, and also aid in improving secondary complications associated with DM (Ganguly et al., 2023).

The main aim of the current study is to assess the antidiabetic capacity of *A. adenophora* hydroalcoholic extract in STZ-NA-induced diabetic rats. Ageratina of different species, *Ageratina grandifolia* and *Ageratina petiolaris*, have been cited to possess α -glucosidase inhibitory potential (Gutiérrez-González et al., 2021) and induces hypoglycemic effect (Bustos-brito et al., 2016; Mata-torres and Andrade-cetto, 2020). A report has mentioned the traditional use of *A. adenophora* leaves to treat diabetes in Nigeria (Awah et al., 2012); however, further scientific validation has not been carried out. Another recent work on the *in vitro* antidiabetic activity of *A. adenophora* methanolic extract from Nepal reported an α -amylase inhibitory activity, but further assessment *in vivo* was not implemented (Kapali and Sharma, 2021). Although few preliminary studies have mentioned the antidiabetic effect of *A. adenophora* extract, further extensive validation with animal models is crucial for the development of new drugs. The plant is extensively grown in Manipur as an unattended herb. In spite of the abundance, its therapeutic potential has not been utilized adequately due to lack of limited knowledge. Therefore, considering the preliminary works and reported scientific significances of *A. adenophora*, the current study has been performed to evaluate the phytochemicals, antioxidant, and *in vitro* as well as *in vivo* antidiabetic properties of the plant.

2 Materials and methods

2.1 Materials

α -Glucosidase (from *Saccharomyces cerevisiae*), α -amylase (from *Bacillus subtilis*) and p-nitrophenyl- α -D-glucopyranoside (pNPG), streptozotocin (STZ), chlorogenic acid ($\geq 95\%$), and caffeic acid ($\geq 98.0\%$) were procured from Sigma-Aldrich Co. (St. Louis, United States). Nicotinamide (NA) and metformin

hydrochloride were from Hi media. All other reagents and chemicals used for the study were of analytical grade.

2.2 Plant materials and extraction

The fresh leaves and aerial parts of the plants were collected from Mao, Manipur (latitude: 25°30'24.69"N and longitude: 94°08'03.01"E), during the month of January 2020, growing at an altitude of 1665 m above the sea level. The taxonomic identification of the herbarium was authenticated by the Institute of Bioresources and Sustainable Development (IBSD), India, such as *A. adenophora* (Spreng.) R. M. King & H. Rob., and deposited at the Plant Systematic and Conservation Laboratory, IBSD (Herbarium No. Institute of Bioresources and Sustainable Development/M-274). The collected sample was washed, shade-dried, powdered, and kept for a week by macerating with methanol:water (70:30 v/v), and the macerate was filtered at the end of the time point. Finally, the filtrate was evaporated with the help of a rotary vacuum evaporator (IKA RV 10) set at 45°C, followed by lyophilization (Scanvac cool safe, labogene scandinavian by design, Denmark) (Alamgeer et al., 2013). In total, 132.3 gm dried crude extract was yielded from 1,500 gm of dried leaf powder. The % yield of the *A. adenophora* hydroalcoholic (AAHY) extract was calculated as

$$\text{Yield (\%)} = \frac{X}{Y} \times 100, \quad (1)$$

where X is weight of the dried crude extract obtained and Y is weight of dried leaves powder used for extraction.

2.3 Qualitative phytochemical analysis

To examine the presence or absence of the major phytochemical group of compounds in the AAHY extract, such as alkaloids, phenols, flavonoids, saponins, tannins, glycosides, terpenoids, quinones, and steroids, we followed standard protocols for screening preliminary qualitative phytochemical profiling (Banu and Cathrine, 2015; Sisay et al., 2022).

2.4 High-performance thin-layer chromatography analysis of the AAHY extract

The percentage content of standard chlorogenic acid and caffeic acid in the AAHY extract was estimated by the high-performance thin-layer chromatography (HPTLC) comparative analysis method with the respective retardation factor (*R_f*) of the standard phytoconstituents. The Camag HPTLC instrument (Muttentz, Switzerland) was used for the analysis of samples. The standard stock solution (1 mg/mL) of chlorogenic acid and caffeic acid was prepared by dissolving 1 mg accurately weighed standard in 1 mL HPLC-grade methanol. All the solutions were vortexed and kept in an ultrasonic bath till dissolved and filtered through a 0.45 μ syringe filter before analysis. The external standard calibration curve for chlorogenic acid and caffeic acid was prepared in a concentration range from 20 to 100 μ g/mL and 100 to 180 μ g/mL, respectively. Then, the solutions were drawn into a

CAMAG LINOMAT V applicator fitted out with a syringe and spotted on aluminum-backed HPTLC plates 10 × 10 cm with 0.2 mm layers of silica gel 60 F₂₅₄. Then, the plates were developed using a suitable mobile phase. The detection of the compounds was performed at 302 nm. The amount of chlorogenic acid and caffeic acid present in the sample was determined through the construction of a calibration curve by plotting the peak area against corresponding concentrations by means of linear regression using visionCATS 3.0 software (Orfali et al., 2021; Chaudhary et al., 2023).

2.5 *In vitro* antioxidant capacity of the AAHY leaf extract

2.5.1 DPPH radical scavenging activity

Measurement of the scavenging effect on 2,2-diphenyl-1-picrylhydrazyl (DPPH) (Sigma-Aldrich) was performed according to the work of Amorati and Valgimigli (2018). 100 µl of 0.2 mM DPPH was prepared in methanol and was mixed with 100 µL of different concentrations of the AAHY extract (1.0, 2.5, 5.0, 10.0, 15.0, 30.0, 60.0, and 100.0 µg/mL). The reaction mixture was shaken well and incubated for 30 min in the dark, and then, the absorbance was measured at 517 nm using a Varioskan LUX multimode microplate reader (ESW version 1.00.38) from Thermo Fisher Scientific.

The percentage of DPPH free radical scavenging capacity was calculated using the following equation:

$$\text{DPPH free radical scavenging capacity (\%)} = \frac{(A_{\text{control}} - A_{\text{sample}})}{A_{\text{control}}} \times 100, \quad (2)$$

where A_{control} is the absorbance of DPPH mixed with methanol and A_{sample} is the absorbance of DPPH mixed with the sample AAHY extract. Experiments were performed thrice ($n = 3$). L-ascorbic acid (Sigma-Aldrich) was used as positive control.

2.5.2 ABTS cation radical scavenging activity

The ABTS radical cation scavenging capacity of the AAHY extract was assayed with 2,2'-azinobis-3-ethylbenzothiazoline-6-sulfonic acid (ABTS) (Sigma-Aldrich) following the work of Floegel et al. (2011). The ABTS radical cation solution was prepared by mixing 7.4 mmol/L ABTS and 2.6 mmol/L potassium persulfate (Sigma-Aldrich). 100 µL of the prepared ABTS radical cation solution was mixed with 100 µL of different concentrations of the AAHY extract (1.0, 2.5, 5.0, 10.0, 15.0, 30.0, 60.0, and 100.0 µg/mL), and after 6 min incubation time, the absorbance was measured at 734 nm using a Varioskan LUX multimode microplate reader (ESW version 1.00.38) from Thermo Fisher Scientific.

The percentage of ABTS⁺ free radical scavenging capacity was calculated using the following equation:

$$\text{ABTS}^+ \text{ radical scavenging capacity (\%)} = \frac{(A_{\text{control}} - A_{\text{sample}})}{A_{\text{control}}} \times 100, \quad (3)$$

where A_{control} is the absorbance of the ABTS with methanol and A_{sample} is the absorbance of the ABTS mixed with the sample AAHY extract. Experiments were performed thrice ($n = 3$). L-ascorbic acid was used as positive control.

2.6 *In vitro* antidiabetic activity

2.6.1 α -Glucosidase inhibition assay

The α -glucosidase inhibition assay was performed following methods previously described by Yao et al. (2013); Kim et al., 2004. Different concentrations of standard inhibitor acarbose and the sample AAHY extract (20, 40, 60, 80, 100, and 120 µg/mL) were prepared. Then, 50 µL of 0.1 M potassium phosphate buffer (pH: 6.8) and 10 µL of α -glucosidase (1 U/mL) were mixed and incubated. After 20 min of incubation at 37°C, 20 µL of p-nitro phenyl glucopyranoside (pNPG, 5 mM) was added, mixed well, and re-incubated at 37°C for 30 min. The reaction was stopped by adding 40 µL of 0.1 M Na₂ CO₃ solution. The enzyme activity was estimated by measuring the absorbance of the end product p-nitrophenol at 410 nm using a microplate reader (Varioskan LUX multimode microplate reader, ESW version 1.00.38) from Thermo Fisher Scientific. The inhibition assay was performed thrice, and the percentage of inhibition was calculated as follows:

$$\alpha - \text{Glucosidase Inhibitory (\%)} = \left(1 - \frac{A_{\text{sample}}}{A_{\text{control}}} \right) \times 100, \quad (4)$$

where A_{sample} is the absorbance in the presence of both α -glucosidase and sample and A_{control} is the absorbance of the reaction mixture containing the same volume of buffer solution instead of the sample.

2.6.2 α -Amylase inhibition assay

The α -amylase inhibition assay was carried out following the work of Yao et al. (2013) and Telagari and Hullatti (2015). Different concentrations (20, 40, 60, 80, 100, and 120 µg/mL) of standard acarbose and the sample AAHY extract were prepared. 50 µL of sodium phosphate buffer (100 mM, pH 6.8) was mixed with 10 µL α -amylase (2U/mL) soluble starch (1%). After 30 min of incubation at 37°C, 20 µL substrate, 1% soluble starch prepared in phosphate buffer 100 mM (pH: 6.8) was added and further re-incubated at 37°C for 30 min. The reaction was terminated by adding 100 µL dinitrosalicylic acid reagent solution and boiling for 10 min. The enzyme activity was estimated by measuring the absorbance at 540 nm using a microplate reader (Varioskan LUX multimode microplate reader, ESW version 1.00.38) from Thermo Fisher Scientific. The inhibition assay was performed thrice, and the inhibition percentage was calculated as follows:

$$\alpha - \text{Amylase Inhibitory (\%)} = \left(1 - \frac{A_{\text{sample}}}{A_{\text{control}}} \right) \times 100, \quad (5)$$

where A_{sample} is the absorbance in the presence of both α -glucosidase and sample and A_{control} is the absorbance of the reaction mixture containing the same volume of buffer solution instead of the sample.

2.7 *In vivo* antidiabetic activity

2.7.1 Experimental animals

Healthy normoglycemic (80–90 mg/dL) adult male Wistar albino rats (150–200 g) obtained from the registered breeder-Saha Enterprise, Kolkata (Reg. No. 1828/PO/BT/S/15/

CPCSEA), were used for the experimental study. Rats were maintained in polypropylene cages bedded with straws under standard ambient conditions (temperature $25^{\circ}\text{C} \pm 4^{\circ}\text{C}$ with 12/12 h light/dark cycle; 50–70 humidity). The rats were fed on a standard pellet diet and given free access to water *ad libitum*. All the experimental protocols were scrutinized and approved by the university's animal ethical committee (Ref. No. ACE/PHARM/1502/09/2015, Jadavpur University, Kolkata 700032, West Bengal, India).

2.7.2 Acute toxicity study

Swiss albino mice were used to evaluate the acute oral toxicity test of the AAHY extract following instructions by the Organization of Economic Cooperation and Development (OECD), Guideline 425. The animals were observed for general behaviors such as tremors, aggressiveness, hypnosis, convulsions, diarrhea, analgesia, and skin color for the first 24 h after administration of the test sample AAHY extract at a limit dose of 2000 mg/kg b.w (OECD, 2022).

2.7.3 Diabetes induction

Induction of diabetes by intraperitoneal (i.p) injection of streptozotocin (STZ) was given to the 16 h fasted rats; however, water was provided. STZ at a dose of 50 mg/kg b. w was dissolved in 0.1 M cold citrate buffer (pH 4.5) just before administration, and an i. p injection of NA (100 mg/kg b. w) was given 15 min prior to STZ injection. Glucose solution 20% was provided for the first 24 h to STZ-NA-injected rats to prevent initial hypoglycemic mortality. The diabetic condition was confirmed by fasting blood glucose (FBG) measurement of blood drawn from the tail vein using a glucometer (ACCU-Chek active), and FBG ≥ 250 mg/dL was selected for the experiment (Ghasemi et al., 2014; Sisay et al., 2022).

2.7.4 Extract effect on the blood glucose level of normoglycemic rats

Normal healthy rats (80–90 mg/dL) were fasted overnight for 16 h, but water was provided *ad libitum*. The normal control animals received normal saline water, and the treated groups were given predetermined doses of 200 and 400 mg/kg b.w., p.o., of the AAHY extract. The baseline blood glucose level of each rat was measured just prior to treatment (0 min) and after administration at 1, 2, 4, and 6 h, with the blood drawn from the tail vein under aseptic conditions (Birru et al., 2015; Sisay et al., 2022).

2.7.5 Extract effect on blood glucose after the oral glucose tolerance test

Normal healthy rats (80–90 mg/dL) which were fasted for 16 h were used for the oral glucose tolerance test (OGTT). The rats were distributed into groups of three, and six rats were placed in each group ($n = 6$). Group I, designated as the normal control group, was given distilled water (5 mL/kg b.w., p.o.), and group II and III were treated with doses of 200 and 400 mg/kg b.w., p.o., respectively. After 30 min of administration, the rats received glucose (2 g/kg b.w., p.o.). Measurement of blood glucose level was carried out just before (0 min) and after 30, 60, and 120 min following oral glucose administration (Kifle et al., 2020). The blood was drawn from the tail vein and measured using a glucometer (ACCU-Chek active).

2.7.6 Experimental design for antidiabetic activity

The rats were divided into five groups, with six rats in each group ($n = 6$). The experimental study was set up for 28 days.

Group I: Normal control rats received normal saline (0.5 mL/kg, b.w., p.o.).

Group II: The diabetic control group treated with STZ (50 mg/kg, b.w., i.p.) and NA (100 mg/kg, b.w., i.p.).

Group III: STZ-NA-induced diabetic rats treated with the AAHY extract (200 mg/kg b.w.), administered orally for 28 days.

Group IV: STZ-NA-induced diabetic rats treated with the AAHY extract (400 mg/kg b.w.) administered orally for 28 days.

Group V: STZ-NA-induced diabetic rats treated with metformin (150 mg/kg, p.o.) for 28 days.

2.7.7 Glycated hemoglobin estimation

A commercially available glycated hemoglobin kit based on the ion exchange resin method [Coral clinical systems, a Division of Tulip Diagnostics (p) Ltd.] was used to measure glycated hemoglobin (HbA1c) levels in whole blood samples.

2.7.8 Serum biochemical parameter determination

At the end of the experimental design, the rats were fasted overnight for 16 h and on the 29th day, they were anaesthetized using isoflurane and sacrificed by cervical dislocation. The blood sample was drawn and collected from the heart by cardiac puncture. Serum was acquired by centrifugation at 3,000 rpm for 10 min. An array of biochemical parameters such as serum glutamic pyruvic transaminase (SGPT), serum glutamic oxaloacetic transaminase (SGOT), serum alkaline phosphatase (SALP), total protein (TP), creatinine, and urea were measured with the collected serum using commercially available assay kits (Arkray Healthcare Pvt., Ltd., Surat, Gujarat, India).

2.7.9 Serum lipid profile evaluation

Estimation of serum lipid profiles such as total cholesterol (TC), high-density lipoprotein (HDL), and triglycerides (TGs) were determined using commercially available kits (Arkray Healthcare Pvt., Ltd., Surat, Gujarat, India).

2.7.10 Tissue antioxidant parameter estimation

The organs, liver and kidney, were carefully harvested from the rats and cleaned in ice-cold saline to remove blood. The organs were weighed, cut into pieces, and homogenized with phosphate buffer (0.025 M, pH 7.4). The homogenate was centrifuged for 15 min at 10,000 rpm at 4°C . The supernatant was collected and used for estimations of antioxidant parameters such as lipid peroxidation (LPO), reduced glutathione (GSH), and superoxide dismutase (SOD).

Lipid peroxidation (LPO) levels from the supernatant of liver and kidney tissues were determined as per the standard protocols followed by Ohkawa et al. (1979) and Niehaus and Samuelsson (1968). The supernatant, 0.02 M phosphate buffer saline (PBS), and 10% trichloro acetic acid (TCA), in the ratio of 1:1:2 were mixed and incubated for 30 min at room temperature. Then, the mixture was centrifuged at 3,000 rpm

For 10 min, 1 mL of the supernatant was collected and mixed with 250 μL of 1% thiobarbituric acid (TBA) and heated for 60 min at 95°C until a stable pink color was observed. The OD was measured at 532 nm against an appropriate blank and expressed as μM of malondialdehyde (MDA)/mg protein.

The glutathione (GSH) levels of the liver and kidney tissues were assayed according to the methods of [Ellman \(1959\)](#) and [Moron et al. \(1979\)](#). 0.1 mL of respective homogenates mixed with 2.4 mL EDTA were incubated in ice for 10 min, followed by precipitation with 0.5 mL of 50% TCA. The precipitate was discarded by centrifugation at 4°C, 3,000 rpm for 15 min. To 1 mL of the clear supernatant, 1 mL of tris buffer and 0.05 mL of DTNB were added. Absorbance at 412 nm was measured after the reaction mixture had been incubated for 3 min. The amount of glutathione was expressed as μM of GSH utilized/mg protein.

The superoxide dismutase (SOD) activity levels of the tissue supernatants were assayed following the work of [Marklund and Marklund \(1974\)](#) and [Kakkar et al. \(1984\)](#). The reaction mixture contained 600 μL PBS, 60 μL of 186 μM phenazine methosulphate (PMS), 150 μL of 300 μM nitroblue tetrazolium (NBT), and 100 μL each of supernatant and NADH (780 μM). The reaction mixture was incubated for 90 s at 30°C, and the reaction was terminated by adding 500 μL of glacial acetic acid. The absorbance was measured at 560 nm against an appropriate blank and expressed as units/mg protein.

2.7.11 Histopathological studies

The pancreas was carefully harvested from the euthanized rats after the termination of the experiment and subjected to histopathological studies. The tissues were washed with a standard saline solution for 5 min each, followed by 10% formalin fixation for 24 h, then dehydrated by passing through different alcohol solutions successively, and finally, embedded in paraffin. The embedded samples were sliced into ultra-thin (4–5 μm) sections with a semi-automated Thermo Scientific microtome. The sliced tissue samples were gently placed over warm water and carefully glided onto glass slides. The slides were deparaffinized, and the transparent intact tissue sections were stained with hematoxylin–eosin dye to provide structural contrast ([Alturkistani et al., 2015](#)). One or two drops of DPX mounting medium were spread over the tissue specimens on the slides and carefully covered with coverslips for preservation. The prepared stained slides were observed and photographed with the camera attached to the microscope (Nikon eclipse Ni-U). The size of the pancreatic islets from the captured histopathology image was calculated using ImageJ analysis software. The changes in the size have been expressed as relative % compared to the normal control group.

2.8 Statistical analysis

The results were evaluated using the statistical tool, one-way analysis of variance (ANOVA) *post hoc* Dunnett's test using Graph pad prism 8.4.3 software (Graph Pad Software, San Diego United States). The size of the histopathology image was analyzed using ImageJ software. The data were represented as mean \pm standard error of mean (SEM). The statistical significance was set at $p < 0.05$.

3 Results

3.1 Extraction yield of the AAHY extract

The yield of the AAHY extract was 8.82%.

3.2 Qualitative phytochemical analysis

The outcomes of the types of tests performed, the changes observed, and the inferences of the preliminary phytoconstituent analysis are summarized in [Table 1](#).

3.3 HPTLC analysis of the AAHY extract

The developed plate was scanned 302 nm using a CAMAG TLC Scanner IV in the absorbance mode. The picture of the developed plate was captured by using CAMAG Reprostar 3. The photo documentation was carried out using the CAMAG TLC visualizer 2 under white, 254 and 366 nm ([Figure 1](#)). The standard compound (chlorogenic acid and caffeic acid) expressed a good linearity between concentrations and the peak area. The mobile phase toluene–ethyl acetate–formic acid (5:4:1, v/v) and ethyl acetate–acetic acid–formic acid–water (100:1.1:1.1:2.6, v/v) were found to produce a compact spot for chlorogenic acid and caffeic acid at R_f 0.43 and 0.72, respectively. A good linear precision relationship between the concentrations and peak areas was obtained with the correlation coefficient (r^2) > 0.997 and 0.998 for chlorogenic acid and caffeic acid, respectively. The amount of chlorogenic acid and caffeic acid was found to be 6.47% and 3.28 w/w in the AAHY extract, respectively.

3.4 Antioxidant activity

The AAHY extract exerted DPPH as well as ABTS free radical scavenging activities in a dose-dependent manner [Figure 1](#). The % inhibitory concentrations (IC_{50}) of the AAHY extract and L-ascorbic acid were $44.52 \pm 1.23 \mu\text{g/mL}$ and $15.12 \pm 0.11 \mu\text{g/mL}$, respectively, as determined by DPPH radical scavenging assay [Figure 2A](#), whereas IC_{50} was $9.75 \pm 0.33 \mu\text{g/mL}$ for L-ascorbic acid and $33.33 \pm 0.66 \mu\text{g/mL}$ for the AAHY extract, respectively, when the scavenging capacity was assessed by ABTS cation radical scavenging assay [Figure 2B](#).

3.5 *In vitro* α -glucosidase and α -amylase inhibition assays

The sample AAHY extract exhibited a dose-dependent inhibition of α -glucosidase and α -amylase activities. The inhibitory effects were compared with a standard inhibitor, acarbose. The α -glucosidase inhibition results of the extract and acarbose are shown in [Figure 3A](#). The corresponding concentration for 50% inhibition (IC_{50}) of the AAHY extract and acarbose was 93.47 ± 2.56 and $46.77 \pm 1.31 \mu\text{g/mL}$, respectively. α -Amylase inhibitory activities of the AAHY extract and acarbose are shown in [Figure 3B](#), and the corresponding IC_{50} values were found to be 116.32 ± 1.15 and $70.62 \pm 0.52 \mu\text{g/mL}$, respectively.

3.6 Acute toxicity study

The study was performed by oral administration (p.o.) of the AAHY extract at a dose of 2000 mg/kg b.w. in mice. There were no toxicity signs, and none of the animals died till the end of the experiment. Since the animals were not toxic up to the dose of

TABLE 1 Preliminary qualitative phytochemical analysis of the AAHY extract.

Phytochemicals	Tests performed	Appearance	Inference
Alkaloids	Mayer's	Reddish brown precipitate seen	+
Phenolics	Ferric chloride	Blue-black color seen	+
Flavonoids	Lead acetate	Yellow precipitate formed	+
Tannins	Braemer's	Bluish-green color seen	+
Glycosides	Keller-Kiliani	Brown ring at the interface seen	+
Saponins	Foam test	Foam observed	–
Terpenoids	Salkowski's	Dark bluish black observed	+
Quinones	Borntrager's	Red color seen	+
Steroids	Liebermann-Burchard	Pink-to-reddish color not seen	–

(+): detected; (–): not detected.

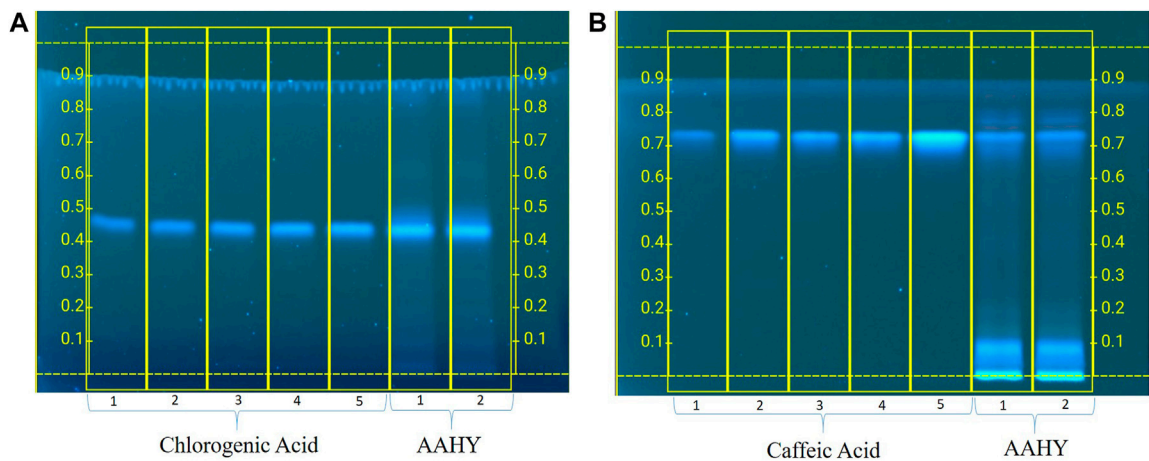


FIGURE 1 Standardization of the AAHY extract for the presence of (A) chlorogenic acid and (B) caffeic acid as the standard phytomarker through HPTLC analysis.

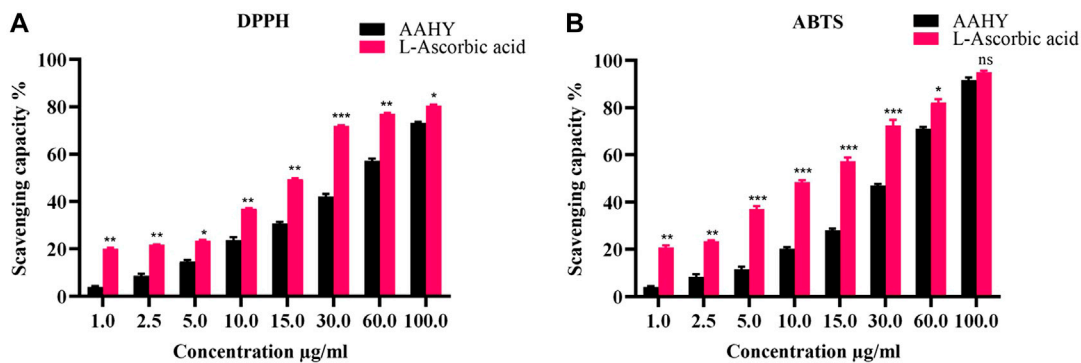


FIGURE 2 (A) DPPH and (B) ABTS free radical scavenging activities (%). A comparison of different concentrations of the AAHY extract and ascorbic acid is shown. Data are represented as mean ± SEM, and experiments were performed thrice ($n = 3$). * $p < 0.05$, ** $p < 0.01$, and *** $p < 0.001$ versus the AAHY extract. SEM: standard error of mean.

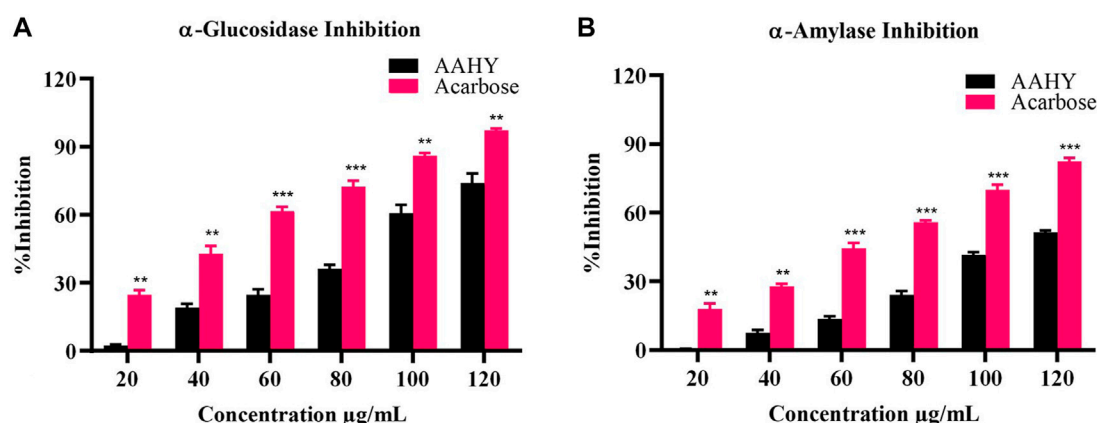


FIGURE 3

In vitro (A) α -glucosidase and (B) α -amylase activities of the AAHY extract. % inhibitions are expressed as mean \pm SEM, and $n = 3$. * $p < 0.05$, ** $p < 0.01$, and *** $p < 0.001$ versus the AAHY extract. SEM: standard error of mean.

TABLE 2 Effect of the AAHY extract in the oral glucose tolerance test.

Groups	Fasting blood glucose level (mg/dL)			
	0 min	30 min	60 min	120 min
Normal control	84.33 \pm 1.14	130.25 \pm 3.09	123.5 \pm 2.5	117.75 \pm 3.35
AAHY extract 200 mg/kg	81.33 \pm 2.81 ^{ns}	126.75 \pm 2.49 ^{ns}	113.25 \pm 2.39 ^{a*}	104.5 \pm 2.32 ^{a**}
AAHY extract 400 mg/kg	82.16 \pm 2.44 ^{ns}	120.75 \pm 2.52 ^{a*}	107.75 \pm 1.6 ^{a**}	92.75 \pm 2.09 ^{a**}
Metformin 150 mg/kg	84 \pm 1.36 ^{ns}	108.25 \pm 2.78 ^{a**}	93.75 \pm 2.86 ^{a***}	86.5 \pm 2.06 ^{a***}

The values are represented as mean \pm SEM, and $n = 6$ for each group.

^aAll treated groups versus the normal control group at the corresponding time point.

^{ns}No significant difference was observed.

^{***}No significant difference observed when all treated groups were compared to the normal control group at the corresponding time point. SEM, standard error of mean; AAHY extract, *Ageratina adenophora* hydroalcoholic extract. * $p < 0.05$, ** $p < 0.01$, and *** $p < 0.001$.

2000 mg/kg b.w., further hypoglycemic experiments were carried out at doses of 200 and 400 mg/kg b.w, respectively.

3.7 Oral glucose tolerance test

The OGTT showed that the BGLs of normoglycemic rats were elevated in the first 30 min after the oral administration of glucose and gradually decreased. However, the AAHY extract (200 and 400 mg/kg b.w.) significantly reduced blood glucose levels at 60 and 120 min in glucose-loaded rats compared to untreated normal control rats (Table 2).

3.8 Effect of the AAHY extract on fasting blood glucose and body weight

The fasting blood glucose levels of STZ-NA-induced diabetic rats (group II) were significantly elevated compared to normal control rats (group I) during the experimental study. Daily oral administration of the AAHY extract at the doses of 200 mg/kg b.w. (group III) and 400 mg/kg b.w. (group IV) to the diabetic rats significantly reduced FBG near to the normal level (group I) compared to the diabetic control rats

(group II) in a dose-dependent manner. The standard metformin (150 mg/kg b.w.)-treated rats (group V) showed reduced FBG compared to the diabetic control (Table 3).

The body weight of STZ-NA-induced diabetic rats (group II) gradually decreased, whereas the groups (III and IV) administered with the AAHY extract at the doses of 200 and 400 mg/kg b.w. showed gradual improvement as compared to normal control rats (group I). The rats treated with drug standard metformin at 150 mg/kg b.w. (group V) also exhibited a gradual increase in body weight. The study data are shown in Table 4.

3.9 Hypoglycemic activity on normoglycemic rats

There was no significant difference in blood glucose levels between the groups prior to treatments. In fact, 2 h after the administration of the extracts and metformin, the FBG level was lowered. Following 6 h of treatment, both the extracts (200 and 400 mg/kg) and metformin (150 mg/kg) were able to significantly reduce FBG levels of the normoglycemic rats compared to the 2 h time point (Table 5).

TABLE 3 Effect of the AAHY extract on fasting blood glucose (mg/dL).

Groups	Fasting blood glucose level (mg/dL)				
	Day 0	Day 7	Day 14	Day 21	Day 28
I Normal control	93 ± 2.04	83 ± 1.04	89 ± 2.04	92 ± 2.21	96 ± 1.21
II Diabetic control	372 ± 2.18 ^{a***}	346 ± 3.51 ^{a***}	364 ± 2.74 ^{a***}	349 ± 3.45 ^{a***}	324 ± 2.94 ^{a***}
III Diabetic + AAHY extract 200 mg/kg	354 ± 1.36 ^{bns}	274 ± 2.89 ^{b*}	155 ± 3.45 ^{b**}	135 ± 1.01 ^{b**}	103 ± 3.2 ^{b***}
IV Diabetic + AAHY extract 400 mg/kg	337 ± 3.3 ^{bns}	231 ± 1.5 ^{b*}	120 ± 3.71 ^{b**}	108 ± 2.48 ^{b***}	93 ± 2.04 ^{b***}
V Diabetic + metformin 150 mg/kg	349 ± 2.12 ^{bns}	217 ± 3.47 ^{b*}	122 ± 1.78 ^{b**}	101 ± 2.69 ^{b***}	84 ± 1.27 ^{b***}

The data are represented as mean ± SEM, and $n = 6$ for each group.

^aThe normal control group versus the diabetic control group.

^bAll treated groups versus the diabetic control group at the corresponding time point.

^{bns}No significant difference was observed.

^{bns}No significant difference observed when all treated groups were compared to the diabetic control group at the corresponding time point. SEM, standard error of mean; AAHY extract, *Ageratina adenophora* hydroalcoholic extract; diabetic: streptozotocin (50 mg/kg, b.w.) + nicotinamide (100 mg/kg, b.w.). * $p < 0.05$, ** $p < 0.01$, and *** $p < 0.001$.

TABLE 4 Effect of the AAHY extract on the body weight of experimental rats (g).

Groups	Body weight (g)				
	Day 0	Day 7	Day 14	Day 21	Day 28
I Normal control	179 ± 1.91	177 ± 1.96	173 ± 2.16	178 ± 1.28	181 ± 2.9
II Diabetic control	188 ± 2.19 ^{ans}	169 ± 1.37 ^{ans}	149 ± 3.08 ^{a**}	132 ± 1.51 ^{a**}	119 ± 2.98 ^{a***}
III Diabetic + AAHY extract (200 mg/kg)	182 ± 2.08 ^{bns}	167 ± 1.7 ^{bns}	152 ± 0.93 ^{bns}	149 ± 0.85 ^{b*}	146 ± 3.02 ^{b**}
IV Diabetic + AAHY extract (400 mg/kg)	185 ± 3.02 ^{bns}	173 ± 1.51 ^{bns}	159 ± 2.3 ^{bns}	158 ± 0.97 ^{b*}	162 ± 1.28 ^{b**}
V Diabetic + metformin (150 mg/kg)	177 ± 1.97 ^{bns}	169 ± 0.98 ^{bns}	166 ± 1.87 ^{b*}	164 ± 2.31 ^{b**}	168 ± 1.97 ^{b**}

The values are represented as mean ± SEM, and $n = 6$ for each group.

^aThe normal control group versus the diabetic control group.

^bAll treated groups versus the diabetic control group on the corresponding day.

^{bns}No significant difference was observed.

^{ans}No significant difference observed when all treated groups were compared to the normal control group at the corresponding time point.

^{bns}No significant difference observed when all treated groups were compared to the diabetic control group at the corresponding time point. SEM, standard error of mean; AAHY extract, *Ageratina adenophora* hydroalcoholic extract; diabetic: streptozotocin (50 mg/kg, b. w.) + nicotinamide (100 mg/kg, b.w.). * $p < 0.05$, ** $p < 0.01$, and *** $p < 0.001$.

3.10 Glycated hemoglobin

After the termination of the experiment, the blood samples were examined for glycated hemoglobin (HbA1c). The HbA1c level of the STZ-NA-induced diabetic control rats was elevated compared to normal control rats. However, the HbA1c level of the STZ-NA-induced diabetic rats treated with doses of the AAHY extract 200 and 400 mg/kg b.w and metformin 150 mg/kg b.w. was reduced compared to the diabetic control rats. The activity observed with the AAHY extract dose of 400 mg/kg b.w was comparable with the standard drug metformin (Figure 4).

3.11 Serum biochemical parameters

The efficacy of the AAHY extract on serum biochemical parameters such as SGPT, SGOT, SALP, TP, creatinine, and urea is shown in Figure 3. In STZ-NA-induced diabetic rats, oral administration of the AAHY extract and metformin significantly reduced SGPT, SGOT, SALP, creatinine, and urea, when compared to diabetic control rats. However, the total protein (TP) content

increased in the AAHY extract- and metformin-administered groups (Figure 5).

3.12 Serum lipid profile

In STZ-NA-induced diabetic control rats, the serum lipid profile, such as triglyceride and total cholesterol (TC) levels, was high. However, the HDL level was low compared to normal control rats. In diabetic rats, oral administration of the AAHY extract at the doses of 200 and 400 mg/kg b. w. and metformin at 150 mg/ml b. w. showed a gradual reduction in TG and TC levels, but HDL levels increased compared to the diabetic control group (Figure 6).

3.13 Tissue antioxidant parameters

The liver and kidney antioxidant data are shown in Figure 7. The SOD and GSH levels of STZ-NA-induced diabetic control rats were low, whereas an increased level of MDA was observed compared to the normal control group. These antioxidant parameters were

TABLE 5 Hypoglycemic activity of the AAHY extract in normoglycemic rats.

Group	Blood glucose level (mg/dL)				
	0 h	1 h	2 h	4 h	6 h
Normal control	86 ± 1.26	85.91 ± 0.4	87.58 ± 0.64	86.71 ± 1.21	87.01 ± 0.54
AAHY extract 200 mg/kg	87.41 ± 2.17 ^{ans}	83.02 ± 1.05 ^{ans}	78.2 ± 0.51 ^{ans}	72.61 ± 0.28 ^{a*}	69.48 ± 0.14 ^{a*}
AAHY extract 400 mg/kg	82.9 ± 0.97 ^{ans}	79.73 ± 0.21 ^{ans}	67.54 ± 1.24 ^{a*}	61.37 ± 0.57 ^{a**}	57.21 ± 0.31 ^{a**}
Metformin (150 mg/kg)	84.34 ± 0.82 ^{ans}	75.41 ± 0.54 ^{ans}	65.17 ± 1.27 ^{a*}	57.24 ± 0.48 ^{a**}	51.08 ± 0.16 ^{a**}

The values are represented as mean ± SEM, and n = 6 for each group.

^aAll treated groups versus the normal control group at the corresponding time period.

^{ans}No significant difference.

^{ans}No significant difference observed when all treated groups were compared to the normal control group at the corresponding time point. SEM, standard error of mean; AAHY extract, *Ageratina adenophora* hydroalcoholic extract. **p* < 0.05; ***p* < 0.01.

significantly improved near to normal levels after administering the AAHY extract 200 and 400 mg/kg b.w. doses and metformin at 150 mg/ml b.w, compared to diabetic control rats.

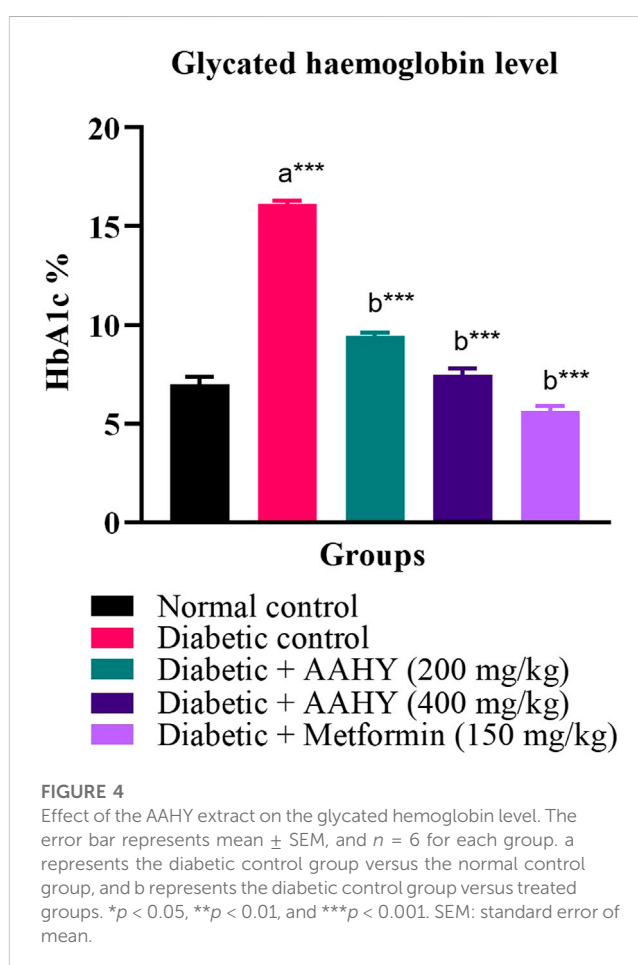
3.14 Histopathological studies

The histology of the pancreas was examined after the end of the experimental design. The hematoxylin and eosin-dyed pancreatic tissue photomicrographs of normal control rats depicted normal islet cells (Figure 8A). On the contrary, the diabetic control pancreatic islet cells were degranulated, disrupted, noticeably depleted, and dilated compared to the normal islet architecture (Figure 8B). However, the AAHY extract 200- and 400 mg/kg b.w.-treated groups exhibited gradual improvement in islet cell density and showed regeneration of cell and granulation in a dose-dependent manner compared to diabetic control rats (Figures 8C, D). The metformin-treated group showed protective response as evident from the increased pancreatic islets size close to the normal histology of the normal control group (Figure 8E). A remarkable difference was observed in the relative pancreatic islets size of the diabetic and treated groups when compared with that of the normal control. The islets sizes in the diabetic group were significantly deduced showing depleted cells ($6.78\% \pm 0.39\%$). A gradual improvement in the histology of the pancreatic islets was observed in the AAHY extract ($17.23\% \pm 1.25\%$ and $35.46\% \pm 2.96\%$, respectively)-treated group and there was a significant improvement in the metformin ($71.1\% \pm 2.04\%$)-treated group when relatively compared with that of the normal group (Figure 9).

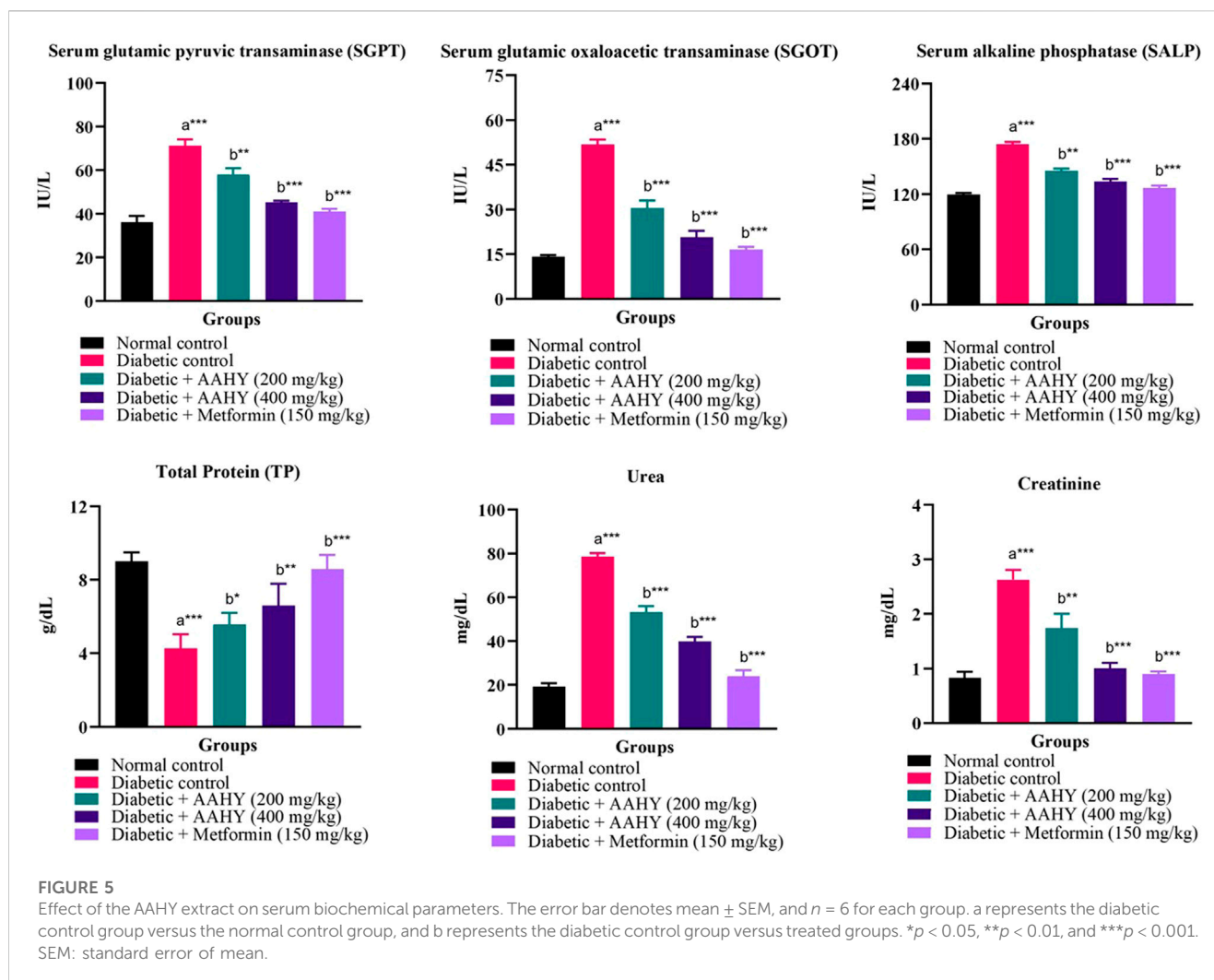
4 Discussions

Although there have been significant advances in the development of antidiabetic drugs, these therapies are often regarded as ineffective since they fail to prevent T2DM-related secondary problems, have adverse effects, and are expensive. Therefore, it is encouraging to look into medicinal plants and other natural remedies as therapeutic alternatives.

The current study has been conducted to evaluate the capacity of *Ageratina adenophora* hydroalcoholic extract administered orally, for antihyperglycemic and antihyperlipidemic activities in normal, oral



glucose-loaded, and STZ-NA-induced diabetic rats, and quantification of phytochemicals chlorogenic and caffeic acids present in the extract. Before conducting *in vivo* animal studies in Wistar albino rats, *in vitro* enzymatic assays, α-glucosidase and α-amylase, were performed. T2DM is characterized by faulty insulin secretion or deficiency and defective metabolism of carbohydrates and lipids in tissues, leading to an increase in postprandial hyperglycemia levels. The pancreatic enzymes α-glucosidase and α-amylase hydrolyze starch and oligosaccharides resulting in fast uptake of glucose in the intestine, thereby increasing the postprandial blood glucose level. Inhibition of these enzymes is a



promising method for reducing such postprandial hyperglycemia, which is crucial in T2DM (Dong et al., 2012). The findings suggest that the AAHY extract possesses good suppressive activities on pancreatic α -glucosidase and α -amylase enzymes, thereby inhibiting carbohydrate metabolism and decreasing the postprandial glucose level.

Prior to the advancement of *in vivo* experiments, the acute toxicity test was performed. Oral administration of the AAHY extract at a dose of 2,000 mg/kg b. w. in mice did not show any toxicity effect. So, further downstream experiments were carried out at doses of 200 and 400 mg/kg b.w, respectively. The oral glucose tolerance test is one of the important assessments for the identification and diagnosis of impaired glucose tolerance, insulin resistance, and sensitivity for T2DM prevention in patients who are at high risk (Kuo et al., 2021). So, it can be interpreted that the AAHY extract has a significant glucose tolerance activity compared to the normal control groups. Oral administration of the AAHY extract at doses of 200 and 400 mg/kg b.w. for consecutive 28 days significantly reduced FBG compared to the diabetic control groups. This might be due to the potential of the extract to induce pancreatic secretion of insulin by the existing and regenerated β -cells. The body weight of the STZ-NA-induced diabetic rats was decreased compared to normal group rats, which could be possibly due to low glycemic grade. In untreated diabetic

rats, there is an extensive breakdown of proteins to provide amino acids for gluconeogenesis during insulin deficiency resulting in muscle wasting and weight loss (Kasetti et al., 2010). The body weight of the treated diabetic groups gradually improved after the administration of the AAHY extract.

Antioxidants play a protective role against the development of many chronic diseases caused by the overproduction of oxidants. Antioxidant phytochemicals are present in several medicinal plants that can scavenge free radicals (Yao et al., 2013). Plant polyphenolic compounds are known to possess antioxidant properties and modulate the hyperglycemic state by inhibiting α -amylase and α -glucosidase activities, thereby managing T2DM (Sekhon-Loodu and Rupasinghe, 2019). Chlorogenic and caffeic acids are natural antioxidant phenolic compounds that prevent oxidative stress-induced diseases such as DM (Stagos, 2020). Chen et al. reported the synergistic effect of chlorogenic and caffeic acids isolated from *Sonchus oleraceus* Linn. in modulating glucose utilization via the PI3K/AKT/GLUT4 inactivation pathway in HepG2 cells (Chen et al., 2019). The phenolic compound, chlorogenic acid, is found to be abundant in the leaves of *A. adenophora* (Liu et al., 2016). Quantification of chlorogenic acid and its associate, caffeic acid, was standardized using HPTLC analysis and was found to be 6.47% w/w and 3.28% w/w, respectively. The antioxidant and antiinflammatory

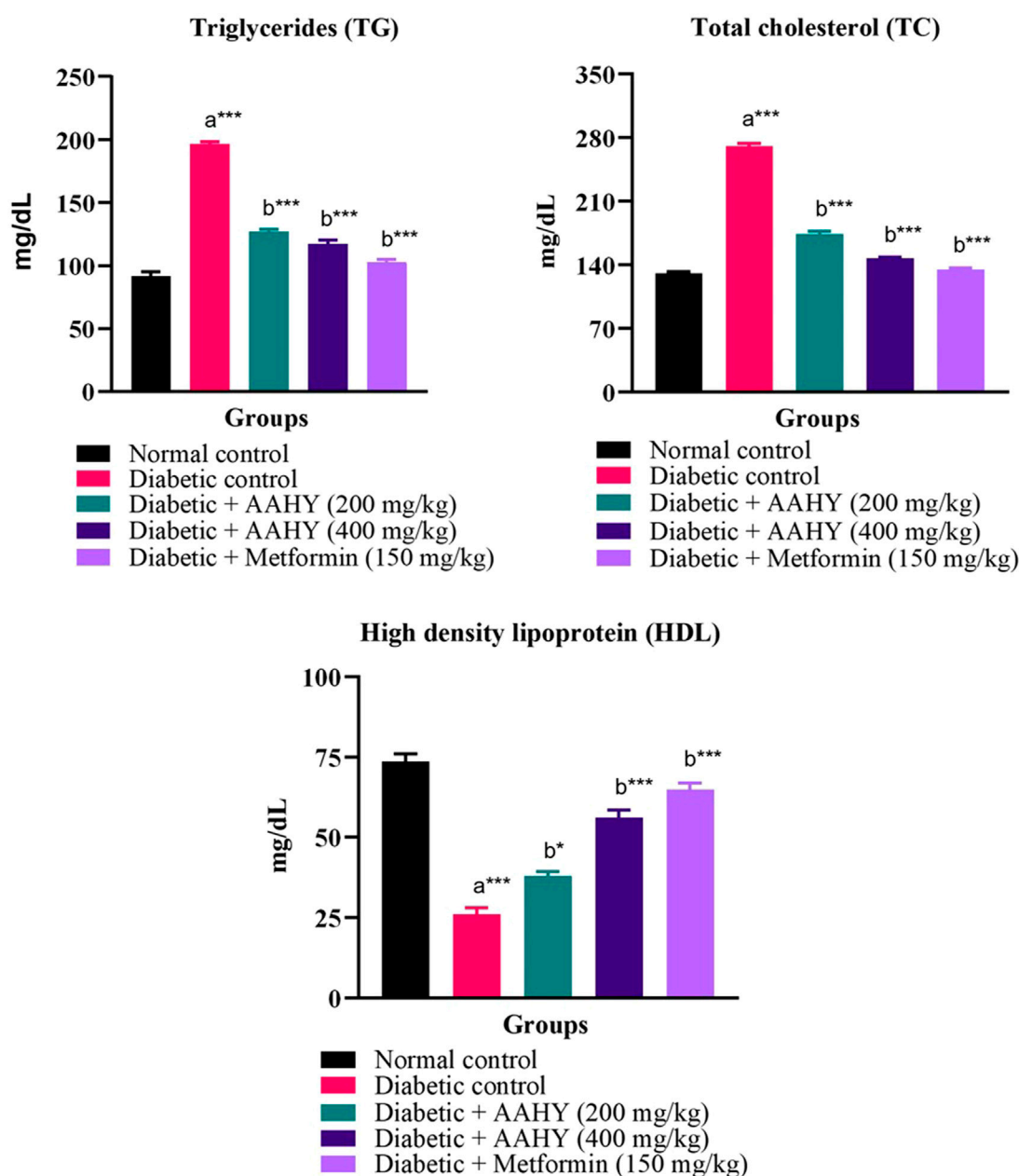


FIGURE 6

Effect of the AAHY extract on the serum lipid profile. The error bar denotes mean \pm SEM and $n = 6$ for each group. a represents the diabetic control group versus the normal control group, and b represents the diabetic control group versus treated groups. * $p < 0.05$, ** $p < 0.01$, and *** $p < 0.001$. SEM: standard error of mean.

properties of these compounds are well reported and also aid in the management of chronic metabolic diseases (Dos Santos et al., 2006; Santana-Gálvez et al., 2017). Previous research showed a variety of plant polyphenolics possessing antioxidant properties that protect pancreatic β -cells (Belayneh et al., 2019). Similarly, the AAHY extract showed antioxidant property in the present study, suggesting the ability to protect β -cells and contribute to antihyperglycemic activity in STZ-NA-induced diabetic rats. The protective role might be attributed to the presence of various groups of secondary metabolites such as alkaloids, phenolics, flavonoids, tannins, glycosides, terpenoids, and quinones, as revealed from the

preliminary qualitative profiling of phytochemicals of the AAHY leaf extract (Zhang et al., 2015). The aforementioned phytoconstituent results are also consistent with the reported studies (André et al., 2019; Poudel et al., 2020). The alkaloids have been reported to regulate hyperglycemia via α -glucosidase and α -amylase inhibition, sensitizing insulin production, inhibition of PTP-1B and DPP-4 pathways, and managing oxidative stress condition (Adhikari, 2021; Ajebli et al., 2021). Terpenoids also help in the management of T2DM via the activation of the AMP-activated protein kinase pathway (Grace et al., 2019). Phenolics and flavonoids are polyphenols possessing antioxidant properties that protect the pancreatic islets of

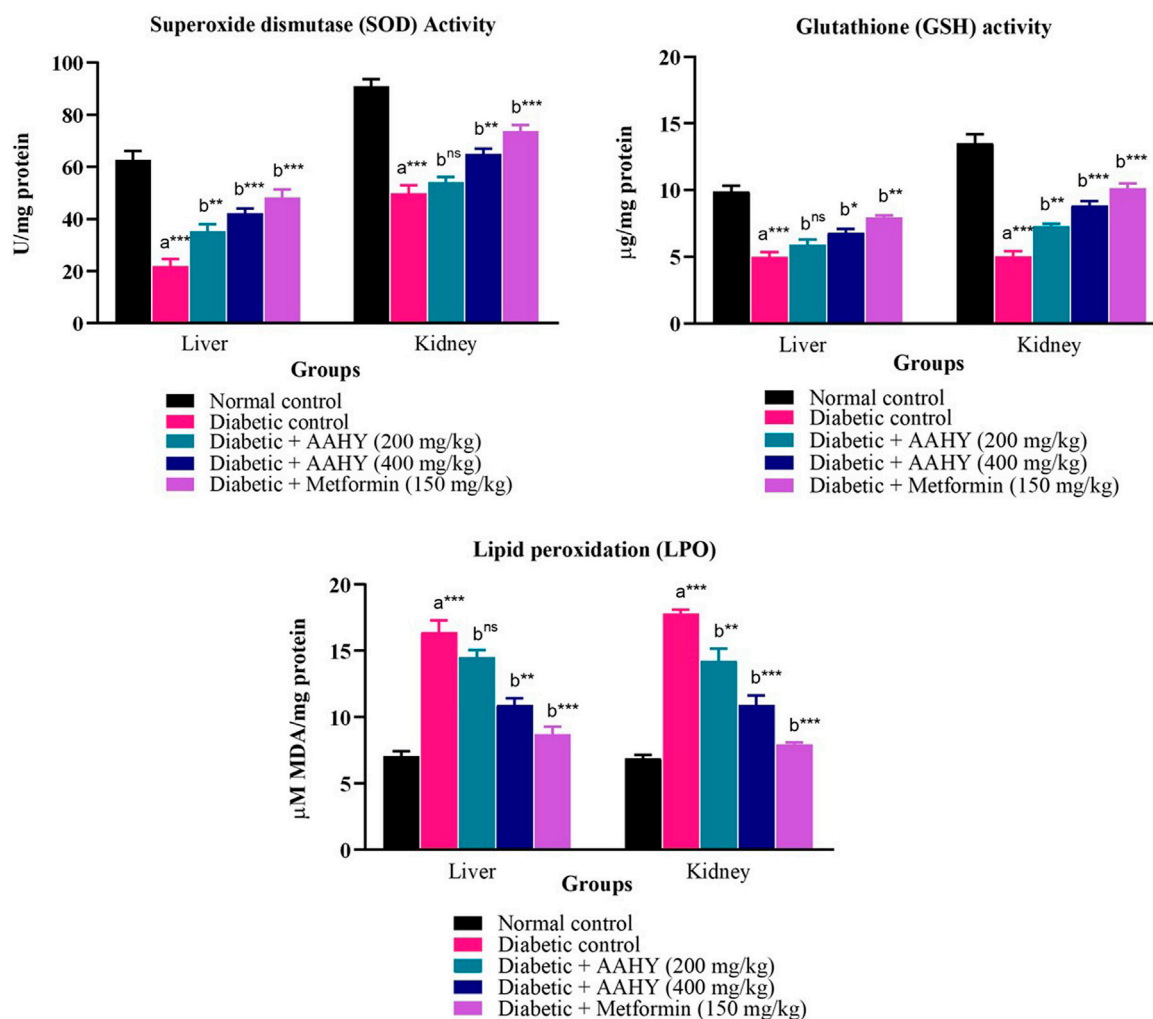


FIGURE 7

Effect of the AAHY extract on liver and kidney tissue antioxidant parameters. The error bar denotes mean \pm SEM, and $n = 6$ for each group. a represents the diabetic control group versus the normal control group, and b represents the diabetic control group versus treated groups. * $p < 0.05$, ** $p < 0.01$, and *** $p < 0.001$. SEM: standard error of mean.

Langerhans (Praparatana et al., 2022). Likewise, tannins (Ajebl and Eddouks, 2019), glycosides (Sumaira and Khan, 2018), and quinones (Demir et al., 2019) have also been reported to have a hypoglycemic effect. These phytochemicals offer significant potential for metabolic homeostasis. Thus, the presence of these secondary metabolites might have synergistically contributed to the antihyperglycemic effect of the AAHY extract. Despite several *in vitro* and *in vivo* experiments demonstrating the promising therapeutic role of bioactive compounds, only few have reached clinical trials (Adhikari, 2021). So, based on the findings, proper evaluation of the diverse functions of these phytochemicals is still critically required for advancement in antidiabetic drug discovery.

The key factors for the pathogenesis and advancement of DM are associated with oxidative stress and inflammation of the pancreas. Induction of diabetes by STZ-NA in rats caused grave damage to pancreatic β -cells due to excessive generation of free radicals such as reactive oxygen and nitrogen species (Bhatti et al., 2022). In consistency with the aforementioned study, the key

antioxidant enzymes', SOD and GSH, levels were significantly reduced, while lipid peroxidation levels were elevated as evidenced by the increased MDA, in the liver and kidney tissues of the diabetic control group, which is an indication of STZ-NA-induced oxidative stress. However, treatment of the AAHY extract 200 and 400 mg/kg b.w. doses and metformin at 150 mg/ml b.w significantly improved the enzyme levels comparable to normal levels, demonstrating the capabilities of the AAHY extract and metformin to decrease oxidative stress.

Glycated hemoglobin (HbA1c) concentration in the blood is a reliable diagnostic marker for the determination of diabetes (WHO, 2011). The American Diabetes Association (ADA) suggested HbA1c level $\geq 6.5\%$ as a high-risk glycemic state and is directly proportional to the blood plasma glucose content. HbA1c indicates a cumulative history of blood glucose levels over the last 2–3 months (Sherwani et al., 2016). However, the threshold point of the HbA1c test is still controversial among different expertised organizations. HbA1c is influenced by several physiological and pathological conditions. So,

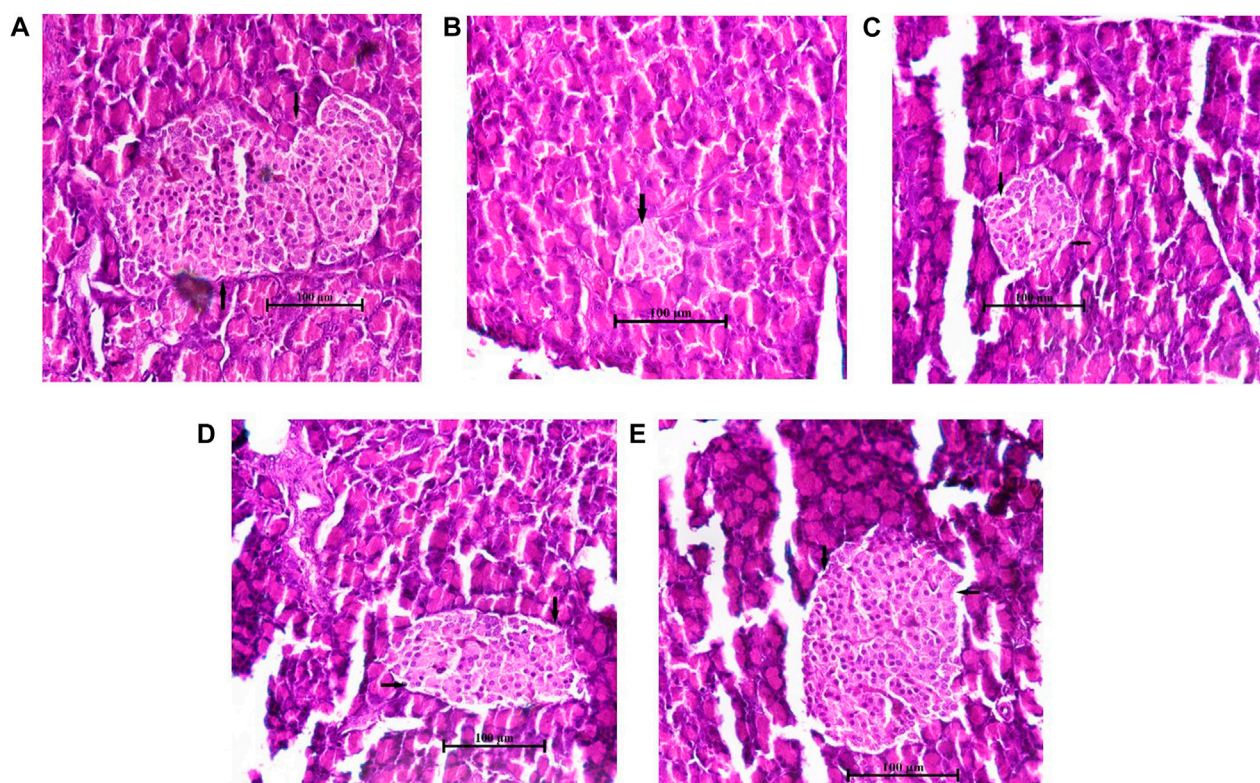


FIGURE 8

Histopathological features of the pancreatic islets of normal and STZ–NA-induced diabetic Wistar albino rats. **(A)** Normal control group depicting the normal histology of the pancreas, **(B)** diabetic pancreas showing a depleted, distorted β -cell structure and greatly reduced islets size, **(C)** diabetic + AAHY extract 200 mg/kg b.w.-treated pancreas revealing mild improvement, **(D)** diabetic + AAHY extract 400 mg/kg b.w.-treated pancreas revealing gradual regeneration of β -cells, thereby improving islets size, and **(E)** diabetic + metformin 150 mg/kg b.w.-treated pancreas showing the nearly normal structure of the islets. A representative photomicrograph of each group is shown ($n = 6$). Scale bar = 100 μ m.

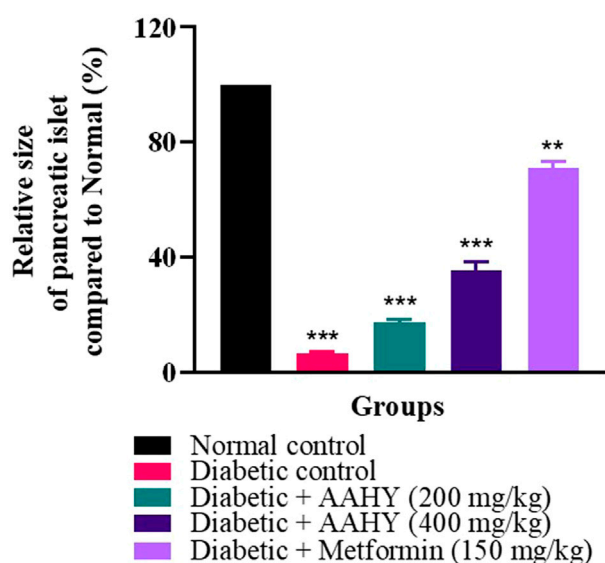


FIGURE 9

Graph showing the relative size of the pancreatic islets compared to that of the normal control. The error bar denotes mean \pm SEM, and $n = 6$ for each group. ** $p < 0.01$ and *** $p < 0.001$ versus the normal control group. SEM: standard error of mean.

the test is preferably taken in conjunction with other tests such as the fasting blood glucose and oral glucose tolerance test for appropriate diagnosis (Hussain, 2016). In the present experimental study, the OGTT and FBG test showed reduction in blood glucose levels after administration of the AAHY extract and metformin. HbA1c was also reduced in the treated groups compared to that of the diabetic group. The decrease in HbA1c and FBG levels in treated diabetic rats is an indication of improving glycemia.

The liver is the largest vital organ for metabolism, excretion, and detoxification. Liver damage is linked with necrotic cells, a hike in tissue lipid peroxidation, and a decrease in reduced glutathione levels, in addition to an increase in serum biochemical markers such as SGPT, SGOT, SALP, triglycerides, and cholesterol (Abou Seif, 2016). The liver of the STZ–NA-induced rats was damaged, and thus, the elevated serum biochemical markers of liver function might be primarily due to the enzymes leaking from the liver cytosol into the bloodstream (Kasetti et al., 2010). Administration of the extract and metformin showed significant reduction in the serum biochemical parameters compared to the diabetic control groups. The diabetic control rats showed the presence of significantly elevated levels of urea and creatinine in serum, which are known markers for kidney dysfunction (Gowda et al., 2010). The serum urea and creatinine levels, presented in the current study of the diabetic treated rats were reduced, indicating the gradual improvement of renal damage compared to the untreated rats.

Abnormal metabolism of enzyme lipoprotein lipase leads to accumulation of triglycerides and total cholesterol (TC), but decreased HDL cholesterol, which are commonly linked with DM and result in diabetic dyslipidemia. Increased levels of TG and TC and decreased HDL are also significant risk factors for cardiovascular diseases (CVDs). Elevated HDL aids in transportation of cholesterol to the liver, which is the primary site for fatty acid metabolism, thus reducing the risk of CVDs. So, in the diabetic condition, there is insulin deficiency due to which lipoproteins are unable to hydrolyze the lipids resulting in the systemic imbalance of synthesis, release, and rate of clearance of lipids (Moodley et al., 2015) (Sisay et al., 2022). In consistency with the reported data, we found elevated levels of TG and TC and decreased HDL cholesterol in the untreated STZ-NA-induced diabetic control group. Administering daily doses of the AAHY extract and metformin significantly decreased TG and TC, while increasing HDL cholesterol in the diabetic rats, indicating that the plant extract improves diabetes dyslipidemic conditions.

Histopathological examination of the STZ-NA-induced diabetic pancreas showed drastic damage to the β -cells, thereby reducing the number and size of the islets. The AAHY extract and metformin treatment groups improved the structure, number, and size of the pancreatic islets. The relative sizes of the treated pancreatic islets increased from $6.78\% \pm 0.39\%$ in diabetic to $17.23\% \pm 1.25\%$ and $35.46\% \pm 2.96\%$ in the AAHY extract 200 and 400 mg/kg b.w.-treated groups when compared with the normal group. Regeneration and restoration of normal β -cell function are critically required for a successful prevention and treatment of diabetes (Chen et al., 2017). A gradual improvement observed in the pancreatic histology of treatment groups suggests the potential preventive and protective nature of the extract against STZ-induced diabetic rats. However, the mechanistic pathway whether the effective nature was due to insulin production or sensitization following administration of the AAHY extract needs to be further assessed.

5 Conclusion

From this study, it can be concluded that the hydroalcoholic extract of *A. adenophora* has significant blood glucose lowering capacity on nomoglycemic, diabetic, and oral glucose-loaded Wistar albino rats while maintaining the body weight of diabetic rats. The experimental results verified that the *A. adenophora* hydroalcoholic extract has beneficial effects in inhibiting α -glucosidase and α -amylase activities and restored the altered blood glucose level, glycated hemoglobin, body weight, serum enzymes (SGOT, SGPT, and ALP), total protein, urea, and creatinine levels close to the normal range in treated STZ-NA-induced diabetic rats. The AAHY extract significantly enhanced tissue antioxidant parameters (SOD, GSH, and LPO) close to the normal level. The presence of high quantity of chlorogenic and caffeic acids as some of the major phytoconstituents may contribute to the improvement of glucose tolerance, insulin resistance, cellular oxidative stress, and obesity in STZ-induced diabetic rats. However, purification of chlorogenic and caffeic acids, as well as their novel mechanisms of lowering the hyperglycemic condition in T2DM, needs detailed evaluation. In addition, the bioactivity of other groups of secondary metabolites

alone or synergistic effect needs scientific evaluation. Even though the results provide scientific support for the traditional use of the plant to treat diabetes, elaborative research is obligatory for safety assessment in the long run. Although the preventive role of the AAHY extract against T2DM is undeniable, further pharmacokinetic and mechanistic pathway studies are needed to determine the extract metabolism, normalization of blood glucose, and biochemical parameters, as well as insulin production or sensitization following administration of the AAHY extract. The present study could play a promoting role in the discovery and development of a new antidiabetic agent from *A. adenophora*.

Data availability statement

The original contributions presented in the study are included in the article/Supplementary Material; further inquiries can be directed to the corresponding author.

Ethics statement

The animal study was reviewed and approved by the Animal Ethical Committee (Ref No. ACE/PHARM/1502/09/2015, Jadavpur University, Kolkata 700032, West Bengal, India).

Author contributions

Conceptualization: KC and VK; data curation: KC, VK, and SC; formal analysis: KC and SC; investigation: KC, VK, SG, and SC; methodology: KC and SC; project administration: NS and PH; resources: KC; software: KC; supervision: NS and PH; validation: KC and VK; visualization: KC, SC, PH, and PM; writing—original draft: KC; and writing—review and editing: KC, VK, SC, SG, NS, PH, and PM.

Funding

This research was funded by the “Himalayan Bioresources Mission,” under the Department of Biotechnology, Grant No. BT/PR45281/NER/95/1934/2022.

Acknowledgments

The authors acknowledge Biseswhori Thongam (Scientist, IBSD) for identification and authentication of the plant sample. They also appreciate the laboratory members for their assistance in the experimental setup.

Conflict of interest

The authors declare that the research was conducted in the absence of any commercial or financial relationships that could be construed as a potential conflict of interest.

Publisher's note

All claims expressed in this article are solely those of the authors and do not necessarily represent those of their affiliated

References

- Abou Seif, H. S. (2016). Physiological changes due to hepatotoxicity and the protective role of some medicinal plants. *Beni-Suef Univ. J. Basic Appl. Sci.* 5 (2), 134–146. doi:10.1016/j.bjbas.2016.03.004
- Adhikari, B. (2021). Roles of alkaloids from medicinal plants in the management of diabetes mellitus. *J. Chem.* 2021, 1–10. doi:10.1155/2021/2691525
- Ajebli, M., and Eddouks, M. (2019). The promising role of plant tannins as bioactive antidiabetic agents. *Curr. Med. Chem.* 26 (25), 4852–4884. doi:10.2174/0929867325666180605124256
- Ajebli, M., Khan, H., and Eddouks, M. (2021). Natural alkaloids and diabetes mellitus: A review. *Endocr. Metab. Immune Disord. Drug Targets* 21 (1), 111–130. doi:10.2174/1871530320666200821124817
- Alamgeer, A., Akhtar, M. S., Jabeen, Q., Akram, M., Khan, H. U., Karim, S., et al. (2013). Antihypertensive activity of aqueous-methanol extract of *Berberis orthobotrys* Bien Ex Aitch in rats. *Trop. J. Pharm. Res.* 12 (3), 393–399. doi:10.4314/tjpr.v12i3.18
- Alturkistani, H. A., Tashkandi, F. M., and Mohammedsah, Z. M. (2015). Histological stains: A literature review and case study. *Glob. J. health Sci.* 8 (3), 72–79. doi:10.5539/gjhs.v8n3p72
- Amorati, R., and Valgimigli, L. (2018). Methods to measure the antioxidant activity of phytochemicals and plant extracts. *J. Agric. Food Chem.* 66 (13), 3324–3329. doi:10.1021/acs.jafc.8b01079
- André, R., Catarro, J., Freitas, D., Pacheco, R., Oliveira, M. C., Serralheiro, M. L., et al. (2019). Action of euptox A from *Ageratina adenophora* juice on human cell lines: A top-down study using ftr spectroscopy and protein profiling. *Toxicol. Vitro* 57, 217–225. doi:10.1016/j.tiv.2019.03.012
- Awah, F. M., Uzoegwu, P. N., Ifeonu, P., Oyugi, J. O., Rutherford, J., Yao, X., et al. (2012). Free radical scavenging activity, phenolic contents and cytotoxicity of selected Nigerian medicinal plants. *Food Chem.* 131 (4), 1279–1286. doi:10.1016/j.foodchem.2011.09.118
- Bailey, C. J., and Day, C. (2004). Metformin: Its botanical background. *Pract. Diabetes Int.* 21 (3), 115–117. doi:10.1002/pdi.606
- Banu, K. S., and Cathrine, L. (2015). General techniques involved in phytochemical analysis. *Int. J. Adv. Res. Chem. Sci.* 2 (4), 25–32.
- Belayneh, Y. M., Birhanu, Z., Birru, E. M., and Getenet, G. (2019). Evaluation of *in vivo* antidiabetic, antidiyslipidemic, and *in vitro* antioxidant activities of hydromethanolic root extract of *datura stramonium* L. (Solanaceae). *J. Exp. Pharmacol.* 11, 29–38. doi:10.2147/JEP.S192264
- Bhatti, J. S., Sehrawat, A., Mishra, J., Sidhu, I. S., Navik, U., Khullar, N., et al. (2022). Oxidative stress in the pathophysiology of type 2 diabetes and related complications: Current therapeutics strategies and future perspectives. *Free Radic. Biol. Med.* 184, 114–134. doi:10.1016/j.freeradbiomed.2022.03.019
- Birru, E. M., Abdelwuhab, M., and Shewamene, Z. (2015). Effect of hydroalcoholic leaves extract of *Indigofera spicata* Forssk. on blood glucose level of normal, glucose loaded and diabetic rodents. *BMC Complementary Altern. Med.* 15 (1), 321–328. doi:10.1186/s12906-015-0852-8
- Blonde, L. (2009). Current antihyperglycemic treatment strategies for patients with type 2 diabetes mellitus. *Cleavel. Clin. J. Med.* 76 (5), 4–11. doi:10.3949/ccjm.76.s5.02
- Bustos-brito, C., Andrade-Cetto, A., Giraldo-Aguirre, J. D., Moreno-Vargas, A. D., and Quijano, L. (2016). Acute hypoglycemic effect and phytochemical composition of *Ageratina petiolaris*. *J. Ethnopharmacol.* 185, 341–346. doi:10.1016/j.jep.2016.03.048
- Carles, M., Hubert, S., Massa, H., and Raucoules-Aimé, M. (2008). Use of oral antidiabetic agents. *Prat. Anesthésie Reanim.* 12 (6), 448–455. doi:10.1016/j.pratan.2008.10.010
- Chan, N. N., Kong, A. P. S., and Chan, J. C. N. (2005). Metabolic syndrome and type 2 diabetes: The Hong Kong perspective. *Clin. Biochem. Rev./Aust. Assoc. Clin. Biochem.* 26 (3), 51–57.
- Chaudhary, S. K., Kar, A., Bhardwaj, P. K., Sharma, N., Indira Devi, S., and Mukherjee, P. K. (2023). A validated high-performance thin-layer chromatography method for the quantification of chlorogenic acid in the hydroalcoholic extract of *Gynura cusimbua* leaves. *JPC-journal Planar Chromatogr. TLC* 36, 1–9. doi:10.1007/s00764-023-00230-7
- Chaudhury, A., Duvoor, C., Reddy Dendi, V. S., Kraleiti, S., Chada, A., Ravilla, R., et al. (2017). Clinical review of antidiabetic drugs: Implications for type 2 diabetes mellitus management. *Front. Endocrinol.* 8, 6. doi:10.3389/fendo.2017.00006
- Chen, C., Cohrs, C. M., Stertmann, J., Bozsak, R., and Speier, S. (2017). Human beta cell mass and function in diabetes: Recent advances in knowledge and technologies to understand disease pathogenesis. *Mol. Metab.* 6 (9), 943–957. doi:10.1016/j.molmet.2017.06.019
- Chen, L., Teng, H., and Cao, H. (2019). Chlorogenic acid and caffeic acid from *Sonchus oleraceus* Linn synergistically attenuate insulin resistance and modulate glucose uptake in HepG2 cells. *Food Chem. Toxicol.* 127, 182–187. doi:10.1016/j.fct.2019.03.038
- Cho, A. S., Jeon, S. M., Kim, M. J., Yeo, J., Seo, K. I., Choi, M. S., et al. (2010). Chlorogenic acid exhibits anti-obesity property and improves lipid metabolism in high-fat diet-induced-obese mice. *Food Chem. Toxicol.* 48 (3), 937–943. doi:10.1016/j.fct.2010.01.003
- Cho, N. H., Shaw, J. E., Karuranga, S., Huang, Y., da Rocha Fernandes, J. D., Ohlrogge, A. W., et al. (2018). IDF Diabetes Atlas: Global estimates of diabetes prevalence for 2017 and projections for 2045. *Diabetes Res. Clin. Pract.* 138, 271–281. doi:10.1016/j.diabres.2018.02.023
- Dahlén, A. D., Dashi, G., Maslov, I., Attwood, M. M., Jonsson, J., Trukhan, V., et al. (2022). Trends in antidiabetic drug discovery: FDA approved drugs, new drugs in clinical trials and global sales. *Front. Pharmacol.* 12, 807548–807616. doi:10.3389/fphar.2021.807548
- Demir, Y., Özasan, M. S., Duran, H. E., Küfrevioğlu, Ö. İ., and Beydemir, Ş. (2019). Inhibition effects of quinones on aldose reductase: Antidiabetic properties. *Environ. Toxicol. Pharmacol.* 70, 103195. doi:10.1016/j.etap.2019.103195
- Dong, H. Q., Zhu, F., Liu, F. L., and Huang, J. B. (2012). Inhibitory potential of trilobatin from *Lithocarpus polystachyus* Rehd against α -glucosidase and α -amylase linked to type 2 diabetes. *Food Chem.* 130 (2), 261–266. doi:10.1016/j.foodchem.2011.07.030
- Dos Santos, M. D., Almeida, M. C., Lopes, N. P., and de Souza, G. E. P. (2006). Evaluation of the anti-inflammatory, analgesic and antipyretic activities of the natural polyphenol chlorogenic acid. *Biol. Pharm. Bull.* 29 (11), 2236–2240. doi:10.1248/bpb.29.2236
- Dowarah, J., and Singh, V. P. (2020). Anti-diabetic drugs recent approaches and advancements. *Bioorg. Med. Chem.* 28 (5), 115263. doi:10.1016/j.bmc.2019.115263
- Drucker, D. J. (2006). The biology of incretin hormones. *Cell Metab.* 3 (3), 153–165. doi:10.1016/j.cmet.2006.01.004
- Ekor, M. (2014). The growing use of herbal medicines: Issues relating to adverse reactions and challenges in monitoring safety. *Front. Neurology* 4, 177–210. doi:10.3389/fphar.2013.00177
- Ellman, G. L. (1959). Tissue sulfhydryl groups. *Archives Biochem. Biophysics* 82, 70–77. doi:10.1016/0003-9861(59)90090-6
- Feldman, J. M. (1985). Glyburide: A second-generation sulfonylurea hypoglycemic agent: History, chemistry, metabolism, pharmacokinetics, clinical use and adverse effects. *Pharmacother. J. Hum. Pharmacol. Drug Ther.* 5 (2), 43–62. doi:10.1002/j.1875-9114.1985.tb03404.x
- Floegel, A., Kim, D. O., Chung, S. J., Koo, S. I., and Chun, O. K. (2011). Comparison of ABTS/DPPH assays to measure antioxidant capacity in popular antioxidant-rich US foods. *J. Food Compos. Analysis* 24 (7), 1043–1048. doi:10.1016/j.jfca.2011.01.008
- Ganguly, R., Singh, S. V., Jaiswal, K., Kumar, R., and Pandey, A. K. (2023). Modulatory effect of caffeic acid in alleviating diabetes and associated complications. *World J. Diabetes* 14 (2), 62–75. doi:10.4239/wjd.v14.i2.62
- Ghasemi, A., Khalifi, S., and Jedi, S. (2014). Streptozotocin-nicotinamide-induced rat model of type 2 diabetes (review). *Acta Physiol. Hung.* 101 (4), 408–420. doi:10.1556/APhysiol.101.2014.4.2
- Gowda, S., Desai, P. B., Kulkarni, S. S., Hull, V. V., Math, A. A. K., and Vernekar, S. N. (2010). Markers of renal function tests. *North Am. J. Med. Sci.* 2 (4), 170–173.
- Grace, S. R. S., Chandran, G., and Chauhan, J. B. (2019). Terpenoids: An activator of “fuel-sensing enzyme AMPK” with special emphasis on antidiabetic activity. *Plant Hum. Health* 2, 227–244.
- Gutiérrez-González, J. A., Pérez-Vásquez, A., Torres-Colín, R., Rangel-Grimaldo, M., Rebollar-Ramos, D., and Mata, R. (2021). α -glucosidase inhibitors from *Ageratina grandifolia*. *J. Nat. Prod.* 84 (5), 1573–1578. doi:10.1021/acs.jnatprod.1c00105
- He, J. H., Chen, L. X., and Li, H. (2019). Progress in the discovery of naturally occurring anti-diabetic drugs and in the identification of their molecular targets. *Fitoterapia* 134, 270–289. doi:10.1016/j.fitote.2019.02.033
- Hussain, N. (2016). Implications of using HBA1 C as a diagnostic marker for diabetes. *Diabetol. Int.* 7 (1), 18–24. doi:10.1007/s13340-015-0244-9

- Kakkar, P., Das, B., and Viswanathan, P. N. (1984). A modified spectrophotometric assay of superoxide dismutase. *Indian J. Biochem. Biophysics* 21 (2), 130–132.
- Kapali, J., and Sharma, K. R. (2021). Estimation of phytochemicals, antioxidant, antidiabetic and brine shrimp lethality activities of some medicinal plants growing in Nepal. *J. Med. Plants* 20 (80), 102–116. doi:10.52547/jmp.20.80.102
- Kasetti, R. B., Rajasekhar, M. D., Kondeti, V. K., Fatima, S. S., Kumar, E. G. T., Swapna, S., et al. (2010). Antihyperglycemic and antihyperlipidemic activities of methanol: Water (4 : 1) fraction isolated from aqueous extract of *Syzygium alternifolium* seeds in streptozotocin induced diabetic rats. *Food Chem. Toxicol.* 48 (4), 1078–1084. doi:10.1016/j.fct.2010.01.029
- Khurshed, R., Singh, S. K., Wadhwa, S., Kapoor, B., Gulati, M., Kumar, R., et al. (2019). Treatment strategies against diabetes: Success so far and challenges ahead. *Eur. J. Pharmacol.* 862 172625. doi:10.1016/j.ejphar.2019.172625
- Kifle, Z. D., Yesuf, J. S., and Atnafie, S. A. (2020). Evaluation of *in vitro* and *in vivo* anti-diabetic, anti-hyperlipidemic and anti-oxidant activity of flower crude extract and solvent fractions of *Hagenia abyssinica* (Rosaceae). *J. Exp. Pharmacol.* 12, 151–167. doi:10.2147/JEP.S249964
- Kim, Y. M., Wang, M. H., and Rhee, H. I. (2004). A novel alpha-glucosidase inhibitor from pine bark. *Carbohydr. Res.* 339 (3), 715–717. doi:10.1016/j.carres.2003.11.005
- Kuo, F. Y., Cheng, K. C., Li, Y., and Cheng, J. T. (2021). Oral glucose tolerance test in diabetes, the old method revisited. *World J. Diabetes* 12 (6), 786–793. doi:10.4239/wjd.12.6.786
- Lebovitz, H. E., and Banerji, M. A. (2001). Insulin resistance and its treatment by thiazolidinediones. *Recent Prog. Hormone Res.* 56, 265–294. doi:10.1210/rp.56.1.265
- Liu, B., Dong, B., Yuan, X., Huang, Q., Zhao, Q., Yang, M., et al. (2016). Enrichment and separation of chlorogenic acid from the extract of *Eupatorium adenophorum* Spreng by macroporous resin. *J. Chromatogr. B Anal. Technol. Biomed. Life Sci.* 1008, 58–64. doi:10.1016/j.jchromb.2015.10.026
- Liu, P. Y., Liu, D., Li, W. H., Zhao, T., Sauriol, F., Gu, Y. C., et al. (2015). Chemical constituents of plants from the genus *Eupatorium* (1904–2014). *Chem. Biodivers.* 12 (10), 1481–1515. doi:10.1002/cbdv.201400227
- Liu, Y., Sun, J., Rao, S., Su, Y., and Yang, Y. (2013). Antihyperglycemic, antihyperlipidemic and antioxidant activities of polysaccharides from *Catathelasma ventricosum* in streptozotocin-induced diabetic mice. *Food Chem. Toxicol.* 57, 39–45. doi:10.1016/j.fct.2013.03.001
- Marklund, S., and Marklund, G. (1974). Involvement of the superoxide anion radical in the autooxidation of pyrogallol and a convenient assay for superoxide dismutase. *Eur. J. Biochem.* 47 (3), 469–474. doi:10.1111/j.1432-1033.1974.tb03714.x
- Mata-torres, G., Andrade-cetto, A., Espinoza-Hernández, F. A., and Cárdenas-Vázquez, R. (2020). Hepatic glucose output inhibition by Mexican plants used in the treatment of type 2 diabetes. *Front. Pharmacol.* 11, 215. doi:10.3389/fphar.2020.00215
- Matboli, M., Eissa, S., Ibrahim, D., Hegazy, M. G. A., Imam, S. S., and Habib, E. K. (2017). Caffeic acid attenuates diabetic kidney disease via modulation of autophagy in a high-fat diet/streptozotocin-induced diabetic rat. *Sci. Rep.* 7 (1), 2263–2312. doi:10.1038/s41598-017-02320-z
- Meng, S., Cao, J., Feng, Q., Peng, J., and Hu, Y. (2013). Roles of chlorogenic acid on regulating glucose and lipids metabolism: A review. *Evidence-based Complementary Altern. Med.* 2013, 801457. doi:10.1155/2013/801457
- Moodley, K., Joseph, K., Naidoo, Y., Islam, S., and Mackraj, I. (2015). Antioxidant, antidiabetic and hypolipidemic effects of *Tulbaghia violacea* Harv. (wild garlic) rhizome methanolic extract in a diabetic rat model. *BMC Complementary Altern. Med.* 15 (1), 408–413. doi:10.1186/s12906-015-0932-9
- Moron, M. S., Depierre, J. W., and Mannervik, B. (1979). Levels of glutathione, glutathione reductase and glutathione S-transferase activities in rat lung and liver. *Biochimica Biophysica Acta* 582 (1), 67–78. doi:10.1016/0304-4165(79)90289-7
- Muniappan, R., Raman, A., and Reddy, G. V. P. (2009). “*Ageratina adenophora* (sprengel) king and robinson (Asteraceae),” in *Biological control of tropical weeds using arthropods* (Cambridge, UK: Cambridge University Press), 63–73. March 2009. doi:10.1017/CBO9780511576348.004
- Naveed, M., Hejazi, V., Abbas, M., Kamboh, A. A., Khan, G. J., Shumzaid, M., et al. (2018). Chlorogenic acid (cga): A pharmacological review and call for further research. *Biomed. Pharmacother.* 97, 67–74. doi:10.1016/j.biopha.2017.10.064
- Niehaus, W. G., and Samuelsson, B. (1968). Formation of malonaldehyde from phospholipid arachidonate during microsomal lipid peroxidation. *Eur. J. Biochem.* 6 (1), 126–130. doi:10.1111/j.1432-1033.1968.tb00428.x
- OECD (2022). *Test guideline 425: Acute oral toxicity - up-and-down procedure*. OECD Guideline for Testing of Chemicals, Paris, France, OECD Publishing 26.
- Oguntibeju, O. O. (2019). Type 2 diabetes mellitus, oxidative stress and inflammation: Examining the links. *Int. J. physiology, Pathophysiol. Pharmacol.* 11 (3), 45–63.
- Ohkawa, H., Ohishi, N., and Yagi, K. (1979). Assay for lipid peroxides in animal tissues by thiobarbituric acid reaction. *Anal. Biochem.* 95 (2), 351–358. doi:10.1016/0003-2697(79)90738-3
- Orfali, R., Perveen, S., Aati, H. Y., Alam, P., Noman, O. M., Palacios, J., et al. (2021). High-performance thin-layer chromatography for rutin, chlorogenic acid, caffeic acid, ursolic acid, and stigmasterol analysis in periploca aphylla extracts. *Separations* 8 (4), 44–12. doi:10.3390/separations8040044
- Osadebe, P., Odoh, E., and Uzor, P. (2014). Natural products as potential sources of antidiabetic drugs. *Br. J. Pharm. Res.* 4 (17), 2075–2095. doi:10.9734/bjpr/2014/8382
- Padhi, S., Nayak, A. K., and Behera, A. (2020). Type II diabetes mellitus: A review on recent drug based therapeutics. *Biomed. Pharmacother.* 131, 110708. doi:10.1016/j.biopha.2020.110708
- Poudel, R., Neupane, N. P., Muker, I. H., Alok, S., and Verma, A. (2020). An updated review on invasive nature, phytochemical evaluation, and pharmacological activity of *Ageratina adenophora* introduction: *Ageratina adenophora*. *Int. J. Pharm. Sci. Res.* 11 (6), 2510–2520. doi:10.13040/IJPSR.0975-8232.11(6).2510-20
- Praparatana, R., Maliyam, P., Barrows, L. R., and Puttarak, P. (2022). Flavonoids and phenols, the potential anti-diabetic compounds from *Bauhinia strychnifolia* craib. *Stem. Molecules* 27 (8), 2393–2416. doi:10.3390/molecules27082393
- Ringmichon, C., and Gopalkrishnan, B. (2017). Antipyretic activity of *Eupatorium adenophorum* leaves. *Int. J. Appl. Biol. Pharm. Technol.* 8 (3), 1–4. doi:10.21276/Ijabpt
- Santana-Gálvez, J., Cisneros-Zevallos, L., and Jacobo-Velázquez, D. A. (2017). Chlorogenic Acid: Recent advances on its dual role as a food additive and a nutraceutical against metabolic syndrome. *Molecules* 22 (3), 358. doi:10.3390/molecules22030358
- Sekhon-Loodu, S., and Rupasinghe, H. P. V. (2019). Evaluation of antioxidant, antidiabetic and antiobesity potential of selected traditional medicinal plants. *Front. Nutr.* 6, 53–11. doi:10.3389/fnut.2019.00053
- Sherwani, S. I., Khan, H. A., Ekhzaimy, A., Masood, A., and Sakharkar, M. K. (2016). Significance of HbA1c test in diagnosis and prognosis of diabetic patients. *Biomark. Insights* 11, 95–104. doi:10.4137/BMLS38440
- Sisay, W., Andargie, Y., Molla, M., Tessema, G., and Singh, P. (2022). *Glinus lotoides* linn. Seed extract as antidiabetic agent: *In vitro* and *in vivo* anti-glucolipotoxicity efficacy in type-II diabetes mellitus. *Metab. Open* 14, 100189. doi:10.1016/j.metop.2022.100189
- Stagos, D. (2020). Antioxidant activity of polyphenolic plant extracts. *Antioxidants* 9 (1), 19. doi:10.3390/antiox9010019
- Sumaira, K., and Khan, H. (2018). Phyto-glycosides as therapeutic target in the treatment of diabetes. *Mini Rev. Med. Chem.* 18 (3), 208–215. doi:10.2174/138957516666160909112751
- Tahrani, A. A., Bailey, C. J., Del Prato, S., and Barnett, A. H. (2011). Management of type 2 diabetes: New and future developments in treatment. *Lancet* 378 (9786), 182–197. doi:10.1016/S0140-6736(11)60207-9
- Telagari, M., and Hullatti, K. (2015). *In-vitro* α-amylase and α-glucosidase inhibitory activity of *Adiantum caudatum* Linn. and *Celosia argentea* Linn. extracts and fractions. *Indian J. Pharmacol.* 47 (4), 425–429. doi:10.4103/0253-7613.161270
- Triggle, C. R., Mohammed, I., Bshesh, K., Marei, I., Ye, K., Ding, H., et al. (2022). Metformin: Is it a drug for all reasons and diseases. *Metabolism* 133, 155223. doi:10.1016/j.metabol.2022.155223
- Wan, F. H., Liu, W., Guo, J., Qiang, S., Li, B., Wang, J., et al. (2010). Invasive mechanism and control strategy of *Ageratina adenophora* (Sprengel). *Sci. China Life Sci.* 53 (11), 1291–1298. doi:10.1007/s11427-010-4080-7
- WHO (2011). *Use of glycated haemoglobin (HbA1c) in the diagnosis of diabetes mellitus: Abbreviated report of a WHO consultation. Approved by the guidelines review committee*. Geneva, Switzerland: World Health Organization, 299–309.
- Xu, L., Li, Y., Dai, Y., and Peng, J. (2018). Natural products for the treatment of type 2 diabetes mellitus: Pharmacology and mechanisms. *Pharmacol. Res.* 130, 451–465. doi:10.1016/j.phrs.2018.01.015
- Yao, X., Zhu, L., Chen, Y., Tian, J., and Wang, Y. (2013). *In vivo* and *in vitro* antioxidant activity and α-glucosidase, α-amylase inhibitory effects of flavonoids from *Cichorium glandulosum* seeds. *Food Chem.* 139 (1–4), 59–66. doi:10.1016/j.foodchem.2012.12.045
- Zhang, Y. J., Gan, R. Y., Li, S., Zhou, Y., Li, A. N., Xu, D. P., et al. (2015). Antioxidant phytochemicals for the prevention and treatment of chronic diseases. *Molecules* 20 (12), 21138–21156. doi:10.3390/molecules201219753
- Zhao, X., Liu, Z., Liu, H., Guo, J., and Long, S. (2022). Hybrid molecules based on caffeic acid as potential therapeutics: A focused review. *Eur. J. Med. Chem.* 243, 114745–114815. doi:10.1016/j.ejmech.2022.114745



OPEN ACCESS

EDITED BY

Ochuko Lucky Erukainure,
University of the Free State, South Africa

REVIEWED BY

Okukwe Obode,
Federal Institute of Industrial Research
Oshodi, Nigeria
Marvellous Acho,
Landmark University, Nigeria

*CORRESPONDENCE

Yi Li,
✉ peach_adore@hotmail.com/liyi@
wchscu.cn

RECEIVED 17 March 2023

ACCEPTED 10 April 2023

PUBLISHED 24 April 2023

CITATION

Wang D and Li Y (2023), Pharmacological
effects of baicalin in lung diseases.
Front. Pharmacol. 14:1188202.
doi: 10.3389/fphar.2023.1188202

COPYRIGHT

© 2023 Wang and Li. This is an open-
access article distributed under the terms
of the [Creative Commons Attribution
License \(CC BY\)](#). The use, distribution or
reproduction in other forums is
permitted, provided the original author(s)
and the copyright owner(s) are credited
and that the original publication in this
journal is cited, in accordance with
accepted academic practice. No use,
distribution or reproduction is permitted
which does not comply with these terms.

Pharmacological effects of baicalin in lung diseases

Duoning Wang^{1,2} and Yi Li ^{2*}

¹Chengdu Hi-tech Nanxili Jiuzheng Clinic, Chengdu, Sichuan, China, ²Department of Respiratory and Critical Care Medicine, Institute of Respiratory Health, Precision Medicine Key Laboratory, West China Hospital, Sichuan University, Chengdu, Sichuan, China

The flavonoids baicalin and baicalein were discovered in the root of *Scutellaria baicalensis* Georgi and are primarily used in traditional Chinese medicine, herbal supplements and healthcare. Recently, accumulated investigations have demonstrated the therapeutic benefits of baicalin in treating various lung diseases due to its antioxidant, anti-inflammatory, immunomodulatory, antiapoptotic, anticancer, and antiviral effects. In this review, the PubMed database and ClinicalTrials website were searched with the search string “baicalin” and “lung” for articles published between September 1970 and March 2023. We summarized the therapeutic role that baicalin plays in a variety of lung diseases, such as chronic obstructive pulmonary disease, asthma, pulmonary fibrosis, pulmonary hypertension, pulmonary infections, acute lung injury/acute respiratory distress syndrome, and lung cancer. We also discussed the underlying mechanisms of baicalin targeting in these lung diseases.

KEYWORDS

baicalin, lung disease, lung infection, lung injury, lung cancer

Introduction

Lung disease is a major global health concern, affecting millions of people worldwide. Baicalin is a flavonoid compound isolated from the root of *Scutellaria baicalensis* Georgi. Baicalein is a flavone, a type of polyphenolic flavonoid, while baicalin is a flavone glycoside, the glucuronide of baicalein, which is obtained through the binding of glucuronic acid to baicalein. As a natural medicine, baicalin has thus been widely used in the treatment of clinical diseases such as cardiovascular and liver disease, diabetes, and neurodegenerative disorders. Baicalin has been shown to have potent antioxidant, anti-inflammatory, immunomodulatory, and antiapoptotic effects, making it a promising candidate for the treatment of several disease conditions. It thus has wide applications in medicine, healthcare, and food industries and has become a focused issue and trend in research worldwide in recent years. It has also been widely studied for its potential therapeutic benefits in treating various lung diseases, including chronic obstructive pulmonary disease (COPD), asthma and acute lung injury (ALI). The pharmacological contributions of baicalin to multiple lung diseases are being revealed (He et al., 2021) but are not fully understood. Baicalin exhibits anti-inflammatory and immunomodulatory effects by targeting several signaling pathways, including nuclear factor- κ B (NF- κ B), phosphatidylinositol-3-kinase (PI3K)/AKT, mitogen-activated protein kinases (MAPKs), and Toll-like receptors (TLRs), leading to a reduction in the production of proinflammatory cytokines and chemokines and subsequent development of inflammation in lung diseases (Figure 1, Table 1). In addition, baicalin has been found to have antioxidant and anti-apoptotic properties, which help prevent oxidative damage to

Main mechanisms underlying Baicalin

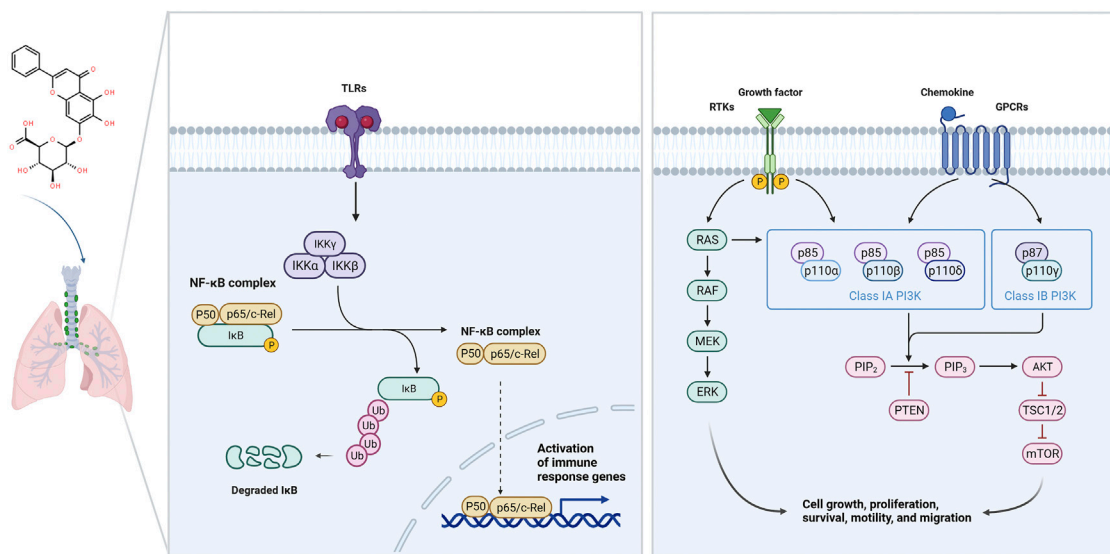


FIGURE 1
Regulatory signaling pathways implicated in baicalin.

cells and tissues. In addition, baicalin has been shown to have anticancer effects through its ability to inhibit the proliferation, migration, and invasion of cancer cells, including lung cancer cells, by inducing apoptosis and cell cycle arrest. Moreover, baicalin also exhibits antiviral effects against respiratory viruses such as influenza and severe acute respiratory syndrome coronavirus (SARS-CoV) by suppressing replication. In conclusion, baicalin shows great potential in the treatment of various lung diseases due to its anti-inflammatory, antioxidant, anticancer and antiviral properties. In this review, we will outline the recent understanding of baicalin treatment in lung diseases and its underlying mechanisms (Figure 2).

Methods

The PubMed database and ClinicalTrials website were searched for articles published between September 1970 and March 2023 using the following search string: (baicalin) and (lung). Studies of all designs that were accessible online were included if they met the following criteria: 1) published in English, 2) randomized control trials, other controlled trials, descriptive and comparative studies, evidence-based practice and 3) full-text available.

COPD

The prevalence of COPD, which is currently the fourth largest cause of morbidity and mortality worldwide, is rising (Barnes et al., 2015; Barnes et al., 2019). Chronic airway inflammation, lung damage, and remodeling are its hallmarks, all of which lead to an

irreversible blockage of airflow. Baicalin has been shown in studies to have anti-inflammatory and antioxidant effects that can help lessen the intensity of COPD symptoms. Moreover, baicalin has been shown to enhance lung health and lessen mucus formation in clinical practice, although there have been no reports to date. Additionally, it might protect the lungs from the harm caused by cigarette smoke and other environmental factors.

Baicalin has a variety of biological effects, including antioxidant and anti-inflammatory properties (Li et al., 2022). Mouse and cell models were stimulated by cigarette smoke (CS) and CS extract to investigate the effects and underlying mechanisms of baicalin on COPD. According to the findings, baicalin may control the balance between pro- and anti-inflammatory responses and significantly improve lung function in COPD patients (Lixuan et al., 2010; Li et al., 2012; Wang et al., 2018; Zhang et al., 2021a; Hao et al., 2021). The anti-inflammatory effect was probably caused by the inhibition of NF-κB activation (Lixuan et al., 2010), the upregulation of histone deacetylase 2 (HDAC2) activity (Li et al., 2012), and the modulation of the HDAC2/NF-κB/plasminogen activator inhibitor 1 (PAI-1) signaling pathways (Zhang et al., 2021a). Hao et al. (2021) demonstrated that baicalin upregulated the expression of heat shock protein 72 (HSP72), resulting in the inhibition of c-Jun N-terminal kinase (JNK) signaling activation and ultimately relieving COPD. Recently, Ju et al. (2022) proved that baicalin controlled the TLR2/myeloid differentiation primary response gene 88 (MYD88)/NF-κB p65 signaling pathway to reduce oxidative stress and the inflammatory response in COPD rats. Through regulating oropharyngeal microbiota and influencing the expression of the High Mobility Group Protein 1 (HMGB1)/Caspase1 pathway, baicalin may also mitigate mouse lung inflammatory injury caused by exposure to PM2.5 (Deng et al., 2022).

TABLE 1 Application of baicalin in experimental models of lung diseases.

Disease	Species	Model	Target/Pathway	References
COPD	Rat	CS	NF- κ B↓	Lixuan et al. (2010)
	Mouse	CS	HDAC2 activity↑	Li et al. (2012)
	Rat	CS	Inflammatory cytokine regulation	Li et al. (2012), Wang et al. (2018)
	Rat	CS	HDAC2↑, NF- κ B/PAI-1↓	Zhang et al. (2021a)
	Mouse	CS	HSP72↑, JNK↓	Hao et al. (2021)
	Rat	CS, LPS, cold stimulation	TLR2/MYD88/NF- κ B p65↓	Ju et al. (2022)
	Mouse	PM2.5	Oropharyngeal microbiota balance	Deng et al. (2022)
			HMGB1/Caspase1↓	
Asthma	Mouse	OVA	ERK↓	Sun et al. (2013)
	Mouse	OVA	Th17 cells↓	Ma et al. (2014)
	Mouse	OVA + LPS	Th17/Treg balance	Xu et al. (2017a)
	Mouse	OVA	NF- κ B, CCR7/CCL19/CCL21↓	Park et al. (2016)
	Mouse	OVA	miR-103↑, TLR4/NF- κ B↓	Zhai and Wang (2022)
	Mouse	OVA	RAS↓	Hu et al. (2023)
PF	Mouse	Silica	Th17/Treg balance	Liu et al. (2015a)
	Rat	BLM	miR-21, TGF- β /Smad↓	Gao et al. (2013)
	Mouse	BLM	A2aR↑, TGF- β 1, ERK1/2↓	Huang et al. (2016)
	Rat	BLM	GPX, SOD, GSH↑	Huang et al. (2016)
	Mouse	Radiation	CysLTs/CysLT1↓	Bao et al. (2022)
	Rat	BLM	SOD↑, MDA, HYP↓	Chang et al. (2021)
PH	Rat	Hypoxia	p38 MAPK/MMP-9↓	Yan et al. (2016)
	Rat	Hypoxia	AKT↑, HIF-1 α ↓, p27↑	Zhang et al. (2014)
	Rat	Hypoxia	ADAMTS-1↑, Collagen I↓	Liu et al. (2015b)
	Rat	MCT	NF- κ B↓	Zhang et al. (2017a)
	Rat	MCT	TNF- α ↓, BMPR2↑	Xue et al. (2021)
	Rat	MCT	AKT, eNOS↑, ERK, NF- κ B↓	Yan et al. (2019)
Lung infection	Rat	<i>Pseudomonas aeruginosa</i>	Lung bacterial clearance↑	Zhang et al. (2021b)
	Mouse	<i>Staphylococcus aureus</i>	Lung microbial load↓	Brackman et al. (2011)
	Mouse	Streptozotocin-induced diabetes mellitus	Lung microbial dysbiosis	Wang et al. (2021a)
	Chicken	Avian pathogenic <i>Escherichia coli</i>	NF- κ B↓	Peng et al. (2019)
	Chicken	<i>Mycoplasma gallisepticum</i>	TLR2/NF- κ B↓	Wu et al. (2019)
	Chicken	<i>Mycoplasma gallisepticum</i>	Inflammatory injury alleviation	Wang et al. (2021b)
	Mouse	<i>Staphylococcus aureus</i>	Inflammatory injury alleviation	Liu et al. (2017)
	Mouse	<i>Mycoplasma pneumoniae</i>	miR-221, TLR4/NF- κ B↓	Zhang et al. (2021c)
	Mouse	Influenza A/FM1/1/47(H1N1) virus	Lung virus titer↓	Xu et al. (2010)
	Rat			
	Mouse	H1N1 virus	Lung virus titer↓	Li and Wang (2019)
	Mouse	H1N1-H275Y	Neuraminidase activity↓	Jin et al. (2018)

(Continued on following page)

TABLE 1 (Continued) Application of baicalin in experimental models of lung diseases.

Disease	Species	Model	Target/Pathway	References
	Mouse	Influenza A (H1N1/H3N2)	Neuraminidase↓	Ding et al. (2014)
	Mouse	H1N1-pdm09	NS1↓	Nayak et al. (2014)
	Mouse	Influenza A	TLR7/MYD88↓	Wan et al. (2014)
	Mouse	Influenza A	IFN-γ↑, JAK/STAT-1↑	Chu et al. (2015)
	Mouse	Influenza A	RLR↓	Pang et al. (2018)
	Mouse	Influenza A	Inflammatory cytokine regulation	Zhi et al. (2019)
	Mouse	Influenza A	macrophage M1 polarization	Geng et al. (2020)
			IFN↑	
ALI/ARDS	Mouse	RSV	Antiviral, anti-inflammatory	Shi et al. (2016)
	Mouse	Staphylococcal enterotoxin B	Tryptophan metabolism regulation	Hu et al. (2022)
	Mouse	CLP	HMGB1↓	Wang and Liu (2014)
	Rat	LPS	Inflammatory cytokine regulation	Huang et al. (2008)
	Mouse	LPS	NF-κB↓	Shin et al. (2015)
	Rat	SAP	Amylase, NO, MDA, TNF-α↓	Zhang et al. (2008)
	Mouse	SAP	TLR4↓	Li et al. (2009a)
	Mouse	LPS	TLR4/NF-κB↓	Zhang et al. (2021d)
	Mouse	LPS	CX3CL1-CX3CR1, NF-κB↓	Ding et al. (2016)
	Mouse	LPS	Nrf2/HO-1↑	Meng et al. (2019)
	Mouse	LPS	TLR4/NF-κB, JNK/ERK↓	Long et al. (2020)
	Rat	LPS	TLR4/MYD88/NF-Kb, MAPK↓	Changle et al. (2022)
	Rat	LPS	Alveolar fluid clearance, α-ENaC↑	Deng et al. (2017)
	Rat	LHP	Lipid-peroxidation in mitochondria↓	Liau et al. (2019)
	Rat	Air embolism	NF-κB↓	Li et al. (2009b)
	Rat	Severe burn	HMGB1, NLRP3, caspase-1, NF-κB, MMP-9↓	Bai et al. (2018)
	Mouse	Hyperoxia	Cpt1a↑	Chang et al. (2022)
	Mouse	LPS	TLR4/NF-κB, MMP-9↓	Zhang et al. (2016)
	Mouse	LPS	TLR4/p-NF-κB↓	Feng et al. (2018)
Lung cancer	Mouse	A549, LLC	HIF-1α↓, SOD↑	Du et al. (2010)
	Mouse	A549	Antitumor	Wei et al. (2017)
	Mouse	A549	Invasion, migration, angiogenesis↓	Yan et al. (2020)
	Mouse	H1299, H1650	Akt/mTOR↓	Sui et al. (2020)
	Mouse	A549, H1299	Id1↓	Zhao et al. (2019)
	Mouse	H460	EMT, PDK1/AKT↓	Chen et al. (2021)

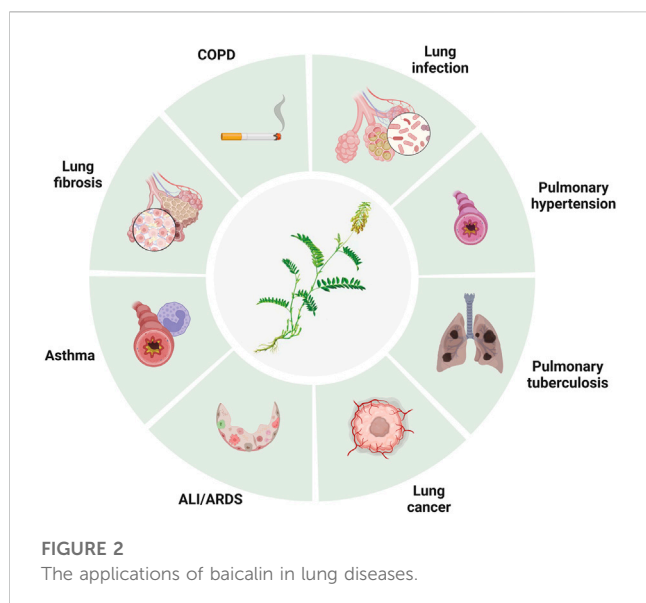
CS: cigarette smoke; LPS: lipopolysaccharide; OVA: ovalbumin; BLM: bleomycin; MCT: monocrotaline; CLP: cecal ligation and puncture; SAP: severe acute pancreatitis; LHP: linoleic acid hydroperoxide.

Asthma

Asthma is a chronic inflammatory respiratory disorder that results in intermittent episodes of wheezing, breathlessness, chest stuffiness, and cough. Chronic bronchial inflammation, bronchial

smooth muscle cell hypertrophy and hyperreactivity, as well as increased mucus output, are the disease’s defining characteristics (Papi et al., 2018).

In animal models of asthma, baicalin has been demonstrated to lower airway inflammation and enhance lung function (Sun et al.,



2013), in part by modulating the Th17/Treg imbalance (Ma et al., 2014; Xu et al., 2017a). Additionally, baicalin has also been demonstrated to lessen mucus production in the airways and inhibit the contraction of bronchial smooth muscle, which might lessen airway narrowing and improve breathing (Xu et al., 2017a). In a previous study, baicalin pretreatment inhibited the MAPK signaling pathway, significantly reducing the proliferation and migration of airway smooth muscle cells (ASMCs) stimulated by platelet-derived growth factor (PDGF) (Yang et al., 2015). Baicalin administration reduced inflammatory cell infiltration and tumor necrosis factor- α (TNF- α) levels in bronchoalveolar lavage fluids in an animal model of allergic asthma, demonstrating that the anti-inflammatory actions of baicalin *in vivo* are due to its capacity to inhibit phosphodiesterase 4 (PDE4) (Park et al., 2016). By inhibiting NF- κ B and reducing CC-chemokine receptor 7 (CCR7)/C-C motif chemokine ligand 19 (CCL19)/CCL21, Liu et al. showed that oral treatment with baicalin greatly enhanced pulmonary function and reduced inflammatory cell infiltration into the lungs (Liu et al., 2016), and Zhai et al. found that baicalin increased miRNA-103 and mediated the TLR4/NF- κ B pathway to successfully reverse ovalbumin (OVA)-induced oxidative stress, inflammation, and changes in the amount of total cells, eosinophils, and neutrophils in bronchoalveolar lavage fluid (BALF) as well as collagen deposition (Zhai and Wang, 2022).

Baicalin significantly decreased the infiltration of inflammatory cells in lung tissue, attenuated airway resistance, and reduced the levels of remodeling-related cytokines such as interleukin (IL-13), vascular endothelial growth factor (VEGF), transforming growth factor- β 1 (TGF- β 1), matrix metalloproteinase 9 (MMP9), and tissue inhibitor of metalloproteinase 1 (TIMP1) at both the mRNA and protein levels. In an OVA-induced asthmatic mouse model, baicalin administration suppressed the RAS signaling pathway to prevent airway remodeling and ASMC proliferation by regulating the activation of protein kinase C- α (PKC- α), A-rapidly accelerated fibrosarcoma (A-RAF), mitogen activated protein kinase 2 (MEK2), extracellular regulated MAP kinase (ERK), MAPK interacting serine/threonine kinase 1 (MNK1), and ETS transcription factor 1 (ELK1) (Hu et al., 2023). Baicalin has recently been demonstrated

to inhibit type 2 immunity by severing the interaction between mast cells and airway epithelial cells, suggesting that it may be a useful alternative therapy for the management of asthma (Yoshida et al., 2021). Baicalin may therefore be an effective medication for treating allergic and asthmatic disorders in humans by regulating NF- κ B activity and other signaling pathways.

Pulmonary fibrosis

Pulmonary fibrosis (PF) is a progressive, resistant pulmonary fibrotic condition with no known cause. Patchy but progressive bilateral interstitial fibrosis is the defining feature of PF, and in advanced cases, it can cause severe hypoxia and cyanosis (Lederer et al., 2018).

Treatment with baicalin in a mouse model of silicosis reduced the buildup of inflammatory cells by balancing the Th17 and Treg responses, which also resulted in fewer clinical inflammatory and fibrotic alterations in lung tissues (Liu et al., 2015a). Baicalin oral administration significantly reduced miR-21 levels, increased TGF- β 1 and p-smad2/3 expression, and decreased hydroxyproline content and α -smooth muscle actin (α -SMA) levels in lung tissue, which is important for myofibroblast activation and collagen deposition in the extracellular matrix (Gao et al., 2013). In a different study, Huang et al. hypothesized that baicalin exerts its antifibrotic effects by modulating the expression of the adenosine A2a receptor (A2aR) gene, which regulates inflammation by lowering the levels of increased TGF- β 1 and p-ERK1/2 (Huang et al., 2016). Subsequent research showed that baicalin considerably boosted serum levels of glutathione peroxidase (GPX), superoxide dismutase (SOD), and glutathione (GSH) while significantly lowering serum levels of malondialdehyde (MDA). Baicalin also controlled cyclin A, D, and E, proliferating cell nuclear antigen, p-AKT, and p-calcium/calmodulin dependent protein kinase type, suppressing the transition of cells from the G0/G1 phase to the G2/M and S phases and lowering the intracellular Ca^{2+} concentration to suppress bleomycin-induced pulmonary fibrosis and fibroblast proliferation (Zhao et al., 2020). By modulating the TGF- β and ERK/glycogen synthase kinase (GSK3 β) signaling pathways (Lu et al., 2017), as well as the cysteinyl leukotriene (CysLTs)/CysLT1 pathway (Bao et al., 2022), baicalin alleviates radiation-induced epithelial-mesenchymal transition of primary type II alveolar epithelial cells. Hong et al. revealed the antifibrotic mechanisms of baicalin, which involve the regulation of four key biomarkers involved in the metabolism of taurine, hypotaurine, glutathione and glycerophospholipids (Chang et al., 2021). Studies have shown that baicalin treatment can improve lung function and reduce symptoms; thus, it may be a useful alternative therapy for the management of PF.

Pulmonary hypertension

Pulmonary hypertension (PH) is usually secondary to a reduction in vessel diameter or an increase in blood flow in the pulmonary vascular bed (Vonk Noordegraaf et al., 2016). Most kinds of PH are thought to have a potential basis in the malfunctioning of pulmonary endothelial cells and/or vascular smooth muscle cells. The entire pulmonary arterial tree thickens the intima and media while

narrowing the lumen as a result of endothelial and smooth muscle cell proliferation (Cui et al., 2022). Pretreatment with baicalin in chronic hypoxic rats attenuated PH and right-sided heart dysfunction by reducing p38 MAPK activation, reducing the elevated levels of the proinflammatory cytokines IL-1, IL-6 and TNF- α and downregulating the expression of MMP9 in the pulmonary arteriole walls (Yan et al., 2016).

Baicalin decreased hypoxia inducible factor-1 (HIF-1) production in a model of hypoxia-induced PH by modulating the AKT signaling pathway to stop p27 degradation. Increased p27 levels thereby inhibited pulmonary artery smooth muscle cell (PASMC) proliferation, preventing hypoxia-induced increased pulmonary arterial pressure and pulmonary vascular remodeling (Zhang et al., 2014). Another study found that baicalin suppressed the HIF-1 α and aryl hydrocarbon receptor (AhR) pathways, which prevented TGF- β 1-induced phenotypic switching and consequently the excessive growth of pulmonary arterial smooth muscle cells (Huang et al., 2014). One study indicated that baicalin provided protection for rats suffering from hypoxic PH. The mechanism may involve an increase in ADAM metalloproteinase with thrombospondin type 1 motif 1 (ADAMTS-1) expression, which inhibits collagen I synthesis and expression (Liu et al., 2015b).

By inhibiting the inflammatory response and downregulating the NF- κ B signaling pathway, baicalin can considerably lower the expression of TGF- β 1 in lung tissues and pulmonary arterial pressure, lessen right ventricular hypertrophy and injury, and attenuate pulmonary vascular remodeling (Luan et al., 2015). Baicalin has been found in numerous studies to significantly reduce P38 MAPK and MMP-9 expression. It effectively improved hypoxia-induced PH in a rat model by blocking the p38 MAPK signaling pathway and MMP-9 in the small pulmonary arteries (Yan et al., 2016).

An earlier study revealed that baicalin had a therapeutic effect on the hypoxia-induced PH rat model, at least in part because it activates peroxisome proliferator-activated receptor γ (PPAR γ) and blocks the HMGB1/receptor for advanced glycation end-products (RAGE) inflammatory signaling pathway (Chen and Wang, 2017). In another study, baicalin exhibited increased A2aR activity and decreased stromal cell derived factor-1 (SDF-1)/C-X-C motif chemokine receptor 4 (CXCR4)-induced PI3K/AKT signaling to protect against hypoxia-induced PH (Huang et al., 2017).

Baicalin can inhibit monocrotaline (MCT)-induced PH in rats by upregulating bone morphogenetic protein 4 (BMP4), BMP9, BMP receptor 2 (BMPR2) and p-Smad1/5/8 expression, according to recent research. Baicalin greatly reduces the expression of NF- κ B, TNF- α , IL-6 and IL-1. Baicalin, on the other hand, may reduce pulmonary vascular remodeling by preventing ERK and NF- κ B phosphorylation and expression, as well as by suppressing endothelial-to-mesenchymal transition (EndMT) via the BMP/Smad axis and NF- κ B signaling (Zhang et al., 2017a; Xue et al., 2021). By decreasing p-p65 and p-ERK expression and encouraging p-AKT and p-endothelial nitric oxide synthase (eNOS) expression, baicalin ameliorated pulmonary vascular remodeling and cardiorespiratory injury in the development of pulmonary arterial hypertension through the AKT/eNOS, ERK and NF- κ B signaling pathways (Yan et al., 2019; Xue et al., 2021). By boosting the expression of ADAMTS-1, which inhibits the synthesis of type I collagen and its mRNA expression, baicalin administration

significantly decreased pulmonary artery pressure and slowed the remodeling of the pulmonary artery under hypoxic conditions, according to Liu et al. (Liu et al., 2015b).

Pulmonary infections

Pneumonia-related deaths from lung infections are common worldwide (McAllister et al., 2019). The lung's epithelial surfaces are constantly exposed to microbial pollutants in the open air, and other frequent lung conditions and bad lifestyle choices, such smoking and drinking, make the lung parenchyma susceptible to pathogenic organisms.

Treatment with baicalin considerably lessened the severity of lung pathology and sped up the clearance of *Pseudomonas aeruginosa* from the lungs. After baicalin treatment, the Th1-induced inflammatory response and decreased cell infiltration in the lung around the implants were observed (Zhang et al., 2021b). In a different investigation, tobramycin treatment in combination with baicalin hydrate reduced the microbial load in mouse lungs infected with *Burkholderia cenocepacia* more than tobramycin treatment alone (Brackman et al., 2011). Via an NF- κ B signaling pathway, baicalin might also treat the microbial dysbiosis of the lungs and the subsequent fibrogenesis in streptozotocin-induced diabetic mice (Wang et al., 2021a). Baicalin has also been shown to control the same pathway in avian pathogenic *Escherichia coli*-induced acute lung injury (Peng et al., 2019). Baicalin alleviates lung inflammatory injury in *Mycoplasma gallisepticum* infection models by inhibiting the TLR2/NF- κ B pathway (Wu et al., 2019) and regulates gut microbiota and phenylalanine metabolism by modulating the gga-miR-190a-3p-Fas-associated death domain (FADD) axis in HD11 macrophages (Wang et al., 2021b). Baicalin also inhibits the development of *Staphylococcus aureus* pneumonia (Liu et al., 2017).

Among chronic pneumonias, pulmonary tuberculosis is a dangerous infectious illness that poses a substantial threat to human health. According to the World Health Organization, it kills 6% of people worldwide and is now getting worse. Th1 cells are primarily responsible for driving immunity against tuberculosis infection by causing macrophages to kill bacteria (Jasenosky et al., 2015). Re-exposure to *Mycobacterium tuberculosis* (Mtb) or the reactivation of the infection in a previously sensitized host triggers a rapid defense response, although hypersensitivity also accelerates tissue necrosis and destruction. The findings showed that baicalin did not affect the phosphorylation of p38, JNK, or ERK in either Raw264.7 or primary peritoneal macrophages but did decrease the levels of p-AKT and p-mammalian target of rapamycin (mTOR) at Ser473 and Ser2448, respectively. Moreover, baicalin increased the colocalization of inflammasomes with autophagosomes to exert an autophagic degradative effect on reducing inflammasome activation and exerted an inhibitory effect on NF- κ B activity. Via the PI3K/AKT/mTOR pathway, baicalin causes autophagy activation in Mtb-infected macrophages. Moreover, baicalin inhibited the PI3K/AKT/NF- κ B signaling pathway, and both autophagy induction and NF- κ B inhibition contributed to limiting the activity of the NOD-like receptor

thermal protein domain associated protein 3 (NLRP3) inflammasome and the resultant release of the proinflammatory cytokine IL-1 β (Zhang et al., 2017b).

Another study showed that baicalin might limit protein kinase R-like endoplasmic reticulum kinase (PERK)/eukaryotic translation initiation factor 2 (eIF2) pathway activation, which would then downregulate thioredoxin interacting protein (TXNIP) expression and reduce the activation of the NLRP3 inflammasome, resulting in reduced pyroptosis in macrophages with Mtb infection (Fu et al., 2021). Baicalin relieves *Mycoplasma pneumoniae* infection-induced lung injury by blocking miRNA-221 to regulate the TLR4/NF- κ B signaling pathway (Zhang et al., 2021c).

Baicalin exhibits inhibitory effects on various strains of influenza virus and SARS-CoV, both *in vitro* and *in vivo* (Limanaqi et al., 2020). Oral administration of baicalin to mice infected with the influenza virus increased the average survival time, reduced lung inflammation, and dose-dependently decreased the lung viral titer. These effects are probably caused by baicalin, which has been demonstrated to impede the replication of SARS-CoV and influenza virus *in vitro* (Chen et al., 2004; Xu et al., 2010). Via the TNF receptor associated factor 6 (TRAF6)-dependent production of Type-I interferons (IFNs), baicalin has been demonstrated to suppress influenza virus replication, which correlates with protection from acute lung injury in infected mice (Li and Wang, 2019). This is noteworthy because, in SARS-CoV, similar to what was observed in the influenza virus, alterations in mitochondrial homeostasis and autophagy were eventually caused by abnormal ubiquitin proteasome system (UPS)-dependent degradation, which was related to the suppression of inhibition of TRAF6-dependent expression of Type-I IFNs (Shi et al., 2014).

Baicalin suppresses influenza virus infection both *in vitro* and *in vivo* by directly inhibiting the neuraminidase surface glycoprotein, which is necessary for viral replication and the release of virions from infected cells (Ding et al., 2014; Jin et al., 2018). While baicalin strengthens the antiviral activity of the neuraminidase inhibitor zanamivir, sodium baicalin is also effective against oseltamivir-resistant mutant influenza virus strains (Sithisarn et al., 2013). The anti-neuraminidase activity of baicalin is accompanied by a reduction in TNF- α , IL-6, and IL-8, which is associated with inhibition of the NF- κ B and PI3K/AKT pathways and may indicate autophagy is being activated (Sithisarn et al., 2013). This makes sense given that baicalin has been demonstrated to directly target the NS1 protein of the influenza virus, which has been proven to impair autophagy by activating PI3K/AKT (Nayak et al., 2014). Baicalin inhibited virus replication and reduced the activity of major factors of the RIG-I-like receptor (RLR) signaling pathway components, including retinoic-acid-inducible gene I (RIG-I), IFN regulatory factor 3 (IRF3), IRF7, NF- κ B, inflammatory responses, and macrophage polarization, in an influenza A virus infection model (Wan et al., 2014; Chu et al., 2015; Zhu et al., 2015; Pang et al., 2018; Zhi et al., 2019; Geng et al., 2020). Treatment with baicalin can also moderately lower respiratory syncytial virus titers recovered from lung tissues with a decrease in T lymphocyte infiltration and proinflammatory factor gene expression (Shi et al., 2016).

The pathologic mechanism of the coronavirus disease (COVID-19) outbreak caused by SARS-CoV-2 is still not completely clear (Huang et al., 2020; Wang et al., 2020). The most common cause of death in severe COVID-19 cases is respiratory failure, and conditions

such as acute respiratory distress syndrome (ARDS), septic shock, severe metabolic acidosis, and a hypercoagulable state can be fatal. Baicalin, herbacetin, and pectolinarin have been found to effectively inhibit the proteolytic activity of the main protease, 3-chymotrypsin-like protease (3CLpro), and show effective inhibitory activity against SARS-CoV-2 3CLpro (Jo et al., 2020). It was predicted that baicalin would bind to papain-like protease (PLpro) (Lin et al., 2021) and the S protein (Boozari and Hosseinzadeh, 2021) with considerable affinity. Baicalin is an intriguing prospective therapeutic candidate for future study against SARS-CoV-2 that has been shown to bind the N-terminus and C-terminus of the homology model of the SARS-CoV-2 proteins non-structural protein 14 (Nsp14) and 3CLpro (Su et al., 2020; Liu et al., 2021). Baicalin and ascorbic acid can work together to reduce SARS-CoV-2 entrance by inhibiting the production of angiotensin-converting enzyme II in human small alveolar epithelial cells (Lai et al., 2021). When used to treat COVID-19, certain traditional Chinese medications containing baicalin have been shown to have immunological modulation, anti-infection, anti-inflammation, and multiorgan protection mechanisms (Su et al., 2020; Zhao et al., 2021a; Huang et al., 2022; Wei et al., 2022).

Acute lung injury/acute respiratory distress syndrome

Damage to the alveolar capillary membrane, which is made up of the microvascular endothelium and the alveolar epithelium, results in pulmonary infiltrates in ALI. In the presence of sepsis, severe trauma, or extensive lung infection, ALI can progress to ARDS, which is more serious diffuse alveolar injury (Matthay et al., 2012).

By regulating the composition of the gut microbiota, increasing the production of short-chain fatty acids, and altering the fecal metabolite profiles via the lung-gut axis, baicalin can ameliorate staphylococcal enterotoxin B-induced ARDS (Hu et al., 2022). Baicalin inhibits the release of HMGB1 and cytokines from macrophages, improves survival and reduces tissue injury in septic mice induced by lipopolysaccharide (LPS) (Wang and Liu, 2014). By inhibiting TLR4, baicalin has a therapeutic impact on LPS-induced ALI (Huang et al., 2008; Shin et al., 2015) as well as acute pancreatitis-associated lung injury (Zhang et al., 2008; Li et al., 2009a; Zhang et al., 2021d). Ding et al. (2016) explained the crosstalk between the C-X3-C motif chemokine ligand 1 (CX3CL1)-C-X3-C motif chemokine receptor 1 (CX3CR1) axis and NF- κ B pathway, while Meng et al. revealed that oxidative stress and inflammation were reduced via the activation of the nuclear factor erythroid 2-related factor 2 (NRF2)-mediated heme oxygenase 1 (HO-1) signaling pathway (Meng et al., 2019). Meanwhile, Long and Zhu et al. demonstrated that the mechanism involves the inhibition of the TLR4/NF- κ B p65 and ERK/JNK signaling pathways (Long et al., 2020) as well as the TLR4/MyD88/NF- κ B/NLRP3 signaling pathway and the MAPK signaling pathway (Changle et al., 2022). Duan et al. (2021) demonstrated that it can attenuate follistatin-like protein 1 (FSTL1) and the ERK/JNK signaling pathway by upregulating miR-200b-3p expression. It may also prevent LPS-induced reduction of alveolar fluid clearance by upregulating epithelial sodium channel α -epithelial sodium channel (α -ENaC) protein through activation of the cyclic adenosine monophosphate (cAMP)/protein kinase A (PKA) signaling pathway to attenuate lung edema (Deng et al., 2017). Another

investigation demonstrated that baicalin can reduce lung mitochondrial lipid peroxidation and antioxidant activity induced by linoleic acid hydroperoxide (LHP) *in vitro* (Liau et al., 2019).

Baicalin attenuated air embolism-induced acute lung injury (Li et al., 2009b) and severe burn-induced remote acute lung injury through the NLRP3 signaling pathway (Bai et al., 2018) and attenuated neonatal hyperoxia-induced endothelial cell dysfunction and alveolar and vascular simplification in adult mice by upregulating carnitine palmitoyltransferase 1a (Cpt1a) (Chang et al., 2022). These results suggest possible treatment approaches for employing baicalin to prevent persistent lung injury in some illnesses and injuries.

Pharmacological studies have shown suppression of TLR4-mediated NF- κ B activation (Zhang et al., 2016; Feng et al., 2018), downregulation of MMP9 expression (Zhang et al., 2016), inhibition of p-Src in LPS-activated neutrophils and formation of neutrophil extracellular traps (NETs) in Phorbol 12-myristate 13-acetate (PMA)-induced neutrophils (Xiao et al., 2022) in response to traditional Chinese medications containing baicalin.

Lung cancer

Baicalin has inhibitory effects on the proliferation and migration of various tumor cells. It can promote tumor cell apoptosis through multiple pathways and enhance the effectiveness of chemotherapy and radiotherapy (Zhang et al., 2017c; Singh et al., 2021). Baicalin can prevent lung cancer cells from growing and spreading by inducing apoptosis and cell cycle arrest and inhibiting the production of proinflammatory and protumor cytokines, according to research conducted on animals and in cell culture (Mizushima et al., 1995; Cheng et al., 2003; Himeji et al., 2007; Du et al., 2010; Jangid et al., 2020), and formulations and derivatives are emerging (Zhang et al., 2017c; Li et al., 2017; Wei et al., 2017; Jangid et al., 2020). By activating p38 MAPK and generating intracellular reactive oxygen species, baicalin enhances TNF-related apoptosis-inducing ligand (TRAIL)-induced apoptosis (Zhang et al., 2017c).

The antitumor effects of baicalin mainly include inhibiting the proliferation of tumor cells by blocking the cell cycle, inducing apoptosis in tumor cells by producing cytotoxicity, and suppressing the erosion and metastasis of tumor cells (Sui et al., 2020; Yan et al., 2020). According to reports, baicalin can block cell cycle progression in the S phase by suppressing cyclin A, but in SKLU1, SKMES1 and DU145 cells, baicalin suppresses the expression of cyclin D1, leading to cell cycle arrest in the G1 phase (Gao et al., 2011). Baicalin stimulates the sirtuin 1 (SIRT1)/AMP-activated protein kinase (AMPK) signaling pathway (You et al., 2018), inhibits p-AKT in tumor cells, and attenuates cisplatin resistance in lung cancer by downregulating MARK2 and p-AKT (Xu et al., 2017b). Yin et al. reported that baicalin attenuates X-ray cross complementing 1 (XRCC1)-mediated DNA repair to enhance the sensitivity of lung cancer cells to cisplatin. Baicalin activated Rap1-GTP binding and dephosphorylated AKT and Src by suppressing $\alpha 7$ nicotinic acetylcholine receptor ($\alpha 7$ nAChR), consequently triggering inhibition of inhibitor of differentiation factor 1 (Id1) (Zhao et al., 2019). Diao et al. demonstrated that baicalin inhibits lung

cancer growth by targeting PDZ-binding kinase/T-LAK cell-originated protein kinase (PBK/TOPK) (Yan et al., 2020), while Chen et al. revealed that baicalin prevents epithelial-mesenchymal transition (EMT) by blocking the pyruvate dehydrogenase kinase 1 (PDK1)/AKT pathway in human non-small cell lung cancer (NSCLC) (Chen et al., 2021). Baicalin's antitumor effects were shown by Zhao et al. to be mediated through the miR-340-5p-neuroepithelial cell transforming 1 (NET1) axis (Zhao et al., 2021b). Follow-up research can carry out more effective and precise interventions in the above and other regulatory pathways, inhibiting the growth and metastasis of lung cancer cells and prolonging the survival of patients.

Conclusion and future directions

The evidence thus far suggests baicalin may be a promising option for managing symptoms and preventing disease progression of various lung diseases due to its anti-inflammatory, antioxidant, anticancer and antiviral properties, although research on baicalin as a treatment for lung disease is still ongoing. While research on baicalin for the treatment of lung disease holds potential, there are still limitations to be addressed. First, many of the studies have focused on animal models; thus, more human clinical trials are needed to evaluate the efficacy and safety of baicalin in treating lung diseases. Baicalin has been found to be a safe and well-tolerated treatment for lung disease with a low incidence of adverse effects. Further research is needed to confirm its long-term safety and therapeutic benefits and to optimize its use as a treatment for lung disease. Additionally, the optimal dose and duration of treatment need to be determined, as well as the potential for drug interactions with other medications. With greater research into its mechanisms of action, long-term effects, application domains, and the continual expansion of its application, its value will continue to be unearthed and investigated.

Author contributions

DW collected and analyzed the data and wrote the manuscript. YL collected and analyzed the data and conceived the study. All authors commented on previous versions of the manuscript and read and approved the final manuscript.

Funding

The research leading to these results has received funding from Sichuan University Full-time Postdoctoral Research and Development Fund, Grant/Award Number: 2020SCU12023; PostDoctor Research Project, West China Hospital, Sichuan University, Grant/Award Number: 2018HXBH041. Financial support was received by YL.

Conflict of interest

The authors declare that the research was conducted in the absence of any commercial or financial relationships that could be construed as a potential conflict of interest.

Publisher's note

All claims expressed in this article are solely those of the authors and do not necessarily represent those of their affiliated

References

- Bai, C., Li, T., Sun, Q., Xin, Q., Xu, T., Yu, J., et al. (2018). Protective effect of baicalin against severe burn-induced remote acute lung injury in rats. *Mol. Med. Rep.* 17 (2), 2689–2694. doi:10.3892/mmr.2017.8120
- Bao, W. A., Wang, Y. Z., Zhu, X., Lin, J., Fan, J. F., Yang, Y., et al. (2022). Baicalin ameliorates radiation-induced lung injury by inhibiting the CysLTs/CysLT1 signaling pathway. *Evid. Based Complement. Altern. Med.* 2022, 2765354. doi:10.1155/2022/2765354
- Barnes, P. J., Baker, J., and Donnelly, L. E. (2019). Cellular senescence as a mechanism and target in chronic lung diseases. *Am. J. Respir. Crit. Care Med.* 200 (5), 556–564. doi:10.1164/rccm.201810-1975TR
- Barnes, P. J., Burney, P. G. J., Silverman, E. K., Celli, B. R., Vestbo, J., Wedzicha, J. A., et al. (2015). Chronic obstructive pulmonary disease. *Nat. Rev. Dis. Prim.* 1 (1), 15076. doi:10.1038/nrdp.2015.76
- Boozari, M., and Hosseinzadeh, H. (2021). Natural products for COVID-19 prevention and treatment regarding to previous coronavirus infections and novel studies. *Phytother. Res.* 35 (2), 864–876. doi:10.1002/ptr.6873
- Brackman, G., Cos, P., Maes, L., Nelis, H. J., and Coenye, T. (2011). Quorum sensing inhibitors increase the susceptibility of bacterial biofilms to antibiotics *in vitro* and *in vivo*. *Antimicrob. Agents Chemother.* 55 (6), 2655–2661. doi:10.1128/AAC.00045-11
- Chang, H., Meng, H. Y., Bai, W. F., and Meng, Q. G. (2021). A metabolomic approach to elucidate the inhibitory effects of baicalin in pulmonary fibrosis. *Pharm. Biol.* 59 (1), 1016–1025. doi:10.1080/13880209.2021.1950192
- Chang, J. L., Gong, J., Rizal, S., Peterson, A. L., Yao, C., Dennery, P. A., et al. (2022). Upregulating carnitine palmitoyltransferase 1 attenuates hyperoxia-induced endothelial cell dysfunction and persistent lung injury. *Respir. Res.* 23 (1), 205. doi:10.1186/s12931-022-02135-1
- Changle, Z., Cuiling, F., Feng, F., Xiaoqin, Y., Guishu, W., Liangtian, S., et al. (2022). Baicalin inhibits inflammation of lipopolysaccharide-induced acute lung injury toll like receptor-4/myeloid differentiation primary response 88/nuclear factor-kappa B signaling pathway. *J. Tradit. Chin. Med.* 42 (2), 200–212. doi:10.19852/j.cnki.jtcm.20211214.004
- Chen, F., Chan, K. H., Jiang, Y., Kao, R. Y. T., Lu, H. T., Fan, K. W., et al. (2004). *In vitro* susceptibility of 10 clinical isolates of SARS coronavirus to selected antiviral compounds. *J. Clin. Virol.* 31 (1), 69–75. doi:10.1016/j.jcv.2004.03.003
- Chen, J., Yuan, C. B., Yang, B., and Zhou, X. (2021). Baicalin inhibits EMT through PDK1/AKT signaling in human non-small cell lung cancer. *J. Oncol.* 2021, 4391581. doi:10.1155/2021/4391581
- Chen, Z., and Wang, Q. (2017). Activation of PPAR γ by baicalin attenuates pulmonary hypertension in an infant rat model by suppressing HMGB1/RAGE signaling. *FEBS Open Bio* 7 (4), 477–484. doi:10.1002/2211-5463.12180
- Cheng, K. T., Hou, W. C., Huang, Y. C., and Wang, L. F. (2003). Baicalin induces differential expression of cytochrome C oxidase in human lung H461 cell. *J. Agric. Food Chem.* 51 (25), 7276–7279. doi:10.1021/jf0301549
- Chu, M., Xu, L., Zhang, M. B., Chu, Z. Y., and Wang, Y. D. (2015). Role of baicalin in anti-influenza virus A as a potent inducer of IFN- γ . *Biomed. Res. Int.* 2015, 263630. doi:10.1155/2015/263630
- Cui, L., Yuan, T., Zeng, Z., Liu, D., Liu, C., Guo, J., et al. (2022). Mechanistic and therapeutic perspectives of baicalin and baicalein on pulmonary hypertension: A comprehensive review. *Biomed. Pharmacother.* 151, 113191. doi:10.1016/j.biopha.2022.113191
- Deng, J., Wang, D. X., Liang, A. L., Tang, J., and Xiang, D. K. (2017). Effects of baicalin on alveolar fluid clearance and α -ENaC expression in rats with LPS-induced acute lung injury. *Can. J. Physiol. Pharmacol.* 95 (2), 122–128. doi:10.1139/cjpp-2016-0212
- Deng, L., Ma, M., Li, S., Zhou, L., Ye, S., Wang, J., et al. (2022). Protective effect and mechanism of baicalin on lung inflammatory injury in BALB/c mice induced by PM_{2.5}. *Ecotoxicol. Environ. Saf.* 248, 114329. doi:10.1016/j.ecoenv.2022.114329
- Ding, X. M., Pan, L., Wang, Y., and Xu, Q. Z. (2016). Baicalin exerts protective effects against lipopolysaccharide-induced acute lung injury by regulating the crosstalk between the CX3CL1-CX3CR1 axis and NF- κ B pathway in CX3CL1-knockout mice. *Int. J. Mol. Med.* 37 (3), 703–715. doi:10.3892/ijmm.2016.2456
- Ding, Y., Dou, J., Teng, Z., Yu, J., Wang, T., Lu, N., et al. (2014). Antiviral activity of baicalin against influenza A (H1N1/H3N2) virus in cell culture and in mice and its inhibition of neuraminidase. *Arch. Virol.* 159 (12), 3269–3278. doi:10.1007/s00705-014-2192-2
- Du, G., Han, G., Zhang, S., Lin, H., Wu, X., Wang, M., et al. (2010). Baicalin suppresses lung carcinoma and lung metastasis by SOD mimic and HIF-1 α inhibition. *Eur. J. Pharmacol.* 630 (1–3), 121–130. doi:10.1016/j.ejphar.2009.12.014
- Duan, X. Y., Sun, Y., Zhao, Z. F., Shi, Y. Q., Ma, X. Y., Tao, L., et al. (2021). Baicalin attenuates LPS-induced alveolar type II epithelial cell A549 injury by attenuation of the FSTL1 signaling pathway via increasing miR-200b-3p expression. *Innate Immun.* 27 (4), 294–312. doi:10.1177/17534259211013887
- Feng, L., Yang, N., Li, C., Tian, G., Wang, J., Dong, Z. B., et al. (2018). Pudin xiaoyan oral liquid alleviates LPS-induced respiratory injury through decreasing nitrooxidative stress and blocking TLR4 activation along with NF- κ B phosphorylation in mice. *J. Ethnopharmacol.* 214, 292–300. doi:10.1016/j.jep.2017.07.009
- Fu, Y., Shen, J., Li, Y., Liu, F., Ning, B., Zheng, Y., et al. (2021). Inhibition of the PERK/TXNIP/NLRP3 Axis by baicalin reduces NLRP3 inflammasome-mediated pyroptosis in macrophages infected with *Mycobacterium tuberculosis*. *Mediat. Inflamm.* 2021, 1805147. doi:10.1155/2021/1805147
- Gao, J., Morgan, W. A., Sanchez-Medina, A., and Corcoran, O. (2011). The ethanol extract of *Scutellaria baicalensis* and the active compounds induce cell cycle arrest and apoptosis including upregulation of p53 and Bax in human lung cancer cells. *Toxicol. Appl. Pharmacol.* 254 (3), 221–228. doi:10.1016/j.taap.2011.03.016
- Gao, Y., Lu, J., Zhang, Y., Chen, Y., Gu, Z., and Jiang, X. (2013). Baicalein attenuates bleomycin-induced pulmonary fibrosis in rats through inhibition of miR-21. *Pulm. Pharmacol. Ther.* 26 (6), 649–654. doi:10.1016/j.pupt.2013.03.006
- Geng, P., Zhu, H., Zhou, W., Su, C., Chen, M., Huang, C., et al. (2020). Baicalin inhibits influenza A virus infection via promotion of M1 macrophage polarization. *Front. Pharmacol.* 11, 01298. doi:10.3389/fphar.2020.01298
- Hao, D., Li, Y., Shi, J., and Jiang, J. (2021). Baicalin alleviates chronic obstructive pulmonary disease through regulation of HSP72-mediated JNK pathway. *Mol. Med.* 27 (1), 53. doi:10.1186/s10020-021-00309-z
- He, Y. Q., Zhou, C. C., Yu, L. Y., Wang, L., Deng, J. L., Tao, Y. L., et al. (2021). Natural product derived phytochemicals in managing acute lung injury by multiple mechanisms. *Pharmacol. Res.* 163, 105224. doi:10.1016/j.phrs.2020.105224
- Himeji, M., Ohtsuki, T., Fukazawa, H., Tanaka, M., Yazaki, S. I., Ui, S., et al. (2007). Difference of growth-inhibitory effect of *Scutellaria baicalensis*-producing flavonoid wogonin among human cancer cells and normal diploid cell. *Cancer Lett.* 245 (1–2), 269–274. doi:10.1016/j.canlet.2006.01.011
- Hu, L., Li, L., Wang, C., Cao, Y., Duan, X., and Sun, J. (2023). Baicalin inhibits airway smooth muscle cells proliferation through the RAS signaling pathway in murine asthmatic airway remodeling model. *Oxid. Med. Cell Longev.* 2023, 4144138. doi:10.1155/2023/4144138
- Hu, T., Zhu, Y., Zhu, J., Yang, M., Wang, Y., and Zheng, Q. (2022). Wine-processed radix *scutellariae* alleviates ARDS by regulating tryptophan metabolism through gut microbiota. *Front. Pharmacol.* 13, 1104280. doi:10.3389/fphar.2022.1104280
- Huang, C., Wang, Y., Li, X., Ren, L., Zhao, J., Hu, Y., et al. (2020). Clinical features of patients infected with 2019 novel coronavirus in Wuhan, China. *Lancet* 395 (10223), 497–506. doi:10.1016/S0140-6736(20)30183-5
- Huang, K. L., Chen, C. S., Hsu, C. W., Li, M. H., Chang, H., Tsai, S. H., et al. (2008). Therapeutic effects of baicalin on lipopolysaccharide-induced acute lung injury in rats. *Am. J. Chin. Med.* 36 (2), 301–311. doi:10.1142/S0192415X08005783
- Huang, S., Chen, P., Shui, X., He, Y., Wang, H., Zheng, J., et al. (2014). Baicalin attenuates transforming growth factor- β -induced human pulmonary artery smooth muscle cell proliferation and phenotypic switch by inhibiting hypoxia inducible factor-1 α and aryl hydrocarbon receptor expression. *J. Pharm. Pharmacol.* 66 (10), 1469–1477. doi:10.1111/jphp.12273
- Huang, X., He, Y., Chen, Y., Wu, P., Gui, D., Cai, H., et al. (2016). Baicalin attenuates bleomycin-induced pulmonary fibrosis via adenosine A2a receptor related TGF- β 1-induced ERK1/2 signaling pathway. *BMC Pulm. Med.* 16 (1), 132. doi:10.1186/s12890-016-0294-1
- Huang, X., Wu, P., Huang, F., Xu, M., Chen, M., Huang, K., et al. (2017). Baicalin attenuates chronic hypoxia-induced pulmonary hypertension via adenosine A(2A) receptor-induced SDF-1/CXCR4/PI3K/AKT signaling. *J. Biomed. Sci.* 24 (1), 52. doi:10.1186/s12929-017-0359-3
- Huang, Y. X., Li, N. F., Li, C. Y., Zheng, F. P., Yao, X. Y., Lin, B. H., et al. (2022). Clinical features and effectiveness of Chinese medicine in patients with COVID-19 from overseas: A retrospective study in xiamen, China. *Front. Public Health* 10, 1038017. doi:10.3389/fpubh.2022.1038017

- Jangid, A. K., Agrawal, H., Rai, D. B., Jain, P., Yadav, U. C., Pooja, D., et al. (2020). Baicalin encapsulating lipid-surfactant conjugate based nanomimicelles: Preparation, characterization and anticancer activity. *Chem. Phys. Lipids* 233, 104978. doi:10.1016/j.chemphyslip.2020.104978
- Jasenosky, L. D., Scriba, T. J., Hanekom, W. A., and Goldfeld, A. E. (2015). T cells and adaptive immunity to *Mycobacterium tuberculosis* in humans. *Immunol. Rev.* 264 (1), 74–87. doi:10.1111/imr.12274
- Jin, J., Chen, Y., Wang, D., Ma, L., Guo, M., Zhou, C., et al. (2018). The inhibitory effect of sodium baicalin on oseltamivir-resistant influenza A virus via reduction of neuraminidase activity. *Arch. Pharm. Res.* 41 (6), 664–676. doi:10.1007/s12272-018-1022-6
- Jo, S., Kim, S., Kim, D. Y., Kim, M. S., and Shin, D. H. (2020). Flavonoids with inhibitory activity against SARS-CoV-2 3CLpro. *J. Enzyme Inhib. Med. Chem.* 35 (1), 1539–1544. doi:10.1080/14756366.2020.1801672
- Ju, J., Li, Z., and Shi, Q. (2022). Baicalin inhibits inflammation in rats with chronic obstructive pulmonary disease by the TLR2/MYD88/NF- κ Bp65 signaling pathway. *Evid. Based Complement. Altern. Med.* 2022, 7273387. doi:10.1155/2022/7273387
- Lai, Y. J., Chang, H. S., Yang, Y. P., Lin, T. W., Lai, W. Y., Lin, Y. Y., et al. (2021). The role of micronutrient and immunomodulation effect in the vaccine era of COVID-19. *J. Chin. Med. Assoc.* 84 (9), 821–826. doi:10.1097/JCMA.0000000000000587
- Lederer, D. J., Longo, D. L., and Martinez, F. J. (2018). Idiopathic pulmonary fibrosis. *N. Engl. J. Med.* 378 (19), 1811–1823. doi:10.1056/NEJMra1705751
- Li, L., Bao, H., Wu, J., Duan, X., Liu, B., Sun, J., et al. (2012). Baicalin is anti-inflammatory in cigarette smoke-induced inflammatory models *in vivo* and *in vitro*: A possible role for HDAC2 activity. *Int. Immunopharmacol.* 13 (1), 15–22. doi:10.1016/j.intimp.2012.03.001
- Li, L. Y., Zhang, C. T., Zhu, F. Y., Zheng, G., Liu, Y. F., Liu, K., et al. (2022). Potential natural small molecular compounds for the treatment of chronic obstructive pulmonary disease: An overview. *Front. Pharmacol.* 13, 821941. doi:10.3389/fphar.2022.821941
- Li, M. H., Huang, K. L., Wu, S. Y., Chen, C. W., Yan, H. C., Hsu, K., et al. (2009). Baicalin attenuates air embolism-induced acute lung injury in rat isolated lungs. *Br. J. Pharmacol.* 157 (2), 244–251. doi:10.1111/j.1476-5381.2009.00139.x
- Li, R., and Wang, L. (2019). Baicalin inhibits influenza virus A replication via activation of type I IFN signaling by reducing miR-146a. *Mol. Med. Rep.* 20 (6), 5041–5049. doi:10.3892/mmr.2019.10743
- Li, S., Wang, L., Liu, Y., and Su, H. (2017). Combination lung cancer chemotherapy: Design of a pH-sensitive transferrin-PEG-Hz-lipid conjugate for the co-delivery of docetaxel and baicalin. *Biomed. Pharmacother.* 95, 548–555. doi:10.1016/j.biopha.2017.08.090
- Li, Z., Xia, X., Zhang, S., Zhang, A., Bo, W., and Zhou, R. (2009). Up-regulation of Toll-like receptor 4 was suppressed by emodin and baicalin in the setting of acute pancreatitis. *Biomed. Pharmacother.* 63 (2), 120–128. doi:10.1016/j.biopha.2008.01.003
- Liau, P. R., Wu, M. S., and Lee, C. K. (2019). Inhibitory effects of Scutellaria baicalensis root extract on linoleic acid hydroperoxide-induced lung mitochondrial lipid peroxidation and antioxidant activities. *Molecules* 24 (11), 2143. doi:10.3390/molecules24112143
- Limanaqi, F., Busceti, C. L., Biagioni, F., Lazzeri, G., Forte, M., Schiavon, S., et al. (2020). Cell clearing systems as targets of polyphenols in viral infections: Potential implications for COVID-19 pathogenesis. *Antioxidants (Basel)* 9 (11), 1105. doi:10.3390/antiox9111105
- Lin, C., Tsai, F. J., Hsu, Y. M., Ho, T. J., Wang, G. K., Chiu, Y. J., et al. (2021). Study of baicalin toward COVID-19 treatment: *In silico* target analysis and *in vitro* inhibitory effects on SARS-CoV-2 proteases. *Biomed. Hub.* 6 (3), 122–137. doi:10.1159/000519564
- Liu, C., Zhu, X., Lu, Y., Zhang, X., Jia, X., and Yang, T. (2021). Potential treatment with Chinese and Western medicine targeting NSP14 of SARS-CoV-2. *J. Pharm. Anal.* 11 (3), 272–277. doi:10.1016/j.jpba.2020.08.002
- Liu, J., Wei, Y., Luo, Q., Xu, F., Zhao, Z., Zhang, H., et al. (2016). Baicalin attenuates inflammation in mice with OVA-induced asthma by inhibiting NF- κ B and suppressing CCR7/CCL19/CCL21. *Int. J. Mol. Med.* 38 (5), 1541–1548. doi:10.3892/ijmm.2016.2743
- Liu, P., Yan, S., Chen, M., Chen, A., Yao, D., Xu, X., et al. (2015). Effects of baicalin on collagen I and collagen III expression in pulmonary arteries of rats with hypoxic pulmonary hypertension. *Int. J. Mol. Med.* 35 (4), 901–908. doi:10.3892/ijmm.2015.2110
- Liu, S., Liu, B., Luo, Z. Q., Qiu, J., Zhou, X., Li, G., et al. (2017). The combination of osthole with baicalin protects mice from *Staphylococcus aureus* pneumonia. *World J. Microbiol. Biotechnol.* 33 (1), 11. doi:10.1007/s11274-016-2162-9
- Liu, T., Dai, W., Liu, F., Chen, Y., Weng, D., et al. (2015). Baicalin alleviates silica-induced lung inflammation and fibrosis by inhibiting the Th17 response in C57bl/6 mice. *J. Nat. Prod.* 78 (12), 3049–3057. doi:10.1021/acs.jnatprod.5b00868
- Lixuan, Z., Jingcheng, D., Wenqin, Y., Jianhua, H., Baojun, L., and Xiaotao, F. (2010). Baicalin attenuates inflammation by inhibiting NF- κ B activation in cigarette smoke induced inflammatory models. *Pulm. Pharmacol. Ther.* 23 (5), 411–419. doi:10.1016/j.pupt.2010.05.004
- Long, Y., Xiang, Y., Liu, S., Zhang, Y., Wan, J., Yang, Q., et al. (2020). Baicalin liposome alleviates lipopolysaccharide-induced acute lung injury in mice via inhibiting TLR4/JNK/ERK/NF- κ B pathway. *Mediat. Inflamm.* 2020, 8414062. doi:10.1155/2020/8414062
- Lu, J., Zhong, Y., Lin, Z., Lin, X., Chen, Z., Wu, X., et al. (2017). Baicalin alleviates radiation-induced epithelial-mesenchymal transition of primary type II alveolar epithelial cells via TGF- β and ERK/GSK3 β signaling pathways. *Biomed. Pharmacother.* 95, 1219–1224. doi:10.1016/j.biopha.2017.09.037
- Luan, Y., Chao, S., Ju, Z. Y., Wang, J., Xue, X., Qi, T. G., et al. (2015). Therapeutic effects of baicalin on monocrotaline-induced pulmonary arterial hypertension by inhibiting inflammatory response. *Int. Immunopharmacol.* 26 (1), 188–193. doi:10.1016/j.intimp.2015.01.009
- Ma, C., Ma, Z., and Fu, Q. (2014). Anti-asthmatic effects of baicalin in a mouse model of allergic asthma. *Phytother. Res.* 28 (2), 231–237. doi:10.1002/ptr.4983
- Matthay, M. A., Ware, L. B., and Zimmerman, G. A. (2012). The acute respiratory distress syndrome. *J. Clin. investigation* 122 (8), 2731–2740. doi:10.1172/JCI60331
- McAllister, D. A., Liu, L., Shi, T., Chu, Y., Reed, C., Burrows, J., et al. (2019). Global, regional, and national estimates of pneumonia morbidity and mortality in children younger than 5 years between 2000 and 2015: A systematic analysis. *Lancet Glob. Health* 7 (1), e47–e57. doi:10.1016/S2214-109X(18)30408-X
- Meng, X., Hu, L., and Li, W. (2019). Baicalin ameliorates lipopolysaccharide-induced acute lung injury in mice by suppressing oxidative stress and inflammation via the activation of the Nrf2-mediated HO-1 signaling pathway. *Naunyn Schmiedeb. Arch. Pharmacol.* 392 (11), 1421–1433. doi:10.1007/s00210-019-01680-9
- Mizushima, Y., Kashii, T., Tokimitsu, Y., and Kobayashi, M. (1995). Cytotoxic effect of herbal medicine sho-saiko-to on human lung-cancer cell-lines *in-vitro*. *Oncol. Rep.* 2 (1), 91–94. doi:10.3892/or.2.1.91
- Nayak, M. K., Agrawal, A. S., Bose, S., Naskar, S., Bhowmick, R., Chakrabarti, S., et al. (2014). Antiviral activity of baicalin against influenza virus H1N1-pdm09 is due to modulation of NS1-mediated cellular innate immune responses. *J. Antimicrob. Chemother.* 69 (5), 1298–1310. doi:10.1093/jac/dkt534
- Pang, P., Zheng, K., Wu, S., Xu, H., Deng, L., Shi, Y., et al. (2018). Baicalin downregulates RLRs signaling pathway to control influenza A virus infection and improve the prognosis. *Evid. Based Complement. Altern. Med.* 2018, 4923062. doi:10.1155/2018/4923062
- Papi, A., Brightling, C., Pedersen, S. E., and Reddel, H. K. (2018). Asthma. *Lancet* 391 (10122), 783–800. doi:10.1016/S0140-6736(17)33311-1
- Park, K., Lee, J. S., Choi, J. S., Nam, Y. J., Han, J. H., Byun, H. D., et al. (2016). Identification and characterization of baicalin as a phosphodiesterase 4 inhibitor. *Phytother. Res.* 30 (1), 144–151. doi:10.1002/ptr.5515
- Peng, L. Y., Yuan, M., Song, K., Yu, J. L., Li, J. H., Huang, J. N., et al. (2019). Baicalin alleviated APEC-induced acute lung injury in chicken by inhibiting NF- κ B pathway activation. *Int. Immunopharmacol.* 72, 467–472. doi:10.1016/j.intimp.2019.04.046
- Shi, C. S., Qi, H. Y., Boularan, C., Huang, N. N., Abu-Asab, M., Shelhamer, J. H., et al. (2014). SARS-coronavirus open reading frame-9b suppresses innate immunity by targeting mitochondria and the MAVS/TRAF3/TRAF6 signalosome. *J. Immunol.* 193 (6), 3080–3089. doi:10.4049/jimmunol.1303196
- Shi, H., Ren, K., Lv, B., Zhang, W., Zhao, Y., Tan, R. X., et al. (2016). Baicalin from Scutellaria baicalensis blocks respiratory syncytial virus (RSV) infection and reduces inflammatory cell infiltration and lung injury in mice. *Sci. Rep.* 6, 35851. doi:10.1038/srep35851
- Shin, Y. O., Park, C. H., Lee, G. H., Yokozawa, T., Roh, S. S., and Rhee, M. H. (2015). Heat-Processed scutellariae radix enhances anti-inflammatory effect against lipopolysaccharide-induced acute lung injury in mice via NF- κ B signaling. *Evid. Based Complement. Altern. Med.* 2015, 456846. doi:10.1155/2015/456846
- Singh, S., Meena, A., and Luqman, S. (2021). Baicalin mediated regulation of key signaling pathways in cancer. *Pharmacol. Res.* 164, 105387. doi:10.1016/j.phrs.2020.105387
- Sithisarn, P., Michaelis, M., Schubert-Zsilavecz, M., and Cinatl, J. (2013). Differential antiviral and anti-inflammatory mechanisms of the flavonoids biochanin A and baicalin in H5N1 influenza A virus-infected cells. *Antivir. Res.* 97 (1), 41–48. doi:10.1016/j.antiviral.2012.10.004
- Su, H. X., Yao, S., Zhao, W. F., Li, M. J., Liu, J., Shang, W. J., et al. (2020). Anti-SARS-CoV-2 activities *in vitro* of Shuanghuanglian preparations and bioactive ingredients. *Acta Pharmacol. Sin.* 41 (9), 1167–1177. doi:10.1038/s41401-020-0483-6
- Sui, X., Han, X., Chen, P., Wu, Q., Feng, J., Duan, T., et al. (2020). Baicalin induces apoptosis and suppresses the cell cycle progression of lung cancer cells through downregulating akt/mTOR signaling pathway. *Front. Mol. Biosci.* 7, 602282. doi:10.3389/fmolb.2020.602282
- Sun, J., Li, L., Wu, J., Liu, B., Gong, W., Lv, Y., et al. (2013). Effects of baicalin on airway remodeling in asthmatic mice. *Planta Med.* 79 (3-4), 199–206. doi:10.1055/s-0032-1328197

- Vonk Noordegraaf, A., Groeneveldt, J. A., and Bogaard, H. J. (2016). Pulmonary hypertension. *Eur. Respir. Rev.* 25 (139), 4–11. doi:10.1183/16000617.0096-2015
- Wan, Q., Wang, H., Han, X., Lin, Y., Yang, Y., Gu, L., et al. (2014). Baicalin inhibits TLR7/MYD88 signaling pathway activation to suppress lung inflammation in mice infected with influenza A virus. *Biomed. Rep.* 2 (3), 437–441. doi:10.3892/br.2014.253
- Wang, C., Horby, P. W., Hayden, F. G., and Gao, G. F. (2020). A novel coronavirus outbreak of global health concern. *Lancet* 395 (10223), 470–473. doi:10.1016/S0140-6736(20)30185-9
- Wang, G., Hu, Y. X., He, M. Y., Xie, Y. H., Su, W., Long, D., et al. (2021). Gut-lung dysbiosis accompanied by diabetes mellitus leads to pulmonary fibrotic change through the NF- κ B signaling pathway. *Am. J. Pathol.* 191 (5), 838–856. doi:10.1016/j.ajpath.2021.02.019
- Wang, G., Mohammadtursun, N., Lv, Y., Zhang, H., Sun, J., and Dong, J. (2018). Baicalin exerts anti-airway inflammation and anti-remodelling effects in severe stage rat model of chronic obstructive pulmonary disease. *Evid. Based Complement. Altern. Med.* 2018, 7591348. doi:10.1155/2018/7591348
- Wang, H., and Liu, D. (2014). Baicalin inhibits high-mobility group box 1 release and improves survival in experimental sepsis. *Shock* 41 (4), 324–330. doi:10.1097/SHK.0000000000000122
- Wang, J., Ishfaq, M., and Li, J. (2021). Baicalin ameliorates Mycoplasma gallisepticum-induced inflammatory injury in the chicken lung through regulating the intestinal microbiota and phenylalanine metabolism. *Food Funct.* 12 (9), 4092–4104. doi:10.1039/d1fo00055a
- Wei, W. C., Liaw, C. C., Tsai, K. C., Chiou, C. T., Tseng, Y. H., Chiou, W. F., et al. (2022). Targeting spike protein-induced TLR/NET axis by COVID-19 therapeutic NR1CM102 ameliorates pulmonary embolism and fibrosis. *Pharmacol. Res.* 184, 106424. doi:10.1016/j.phrs.2022.106424
- Wei, Y., Liang, J., Zheng, X., Pi, C., Liu, H., Yang, H., et al. (2017). Lung-targeting drug delivery system of baicalin-loaded nanoliposomes: Development, biodistribution in rabbits, and pharmacodynamics in nude mice bearing orthotopic human lung cancer. *Int. J. Nanomedicine* 12, 251–261. doi:10.2147/IJN.S119895
- Wu, Z., Chen, C., Miao, Y., Liu, Y., Zhang, Q., Li, R., et al. (2019). Baicalin attenuates Mycoplasma gallisepticum-induced inflammation via inhibition of the TLR2-NF- κ B pathway in chicken and DF-1 cells. *Infect. Drug Resist* 12, 3911–3923. doi:10.2147/IDR.S231908
- Xiao, S., Liu, L., Sun, Z., Liu, X., Xu, J., Guo, Z., et al. (2022). Network Pharmacology and experimental validation to explore the mechanism of qing-jin-hua-tan-decoction against acute lung injury. *Front. Pharmacol.* 13, 891889. doi:10.3389/fphar.2022.891889
- Xu, G., Dou, J., Zhang, L., Guo, Q., and Zhou, C. (2010). Inhibitory effects of baicalin on the influenza virus *in vivo* is determined by baicalin in the serum. *Biol. Pharm. Bull.* 33 (2), 238–243. doi:10.1248/bpb.33.238
- Xu, L., Li, J., Zhang, Y., Zhao, P., and Zhang, X. (2017). Regulatory effect of baicalin on the imbalance of Th17/Treg responses in mice with allergic asthma. *J. Ethnopharmacol.* 208, 199–206. doi:10.1016/j.jep.2017.07.013
- Xu, Z., Mei, J., and Tan, Y. (2017). Baicalin attenuates DDP (cisplatin) resistance in lung cancer by downregulating MARK2 and p-Akt. *Int. J. Oncol.* 50 (1), 93–100. doi:10.3892/ijo.2016.3768
- Xue, X., Zhang, S., Jiang, W., Wang, J., Xin, Q., Sun, C., et al. (2021). Protective effect of baicalin against pulmonary arterial hypertension vascular remodeling through regulation of TNF- α signaling pathway. *Pharmacol. Res. Perspect.* 9 (1), e00703. doi:10.1002/prp2.703
- Yan, G., Wang, J., Yi, T., Cheng, J., Guo, H., He, Y., et al. (2019). Baicalin prevents pulmonary arterial remodeling *in vivo* via the AKT/ERK/NF- κ B signaling pathways. *Pulm. Circ.* 9 (4), 2045894019878599. doi:10.1177/2045894019878599
- Yan, S., Wang, Y., Liu, P., Chen, A., Chen, M., Yao, D., et al. (2016). Baicalin attenuates hypoxia-induced pulmonary arterial hypertension to improve hypoxic cor pulmonale by reducing the activity of the p38 MAPK signaling pathway and MMP-9. *Evid. Based Complement. Altern. Med.* 2016, 2546402. doi:10.1155/2016/2546402
- Yan, Y., Yao, L., Sun, H., Pang, S., Kong, X., Zhao, S., et al. (2020). Effects of wogonoside on invasion and migration of lung cancer A549 cells and angiogenesis in xenograft tumors of nude mice. *J. Thorac. Dis.* 12 (4), 1552–1560. doi:10.21037/jtd-20-1555
- Yang, G., Li, J., Bo, J. P., Wang, B., Tian, X. R., Liu, T. Z., et al. (2015). Baicalin inhibits PDGF-induced proliferation and migration of airway smooth muscle cells. *Int. J. Clin. Exp. Med.* 8 (11), 20532–20539.
- Yin, Z., Chen, E., Cai, X., Gong, E., Li, Y., Xu, C., et al. (2022). Baicalin attenuates XRCC1-mediated DNA repair to enhance the sensitivity of lung cancer cells to cisplatin. *J. Recept. Signal Transduct. Res.* 42 (3), 215–224. doi:10.1080/10799893.2021.1892132
- Yoshida, K., Takabayashi, T., Kaneko, A., Takiyama, M., Sakashita, M., Imoto, Y., et al. (2021). Baicalin suppresses type 2 immunity through breaking off the interplay between mast cell and airway epithelial cell. *J. Ethnopharmacol.* 267, 113492. doi:10.1016/j.jep.2020.113492
- You, J., Cheng, J., Yu, B., Duan, C., and Peng, J. (2018). Baicalin, a Chinese herbal medicine, inhibits the proliferation and migration of human non-small cell lung carcinoma (NSCLC) cells, A549 and H1299, by activating the SIRT1/AMPK signaling pathway. *Med. Sci. Monit.* 24, 2126–2133. doi:10.12659/msm.909627
- Zhai, C., and Wang, D. (2022). Baicalin regulates the development of pediatric asthma via upregulating microRNA-103 and mediating the TLR4/NF- κ B pathway. *J. Recept. Signal Transduct. Res.* 42 (3), 230–240. doi:10.1080/10799893.2021.1900865
- Zhang, H., Li, X., Wang, J., Cheng, Q., Shang, Y., and Wang, G. (2021). Baicalin relieves Mycoplasma pneumoniae infection-induced lung injury through regulating microRNA-221 to inhibit the TLR4/NF- κ B signaling pathway. *Mol. Med. Rep.* 24 (2), 571. doi:10.3892/mmr.2021.12210
- Zhang, H., Pu, Z., Wang, J., Jiang, S., Wu, J. F., Qi, C. H., Mohammadtursun, N., et al. (2021). Baicalin ameliorates cigarette smoke-induced airway inflammation in rats by modulating HDAC2/NF- κ B/PAI-1 signalling. *Pulm. Pharmacol. Ther.* 70, 102061. doi:10.1016/j.pupt.2021.102061
- Zhang, L., Pu, Z., Wang, J., Zhang, Z., Hu, D., and Wang, J. (2014). Baicalin inhibits hypoxia-induced pulmonary artery smooth muscle cell proliferation via the AKT/HIF-1 α /p27-associated pathway. *Int. J. Mol. Sci.* 15 (5), 8153–8168. doi:10.3390/ijms15058153
- Zhang, L., Wang, X., Wang, R., Zheng, X., Li, H., et al. (2017). Baicalin potentiates TRAIL-induced apoptosis through p38 MAPK activation and intracellular reactive oxygen species production. *Mol. Med. Rep.* 16 (6), 8549–8555. doi:10.3892/mmr.2017.7633
- Zhang, L., Yang, L., Xie, X., Zheng, H., Zheng, H., et al. (2021). Baicalin magnesium salt attenuates lipopolysaccharide-induced acute lung injury via inhibiting of TLR4/NF- κ B signaling pathway. *J. Immunol. Res.* 2021, 6629531. doi:10.1155/2021/6629531
- Zhang, P., Guo, Q., Wei, Z., Yang, Q., Guo, Z., Shen, L., et al. (2021). Baicalin represses type three secretion system of *Pseudomonas aeruginosa* through PQS system. *Molecules* 26 (6), 1497. doi:10.3390/molecules26061497
- Zhang, Q., Sun, J., Wang, Y., He, W., Wang, L., Zheng, Y., et al. (2017). Antimycobacterial and anti-inflammatory mechanisms of baicalin via induced autophagy in macrophages infected with *Mycobacterium tuberculosis*. *Front. Microbiol.* 8, 2142. doi:10.3389/fmicb.2017.02142
- Zhang, X. P., Zhang, L., Yang, P., Zhang, R. P., and Cheng, Q. H. (2008). Protective effects of baicalin and octreotide on multiple organ injury in severe acute pancreatitis. *Dig. Dis. Sci.* 53 (2), 581–591. doi:10.1007/s10620-007-9868-3
- Zhang, X., Sun, C. Y., Zhang, Y. B., Guo, H. Z., Feng, X. X., Peng, S. Z., et al. (2016). Kegan Liyan oral liquid ameliorates lipopolysaccharide-induced acute lung injury through inhibition of TLR4-mediated NF- κ B signaling pathway and MMP-9 expression. *J. Ethnopharmacol.* 186, 91–102. doi:10.1016/j.jep.2016.03.057
- Zhang, Z., Zhang, L., Sun, C., Kong, F., Wang, J., Xin, Q., et al. (2017). Baicalin attenuates monocrotaline-induced pulmonary hypertension through bone morphogenetic protein signaling pathway. *Oncotarget* 8 (38), 63430–63441. doi:10.18632/oncotarget.18825
- Zhao, F., Zhao, Z., Han, Y., Li, S., Liu, C., and Jia, K. (2021). Baicalin suppresses lung cancer growth phenotypes via miR-340-5p/NET1 axis. *Bioengineered* 12 (1), 1699–1707. doi:10.1080/21655979.2021.1922052
- Zhao, H., Li, C., Li, L., Liu, J., Gao, Y., Mu, K., et al. (2020). Baicalin alleviates bleomycin-induced pulmonary fibrosis and fibroblast proliferation in rats via the PI3K/AKT signaling pathway. *Mol. Med. Rep.* 21 (6), 2321–2334. doi:10.3892/mmr.2020.11046
- Zhao, J., Tian, S., Lu, D., Yang, J., Zeng, H., Zhang, F., et al. (2021). Systems pharmacological study illustrates the immune regulation, anti-infection, anti-inflammation, and multi-organ protection mechanism of Qing-Fei-Pai-Du decoction in the treatment of COVID-19. *Phytomedicine* 85, 153315. doi:10.1016/j.phymed.2020.153315
- Zhao, Z., Liu, B., Sun, J., Liu, L., Liu, L., Qiu, J., et al. (2019). Scutellaria flavonoids effectively inhibit the malignant phenotypes of non-small cell lung cancer in an id1-dependent manner. *Int. J. Biol. Sci.* 15 (7), 1500–1513. doi:10.7150/ijbs.33146
- Zhi, H. J., Zhu, H. Y., Zhang, Y. Y., Lu, Y., Li, H., and Chen, D. F. (2019). *In vivo* effect of quantified flavonoids-enriched extract of Scutellaria baicalensis root on acute lung injury induced by influenza A virus. *Phytomedicine* 57, 105–116. doi:10.1016/j.phymed.2018.12.009
- Zhu, H. Y., Han, L., Shi, X. L., Wang, B. L., Huang, H., Wang, X., et al. (2015). Baicalin inhibits autophagy induced by influenza A virus H3N2. *Antivir. Res.* 113, 62–70. doi:10.1016/j.antiviral.2014.11.003



OPEN ACCESS

EDITED BY

Aliyu Muhammad,
Ahmadu Bello University, Nigeria

REVIEWED BY

Tijjani Salihu,
Kampala International University, Uganda
Ibrahim Babangida Abubakar,
Kebbi State University of Science and
Technology Aliero, Nigeria

*CORRESPONDENCE

Maryam Mazhar,
✉ maryam@swmu.edu.cn
Wei Ren,
✉ renwei1991@swmu.edu.cn
Sijin Yang,
✉ ysjimn@sina.com

RECEIVED 31 March 2023

ACCEPTED 24 May 2023

PUBLISHED 07 June 2023

CITATION

Mazhar M, Yang G, Xu H, Liu Y, Liang P,
Yang L, Spáčil R, Shen H, Zhang D, Ren W
and Yang S (2023), Zhilong Huoxue
Tongyu capsule attenuates intracerebral
hemorrhage induced redox imbalance by
modulation of Nrf2 signaling pathway.
Front. Pharmacol. 14:1197433.
doi: 10.3389/fphar.2023.1197433

COPYRIGHT

© 2023 Mazhar, Yang, Xu, Liu, Liang,
Yang, Spáčil, Shen, Zhang, Ren and Yang.
This is an open-access article distributed
under the terms of the [Creative
Commons Attribution License \(CC BY\)](#).
The use, distribution or reproduction in
other forums is permitted, provided the
original author(s) and the copyright
owner(s) are credited and that the original
publication in this journal is cited, in
accordance with accepted academic
practice. No use, distribution or
reproduction is permitted which does not
comply with these terms.

Zhilong Huoxue Tongyu capsule attenuates intracerebral hemorrhage induced redox imbalance by modulation of Nrf2 signaling pathway

Maryam Mazhar^{1,2*}, Guoqiang Yang^{3,4}, Houping Xu⁵, Yulin Liu^{2,6},
Pan Liang^{1,2}, Luyin Yang^{1,2}, Roman Spáčil⁷, Hongping Shen^{1,2},
Dechou Zhang^{1,2}, Wei Ren^{1,2*} and Sijin Yang^{1,2*}

¹National Traditional Chinese Medicine Clinical Research Base and Drug Research Center, the Affiliated Traditional Chinese Medicine Hospital of Southwest Medical University, Luzhou, China, ²Institute of Integrated Chinese and Western Medicine of Southwest Medical University, Luzhou, China, ³Research Center for Integrated Chinese and Western Medicine, the Affiliated Traditional Chinese Medicine Hospital of Southwest Medical University, Luzhou, Sichuan, China, ⁴Molecular Imaging and Therapy Research Unit, Center of Radiation Research and Medical Imaging, Department of Radiologic Technology, Faculty of Associated Medical Sciences, Chiang Mai University, Chiang Mai, Thailand, ⁵Preventive Treatment Center, the Affiliated Traditional Chinese Medicine Hospital of Southwest Medical University, Luzhou, China, ⁶Chengdu University of Traditional Chinese Medicine, Chengdu, Sichuan, China, ⁷The Czech Center for Traditional Chinese Medicine, Olomouc, Czechia

Background: One of the severely debilitating and fatal subtypes of hemorrhagic stroke is intracerebral hemorrhage (ICH), which lacks an adequate cure at present. The *Zhilong Huoxue Tongyu* (ZLHXTY) capsule has been utilized effectively since last decade to treat ICH, in some provinces of China but the scientific basis for its mechanism is lacking. **Purpose:** To investigate the neuroprotective role of ZLHXTY capsules for ICH-induced oxidative injury through the regulation of redox imbalance with the Nrf2 signaling pathway.

Methods: Autologous blood injection model of ICH in C57BL/6J mice was employed. Three treatment groups received ZLHXTY once daily through oral gavage at doses 0.35 g/kg, 0.7 g/kg, and 1.4 g/kg, started after 2 h and continued for 72 h of ICH induction. The neurological outcome was measured using a balance beam test. Serum was tested for inflammatory markers IL-1 β , IL-6, and TNF- α through ELISA, oxidative stress through hydrogen peroxide content assay, and antioxidant status by total antioxidant capacity (T-AOC) assay. Nuclear extract from brain tissue was assayed for Nrf2 transcriptional factor activity. RT-qPCR was performed for Nfe2l2, Sod1, Hmox1, Nqo1, and Mgst1; and Western blotting for determination of protein expression of Nrf2, p62, Pp62, Keap, HO1, and NQO1. Fluoro-jade C staining was also used to examine neuronal damage.

Results: ZLHXTY capsule treatment following ICH demonstrated a protective effect against oxidative brain injury. Neurological scoring showed improvement in behavioral outcomes. ELISA-based identification demonstrated a significant decline in the expression of serum inflammatory markers. Hydrogen peroxide content in serum was found to be reduced. The total antioxidant capacity was also reduced in serum, but the ZLHXTY extract showed a concentration-dependent increase in T-AOC speculating at its intrinsic antioxidant potential. Nrf2 transcriptional factor activity, mRNA and protein expression analyses

revealed normalization of Nrf2 and its downstream targets, which were previously elevated as a result of oxidative stress induced by ICH. Neuronal damage was also reduced markedly after ZLHXTY treatment as revealed by Fluoro-jade C staining. **Conclusion:** ZLHXTY capsules possess an intrinsic antioxidant potential that can modulate the ICH-induced redox imbalance in the brain as revealed by the normalization of Nrf2 and its downstream antioxidant targets.

KEYWORDS

intracerebral haemorrhage, traditional Chinese medicine, Nrf2 signalling, redox imbalance, antioxidants

Highlights

- Nrf2 signaling activates in response to oxidative stress after ICH-induced brain injury.
- ZLHXTY capsules possess an intrinsic antioxidant potential that regulates the ICH-induced redox imbalance in the brain.
- ZLHXTY capsules mediate neuroprotection through anti-inflammatory and anti-oxidant pathways.

Introduction

Among the subtypes of hemorrhagic stroke, intracerebral hemorrhage (ICH) is the most seriously debilitating and fatal, associated with high morbidity and mortality, inflicting 5 million people each year worldwide (An et al., 2017). Primarily, ICH injury is due to the rupture of blood vessels releasing massive blood volumes into the surrounding parenchyma, causing high intracranial pressure and inflammatory injury to the brain tissue (Keep et al., 2012). Preclinical and clinical studies have evidenced the key role of reactive oxygen species (ROS) mediated oxidative stress and inflammation in the progression of ICH-induced early brain injury (Lan et al., 2019). However, inflammatory responses can be modulated by oxidative stress through the activation of nuclear factor erythroid 2-related factor 2 (Nrf2) (He et al., 2020). Nrf2 is known to be a master regulator of the antioxidant system in our body and a fundamental transcriptional factor for genes regulated by antioxidant response element (ARE). This system is triggered on exposure to oxidative stress response to protect many organs including the brain, by the upregulation of cytoprotective and antioxidant genes and regulation of the cell survival (Ma, 2013; Saha and Buttari, 2020). Several studies have reported the activation of Nrf2 signaling after induction of intracerebral hemorrhage to provide protection against aggravation of early brain injury (Zhao et al., 2007; Zhao and Aronowski, 2013; Zhao et al., 2015; Chen-Roetling and Regan, 2017).

The lack of effective therapeutic options for ICH in clinics is impelling researchers to develop potent remedies (Liddle et al., 2020). Recently, the use of traditional Chinese medicine (TCM) has become popular as a sole or adjunct therapy for the treatment of various illnesses not only in China but all around the globe (Zhao et al., 2021). In 2019, TCM was accepted in the 11th revision of the International Statistical Classification of Diseases and Related Health Problems (ICD-11) as an effective therapeutic category (Lam et al., 2019). Moreover, in order to accomplish universal health coverage (UHC) as a Sustainable Development Goal 3

(SDG 3), the allocation of traditional and complementary medicines in mainstream healthcare and medical services has also been encouraged by World Health Organization (World Health Organization, 2019). Zhilong Huoxue Tongyu (ZLHXTY) capsule is a TCM formula containing a mixture of five Chinese medicines: *Pheretima Aspergillum* (E. Perrier), *Hirudo nipponica* Whitman, *Astragalus membranaceus* Fisch. ex Bunge, *Sargentodoxa cuneata* (Oliv.) Rehder and E.H. Wilson, and *Cinnamomum cassia* (L.) J. Presl (Table 1). Interestingly, antioxidant activity is common among all of these components (Yang et al., 2012; Rao and Gan, 2014; Durazzo et al., 2021; Li et al., 2021; Samuel et al., 2021; Zhang et al., 2021; Xu et al., 2022). According to TCM theory, the combination of these five drugs work in concert to reduce inflammation, resist oxidation, and fight against aging by enriching Qi, eliminating phlegm and blood stasis, and promoting blood circulation; thereby suitable for the treatment of stroke, atherosclerosis, and other related cardiovascular and cerebrovascular conditions (Liang et al., 2021).

Our previous research has demonstrated that ZLHXTY capsules inhibit inflammation after ICH by regulating the NFκB pathway (Mazhar et al., 2022). In this study, we further investigate the extensive mechanisms of the ZLHXTY capsule for ICH therapy, by exploring its modulatory role on the redox environment of the Nrf2 signaling pathway, during the early stages of ICH.

Materials and methods

Materials

Zhilong Huoxue Tongyu (ZLHXTY) capsules were obtained from the pharmacy department of the Affiliated TCM Hospital of Southwest Medical University, Luzhou, Sichuan, China. ZLHXTY capsule is a hospital preparation of the Affiliated Traditional Chinese Medicine Hospital, Southwest Medical University, Luzhou China. The formula is adapted by Prof. Sijin Yang according to the Buyang Huanwu decoction method, which is approved by the State Intellectual Property Office of the People's Republic of China (Patent No. 200810147774.1). Briefly, the Chinese herbs were obtained from various sources (Table 1) that were authenticated by Prof. Qingrong Pu, Director of TCM Preparation Room of The Affiliated Chinese Medicine Hospital of Southwest Medical University. Dried whole bodies of *H. nipponica* Whitman (0.32g) and *Pheretima aspergillum* (E. Perrier) (1.7g) were soaked in 2.85 ml of 60% ethanol for 7 days, followed by filtration and collection of filtrate A. The three herbal

TABLE 1 Composition of Zhilong Huoxue Tongyu capsule.

Components	1	2	3	4	5
Scientific Name	<i>Hirudo nipponica</i> Whitman	<i>Pheretima aspergillum</i> (E. Perrier)	<i>Astragalus membranaceus</i> Fisch. ex Bunge	<i>Cinnamomum cassia</i> L.) J. Presl	<i>Sargentodoxa cuneata</i> (Oliv.) Rehder and E.H. Wilson
Synonyms	Not applicable	<i>Amyntas aspergillum</i> (Perrier)	<i>Astragalus mongholicus</i> Bunge	<i>Neolitsea cassia</i> L.) Kosterm.	<i>Holboellia cuneata</i> Oliv.
English Name	Leech	Earthworm	Astragalus	Cassia	Sargentgloryvine
Chinese Name	ShuiZhi	Guang Dilong	Huang Qi	GuiZhi	Da XueTeng
Family	Hirudideae	Megascolecidae	Fabaceae	Lauraceae	Lardizabalaceae
Parts Used	Dried whole animal	Dried whole animal	Dried Roots	Dried Stem/Twig	Dried Stem/Twig
Dry Weight in ZLHXTY Capsule (grams)	0.32	1.7	2.3	0.86	1.7
Source	Chengdu Renjihong Pharmaceutical Co., Ltd.	Chengdu Renjihong Pharmaceutical Co., Ltd.	Sichuan Jinfang Biomedical Technology Co., Ltd.	Sichuan Tianzhi Traditional Chinese Medicine Co., Ltd.	Sichuan Jinfang Biomedical Technology Co., Ltd.
Batch Number	190101	190301	190501	20030101	190402
Origin	Anhui, China	Guangxi, China	Gansu, China	Anhui, China	Guangxi, China

components, i.e., dried roots of *A. membranaceus* Fisch. ex Bunge (2.3g), dried twigs of *C. cassia* L.) J. Presl (0.86g) and *S. cuneata* (Oliv.) Rehder and E.H. Wilson (1.7g), were decocted twice with 13.51 ml of water for 1 h each time and the volatile components were also collected. The decoctions collected in two steps were combined together and filtered. The filtrate was concentrated at 80 °C to a relative density of $1.05 \leq 1.10$. Later, ethanol was added to the concentrate to make the alcohol content up to 50%, and was kept standing for 12 h followed by filtration. The resulting filtrate B was combined with the ethanolic infusion A. After the alcohol was recovered, the resulting mixture was boiled and concentrated at 80 °C to a relative density of 1.20. The concentrate was added with 0.2g of dextrin as an excipient, boiled, granulated, and crushed into a fine powder and sprayed and mixed with volatile components collected previously. Finally, 0.4g of the powdered mixture was filled in a capsule shell to make one capsule dosage form. The whole drug extract ratio (DER) is 12.9%. All the procedures were performed following good laboratory practices (GLP). The HPLC-HR-MS analysis of the ZLHXTY capsule has been performed previously and can be referred to in our previous publication (Mazhar et al., 2022) (Supplementary Table S1; Supplementary Figure S1).

Animals

Male C57BL/6J mice weighing 20–22g, and 7–8 weeks old, were raised in the controlled environment of an animal house facility regulated at a temperature of 22 °C, and humidity of 55%, with alternate 12-h light and dark cycles. All animals were provided with normal rodent food and plain water *ad libitum*. The study design was approved by the Animal Research Committee of Southwest Medical University, Luzhou, China; and all the procedures were conducted in accordance with the National Institute of Health (NIH) Guide for the Care and Use of Laboratory Animals.

Intracerebral hemorrhage model

The autologous blood injection model of ICH was employed in this study. Briefly, animals were anesthetized with sodium pentobarbital (dose 50 mg/kg) intraperitoneal injection. The mouse head was fixed in a stereotaxic frame with a small incision made on the skin. A sterile cotton bud soaked in 30% H₂O₂ was applied on the surface of the skull to remove the periosteum. At co-ordinates of 2.5 mm lateral and 0.2 mm anterior to the bregma, a 1-mm burr hole was drilled in the right striatum, through which a volume of 25 µL autologous blood obtained from the tail vein was injected at a rate of 5 µL/min, with a needle insertion depth of 3 mm. To prevent backflow of blood, the needle was held steady for 5 min after the completion of injection and then withdrawn gently. The incision was sutured in aseptic conditions. The animals were observed for vital signs and maintained in a warm environment at 37 °C until consciousness was regained.

Treatment groups

There were five experimental groups with six mice in each, distributed randomly. The experiments were repeated three independent times. The groups were as follows i) normal control, ii) ICH model group, iii) Low dose (0.35 g/kg) ZLHXTY-LD, iv) Medium dose (0.7 g/kg) ZLHXTY-MD, and v) High dose (1.4 g/kg) ZLHXTY-HD.

The first ZLHXTY dose was given by oral gavage after 2 h of ICH induction, followed by once daily dosing for three consecutive days. The mice in the normal and ICH model groups were orally gavaged with normal saline. The animals from respective groups were sacrificed after 24 and 72 h, for subsequent assays and molecular analysis. From the previous experiments, the dose-dependent effect of ZLHXTY capsules on ICH recovery has been established. To be

TABLE 2 Neurological scoring scale for beam walking test^a.

Score	Performance on the beam
7	Traverses beam normally with both affected paws on horizontal beam surface, neither paw ever grasps the side surface, and there are no more than two footslips; toe placement style is the same as preinjury
6	Traverses beam successfully and uses affected limbs to aid >50% of steps along beam.
5	Traverses beam successfully but uses affected limbs in <50% of steps along beam.
4	Traverses beam and, at least once, places affected limbs on horizontal beam surface.
3	Traverses beam by dragging affected hindlimbs.
2	Unable to traverse beam but places affected limbs on horizontal beam surface and maintains balance for ≥5 s.
1	Unable to traverse beam; cannot place affected limbs on horizontal beam surface.

^aAdapted from the method of Feeney et al. (25) used to evaluate unilateral lesions of sensory cortex in rats.

concise, only the highest dose data with the best effective results are presented here, except for neurological scoring outcomes showing the three dosing groups of ZLHXTY capsule treatment.

Balance beam test with neurological scoring

The animals were examined for neurological scoring on a balance beam (Feeney et al., 1982; Liu et al., 2020) 2 days prior to the induction of ICH and continued after 3 h s, 24 h s, 48 h s, and 72 h s of ICH induction. Briefly, the mice were allowed to cross the 2 cm long beam, and the latency period from the starting point to the terminal box was noted, within 60 s of the maximum limit (Liu et al., 2020). The general behavior and gait of the animal while walking on the beam such as the number of paw slips were also recorded according to the scoring criteria (Table 2) (Feeney et al., 1982). The average score was calculated from the observations of two independent observers.

Animal surgery and specimen preparation

Following the ZLHXTY treatment regimen for 1 and 3 days, the mice in respective groups were euthanized with sodium pentobarbital overdose for dissection. A cardiac puncture was performed to collect blood in a vacutainer that was centrifuged to obtain serum. The brain tissues were collected in 1.5 ml eppendorf tubes and were snap-frozen by immersion in liquid nitrogen. Both the serum and brain tissue samples were stored at −80 °C for later use.

ELISA for IL-1β, IL-6 and TNF-α

Sera were assayed for IL-1β, IL6, and TNF-α following the manufacturer's procedure provided by commercially available ELISA kits (Cat# PI301, PI326, PT512) purchased from Beyotime Biotechnology, Shanghai, China. Briefly, 100 μl of each six standard dilutions, standard diluent buffer, and samples were added respectively into the wells of the ELISA plate and incubated for 2 h at room temperature. Then, the wells were rinsed 5x with washing solution, followed by incubation in 100 μl biotinylated

antibody for 1 h. Followed by washing 5x, wells were incubated in 100 μl horseradish peroxidase-labeled streptavidin solution for 20 min in the dark at room temperature. Followed by another washing step 5x, 100 μl of chromogenic reagent TMB solution was added and allowed to react for 20 min at room temperature in the dark. Finally, 50 μl of stop solution was added and mixed well, followed by absorbance measurement at 450 nm under a microplate reader. The target protein concentration was calculated by plotting the standard curve graph.

Hydrogen peroxide content assay

Oxidative stress was evaluated by determining the level of hydrogen peroxide (H₂O₂) in the serum samples using the hydrogen peroxide content assay kit (Solarbio, Beijing, China, Cat#BC3595). All the steps were performed according to the manufacturer's protocol and finally, the samples were measured at the absorbance of 415 nm under BioTek Synergy 2 microplate reader.

Total antioxidant capacity (T-AOC) assay

The antioxidant capacity was determined in serum samples using a total antioxidant capacity test kit (T-AOC) purchased from Solarbio, Beijing, China (Cat#BC1315) according to the manufacturer's protocol. Four graded concentrations of ZLHXTY water extract, i.e., 0.07, 0.14, 0.28, and 0.42g per 1 ml of extraction solution, were also evaluated for their intrinsic antioxidant potential and all the samples were measured under BioTek Synergy 2 microplate reader at the absorbance of 593 nm.

Nrf2 transcriptional factor activity assay

The transcriptional activity of Nrf2 was measured with RayBio[®] Mouse Nrf2 TF-Activity Assay Kit (Catalog #: TFEM-Nrf2, Norcross, GA 30092, United States). Nuclear protein was extracted from the brain samples using a nuclear and cytoplasmic protein extraction kit according to the

TABLE 3 Primer sequences (5' - 3').

Gene name	Primer sequence	Product length
Nfe2l2	F: TCTTGAGTAAGTCGAGA AGTGT	23
	R: GTTGAACTGAGCGAAAAAGGC	22
Sod1	F: GCCCGCTAAGTGCTGAGTC	19
	R: CCAGAAGGATAACGGATGCCA	21
Nqo1	F: AGGATGGGAGGTACTCGAATC	21
	R: AGGCGTCCTTCCTTATATGCTA	22
Hmox1	F: AAGCCGAGAATGCTGAGTTCA	21
	R: GCCGTGTAGATATGGTAC AAGGA	23
Mgst1	F: CTCAGGCAGCTCATGGACAAT	21
	R: GTTATCCTCTGGAATGCGGTC	21
GAPDH	F: CGGAGTCAACGGATTGG TCGTAT	24
	R: AGCCTTCTCCATGGTGGT GAAGAC	24

manufacturer's instructions (Sangon Biotech, Shanghai, China, Cat# C510001). The procedures were performed following the manufacturer's protocol.

Quantitative real time polymerase chain reaction (qRT-PCR)

The qRT-PCR analysis for mRNA expression was performed for the following set of genes: Nfe2l2, Hmox1, Nqo1, Mgst1, and Sod1, the primer sequences of which are given in Table 3. Briefly, the brain tissues from the hemorrhagic cortex were homogenized in Trizol reagent (Beyotime Biotechnology, China, Cat# R0016) to extract total RNA. The absorbance was measured under a UV spectrophotometer at 260 and 280 nm, considering a ratio value > 1.8 for OD260/OD280 as appropriate for RNA sample quality. Reverse transcription of total RNA into cDNA was performed with HiScript III RT SuperMix for qPCR (+gDNA wiper) kit (Vazyme Biotech Co., Ltd, China, Cat. No. R323-01). The qRT-PCR was carried out in the presence of a fluorescent dye ChamQ universal SYBR qPCR Master Mix (Vazyme Biotech Co., Ltd, China, Cat. No. Q711-02/03) on the LightCycler® 480 Instrument II (Roche, United States). The gene expression values were obtained through a cDNA standard curve. The mRNA levels were normalized to the GAPDH expression and calculated by the $2^{-\Delta\Delta Ct}$ method.

Western blot analysis

Samples of brain tissues were lysed and homogenized in RIPA buffer containing 1 mM PMSF on ice. The homogenized samples

were centrifuged, and supernatants were collected in new eppendorf tubes. The supernatants containing protein were measured using a BCA protein concentration assay kit (enhanced) assay method (Beyotime, Shanghai, China, Cat#P0010S). Each sample containing 40 µg protein was prepared with loading buffer and subjected to electrophoresis on 12% SDS-PAGE gel, and then transferred to nitrocellulose membranes under appropriate voltage and time for specific proteins. The blots underwent blocking with 5% skimmed milk/TBST with gentle shaking for 1 h at room temperature. Later, the blots were incubated overnight with respective primary antibodies (listed in Table 4) with gentle shaking. The following day, after recovering the primary antibody solutions, the membranes were washed with TBST 5min x3, and subsequently incubated in Alexa Fluor 790 and Alexa Fluor 680 fluorescently labeled secondary antibodies (Invitrogen Life Technologies, United States, Cat#A11357 and A21109); at dilution ratio 1:10,000, for 1 h at room temperature. Membranes were then washed with TBST 5min x3 and observed under a laser scanner (Amersham Typhoon™, Cytiva, United States) for NIR fluorescent signal detection. The optical density was measured using the ImageJ software (NIH, Bethesda, MA, United States), and the values were normalized with respect to GAPDH.

Fluoro-jade C staining

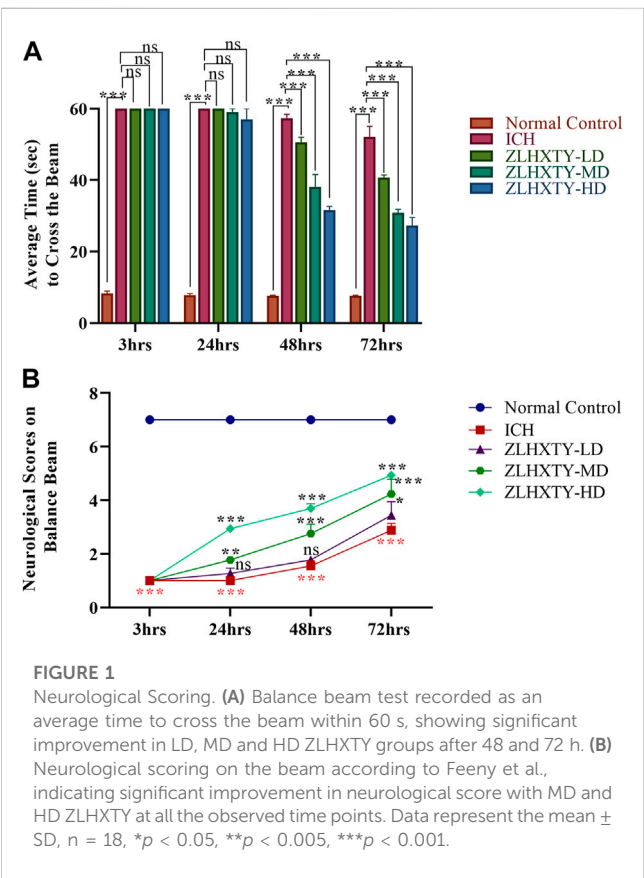
Frozen brain tissues were cryo-sectioned and fixed in 4% paraformaldehyde for 30 min, with subsequent 5 min rehydration in 80% ethanol and NaOH solution mixed in a 9:1 ratio; followed by immersion in 70% ethanol and then distilled water, for 2 min in each. The blocking was carried out in KMnO₄ solution diluted in distilled water (1:9 ratio), for 10 min. After blocking, the slides were rinsed with distilled water for 2 min, followed by fluoro-jade C staining (along with DAPI) for 10 min in the dark (Fluoro-Jade C RTD Stain Reagent, Biosensis, Australia, Cat#TR-100-FJ). Later, the slides were rinsed with distilled water for 1 min x 3. The slides were dried in an oven preheated at 50°C, for 5 min in the dark, and then dehydrated in xylene for 1 min. A drop of non-fluorescent mounting medium was placed on the tissue and clean coverslips were carefully placed over it. The slides were kept in the dark and observed under a Leica DM4 B fluorescence microscope equipped with a Leica DMC6200 camera. The photomicrographs were acquired at magnification ×200 (Objective lens ×20 and eyepiece lens 10x), using Leica application suite X software. The photomicrographs were adjusted for background and contrast using adobe photoshop software version 7.0.

Statistical analysis

Results are expressed as mean ± S.D. Statistical analysis was performed by GraphPad Prism-5 statistic software Version 8.0.1 software (GraphPad Software Inc., La Jolla, CA, United States). The statistical comparisons were analyzed by ANOVA followed by Tukey *post hoc* test. Differences with **p* < 0.05, ***p* < 0.005, and ****p* < 0.001 were considered statistically significant.

TABLE 4 Primary antibodies.

Antibody	Type	Dilution	Uniprot RRIIDs	Catalogue number	Source
NRF2(D1Z9C)XP	Monoclonal	1:1000	Q16236	12721	Cell Signaling Technologies Inc., Shanghai, China.
SQSTM1/p62 (D6M5X)	Monoclonal	1:1000	Q64337	23214	
Phospho-SQSTM1/p62(Ser349) (E7M1A)	Monoclonal	1:1000	Q13501	16177	
Keap1(F-10)	Monoclonal	1:1000	Q9Z2X8	sc-514914	Santa Cruz Biotechnology, Inc., CA, United States.
HO1(F-4)	Monoclonal	1:1000	P14901	sc-390991	
NQO1 (A180)	Monoclonal	1:1000	Q64669	sc-32793	
GAPDH	Monoclonal	1:10 000	P04406	AB0037	Abways Technology, Inc., Shanghai, China.



Results

ZLHXTY capsule ameliorates the neurological outcome after ICH

The balance beam test with neurological scoring was performed to evaluate the protective effect of ZLHXTY on the restoration of neurobehavioural outcomes after ICH. The ICH model animals demonstrated a complete inability to walk with significant fearfulness and shivering while on the beam when

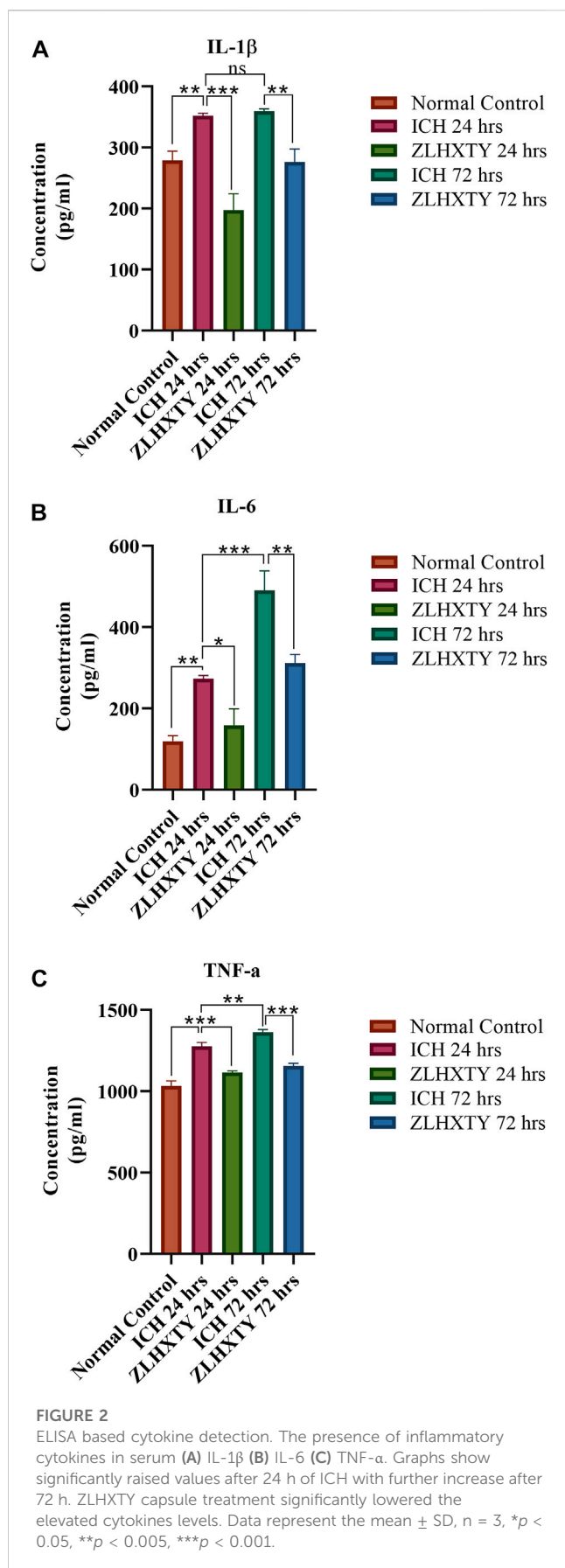
observed after 3 and 24 h, however, after 48 and 72 h animals showed to stumble on the beam with frequent paw slips ($**p < 0.005$, $***p < 0.001$). The mice in 24 h ZLHXTY treatment group also demonstrated enhanced fear and frequent paw slips while limping on the beam, however, the overall behavior and the walking ability were significantly improved ($***p < 0.001$) after 48 h and 72 h (Figure 1A). The behavioral score on the balance beam is shown in Figure 1B.

ZLHXTY capsule reduces the inflammation after ICH

As identified previously, the treatment with ZLHXTY capsule after ICH protected from aggravated inflammatory brain injury by inhibition of the NF κ B signaling pathway and its downstream targets (Mazhar et al., 2022). Similarly, the ELISA-based evaluation revealed significant elevation of inflammatory mediators IL-1 β , IL-6, and TNF- α in the sera of ICH mice ($**p < 0.005$, $***p < 0.001$) both after 24 and 72 h, as compared to normal mice. However, ZLHXTY treatment after 24 h and 72 h significantly lowered the serum levels of IL-1 β , IL-6, and TNF- α as compared to the elevated expression observed after ICH ($***p < 0.001$) (Figures 2A–C).

ZLHXTY capsule resist the oxidative stress after ICH

During primary ICH injury, excessive generation of reactive oxygen species including hydrogen peroxide (H_2O_2) leads to oxidative stress, which is the key phenomenon leading to secondary damage resulting from the apoptosis, autophagy, inflammatory response, and blood-brain barrier (BBB) disruption (Yao et al., 2021). In our study, we found that the serum H_2O_2 content was significantly elevated after ICH ($***p < 0.001$) as compared to the normal group. Whereas, the ZLHXTY capsule significantly reduced the serum H_2O_2 content in the treatment groups ($***p < 0.001$). The results of an assay for hydrogen peroxide (H_2O_2) content as a marker of oxidative stress are shown in Figure 3A.



ZLHXTY capsules possess intrinsic antioxidant potential

Supporting the results of H₂O₂ content that were significantly elevated after ICH, the results of the T-AOC assay revealed that antioxidant capacity was also increased after ICH (* $p < 0.05$ compared to normal). Inconsistently, after ZLHXTY treatment the serum antioxidant capacity was reduced as compared to ICH and the normal group (*** $p < 0.001$) (Figure 3B). On the other hand, the four different concentrations of ZLHXTY water extract showed that ZLHXTY antioxidant potential increases with increasing concentration, indicating the intrinsic antioxidant potential of the ZLHXTY capsule (Figure 3C).

ZLHXTY capsule regulates the Nrf2 transcriptional activity after ICH

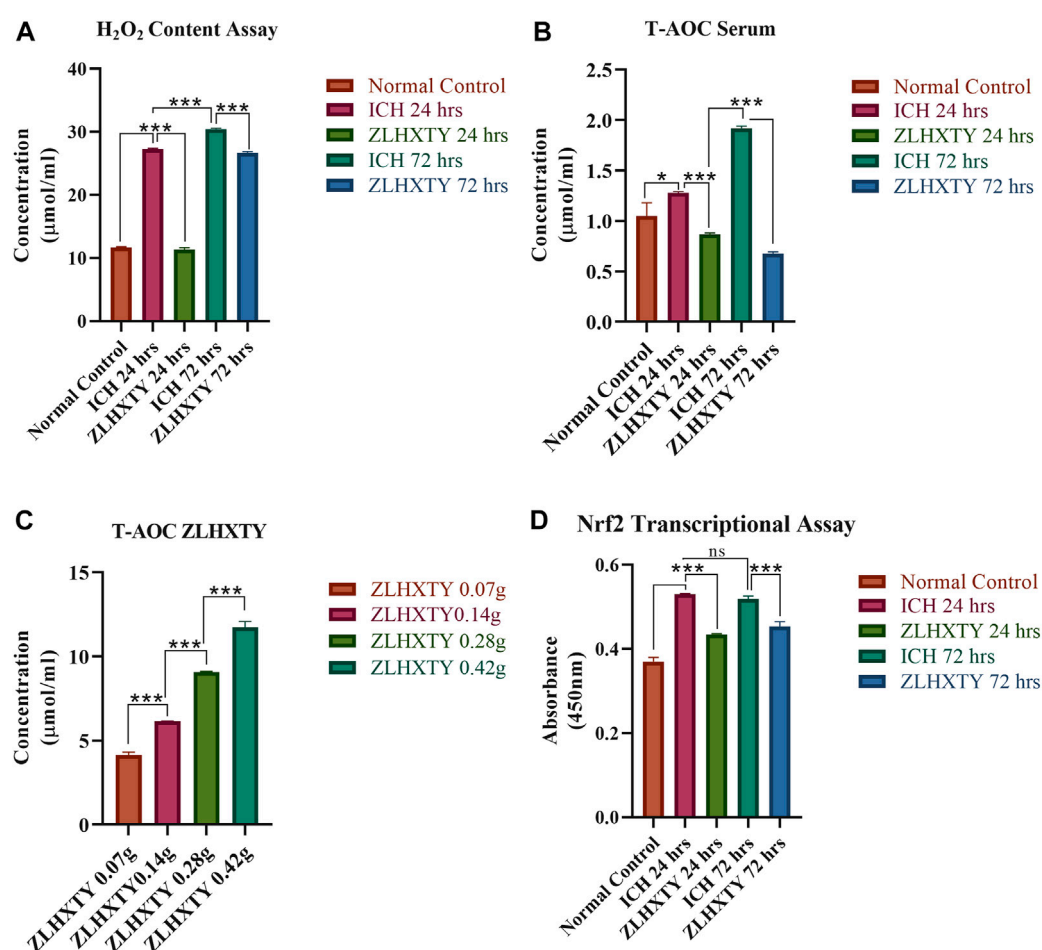
It was observed that Nrf2 transcriptional factor activity was significantly upregulated after ICH induction after 24 h (*** $p < 0.001$) as compared to the normal group, which was further exaggerated after 72 h non-significantly, in response to resulting oxidative and inflammatory stress. However, following ZLHXTY capsule treatment both at 24 h and 72 h, the Nrf2 transcription was restored to normal levels that might correlate with the intrinsic antioxidant potential of ZLHXTY capsules (*** $p < 0.001$). This result further supports that the ZLHXTY capsule exerts its neuroprotection via its antioxidant property while modulating the Nrf2 antioxidant defense mechanism after ICH-induced oxidative stress (Figure 3D).

ZLHXTY capsule normalizes the mRNA levels of Nrf2 and its downstream antioxidant target genes

The mRNA expression levels of Nfe2l2 coding for transcription factor Nrf2, and its downstream antioxidant target genes such as Nqo1, Hmox1, Sod1, and Mgst1 were tested. After 24 h of ICH, the measured values of Nfe2l2, Nqo1, Hmox1, Sod1, and Mgst1 were significantly elevated as compared to the normal control group (*** $p < 0.001$), which continued to be elevated until after 72 h of ICH. However, following ZLHXTY treatment both after 24 and 72 h have been shown to reduce their expression down towards normal (*** $p < 0.001$ as compared to the ICH group), (Figures 4A–E).

ZLHXTY capsules regulation of Nrf2 signaling revealed by protein expression

The Western blot analysis was performed for analysis of protein expression of Nrf2, p62, Pp62, Keap, and downstream antioxidant proteins HO1 and NQO1, shown in Figures 5A–G. After 24 h of ICH, the protein expression of Nrf2 and p62 were significantly elevated (*** $p < 0.001$) as compared to the normal group. However,

**FIGURE 3**

Oxidative and Antioxidant Assays. (A) H₂O₂ content assay of serum revealed significant elevation of hydrogenperoxide after 24 h with further increase after 72 h of ICH, which is reduced after ZLHXTY treatment. (B) Total antioxidant capacity assay revealed increased antioxidant capacity after ICH 24 h and further elevation at 72 h, while ZLHXTY treatment reduced the antioxidant capacity in serum. (C) Total antioxidant capacity of graded concentrations of ZLHXTY revealed increase in antioxidant capacity in a concentration dependent manner. (D) Nrf2 transcriptional assay revealed actively increased Nrf2 transcription after ICH which is downregulated to normal by ZLHXTY capsule. Data represent the mean \pm SD, $n = 3$, * $p < 0.05$, ** $p < 0.005$, *** $p < 0.001$.

after ZLHXTY treatment for 24 h, the Nrf2 expression was significantly decreased (** $p < 0.005$), as well as the expression of p62 was also lowered more significantly (*** $p < 0.001$). The expression of p62 is supported by the parallel expression of phosphorylated p62, Pp62, indicating an active form of p62 regulating the ICH and ZLHXTY action mechanism. In contrast, the levels of keap1 were maintained at the same level in all the groups without significant alteration except in ICH 72 h group where it was slightly elevated. The expression pattern of downstream targets NQO1 and HO1 follow similarity with Nrf2 expression, i.e., significant elevation (*** $p < 0.001$) after 24 h of ICH and downregulation after ZLHXTY 24 h treatment. However, all the proteins such as Nrf2, p62, Pp62, HO1, and NQO1 show significantly higher expression (*** $p < 0.001$) after 72 h of ICH indicating the critical time point for regulation of disease mechanism. The effect was regulated by ZLHXTY treatment for 72 h, decreasing the protein expression to resume normal levels.

ZLHXTY capsules control neuronal damage

The neuronal damage was evaluated by using Fluoro-jade C staining on brain tissue sections. In normal tissues (Figures 6A,D) there was no sign of neuronal damage in the brain tissue slides around the basal ganglia region in the right hemisphere. After 24 h of ICH, the neuronal damage in the perihematomal region was obvious, and an increase in the green fluorescent signals was observed (Figure 6B). However, after ZLHXTY treatment for 24 h, the neuronal damage was significantly controlled as compared to ICH 24 h model (Figure 6C). The extent of neuronal damage was markedly increased even higher than that after 24 h of ICH injury as evidenced by the increased number of green fluorescent signals in the brain tissue (Figure 6E). Following ZLHXTY treatment for 72 h, the neuronal damage was significantly controlled and few to negligible green fluorescent signals were found as an indicator of neuronal damage (Figure 6F).

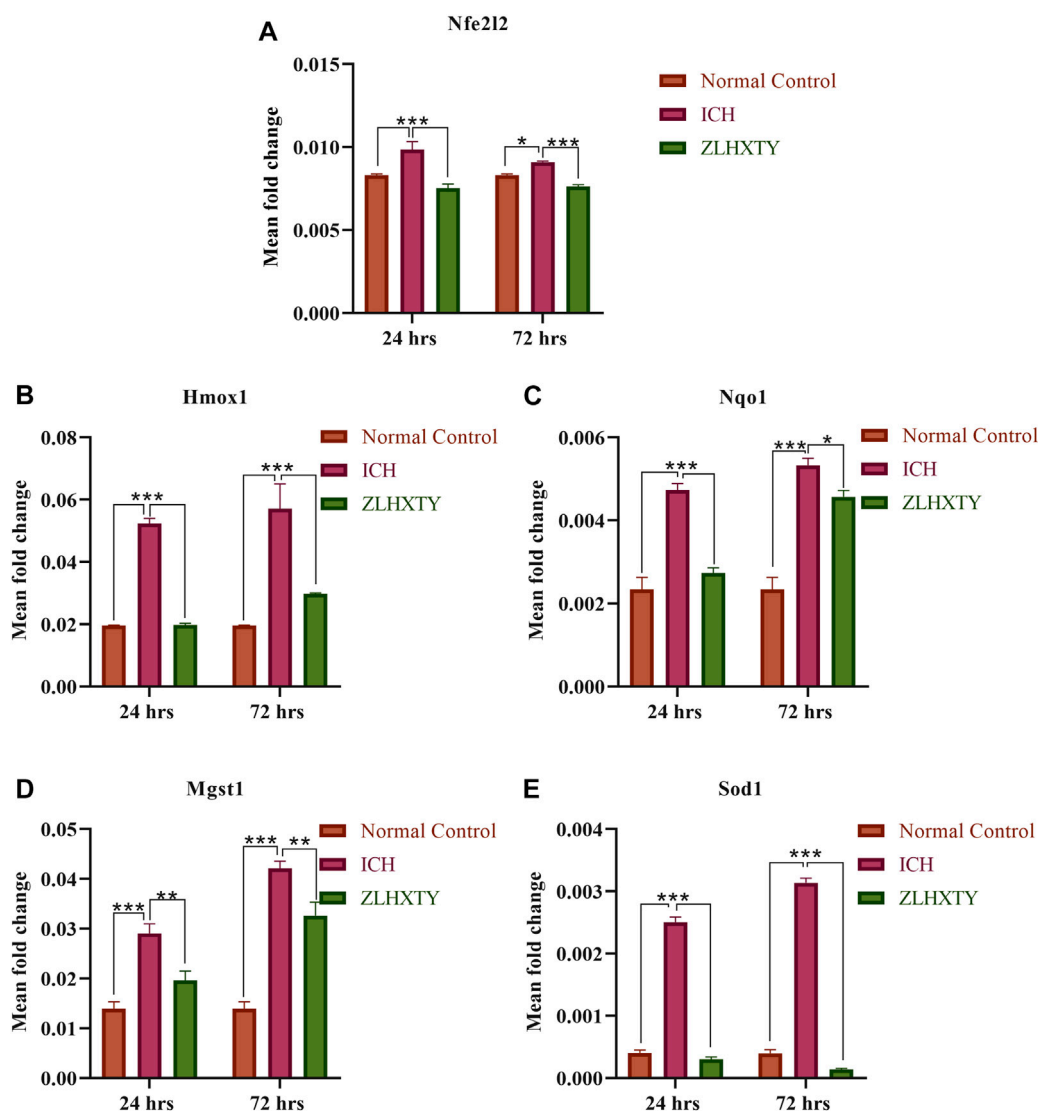


FIGURE 4

RT-qPCR (A) Nfe2l2 (B) Hmox1 (C) Nqo1 (D) Mgst1 (E) Sod1, showing significant elevation after 24 h with further increase after 72 h of ICH whereas, ZLHXTY capsule treatment caused downregulation. Data represent the mean \pm SD, $n = 9$, * $p < 0.05$, ** $p < 0.005$, *** $p < 0.001$.

Discussion

Oxidative stress following intracerebral hemorrhage is a key phenomenon underlying aggravated brain injury. The redox imbalance due to the excessive production of reactive oxygen species activates antioxidant defense pathways such as Nrf2 signaling to combat the oxidative stress (Yao et al., 2021). In the present study, we tested the hypothesis that ZLHXTY capsules alleviate intracerebral hemorrhage-induced brain injury in a mouse model by combating oxidative stress and inflammation, on its early administration, i.e., within 2 h of ICH induction. It is presumed that the neuroprotective effect of ZLHXTY capsules may partially involve its intrinsic antioxidant potential that regulates redox imbalance and maintain Nrf2 transcription and antioxidant response elements after ICH. This study is further proof of evidence to

our previous research on exploring the anti-inflammatory role of ZLHXTY capsules in inhibiting TNF α -NF κ B canonical signaling after ICH.

Oxidative stress damage mediated by reactive oxygen species-mediated plays a crucial role in deciding the course of disease in severe brain injury in humans (Paolin et al., 2002). A similar finding was also evidenced in our experiment indicating poor neurological outcomes after ICH due to a high oxidative stress environment. Accumulated research evidence indicates a direct relationship between high ROS/oxidative stress in plasma/serum and poor neurological outcome/mortality after traumatic brain injury (Nayak et al., 2008; Hohl et al., 2012; Lorente et al., 2019; Park et al., 2022). Maintaining antioxidant levels can effectively control the oxidative stress that induces damage and therefore, improve the neurological outcome (Park et al., 2022), as is also observed after ZLHXTY capsule treatment after ICH in our experiment.

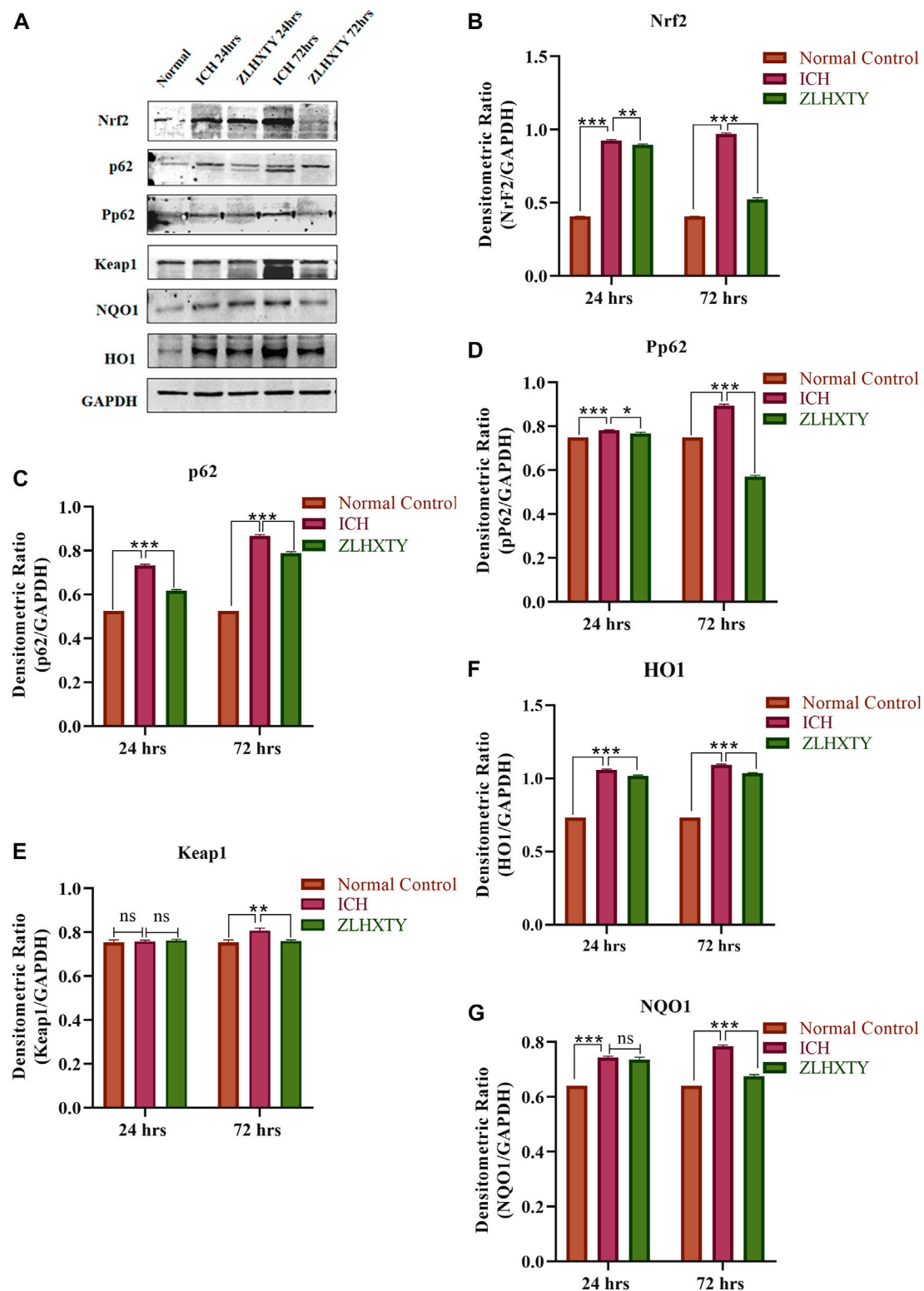


FIGURE 5

Western blotting (A) Representative immunoblots; graphical representation of measured densitometric ratio of specific proteins and GAPDH (B) Nrf2 (C) p62 (D) Pp62 (E) Keap1 (F) HO1 (G) NQO1, showing significant increase in expression after 24 h and farther after 72 h of ICH followed by regulatory effect of ZLHXTY capsule treatment. Data represent the mean \pm SD, $n = 3$, * $p < 0.05$, ** $p < 0.005$, *** $p < 0.001$.

Fluoro-Jade C Staining

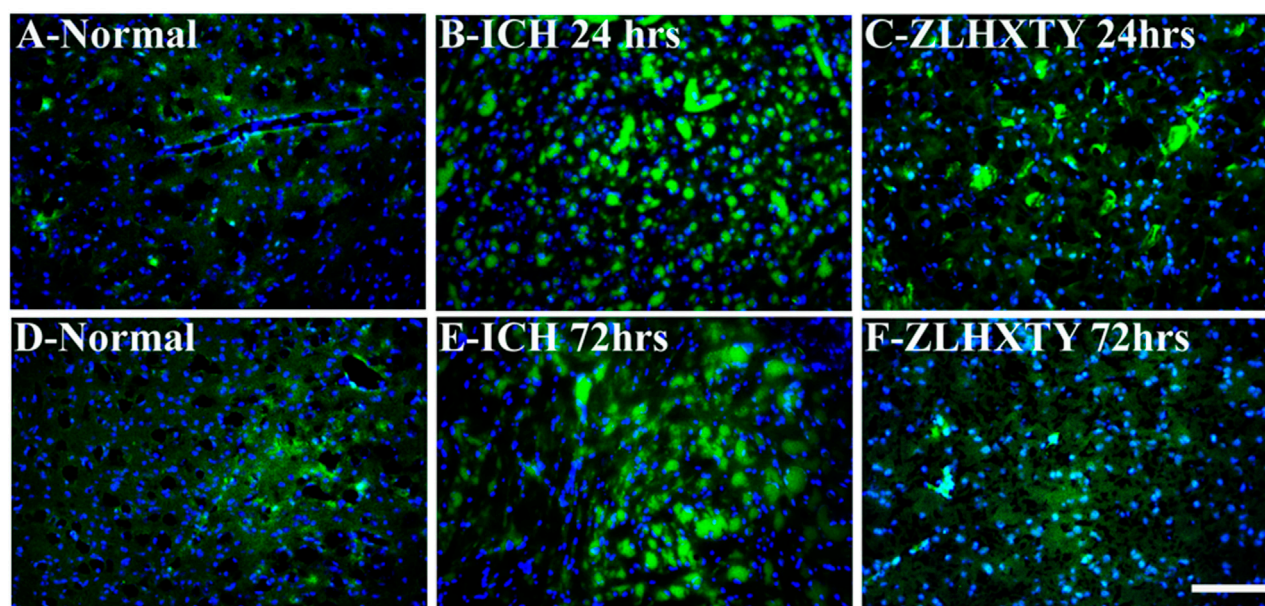


FIGURE 6

Fluoro-Jade C Staining. Brain sections stained with Fluoro-Jade C (green) to identify neuronal damage, and DAPI (blue) to mark nucleus. (A, D) Normal brain sections, without any sign of neuronal damage. (B) ICH 24 h group reveal obvious neuroal damage with increased number and signal of green fluorescence. (C) ZLHXTY 24 h group show significant control over neuronal damage. (E) ICH 72 h show excessive neuronal damage, even higher than that observed in ICH 24 h group. (F) ZLHXTY 72 h group show only few damaged neuronal cells, indicating significant control over neuronal damage. 50µm scale bar corresponds to x200 magnification.

Excessive production of reactive oxygen species is known to progress primary hemorrhage into aggravated secondary injury. In our experiments, we also observed significant ROS production through hydrogen peroxide content assay after 24 and 72 h of ICH, which was subsided by ZLHXTY capsule treatment. Soon after hemorrhage, the infiltration of reactive leukocytes and microglia/macrophages secreting various cytokines and chemokines, act as a major source of ROS causing damage to perihematoma tissue (Zhou et al., 2014). Available data from both clinical and preclinical resources support the contribution of activated leukocytes and microglia/macrophages in the progression of ICH-induced early brain injury (Keep et al., 2012). In addition, hemoglobin and its metabolites: iron, carbon monoxide, and biliverdin; released via erythrolysis further contribute to ICH brain injury (Keep et al., 2012). Subsequently, iron accumulation in the brain leads to abundant ROS generation via Fenton reaction, causing neurotoxicity (Xiong et al., 2014). Together these mechanisms interact resulting in disruption of the blood-brain barrier (BBB), neuronal damage, and gliosis with lasting neurological deficits (Hu et al., 2016).

To further confirm our result, we performed a total antioxidant capacity assay and observed that ZLHXTY capsules possess intrinsic antioxidant activity which increases with increasing concentration. This can be further explained by the constitution of the ZLHXTY capsule, which is a mixture of five Chinese medicines derived from natural origin with multiple constituents and rich antioxidant potential. Extensive research studies have identified the antioxidant properties of *A.*

membranaceus Fisch. ex Bunge (Durazzo et al., 2021; Samuel et al., 2021), *C. cassia* L.) J. Presl (Yang et al., 2012; Rao and Gan, 2014), and *S. cuneata* (Oliv.) Rehder and E.H. Wilson (Zhang et al., 2021), displaying significant prevention from tissue injury via antioxidant mechanisms. In addition, two constituents of the ZLHXTY capsule are of animal origin, i.e., *H. nipponica* Whitman and *P. aspergillum* (E. Perrier), that have also been shown to act through antioxidant mechanisms (Li et al., 2021; Xu et al., 2022).

As explained in a previous study, the absorption of antioxidants after their consumption must be reflected as the increment in total antioxidant capacity in serum. However, the total antioxidant capacity in plasma/serum is under strict regulatory control and the increased levels usually reflect the adaptation to increased oxidative stress (Lorente et al., 2015; Morimoto et al., 2019). Similarly, we observed an increased T-AOC in the serum of ICH groups both at 24 and 72 h, probably as a physiological mechanism to counter the increased ROS production. However, the ZLHXTY treatment decreased the total antioxidant capacity more than the ICH groups. Elevated serum antioxidant capacity may not necessarily be a desirable condition, probably indicating an underlying ongoing pathological process in the body, as yet the decreased levels might be in response to decreased production of reactive species *in vivo* (Ogawa et al., 2011; Lorente et al., 2015; Morimoto et al., 2019). Therefore, as a net result of the two methods, i.e., hydrogen peroxide content and total antioxidant capacity, we can assume that ZLHXTY maintains the redox imbalance and counter the ROS production after ICH.

Nrf2 has a crucial function in limiting the cascade of events originating from oxidative stress, leading to ICH-induced early brain injury. Nrf2 is a major transcription factor responsible to induce phase II detoxification enzymes through upregulation of antioxidant response element (ARE) mediated antioxidant genes expression such as NAD(P)H: quinone oxidoreductase 1 (NQO1), heme oxygenase 1 (HO-1), glutathione S-transferase (GST), glutamylcysteine ligase (the rate-limiting enzyme in glutathione synthesis), thioredoxin reductase 1, and thioredoxin (Keep et al., 2012). Accumulated research reported that Nrf2 expression gradually increased within 2 h following ICH, reaching its peak at 24 h, mediating the induction of antioxidant and detoxification enzymes/proteins expression, resulting in an improved neurological outcome, alleviated cerebral edema, and decreased inflammation (Shang et al., 2013). We also identified the same observation of increased Nrf2 transcriptional activity after 24 h and further increment at 72 h of ICH, which was further confirmed through RT-qPCR and Western blot. The downstream antioxidant targets, i.e., HO1, NQO1 and MGST1 were also expressed concordantly as Nrf2, as observed at the transcriptional and protein levels. Previous studies have also documented the protective role of the Nrf2 gene, by identifying more neuronal vulnerability to oxidative stress and aggravated brain damage following ICH in Nrf2^{-/-} mice, compared with WT mice, because of decreased NQO1 and GST activities (Kensler et al., 2006). Furthermore, neuroblastoma cell lines with Nrf2 silencing or gene knockout were found to be more susceptible to apoptosis than the vector-only transfected cells, due to the suppression of ARE-mediated genes (Zhao et al., 2006).

Nrf2 activation is regulated by two mechanisms, i.e., canonical and non-canonical mechanisms. During basal conditions, Nrf2 levels are mainly regulated by Kelch-like ECH-associated protein 1 (Keap1) i.e., E3 ubiquitin ligase substrate adaptor, mediating Nrf2 polyubiquitination and constant degradation through the proteasomal pathway. However, some molecules of Nrf2 evade Keap1-dependent degradation and translocate into the nucleus generating a constitutive and weak signal of target genes expression. This ubiquitin ligase activity of Keap1-dependent Nrf2 degradation is regulated in a redox-sensitive manner. During oxidative stress or in the presence of electrophilic compounds, a conformational change occurs at specific cysteine residues of Keap1 that are oxidized, causing inhibition of the E3 ubiquitin ligase activity. This inhibition of Keap activity allows newly synthesized Nrf2 molecules to translocate into the nucleus and bind to the ARE for induction of target gene expression. This mechanism is called the canonical activation of Nrf2, which requires the oxidation of cysteine residues of Keap1 (Hennig et al., 2018). However, Nrf2 activation upon the disruption of Keap1-Nrf2 complex by phosphoactivation of p62 and some other proteins such as DPP3, WTX, PALB2, p21, and BRCA1 is termed as non-canonical Nrf2 activation (Silva-Islas and Maldonado, 2018). In our experiment, it is observed that both the transcriptional and protein expression of p62 and Pp62 was found to be upregulated after ICH but not the Keap transcriptional and protein expression in response to increased Nrf2 activity. A ubiquitin-binding protein p62, serves as a cargo receptor during autophagy

(Katsuragi et al., 2016). Under normal physiological conditions, p62 interacts with autophagic ubiquitinated substrates and delivers them to autophagosomes for degradation. However, under conditions of oxidative stress when the autophagy is impaired, p62 gets accumulated in the cytoplasm and gets phosphorylated for selective binding to the ubiquitinated autophagic cargos (such as damaged mitochondria, protein aggregates, and invasive bacteria). When p62 is phosphorylated at S351 of the KIR, in an mTORC1-dependent manner, its affinity for Keap1 increases, leading to sequestration of Keap1 on autophagic cargos for degradation. Consequently, Nrf2 molecules are stabilized allowing more molecules to translocate into the nucleus and bind to the target site on DNA for induction of cytoprotective target genes (Lau et al., 2010; Ichimura et al., 2013; Ahmed et al., 2017). Since p62 is a target of Nrf2, there exists a positive feedback loop in the p62-Keap1-Nrf2 axis. Moreover, p62 also regulates NF- κ B expression that, successively, increases Nrf2 expression (Hennig et al., 2018).

Our results demonstrated the downregulation of Nrf2 and its downstream antioxidant targets to normal levels in ICH animals that have undergone treatment with ZLHXTY capsule possessing intrinsic antioxidant activity. To explain this, we assume that an autoregulatory feedback loop mechanism in the Nrf2 pathway was activated upon antioxidant exposure where excessive Nrf2 leads to an increase in INrf2 (Keap1) gene expression that leads to ubiquitination and degradation of Nrf2 reducing its levels to normal (Lee et al., 2007).

Conclusion

To conclude, we have demonstrated that ZLHXTY capsules hold antioxidant potential through which it can improve neurological outcomes, and inhibit redox imbalance and inflammation following ICH injury as shown by its modulation of Nrf2 signaling.

Data availability statement

The raw data supporting the conclusion of this article will be made available by the authors, without undue reservation.

Ethics statement

The animal study was reviewed and approved by the Animal Ethics Research Committee of Southwest Medical University, Luzhou, China.

Author contributions

MM contributed to the conception and design of the study and wrote the manuscript. MM and GY performed the experiments, acquired and interpreted the data. WR, YL and PL wrote the sections of the manuscript. RS, HS and DZ contributed to the conception and design of study. HX and SY provided intellectual research guidance and critically revised and approved the final manuscript for

publication. All the authors contributed to the manuscript drafting, revision, read, and approved the submitted version.

Funding

This work was funded by the Science & Technology Department of Sichuan Province (Grant No. 2022ZDZX0022, 2022YFS0635, and 2022YFS0613); a Technology strategic cooperation project between Luzhou Municipal People's Government and Southwest Medical University (2019LZXNYDC02); Innovation Team and Talents Cultivation Program of National Administration of Traditional Chinese Medicine (Number: ZYYCXTD-C-202207), Innovation Team of Sichuan Provincial Administration of Traditional Chinese Medicine (Number: 2022C007).

Conflict of interest

The authors declare that the research was conducted in the absence of any commercial or financial relationships that could be construed as a potential conflict of interest.

References

- Ahmed, S. M. U., Luo, L., Namani, A., Wang, X. J., and Tang, X. (2017). Nrf2 signaling pathway: Pivotal roles in inflammation. *Biochimica Biophysica Acta (BBA) - Mol. Basis Dis.* 1863 (2), 585–597. doi:10.1016/j.bbdis.2016.11.005
- An, S. J., Kim, T. J., and Yoon, B. W. (2017). Epidemiology, risk factors, and clinical features of intracerebral hemorrhage: An update. *J. Stroke* 19 (1), 3–10. doi:10.5853/jos.2016.00864
- Chen-Roetling, J., and Regan, R. F. (2017). Targeting the nrf2-heme oxygenase-1 Axis after intracerebral hemorrhage. *Curr. Pharm. Des.* 23 (15), 2226–2237. doi:10.2174/1381612822666161027150616
- Durazzo, A., Nazhand, A., Lucarini, M., Silva, A. M., Souto, S. B., Guerra, F., et al. (2021). Astragalus (*Astragalus membranaceus* Bunge): Botanical, geographical, and historical aspects to pharmaceutical components and beneficial role. *Rendiconti Lincei Sci. Fis. Nat.* 32 (3), 625–642. doi:10.1007/s12210-021-01003-2
- Feeney, D. M., Gonzalez, A., and Law, W. A. (1982). Amphetamine, haloperidol, and experience interact to affect rate of recovery after motor cortex injury. *Science* 217 (4562), 855–857. doi:10.1126/science.7100929
- He, F., Ru, X., and Wen, T. (2020). NRF2, a transcription factor for stress response and beyond. *Int. J. Mol. Sci.* 21 (13), 4777. doi:10.3390/ijms21134777
- Hennig, P., Garstkiewicz, M., Grossi, S., Di Filippo, M., French, L. E., and Beer, H. D. (2018). The crosstalk between Nrf2 and inflammasomes. *Int. J. Mol. Sci.* 19 (2), 562. doi:10.3390/ijms19020562
- Hohl, A., Gullo, J. S., Silva, C. C. P., Bertotti, M. M., Felisberto, F., Nunes, J. C., et al. (2012). Plasma levels of oxidative stress biomarkers and hospital mortality in severe head injury: A multivariate analysis. *J. Crit. Care* 27 (5), e11–e19. doi:10.1016/j.jcrc.2011.06.007
- Hu, X., Tao, C., Gan, Q., Zheng, J., Li, H., and You, C. (2016). Oxidative stress in intracerebral hemorrhage: Sources, mechanisms, and therapeutic targets. *Oxid. Med. Cell. Longev.* 2016, 3215391. doi:10.1155/2016/3215391
- Ichimura, Y., Waguri, S., Sou, Y. S., Kageyama, S., Hasegawa, J., Ishimura, R., et al. (2013). Phosphorylation of p62 activates the Keap1-Nrf2 pathway during selective autophagy. *Mol. Cell.* 51 (5), 618–631. doi:10.1016/j.molcel.2013.08.003
- Katsuragi, Y., Ichimura, Y., and Komatsu, M. (2016). Regulation of the Keap1-Nrf2 pathway by p62/SQSTM1. *Curr. Opin. Toxicol.* 1, 54–61. doi:10.1016/j.cotox.2016.09.005
- Keep, R. F., Hua, Y., and Xi, G. (2012). Intracerebral haemorrhage: Mechanisms of injury and therapeutic targets. *Lancet Neurology* 11 (8), 720–731. doi:10.1016/S1474-4422(12)70104-7
- Kensler, T. W., Wakabayashi, N., and Biswal, S. (2006). Cell survival responses to environmental stresses via the Keap1-Nrf2-ARE pathway. *Annu. Rev. Pharmacol. Toxicol.* 47, 89–116. doi:10.1146/annurev.pharmtox.46.120604.141046
- Lam, W. C., Lyu, A., and Bian, Z. (2019). ICD-11: Impact on traditional Chinese medicine and World healthcare systems. *Pharm. Med.* 33 (5), 373–377. doi:10.1007/s40290-019-00295-y
- Lan, X., Han, X., Liu, X., and Wang, J. (2019). Inflammatory responses after intracerebral hemorrhage: From cellular function to therapeutic targets. *J. Cereb. blood flow metabolism* 39 (1), 184–186. doi:10.1177/0271678X18805675
- Lau, A., Wang, X. J., Zhao, F., Villeneuve, N. F., Wu, T., Jiang, T., et al. (2010). A noncanonical mechanism of Nrf2 activation by autophagy deficiency: Direct interaction between Keap1 and p62. *Mol. Cell. Biol.* 30 (13), 3275–3285. doi:10.1128/MCB.00248-10
- Lee, O. H., Jain, A. K., Papusha, V., and Jaiswal, A. K. (2007). An auto-regulatory loop between stress sensors INrf2 and Nrf2 controls their cellular abundance. *J. Biol. Chem.* 282 (50), 36412–36420. doi:10.1074/jbc.M706517200
- Li, P., Lin, B., Tang, P., Ye, Y., Wu, Z., Gui, S., et al. (2021). Aqueous extract of *Whitmania pigra* Whitman ameliorates ferric chloride-induced venous thrombosis in rats via antioxidation. *J. Thrombosis Thrombolysis* 52 (1), 59–68. doi:10.1007/s11239-020-02337-8
- Liang, P., Mao, L., Ma, Y., Ren, W., and Yang, S. (2021). A systematic review on Zhilong Huoxue Tongyu capsule in treating cardiovascular and cerebrovascular diseases: Pharmacological actions, molecular mechanisms and clinical outcomes. *J. Ethnopharmacol.* 277, 114234. doi:10.1016/j.jep.2021.114234
- Liddle, L. J., Ralhan, S., Ward, D. L., and Colbourne, F. (2020). Translational intracerebral hemorrhage research: Has current neuroprotection research ARRIVED at a standard for experimental design and reporting? *Transl. Stroke. Res.* 11 (6), 1203–1213. doi:10.1007/s12975-020-00824-x
- Liu, Y., Yang, S., Cai, E., Lin, L., Zeng, P., Nie, B., et al. (2020). Functions of lactate in the brain of rat with intracerebral hemorrhage evaluated with MRI/MRS and *in vitro* approaches. *CNS Neurosci. Ther.* 26 (10), 1031–1044. doi:10.1111/cns.13399
- Lorente, L., Martín, M. M., Abreu-González, P., Ramos, L., Cáceres, J. J., Argüeso, M., et al. (2019). Maintained high sustained serum malondialdehyde levels after severe brain trauma injury in non-survivor patients. *BMC Res. notes* 12 (1), 789. doi:10.1186/s13104-019-4828-5
- Lorente, L., Martín, M. M., Almeida, T., Abreu-González, P., Ramos, L., Argüeso, M., et al. (2015). Total antioxidant capacity is associated with mortality of patients with severe traumatic brain injury. *BMC Neurol.* 15 (1), 115. doi:10.1186/s12883-015-0378-1
- Ma, Q. (2013). Role of nrf2 in oxidative stress and toxicity. *Annu. Rev. Pharmacol. Toxicol.* 53, 401–426. doi:10.1146/annurev-pharmtox-011112-140320
- Mazhar, M., Yang, G., Mao, L., Liang, P., Tan, R., Wang, L., et al. (2022). Zhilong Huoxue capsules ameliorate early brain inflammatory injury induced by intracerebral hemorrhage via inhibition of canonical NF- κ B signalling pathway. *Front. Pharmacol.* 13, 850060. doi:10.3389/fphar.2022.850060
- Morimoto, M., Hashimoto, T., Tsuda, Y., Kitaoka, T., and Kyotani, S. (2019). Evaluation of oxidative stress and antioxidant capacity in healthy children. *J. Chin. Med. Assoc.* 82 (8), 651–654. doi:10.1097/JCMA.0000000000000045
- Nayak, C., Nayak, D., Raja, A., and Rao, A. (2008). Relationship between markers of lipid peroxidation, thiol oxidation and Glasgow coma scale scores of moderate head

Publisher's note

All claims expressed in this article are solely those of the authors and do not necessarily represent those of their affiliated organizations, or those of the publisher, the editors and the reviewers. Any product that may be evaluated in this article, or claim that may be made by its manufacturer, is not guaranteed or endorsed by the publisher.

Supplementary material

The Supplementary Material for this article can be found online at: <https://www.frontiersin.org/articles/10.3389/fphar.2023.1197433/full#supplementary-material>

SUPPLEMENTARY FIGURE S1

UPLC-HRMS chromatogram for ZLHXTY capsule characterization. (A) ZLHXTY capsule chromatogram in positive ion modes, m/z range 150–1500, resolution 70,000; (B) Chemical standards; L-epicatechin, calycosin-7-O- β -glucoside, coumarin, ononin, calycosin, cinnamaldehyde, formononetin, and wogonin.

injury patients in the 7 day post-traumatic period. *Neurological Res.* 30 (5), 461–464. doi:10.1179/016164107X251790

Ogawa, F., Shimizu, K., Muroi, E., Hara, T., and Sato, S. (2011). Increasing levels of serum antioxidant status, total antioxidant power, in systemic sclerosis. *Clin. Rheumatol.* 30 (7), 921–925. doi:10.1007/s10067-011-1695-4

Paolin, A., Nardin, L., Gaetani, P., Rodriguez, Y. B. R., Pansarasa, O., and Marzatico, F. (2002). Oxidative damage after severe head injury and its relationship to neurological outcome. *Neurosurgery* 51 (4), 949–954. doi:10.1097/00006123-200210000-00018

Park, G. J., Ro, Y. S., Yoon, H., Lee, S. G. W., Jung, E., Moon, S. B., et al. (2022). Serum vitamin E level and functional prognosis after traumatic brain injury with intracranial injury: A multicenter prospective study. *Front. neurology* 13, 1008717. doi:10.3389/fneur.2022.1008717

Rao, P. V., and Gan, S. H. (2014). Cinnamon: A multifaceted medicinal plant. *Evidence-Based Complementary Altern. Med.* 2014, 642942. doi:10.1155/2014/642942

Saha, S., Buttari, B., Panieri, E., Profumo, E., and Saso, L. (2020). An overview of Nrf2 signaling pathway and its role in inflammation. *Molecules* 25 (22), 5474. doi:10.3390/molecules25225474

Samuel, A. O., Huang, B.-T., Chen, Y., Guo, F.-X., Yang, D.-D., and Jin, J.-Q. (2021). Antioxidant and antibacterial insights into the leaves, leaf tea and medicinal roots from *Astragalus membranaceus* (Fisch) Bge. *Sci. Rep.* 11 (1), 19625. doi:10.1038/s41598-021-97109-6

Shang, H., Yang, D., Zhang, W., Li, T., Ren, X., Wang, X., et al. (2013). Time course of keap1-nrf2 pathway expression after experimental intracerebral haemorrhage: Correlation with brain oedema and neurological deficit. *Free Radic. Res.* 47 (5), 368–375. doi:10.3109/10715762.2013.778403

Silva-Islas, C. A., and Maldonado, P. D. (2018). Canonical and non-canonical mechanisms of Nrf2 activation. *Pharmacol. Res.* 134, 92–99. doi:10.1016/j.phrs.2018.06.013

World Health Organization (2019). WHO global report on traditional and complementary medicine. Available at: <https://www.who.int/traditionalcomplementaryintegrativemedicine/WhoGlobalReportOnTraditionalAndComplementaryMedicine2019>.

Xiong, X.-Y., Wang, J., Qian, Z.-M., and Yang, Q.-W. (2014). Iron and intracerebral hemorrhage: From mechanism to translation. *Transl. stroke Res.* 5 (4), 429–441. doi:10.1007/s12975-013-0317-7

Xu, T., Liu, X., Wang, S., Kong, H., Yu, X., Liu, C., et al. (2022). Effect of *Pheretima aspergillum* on reducing fibrosis: A systematic review and meta-analysis. *Front. Pharmacol.* 13, 1039553. doi:10.3389/fphar.2022.1039553

Yang, C. H., Li, R. X., and Chuang, L. Y. (2012). Antioxidant activity of various parts of *Cinnamomum cassia* extracted with different extraction methods. *Mol. (Basel, Switz.* 17 (6), 7294–7304. doi:10.3390/molecules17067294

Yao, Z., Bai, Q., and Wang, G. (2021). Mechanisms of oxidative stress and therapeutic targets following intracerebral hemorrhage. *Oxidative Med. Cell. Longev.* 2021, 8815441. doi:10.1155/2021/8815441

Zhang, W., Sun, C., Zhou, S., Zhao, W., Wang, L., Sheng, L., et al. (2021). Recent advances in chemistry and bioactivity of *Sargentodoxa cuneata*. *J. Ethnopharmacol.* 270, 113840. doi:10.1016/j.jep.2021.113840

Zhao, J., Kobori, N., Aronowski, J., and Dash, P. K. (2006). Sulforaphane reduces infarct volume following focal cerebral ischemia in rodents. *Neurosci. Lett.* 393, 108–112. doi:10.1016/j.neulet.2005.09.065

Zhao, X., and Aronowski, J. (2013). Nrf2 to pre-condition the brain against injury caused by products of hemolysis after ICH. *Transl. stroke Res.* 4 (1), 71–75. doi:10.1007/s12975-012-0245-y

Zhao, X., Sun, G., Ting, S. M., Song, S., Zhang, J., Edwards, N. J., et al. (2015). Cleaning up after ICH: The role of Nrf2 in modulating microglia function and hematoma clearance. *J. Neurochem.* 133 (1), 144–152. doi:10.1111/jnc.12974

Zhao, X., Sun, G., Zhang, J., Strong, R., Dash, P. K., Kan, Y. W., et al. (2007). Transcription factor Nrf2 protects the brain from damage produced by intracerebral hemorrhage. *Stroke* 38 (12), 3280–3286. doi:10.1161/STROKEAHA.107.486506

Zhao, X., Tan, X., Shi, H., and Xia, D. (2021). Nutrition and traditional Chinese medicine (TCM): A system's theoretical perspective. *Eur. J. Clin. Nutr.* 75 (2), 267–273. doi:10.1038/s41430-020-00737-w

Zhou, Y., Wang, Y., Wang, J., Anne Stetler, R., and Yang, Q. W. (2014). Inflammation in intracerebral hemorrhage: From mechanisms to clinical translation. *Prog. Neurobiol.* 115, 25–44. doi:10.1016/j.pneurobio.2013.11.003



OPEN ACCESS

EDITED BY

Chika Ifeanyi Chukwuma,
Central University of Technology, South
Africa

REVIEWED BY

Jude Akinyelu,
Federal University Oye-Ekiti, Nigeria
Londiwe Mbatha,
Durban University of Technology, South
Africa

*CORRESPONDENCE

Ayman M. Mahmoud,
✉ ayman.mahmoud@science.bsu.edu.eg,
✉ a.mahmoud@mmu.ac.uk

RECEIVED 12 April 2023

ACCEPTED 01 June 2023

PUBLISHED 16 June 2023

CITATION

Alruhaimi RS, Mostafa-Hedeab G,
Abduh MS, Bin-Amman A,
Hassanein EHM, Kamel EM and
Mahmoud AM (2023), A flavonoid-rich
fraction of *Euphorbia peplus* attenuates
hyperglycemia, insulin resistance, and
oxidative stress in a type 2 diabetes
rat model.
Front. Pharmacol. 14:1204641.
doi: 10.3389/fphar.2023.1204641

COPYRIGHT

© 2023 Alruhaimi, Mostafa-Hedeab,
Abduh, Bin-Amman, Hassanein, Kamel
and Mahmoud. This is an open-access
article distributed under the terms of the
[Creative Commons Attribution License](https://creativecommons.org/licenses/by/4.0/)
(CC BY). The use, distribution or
reproduction in other forums is
permitted, provided the original author(s)
and the copyright owner(s) are credited
and that the original publication in this
journal is cited, in accordance with
accepted academic practice. No use,
distribution or reproduction is permitted
which does not comply with these terms.

A flavonoid-rich fraction of *Euphorbia peplus* attenuates hyperglycemia, insulin resistance, and oxidative stress in a type 2 diabetes rat model

Reem S. Alruhaimi¹, Gomaa Mostafa-Hedeab^{2,3},
Maisa Siddiq Abduh^{4,5}, Albandari Bin-Amman⁶,
Emad H. M. Hassanein⁷, Emadeldin M. Kamel⁸ and
Ayman M. Mahmoud^{9,10*}

¹Department of Biology, College of Science, Princess Nourah Bint Abdulrahman University, Riyadh, Saudi Arabia, ²Pharmacology Department, Medical College, Jouf University, Sakaka, Saudi Arabia, ³Pharmacology Department, Faculty of Medicine, Beni-Suef University, Beni-Suef, Egypt, ⁴Immune Responses in Different Diseases Research Group, Department of Medical Laboratory Sciences, Faculty of Applied Medical Sciences, King Abdulaziz University, Jeddah, Saudi Arabia, ⁵Center of Excellence in Genomic Medicine Research, King Abdulaziz University, Jeddah, Saudi Arabia, ⁶Department of Clinical Nutrition, College of Applied Medical Sciences, University of Hail, Hail, Saudi Arabia, ⁷Department of Pharmacology and Toxicology, Faculty of Pharmacy, Al-Azhar University, Assiut, Egypt, ⁸Chemistry Department, Faculty of Science, Beni-Suef University, Beni-Suef, Egypt, ⁹Department of Life Sciences, Faculty of Science and Engineering, Manchester Metropolitan University, Manchester, United Kingdom, ¹⁰Physiology Division, Zoology Department, Faculty of Science, Beni-Suef University, Beni-Suef, Egypt

Background: Type 2 diabetes (T2D) is a metabolic disorder characterized by insulin resistance (IR) and hyperglycemia. Plants are valuable sources of therapeutic agents for the management of T2D. *Euphorbia peplus* has been widely used as a traditional medicine for the treatment of various diseases, but its beneficial role in T2D has not been fully explored.

Methods: The anti-diabetic efficacy of *E. peplus* extract (EPE) was studied using rats with T2D induced by high-fat diet (HFD) and streptozotocin (STZ). The diabetic rats received 100, 200, and 400 mg/kg EPE for 4 weeks.

Results: Phytochemical fractionation of the aerial parts of *E. peplus* led to the isolation of seven known flavonoids. Rats with T2D exhibited IR, impaired glucose tolerance, decreased liver hexokinase and glycogen, and upregulated glycogen phosphorylase, glucose-6-phosphatase (G-6-Pase), and fructose-1,6-bisphosphatase (F-1,6-BPase). Treatment with 100, 200, and 400 mg/kg EPE for 4 weeks ameliorated hyperglycemia, IR, liver glycogen, and the activities of carbohydrate-metabolizing enzymes. EPE attenuated dyslipidemia, serum transaminases, tumor necrosis factor (TNF)- α , interleukin (IL)-1 β and liver lipid accumulation, nuclear factor (NF)- κ B p65, and lipid peroxidation, nitric oxide and enhanced antioxidants. All EPE doses upregulated serum adiponectin and liver peroxisome proliferator-activated receptor γ (PPAR γ) in HFD/STZ-induced rats. The isolated flavonoids showed *in silico* binding affinity toward hexokinase, NF- κ B, and PPAR γ .

Conclusion: *E. peplus* is rich in flavonoids, and its extract ameliorated IR, hyperglycemia, dyslipidemia, inflammation and redox imbalance, and upregulated adiponectin and PPAR γ in rats with T2D.

KEYWORDS

Euphorbia, diabetes, insulin resistance, oxidative stress, inflammation

1 Introduction

Diabetes mellitus (DM) is a common metabolic disorder associated with several complications, including nephropathy, neuropathy, and cardiomyopathy. This disorder includes type 1 (T1DM) and type 2 (T2DM) forms of the disease where T1DM is characterized by insulin insufficiency, whereas insulin resistance (IR) is the characteristic feature of T2DM. Both insulin deficiency and IR lead to the accumulation of glucose in the blood (hyperglycemia) (American Diabetes Association, 2021). DM is a fast-increasing disease worldwide, and the number of patients with diabetes is expected to reach 700 million by 2045 (Saeedi et al., 2019). T2DM is the most common form of the disease characterized by hyperglycemia and IR (Kahn et al., 2014). IR increases the risk of hypertension, dyslipidemia, and atherosclerosis (Guzik and Cosentino, 2018). Oxidative stress (OS) and inflammation mediated by excess reactive oxygen species (ROS) and inflammatory mediators produced under hyperglycemic conditions are implicated in the pathophysiology of DM and its complications (Mahmoud et al., 2012). Excess ROS can damage cellular macromolecules and work in concert with inflammatory mediators to provoke cell death. ROS and inflammatory mediators impair insulin signaling by provoking β -cell death, alter peripheral glucose uptake, and increase gluconeogenesis (Jheng et al., 2012). Therefore, mitigation of OS and inflammation could be beneficial to prevent IR and hyperglycemia in T2DM.

Plants of the genus *Euphorbia* include numerous known species with chemical diversity and multiple biological and commercial uses (Shi et al., 2008). The latex of plants of the family *Euphorbiaceae* was acknowledged for its various phytoconstituents that possess both commercial and pharmacological importance such as triterpene alcohols (Giner and Schroeder, 2015). Because of its toxic nature and unpleasantness, the latex protects the plants against the attack of animals (Al-Sultan and Hussein, 2006). Steroids, flavonoids, sesquiterpenoids, glycerols, and cerebrosides are among the phytoconstituents reported in plants of the genus *Euphorbia* (Shi et al., 2008; Kamel et al., 2022). With this rich content, *Euphorbia* plants found their way to be employed in folkloric medicine to treat migraine, intestinal parasites, gonorrhea, and skin disorders (Singla and Kamla, 1990), and studies have reported their wound-healing potential (Pattanaik et al., 2014; Ahmed et al., 2016). Recent work from our laboratory revealed the inhibitory activity of *E. peplus* on xanthine oxidase (XO) and hyperuricemia in rats (Kamel et al., 2022). Other studies showed the possible beneficial effects of *E. royleana* stem extract (Zafar et al., 2021) and *E. hirta* flower extract (Kumar et al., 2010) in rats with streptozotocin (STZ)- and alloxan-induced diabetes, respectively. These studies revealed the ability of *E. royleana* and *E. hirta* to ameliorate hyperglycemia and oxidative damage. Another recent study highlighted the anti-hyperglycemic effect of *E. helioscopia* methanolic extract in sucrose-supplemented rats (Mustafa et al., 2022). Owing to the promising therapeutic value of plants of this genus, this study explored the phytochemical constituents and the effect of *E. peplus* extract (EPE) on hyperglycemia, IR, OS, and inflammation in rats with T2D induced by high-fat diet (HFD) and STZ.

2 Materials and methods

2.1 Phytochemical investigation

2.1.1 General

Proton nuclear magnetic resonance (^1H NMR) and ^{13}C NMR (500 MHz and 125 MHz, respectively) spectra were recorded on the Bruker AV-500 spectrometer using TMS as an internal standard. The optical rotation of isolated flavonoids was obtained using a Rudolph Autopol III polarimeter. Ultraviolet (UV) spectral data were measured using the Shimadzu UV-vis 160i spectrophotometer, and the HREIMS and EIMS spectral data were recorded using the Finnigan MAT TSQ 700 mass spectrometer. Infrared spectral data were obtained through KBr pellets on the Shimadzu FTIR-8400 instrument.

2.1.2 Plant collection, extraction, and isolation

The plant was collected from Beni Suef Governorate in March 2021 and identified by a taxonomist and a voucher specimen (EP-038021-2) was stored. The aerial parts (2.75 kg) were extracted four times using 70% acetone followed by the removal of the solvent under reduced pressure, resulting in 904 g of extract. Thereafter, the extract was dissolved in water and successively partitioned using chloroform, ethyl acetate (EA), and *n*-butanol (3L x 2, each). The EA fraction (69.7 g) was subjected to chromatographic fractionation over a silica gel column (120 × 4 cm, 1.1 kg) and eluted with dichloromethane (DCM)/acetone mixture of increasing polarity. To track the movement of the bands along the column and to regulate the collection of fractions, a UV lamp was employed. A total of 22 fractions were collected and combined into seven main subfractions (F1–F7) according to their similar thin-layer chromatography (TLC) profiles. Subfraction F3 was chromatographed over silica gel using chloroform–EA of gradient elution to afford nine subfractions (F3.1–F3.9). Subfractions F3.3–F3.7 were combined and applied to the Sephadex LH-20 column eluted with methanol (MeOH):water (50:50→100:0) to give seven TLC-monitored subfractions (E1–E7). Subfractions (E2–E5) were combined and purified over a Sephadex LH-20 column eluted with MeOH to yield the purified compounds 2 (22 mg), 3 (17 mg), and 4 (14 mg). Subfraction F4 was fractionated over a polyamide 6S column eluted with the MeOH–water solvent mixture of increasing polarity to afford eleven subfractions (F4.1–F4.11). Subfraction F4.6 was purified over the Sephadex LH-20 column eluted with MeOH to yield purified compound 1 (23 mg). Subfractions F4.8–F4.10 were combined and re-chromatographed using the Sephadex LH-20 column eluted with MeOH to give compound 5 (19 mg). Subfraction F5 was partitioned by means of the Sephadex LH-20 column using MeOH–water (2:8, 3:7→10:0) to afford six subfractions (F5.1–F5.6). Compound 6 (23 mg) was obtained from the chromatographic fractionation of F5.3–F5.5 over two consecutive Sephadex LH-20 columns using 30% MeOH as an eluent. Subfraction F7 was subjected to silica gel column chromatography eluted with the solvent system chloroform–MeOH–water (lower layer, 28:9:6 and 6:3:1) to yield

five subfractions (F7.1–F7.5). Compound 7 (24 mg) was obtained from the recombination and purification of subfractions F7.1–F7.3 over Sephadex LH-20 and eluted with MeOH (Supplementary Figure S1).

2.2 *In vitro* radical-scavenging activity

The RSA activity of EPE was measured using 2,2-diphenyl-1-picrylhydrazyl (DPPH) and 2,2-azinobis (3-ethylbenzothiazoline-6-sulfonic acid) (ABTS) assays following the methods of Brand-Williams et al. (1995) and Re et al. (1999), respectively, using ascorbic acid as a standard.

2.3 Experimental animals and treatments

Male Wistar rats weighing 170–190 g were included in this investigation. The rats were maintained under standard conditions of temperature ($23^{\circ}\text{C} \pm 1^{\circ}\text{C}$) and humidity (50%–60%) on a 12-h light/dark cycle with free access to food and water. The animal study protocol was approved by the Research Ethics Committee of Al-Azhar University (ZA-AS/PH/18/C/2023). The rats received a normal diet and a single intraperitoneal (i.p.) injection of freshly prepared citrate buffer (pH 4.5) to serve as a control. Other rats were fed a HFD (58% fat, 17% carbohydrate, and 25% protein) for 28 days and received a single i.p. dose of STZ (35 mg/kg; Sigma, United States) dissolved in freshly prepared citrate buffer (pH 4.5) to induce T2D (Germoush et al., 2019). After 7 days, T2D was confirmed by measuring blood glucose (BG) for 2 h after supplementing the overnight fasted rats with 3 g/kg glucose orally. The rats exhibited BG higher than 250 mg/kg were included in the investigation.

To investigate the antidiabetic effects of the EA fraction of *E. peplus* extract (EPE; dissolved in 0.5% carboxymethyl cellulose (CMC) as a vehicle), 30 diabetic and 12 normal rats were allocated into seven groups ($n = 6$) as follows:

Group I (control): received 0.5% CMC.

Group II (EPE): received 400 mg/kg EPE.

Group III (diabetic): received 0.5% CMC.

Group IV (diabetic + 100 mg/kg EPE): received 100 mg/kg EPE.

Group V (diabetic + 200 mg/kg EPE): received 200 mg/kg EPE.

Group VI (diabetic + 400 mg/kg EPE): received 400 mg/kg EPE.

Group VII (diabetic + PIO): received 10 mg/kg of the antidiabetic pioglitazone (PIO) (Abd El-Twab et al., 2016).

EPE, 0.5% CMC, and PIO were supplemented orally for 4 weeks. A day before the end of the experiment, the rats were fasted overnight and then supplemented with 3 g/kg glucose solution, and the blood was collected from the tail vein over 2 h for the determination of BG using a Spinreact (Spain) kit (Trinder, 1969). At the end of treatments, the animals were euthanized under ketamine anesthesia (100 mg/kg i.p.), and blood and liver samples were collected. Serum was separated following centrifugation of blood, and samples from the liver were homogenized in Tris-HCl buffer (pH = 7.4). Other samples

were fixed in 10% neutral buffered formalin (NBF) or stored at -80°C .

2.4 Biochemical assays

Serum insulin, transaminases (ALT and AST), adiponectin and cytokines (TNF- α and IL-1 β) were determined using kits from RayBiotech (United States), Spinreact (Spain), and R&D Systems (United States), respectively. NF- κB p65 in liver homogenate was determined using the kit from R&D Systems (United States). All assays were performed according to the manufacturers' instructions.

The homeostasis model assessment of IR (HOMA-IR) was calculated as previously described by Haffner (2000) using the following equation:

$$\text{HOMA-IR} = \frac{\text{Fasting insulin } \left(\frac{\mu\text{U}}{\text{ml}}\right) \times \text{Fasting glucose } \left(\frac{\text{mmol}}{\text{L}}\right)}{22.5}$$

Liver glycogen content was determined as previously described (Seifter and Dayton, 1950). Liver homogenate was centrifuged, and the clear supernatant was used to assess the activities of hexokinase (Brandstrup et al., 1957), G-6-Pase (Koide and Oda, 1959), F-1,6-BPase (Freedland and Harper, 1959), and glycogen phosphorylase (Stalmans and Hers, 1975). Malondialdehyde (MDA) (Ohkawa et al., 1979), nitric oxide (NO) (Green et al., 1982), reduced glutathione (GSH) (Beutler et al., 1963), and the activities of superoxide dismutase (SOD) (Marklund and Marklund, 1974), catalase (CAT) (Aebi, 1984), and glutathione peroxidase (GPx) (Flohé and Günzler, 1984) were determined in the supernatant of the homogenized liver. Liver triglycerides (TGs) and cholesterol were assayed using Spinreact (Spain) kits after extracting the lipids using chloroform/MeOH mixture (2:1, v/v) as described by Folch et al. (1957). Serum TG, total cholesterol (TC), and high-density lipoprotein (HDL)-C were assayed using kits from Spinreact (Spain). Low-density lipoprotein (LDL)-C, very low-density lipoprotein (vLDL)-C, and atherogenic index of plasma (AIP) were calculated according to the following equations:

$$\text{vLDL-C} = \text{TG}/5,$$

$$\text{LDL-C} = \text{TC} - (\text{HDL-C} + \text{vLDL-C}),$$

$$\text{AIP} = \log \left(\frac{\text{TG}}{\text{HDL}} \right).$$

2.5 Histopathological study

Samples from the liver fixed in 10% NBF for 24 h were dehydrated, cleared, and embedded in paraffin wax. Sections of 5 μm thickness were cut for routine staining with hematoxylin and eosin (H&E) (Bancroft and Gamble, 2008) and examined under a light microscope.

2.6 Quantitative real-time polymerase chain reaction

To determine the changes in PPAR γ mRNA, RNA was isolated from the frozen liver using TRIzol and quantified, and samples with

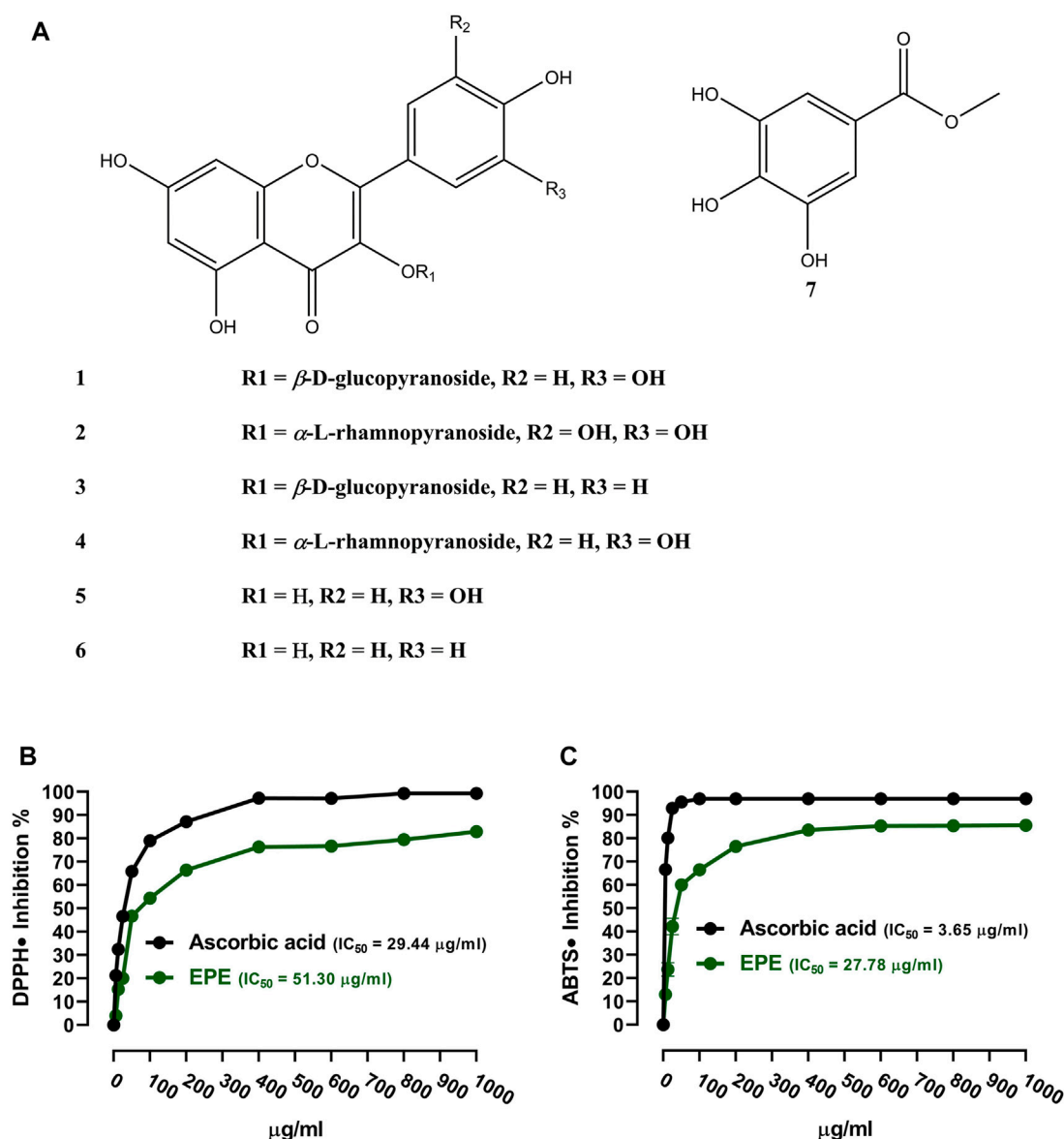


FIGURE 1

(A) Chemical structure of the isolated compounds. (B, C) DPPH and ABTS radical-scavenging activities of EPE. Data are mean \pm SD (N = 3).

OD_{260/280} \geq 1.8 were reverse-transcribed into cDNA using a cDNA synthesis kit (Thermo Scientific, United States). cDNA amplification was carried out using SYBR Green Master Mix (Thermo Scientific, United States), and the primers used in the qRT-PCR experiment are listed in [Supplementary Table S1](#). The Ct values were analyzed by using the $2^{-\Delta\Delta C_t}$ method (Livak and Schmittgen, 2001).

2.7 *In silico* molecular docking

The binding of *E. peplus* compounds with hexokinase II (PDB ID: 2NZT), NF- κ B-DNA complex (PDB ID 1LE9), and PPAR γ (PDB ID: 2PRG) was investigated as previously reported (Supplementary Material) (Sami et al., 2022; Abduh et al., 2023).

2.8 Statistical analysis

The obtained results are presented as mean \pm standard deviation (SD), and all statistical comparisons were made using one-way ANOVA followed by *post hoc* Tukey's test on GraphPad Prism 8 software. *p*-values < 0.05 were considered statistically significant.

3 Results

3.1 Phytochemical investigation and *in vitro* RSA

The analysis of the EA fraction of *E. peplus* led to the isolation of seven known flavonoids. Structures of isolated

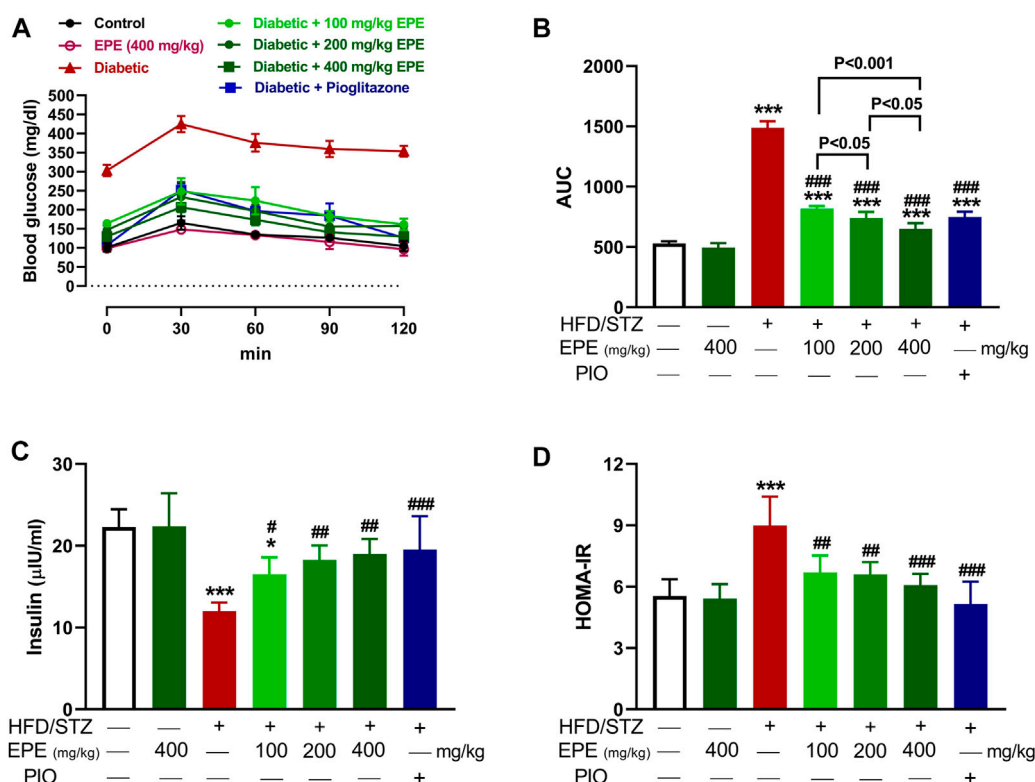


FIGURE 2

EPE ameliorated glucose intolerance (A and B), serum insulin (C), and HOMA-IR (D) in diabetic rats. Data are mean \pm SD ($n = 6$). * $p < 0.05$ and *** $p < 0.001$ vs. control. # $p < 0.05$, ## $p < 0.01$, and ### $p < 0.001$ vs. diabetic.

compounds (1-7) were elucidated based on spectroscopic data (Supplementary Figures S2–15) and by comparison with those previously reported. The isolated flavonoids (Figure 1A) were identified as isoquercetin (1) (Han et al., 2004), myricitrin (2) (Fu et al., 2013), astragalin (3) (Wei et al., 2011), quercitrin (4) (Tatsis et al., 2007), quercetin (5) (Mabry et al., 1970), kaempferol (6) (Mabry et al., 1970; Elsayed et al., 2020), and methyl gallate (7) (Ma et al., 2005). The *in vitro* RSA showed a concentration-dependent antioxidant activity of EPE against DPPH (Figure 1C) and ABTS (Figure 1D) radicals with IC_{50} values of 51.30 and 27.78 μ g/ml, respectively.

3.2 EPE ameliorates glucose intolerance and IR in diabetic rats

OGTT was performed, and insulin was measured to determine the anti-hyperglycemic effect of EPE. The HFD/STZ-induced diabetic rats exhibited significant elevation in BG (Figure 2A, B). Treatment with EPE and PIO effectively ameliorated BG levels in diabetic rats ($p < 0.001$). Insulin was declined in diabetic rats ($p < 0.001$; Figure 2C), and the value of HOMA-IR was elevated (Figure 2D). All doses of EPE effectively alleviated insulin and HOMA-IR ($p < 0.001$). EPE didn't alter glucose and insulin in normal animals.

3.3 EPE modulates carbohydrate-metabolizing enzymes in diabetic rats

The activity of hexokinase (Figure 3A) was decreased, and G-6-Pase (Figure 3B), F-1,6-BPase (Figure 3C), and glycogen phosphorylase (Figure 3D) were activated in the diabetic rat liver ($p < 0.001$). Liver glycogen was decreased in diabetic rats as compared to the non-diabetic animals ($p < 0.001$; Figure 3E). EPE remarkably increased hexokinase and glycogen and suppressed other enzymes in diabetic rats.

MD simulations showed the binding affinity of EPE flavonoids with hexokinase as shown in Table 1 and Figure 4 and Supplementary Figure S16. Compounds 3, 4, 5, and 6 exhibited the lowest binding energy (−7.4, −7.3, −8.1, and −7.8 kcal/mol, respectively) and formed multiple polar bonding and hydrophobic interactions with different amino acid residues (Table 1).

3.4 EPE ameliorates dyslipidemia and liver lipid accumulation in diabetic rats

TG, TC, LDL-C, and vLDL-C were increased in the serum of diabetic rats ($p < 0.001$) as shown in Figures 5A–D. HDL-C was decreased ($p < 0.01$; Figure 5E), and AIP was elevated ($p < 0.001$;

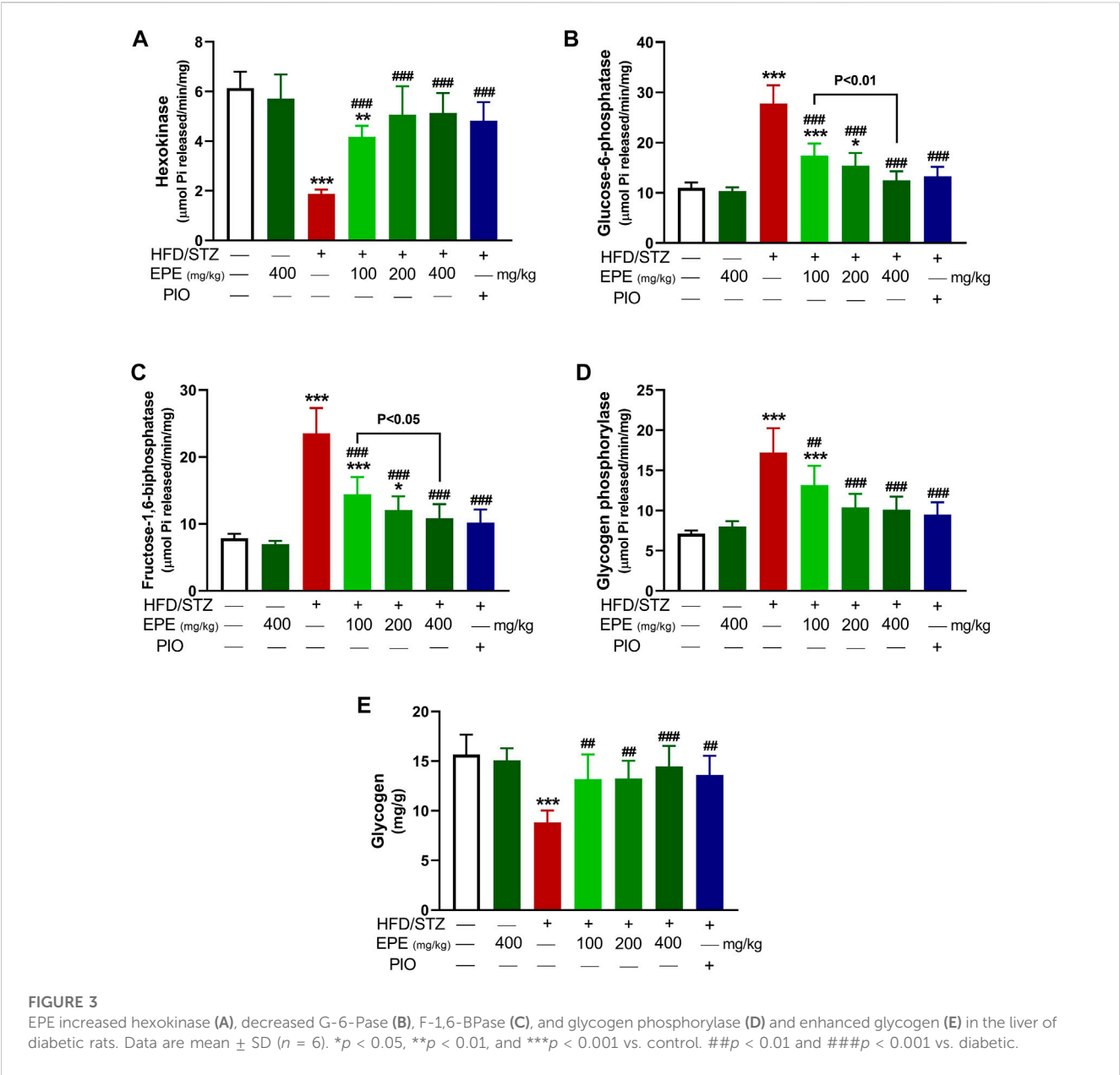


TABLE 1 Binding affinities, interacting polar residues, and hydrophobic interactions of the compounds isolated from *E. peplus* with hexokinase.

Compound	Binding energy (kcal/mol)	Polar bond	Hydrophobic interaction
1	-6.9	Gly535, Thr536, Gly747, Glu783, Thr784, and Thr863	Thr680, Met748, and Gly780
2	-7.0	Leu617 and Gln739	Ala505, Ser506, Ala507, Pro508, Lys510, Pro605, Lys618, Glu708, Ala711, Asp714, Asn715, and Lys738
3	-7.4	Asp532, Asp657, Glu864, and Ser897	Arg539, Ile677, Asp861, Thr863, Lys866, Asp895, and Gly896
4	-7.3	Glu877, Cys886, Val888, and Ser886	Lys873, His876, Lys880, and Asp887
5	-8.1	Asp657, Thr680, Thr863, and Ser897	Asp532, Thr536, Arg539, Ile677, Gly679, Asp861, Asp895, and Gly896
6	-7.8	Asp657, Thr680, Thr863, and Ser897	Asp532, Thr536, Arg539, Ile677, Gly679, Asp861, Asp895, and Gly896
7	-6.1	Asp532, Thr661, and Ser897	Gly535, Thr536, Ile677, Gly679, Thr680, Asp861, Gly862, and Thr863

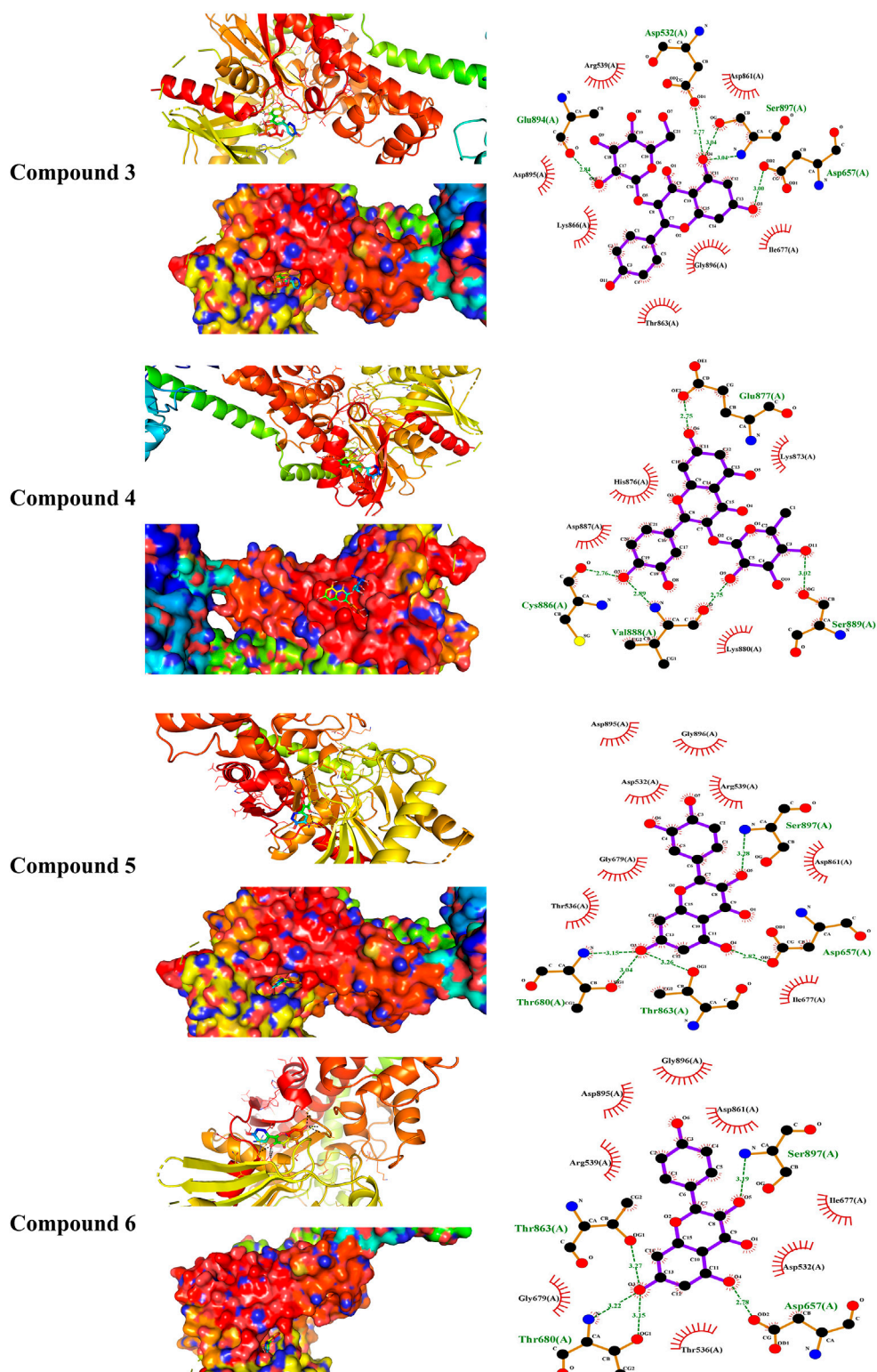


FIGURE 4

Molecular docking showing the binding modes of compounds 3, 4, 5, and 6 with hexokinase.

Figure 5F) in diabetic animals. All doses of EPE decreased serum lipids and AIP and increased HDL-C in diabetic rats. Dyslipidemia was associated with increased liver TG

(Figure 6A) and cholesterol (Figure 6B). Likewise, the stained sections of the liver of diabetic rats revealed the deposition of lipids (Figure 6C) along with increased circulating transaminases

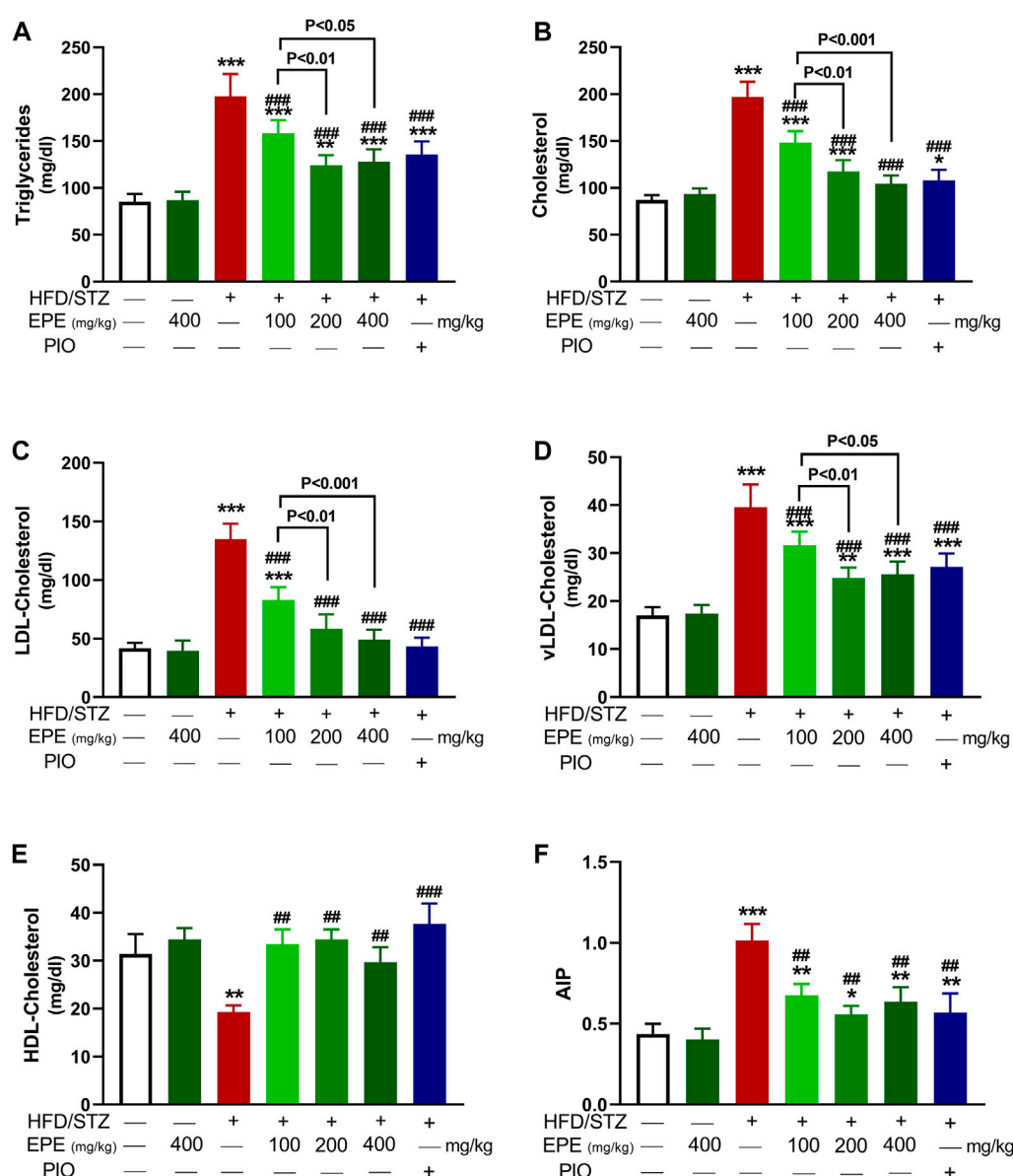


FIGURE 5

EPE decreased serum TG (A), TC (B), LDL-C (C), vLDL-C (D), and AIP (F) and increased HDL-C (E) in diabetic rats. Data are mean \pm SD ($n = 6$). * $p < 0.05$, ** $p < 0.01$, and *** $p < 0.001$ vs. control. ## $p < 0.01$ and ### $p < 0.001$ vs. diabetic.

(Figures 6D,E; $p < 0.001$). All doses of EPE decreased liver lipids and serum transaminases in diabetic rats.

3.5 EPE mitigates oxidative stress in diabetic rats

MDA and NO were elevated in HFD/STZ-induced rats ($p < 0.001$) as compared to the control rats (Figures 7A,B). In contrast, GSH (Figure 7C), SOD (Figure 7D), CAT (Figure 7E), and GPx (Figure 7F) were decreased in diabetic animals. EPE decreased MDA and NO and increased antioxidants effectively in diabetic rats while showing no effect on normal animals.

3.6 EPE attenuates inflammation in diabetic rats

Liver NF- κ B p65 and serum TNF- α and IL-1 β were upregulated in diabetic rats as depicted in Figures 8A–C. Treatment with EPE noticeably decreased the assayed inflammatory markers in rats with diabetes. The binding affinity of the isolated flavonoids toward NF- κ B was investigated with MD (Table 2; Figure 9 and Supplementary Figure S17). All compounds showed binding affinity marked by the polar bonding and hydrophobic interactions, and compounds 2, 3, 4, and 5 showed the lowest binding energy (−9.5, −10.6, −9.8, and −9.6 kcal/mol, respectively).

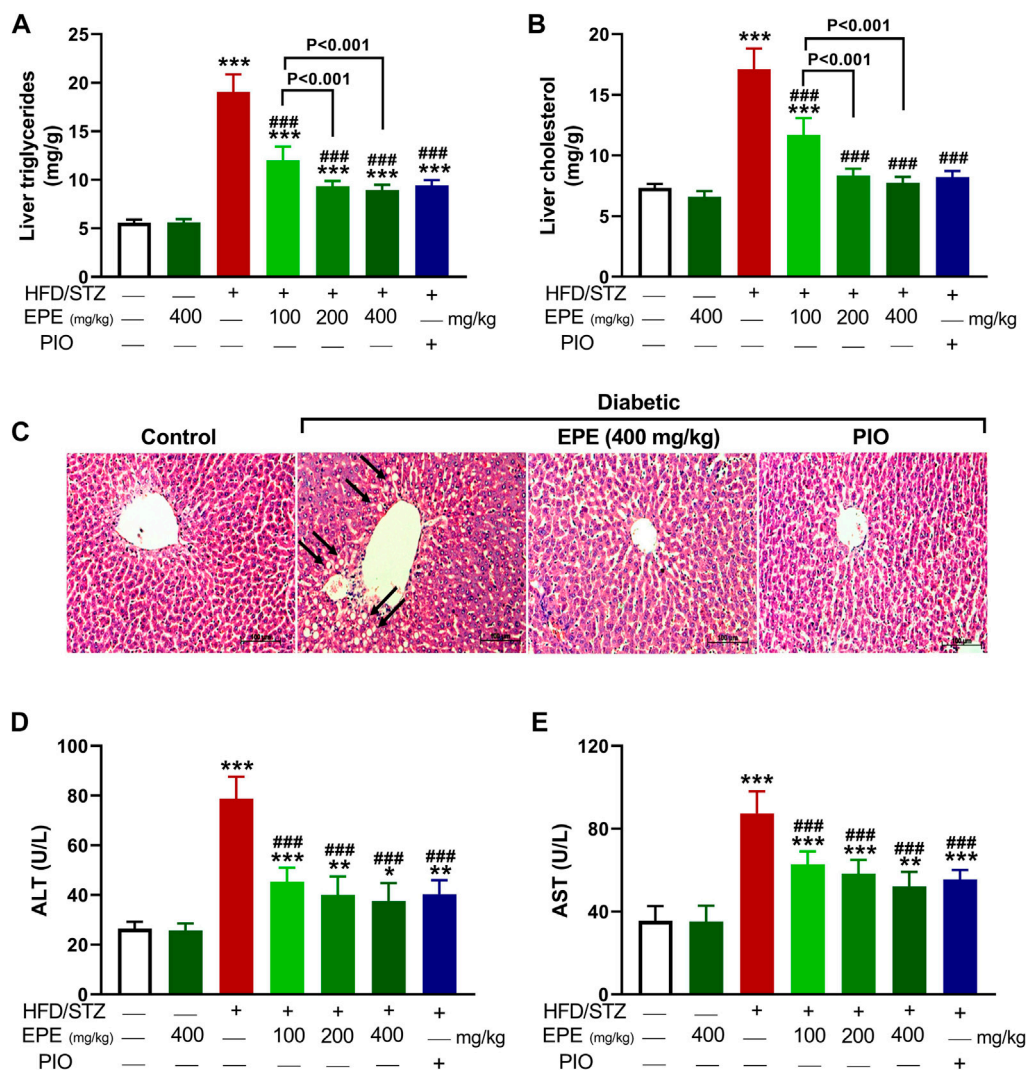


FIGURE 6

EPE decreased liver TG (A) and cholesterol (B), prevented lipid deposition (C), and ameliorated serum ALT (D) and AST (E) in diabetic rats. Data are mean \pm SD ($n = 6$). * $p < 0.05$, ** $p < 0.01$, and *** $p < 0.001$ vs. control. ### $p < 0.001$ vs. diabetic.

3.7 EPE upregulates adiponectin and PPAR γ in diabetic rats

Circulating adiponectin was declined in rats with diabetes, and all EPE doses effectively restored its levels (Figure 10A). The effect of EPE on PPAR γ and the binding affinity of the isolated flavonoids were determined using qRT-PCR and MD, respectively. As shown in Figure 10B, diabetic rats exhibited significant downregulation of liver PPAR γ , an effect that was reversed following treatment with all doses of EPE and the PPAR γ agonist PIO. MD revealed the affinity of *E. peplus* flavonoids toward PPAR γ , and compounds 3, 4, and 5 exhibited the lowest binding energy (−8.7, −8.0, and −8.0 kcal/mol, respectively) (Table 3; Figure 10C and Supplementary Figure S18I).

4 Discussion

Plants of the genus *Euphorbia* showed a very promising anti-diabetic effect in STZ-, alloxan-, and sucrose-induced DM in rats (Kumar et al., 2010; Zafar et al., 2021; Mustafa et al., 2022), and the LD₅₀ of most *Euphorbia* species was estimated to exceed 5,000 mg/kg (Abd-Elhakim et al., 2019). Herein, we explored the ameliorative effect of the flavonoid-rich fraction of *E. peplus* on hyperglycemia, IR, OS, and inflammation in HFD/STZ-induced T2D rats. The *in vitro* assays showed that EPE scavenged DPPH radicals in a concentration-dependent manner. Previous studies showed the DPPH radical-scavenging efficacy of plants of the genus *Euphorbia* such as *E. royleana* (Zafar et al., 2021). The DPPH assay data were supported by the ability of EPE to scavenge ABTS radicals, demonstrating its powerful RSA.

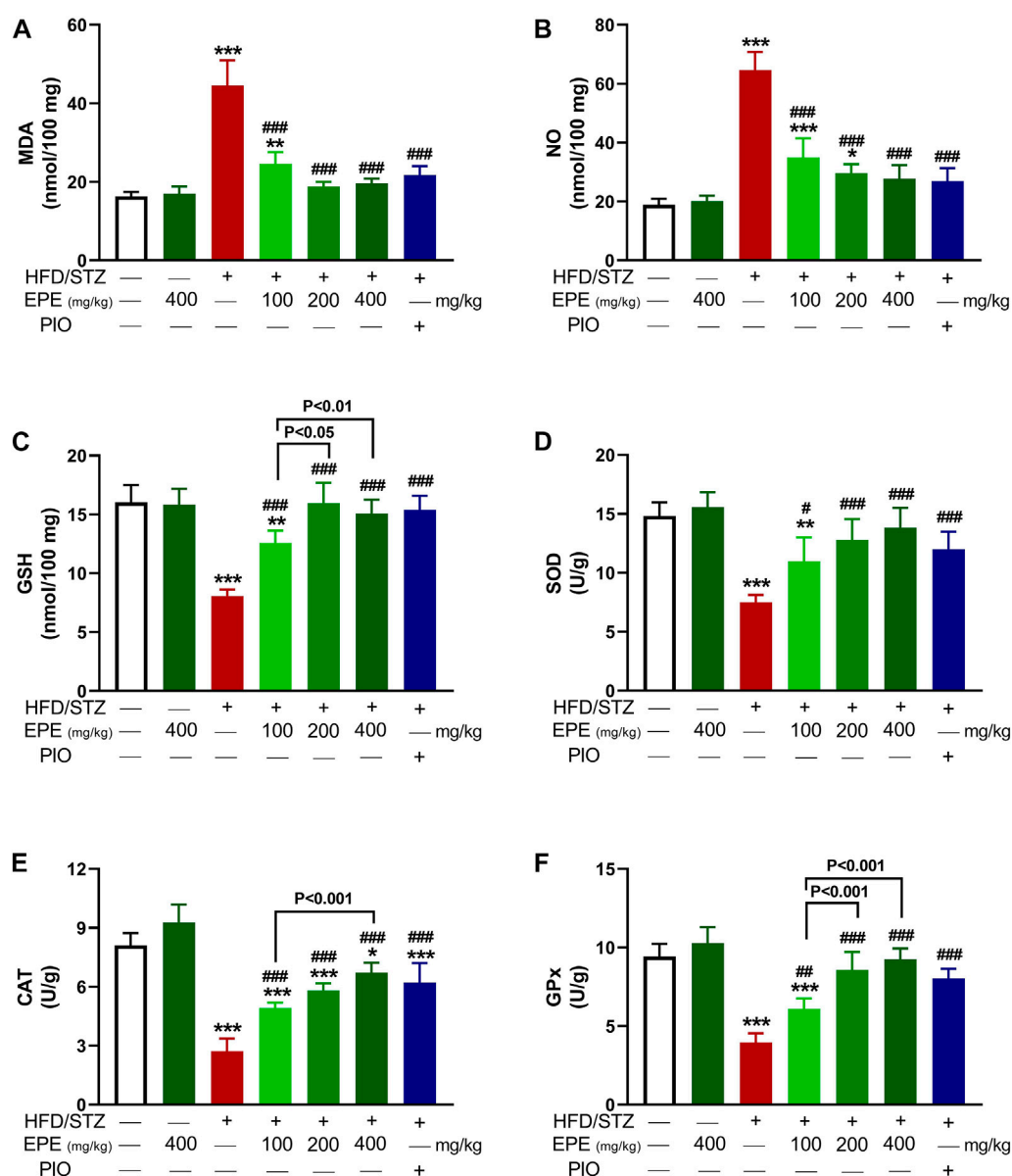


FIGURE 7

EPE decreased liver MDA (A) and NO (B) and increased GSH (C), SOD (D), CAT (E), and GPx (F) in diabetic rats. Data are mean \pm SD ($n = 6$). * $p < 0.05$, ** $p < 0.01$, and *** $p < 0.001$ vs. control. # $p < 0.05$, ## $p < 0.01$, and ### $p < 0.001$ vs. diabetic.

ABTS assay is more reliable and accurate for the evaluation of RSA of phytoconstituents than DPPH (Floegel et al., 2011). The RSA of EPE could be directly related to the rich content of flavonoids that possess potent scavenging properties against free radicals (Kamel et al., 2016; Elsayed et al., 2020).

The effect of EPE on glucose intolerance and IR was investigated *in vivo* in rats with HFD/STZ-induced diabetes. HFD and STZ were employed to induce T2D as this model showed similarities to the disease in humans. Feeding a HFD results in IR, and STZ decreases insulin release by damaging β -cells (Breyer et al., 2005; Lee et al., 2011), leading to hyperglycemia. Together with IR, hyperglycemia is a characteristic feature of T2D and should be managed to prevent complications in different

organs (Jellinger, 2007). Here, HFD/STZ-challenged animals showed hyperglycemia marked by glucose intolerance and IR. The developed T2D was consistent with our previous investigations, showing IR and hyperglycemia in HFD/STZ-induced rats (Mahmoud et al., 2012; Germoush et al., 2019; Elsayed et al., 2020; Abduh et al., 2023). The chronic hyperglycemia in this model was supported by the values of HbA1c%, a reliable marker for both diagnosis and prognosis of DM (American Diabetes Association, 2014) reported in our recent work (Abduh et al., 2023). Hyperglycemia was associated with hypoinsulinemia, and the development of IR as the value of HOMA-IR was revealed. Similar to these findings, elevated glucose, HbA1c%, and HOMA-IR along with decreased insulin

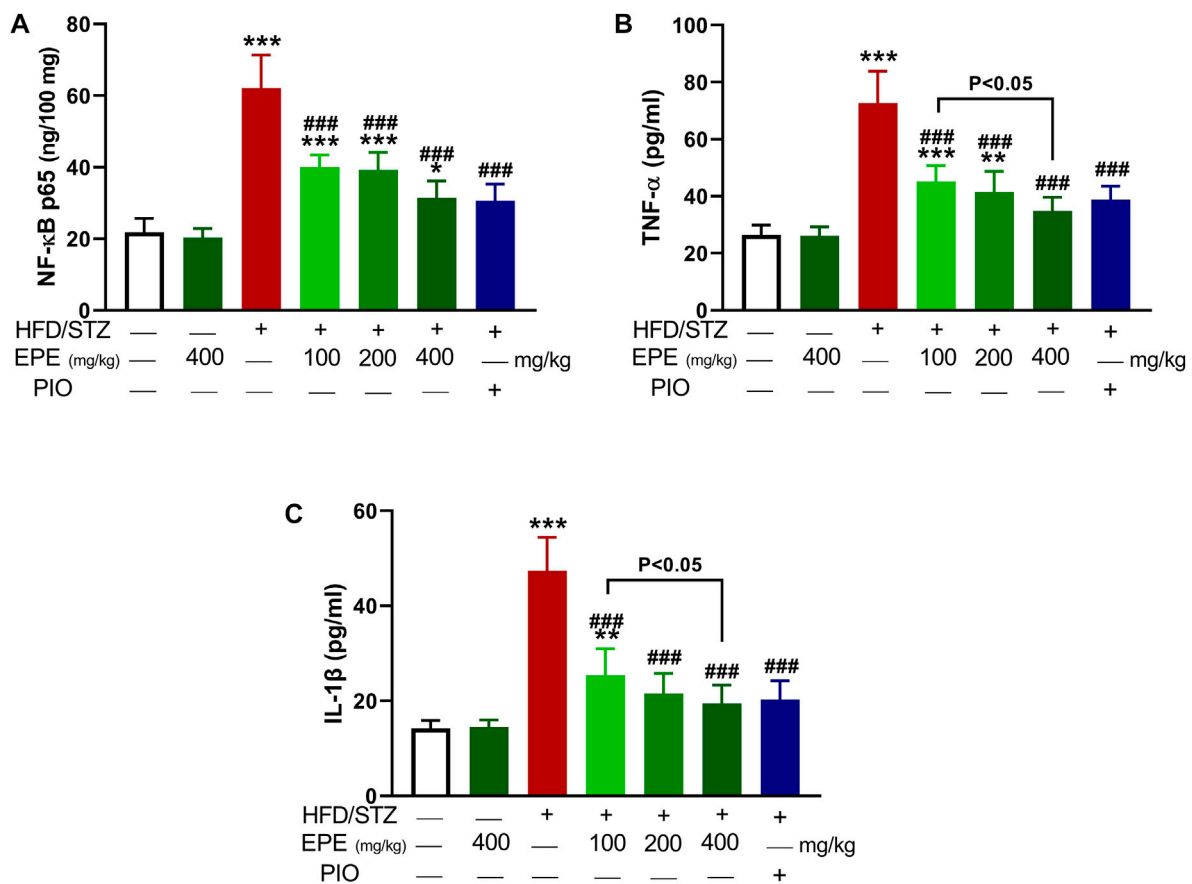


FIGURE 8

EPE decreased liver NF-κB p65 (A) and serum TNF-α (B) and IL-1β (C) in diabetic rats. Data are mean \pm SD ($n = 6$). * $p < 0.05$, ** $p < 0.01$, and *** $p < 0.001$ vs. control. ### $p < 0.001$ vs. diabetic.

TABLE 2 Binding affinities, interacting polar residues, and hydrophobic interactions of the compounds isolated from *E. pepplus* with the NF-κB-DNA complex.

Compound	Binding energy (kcal/mol)	Polar bond	Hydrophobic interaction
1	−8.9	Gln274 and two DNA units	Five DNA units
2	−9.5	Four DNA units	Gln274 and four DNA units
3	−10.6	Asp217, Lys218, and four DNA units	Asn186, Arg187, Arg305, and one DNA unit
4	−9.8	Glu222 and four DNA units	Three DNA units
5	−9.6	Lys241, Ser246, Arg246, Asn247, and three DNA units	Asp271, Lys272, and one DNA unit
6	−9.1	Lys241, Asp271, Arg246, Asn247, and three DNA units	Ser246, Lys272, and one DNA unit
7	−6.4	Lys241 and three DNA units	Arg246, Lys272, and two DNA units

were reported in HFD/STZ-challenged rats (Abduh et al., 2023). The declined insulin is due to damage caused to the pancreatic islets induced by STZ-mediated ROS generation and DNA damage (Lenzen, 2008). Although the early phase of damage is associated with increased insulin release as a compensatory mechanism, prolonged hyperglycemia and ROS release deteriorate the

pancreatic islets and promote more β -cell damage and ultimately reduced insulin release (Ntimbane et al., 2016). The effects of excessive ROS include enhanced lipid peroxidation (LPO), massively increased cytosolic Ca^{2+} , and diminished pancreatic antioxidants, effects that enhance the destruction of β -cells (Nahdi et al., 2017).



the previously reported anti-hyperglycemic activity of plants of the same genus. For instance, *E. royleana* stem extract decreased fasting BG (FBG) and ameliorated glucose intolerance in diabetic

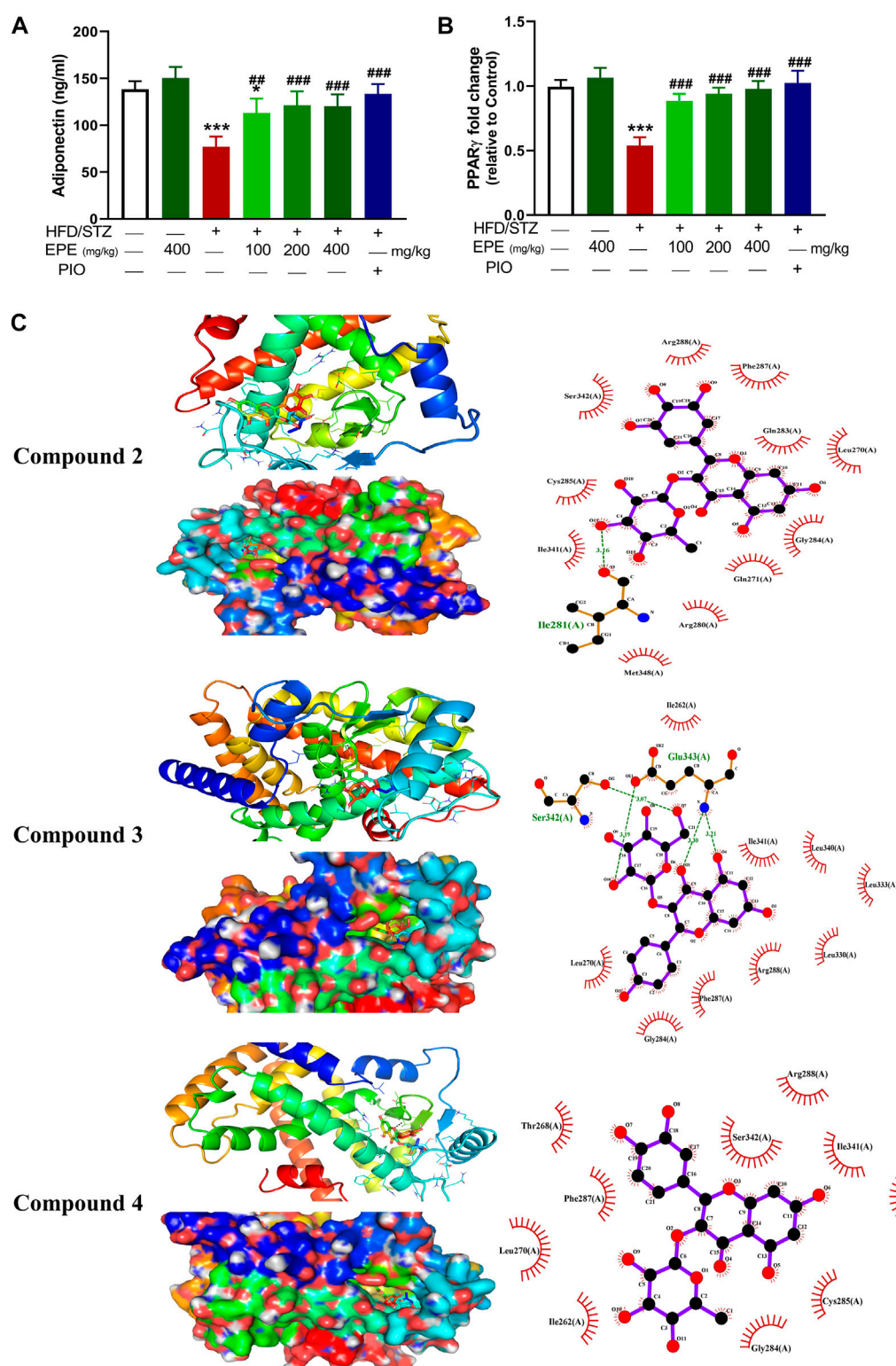


FIGURE 10

EPE increased serum adiponectin (A) and upregulated liver PPARγ mRNA (B) in diabetic rats. Data are mean \pm SD ($n = 6$). * $p < 0.05$ and *** $p < 0.001$ vs. control. ## $p < 0.01$ and ### $p < 0.001$ vs. diabetic. (C) Molecular docking showing the binding modes of compounds 2, 3, and 4 with PPARγ.

rats (Zafar et al., 2021), and *E. helioscopia* alleviated BG and insulin in sucrose-fed rats (Mustafa et al., 2022). The ameliorative effect of EPE on hyperglycemia is a direct result of increased

insulin secretion. Impaired insulin release and IR increase hepatic glucose output due to suppressed glycolysis and glycogenesis. Impaired insulin release and IR can also impair

TABLE 3 Binding affinities, interacting polar residues, and hydrophobic interactions of the compounds isolated from *E. peplus* with PPAR γ .

Compound	Binding energy (kcal/mol)	Polar bond	Hydrophobic interaction
1	−7.9	Gln271, Glu272, and Ser342	Ile262, Leu270, Gly284, Phe287, Arg288, Ile341, and Met348
2	−8.7	Ile281	Leu270, Gln271, Arg280, Gln283, Gly284, Cys285, Phe287, Arg288, Ile341, Ser342, and Met348
3	−8.0	Ser342 and Glu343	Ile262, Leu270, Gly284, Phe287, Arg288, Leu330, Leu333, Leu340, and Ile341
4	−8.0		Ile262, Thr268, Leu270, Gln271, Arg280, Gly284, Cys285, Phe287, Arg288, Ile341, and Ser342
5	−7.5	Glu259, Gln271, Arg280, and Glu291	Leu270, Gly284, Phe287, and Arg288
6	−7.4		Leu270, Gln271, Arg280, Gln283, Gly284, Phe287, Arg288, and Glu291
7	−5.8	Ser289, His323, and Met364	Cys285, Tyr327, Phe363, His449, Leu469, and Tyr473

peripheral glucose uptake and hepatic gluconeogenesis, resulting in hyperglycemia (Nordlie et al., 1999). By alleviating insulin release and IR, EPE effectively ameliorated hyperglycemia possibly by modulating enzymes involved in glycogenesis and gluconeogenesis. This notion was supported by the findings of this study where EPE increased hexokinase and suppressed F-1,6-BPase, G-6-Pase, and glycogen phosphorylase, resulting in increased liver glycogen content. Hexokinase is involved in glucose oxidation and suppressed by IR and insulin deficiency. Suppressed hexokinase activity decreases glycolysis, and hence glucose accumulates in the blood (Gupta et al., 1999). Along with hexokinase suppression, insulin insufficiency activates G-6-Pase, F-1,6-BPase, and glycogen phosphorylase, resulting in enhanced gluconeogenesis and glycogenolysis (Rodén and Bernroider, 2003). The improved insulin sensitivity and levels of EPE decreased glycogenolysis and gluconeogenesis and enhanced liver glycogen by modulating the activity of the involved enzymes. In addition to the determined enzymes, insulin activates glycogen synthase and suppresses glycogen phosphorylase (Postic et al., 2004), and this explains the alleviated glycogen levels following treatment with EPE. Owing to its role in glucose oxidation, the ameliorated FBG following EPE supplementation is a result of enhanced hexokinase activity. To further explore the effect of EPE on hexokinase activity, we carried out MD simulations of the binding affinity of the contained flavonoids toward the enzyme. All flavonoids revealed binding affinity marked by polar bonding toward important residues in the active site and dense hydrophobic interactions. Recent findings showed improvements in glycemic status and insulin sensitivity by plant extracts that modulate the carbohydrate-metabolizing enzymes (Germoush et al., 2019; Elsayed et al., 2020). In this context, Mustafa et al. (2022) related the anti-hyperglycemic effect of *E. helioscopia* in sucrose-fed rats to its ability to modulate the activities of pyruvate kinase, glucokinase, and phosphofructokinase.

In addition to hyperglycemia, dyslipidemia is found in T2D and can increase atherogenicity and the risk of cardiovascular disease (Reaven, 2005). Elevated serum lipids and decreased

HDL-C in this study represent an atherogenic profile as previously described (Germoush et al., 2019). AIP, a marker of lipoprotein particle size that possesses a predictive value beyond that of the assayed lipids (Dobiášová, 2006), was increased in diabetic rats. The observed dyslipidemia is a direct result of IR and the enhanced lipolysis and decreased lipogenesis (Carpentier, 2021). Increased lipolysis provokes liver lipid accumulation which is also promoted by increased synthesis of free fatty acids (FFAs) that provoke lipogenesis within hepatocytes (Mohamed et al., 2016). Lipid accumulation in hepatocytes causes cell injury, thereby aggravating IR, hyperglycemia, and dyslipidemia (Levinthal and Tavill, 1999). Herein, lipids were increased in the liver, and circulating transaminases were elevated in diabetic rats as previously reported (Elsayed et al., 2020; Abduh et al., 2023). EPE effectively ameliorated serum and liver lipids, effects that were directly related to the enhanced insulin release and sensitivity.

Owing to the involvement of OS and inflammation in provoking IR and the complications of DM (Mahmoud et al., 2012; Mahmoud, 2017), we explored the ability of EPE to suppress these pathological processes. Diabetic rats showed OS and inflammatory reactions marked by elevated MDA, NO, NF- κ B, TNF- α , and IL-1 β and declined antioxidants. OS, defined by excess ROS and decreased antioxidants, is a key mechanism in IR and can damage cells and alter multiple signaling pathways. Hyperglycemia can increase the production of ROS and lead to OS by activating NADPH oxidases and promoting mitochondrial dysfunction (Jimenez et al., 2018). Excess ROS can activate pathways related to increased pro-inflammatory cytokines, and both can impair insulin signaling, leading to IR and glucose accumulation in the blood (Rösen et al., 2001). The altered insulin levels shift the signaling where PI3K phosphorylates Rac, resulting in increased NADPH oxidase 4-mediated ROS generation (Campa et al., 2015). Excess ROS activates casein kinase-2 followed by retromer that alters glucose transporter-4 membrane translocation and impair glucose uptake (Ma et al., 2014). ROS can also increase mitochondrial fission that stimulates stress responses and

impairs insulin signaling and has been linked to IR as well as apoptosis (Jheng et al., 2012). Pro-inflammatory cytokines trigger IR by altering insulin signaling and many kinases. The elevated IL-1 β and TNF- α reported in this study can impair insulin-stimulated uptake of glucose, stimulate lipolysis and gluconeogenesis, and inhibit tyrosine phosphorylation of insulin receptor substrate-1 and protein kinase B activation (Green et al., 1994; Del Aguila et al., 1999; Jager et al., 2007). Therefore, attenuation of OS and pro-inflammatory cytokines can attenuate IR and increase insulin signaling, activity, and stimulated glucose uptake.

EPE enhanced antioxidants and prevented OS and inflammation in diabetic rats in this investigation. In addition to its *in vitro* RSA, EPE prevented LPO, enhanced antioxidants, and suppressed NF- κ B and cytokines in diabetic rats. The suppression of inflammation following EPE supplementation was supported by *in silico* investigations that showed the ability of flavonoids to bind strongly with NF- κ B through multiple polar bonding and hydrophobic interactions. The attenuation of these pathological processes contributed to the anti-hyperglycemic and insulin-sensitizing effects of EPE. Numerous studies showed the beneficial effects of antioxidants and plant extracts that are rich in antioxidant phytochemicals against hyperglycemia and IR (Mahmoud, 2013; Mahmoud et al., 2017; Germoush et al., 2019). The antioxidant and anti-inflammatory role of EPE is related to its content of flavonoids which possess potent RSA and showed benefits against DM (Mahmoud, 2013; Mahmoud et al., 2017; Germoush et al., 2019; Abukhalil et al., 2021). In diabetic patients, the supplementation of flavonoids improved glycemic and lipidemic statuses and antioxidants and decreased inflammatory markers (Li et al., 2015). In obese patients, the consumption of flavonoids positively affected the metabolic status by lowering systemic oxidation and enhancing insulin sensitivity (Suliburska et al., 2012).

The beneficial effects of EPE could also be linked to the upregulation of adiponectin and PPAR γ . EPE increased serum adiponectin that participated, at least in part, in the amelioration of hyperglycemia. Adiponectin exerts insulin-sensitizing effects and possesses anti-inflammatory activity, and experimental evidence revealed that it ameliorated hyperglycemia in HFD-fed rodents (Fruebis et al., 2001; Yamauchi et al., 2001). Despite its ameliorated hyperglycemia in T1D and T2D in rodents, high adiponectin doses didn't affect BG in normal animals. These findings suggested that the downregulation of glycogenolysis and gluconeogenesis mediated its anti-hyperglycemic effects. Accordingly, adiponectin decreased glucose production in rat hepatocytes and G-6-Pase mRNA abundance in mice (Berg et al., 2001; Combs et al., 2001). It can also upregulate liver CD36, PPAR α , and UCP-2, effects that were related to the increase in insulin sensitivity (Yamauchi et al., 2001). EPE upregulated liver PPAR γ , and its flavonoids were shown to dock into the PPAR γ active site through polar bonding and hydrophobic interactions. The activation of PPAR γ is a key mechanism for ameliorating hyperglycemia, and IR and PPAR γ agonists, such as PIO, increase insulin sensitivity and ameliorate hyperglycemia,

dyslipidemia, OS, and inflammation (Tontonoz and Spiegelman, 2008). PPAR γ suppresses OS and inflammation by enhancing antioxidant enzymes (Okuno et al., 2010), inhibiting the activation of NF- κ B both directly and indirectly (Kersten et al., 2000; Remels et al., 2009), and preventing ROS generation from NADPH oxidases (Hwang et al., 2005). However, the lack of PPAR γ protein expression data could be considered a limitation to this study.

5 Conclusion

This investigation introduces new information that *E. peplus* is rich in flavonoids and possesses potent radical-scavenging and anti-diabetic efficacies. EPE ameliorated hyperglycemia, IR, OS, dyslipidemia, and inflammation in rats with T2D. In addition, EPE modulated carbohydrate-metabolizing enzymes and enhanced antioxidants, adiponectin, and PPAR γ . *In silico* findings revealed the binding affinity of *E. peplus* constituents toward hexokinase, NF- κ B, and PPAR γ . Therefore, *E. peplus* could be a promising candidate for the development of a potent anti-hyperglycemic and insulin-sensitizing agent. However, further investigations to determine other molecular mechanism(s) of action are needed.

Data availability statement

The original contributions presented in the study are included in the article/Supplementary Material; further inquiries can be directed to the corresponding author.

Ethics statement

The animal study was reviewed and approved by the Research Ethics Committee of Al-Azhar University.

Author contributions

Conceptualization, AM, EK, and RA; methodology, AM, RA, MA, GM-H, AB-A, and EK; software, AM and EK; validation, AM; formal analysis, RA, MA, AM, and EK; investigation, RA, AM, GM-H, MA, AB-A, and EK; resources, RA, GM-H, MA, and EH; data curation, AM, EK, and RA; writing—original draft and preparation, AM, GM-H, and EK; writing—review and editing, AM; visualization, AM; supervision, AM; project administration, RA and AM; funding acquisition, RA. All authors contributed to the article and approved the submitted version.

Funding

This research was funded by the Nourah Bint Abdulrahman University Researchers Supporting Project (grant number PNURSP

2023R381), Princess Nourah Bint Abdulrahman University, Riyadh, Saudi Arabia.

Acknowledgments

Princess Nourah bint Abdulrahman University Researchers Supporting Project number (PNURSP2023R381), Princess Nourah bint Abdulrahman University, Riyadh, Saudi Arabia.

Conflict of interest

The authors declare that the research was conducted in the absence of any commercial or financial relationships that could be construed as a potential conflict of interest.

References

- Abd El-Twab, S. M., Mohamed, H. M., and Mahmoud, A. M. (2016). Taurine and pioglitazone attenuate diabetes-induced testicular damage by abrogation of oxidative stress and up-regulation of the pituitary-gonadal axis. *Can. J. Physiol. Pharmacol.* 94, 651–661. doi:10.1139/cjpp-2015-0503
- Abd-Elhakim, Y. M., Abdo Nassan, M., Salem, G. A., Sasi, A., Aldhahrani, A., Ben Issa, K., et al. (2019). Investigation of the *in-vivo* cytotoxicity and the *in silico*-prediction of MDM2-p53 inhibitor potential of *Euphorbia peplus* methanolic extract in rats. *Toxins (Basel)* 11, 642. doi:10.3390/toxins11110642
- Abduh, M. S., Alzoghaibi, M. A., Alzoghaibi, A. M., Bin-Ammar, A., Alotaibi, M. F., Kamel, E. M., et al. (2023). Arbutin ameliorates hyperglycemia, dyslipidemia and oxidative stress and modulates adipocytokines and PPAR γ in high-fat diet/streptozotocin-induced diabetic rats. *Life Sci.* 321, 121612. doi:10.1016/j.lfs.2023.121612
- Abukhalil, M. H., Althunibat, O. Y., Aladaileh, S. H., Al-Amarat, W., Obeidat, H. M., Al-Khawalde, A. a. A., et al. (2021). Galangin attenuates diabetic cardiomyopathy through modulating oxidative stress, inflammation and apoptosis in rats. *Biomed. Pharmacother.* 138, 111410. doi:10.1016/j.biopha.2021.111410
- Aebi, H. (1984). “[13] catalase *in vitro*,” in *Methods in enzymology* (Cambridge: Academic Press), 121–126.
- Ahmed, S., Yousaf, M., Mothana, R. A., and Al-Rehaily, A. J. (2016). Studies on wound healing activity of some EUPHORBIA species on experimental rats. *Afr. J. Tradit. Complement. Altern. Med.* 13, 145–152. doi:10.21010/ajtcam.v13i5.19
- Al-Sultan, S., and Hussein, Y. A. (2006). Acute toxicity of *Euphorbia helioscopia* in rats. *Pak. J. Nutr.* 5, 135–140. doi:10.3923/pjn.2006.135.140
- American Diabetes Association (2021). 2. Classification and diagnosis of diabetes: Standards of medical care in diabetes-2021. *Diabetes Care* 44, S15–S33. doi:10.2337/dc21-S002
- American Diabetes Association (2014). Standards of medical care in diabetes-2014. *Diabetes Care* 37, S14–S80. doi:10.2337/dc14-S014
- Bancroft, J. D., and Gamble, M. (2008). *Theory and practice of histological techniques*. Netherlands: Elsevier health sciences.
- Berg, A. H., Combs, T. P., Du, X., Brownlee, M., and Scherer, P. E. (2001). The adipocyte-secreted protein Acrp30 enhances hepatic insulin action. *Nat. Med.* 7, 947–953. doi:10.1038/90992
- Beutler, E., Duron, O., and Kelly, B. M. (1963). Improved method for the determination of blood glutathione. *J. laboratory Clin. Med.* 61, 882–888.
- Brand-Williams, W., Cuvelier, M. E., and Berset, C. (1995). Use of a free radical method to evaluate antioxidant activity. *LWT - Food Sci. Technol.* 28, 25–30. doi:10.1016/s0023-6438(95)80008-5
- Brandstrup, N., Kirk, J. E., and Bruni, C. (1957). The hexokinase and phosphoglucosomerase activities of aortic and pulmonary artery tissue in individuals of various ages. *J. Gerontol.* 12, 166–171. doi:10.1093/geronj/12.2.166
- Breyer, M. D., Böttinger, E., Brosius, F. C., Iii, Coffman, T. M., Harris, R. C., Heilig, C. W., et al. (2005). Mouse models of diabetic nephropathy. *J. Am. Soc. Nephrol.* 16, 27–45. doi:10.1681/ASN.2004080648
- Campa, C. C., Ciralo, E., Ghigo, A., Germa, G., and Hirsch, E. (2015). Crossroads of PI3K and rac pathways. *Small GTPases* 6, 71–80. doi:10.4161/21541248.2014.989789
- Carpentier, A. C. (2021). 100th anniversary of the discovery of insulin perspective: Insulin and adipose tissue fatty acid metabolism. *Am. J. Physiology-Endocrinology Metabolism* 320, E653–E670. doi:10.1152/ajpendo.00620.2020
- Combs, T. P., Berg, A. H., Obici, S., Scherer, P. E., and Rossetti, L. (2001). Endogenous glucose production is inhibited by the adipose-derived protein Acrp30. *J. Clin. Invest.* 108, 1875–1881. doi:10.1172/JCI14120
- Del Aguila, L. F., Claffey, K. P., and Kirwan, J. P. (1999). TNF- α impairs insulin signaling and insulin stimulation of glucose uptake in C2C12 muscle cells. *Am. J. Physiology - Endocrinol. Metabolism* 276, E849–E855. doi:10.1152/ajpendo.1999.276.5.E849
- Dobiášová, M. (2006). AIP-atherogenic index of plasma as a significant predictor of cardiovascular risk: From research to practice. *Vnitr Lek.* 52, 64–71.
- Elsayed, R. H., Kamel, E. M., Mahmoud, A. M., El-Bassuony, A. A., Bin-Jumah, M., Lamsabhi, A. M., et al. (2020). Rumex dentatus L. phenolics ameliorate hyperglycemia by modulating hepatic key enzymes of carbohydrate metabolism, oxidative stress and PPAR γ in diabetic rats. *Food Chem. Toxicol.* 138, 111202. doi:10.1016/j.fct.2020.111202
- Floegel, A., Kim, D.-O., Chung, S.-J., Koo, S. I., and Chun, O. K. (2011). Comparison of ABTS/DPPH assays to measure antioxidant capacity in popular antioxidant-rich US foods. *J. food Compos. analysis* 24, 1043–1048. doi:10.1016/j.jfca.2011.01.008
- Flohé, L., and Günzler, W. A. (1984). Assays of glutathione peroxidase. *Methods Enzymol.* 105, 114–121. doi:10.1016/s0076-6879(84)05015-1
- Folch, J., Lees, M., and Sloane Stanley, G. H. (1957). A simple method for the isolation and purification of total lipides from animal tissues. *J. Biol. Chem.* 226, 497–509. doi:10.1016/s0021-9258(18)64849-5
- Freedland, R. A., and Harper, A. E. (1959). Metabolic adaptations in higher animals. *J. Biol. Chem.* 234, 1350–1354. doi:10.1016/s0021-9258(18)70010-0
- Fruebis, J., Tsao, T. S., Javorschi, S., Ebbets-Reed, D., Erickson, M. R., Yen, F. T., et al. (2001). Proteolytic cleavage product of 30-kDa adipocyte complement-related protein increases fatty acid oxidation in muscle and causes weight loss in mice. *Proc. Natl. Acad. Sci. U. S. A.* 98, 2005–2010. doi:10.1073/pnas.041591798
- Fu, Y., Li, Z., Si, J., Chang, Q., Li, Z., and Pan, R. (2013). Separation and purification of myricitrin from bayberry tree bark by high-speed counter-current chromatography. *J. Liq. Chromatogr. Relat. Technol.* 36, 1503–1512. doi:10.1080/10826076.2012.692147
- Germoush, M. O., Elgebaly, H. A., Hassan, S., Kamel, E. M., Bin-Jumah, M., and Mahmoud, A. M. (2019). Consumption of terpenoids-rich padina pavonia extract attenuates hyperglycemia, insulin resistance and oxidative stress, and upregulates PPAR γ in a rat model of type 2 diabetes. *Antioxidants (Basel)* 9, 22. doi:10.3390/antiox9010022
- Giner, J. L., and Schroeder, T. N. (2015). Polygonifoliol, a new tirucallane triterpene from the latex of the seaside sandmat *Euphorbia polygonifolia*. *Chem. Biodivers.* 12, 1126–1129. doi:10.1002/cbdv.201400426
- Green, A., Dobias, S. B., Walters, D. J. A., and Brasier, A. R. (1994). Tumor necrosis factor increases the rate of lipolysis in primary cultures of adipocytes without altering levels of hormone-sensitive lipase. *Endocrinology* 134, 2581–2588. doi:10.1210/endo.134.6.8194485
- Green, L. C., Wagner, D. A., Glogowski, J., Skipper, P. L., Wishnok, J. S., and Tannenbaum, S. R. (1982). Analysis of nitrate, nitrite, and [15N]nitrate in biological fluids. *Anal. Biochem.* 126, 131–138. doi:10.1016/0003-2697(82)90118-x

Publisher's note

All claims expressed in this article are solely those of the authors and do not necessarily represent those of their affiliated organizations, or those of the publisher, the editors, and the reviewers. Any product that may be evaluated in this article, or claim that may be made by its manufacturer, is not guaranteed or endorsed by the publisher.

Supplementary material

The Supplementary Material for this article can be found online at: <https://www.frontiersin.org/articles/10.3389/fphar.2023.1204641/full#supplementary-material>

- Gupta, D., Raju, J., Prakash, J., and Baquer, N. Z. (1999). Change in the lipid profile, lipogenic and related enzymes in the livers of experimental diabetic rats: Effect of insulin and vanadate. *Diabetes Res. Clin. Pract.* 46, 1–7. doi:10.1016/s0168-8227(99)00067-4
- Guzik, T. J., and Cosentino, F. (2018). Epigenetics and immunometabolism in diabetes and aging. *Antioxid. Redox Signal* 29, 257–274. doi:10.1089/ars.2017.7299
- Haffner, S. M. (2000). Coronary heart disease in patients with diabetes. *N. Engl. J. Med.* 342, 1040–1042. doi:10.1056/NEJM200004063421408
- Han, J.-T., Bang, M.-H., Chun, O.-K., Kim, D.-O., Lee, C.-Y., and Baek, N.-I. (2004). Flavonol glycosides from the aerial parts of *Aceriphyllum rossii* and their antioxidant activities. *Archives Pharmacol. Res.* 27, 390–395. doi:10.1007/BF02980079
- Hwang, J., Kleinhenz, D. J., Lassegue, B., Griendling, K. K., Dikalov, S., and Hart, C. M. (2005). Peroxisome proliferator-activated receptor-gamma ligands regulate endothelial membrane superoxide production. *Am. J. Physiol. Cell Physiol.* 288, C899–C905. doi:10.1152/ajpcell.00474.2004
- Jager, J., Grémeaux, T., Cormont, M., Le Marchand-Brustel, Y., and Tanti, J. F. (2007). Interleukin-1 β -induced insulin resistance in adipocytes through down-regulation of insulin receptor substrate-1 expression. *Endocrinology* 148, 241–251. doi:10.1210/en.2006-0692
- Jellinger, P. S. (2007). Metabolic consequences of hyperglycemia and insulin resistance. *Clin. Cornerstone* 8, S30–S42. doi:10.1016/s1098-3597(07)80019-6
- Jheng, H. F., Tsai, P. J., Guo, S. M., Kuo, L. H., Chang, C. S., Su, I. J., et al. (2012). Mitochondrial fission contributes to mitochondrial dysfunction and insulin resistance in skeletal muscle. *Mol. Cell Biol.* 32, 309–319. doi:10.1128/MCB.05603-11
- Jimenez, R., Toral, M., Gómez-Guzmán, M., Romero, M., Sanchez, M., Mahmoud, A. M., et al. (2018). The role of Nrf2 signaling in ppar β / δ -mediated vascular protection against hyperglycemia-induced oxidative stress. *Oxid. Med. Cell Longev.* 2018, 5852706. doi:10.1155/2018/5852706
- Kahn, S. E., Cooper, M. E., and Del Prato, S. (2014). Pathophysiology and treatment of type 2 diabetes: Perspectives on the past, present, and future. *Lancet* 383, 1068–1083. doi:10.1016/S0140-6736(13)62154-6
- Kamel, E. M., Ahmed, N. A., El-Bassuony, A. A., Hussein, O. E., Alrashdi, B., Ahmed, S. A., et al. (2022). Xanthine oxidase inhibitory activity of *Euphorbia peplus* L. Phenolics. *Comb. Chem. High. Throughput Screen* 25, 1336–1344. doi:10.2174/1386207324666210609104456
- Kamel, E. M., Mahmoud, A. M., Ahmed, S. A., and Lamsabhi, A. M. (2016). A phytochemical and computational study on flavonoids isolated from *Trifolium resupinatum* L. and their novel hepatoprotective activity. *Food Funct.* 7, 2094–2106. doi:10.1039/c6fo00194g
- Kersten, S., Desvergne, B., and Wahli, W. (2000). Roles of PPARs in health and disease. *Nature* 405, 421–424. doi:10.1038/35013000
- Koide, H., and Oda, T. (1959). Pathological occurrence of glucose-6-phosphatase in serum in liver diseases. *Clin. Chim. Acta* 4, 554–561. doi:10.1016/0009-8981(59)90165-2
- Kumar, S., Malhotra, R., and Kumar, D. (2010). Antidiabetic and free radicals scavenging potential of *Euphorbia hirta* flower extract. *Indian J. Pharm. Sci.* 72, 533–537. doi:10.4103/0250-474X.73921
- Lee, Y. S., Li, P., Huh, J. Y., Hwang, I. J., Lu, M., Kim, J. I., et al. (2011). Inflammation is necessary for long-term but not short-term high-fat diet-induced insulin resistance. *Diabetes* 60, 2474–2483. doi:10.2337/db11-0194
- Lenzen, S. (2008). The mechanisms of alloxan- and streptozotocin-induced diabetes. *Diabetologia* 51, 216–226. doi:10.1007/s00125-007-0886-7
- Levinthal, G. N., and Tavill, A. S. (1999). Liver disease and diabetes mellitus. *Clin. DIABETES* 17, 73–81.
- Li, D., Zhang, Y., Liu, Y., Sun, R., and Xia, M. (2015). Purified anthocyanin supplementation reduces dyslipidemia, enhances antioxidant capacity, and prevents insulin resistance in diabetic patients. *J. Nutr.* 145, 742–748. doi:10.3945/jn.114.205674
- Livak, K. J., and Schmittgen, T. D. (2001). Analysis of relative gene expression data using real-time quantitative PCR and the 2(-Delta Delta C(T)) Method. *Methods* 25, 402–408. doi:10.1006/meth.2001.1262
- Ma, J., Nakagawa, Y., Kojima, I., and Shibata, H. (2014). Prolonged insulin stimulation down-regulates GLUT4 through oxidative stress-mediated retromer inhibition by a protein kinase CK2-dependent mechanism in 3T3-L1 adipocytes. *J. Biol. Chem.* 289, 133–142. doi:10.1074/jbc.M113.533240
- Ma, X., Wu, L., Ito, Y., and Tian, W. (2005). Application of preparative high-speed counter-current chromatography for separation of methyl gallate from *Acer truncatum* Bunge. *J. Chromatogr. A* 1076, 212–215. doi:10.1016/j.chroma.2005.04.077
- Mabry, T. J., Markham, K., Thomas, M., Mabry, T. J., Markham, K., and Thomas, M. (1970). “The NMR spectra of flavonoids,” in *The systematic identification of flavonoids* (Berlin, Heidelberg: Springer), 274–343.
- Mahmoud, A. M., Abd El-Twab, S. M., and Abdel-Reheim, E. S. (2017). Consumption of polyphenol-rich morus alba leaves extract attenuates early diabetic retinopathy: The underlying mechanism. *Eur. J. Nutr.* 56, 1671–1684. doi:10.1007/s00394-016-1214-0
- Mahmoud, A. M., Ashour, M. B., Abdel-Moneim, A., and Ahmed, O. M. (2012). Hesperidin and naringin attenuate hyperglycemia-mediated oxidative stress and proinflammatory cytokine production in high fat fed/streptozotocin-induced type 2 diabetic rats. *J. Diabetes its Complicat.* 26, 483–490. doi:10.1016/j.jdiacomp.2012.06.001
- Mahmoud, A. M. (2017). “Exercise ameliorates metabolic disturbances and oxidative stress in diabetic cardiomyopathy: Possible underlying mechanisms,” in *Exercise for cardiovascular disease prevention and treatment: From molecular to clinical, Part 1*. Editor J. Xiao (Singapore: Springer Singapore), 207–230.
- Mahmoud, A. M. (2013). Hematological alterations in diabetic rats - role of adipocytokines and effect of citrus flavonoids. *Excli J.* 12, 647–657.
- Marklund, S., and Marklund, G. (1974). Involvement of the superoxide anion radical in the autooxidation of pyrogallol and a convenient assay for superoxide dismutase. *FEBS Eur. J. Biochem.* 47, 469–474. doi:10.1111/j.1432-1033.1974.tb03714.x
- Mohamed, J., Nazratun Nafizah, A. H., Zariyante, A. H., and Budin, S. B. (2016). Mechanisms of Diabetes-Induced Liver Damage: The role of oxidative stress and inflammation. *Sultan Qaboos Univ. Med. J.* 16, e132–e141. doi:10.18295/squmj.2016.16.02.002
- Mustafa, I., Anwar, H., Irfan, S., Muzaffar, H., and Ijaz, M. U. (2022). Attenuation of carbohydrate metabolism and lipid profile by methanolic extract of *Euphorbia helioscopia* and improvement of beta cell function in a type 2 diabetic rat model. *BMC Complementary Med. Ther.* 22, 23. doi:10.1186/s12906-022-03507-2
- Nahdi, A. M. T. A., John, A., and Raza, H. (2017). Elucidation of molecular mechanisms of streptozotocin-induced oxidative stress, apoptosis, and mitochondrial dysfunction in rin-5F pancreatic β -cells. *Oxidative Med. Cell. Longev.* 2017, 7054272. doi:10.1155/2017/7054272
- Nordlie, R. C., Foster, J. D., and Lange, A. J. (1999). Regulation of glucose production by the liver. *Annu. Rev. Nutr.* 19, 379–406. doi:10.1146/annurev.nutr.19.1.379
- Ntimbane, T., Mailhot, G., Spahis, S., Rabasa-Lhoret, R., Kleme, M. L., Melloul, D., et al. (2016). CFTR silencing in pancreatic β -cells reveals a functional impact on glucose-stimulated insulin secretion and oxidative stress response. *Am. J. Physiol. Endocrinol. Metab.* 310, E200–E212. doi:10.1152/ajpendo.00333.2015
- Ohkawa, H., Ohishi, N., and Yagi, K. (1979). Assay for lipid peroxides in animal tissues by thiobarbituric acid reaction. *Anal. Biochem.* 95, 351–358. doi:10.1016/0003-2697(79)90738-3
- Okuno, Y., Matsuda, M., Miyata, Y., Fukuhara, A., Komuro, R., Shimabukuro, M., et al. (2010). Human catalase gene is regulated by peroxisome proliferator activated receptor-gamma through a response element distinct from that of mouse. *Endocr. J.* 57, 303–309. doi:10.1507/endocrj.k09e-113
- Pattanaik, S., Si, S. C., Pal, A., Panda, J., and Nayak, S. S. (2014). Wound healing activity of methanolic extract of the leaves of *Crataeva magna* and *Euphorbia nerifolia* in rats. *J. Appl. Pharm. Sci.* 4, 046–049. doi:10.7324/japs.2014.40310
- Postic, C., Dentin, R., and Girard, J. (2004). Role of the liver in the control of carbohydrate and lipid homeostasis. *Diabetes Metabolism* 30, 398–408. doi:10.1016/s1262-3636(07)70133-7
- Re, R., Pellegrini, N., Proteggente, A., Pannala, A., Yang, M., and Rice-Evans, C. (1999). Antioxidant activity applying an improved ABTS radical cation decolorization assay. *Free Radic. Biol. Med.* 26, 1231–1237. doi:10.1016/s0891-5849(98)00315-3
- Reaven, G. M. (2005). Compensatory hyperinsulinemia and the development of an atherogenic lipoprotein profile: The price paid to maintain glucose homeostasis in insulin-resistant individuals. *Endocrinol. Metab. Clin. North Am.* 34, 49–62. doi:10.1016/j.ecl.2004.12.001
- Remels, A. H., Langen, R. C., Gosker, H. R., Russell, A. P., Spaepen, F., Voncken, J. W., et al. (2009). PPARgamma inhibits NF-kappaB-dependent transcriptional activation in skeletal muscle. *Am. J. Physiol. Endocrinol. Metab.* 297, E174–E183. doi:10.1152/ajpendo.90632.2008
- Roden, M., and Bernroider, E. (2003). Hepatic glucose metabolism in humans-its role in health and disease. *Best. Pract. Res. Clin. Endocrinol. Metab.* 17, 365–383. doi:10.1016/s1521-690x(03)00031-9
- Rösen, P., Nawroth, P. P., King, G., Möller, W., Tritschler, H. J., and Packer, L. (2001). The role of oxidative stress in the onset and progression of diabetes and its complications: A summary of a congress series sponsored by UNESCO-MCBN, the American diabetes association and the German diabetes society. *Diabetes/Metabolism Res. Rev.* 17, 189–212. doi:10.1002/dmrr.196
- Saeedi, P., Petersohn, I., Salpea, P., Malanda, B., Karuranga, S., Unwin, N., et al. (2019). Global and regional diabetes prevalence estimates for 2019 and projections for 2030 and 2045: Results from the international diabetes federation diabetes atlas, 9th edition. *Diabetes Res. Clin. Pract.* 157, 107843. doi:10.1016/j.diabres.2019.107843
- Sami, D. H., Soliman, A. S., Khawailed, A. A., Hassanein, E. H., Kamel, E. M., and Mahmoud, A. M. J. L. S. (2022). 7-hydroxycoumarin modulates Nrf2/HO-1 and microRNA-34a/SIRT1 signaling and prevents cisplatin-induced oxidative stress, inflammation, and kidney injury in rats. *Life Sci.* 310, 121104. doi:10.1016/j.lfs.2022.121104
- Seifter, S., Dayton, S., et al. (1950). The estimation of glycogen with the anthrone reagent. *Arch. Biochem.* 25, 191–200.

- Shi, Q. W., Su, X. H., and Kiyota, H. (2008). Chemical and pharmacological research of the plants in genus *Euphorbia*. *Chem. Rev.* 108, 4295–4327. doi:10.1021/cr078350s
- Singla, A., and Kamla, P. (1990). Phytoconstituents of *Euphorbia* species. *Fitoterapia* 41, 483–516.
- Stalmans, W., and Hers, H. G. (1975). The stimulation of liver phosphorylase b by AMP, fluoride and sulfate. A technical note on the specific determination of the a and b forms of liver glycogen phosphorylase. *Eur. J. Biochem.* 54, 341–350. doi:10.1111/j.1432-1033.1975.tb04144.x
- Suliburska, J., Bogdanski, P., Szulinska, M., Stepień, M., Pupek-Musialik, D., and Jabłeczka, A. (2012). Effects of green tea supplementation on elements, total antioxidants, lipids, and glucose values in the serum of obese patients. *Biol. Trace Elem. Res.* 149, 315–322. doi:10.1007/s12011-012-9448-z
- Tatsis, E. C., Boeren, S., Exarchou, V., Trojanis, A. N., Vervoort, J., and Gerothanassis, I. P. (2007). Identification of the major constituents of *Hypericum perforatum* by LC/SPE/NMR and/or LC/MS. *Phytochemistry* 68, 383–393. doi:10.1016/j.phytochem.2006.11.026
- Tontonoz, P., and Spiegelman, B. M. (2008). Fat and beyond: The diverse biology of PPARgamma. *Annu. Rev. Biochem.* 77, 289–312. doi:10.1146/annurev.biochem.77.061307.091829
- Trinder, P. (1969). Determination of glucose in blood using glucose oxidase with an alternative oxygen acceptor. *Ann. Clin. Biochem. An Int. J. Biochem. laboratory Med. Ann. Clin. Biochem. An Int. J. Biochem. laboratory Med.* 6, 24–27. doi:10.1177/000456326900600108
- Wei, Y., Xie, Q., Fisher, D., and Sutherland, I. A. (2011). Separation of patuletin-3-O-glucoside, astragalin, quercetin, kaempferol and isorhamnetin from *Flaveria bidentis* (L.) Kuntze by elution-pump-out high-performance counter-current chromatography. *J. Chromatogr. A* 1218, 6206–6211. doi:10.1016/j.chroma.2011.01.058
- Yamauchi, T., Kamon, J., Waki, H., Terauchi, Y., Kubota, N., Hara, K., et al. (2001). The fat-derived hormone adiponectin reverses insulin resistance associated with both lipodystrophy and obesity. *Nat. Med.* 7, 941–946. doi:10.1038/90984
- Zafar, M., Sharif, A., Khan, D., Akhtar, B., Muhammad, F., Akhtar, M. F., et al. (2021). Preventive effect of *Euphorbia royleana* Boiss on diabetes induced by streptozotocin via modulating oxidative stress and deoxyribonucleic acid damage. *Toxin Rev.* 40, 777–790. doi:10.1080/15569543.2020.1780262



OPEN ACCESS

EDITED BY

Aliyu Muhammad,
Ahmadu Bello University, Nigeria

REVIEWED BY

Murtala Bello Abubakar,
Usmanu Danfodiyo University, Nigeria
Gilead Forcados,
National Veterinary Research Institute
(NVRI), Nigeria

*CORRESPONDENCE

Said Moshawih,
✉ saeedmomo@hotmail.com
Bey Hing Goh,
✉ goh.bey.hing@monash.edu
Andi Hermansyah,
✉ andi-h@ff.unair.ac.id

[†]These authors have contributed equally
to this work

RECEIVED 09 March 2023

ACCEPTED 06 June 2023

PUBLISHED 20 June 2023

CITATION

Shaik Mohamed Sayed UF, Moshawih S,
Goh HP, Kifli N, Gupta G, Singh SK,
Chellappan DK, Dua K, Hermansyah A,
Ser HL, Ming LC and Goh BH (2023),
Natural products as novel anti-obesity
agents: insights into mechanisms of
action and potential for
therapeutic management.
Front. Pharmacol. 14:1182937.
doi: 10.3389/fphar.2023.1182937

COPYRIGHT

© 2023 Shaik Mohamed Sayed,
Moshawih, Goh, Kifli, Gupta, Singh,
Chellappan, Dua, Hermansyah, Ser, Ming
and Goh. This is an open-access article
distributed under the terms of the
[Creative Commons Attribution License
\(CC BY\)](https://creativecommons.org/licenses/by/4.0/). The use, distribution or
reproduction in other forums is
permitted, provided the original author(s)
and the copyright owner(s) are credited
and that the original publication in this
journal is cited, in accordance with
accepted academic practice. No use,
distribution or reproduction is permitted
which does not comply with these terms.

Natural products as novel anti-obesity agents: insights into mechanisms of action and potential for therapeutic management

Ummul Fathima Shaik Mohamed Sayed^{1†}, Said Moshawih^{1*†},
Hui Poh Goh¹, Nurolaini Kifli¹, Gaurav Gupta^{2,3},
Sachin Kumar Singh^{4,5}, Dinesh Kumar Chellappan⁶,
Kamal Dua^{4,7,8}, Andi Hermansyah^{9*}, Hooi Leng Ser¹⁰,
Long Chiau Ming^{1,9,10} and Bey Hing Goh^{11,12*}

¹PAPRSB Institute of Health Sciences, Universiti Brunei Darussalam, Gadong, Brunei, ²School of Pharmacy, Suresh Gyan Vihar University, Jaipur, India, ³Department of Pharmacology, Saveetha Institute of Medical and Technical Sciences, Saveetha Dental College and Hospitals, Saveetha University, Chennai, India, ⁴Faculty of Health, Australian Research Centre in Complementary and Integrative Medicine, University of Technology Sydney, Ultimo, NSW, Australia, ⁵School of Pharmaceutical Sciences, Lovely Professional University, Phagwara, India, ⁶Department of Life Sciences, School of Pharmacy, International Medical University, Kuala Lumpur, Malaysia, ⁷Discipline of Pharmacy, Graduate School of Health, University of Technology Sydney, Ultimo, NSW, Australia, ⁸Uttaranchal Institute of Pharmaceutical Sciences, Uttaranchal University, Dehradun, India, ⁹Department of Pharmacy Practice, Faculty of Pharmacy, Universitas Airlangga Surabaya, Indonesia, ¹⁰School of Medical and Life Sciences, Sunway University, Sunway, Malaysia, ¹¹Biofunctional Molecule Exploratory Research Group, School of Pharmacy, Monash University Malaysia, Bandar Sunway, Malaysia, ¹²College of Pharmaceutical Sciences, Zhejiang University, Hangzhou, China

Obesity affects more than 10% of the adult population globally. Despite the introduction of diverse medications aimed at combating fat accumulation and obesity, a significant number of these pharmaceutical interventions are linked to substantial occurrences of severe adverse events, occasionally leading to their withdrawal from the market. Natural products serve as attractive sources for anti-obesity agents as many of them can alter the host metabolic processes and maintain glucose homeostasis via metabolic and thermogenic stimulation, appetite regulation, pancreatic lipase and amylase inhibition, insulin sensitivity enhancing, adipogenesis inhibition and adipocyte apoptosis induction. In this review, we shed light on the biological processes that control energy balance and thermogenesis as well as metabolic pathways in white adipose tissue browning, we also highlight the anti-obesity potential of natural products with their mechanism of action. Based on previous findings, the crucial proteins and molecular pathways involved in adipose tissue browning and lipolysis induction are uncoupling protein-1, PR domain containing 16, and peroxisome proliferator-activated receptor- γ in addition to Sirtuin-1 and AMP-activated protein kinase pathway. Given that some phytochemicals can also lower proinflammatory substances like TNF- α , IL-6, and IL-1 secreted from adipose tissue and change the production of adipokines like leptin and adiponectin, which are important regulators of body weight, natural products represent a treasure trove for anti-obesity agents. In conclusion, conducting comprehensive research on natural products holds the potential to accelerate the development of an improved

obesity management strategy characterized by heightened efficacy and reduced incidence of side effects.

KEYWORDS

obesity, medicinal plants, adipogenesis, white adipose tissue, brown adipose tissue, WAT browning

1 Introduction

Obesity poses a serious threat to worldwide public health and is defined by a Body mass index (BMI) of 30 kg/m² or higher (Lin and Li, 2021). Obese individuals are at risk of developing various chronic diseases, such as diabetes mellitus, hypertension, cancer, and neurological disorders, which could be severely impacted by the buildup of excess body fat (WHO, 2021). According to the World Health Organization (2021), 13% of the adult population worldwide was obese in 2016, a figure that has tripled since 1975. Currently, more than 1.9 billion adults are overweight (with BMI of 25.0–29.9) and more than 650 million are considered obese (Haththotuwa et al., 2020). In Europe, around 23% of women and 20% of men are obese. In Western nations, the prevalence of obesity and type 2 diabetes mellitus (T2DM) are on the rise (WHO, 2022). Decades of research have been devoted to understanding the relationship between obesity and metabolic problems, as well as the connection between obesity and adipose tissue, which is considered a metabolically active endocrine organ (Xu et al., 2003; Wang Q. et al., 2015; Jiang et al., 2020). As a matter of fact, adipose tissue is also involved in other functions such as the regulation of glucose and lipid metabolism, insulin sensitivity, inflammatory response, non-shivering thermogenesis, and vascular endothelial function (Kwok et al., 2016).

A growing body of research suggests that the dysfunction in adipose tissue drives the development of obesity (Sam and Mazzone, 2014). In general, there are two main types of adipose tissue: a) white adipose tissue (WAT) which is widely distributed in the human body, and b) brown adipose tissue (BAT) which is found in the cervical, supraclavicular, axillary, paravertebral, mediastinal, and upper abdominal regions in adult humans (Maurer et al., 2021). Majority of WAT stored in the subcutaneous region in deep and superficial abdominal parts and the gluteal-femoral regions, but there are also some distribution of WAT in the visceral region such as in the omental, mesenteric, mediastinal, and epicardial regions (Sbarbati et al., 2014). Under the skin, subcutaneous WAT serves as a buffer against mechanical stress from the outside world, and an insulator to keep heat in and prevent dermal infection. On the other hand, visceral WAT wraps around internal organs inside the peritoneum and the rib cage (Zwick et al., 2018). The central role of WAT is to store excess energy as triglycerides which is antagonistic to the function of brown adipose tissue (BAT), which dissipates energy by producing heat and warms up the blood supply to vital organs (Saely et al., 2012). The brown appearance of BAT is due to the presence of high mitochondrion content and dense vascularization. Uncoupled protein 1 (UCP-1) is employed in the inner membrane of the mitochondria to help BAT use and dissipate the energy derived from lipids to generate heat (Cannon and Nedergaard, 2004).

In addition to its role as an energy storage organ, WAT plays major role in obesity because these cells secrete unique regulatory substances with endocrine, paracrine, and autocrine functions (Fruhbeck et al., 2001). Several substances secreted by adipocytes play significant roles in various aspects of physiological control. For instance, leptin and adiponectin contribute to body weight regulation, while TNF- α , IL-6, and IL-1 β are associated with local inflammation resulting from obesity. Additionally, substances like Ang II and PAI-1 impact vascular function, and estrogens are involved in reproductive processes (Gómez-Hernández et al., 2016). WAT modulates metabolic activities in other peripheral tissues and the brain by secreting adipocytokines such as leptin and adiponectin (Kershaw and Flier, 2004). Leptin, a hormone that is mostly secreted by adipocytes, plays an important role in controlling body weight via its central effects on hunger and peripheral effects on regulating energy expenditure (Marti et al., 1999). Adiponectin is another hormone secreted by adipocytes that regulates food intake. Several investigations have reported hypoadiponectinemia in individuals with obesity, diabetes, and coronary artery disease (Arita et al., 1999). Consequently, restoring the regulatory function of WAT appears to be a viable strategy for combating obesity.

Apart from that, numerous studies have pointed out the presence of a subpopulation of WAT that has adapted characteristics of BAT, such as increased UCP-1 expression, adipocyte locularity, mitochondrion density, and vascularization, is known as brite or beige adipose tissue (Harms and Seale, 2013). The process that involves the browning of WAT or what is termed adaptive thermogenesis is usually triggered by low temperatures. In healthy adult humans, metabolically active adipose tissue depots with beige-like features were found in the cervical, supraclavicular, axillary, and paravertebral regions (Nedergaard et al., 2007). The reprogramming of WAT to BAT or even beige adipose tissue garnered much interest in the scientific community as this conversion constitutes a great opening to tackle obesity by increasing energy expenditure and restoring glucose homeostasis balance (Kuryłowicz and Puzianowska-Kuźnicka, 2020).

As an alternative to conventional treatments against obesity and associated problems, natural products, such as medicinal plants in the form of pure compounds or extracts, are widely accessible on the market (Hasani-Ranjbar et al., 2013). Phytochemicals can exert their anti-obesity effects through different mechanisms such as inhibiting digestive enzyme activities (pancreatic lipase and amylase), appetite regulation, and reducing the formation of WAT or increasing WAT browning (Fu et al., 2016). Moreover, the phytoconstituents found in diverse plants have proven to possess a range of additional mechanisms of actions against obesity, including promoting PPAR- α and PPAR- β expression, suppressing ghrelin, and regulating plasma lipid profile (Raouf and Kareem, 2020). Certain nutritional compounds isolated from fruits, vegetables, and edible

plants, such as curcumin from turmeric (Lee et al., 2011), anthocyanins from blueberries, epigallocatechin gallate from green tea and nobiletin from citrus peel, have been found to be useful in treating metabolic diseases (Chan et al., 2021). Typically, these natural substances limit adipose tissue formation by inhibiting adipocyte differentiation and adipogenesis and lowering triacylglycerol levels by boosting lipolysis or decreasing lipogenesis pathways (Sun et al., 2016). The current review aims to an overview of the numerous types of adipose tissues and their specific functions prior to discussing the possibility of natural products to reduce obesity based on their mechanism of action. The current review also presents how certain natural products influence main molecular pathways involved in WAT browning and elucidated action mechanisms that are associated with energy homeostasis and thermogenesis.

1.1 Energy balance and thermogenesis by different adipose tissues

Thermogenesis is essential for the survival of homeotherms. At thermoneutrality or 23°C for an adult man, obligatory thermogenesis is sufficient to sustain normal body temperature and function (Silva, 2003). Adaptive thermogenesis, also known as facultative thermogenic mechanisms requiring or not requiring shivering, is initiated when the ambient temperature falls below thermoneutrality (Yau et al., 2020). The shivering thermogenesis responds to cold by contracting the skeletal muscles to generate heat; this boosts the resting metabolic rate by five-fold in humans (Eyolfson et al., 2001), but it cannot be sustained for an extended period of time (Periasamy et al., 2017). In contrast, non-shivering thermogenesis occurs predominantly in BAT, which oxidizes lipids by activating the lipase enzyme and releases energy as heat during prolonged exposure to cold (Cannon and Nedergaard, 2010). Besides the free fatty acids released from triglycerides by lipases via β -oxidation in BAT, β 3-adrenergic receptors (β 3-AR) present in brown adipocytes increase the expression of thermogenic marker Uncoupling protein 1 (UCP-1) protein via protein kinase A (Tan et al., 2011). Upon activation, these UCP-1 proteins in the inner mitochondrial membrane of brown and beige adipocytes translocate protons (H^+) from the intermembrane space into the mitochondrial matrix. This increases the respiratory chain activity and diminishes the proton motive force utilized by ATP synthase. Due to the conversion of the available energy from substrate oxidation, heat is created (Nicholls, 2006).

1.2 Major metabolic pathways in WAT browning

A condition known as “white fat browning” occurs when specific white adipose tissue drastically raise their gene expression and production of proteins such as the UCP-1 protein, thus, giving them the ability to burn fat and produce energy. White adipocyte browning results in the formation of beige also known as brite adipocytes that resemble the brown adipocyte phenotype but are present within the WAT. The conversion of white adipocytes into beige adipocytes may be caused by various stimuli (Bargut et al.,

2017). Subcutaneous adipocytes are more likely to undergo browning than visceral adipocytes because they are predominantly smaller and have a greater potential to differentiate (Gustafson and Smith, 2015). UCP-1 protein has key roles in thermogenesis, nonetheless, it depends on the tissue and the type of stimulus. As reviewed previously, UCP-1 protein levels in mitochondria isolated from the “white” adipose depot of cold-induced adipocytes were nearly identical to those in brown-fat mitochondria. The thermogenic function of UCP-1 protein was evidenced by UCP-1-dependent thermogenesis with lipid or carbohydrate substrates by increasing the canonical guanosine diphosphate (GDP) sensitivity. The thermogenic density of WAT measured by UCP-1-dependant oxygen consumption of WAT was one-fifth that of brown adipose tissue, and the overall quantitative contribution of all white-fat mitochondria was one-third that of brown adipose tissue, indicating that the conventional brown adipose tissue depots would still dominant in thermogenesis (Shabalina et al., 2013; Ikeda and Yamada, 2020). Among the widely studied pathways for stimulating the browning of white adipocytes are the actions of norepinephrine, which is released by sympathetic nerve terminals and binds with β -adrenergic receptors mainly β 3-AR found on the surface of adipocytes to carry out its functions (Otton et al., 2021).

Stimulation of β 3-AR causes the p38 mitogen-activated protein kinase (p38 MAPK) to stimulate activating transcription factor 2 (ATF-2), thus leading to the transcription of peroxisome proliferator-activated receptor gamma coactivator 1 α (PGC-1 α) (Robidoux et al., 2005). Later, PGC-1 α promotes two pathways leading to the formation of brite adipocytes; mitochondrial biogenesis and peroxisome proliferator-activated receptors (PPAR) activation (Hondares et al., 2011). In mitochondrial biogenesis, the PGC-1 α activates nuclear respiratory factor 1 (NRF1), which links the nucleus with the mitochondrion and generates mitochondrial replication through mitochondrial transcription factor A (TFAM) activation (Piantadosi and Suliman, 2006). Whereas the three isoforms of PPAR, α , β , and γ , are involved in the transcription of UCP1 (Barbera et al., 2001). This protein is present in the inner mitochondrial membrane as a thermogenesis effector, indicating that mitochondrial biogenesis is required for inducing brite adipocytes. It was found that thermogenic-activated brite adipocytes have a considerable number of mitochondria throughout their cytoplasm (Rossato et al., 2014; Jeremic et al., 2017). Also, the PPAR α and β release fatty acids that have multiple roles such as activating UCP-1 and acting as substrates for UCP-1-mediated thermogenesis (Cannon and Nedergaard, 2004), as well as, modulating the transcriptional control (Villarroya et al., 2007). PPAR γ is important for adipocyte differentiation (Wu et al., 1999a). It regulates adipogenesis and genes that are involved in the uptake and storage of FAs in WAT (Hansen and Kristiansen, 2006). Furthermore, PGC-1 α is a cofactor for the receptor PPAR γ , which is required for adaptive thermogenesis in response to decreasing temperatures and is associated with tissue-specific metabolic pathways in the adaptive response to nutritional and environmental stimuli (Ruschke et al., 2010).

Moreover, the commonly agreed pathways that take part in differentiating brite adipocytes from white adipocytes is by detecting the expression of UCP-1 and PR domain containing 16 (PRDM16)

(Spiegelman, 2013). It is worth noting that UCP-1 is the protein responsible for thermogenesis, while PRDM16 acts as a stimulus that maintains the brite adipocyte phenotype (Shabalina et al., 2013). It has been shown that at low PRDM16 expression, the brite adipocytes convert back to white adipocytes, thus, PRDM16 is an important molecule for inducing browning and maintaining the thermogenic activity of brite adipocytes (Cohen et al., 2014). The importance of PRDM16 in the browning of subcutaneous white adipocytes is shown by *in vitro* decreasing the amount of small hairpin RNA expressed by PRDM16, which results in a decrease in the expression of thermogenic genes and uncoupled respiration (Seale et al., 2011). The PRDM16 is involved in both the induction of BAT genes and the repression of WAT genes. The induction of BAT-specific genes occurs when PRDM16 binds to the transcriptional coactivators PGC-1 α and PGC-1 β . Contrarily, the repression of WAT-specific genes is caused by the interaction of PRDM16 with C-terminal binding protein (CtBP) 1 and 2 at the promoter domains of WAT genes (Kajimura et al., 2008). In response to cold, overfeeding in addition to chronic activation of PPAR γ , and PRDM16 facilitates the activation of PGC-1 α and UCP-1 in WAT by suppressing white fat genes (Seale et al., 2011) (Figure 1).

SIRT1 is a crucial regulator involved in WAT browning (Qiang et al., 2012) and it facilitates erythropoietin production to enhance metabolic activity (Wang et al., 2013). SIRT1 suppresses WAT by inhibiting the nuclear receptor PPAR γ (Tamori et al., 2002). PPAR γ stimulates the binding of CCAAT/enhancer-binding protein (C/EBP α) and CtBP (1 and 2) and inhibits transcription of WAT-specific genes (Vernochet et al., 2009). It has been reported that browning of subcutaneous WAT is promoted by SIRT1-dependent PPAR γ deacetylation via the regulation of ligand-dependent coactivator or corepressor exchange at PPAR γ transcriptional complex. Additionally, SIRT1-dependent PPAR γ deacetylation is found to regulate energy homeostasis, and promote energy expenditure from energy storage (Qiang et al., 2012). Other than that, SIRT1 promotes threonine phosphorylation, which activates the AMPK signaling pathway and AMPK is known to play a key role in the initiation of adipocyte lipolysis. Besides, PPAR α is activated by AMPK via the PGC-1 α ligand, which in turn upregulates the gene expression of several key β -oxidation enzymes and promotes fatty acid oxidation (Liu L. et al., 2020). Genes that are responsible for thermogenesis such as UCP1 and PGC-1 α , are found to be related by AMPK activation, while SIRT1 was found to promote mitochondrial biogenesis through the activation of PGC-1 α (Wu et al., 1999b). In conclusion, the upregulation of SIRT1 mRNA, which reduces PPAR γ , was linked to the downregulation of adipogenesis (Feng et al., 2016).

2 Pharmacological treatment for obesity

Individuals who are overweight or obese may benefit from bariatric surgery, pharmaceutical treatment, behavioral modifications, and dietary changes, among others. General practitioners and multidisciplinary support teams are vital in assisting patients in losing weight in a healthy, long-term manner. Life expectancy drops by 1 year for every two

percentage points increase in its average BMI, accordingly to a modeling study (Semlitsch et al., 2019). Therefore, structured guidelines were developed to create a clinical pathway for the management of overweight and obesity in primary care as reviewed by (Semlitsch et al., 2019). Numerous drugs, such as serotonin receptor agonists have been discovered to be useful in weight loss. In the 1970s, it was revealed that serotonin or 5-hydroxytryptamine (5-HT) possesses anorectic properties, as heightened brain serotonin levels was associated with increased satiety (Blundell, 1977). For instance, fenfluramine and d-fenfluramine, which are the direct agonists of 5-HT receptors exhibited anti-obesity properties by increasing the release of serotonin in the synaptic cleft. Both compounds modify eating behavior in a manner consistent with satiety (Halford et al., 2005). However, these medications were taken off the market due to arising valvular heart disease (Elliot and Chan, 1997). On the other hand, selective serotonin reuptake inhibitors (SSRIs) could also be administered to increase serotonin levels in obesity treatment by blocking its reuptake into the nerve terminals (Leibowitz et al., 1990). The SSRI fluoxetine decreases food intake and improves satiety feeling (Halford et al., 1998), but it may induce adverse symptoms such as headache, nausea, somnolence, asthenia, diarrhea, sleeplessness, anxiety, sweating, and tremor (Wise, 1992). In addition, 30%–70% of individuals using fluoxetine experienced sexual dysfunction, including erectile dysfunction, anorgasmia, and diminished libido, resulting in non-compliance with the treatment (Colman et al., 2012; Wenthur et al., 2014). Another compound from this class with anti-obesity has been used is sibutramine, which works similarly like fluoxetine as SSRI, but sibutramine also blocks the reuptake of norepinephrine and partially dopamine, both of which have been shown to have anorectic effects *in vivo* (Balcioglu and Wurtman, 2000). However, sibutramine was pulled off the market due to the increased risk of cardiovascular disease in obese patients (Czernichow and Batty, 2010).

Differently, rimonabant, a Cannabinoid receptor type 1 (CB1) antagonist has been used in the management of obesity. In response to fasting, the two potent appetite-stimulating hormones, cannabinoid and ghrelin, are known to rise in concentration in the gastrointestinal tract. The administration of CB1 receptor inverse agonist leads to decreased levels of these two hormones, which subsequent resulting in decreased food intake as observed in the 24-h food-starved rats and partially satisfied rats (Gómez et al., 2002). Rimonabant also prevents fat storage in adipocytes by regulating the level of adipose tissue lipoprotein lipase, which is augmented by cannabinoid treatment (Bensaid et al., 2003). Despite that, in Europe and India, rimonabant was withdrawn from the market in 2007 owing to its unwanted psychiatric side effects which included anxiety and depression (Onakpoya et al., 2016).

At the time of writing, orlistat is the only anti-obesity medication that functions independently of the central nervous system and does not enter the bloodstream. In addition, it is the only pancreatic lipase inhibitor treatment that is presently being used in clinical practice (Ballinger and Peikin, 2002). In order to exert its therapeutic effect, it forms a covalent connection with the active serine residue of gastric and pancreatic lipases in the lumen of the digestive system. This action then prevents the hydrolysis of dietary fat (in the form of triglycerides) into absorbable free fatty acids and monoglycerols

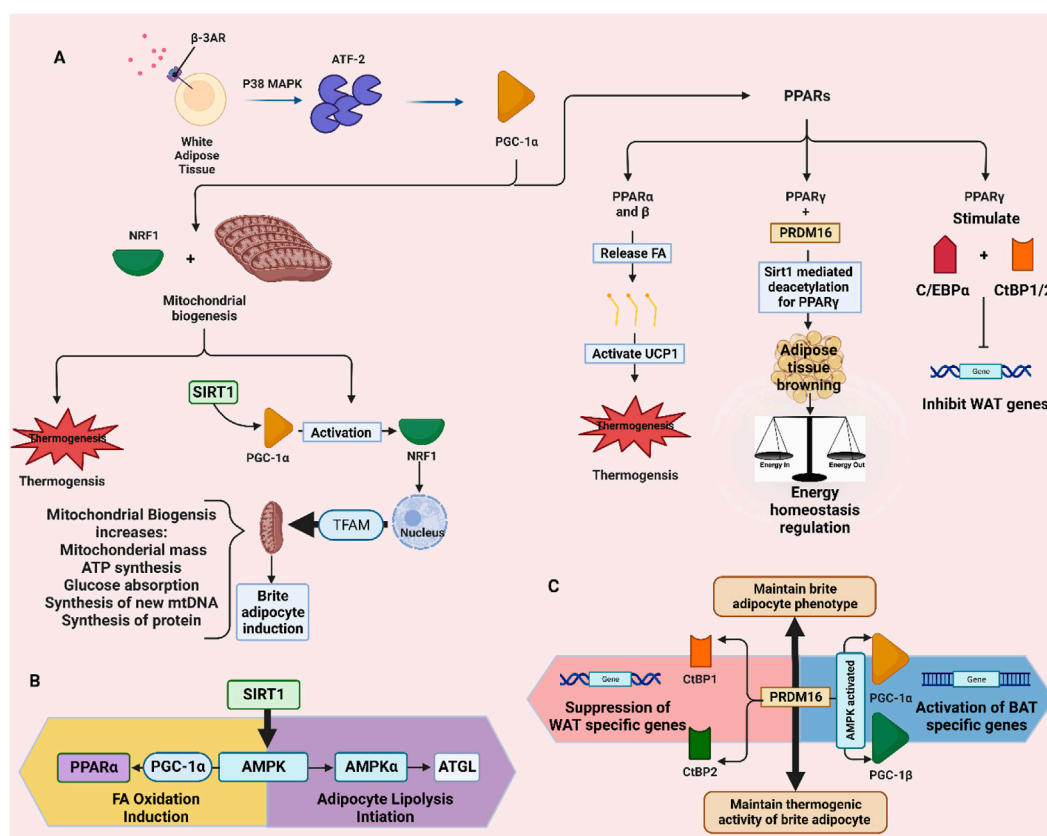


FIGURE 1

Pathways involved in the browning of white adipose tissue and producing brite adipocytes. (A) stimulation of thermogenesis and adipose tissue browning through PPARs and mitochondrial biogenesis. (B) SIRT1-AMPK pathway for lipolysis and fatty acid oxidation. (C) PRDM16-CtBP1/2 and -PGC-1 α and β pathways for suppressing WAT genes and activating BAT genes. ATGL: adipose triglyceride lipase.

(Ransac et al., 1991). The side effects associated with orlistat commonly emerge during the initial stages of therapy and tend to attenuate with the progression of treatment. The gastrointestinal tract is primarily affected by these side effects, which can include the presence of oily stool (Liu T.-T. et al., 2020). Another anti-obesity drug that is currently available is liraglutide, which is a glucagon-like peptide-1 (GLP-1) receptor agonist. The weight reduction effects of GLP-1 are assumed to be due to appetite suppression and delayed stomach emptying (Jelsing et al., 2012). The common adverse events of liraglutide involve the gastrointestinal tract such as nausea (Burcelin and Gourdy, 2017). In clinical studies, gastrointestinal intolerance was the most frequent reason for liraglutide discontinuation in individuals reported adverse events (Mehta et al., 2017). Meanwhile, exenatide, another GLP-1 agonist approved for obesity treatment, showed a higher reduction in body weight when lifestyle modifications were adopted (Rosenstock et al., 2010).

3 Plant-derived natural products as anti-obesogenic agents

Having seen the adverse effects caused by the bulk of the drugs now used for the treatment of obesity, researchers are now turning to

natural resources in a quest of compounds with fewer side effects for the management of obesity. Plant-derived natural products have been demonstrated to have anti-obesity effects via a variety of pathways, including metabolic and thermogenic stimulants, appetite regulators, pancreatic lipase and amylase inhibitors, insulin sensitivity enhancers, and adipogenesis inhibitors and adipocytes apoptosis inducers.

3.1 Plant-derived natural products as metabolic and thermogenic stimulants

Natural products such as caffeine, ephedrine, capsaicin, and green tea have been suggested for obesity management since they may increase energy expenditure and counterbalance the decrease in metabolic rate that occurs with/after weight loss (Figure 2). Despite being in the same category, the combination of caffeine and ephedrine assists people to lose weight over the long run (Astrup et al., 1992). This is likely due to the fact that two substances inhibit different enzymes that may work synergistically, as the former exerts its effect by inhibiting cAMP degradation caused by phosphodiesterase, while the latter stimulates metabolism by enhancing catecholamine release in the sympathetic nervous system (Diepvens et al., 2007a).

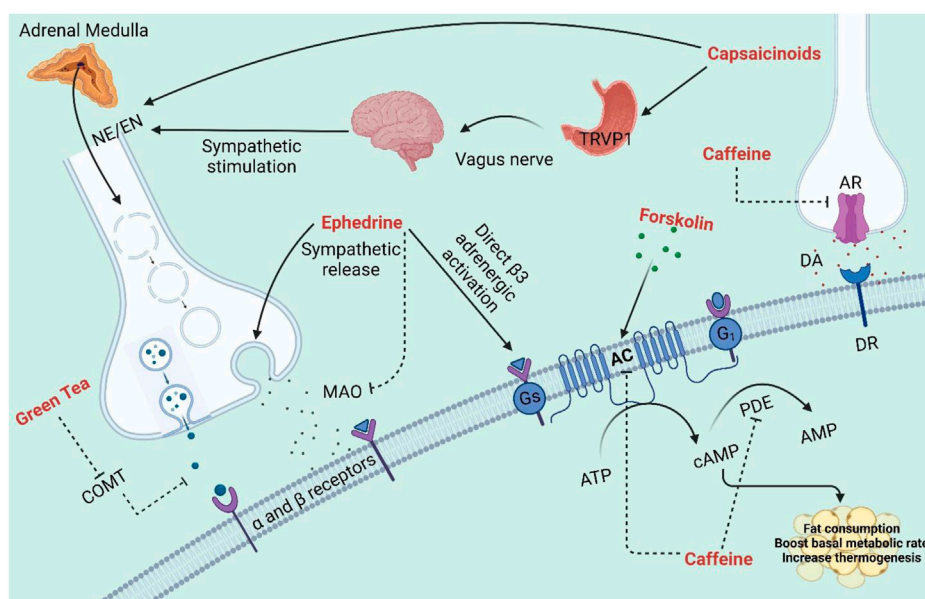


FIGURE 2

The effects of several NPs on diverse physiological pathways as metabolic and thermogenic stimulants. AC: Adenyl cyclase; AR: Adenosine receptor; DA: Dopamine; DR: Dopamine receptors; MAO: Monoamine oxidase; PDE: Phosphodiesterase; TRPV1: Transient receptor potential vanilloid-1; NE: Norepinephrine; EN: Epinephrine; COMT: Catechol-O-methyltransferase.

3.1.1 Caffeine from *Coffea arabica*

Caffeine is the most consumed stimulant worldwide due to its various effects and mechanisms of action (Ferreira et al., 2019). In fact, the two most used coffee beans in the genus *Coffea* are *Coffea arabica* L. and *Coffea canephora* Pierre. Caffeine has been explored as a possible thermogenic agent for body weight reduction and it may alter thermogenesis by preventing the phosphodiesterase-induced degradation of intracellular cyclic AMP (cAMP) (Diepvens et al., 2007b). In the liver, one of the enzymes under the cytochrome P450 oxidase enzyme family, CYP1A2 metabolizes caffeine into three primary metabolites: paraxanthine (84%), theobromine (12%) and theophylline (4%) (Schwarzschild et al., 2003). Due to the structural similarity, the primary pharmacological action of caffeine is to antagonize adenosine receptors and modulate the purinergic system (Van Dam et al., 2020). There are four types of adenosine receptors highly expressed in the human body, namely, A1, A2A, A2B and A3. A1 and A3 receptors inhibit adenylyl cyclase by binding to Gi proteins, whereas A2A and A2B stimulates cAMP production by binding Gs protein (Ortweiler et al., 1985). These receptors have been linked to numerous physiological and pathological processes, including heart rhythm and circulation, lipolysis, renal blood flow, immunological function, sleep regulation, angiogenesis, inflammatory diseases, ischemia-reperfusion, and neurodegenerative disorders (Chen et al., 2013).

3.1.2 Ephedrine from *Ephedra sinica*

Ephedrine is one of the four isomers contained in the shrub known as *Ephedra sinica* which is native to China and Mongolia (Saper et al., 2004). It is a phenylpropylamine protoalkaloid and a sympathomimetic agent that functions as a stimulant and a thermogenic agent (Stohs and Badmaev, 2016). Ephedrine

increases energy expenditure and promotes weight loss, as reported in several human studies (Astrup, 2000). The main thermogenic effect of ephedrine is mediated by increasing the sympathetic neuronal release of norepinephrine (NE) and epinephrine (Dulloo, 1993). By inhibiting monoamine oxidase, ephedrine also decreases the breakdown of norepinephrine. The interaction of ephedrine with β-3 adrenergic receptors is implicated in the induction of thermogenesis that promotes breakdown of fats and glucose metabolism modulation (Carey et al., 2015). Similarly, the interactions of ephedrine with β-1 and β-2 adrenergic receptors have also been shown to contribute to some of its thermogenic effects (Liu et al., 1995).

3.1.3 Capsaicinoids from *Capsicum annuum*

Hot red peppers of the species *Capsicum annuum* L. (*Capsicum frutescens*), contain a group of pungent chemicals known as capsaicinoids with capsaicin being the primary pungent component (Barceloux, 2009). According to studies conducted by Reinbach et al. (2010) and Ludy et al. (2012), capsaicin has been found to increase the production of catecholamines, norepinephrine, and epinephrine from the adrenal medulla, which in turn stimulates thermogenesis by acting on adrenergic receptors (Reinbach et al., 2010; Ludy et al., 2012). However, capsaicinoids also have the capacity to modify metabolism through the activation of transient receptor potential vanilloid 1 (TRPV1) receptors, where they are similarly thought to be able to enhance energy expenditure and reduce body fat by boosting catabolic processes in adipose tissues (Yoneshiro and Saito, 2013). Numerous studies in small mice have shown that capsaicin and capsinoids stimulate sympathetically-mediated BAT

thermogenesis and decrease body fatness (Saito, 2015). Notably, it has been found that a single intraperitoneal or intragastric dose of capsaicin or capsinoids can increase the whole-body energy expenditure, activates the adreno-sympathetic nervous system, increases BAT temperature, and increase the core temperature which is all produced in hours (Kawada et al., 1986; Ono et al., 2011). Most of these reactions are significantly diminished in mice lacking TRPV1 or by β -adrenergic inhibition (Kawabata et al., 2009). In one study, it was found that red pepper-containing meals resulted in a greater increase in energy expenditure than control meals (Yoshioka et al., 1995). Additionally, research in both human and non-human animals revealed that an increase in thermogenesis is disrupted when a β -adrenergic blocker like propranolol is administered (Kawada et al., 1986), suggesting that capsaicin-induced thermogenesis is probably based on β -adrenergic activation. Capsaicin administration leads to a rise in lipid mobilization and a fall in adipose tissue bulk (Kawada et al., 1986). It is also found to cause WAT browning by activating SIRT's CaMKII/AMPK-dependent phosphorylation, which stimulates SIRT1. This led to the deacetylation and interaction of proteins to stimulate the browning of WAT in the mouse model (Baskaran et al., 2016).

3.1.4 Forskolin from *Coleus barbatulus*

Forskolin is a labdane diterpene isolated from the roots of the *Coleus forskohlii* Briq, belonging to the Labiatae family (Lamiaceae), which is native to India, while *Plectranthus barbatulus* and *Coleus forskalaei* (Lamiaceae) thought to be the most prevalent species contains forskolin. (Astell et al., 2013). Forskolin acts directly on adenylate cyclase enzyme, which increases cAMP level and eventually drives the lipolysis or the breakdown of fat in adipose tissues (Litosch et al., 1982). Subsequently, fatty acids released from adipose tissue depot also trigger thermogenesis and an increase in the lean tissue. Overall, forskolin may result in a fat reduction without loss of muscle mass (Godard et al., 2005).

3.1.5 Green tea extracts from *Camellia sinensis*

As the most consumed beverage in Southeast Asia, green tea is the decoction of the plant *Camellia sinensis* L. (belonging to the family Theaceae) (Thitimuta et al., 2017). Consuming green tea and green tea extracts have been shown in several studies to improve thermogenesis and fat oxidation (Dulloo et al., 2000; Diepvens et al., 2007b; Westerterp-Plantenga, 2010a; Türközü and Tek, 2017). The composition of green tea extract responsible for the thermogenic effect includes catechins such as epicatechin, epicatechin gallate, epigallocatechin, and epigallocatechin gallate (EGCG); among which, EGCG is the most prevalent catechins, ranges from 50% to 80% of total catechins (Stohs and Badmaev, 2016). It is hypothesized that catechins, especially EGCG, directly inhibit catechol-O-methyltransferase, an enzyme that breaks down norepinephrine, in order to enhance fat oxidation (Borchardt and Huber, 1975). This transient rise in sympathetic nervous system activity results in elevated catecholamine levels, which may enhance fatty acid mobilization and oxidation (Figure 1). Despite the frequent implications of this mechanism in previous studies, there is no clear evidence to support this theory (Jeukendrup and Randell,

2011). Nonetheless, green tea may regulate the PPAR/FGF21/AMPK/UCP1 pathway, which then enhance thermogenic cells induction by reprogramming the first phase of adipocyte differentiation (Bolin et al., 2020). Furthermore, green tea aqueous extract is shown to promote browning markers in inguinal WAT (Li et al., 2021). In line with this, the aqueous extract of green tea markedly increased PGC-1 α activation. This transcriptional activation controls the UCP-1 promoter's activity which increases thermogenesis, fat consumption, and basal metabolic rate (Boström et al., 2012). It was revealed that EGCG-induced adipogenesis suppression could involve the mitogen-activated protein (MAP) kinase, specifically the extracellular signal-regulated kinases (ERKs) which are activated by growth-related signals (Lin et al., 2005).

3.2 Plant-derived natural products as appetite regulators

Food intake is influenced by hunger, satiety, and the physiological mechanisms that balance eating with internal caloric supplies and stable body weight (Sayan and Soumya, 2017). Indeed, anorexic or anorectic agents suppress appetite and reduce body weight, via acting on the satiety centre in the central nervous system, hypothalamus and altering crucial pathways in the neuroendocrine system as well as the brain-gut connection. Various anti-obesity medications including anorexic substances were sold in the past; however, they have all been discontinued due to serious side effects. For instance, the widely used appetite suppressant, sibutramine, was prohibited as anti-obesity agent by Food and Drug Administration and European Medicines Agency due to adverse cardiovascular effects and was discontinued in many countries (James et al., 2010). For further understanding of the mechanism of appetite regulation of pharmacological medicines, it has been found that mild stimulants, such as diethylpropion, phentermine, and bupropion, suppressed food intake, caused weight loss, and modulated neural activity in the nucleus accumbens shell (NAcSh) (Perez et al., 2019), a brain area with strong dopaminergic innervation involved in feeding, sleep, and locomotor behavior (Tellez et al., 2012). It was shown that D1- and D2-like Dopamine (DA) receptor antagonists significantly decreased their anorectic and weight loss effects, contradicting the assumption that they primarily function via norepinephrine and serotonin neurotransmitters (Kalyanasundar et al., 2015). Nonetheless, these drugs are too present some side effects with contraindications for individuals with heart diseases, diabetes, pregnancy, seizure, uncontrolled hypertension, opioid or monoamine oxidase inhibitor use, and may cause vomiting, constipation, dry mouth, or suicidal thoughts (Grunvald et al., 2022). Various phytochemicals aid in inhibiting appetite, with some appetite suppressants having additional benefits such as the browning of WAT that boosts its weight loss efficiency with fewer adverse events encountered as found with the pharmacological intervention (Figure 3).

3.2.1 Khat extracts from *Catha edulis*

Resembling the effect of amphetamine, Khat is a naturally occurring stimulant that is derived from the leaves or young

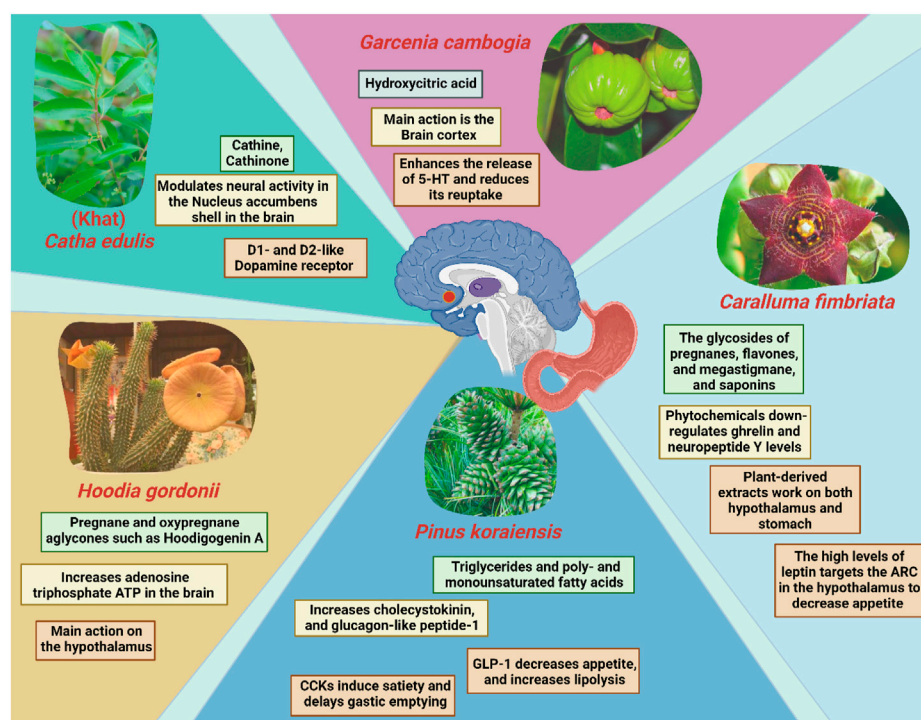


FIGURE 3

Mechanism of action(s) involved in reducing appetite and/or inducing the feeling of satiety exerted by selected plants and their main chemical constituents. ARC; The arcuate nucleus of the hypothalamus; GLP-1: Glucagon-like peptide-1; CCK: Cholecystokinin.

shoots of a flowering plant, *Catha edulis* which is grown in East Africa and the Arabian Peninsula. Although the appetite-suppressing properties of the synthetic amphetamine class stimulants such as pure amphetamine (AMPH) are well known, studies have implicated possibility of the malnutrition and low body mass index due to consumption of these stimulants (Lemieux et al., 2015). To date, very little is known regarding their natural counterpart “khat”. Nevertheless, cultural chewing practice using the leaves of the Khat plant has been known to have appetite-suppressing effects for many years (Halbach, 1972; Zelger and Carlini, 1980). The main active components of *C. edulis* are cathine (D-nor-pseudoephedrine) (NPE) and cathinone (1-aminopropiophenone) (Tucci, 2010). A recent study has supported the idea that NPE-induced food suppression were mediated by dopamine receptors (Fernandes et al., 2020). In another words, NPE has been suggested to have similar anorectic effects as other phenethylamine derivatives like diethylpropion, phentermine, bupropion, and cathinone. This is to no one's surprise, given that these drugs are all structurally linked to amphetamine and predicted to exert their effects via similar pathways (Khan et al., 2012).

3.2.2 Extracts from *Hoodia gordonii*

One of the most is *Hoodia gordonii*, commonly known as Bushman's hat or Kalahari cactus is a popular dietary supplement which is used extensively naturally derived appetite suppressants (Jain and Singh, 2013). It is a succulent plant that is native to Namibia and South Africa and is a member of the

Apocynaceae family (Bruyns, 2005). According to a study by Shukla and team, *H. gordonii* contains large amounts of pregnane, oxypregnane, and steroidal glycosides (Shukla et al., 2009). Numerous oxypregnane glycosides were retrieved from *H. gordonii*, such as P57AS3, also known as P57, which is notable for its common aglycone Hoodigogenin A (12-O-tigloyl-3, 14-dihydroxy-pregn-5-ene-20-one). Hoodigogenin A is suggested to be the substance that actively suppresses appetite and raises the amount of adenosine triphosphate ATP in hypothalamic neurons that control food intake (MacLean and Luo, 2004; Geoffroy et al., 2011). While consuming *H. gordonii* in powder supplements, tea, and energy bars appears to have the intended impact on appetite and weight loss, this effect may at least in part be a secondary effect of the substantial side effects linked to ingesting the large dosages necessary to reach therapeutic clinical benefit (Smith and Krygsman, 2014).

3.2.3 Extracts from *Caralluma fimbriata*

Caralluma adscendens var. *fimbriata* (Wall.), also commonly known as *Caralluma fimbriata* (*C. fimbriata*) is well spread in the dry regions of Asia (Dutt et al., 2012). It is an edible succulent cactus that naturally grows throughout India and is a well-known famine food, hunger suppressant, and thirst quencher (Kuriyan et al., 2007). According to a study, pregnane glycosides, flavone glycosides, megastigmane glycosides, bitter principles, saponins, and numerous other flavonoids are the main phytochemical components of *C. fimbriata*. Pregnane glycosides (Bader et al., 2003). In reality, these compounds are abundant in plants of the

Asclepiadaceae family and may account for Caralluma's appetite-suppressing effects (Schneider et al., 1993). Downregulation of ghrelin production in the stomach and neuropeptide Y (NPY) in the hypothalamus is associated with the appetite reduction effects of *C. fimbriata* extract (CFE), however the precise mechanism of action is yet to be understood fully (Gardiner et al., 2005; Komarnytsky et al., 2013). A clinical study was conducted in 140 overweight adults between 20 and 50 years of age to examine the effects of *C. fimbriata* extract on biomarkers of satiety and body composition (Rao et al., 2021a). There was a significant difference in plasma leptin concentration change between subjects who took the extract and those who did not at week 16. Also, subjects received the treatment had significantly reduced calorie intake from baseline, and consequently a lower waist circumference compared to the placebo group. Furthermore, an increased weight, fat mass, android fat mass, BMI, along with higher level of leptin were reported in the placebo group (when compared to baseline), but not those who undergone extract treatment.

3.2.4 Nut oil from *pinus koraiensis*

Korean pine nuts have a long history of consumption, notably in the Mediterranean and Asia. Fat constitutes over 60% of *Pinus Koraiensis* oil (PNO). The major constituents of PNO includes triglycerides, poly- and monounsaturated fatty acids (PUFAs and MUFAs), such as 4% palmitic acid, 28% oleic acid, 47% linoleic acid, and 14% pinolenic acid (Wolff et al., 2000). Consumption of Korean pine nut-free fatty acids (FFA) promotes release of the satiety hormone, cholecystokinin (CCK) (Pasman et al., 2008). CCK causes a delay in stomach emptying, which results in an enhanced sensation of fullness and a decrease in appetite. Long-chain fatty acids are more potent than medium-chain fatty acids at triggering the release of the satiety hormone, and PUFAs are more potent than MUFAs (McLaughlin et al., 1998). According to a study, CCK-8 and glucagon-like peptide-1 (GLP-1) levels have been demonstrated to rise after overweight postmenopausal women were given pine nut-free fatty acids (Tucci, 2010). In clinical investigations, Korean PNO reduced caloric consumption in overweight women (Hughes et al., 2008), enhanced the release of satiety hormones, and lowered appetite in post-menopausal overweight women (Pasman et al., 2008).

3.2.5 Hydroxycitric acid from *Garcenia cambogia*

Hydroxycitric acid (HCA), a popular natural weight loss drug derived from the dried fruit rind of the Southeast Asian tree *Garcinia cambogia* (family Guttiferae) (Ohia et al., 2002). The dried fruit rind is also referred to as Malabar tamarind, and it is widely utilized for culinary uses in southern India (Sergio, 1988). HCA is a competitive inhibitor of ATP citrate lyase that catalyzes the additional mitochondrial cleavage of citrate to oxaloacetate and acetyl-CoA (Ohia et al., 2002). Recent studies have shown that oral HCA supplementation (as Super CitriMax™, a calcium/potassium salt of 60% HCA that is tasteless, odorless, and extremely water soluble, HCA-SX) is highly bioavailable in human plasma, as determined by a gas chromatography-mass spectrometric approach (Loe et al., 2001). Additionally, HCA (as Super CitriMax™, HCA-SX) enhances the release of 5-HT from rat brain cortex slices

in vitro, allowing researchers to elucidate how HCA might reduce hunger (Ohia et al., 2001). By altering the neuronal absorption of this monoamine, HCA-SX is thought to enhance the release and accessibility of [³H]-5-HT from neuronal serotonergic nerve terminals. These results clearly imply that the influence on 5-HT might be the mechanism underlying the appetite reduction and food intake produced by HCA-SX since elevated brain levels of 5-HT are implicated in regulating sleep, mood changes, and appetite suppression (Ohia et al., 2002). This finally leads to weight reduction due to reduced food intake in addition to other mechanisms such as reduction in body fat percentage, triglycerides, cholesterol and glucose levels, and lipogenesis rate.

3.3 Plant-derived natural products as pancreatic lipase and amylase inhibitors

α -amylase is one of the digestive enzymes secreted by the pancreas and salivary glands. It is engaged in vital biological functions such as carbohydrate digestion, whereas its activity is inhibited by many crude drugs (Kobayashi et al., 2000). It has been shown that natural α -amylase inhibitors are beneficial in lowering post-prandial hyperglycemia by delaying the breakdown of carbohydrates and, as a result, reducing the absorption of glucose. Reducing post-prandial hyperglycemia inhibits the formation and storage of triacylglycerol by preventing glucose absorption into adipose tissue (Maury et al., 1993). On the other hand, it is generally recognized that pancreatic lipase must first be used to break down dietary fat before it can be directly absorbed from the intestine. Fatty acid and 2-monoacylglycerol are the two primary by-products of pancreatic lipase hydrolysis (Rani et al., 2012a). Based on these facts, it can be a useful strategy to block these digestive enzymes for treating obesity. Notably, there are numerous digestive enzyme inhibitors isolated from plants that have been reported in the literature, including crude saponins from *Platycodi radix* (Han L. K. et al., 2002), tea saponin (Han et al., 2001), licochalcone A from *Glycyrrhiza uralensis* roots (WonLicochalcone et al., 2007), dioscin from *Dioscorea nipponica* (Kwon C. S. et al., 2003) and the leaves of *Nelumbo nucifera* containing phenolic components (Ono et al., 2006a).

3.3.1 Extracts from *Stellaria media*

Commonly referred to as "Chickweed," *Stellaria medium* (Linn.) Vill. (Caryophyllaceae) is a favorite salad herb that is found all across the Himalayas up to an altitude of 4,300 m (Sharma, 2003). It is an edible medicinal species that are high in β -carotenes, γ -linolenic acid, phenols, vitamins, and minerals. This species shows dose-dependent inhibitory action against pancreatic α -amylase and lipase. However, lipase was more strongly inhibited by *Stellaria media* than α -amylase (Rani et al., 2012a). Generally, *S. media* may reduce the buildup of fat in adipose tissue caused by a high-fat diet by preventing the intestinal absorption of dietary fat and carbohydrates through the inhibition of both enzymes (Rani et al., 2012a).

3.3.2 Extracts from *Achyranthes aspera*

Achyranthes aspera Linn (Amaranthaceae), commonly known as apamarga, is an herb that grows abundantly in India on roadsides

and waste places. Traditionally, this plant is used as an antimalarial, antileprotic, purgative, diuretic, emmenagogue, oestrogenic, antiarthritic, antispasmodic, cardiogenic, antibacterial, and antiviral agent (Goyal et al., 2007). Oleanane-type triterpenoid saponins have been reportedly found in the extracts of *A. aspera* (EAA) seeds (Hariharan and Rangaswami, 1970) that have elucidated anti-microbial (Peter Amaladhas et al., 2013), wound-healing and anti-inflammatory activities (Hareshbhai, 2021). A study conducted by Rani et al. (2012) showed the effect of phenols, flavonoids, and saponins of *A. aspera* in reducing weight by inhibiting lipases and amylases. The *in vitro* assays employing EAA showed dose-dependent inhibition of lipase and α -amylase activity. EAA inhibited lipase more potently than α -amylase, with an IC_{50} value of 2.34 mg/mL and 3.83 mg/mL respectively. Latha et al. evaluated the hypolipidemic activity of the saponin extract of EAA at 1,200 mg/kg body weight in male Wistar rats fed on a high-fat diet for 8 weeks (Latha, 2011). The result demonstrated that when comparing EAA-treated rats to HF diet-only fed rats, a significant reduction was seen in the food efficiency ratio, body weight gain, visceral organ weight indices, serum total cholesterol, triglycerides, very low-density lipoproteins, low-density lipoproteins, atherogenic index, and hepatic total cholesterol and triglyceride levels. When compared to the HF diet alone fed group, the EAA-treated group showed a significant increase in blood high density lipoproteins, fecal total cholesterol, and triglyceride levels. Comparatively, another study administered EAA to mice at a dosage of 900 mg/kg body weight following an oral administration of olive oil, which dramatically reduced postprandial lipid levels at 3 and 4 h (Rani et al., 2012b). When EAA was fed to mice over an extended period of 6 weeks, the blood parameters significantly changed, with lower levels of total cholesterol, total triglycerides, and LDL cholesterol, but higher levels of HDL cholesterol (Rani et al., 2012b). In both of the aforementioned studies, 5-weeks old male Swiss albino mice were employed for the *in vivo* models to determine the pancreatic amylase and lipase inhibitory activity in using similar experiments. In other words, the anti-obesity effects of *A. aspera* were most likely attributed to the anti-oxidant power delivered by saponins and more studies would be helpful to understand other phytochemicals extracted in different parts of this plant.

3.3.3 Extracts from *Nelumbo nucifera*

Nelumbo nucifera Gaertn. Is a traditional Chinese herb commonly called lotus, that is widely distributed throughout Eastern Asia. Interestingly, all its plant parts including its fruits, leaves, rhizomes, and seeds are edible and have been used for different purposes including obesity management (Mukherjee et al., 2009). Diverse phytochemical groups were isolated from *N. nucifera* such as alkaloids, flavonoids, megastigmanes, vitamins, and elemanolide sesquiterpenes. Two main actions were inhibited by using *N. nucifera* leaves: a) pancreatic lipases and b) T3-L1 preadipocytes differentiation. The inhibition of pancreatic lipases seems to be mediated by benzyloquinoline alkaloids, such as trans-N-coumaroyltyramine and trans-N-feruloyltyramine. Besides that, T3-L1 preadipocytes differentiation was strongly inhibited by alkaloids like roemerine oxide, and liriodenine. Other megastigmanes and flavonoids have also been described to significantly reduce fat accumulation but with lower efficacy

compared to the above-mentioned ones. On the other hand, due to the presence of an epoxy moiety in their structures, the two compounds; 5,6-epoxy-3-hydroxy-7-megastigmen-9-one and annuionone D strongly suppressed adipocyte differentiation, indicating the significance of the epoxy moiety for the antiadipogenic activity of megastigmanes (Ahn et al., 2013).

3.3.4 Extracts from *Dioscorea nipponica* makino

Dioscorea nipponica Makino is a perennial herb belonging to the Dioscoreaceae family that is mostly found in northeastern, northern, eastern, and central China. The Miao and Meng ethnic groups of China have traditionally used this herb's rhizome to treat pain. Saponin and sapogenins in addition to the phenanthrenes that were extracted from the aerial parts are mainly responsible for most of the pharmacological effects of this plant (Ou-Yang et al., 2018). Saponins glycone and aglycone, namely, dioscin and diosgenin, were isolated from *D. nipponica*. Both compounds suppressed the increase in blood triacylglycerol level in a time-dependent manner when orally injected with corn oil to mice, demonstrating their inhibitory potential against fat absorption. Additionally, during an 8-week study, Sprague-Dawley rats fed a high-fat diet that also contained 40% beef tallow and 5% *D. nipponica* Makino grew much less body weight and adipose tissue than the control animals (Kwon C.-S. et al., 2003).

3.3.5 Extracts from *Platycodon Radix*

The root of *Platycodon grandiflorum* known as Platycodi Radix is a rich source of saponins (platycosides) which exhibits potent biological activities. It has been used as a traditional oriental medicine and many biological benefits were attributed to the Platycodi Radix extracts (Ha et al., 2006). Example use of Platycodi Radix as a food and a folk remedy includes bronchitis, asthma and pulmonary tuberculosis, hyperlipidemia, diabetes and inflammatory diseases. The saponins extracted from Platycodi Radix was employed in preventing hypercholesterolemia and hyperlipidemia (Lee and Jeong, 2002). Han et al. (Han L.-K. et al., 2002) discussed the effects of crude saponins isolated from Platycodi Radix on fat storage induced in mice by feeding a high fat diet. A high fat diet supplemented with 10 or 30 g/kg crude saponins reduced adipose tissue gain and hepatic steatosis. However, the oral administration of 375 mg/kg saponins in a lipid emulsion inhibited the increases in triacylglycerol blood levels in rats compared with that of rats which did not receive the saponin extracts. Consequently, it was determined that the anti-obesity effect of the crude saponins in mice fed a high fat diet including the reduction of blood triacylglycerol may be due to the inhibition of intestinal absorption of dietary fat by platycodin D. In a different study, 10 known triterpenoidal saponins were purified from Platycodi Radix, among them; platycodin A, C, D, and deapioplatycodin D, as all of them showed intestinal absorption inhibition of dietary fats mediated by pancreatic lipase inhibition (Xu et al., 2005).

3.3.6 Licochalcone A from *Glycyrrhiza uralensis*

Glycyrrhiza uralensis (Fisher) belongs to the family Leguminosae and is widely prized for its therapeutic capabilities, which include antiviral and anti-tumor benefits. These effects are typically attributed to its main bioactive

component, glycyrrhizin. In addition, other phytochemical classes isolated from the roots of this plant such as polysaccharides, triterpenes, and flavonoids were reported have anti-inflammatory, anticancer, and antioxidant activities (Afreen et al., 2006; Aipire et al., 2020). In 2007, Won and team purified Licochalcone A from the ethyl acetate/n-hexane fraction of the ethyl acetate extract of *G. uralensis* roots (WonLicochalcone et al., 2007). The team subsequently uncovered that licochalcone A inhibited pancreatic lipase activity reversibly and non-competitively with a K_i value of $11.2 \mu\text{g/mL}$ ($32.8 \mu\text{M}$). The same study has also reported pancreatic lipase inhibition mediated the production of oleic acid with both artificial substrate 2,4-dinitrophenyl butyrate and the natural substrate triolein. Intriguingly, licochalcone A extracted from *G. uralensis* increased the browning of inguinal white adipose tissue population in obese mice in addition to inducing the expression of UCP-1 in 3T3-L1 adipocytes (Lee et al., 2018). Figure 4.

3.4 Plant-derived natural products improve insulin sensitivity and induce hypoglycemia

Insulin resistance is directly associated with obesity and physical inactivity (Ginsberg, 2000). Adipose tissue is a highly insulin-responsive organ that significantly affects both glucose and lipid metabolism (Luo and Liu, 2016). Furthermore, the adipose tissue of people with obesity and insulin resistance is characterized by a progressive infiltration of macrophages,

which may increase the secretion of proinflammatory adipokines, resulting in a progressive failure of adipocyte function, the emergence of insulin resistance and eventually T2DM (Goossens, 2008). There are several studies demonstrated the effects of natural products in diabetes management by improving insulin sensitivity and reducing its resistance. The hypothesis postulated to interpret insulin resistance that eventually leads to diabetes is related to inflammation, mitochondrial dysfunction, and hyperinsulinemia. Other active factors in this mechanism are oxidative stress, endoplasmic reticulum stress, genetic factors, aging, and fatty liver. A more plausible interpretation is cell energy surplus signaled by the adenosine monophosphate-activated protein kinase (AMPK) signaling pathway that indicates high ATP production inside cells. Consequently, effective therapies for reducing obesity-associated insulin resistance pass through one of the following approaches: suppressing ATP production or stimulating their utilization, which can be achieved by restricting calories and exercising. Also, medicines and natural products that sensitize cells eventually inhibit ATP production in mitochondria (Ye, 2013). These products sensitize cells to insulin, mainly targeting PPAR γ , which controls several genes that affect the metabolism of glucose and lipids. Those agents improve insulin resistance in humans, specifically by boosting the disposal of insulin-stimulated glucose from skeletal muscle. Besides, individuals with T2DM have illustrated an increase in insulin-stimulated (insulin-resistant substrate) IRS-1-associated PI3K and Akt activity in their skeletal muscle (Choi and Kim, 2010).

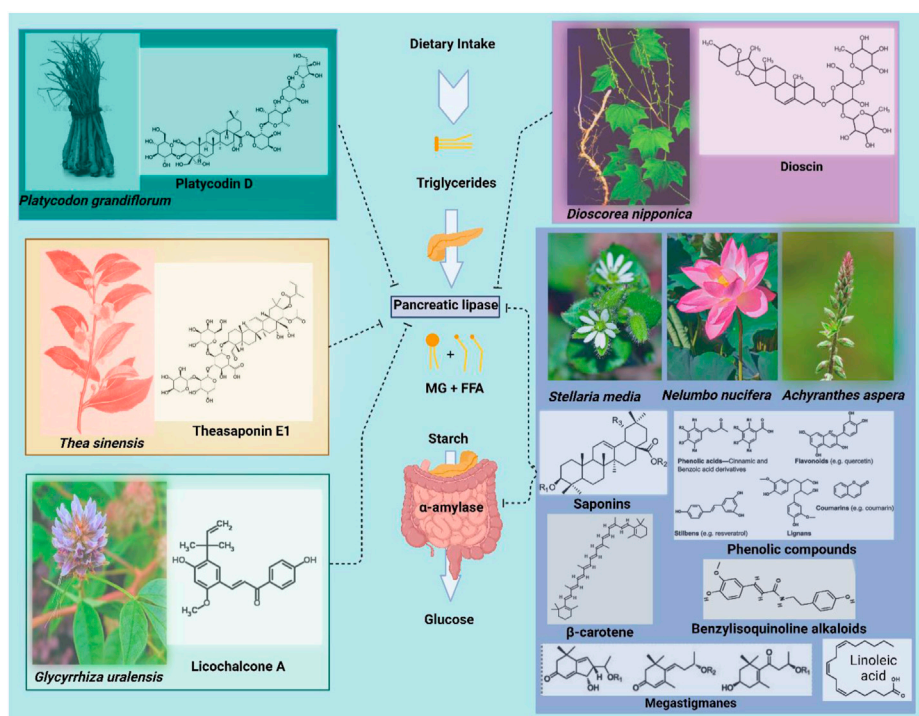


FIGURE 4

Examples of few plant species with the main phytochemicals and/or groups that inhibit lipases and amylases. MG: monoglycerols, FFA: free fatty acids.

3.4.1 Extracts from *Trigonella foenum-graecum*

Fenugreek *Trigonella foenum-graecum* L. originated in India and North America and was also reported in ancient Egypt and Rome for embalming mummies and facilitating labor and delivery (Smith et al., 2003). The chemical constituents extracted from fenugreek include steroidal saponinins such as diosgenin, furostanol glycosides, alkaloids such as trigocoumarin, nicotinic acid, trimethyl coumarin, and trigonelline (Wani and Kumar, 2018). In diabetic patients, fenugreek extract has reduced insulin resistance and improved blood glucose management (Gupta et al., 2001). Its anti-hyperglycemic actions have been linked to potentiating insulin release and improving insulin sensitivity (Puri et al., 2002), in addition to preventing intestinal carbohydrate digestion and absorption (Hannan et al., 2007). The anti-hyperglycemic properties are thought to be caused by steroids, saponins, alkaloids, and fiber in the fenugreek seeds (Snehlata and Payal, 2012). According to a clinical study on 18 individuals, fenugreek seed soaked in hot water significantly lowered fasting blood glucose, triglycerides, and very low-density lipoprotein cholesterol (VLDL-C) levels (Kassaian et al., 2009). In another study, when total fenugreek saponins and sulfonylureas were used together as a therapy, 46 patients with type II diabetes witnessed an improvement in clinical symptoms as compared to 23 controls. The combined treatment reduced blood sugar levels (Lu et al., 2008). Besides, trigonelline displayed great potential in treating obesity as it is involved in the browning of 3T3-L1 white adipocytes. The administration of trigonelline resulted in a considerable upregulation of the expression of BAT signature proteins, including PGC-1 α , PRDM16, and UCP1 as well as the genes that encode these proteins (Ppargc1 α , Prdm16, and Ucp1) in 3T3-L1 white adipocytes (Choi et al., 2021).

3.4.2 Extracts from *Allium sativum*

Garlic (*Allium sativum*) belongs to the Liliaceae family and contains a variety of chemicals, such as organic sulfur compounds, amino acids, vitamins, and minerals. Some organosulfur garlic components are allicin which is very unstable and rapidly decomposes into other sulfur compounds, including ajoene, dithiins, allyl methyl trisulfide, diallyl sulfide, diallyl disulfide, and diallyl trisulfide (Zhang Y. et al., 2020). S-allyl cysteine and diallyl disulfide may have therapeutic benefits on blood glucose, lipid profile, and insulin levels (Agarwal, 1996). The effects of garlic in treating hyperglycemia are investigated by conducting different studies; where in one study, the results showed that garlic decreased serum fructosamine, triglycerides, and fasting blood glucose levels in a 4-week double-blinded placebo-controlled study with 60 T2DM patients (Sobenin et al., 2008). In another study, it was found that in T2DM patients, garlic showed anti-hyperglycemic and anti-hyperlipidemic properties (Ashraf et al., 2005). The mechanisms of garlic are thought to improve hyperglycemia by increasing insulin secretion and enhancing insulin sensitivity (Liu et al., 2005). A randomized study demonstrated that aged garlic extract plus supplement (AGE-S) decreased homocysteine white epicardial adipose tissue (EAT). AGE-S was also found to increase brown EAT and the ratio of brown EAT to white EAT, which was related to the increases in vascular function measured by temperature rebound (Ahmadi et al., 2013). Balogun et al. studied the effect of garlic scape extract in

regulating adipogenesis and lipogenesis in white adipose tissue. On the molecular and genetic level, 3T3-L1 cells treated with the extracts exhibited reduced PPAR- γ , CCAAT/enhancer-binding protein a and b, acetyl-CoA carboxylase, fatty acid synthase, sterol regulatory element binding protein 1c, diacylglycerol acyltransferase 1, and perilipin-1 genes. Furthermore, it was also found that lipid accumulation significantly decreased in cells treated during pre-adipogenesis and post-differentiation but less so in cells treated during adipogenesis and differentiation. Additionally, when cells were exposed to garlic scape extract during differentiation, phosphorylation on AMPK and its downstream proteins increased along with elevated levels of carnitine palmitoyl transferase-1 α and hormone-sensitive lipase (Balogun and Kang, 2022). In parallel, the β -carboline alkaloid; (1R,3S)-1-methyl-1,2,3,4-tetrahydro- β -carboline-3-carboxylic acid, was the active compound isolated from garlic has suppressed the differentiation of adipocytes in the 3T3-L1 preadipocytes by preventing the remodeling of cytoskeleton, which is required for adipogenesis to take place (Baek et al., 2019).

3.4.3 Extracts from *Hypericum perforatum* L.

Hypericum perforatum L., also known as St. John's wort, has been used for many purposes by the public to treat anxiety, depression, insomnia, gastritis, hemorrhoids, wounds, and burns. (Tokgöz and Altan, 2020). The main bioactive compounds in *Hypericum perforatum* L. are hypericin, hyperforin, and adhyperforin (Gray et al., 2000). It was demonstrated that *H. perforatum* L. extract (EHP) inhibited the protein tyrosine phosphatase 1B (PTP1B) by reducing the gene expression and the catalytic activity of the enzyme (Tian et al., 2015). Insulin resistance and lipid metabolic disorders have been linked to PTP1B, the enzyme that negatively regulates the insulin and leptin signaling pathways (Sun et al., 2007; Basavarajappa et al., 2012). PTP1B inhibitors increase insulin sensitivity by increasing the activity of insulin and leptin receptors (Picardi et al., 2008). Thus, it was found that the treatment with EHP improves hyperinsulinemia, hyperglycemia, insulin tolerance, and glucose infusion rate in the hyperinsulinemic-euglycemic clamp test (Tian et al., 2015).

3.4.4 Extracts from *Zingiber officinale*

Ginger is the subterranean stem of *Zingiber officinale* Roscoe, which belongs to Zingiberaceae and most likely originated from Southern China. The primary bioactive ingredients are found to be phenolic and terpene compounds such as gingerols that, under heat and prolonged storage converted to shogaols which are transformed by hydrogenation to paradols (Stoner, 2013; Khandouzi et al., 2015). Gingerol treatment enhanced the adipocyte differentiation in mice and improved insulin sensitivity and glucose uptake; thus, it is anticipated that this may also help the diabetic condition (Sekiya et al., 2004). In an *in vivo* study, animals fed a high-fat diet who had their diets enriched with 2% ginger had considerably higher blood insulin concentrations and greater glucose tolerance (Islam and Choi, 2008). Moreover, ginger nanoparticles were fed with HFD for a year to the mice to examine their power to prevent insulin resistance by restoring homeostasis of the transcription factor *Foxa2* in the gut epithelia (Kumar et al., 2022). The ginger nanoparticle

feeding boosted *Foxa2* protein expression and protected it from Akt-1-mediated phosphorylation and the subsequent inactivation of *Foxa2*, opposite to HFD, that suppressed its expression. Furthermore, compared to gingerols and 6-shogaol, gingerenone A had a stronger inhibitory effect on adipogenesis and lipid accumulation in 3T3-L1 preadipocyte cells. Additionally, gingerenone A may alter fatty acid metabolism *in vivo* by activating AMPK, that minimize diet-induced obesity. The peroxisome proliferator-activated receptor δ (PPAR- δ)-dependent gene expression in cultured skeletal muscle myotubes was increased by 6-shogaol and 6-gingerol, which enhanced cellular fatty acid catabolism. Also, a randomized, double-blind, placebo-controlled study showed a reduction in BMI among female participants when they took 2 g of ginger powder daily (Mao et al., 2019).

3.4.5 Extracts from *Crocus sativus*

Crocus sativus Linn is a member of the Iridaceae family, and its dry stigmas have traditionally been used as a spice or culinary ingredient (Kang et al., 2012). Saffron has a long history of traditional use as a medicinal agent in addition to being a food coloring and aromatic spice. It appeared in ancient writings of prominent scientists like Avicenna as he noted its significant therapeutic effects (Javadi et al., 2013). Saffron extracts include several potent carotenoids, including crocin, and its aglycone crocetin, the monoterpene glycoside picrocrocin, and safranal, which give them pharmacological activities on a diverse range of diseases (Rios et al., 1996). A randomized, double-blind, placebo-controlled clinical trial supported the idea of saffron in treating diabetes, in which it was found that type II diabetes patients who took 100 mg/day of saffron powder for 8 weeks lowered the fasting blood glucose and TNF- α serum levels, along with downregulation of TNF- α and IL-6 mRNA expression (Mobasser et al., 2020a). Additionally, Milajerdi and team conducted a randomized, triple-blind study involving 54 T2DM patients, and discovered that saffron supplementation daily for 8 weeks significantly lowered the individuals' fasting blood glucose levels (Milajerdi et al., 2018). Similarly, another placebo-controlled randomized clinical study by Sepahi found that daily 15 mg of oral crocin administration significantly decreased Hb_{A1C} in diabetic patients compared to the control placebo groups (Sepahi et al., 2018). The underlying mechanisms of action of saffron in diabetes treatment are believed to be insulin sensitivity enhancement, stimulation of insulin signaling pathways, improvement of β -cell activities, promotion of glucose transporter type 4 (GLUT-4) expression, regulation of oxidative stress, repression of inflammatory pathways (Mobasser et al., 2020b).

3.4.6 Extracts from the genus *Panax*

There are several different species of ginseng, all of which are members of the Aaraliaceae plant family. Ginseng from Korea, Japan, and North America belong to the genus *Eleutherococcus*, while Siberian ginseng belongs to the genus *Panax* (Vogler et al., 1999). Ginsenosides, a broad group of steroidal saponins, are primary ingredients in ginseng that target a wide range of tissues and elicit various pharmacological effects. Their capacity to separately target multireceptor systems at the plasma membrane and activate intracellular steroid receptors may explain some of their

complex pharmacological effects (Attele et al., 1999). In several animal models of T2DM, different parts of ginseng (e.g., roots, stems, leaves, and berries) have displayed substantial antihyperglycemic effects. Clinical investigations suggested that ginseng arises as an alternative treatment for T2DM (Vuksan et al., 2000) as it can effectively reduce insulin resistance and fasting blood glucose (Ma et al., 2008). Ginseng possibly reduces blood glucose by increasing insulin production, preserving pancreatic islets, increasing insulin sensitivity, and stimulating glucose uptake (Xie et al., 2011). In particular, by promoting the AMPK pathway, ginseng and ginsenosides decrease energy intake while increasing energy expenditure. Moreover, a study found that black ginseng significantly elevated the expression of brown adipocyte markers (UCP1, PRDM16, and PGC-1) in both types of adipocytes, 3T3-L1 cells and primary white adipocytes. In the same study, administration of the ginsenoside Rb1 enhanced the expression of the brown adipocyte markers in a dose-dependent way in 3T3-L1 cells and primary white adipocytes (Park S. J. et al., 2019). Finally, improving insulin sensitivity and browning the WAT by ginseng chemical constituents can increase the capabilities to reduce weight and prevent obesity.

3.4.7 Essential oils from the genus *Cinnamomum*

Cinnamon is a spice from the Lauraceae family made of the bark of plants from the genus *Cinnamomum* including *Cinnamomum zeylanicum* and *Cinnamomum cassia*. The main active ingredients of cinnamon are the volatile oils extracted from *C. zeylanicum*, and *C. cassia*'s bark, leaves, and roots. Due to the different chemical compositions of distinct plant parts, the pharmacological effects of these volatile oils also vary. Even so, there are few common monoterpene hydrocarbons present in these oils across the three plant parts (i.e., bark, leaves and roots) but in various ratios. The predominant component of the root-bark oil is camphor, while eugenol and cinnamaldehyde present in the leaf oil and bark oil, respectively. Particularly, four oils were extracted from the dried stem bark of *C. cassia*; cinnamaldehyde, cinnamic acid, cinnamyl alcohol, and coumarin (Jayaprakasha and Rao, 2011).

In addition to its traditional and culinary uses, cinnamon has anti-inflammatory, antibacterial, antioxidant, and anticancer properties (Cao et al., 2008; Hariri and Ghiasvand, 2016). Cinnamon enhances insulin sensitivity and has advantageous effects on metabolism (Couturier et al., 2010). In a randomized, controlled clinical trial, cinnamon decreased hemoglobin A1c (Hb_{A1C}) by 0.83% compared to conventional therapy alone, which decreased Hb_{A1C} by 0.37% in individuals with T2DM (Crawford, 2009). Furthermore, cinnamon is also described to promote the browning of white adipose tissue by Kwan and team when they observed that subcutaneous adipocytes derived from obese mice models underwent browning post-cinnamon extract treatment. The WAT browning mechanism was marked by an increase in the expression of UCP1 and other brown adipocyte markers in 3T3-L1 adipocytes as well as subcutaneous adipocytes. Additionally, the cinnamon extract treatment increased mitochondrial protein biogenesis (Kwan et al., 2017).

3.4.8 Capsaicin from *Capsicum annuum*

The active ingredient in chili peppers, capsaicin, is often taken as a spice. It acts as an agonist on vanilloid channel 1's transient

receptor potential (TRPV1) (Saito, 2015). The receptor plays a significant role in the modulation of metabolic syndrome, where insulin resistance and obesity are present and increase the risk of developing cardiovascular disease, T2DM, and non-alcoholic fatty liver disease (Panchal et al., 2018). *In vitro* and pre-clinical studies have shown low-dose dietary capsaicin to be useful in reducing metabolic problems. Capsaicin's activation of TRPV1 protein receptor can subsequently regulate adipocyte thermogenesis, and the activation of metabolic modulators such as AMP-activated protein kinase (AMPK), PPAR α , UCP1, and GLP-1 (Panchal et al., 2018). Capsaicin enhances insulin sensitivity, increases fat oxidation and reduces body fat; all of which are known to be beneficial for liver and heart health. It was also reported to be effective in diabetic neuropathy and has anti-inflammatory and anti-diabetic properties (Aryaeian et al., 2017) (Figure 5). Capsaicin was also found to decrease lipid accumulation by decreasing PPAR γ , C/EBP α , and leptin protein expression, but increased adiponectin expression in 3T3-L1 adipocytes (Hsu and Yen, 2007).

3.4.9 Ursolic acid

The well-known pentacyclic triterpene ursolic acid (3 β -hydroxy-12-urs-12-en-28-oic acid) is frequently utilized in traditional Chinese medicine (Bacanli et al., 2019). The primary sources of ursolic acid include *Malus pumila*, *Ocimum basilicum*, *Vaccinium* spp., *Vaccinium macrocarpon*, *Olea europaea*, *Origanum vulgare*, *Rosmarinus officinalis*, *Salvia officinalis*, and *Thymus vulgaris* (Ikeda et al., 2008). In diabetic rats, it was demonstrated that ursolic acid (0.05% w/w) altered blood glucose levels and enhanced insulin sensitivity and glucose intolerance. It has also been proposed to preserve pancreatic β -cells and thus increase insulin levels (Jang et al., 2009). Ursolic acid inhibits protein tyrosine phosphatase 1B (PTP1B), an enzyme linked to the downregulation of the insulin receptor, hence increasing the

number of insulin receptors and the number of active receptors; it is the mechanism presented in an *in vitro* study, explaining the hypoglycemic activity of ursolic acid (Jung et al., 2007).

3.4.10 Cinnamic acid

The most common sources of cinnamic acid are cinnamon (*C. cassia* L.) J. Presl, citrus fruits, grapes (*Vitis vinifera* L.), tea (*Camellia sinensis* L.) Kuntze, chocolate (*Theobroma cacao* L.), spinach (*Spinacia oleracea* L.), celery (*Apium graveolens* L.), and brassica vegetables (Adisakwattana, 2017). Cinnamic acid (3-phenyl-2-propenoic acid) is an antioxidant phenolic molecule (Bacanli et al., 2019). Cinnamic acid and its derivatives effectively treat diabetes and its complications, among other biological activities. In particular, the impact of cinnamon bark extract on diabetic mice was investigated by Kim et al. (Kim and Choung, 2010). Through the regulation of PPAR-mediated glucose and lipid metabolism, cinnamon extract has been proposed to improve hyperglycemia and hyperlipidemia, increase insulin sensitivity, and lower blood and hepatic lipids. The objective of Lee et al. (Lee et al., 2022) study was to assess the impact of cinnamic acid on obesity, along with its effects on peripheral and hypothalamic inflammation, metabolic profiles, and macrophage-related inflammatory responses in mice fed a high-fat diet (HFD). Results indicated that cinnamic acid-supplement feed reduced obesity and its associated symptoms, such as epididymal fat accumulation, insulin resistance, glucose intolerance, and dyslipidemia, without causing hepatic or renal damage. Additionally, cinnamic acid reduced HFD-induced fat deposition, tumor necrosis factor- α , and macrophage infiltration in the liver and adipose tissue. Moreover, Ly6c^{high} monocytes, M1 adipose tissue macrophages, and hypothalamus microglial activation were all reduced by cinnamic acid. These findings imply that cinnamic acid inhibits the peripheral and

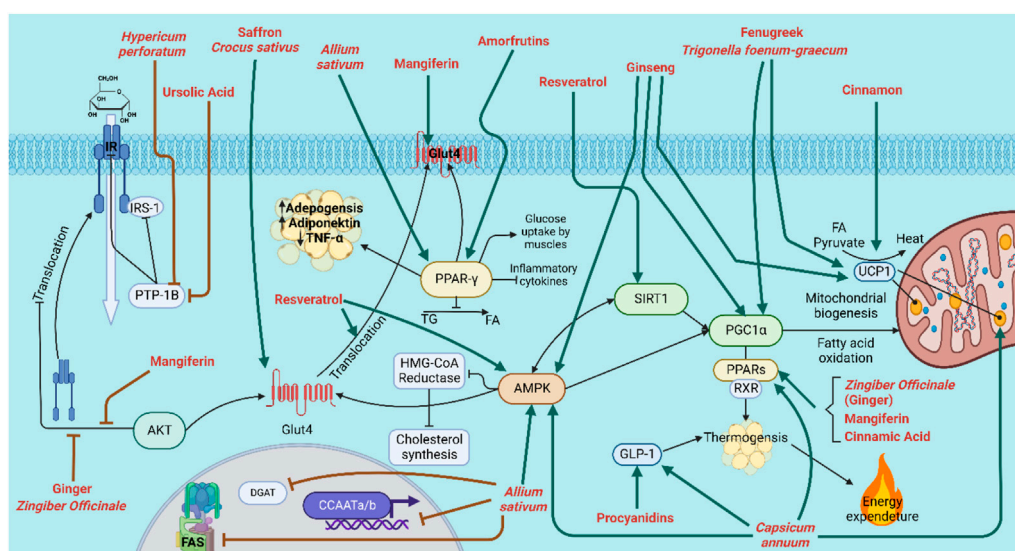


FIGURE 5

Natural products/plant species that enhance insulin resistance and reduce obesity. IR: insulin receptor; IRS-1: insulin receptor subunit-1; GLUT4: Glucose transporter type 4; DGAT: Diglyceride acyltransferase; CCAATa/b: CCAAT/enhancer-binding protein a and b; FAS: Fatty acid synthase; Thick green arrow: increase; Thick red inhibition arrow (□): inhibition.

hypothalamus inflammatory monocyte/macrophage system and improves metabolic problems associated with obesity.

3.4.11 Resveratrol

Resveratrol (3,4,5-trihydroxystilbene), a polyphenolic compound renowned for its antioxidant and anti-inflammatory attributes, has been identified in several plant species, such as *Polygonum cuspidatum*, *Veratrum grandiflorum*, *V. vinifera*, *Arachis hypogaea*, and *Vaccinium oxycoccos*, among others (Bishayee et al., 2010). Due to its multifaceted mechanisms of action, encompassing enhancements in insulin sensitivity, promotion of GLUT4 translocation, mitigation of oxidative stress, regulation of carbohydrate metabolizing enzymes, activation of crucial signaling pathways mediated by SIRT1 and AMPK, and potential downregulation of adipogenic genes, resveratrol exhibits considerable promise as a therapeutic agent for the treatment of diabetes and other severe diseases (Bagul and Banerjee, 2015). Particularly, through the activation of mitochondrial sirtuin proteins, resveratrol controls blood sugar levels. These proteins regulate the metabolism of sugar and fat; therefore, they significantly impact the body's ability to produce energy at various levels. This is achieved by enhancing the thermogenesis processes, which increase energy expenditure by burning more adipose tissue (Moshawih et al., 2019). Consequently, resveratrol has the potential to decrease target organ failure and comorbidities that are related to diabetes (Figure 5).

3.4.12 Procyanidins

Procyanidins are the primary flavonoids, also known as flavan-3-ols or flavanols, under proanthocyanidins or condensed tannins family (Aron and Kennedy, 2008). They are oligomeric structures formed by polymerizing 2 to 10 subunits of the monomeric flavanols catechin and epicatechin. Procyanidins are available in different fruits, vegetables, legumes, grains, and nuts such as *Prunus domestica*, *Prunus salicina*, *Malus domestica*, *V. vinifera*, *Prunus amygdalus*, *Cicer arietinum*, among others (Rue et al., 2018; Bahrin et al., 2022). Few studies have shown the effects of different procyanidins forms on GLP-1. For instance, after being consumed simultaneously with sucrose, berry puree high in proanthocyanidins increased the active GLP-1 levels in healthy adults, leading to a significant decrease in blood glucose levels. Moreover, the administration of another procyanidins derivative, cinnamtannin A2 increases insulin and active GLP-1 secretion in fasting healthy mice. It was previously described that the L-cells found in the intestine, specifically the ileum and large intestine, and the release of GLP-1 (Törrönen et al., 2012; Yamashita et al., 2013). This hormone is important for controlling glucose homeostasis since its major job is to improve the β -cells' responsiveness to glucose. It also increases β -cell mass by encouraging proliferation, lowering apoptosis, and boosting β -cell differentiation. It is also that has been found that enteroendocrine cells such as L-cells is a possible target for procyanidin. They have also been reported to reduce the damage caused by the diet, hence enhancing glycemic status and insulin sensitivity in fructose or high-fat-induced insulin resistant models (González-Abuín et al., 2015).

3.4.13 Mangiferin

Mangiferin (MF) is a glucosylxanthone that is present in the mango tree (*Mangifera indica*), the rhizomes of *Anemarrhena*

asphodeloides (Miura et al., 2001), and the leaves of *Bombax ceiba*. It is proven to have anti-diabetic, cancer-fighting, antiviral, anti-aging, and antioxidant properties (Dar et al., 2005). Studies revealed that MF increased the AMP-activated protein kinase (AMPK) phosphorylation in 3T3-L1 cells, pancreatic β -cell mass, and the amount of glucose and insulin absorption (Han et al., 2015). To elucidate the mechanism of mangiferin in reducing insulin resistance, Qiao Zhang and team induced lipid accumulation in HepG2 and C2C12 cell lines by using palmitic acid and treated them with various concentrations of MF (Zhang et al., 2019). The outcomes demonstrated that MF significantly increased insulin-stimulated glucose uptake and markedly decreased glucose content in HepG2 and C2C12 cells, as a result of phosphorylated protein kinase B (AKT), GLUT2, and GLUT4 protein expressions. MF also significantly reduced intracellular FFA and triglyceride accumulations and boosted FFA uptake. In HepG2 and C2C12 cells, MF increased the fatty acid oxidation rate corresponding to FFA metabolism, and augmented the activity of PPAR protein and its downstream proteins involved in fatty acid translocase (CD36) and carnitine palmitoyltransferase 1 (CPT1). *In vitro*, oral treatment of mangiferin at a dosage of 20 mg/kg improved insulin sensitivity in Streptozotocin-induced diabetic rats, altered lipid profiles, and reduced the amount of adipokine, and consequently, reduced the inflammation and metabolic syndrome development (Saleh et al., 2014).

3.4.14 Amorfrutins

Amorfrutins are non-toxic components of the fruits of *Amorpha fruticosa*, and the edible roots of licorice, *Glycyrrhiza foetida* (Weidner et al., 2012). The plant *A. fruticosa*, in which the molecules were first discovered, is where the term "amorfrutin" originated. The small, lipophilic amorfrutin class contains the 2-hydroxybenzoic acid as the core structure, and it is surrounded by phenyl and isoprenyl moieties (de Groot et al., 2013). They are a class of natural compounds that have recently been discovered to be PPAR γ agonists with selective peroxisome proliferator-activated receptor [y] modulator (SPPAR γ Ms)-like properties (Lefebvre and Staels, 2012). Amorfrutins are found to be potent PPAR γ agonists with a binding affinity range from 236 to 354 nM, in addition to a micromolar affinity for PPAR α and PPAR β/δ . It was reported that the affinity of amorfrutin B to the PPAR γ receptors is twice as strong as the synthetic anti-diabetic drug pioglitazone (Weidner et al., 2012). The widely targeted type II diabetes protein, PPAR γ , is a sensor and regulator that predominates lipid and glucose metabolism and adipose cell differentiation. PPAR γ receptor improves insulin sensitivity via various metabolic actions, including adipokines regulation (Malapaka et al., 2012).

3.5 Plant-derived natural products inhibiting adipogenesis and inducing adipocytes apoptosis

Adipogenesis is described as transforming preadipocytes into adipocytes by arresting preadipocyte development, accumulating lipid droplets, and producing mature adipocytes with certain morphological and biochemical features (Ghaben and Scherer,

2019; Zhang K. et al., 2020). The initial sign of adipogenesis is a change in cell shape, accompanied by modifications in the type and level of expression of cytoskeletal and extracellular matrix components (Gregoire et al., 1998). These events give rise to the production of two categories of transcriptional factors involved in adipogenesis, namely, C/EBP and PPAR. The main transcriptional regulators of adipogenesis are C/EBP α and PPAR γ , which are necessary for producing numerous functional proteins in adipocytes. The terminally differentiated adipocyte phenotype appears predominantly activated and maintained by C/EBP α . At the onset of differentiation, C/EBP β and C/EBP δ are expressed and thought to control C/EBP α synthesis. The PPARs are part of the nuclear hormone receptor superfamily, which contains retinoid, thyroid, and steroid hormone receptors. For example, activation of PPAR α in the liver causes peroxisomes and related enzymes to proliferate, resulting in long-chain fatty acid metabolism via the β -oxidation cycle. Because it is expressed most abundantly in adipose tissue and is activated during the early phase of differentiation of both 3T3-L1 and 3T3-F442A preadipocytes, PPAR γ is thought to play a significant role in controlling adipogenesis (Wu et al., 1996).

On the other hand, inducing apoptosis is a viable method of removing adipocytes in obese people, which can be achieved through suppressing adipogenesis, obstructing fat accumulation, and deleting adipocytes. Notably, adipokines are the hormones that signal changes in fatty-tissue mass and energy balance to regulate energy consumption. They are secreted from the adipose tissue to control fat weight and homeostasis (Muioio and Newgard, 2005). The two most prominent adipokines that can be considered an excellent strategy to be targeted by natural products are leptin and TNF- α . Leptin is produced and secreted by adipocytes to regulate thermogenesis and food intake through both central and peripheral pathways to increase adipose tissue mass. According to a recent study, adipose tissue in rats that had received leptin by intra-cerebroventricular injection decreased quickly and showed signs of apoptosis. Furthermore, the effect of leptin on peripheral tissue was as efficacious as the centrally administered dose (Zhang and Huang, 2012). To further clarify the mechanism, it has been known that leptin can stimulate the production of angiotensin-2 in the adipose tissue, which also

leads to the development of apoptosis in the cells without increasing the vascular endothelial growth factor. To understand the role of the PPAR- γ in this process, Qian and others analyzed its mRNA levels after intra-cerebrovascular administration. They found that the protein levels increased significantly after leptin treatment, which may indicate its involvement in the mechanism (Qian et al., 1998). TNF- α is the second adipokine generated and produced by adipocytes and plays a vital role in regulating and controlling adipocyte mass and number via apoptotic mechanisms. It has been reported that the P55 TNF- α receptor subtype is responsible for the induction of apoptosis of the differentiated brown fat cells when bound with its substrate, TNF- α . According to a recent study, TNF- α decreases the number of mature adipocytes but not preadipocytes by inducing apoptosis, through C/EBP and PPAR γ -mediated inhibition of NF- κ B. Moreover, β -catenin pathway was also found to be involved in the TNF- α regulated 3T3-L1 preadipocyte apoptosis (Cawthorn et al., 2007; Tamai et al., 2010). In short, adipogenesis is tightly regulated by neuroendocrine system. At any rate, natural products and phytochemical affecting enzymes or pathways that are related to hunger or satiety can have the potential to indirectly affects adipogenesis and apoptosis induction, and eventually lead to obesity reduction. The following section further explores additional phytochemicals that exert its anti-obesity effects via inhibiting adipogenesis or inducing apoptosis of adipocytes. Figure 6.

Natural substances, including EGCG, genistein, esculetin, berberine, resveratrol, capsaicin, baicalein, and procyanidins, have been shown to inhibit adipogenesis in several studies. In adipocytes treated with genistein, berberine, and rhein, the protein expression of PPAR and C/EBP was lowered (Rayalam et al., 2008). The isoflavone, genistein was first discovered and isolated from the plant *Genista tinctoria*, or dyer's broom (Mukund et al., 2017), has been demonstrated to reduce PPAR γ expression by activating the Wnt/ β -catenin pathway and inhibiting C/EBP β , while it also regulates PPAR γ transcriptional activity by activating AMPK during adipogenesis. This shows that genistein may be a potent anti-

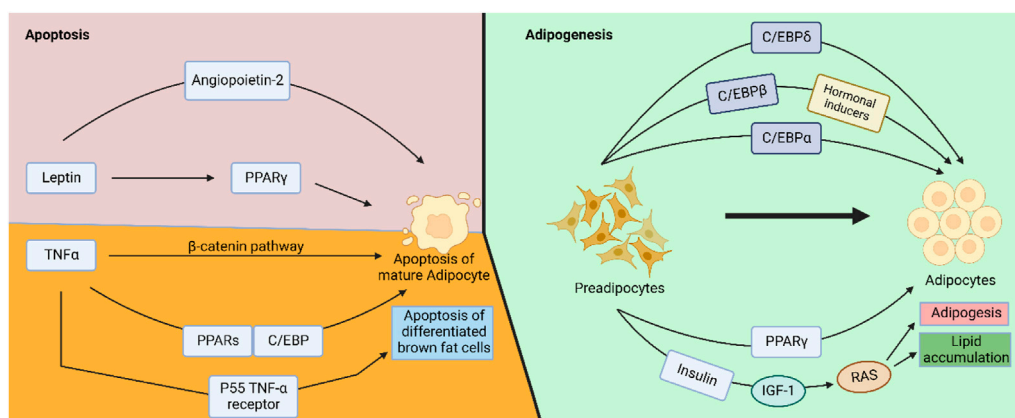


FIGURE 6
The major molecular pathways in adipocytes' apoptosis and adipogenesis.

obesity agent. Differently, berberine (BBR) is the primary component in *Cordis rhizome* and has an anti-bacterial activity utilized in Chinese medicine. The mechanism of BBR shows that it suppresses 3T3-L1 adipocyte differentiation, proliferation, and lipid buildup. These effects may occur due to a variety of molecular targets and intricate pathways, such as suppressing PPAR γ and PPAR α transactivations and inhibiting the mRNA and protein of early transcription factors C/EBP β , PPAR γ , and PPAR α . (Huang et al., 2006). BBR also activates AMPK and stimulates PGC-1 α to cause browning-related UCP1 expression (Zhang et al., 2014).

Moreover, Esculetin is a naturally occurring dihydroxycoumarin primarily obtained from the trunk bark and twig skin of the Chinese plant *Fraxinus rhynchophylla* Hance (Zhang et al., 2022). Esculetin (6,7-dihydroxy-2H-1-benzopyran-2-one) exerts its actions by inhibiting cell proliferation, inducing apoptosis in both preadipocytes and mature adipocytes, in addition to inhibiting adipogenesis of 3T3-L1 preadipocytes. A study found that esculetin inhibited 3T3-L1 adipocyte differentiation by suppressing the accumulation of lipids in a dose-dependent manner (Yang et al., 2006). Similarly, delphinidin, an anthocyanin present in pigmented fruits and vegetables, inhibits adipogenesis by suppressing adipogenesis and lipogenesis markers, inhibiting lipid accumulation, and increasing the expression of fatty acid metabolism genes as illustrated *in vitro* by Park M et al. (Park M. et al., 2019). Furthermore, baicalein, one of the primary flavonoids found in *Scutellaria baicalensis* (Chinese Skullcap), has been linked to many biological activities. The capacity of baicalein to increase the expression of cyclooxygenase-2 (COX-2), which is generally downregulated during adipogenesis, may explain its anti-adipogenic activity (Cha et al., 2006).

The perennial herb *Alchemilla monticola* Opiz (ALM) has been traditionally used to treat inflammatory diseases, wounds, and burns (Tasić-Kostov et al., 2019). *Alchemilla* species are recognized chemically for their flavonoids, flavonoid glycosides, phenolic acids, and tannins (Choi et al., 2018). Remarkably, it was demonstrated that ALM extracts inhibited adipogenesis by interfering with the PI3K/AKT signaling pathway, thereby inhibiting the adipogenic markers PPAR γ , C/EBP α and adiponectin (Mladenova et al., 2021). Another naturally occurring anthraquinone with a wide range of beneficial pharmacological applications is Rhein (Wu et al., 1996). It is isolated from rhizomes of medicinal plants such as *Rheum undulatum*, *Rheum palmatum*, as well as in *Cassia reticulata* (Huang et al., 2021). In 3T3-L1 cells, PPAR γ and C/EBP α protein and mRNA levels produced by differentiation medium were found to be dramatically downregulated by rhein (Liu et al., 2011). In a recent study, rhein treatment in the mitotic clonal expansion stage has slowed down 3T3-L1 differentiation with much fewer lipid droplets accumulation and adipocyte gene expression (Huang et al., 2021). It was also found that Rhein suppresses 3T3-L1 adipocyte development in a dose- and time-dependent way.

Furthermore, turmeric as a commonly used spice in Asian cuisines (*Curcuma longa* Linn.), contains curcumin (also known as diferuloylmethane). Curcumin suppresses adipogenesis and

downregulates the expression of PPAR γ in 3T3-L1 adipocytes by activating AMPK (Lee et al., 2009). Curcumin decreased the activation of MAPK signalling pathways (including ERK, JNK, and p38), which prevented the differentiation of 3T3-L1 cells into adipocytes. Curcumin also restored nuclear translocation of the essential Wnt signaling component β -catenin during differentiation in a dose-dependent manner. The differentiation-stimulated production of CK1 α , GSK-3 β , and Axin, was inhibited by curcumin, all of which are components of the destruction complex that targets β -catenin; consequently, it blocks adipogenesis in 3T3-L1 adipocytes (Ahn et al., 2010). In another study, it was found that in inguinal WAT, curcumin increased the plasma norepinephrine levels and the expression of the β 3AR gene (Wang S. et al., 2015). Both the rapid stimulation of already-existing beige adipocytes and the differentiation of beige adipocytes from their precursors depend on the release of norepinephrine at sympathetic terminals in the adrenal medulla and WAT (Bartelt and Heeren, 2014). Norepinephrine is the primary regulator of adaptive thermogenesis in brown and beige adipose tissues by upregulating PGC-1 α and UCP1 expression through β -adrenergic (mainly β 3) and cAMP-dependent pathways (Nedergaard and Cannon, 2014). Thus, curcumin has the potential to induce WAT browning through the norepinephrine- β 3AR pathway. For a complete summary for the Plant-derived active compounds, source, and mechanism of phytochemicals responsible for obesity management, see Table 1.

4 Safety considerations and limitations of natural products for weight management

Despite the previously demonstrated benefits of plant-derived natural products in weight management with minimal side effects, it is important to acknowledge that isolated phytochemicals and plant extracts can occasionally impose a potential risk on human health. While these substances hold promise as therapeutic agents, their inherent complexity and diverse chemical composition may give rise to unintended consequences when administered in concentrated forms. For instance, despite the short-term increase in thermogenesis associated with caffeine consumption, long-term studies involving obese subjects have shown that it does not lead to greater weight loss compared to a placebo. Interestingly, when a group with habitual high caffeine intake (approximately 300 mg/day) received a combination of green tea and caffeine, there was no significant improvement in body weight maintenance after weight loss, suggesting a potential loss of sensitivity to caffeine over time (Westertep-Plantenga, 2010b). While caffeine has been extensively studied, there is limited research focusing specifically on its long-term effects as an anti-obesity treatment. Most studies have primarily explored short-term effects or specific metabolic changes. Therefore, the efficacy and safety of using caffeine as a long-term anti-obesity strategy remain uncertain. Ephedrine, is another stimulant utilized as an anti-obesity agent for its metabolism-enhancing properties, is accompanied by various limitations and concerns. Its administration can lead to

TABLE 1 Plant-derived active compounds, source, and effects of phytochemicals responsible for obesity management.

Active compound	Source (plant species)	Effects/Mechanism of action	IC ₅₀ value	Dosages employed	Study type
Caffeine	<i>C. arabica</i> L. and <i>C. canephora</i> Pierre (Ferreira et al., 2019)	- Metabolic stimulant - Thermogenic agent (Diepvens et al., 2007b)	-	100 mg/day of caffeine	Clinical trial (Dulloo et al., 1989)
Ephedrine	<i>Ephedra sinica</i> (Saper et al., 2004)	-Metabolic stimulant - Thermogenic agent (Stohs and Badmaev, 2016)	-	1.5 mg/kg/day of ephedrine	Clinical trial (Carey et al., 2015)
Epigallocatechin gallate (EGCG)	<i>Camellia sinensis</i> L. (Thitimuta et al., 2017)	- Enhance fatty acid mobilization and oxidation (Jeukendrup and Randell, 2011) - Promote browning markers (Li et al., 2021) - Inhibit adipogenesis (Lin et al., 2005)	0.45 mg/mL (Lipase Inhibition) (Jamous et al., 2018)	576 mg/day of catechins	Clinical trial (Matsuyama et al., 2008)
Capsaicin	<i>Capsicum annuum</i> L. (Barceloux, 2009)	-Stimulates thermogenesis Reinbach et al. (2010) - Enhance insulin sensitivity, and increase fat oxidation (Aryaeian et al., 2017) -Decreases PPAR γ , C/EBP α and leptin protein expression in 3T3-L1 adipocytes (Hsu and Yen, 2007)	-	1 g/day of red peppers containing 1995 μ g capsaicin, 247 μ g nordihydrocapsaicin and 1,350 μ g dihydrocapsaicin - 400 μ g/day of capsaicin	Clinical trial (Ludy and Mattes, 2011) (Dömötör et al., 2006)
Korean pine nut-free fatty acids (FFA)	<i>Pinus Koraiensis</i> (Wolff et al., 2000)	-Releases cholecystokinin (CCK), thus, enhancing satiety and reducing appetite (Pasman et al., 2008)	-	3 g of Korean pine nut FFA.	Clinical trial (Pasman et al., 2008)
Hydroxycitric acid (HCA)	<i>Garcinia cambogia</i> (S. E Ohia et al., 2002)	Enhances 5-HT release (Ohia et al., 2001)	-	2800 mg/day of HCA.	Clinical trial (Preuss et al., 2004)
Cathine (D-nor-pseudoephedrine) and cathinone (1-aminopropiophenone)	<i>Catha edulis</i> (Lemieux et al., 2015)	Increases dopamine in the brain by acting on the catecholaminergic synapses (Patel, 2000)	-	- 20 mg/kg/day of khat extract -200 and 400 g of fresh khat chewed for 4 h	- <i>In vivo</i> trial (Hesham et al., 2011) - Clinical trial (Walid et al., 2006)
P57 molecule (oxypregnane steroidal glycoside)	<i>Hoodia gordonii</i> (Jain and Singh, 2013)	Increases ATP in hypothalamic neurons (MacLean and Luo, 2004)	-	100–150 mg/kg/day of <i>Hoodia gordonii</i> extract	<i>In vivo</i> trial (Jain and Singh, 2013)
Pregnane glycosides (Schneider et al., 1993)	<i>Caralluma adscendens</i> var. <i>Fimbriata</i> (Wall.) Gravely & Mayur (Dutt et al., 2012)	Downregulation of ghrelin production and neuropeptide Y (NPY) (Gardiner et al., 2005; Komarnytsky et al., 2013)	-	1 g/day of C. Fimbriata extract	Clinical trial (Rao et al., 2021b)
Forskolin	<i>Coleus forskohlii</i> Briq (Astell et al., 2013)	Increase thermogenesis and lipogenesis (Godard et al., 2005)	-	250 mg of 10% forskolin extract twice a day	Clinical trial (Godard et al., 2005)
Beta-carotenes, γ -linolenic acid, and phenols	<i>Stellaria medium</i> (Linn.) Vill. (Sharma, 2003)	Inhibits pancreatic α -amylase and lipase. (Rani et al., 2012a)	-3.71 mg/mL (Lipase inhibition) -4.53 mg/mL (α -amylase inhibition)	900 mg/kg/day of <i>Stellaria medium</i> extract	<i>In vivo</i> trial (Rani et al., 2012a)
Saponins, flavonoids, and phenols		Inhibits lipase and α -amylase activity (Rani et al., 2012b)	-2.34 mg/mL (lipase inhibition)	900 mg/kg/day of <i>Achyranthes aspera</i> extract	<i>In vivo</i> trial (Rani et al., 2012b)

(Continued on following page)

TABLE 1 (Continued) Plant-derived active compounds, source, and effects of phytochemicals responsible for obesity management.

Active compound	Source (plant species)	Effects/Mechanism of action	IC ₅₀ value	Dosages employed	Study type
	<i>Achyranthes aspera</i> (Hariharan and Rangaswami, 1970)		–3.83 mg/mL (α-amylase inhibition)		
Megastigmanes and alkaloids such as <i>trans</i> -N-coumaroyltyramine, <i>trans</i> -N-feruloyltyramine, roemerine oxide, lirioidenine, and annuionone D	<i>Nelumbo nucifera</i> Gaertn	-Inhibits lipase and α-amylase activity	–0.46 mg/mL (Lipase inhibition)	20 g (i.e., 10% yield) of a dark brown, <i>Nelumbo nucifera</i> leaves extract in high fat diet per day	<i>In vivo</i> and <i>In vitro</i> trial (Ono et al., 2006b)
		-Suppresses adipocyte differentiation (Ahn et al., 2013)	–0.82 mg/mL (α-amylase inhibition)		
Saponin, sapogenins and Phenanthrenes such as dioscin and diosgenin	<i>Dioscorea nipponica</i> Makino	-Suppressed blood triacylglycerol level	5–10 µg/mL (Lipase inhibition)	20–50 g/kg/day of methanol extract of <i>Dioscorea nipponica</i> Makino powder (DP)	<i>In vivo</i> trial (Kwon et al., 2003a)
		-Inhibits fat absorption (Kwon et al., 2003a)			
Saponins known as platycosides such as platycodin A, C, D, and deapioplatycodin D	<i>Platycodon grandiflorum</i>	-Reduces hyperlipidemia, diabetes and inflammatory diseases	-	–500 µg/mL/day of total saponin	<i>In vitro</i> trial (Xu et al., 2005)
		-Suppresses hypercholesterolemia and hyperlipidemia by inhibiting intestinal absorption of dietary fats mediated by pancreatic lipase inhibition. (Xu et al., 2005)		–500 µg/mL/day of platycodin	
Licochalcone A and Glycyrrhizin	<i>Glycyrrhiza uralensis</i>	- Inhibits pancreatic lipase activity (WonLicochalcone et al., 2007)	35 µg/mL	2, 4, and 6 mg/ml/day of licochalcone A	<i>In vitro</i> trial (WonLicochalcone et al., 2007)
		- Contributes in browning of inguinal white adipose tissue (Lee et al., 2018)			
Ursolic acid (Bacanli et al., 2019)	<i>Malus pumila</i> , <i>Ocimum basilicum</i> , <i>Vaccinium macrocarpon</i> , <i>Olea europaea</i> , <i>Origanum vulgare</i> , <i>Rosmarinus officinalis</i> , <i>Salvia</i> , and <i>Thymus</i> (Ikeda et al., 2008)	-Enhances insulin sensitivity and glucose intolerance (Jang et al., 2009)	-	0.5 g/kg/day of ursolic acid	<i>In vivo</i> (Jang et al., 2009)
Cinnamic acid	<i>Cinnamomum cassia</i> L.) J.Presl, <i>Vitis vinifera</i> L., <i>Camellia sinensis</i> L.) Kuntze, <i>Theobroma cacao</i> L., <i>Spinacia oleracea</i> L., <i>Apium graveolens</i> L. (Guzman, 2014)	-Improves hyperglycemia and hyperlipidemia. -Increases insulin sensitivity, and lowers blood and hepatic lipids (Kim and Choung, 2010)	-	200 mg/kg/day after of cinnamon extract	<i>In vivo</i> (Kim and Choung, 2010)
Resveratrol	<i>Polygonum cuspidatum</i> , <i>Veratrum grandiflorum</i> , <i>Vitis vinifera</i> , <i>Arachis hypogaea</i> , and <i>Vaccinium oxycoccos</i>	-Improve insulin sensitivity	-	250 mg/day of resveratrol	Clinical trial (Bhatt et al., 2012)
		-Enhance GLUT4 translocation			
		-Reduce oxidative stress			
		-Regulate carbohydrate metabolizing enzymes			
		-Activate SIRT1 and AMPK			
		-Reduce adipogenic genes. (Bagul and Banerjee, 2015)			
Procyanidins	<i>Prunus domestica</i> , <i>Prunus salicina</i> , <i>Malus</i>	-Enhances Insulin sensitivity	-	850 mg flavan-3-ols and 100 mg isoflavones per day	Clinical trial (Curtis et al., 2012)

(Continued on following page)

TABLE 1 (Continued) Plant-derived active compounds, source, and effects of phytochemicals responsible for obesity management.

Active compound	Source (plant species)	Effects/Mechanism of action	IC ₅₀ value	Dosages employed	Study type
	<i>domestica</i> , <i>Vitis vinifera</i> , <i>Prunus amygdalus</i> , and <i>Cicer arietinum</i>	-Increases the active GLP-1 levels and controls glucose homeostasis. (González-Abuin et al., 2015)			
Mangiferin (xanthonoid)	Mango and rhizomes of <i>Anemarrhena asphodeloides</i> (Miura et al., 2001)	-Improve insulin sensitivity -Altered lipid profiles -Reduce the number of adipokines. (Saleh et al., 2014)	-	20 mg/kg/day of mangiferin	<i>In vitro</i> (Saleh et al., 2014)
Ginger extracts such as gingerols, shogaols, paradols, and gingerenone A	<i>Zingiber Officinale</i> (Khandouzi et al., 2015)	-Improve insulin sensitivity and glucose uptake (Sekiya et al., 2004) -6-gingerol decreases PPAR γ , C/EBP α , and FABP4 expression and increases adiponectin expression (Cheng et al., 2022)	-	- 30–1,000 μ M/day of 6-gingerol (insulin sensitivity) -25 mg/kg/day of 6-gingerol (increases adiponectin expression)	- <i>In vitro</i> (Sekiya et al., 2004) - <i>In vivo</i> (Cheng et al., 2022)
Saffron extracts including; carotenoids, crocin, and its aglycone crocetin, picrocrocin, and safranal	<i>Crocus sativus</i> Linn. (Kang et al., 2012)	-Insulin sensitivity enhancement -Stimulation of insulin signaling pathways -Improvement of β -cell activities -Promotion of glucose transporter type 4 (GLUT-4) expression -Regulation of oxidative stress -Repression of inflammatory pathways (Mobasser et al., 2020b)	-	2.5 μ g/ml/day of 47% (w/w) of saffron stigma extract	<i>In vitro</i> (Kang et al., 2012)
Amorfrutin derivatives	Fruits of <i>Amorpha fruticosa</i> , and the edible roots of <i>Glycyrrhiza foetida</i> (Weidner et al., 2012)	-Lipid and glucose metabolism -Improve insulin sensitivity -They are potent PPAR γ agonists -Improve insulin sensitivity and regulate adipokines regulation. (Malapaka et al., 2012)	51 nM	100 mg/kg/day of amorfrutin 1	<i>In vivo</i> (Weidner et al., 2012)
Steroidal saponins called Ginsenosides	Genus <i>Eleutherococcus</i> and genus <i>Panax</i> (Vogler et al., 1999)	-Increase insulin production -Preserve pancreatic islets -Increase insulin sensitivity -Stimulate glucose uptake (Xie et al., 2011) -Elevate the UCP1, PRDM16, and PGC-1 in 3T3-L1 cells and primary white adipocytes	-	6 g/day of Panax ginseng extract	Clinical trial (Vuksan et al., 2008)
Steroidal saponins such as diosgenin, furostanol glycosides, alkaloids such as trigocoumarin,	<i>Trigonella foenum-graecum</i> L. (Gupta et al., 2001)	-Increase insulin release	-	50 mg/kg/day of active hypoglycemic principle isolated from water extract	<i>In vivo</i> (Puri et al., 2002)

(Continued on following page)

TABLE 1 (Continued) Plant-derived active compounds, source, and effects of phytochemicals responsible for obesity management.

Active compound	Source (plant species)	Effects/Mechanism of action	IC ₅₀ value	Dosages employed	Study type
nicotinic acid, trimethyl coumarin, and trigonelline		-Improve insulin sensitivity (Puri et al., 2002)		of seeds of <i>Trigonella foenum graecum</i>	
		- Increase the expression of BAT signature proteins including PGC-1 α , PRDM16, and UCP1 in 3T3-L1 white adipocytes (Choi et al., 2021)			
Allicin, ajoene, dithiins, allyl methyl trisulfide, diallyl sulfide, diallyl disulfide, diallyl trisulfide, and β -carbolide alkaloids	<i>Allium Sativa</i>	-Increase insulin secretion and enhance insulin sensitivity (Liu et al., 2005)	-	-100 mg/kg every other day of gavage garlic oil	<i>In vivo</i> (Liu et al., 2005)
		-Increased phosphorylation on AMPK and its downstream proteins		-40 mg/kg every other day of diallyl trisulfide	
		- β -carboline alkaloid suppressed the differentiation of adipocytes			
Camphor, eugenol, cinnamaldehyde, cinnamic acid, cinnamyl alcohol, and coumarin	<i>Cinnamomum zeylanicum</i> and <i>Cinnamon cassia</i> (Hariri and Ghiasvand, 2016)	-Increase insulin sensitivity (Couturier et al., 2010)	-	-20 g/kg/day of <i>Cinnamon cassia</i> powder (Improve insulin sensitivity)	<i>In vivo</i> trial (Couturier et al., 2010)
		- Increase the expression of UCP1 and other brown adipocyte markers in 3T3-L1 adipocytes and subcutaneous adipocytes		-80 μ g/ml/day of cinnamon extract (increase brown adipocyte markers)	- <i>In vivo</i> , <i>ex vivo</i> , <i>in vitro</i> trial (Kwan et al., 2017)
		-Increase the biogenesis of mitochondrial protein (Kwan et al., 2017)			
Hypericin, hyperforin, and adhyperforin (Gray et al., 2000)	<i>Hypericum perforatum</i> L. (Tokgöz and Altan, 2020)	-Improves hyperinsulinemia, hyperglycemia, insulin tolerance, and glucose infusion rate (GIR) (Tian et al., 2015)	-	50 mg/kg/day and 200 mg/kg/day of <i>H. perforatum</i> L. extracts	<i>In vitro</i> trial (Tian et al., 2015)
Rhein (anthraquinone)	<i>Rheum undulatum</i> , <i>Rheum palmatum</i> , and <i>Cassia reticulata</i> (Huang et al., 2021)	Decrease in PPAR γ , C/EBP α protein and mRNA levels in 3T3-L1 cells (Liu et al., 2011)	-	2.5, 5, and 10 μ M/day of rhein	<i>In vitro</i> trial (Liu et al., 2011)
Genistein	<i>Genista tinctoria</i> (Mukund et al., 2017)	Reduces PPAR γ and downregulated adipogenesis (Feng et al., 2016)	-	100 μ M/day of genistein	<i>In vitro</i> trial (Harmon et al., 2002)
Esculetin	<i>Fraxinus rhynchophylla</i> Hance (Zhang et al., 2022)	-Inhibits cell proliferation	-	100 and 200 μ M/day of esculetin	<i>In vitro</i> trial (Yang et al., 2006)
		-Induces apoptosis in preadipocytes and mature adipocytes			
		-Inhibits adipogenesis in 3T3-L1 preadipocytes. (Yang et al., 2006)			
Berberine	<i>Cortidis rhizome</i> (Huang et al., 2006)	-Suppresses the 3T3-L1 adipocyte differentiation, proliferation, and lipid buildup (Huang et al., 2006)	-	1.25, 2.5, and 5 μ M/day of berberine (Inhibit 3T3-L1 adipocyte differentiation)	<i>In vitro</i> trial (Huang et al., 2006)
		- Increases the expression of browning-related UCP1 (Zhang et al., 2014)			
Baicalein	<i>Scutellaria baicalensis</i> (Cha et al., 2006)	Increase the expression of COX-2 (Cha et al., 2006)	-	100, 150 and 200 μ M/day of baicalein	<i>In vitro</i> trial (Cha et al., 2006)

(Continued on following page)

TABLE 1 (Continued) Plant-derived active compounds, source, and effects of phytochemicals responsible for obesity management.

Active compound	Source (plant species)	Effects/Mechanism of action	IC ₅₀ value	Dosages employed	Study type
Flavonoids, glycosides, phenolic acids, and tannins (Choi et al., 2018)	<i>Alchemilla monticola</i> Opiz. (ALM) (Tasić-Kostov et al., 2019)	Inhibits the adipogenic markers PPAR γ , C/EBP α , and adiponectin (Mladenova et al., 2021)	-	5, 10 and 25 μ g/ml/day of <i>A. monticola</i> extract	<i>In vitro</i> trial (Mladenova et al., 2021)
Delphinidin	Pigmented fruits and vegetables	-Inhibit the production of adipogenesis and lipogenesis markers	-	25, 50 and 100 μ M of Delphinidin-3-O- β -Glucoside	<i>In vitro</i> trial (Park et al., 2019b)
		- Increase the expression of fatty acid metabolism genes in 3T3-L1 adipocytes. (Park et al., 2019b)			
Curcumin	Turmeric (<i>Curcuma longa</i> Linn) (Lee et al., 2009)	-Activate the AMP-activated protein kinase (AMPK) in 3T3-L1 cells (Lee et al., 2009)	-	-10–50 μ M/day of curcumin (Activate AMPK in 3T3-L1 cells)	- <i>In vitro</i> trial (Lee et al., 2009)
		-Increases the plasma norepinephrine levels and the expression of the β 3AR gene (Wang et al., 2015b)		- 50 or 100 mg/kg/day of curcumin (Increase plasma NE levels)	- <i>In vivo</i> trial (Wang et al., 2015b)

noteworthy cardiovascular side effects, such as elevated heart rate and blood pressure, and has been linked to an augmented risk of heart attack, stroke, and withdrawal symptoms upon abrupt cessation. Consequently, due to these safety concerns, the utilization of ephedrine as a weight loss aid is not recommended, resulting in its prohibition or restriction in numerous countries (Gadde and Atkins, 2020). Additionally, a notable limitation linked to capsaicin is the difficulty of achieving a significant weight loss effect solely through dietary intake, due to the challenge of attaining an adequate dosage. Furthermore, at anti-obesity doses, capsaicin possesses the potential to cause gastrointestinal discomfort in specific individuals, thereby limiting its practical utilization (Li et al., 2020).

Differently, appetite suppressants also show limitations on the long-run use. Although khat usage is prevalent, psychosis cases were reported. However, it has been revealed about some cases of psychotic reactions in Somalian males, emphasizing the significance of recognizing the medical and psychiatric complications of khat abuse. Notably, the side effects of khat, such as gastrointestinal discomfort, and its potential involvement in forensic cases of homicide and combined homicide-suicide, warrant concern. Cultural dislocation may further amplify the adverse effects of khat consumption. Similar to other well-known amphetamine-type stimulants, chronic use of synthetic cathinone compounds can significantly impact the central nervous system, leading to acute psychosis, hypomania, paranoid ideation, and delusions (Pantelis et al., 1989; Weinstein et al., 2017). Despite its limited availability and high public demand, *Hoodia gordonii* has been associated with potential side effects including skin reactions, elevated heart rate, and high blood pressure. However, the main focus of scientific studies has been on quality control due to the scarcity of *H. gordonii* plant material resulting from its sparse geographical distribution, slow maturation rate, and the requirement of permits for cultivation and export. The high

demand has led to a significant risk of product adulteration (Vermaak et al., 2011).

Both garlic and fenugreek have a history of safe medicinal use for most individuals. Potential side effects of garlic include gastrointestinal discomfort, sweating, dizziness, allergic reactions such as (allergic contact dermatitis, generalized urticaria, angioedema, pemphigus, anaphylaxis and photoallergy), and bleeding (Borrelli et al., 2007), whereas anecdotal reports suggest less serious side effects such as diarrhea and indigestion for fenugreek. Additionally, the aqueous extract of fenugreek has been shown to inhibit the coagulation process *in vitro*, resulting in a significant prolongation of prothrombin time and inhibition of clot formation (Taj Eldin et al., 2013). Thus, combining both plants and/or extract for the purpose of reducing overweight could pose a bleeding adverse reaction. On the same context, clinical and experimental studies provide evidence supporting the antidepressant-like effects of St. John's Wort due to a non-selective blockade of the reuptake of serotonin, noradrenaline and dopamine. However, it is important to acknowledge the side effects associated with its use, including nausea, rash, fatigue, restlessness, photosensitivity, acute neuropathy, and even episodes of mania and serotonergic syndrome when used concurrently with other antidepressant drugs. These side effects indicate that *H. perforatum* extracts may possess significant pharmacological activity by targeting various neurotransmission systems involved in depression. Nevertheless, there is limited information available regarding the safety of *H. perforatum*, including potential interactions with other medications (Rodríguez-Landa and Contreras, 2003).

Cumulative evidence suggests that under specific conditions, ursolic acid may exhibit adverse reactions, including cytotoxicity. Furthermore, the therapeutic application of ursolic acid is significantly hindered by its poor solubility in aqueous medium and limited bioavailability *in vivo*. Notably, ursolic acid has been

observed to induce inflammation by enhancing the production of nitric oxide and TNF- α in resting macrophages through NF- κ B transactivation, and upregulates IL-1 β , an important pro-inflammatory mediator. In the context of male rat spermatogenesis, the extract of ursolic acid was found to impede the physiological maturation of sperm, evident by decreased sperm count and motility, potentially attributed to the depletion of testosterone at the target level (Sun et al., 2020). Finally, obesity is a multifactorial condition that requires a comprehensive approach for effective management. Relying solely on single plant extract or one phytochemical component without addressing multi-approaches, such as appetite suppression, lipases inhibition, insulin sensitivity enhancement, in addition to other mechanisms, is unlikely to lead to sustainable weight loss. For instance, the weight-loss supplement Buginawa (Bugi) contains twelve different medicinal herbs in a novel water extract combination that improves insulin sensitivity, decreases PPAR γ , and C/EBP α , and inhibits adipogenesis (Park Y.-J. et al., 2019).

5 Conclusion

Recently, obesity affects much more than just physical appearance and is now recognized as a medical condition that should be treated to minimize the risk of developing other metabolic diseases like diabetes. The mechanisms exploited by marketed anti-obesity medicines are appetite suppression by increasing norepinephrine, dopamine, and serotonin in the synaptic clefts, pancreatic lipase, and amylase inhibition, and gastric emptying slowing. However, the occurrence of unwanted, adverse effects affecting cardiovascular, psychological, and gastrointestinal systems urge for more effective treatment plans with minimal risk/complications. Phytochemicals derived from plants seems as a promising source of anti-obesity drugs as majority of them confer benefits via the same mechanisms with fewer adverse events. Exceptionally, some natural products also display other important features that could be essential as anti-obesity drugs, especially WAT browning, thermogenesis and adipocyte apoptosis induction, and adipogenesis inhibition. At least so far, those mechanisms have not been shown by any synthetic anti-obesity agents. Mechanisms explored in natural products are; metabolic and thermogenic stimulation, appetite regulation, pancreatic lipase and amylase inhibition, insulin sensitivity enhancement, and adipogenesis inhibition and

adipocyte apoptosis induction. The phytochemicals involved in fighting obesity usually affect more than one specific mechanism since the fat storage and energy expenditure processes are complicated and intricate. Uncoupling protein UCP-1, PR domain containing 16 (PRDM16), and peroxisome proliferator-activated receptor (PPAR)- γ have a role in the browning of WAT and consequently reducing lipid accumulation. Most plant extracts/isolated compounds have been found to affect more than one of these thermogenic transcriptional factors. Moreover, SIRT1 and AMPK are controlled by phytochemicals and exert their actions on the above-mentioned transcriptional factors through the induction of the β_3 adrenergic receptor that finally induces mitochondrial biogenesis. The strategy that can effectively reduce obesity is to inhibit/activate more than one mechanism with different pathways, can be more effective in addressing obesity. Furthermore, a holistic approach that combines a balanced diet, regular exercise, behavior modifications, and medical guidance, if necessary, is essential for long-term success in weight management.

Author contributions

Conceptualization: SM; Methodology: SM, AH, HS, LM, and BG; Screening: GG, SS, DC, and KD; Original Draft Preparation: US and SM; Writing—Review and Editing: SM, HS, BG, and LM; Supervision: SM and LM; NK and HG: supervision and funding acquisition.

Conflict of interest

The authors declare that the research was conducted in the absence of any commercial or financial relationships that could be construed as a potential conflict of interest.

Publisher's note

All claims expressed in this article are solely those of the authors and do not necessarily represent those of their affiliated organizations, or those of the publisher, the editors and the reviewers. Any product that may be evaluated in this article, or claim that may be made by its manufacturer, is not guaranteed or endorsed by the publisher.

References

- Adisakwattana, S. (2017). Cinnamic acid and its derivatives: Mechanisms for prevention and management of diabetes and its complications. *Nutrients* 9 (2), 163. doi:10.3390/nu9020163
- Afreen, F., Zobayed, S. M., and Kozai, T. (2006). Melatonin in *Glycyrrhiza uralensis*: Response of plant roots to spectral quality of light and UV-B radiation. *J. pineal Res.* 41 (2), 108–115. doi:10.1111/j.1600-079X.2006.00337.x
- Agarwal, K. C. (1996). Therapeutic actions of garlic constituents. *Med. Res. Rev.* 16 (1), 111–124. doi:10.1002/(SICI)1098-1128(199601)16:1<111:AID-MED4>3.0.CO;2-5
- Ahmadi, N., Nabavi, V., Hajsadeghi, F., Zeb, I., Flores, F., Ebrahimi, R., et al. (2013). Aged garlic extract with supplement is associated with increase in Brown adipose, decrease in white adipose tissue and predict lack of progression in coronary atherosclerosis. *Int. J. Cardiol.* 168 (3), 2310–2314. doi:10.1016/j.ijcard.2013.01.182
- Ahn, J. H., Kim, E. S., Lee, C., Kim, S., Cho, S. H., Hwang, B. Y., et al. (2013). Chemical constituents from *Nelumbo nucifera* leaves and their anti-obesity effects. *Bioorg. Med. Chem. Lett.* 23 (12), 3604–3608. doi:10.1016/j.bmcl.2013.04.013
- Ahn, J., Lee, H., Kim, S., and Ha, T. (2010). Curcumin-induced suppression of adipogenic differentiation is accompanied by activation of Wnt/ β -catenin signaling. *Am. J. Physiol. Cell Physiol.* 298 (6), C1510–C1516. doi:10.1152/ajpcell.00369.2009
- Aipire, A., Mahabati, M., Cai, S., Wei, X., Yuan, P., Aimaier, A., et al. (2020). The immunostimulatory activity of polysaccharides from *Glycyrrhiza uralensis*. *PeerJ* 8, e8294. doi:10.7717/peerj.8294
- Arita, Y., Kihara, S., Ouchi, N., Takahashi, M., Maeda, K., Miyagawa, J., et al. (1999). Paradoxical decrease of an adipose-specific protein, adiponectin, in obesity. *Biochem. biophysical Res. Commun.* 257 (1), 79–83. doi:10.1006/bbrc.1999.0255

- Aron, P. M., and Kennedy, J. A. (2008). Flavan-3-ols: Nature, occurrence and biological activity. *Mol. Nutr. food Res.* 52 (1), 79–104. doi:10.1002/mnfr.200700137
- Aryaean, N., Sedei, S. K., and Arablou, T. (2017). Polyphenols and their effects on diabetes management: A review. *Med. J. Islam Repub. Iran.* 31, 134. doi:10.14196/mjiri.31.134
- Ashraf, R., Aamir, K., Shaikh, A. R., and Ahmed, T. (2005). Effects of garlic on dyslipidemia in patients with type 2 diabetes mellitus. *J. Ayub Med. Coll. Abbottabad* 17 (3), 60–64.
- Astell, K. J., Mathai, M. L., and Su, X. Q. (2013). A review on botanical species and chemical compounds with appetite suppressing properties for body weight control. *Plant Foods Hum. Nutr.* 68 (3), 213–221. doi:10.1007/s11130-013-0361-1
- Astrup, A., Breum, L., Toubro, S., Hein, P., and Quaade, F. (1992). The effect and safety of an ephedrine/caffeine compound compared to ephedrine, caffeine and placebo in obese subjects on an energy restricted diet. A double blind trial. *Int. J. Obes. Relat. metabolic Disord.* 16 (4), 269–277.
- Astrup, A. (2000). Thermogenic drugs as a strategy for treatment of obesity. *Endocrinol. Metab. Seoul.* 13, 207–212. doi:10.1385/ENDO:13:2:207
- Attele, A. S., Wu, J. A., and Yuan, C.-S. (1999). Ginseng pharmacology: Multiple constituents and multiple actions. *Biochem. Pharmacol.* 58 (11), 1685–1693. doi:10.1016/S0006-2952(99)00212-9
- Bacanli, M., Dilsiz, S. A., Başaran, N., and Başaran, A. A. (2019). Effects of phytochemicals against diabetes. *Adv. Food Nutr. Res.* 89, 209–238. doi:10.1016/bs.afnr.2019.02.006
- Bader, A., Braca, A., De Tommasi, N., and Morelli, I. (2003). Further constituents from *Caralluma negevensis*. *Phytochemistry* 62, 1277–1281. doi:10.1016/S0031-9422(02)00678-7
- Baek, S. C., Nam, K. H., Yi, S. A., Jo, M. S., Lee, K. H., Lee, Y. H., et al. (2019). Anti-adipogenic effect of β -carboline alkaloids from garlic (*Allium sativum*). *Foods* 8 (12), 673. doi:10.3390/foods8120673
- Bagul, P. K., and Banerjee, S. K. (2015). Application of resveratrol in diabetes: Rationale, strategies and challenges. *Curr. Mol. Med.* 15 (4), 312–330. doi:10.2174/1566524015666150505155702
- Bahrin, A. A., Moshawih, S., Dhaliwal, J. S., Kanakal, M. M., Khan, A., Lee, K. S., et al. (2022). Cancer protective effects of plums: A systematic review. *Biomed. Pharmacother.* 146, 112568. doi:10.1016/j.biopha.2021.112568
- Balcioglu, A., and Wurtman, R. J. (2000). Sibutramine, a serotonin uptake inhibitor, increases dopamine concentrations in rat striatal and hypothalamic extracellular fluid. *Neuropharmacology* 39 (12), 2352–2359. doi:10.1016/S0028-3908(00)00083-6
- Ballinger, A., and Peikin, S. R. (2002). Orlistat: Its current status as an anti-obesity drug. *Eur. J. Pharmacol.* 440 (2–3), 109–117. doi:10.1016/S0014-2999(02)01422-X
- Balogun, O., and Kang, H. W. (2022). Garlic scape (*Allium sativum* L) extract decreases adipogenesis by activating AMK-activated protein kinase during the differentiation in 3T3-L1 adipocytes. *J. Med. Food* 25 (1), 24–32. doi:10.1089/jmf.2021.0014
- Barbera, M. J., Schluter, A., Pedraza, N., Iglesias, R., Villarroya, F., and Giral, M. (2001). Peroxisome proliferator-activated receptor α activates transcription of the Brown fat uncoupling protein-1 gene. A link between regulation of the thermogenic and lipid oxidation pathways in the Brown fat cell. *J. Biol. Chem.* 276 (2), 1486–1493. doi:10.1074/jbc.M006246200
- Barceloux, D. G. (2009). Pepper and capsaicin (*Capsicum* and *piper* species). Pepper capsaicin (*Capsicum Piper* species). Disease-a-month. *DM* 55 (6), 380–390. doi:10.1016/j.disamonth.2009.03.008
- Bargut, T. C. L., Souza-Mello, V., Aguilu, M. B., and Mandarim-de-Lacerda, C. A. (2017). Browning of white adipose tissue: Lessons from experimental models. *Horm. Mol. Biol. Clin. Invest.* 31 (1). doi:10.1515/hmbci-2016-0051
- Bartel, A., and Heeren, J. (2014). Adipose tissue browning and metabolic health. *Nat. Rev. Endocrinol.* 10 (1), 24–36. doi:10.1038/nrendo.2013.204
- Basavarajappa, D. K., Gupta, V. K., and Rajala, R. V. (2012). Protein tyrosine phosphatase 1B: A novel molecular target for retinal degenerative diseases. *Adv. Exp. Med. Biol.* 723, 829–834. doi:10.1007/978-1-4614-0631-0_106
- Baskaran, P., Krishnan, V., Ren, J., and Thyagarajan, B. (2016). Capsaicin induces browning of white adipose tissue and counters obesity by activating TRPV1 channel-dependent mechanisms. *Br. J. Pharmacol.* 173 (15), 2369–2389. doi:10.1111/bph.13514
- Bensaid, M., Gary-Bobo, M., Esclanlon, A., Maffrand, J. P., Le Fur, G., Oury-Donat, F., et al. (2003). The cannabinoid CB1 receptor antagonist SR141716 increases Acpr30 mRNA expression in adipose tissue of obese fa/fa rats and in cultured adipocyte cells. *Mol. Pharmacol.* 63 (4), 908–914. doi:10.1124/mol.63.4.908
- Bhatt, J., Thomas, S., and Nanjan, M. (2012). Resveratrol supplementation improves glycemic control in type 2 diabetes mellitus. *Nutr. Res.* 32 (7), 537–541. doi:10.1016/j.nutres.2012.06.003
- Bishayee, A., Barnes, K. F., Bhatia, D., Darvesh, A. S., and Carroll, R. T. (2010). Resveratrol suppresses oxidative stress and inflammatory response in diethylnitrosamine-initiated rat hepatocarcinogenesis. *Cancer Prev. Res.* 3 (6), 753–763. doi:10.1158/1940-6207.CAPR-09-0171
- Blundell, J. E. (1977). Is there a role for serotonin (5-hydroxytryptamine) in feeding? *Int. J. Obes.* 1 (1), 15–42.
- Bolin, A. P., Sousa-Filho, C. P. B., Dos Santos, G. T. N., Ferreira, L. T., de Andrade, P. B. M., Figueira, A. C. M., et al. (2020). Adipogenic commitment induced by green tea polyphenols remodel adipocytes to a thermogenic phenotype. *J. Nutr. Biochem.* 83, 108429. doi:10.1016/j.jnutbio.2020.108429
- Borchardt, R. T., and Huber, J. A. (1975). Catechol O-methyltransferase. 5. Structure-activity relationships for inhibition by flavonoids. *J. Med. Chem.* 18 (1), 120–122. doi:10.1021/jm00235a030
- Borrelli, F., Capasso, R., and Izzo, A. A. (2007). Garlic (*Allium sativum* L): Adverse effects and drug interactions in humans. *Mol. Nutr. Food Res.* 51 (11), 1386–1397. doi:10.1002/mnfr.200700072
- Boström, P., Wu, J., Jedrychowski, M. P., Korde, A., Ye, L., Lo, J. C., et al. (2012). A PGC1- α -dependent myokine that drives Brown-fat-like development of white fat and thermogenesis. *Nature* 481 (7382), 463–468. doi:10.1038/nature10777
- Bruyns, P. V. (2005). *Stapeliads of southern Africa and Madagascar*. Pretoria: Umdaus Press. Vol. 1.
- Burcelin, R., and Gourdy, P. (2017). Harnessing glucagon-like peptide-1 receptor agonists for the pharmacological treatment of overweight and obesity. *Obes. Rev.* 18 (1), 86–98. doi:10.1111/obr.12465
- Cannon, B., and Nedergaard, J. (2004). Brown adipose tissue: Function and physiological significance. *Physiol. Rev.* 84 (1), 277–359. doi:10.1152/physrev.00015.2003
- Cannon, B., and Nedergaard, J. (2010). Metabolic consequences of the presence or absence of the thermogenic capacity of Brown adipose tissue in mice (and probably in humans). *Int. J. Obes. (Lond)* 34 (1), S7–S16. doi:10.1038/ijo.2010.177
- Cao, H., Urban, J. F., Jr., and Anderson, R. A. (2008). Cinnamon polyphenol extract affects immune responses by regulating anti- and proinflammatory and glucose transporter gene expression in mouse macrophages. *J. Nutr.* 138 (5), 833–840. doi:10.1093/jn/138.5.833
- Carey, A., Paitak, R., Formosa, M., Van Every, B., Bertovic, D. A., Anderson, M. J., et al. (2015). Chronic ephedrine administration decreases Brown adipose tissue activity in a randomised controlled human trial: Implications for obesity. *Diabetol. Metab. Syndr.* 58, 1045–1054. doi:10.1007/s00125-015-3543-6
- Cawthorn, W., Heyd, F., Hegyi, K., and Sethi, J. K. (2007). Tumour necrosis factor- α inhibits adipogenesis via a beta-catenin/TCF4(TCF7L2)-dependent pathway. *Cell Death Differ.* 14 (7), 1361–1373. doi:10.1038/sj.cdd.4402127
- Cha, M.-H., Kim, I. C., Lee, B. H., and Yoon, Y. (2006). Baicalein inhibits adipocyte differentiation by enhancing COX-2 expression. *J. Med. Food* 9 (2), 145–153. doi:10.1089/jmf.2006.9.145
- Chan, Y., Ng, S. W., Tan, J. Z. X., Gupta, G., Negi, P., Thangavelu, L., et al. (2021). Natural products in the management of obesity: Fundamental mechanisms and pharmacotherapy. *South Afr. J. Bot.* 143, 176–197. doi:10.1016/j.sajb.2021.07.026
- Chen, J., Eltzschig, H., and Fredholm, B. (2013). Adenosine receptors as drug targets – what are the challenges? *Nat. Rev. Drug Discov.* 12, 265–286. doi:10.1038/nrd3955
- Cheng, Z., Xiong, X., Zhou, Y., Wu, F., Shao, Q., Dong, R., et al. (2022). 6-gingerol ameliorates metabolic disorders by inhibiting hypertrophy and hyperplasia of adipocytes in high-fat-diet induced obese mice. *Biomed. Pharmacother.* 146, 112491. doi:10.1016/j.biopha.2021.112491
- Choi, J., Park, Y. G., Yun, M. S., and Seol, J. W. (2018). Effect of herbal mixture composed of *Alchemilla vulgaris* and *mimosa* on wound healing process. *Biomed. Pharmacother.* 106, 326–332. doi:10.1016/j.biopha.2018.06.141
- Choi, K., and Kim, Y.-B. (2010). Molecular mechanism of insulin resistance in obesity and type 2 diabetes. *Korean J. Intern. Med.* 25 (2), 119–129. doi:10.3904/kjim.2010.25.2.119
- Choi, M., Mukherjee, S., and Yun, J. W. (2021). Trigonelline induces browning in 3T3-L1 white adipocytes. *Phytother. Res.* 35 (2), 1113–1124. doi:10.1002/ptr.6892
- Cohen, P., Levy, J. D., Zhang, Y., Frontini, A., Kolodin, D. P., Svensson, K. J., et al. (2014). Ablation of PRDM16 and beige adipose causes metabolic dysfunction and a subcutaneous to visceral fat switch. *Cell* 156 (1–2), 304–316. doi:10.1016/j.cell.2013.12.021
- Colman, E., Golden, J., Roberts, M., Egan, A., Weaver, J., and Rosebraugh, C. (2012). The FDA's assessment of two drugs for chronic weight management. *N. Engl. J. Med.* 367 (17), 1577–1579. doi:10.1056/NEJMp1211277
- Couturier, K., Batandier, C., Awada, M., Hininger-Favre, I., Canini, F., Anderson, R. A., et al. (2010). Cinnamon improves insulin sensitivity and alters the body composition in an animal model of the metabolic syndrome. *Arch. Biochem. Biophys.* 501 (1), 158–161. doi:10.1016/j.abb.2010.05.032
- Crawford, P. (2009). Effectiveness of cinnamon for lowering hemoglobin A1C in patients with type 2 diabetes: A randomized, controlled trial. *J. Am. Board Fam. Med.* 22 (5), 507–512. doi:10.3122/jabfm.2009.05.080093
- Curtis, P. J., Sampson, M., Potter, J., Dhataria, K., Kroon, P. A., and Cassidy, A. (2012). Chronic ingestion of flavan-3-ols and isoflavones improves insulin sensitivity and lipoprotein status and attenuates estimated 10-year CVD risk in medicated postmenopausal women with type 2 diabetes: A 1-year, double-blind, randomized, controlled trial. *Diabetes care* 35 (2), 226–232. doi:10.2337/dc11-1443

- Czernichow, S., and Batty, G. D. (2010). Withdrawal of sibutramine for weight loss: Where does this leave clinicians? *Obes. Facts* 3 (3), 155–156. doi:10.1159/000316508
- Dar, A., Faizi, S., Naqvi, S., Roome, T., Zikr-ur-Rehman, S., Ali, M., et al. (2005). Analgesic and antioxidant activity of mangiferin and its derivatives: The structure activity relationship. *Biol. Pharm. Bull.* 28 (4), 596–600. doi:10.1248/bpb.28.596
- de Groot, J. C., Weidner, C., Krausze, J., Kawamoto, K., Schroeder, F. C., Sauer, S., et al. (2013). Structural characterization of amorfrutins bound to the peroxisome proliferator-activated receptor γ . *J. Med. Chem.* 56 (4), 1535–1543. doi:10.1021/jm3013272
- Diepvens, K., Westerterp, K. R., and Westerterp-Plantenga, M. S. (2007a). Obesity and thermogenesis related to the consumption of caffeine, ephedrine, capsaicin, and green tea. *Am. J. physiology-Regulatory* 292, R77–R85. doi:10.1152/ajpregu.00832.2005
- Diepvens, K., Westerterp, K. R., and Westerterp-Plantenga, M. S. (2007b). Obesity and thermogenesis related to the consumption of caffeine, ephedrine, capsaicin, and green tea. *Am. J. Physiol. Regul. Integr. Comp. Physiol.* 292 (1), R77–R85. doi:10.1152/ajpregu.00832.2005
- Dömötör, A., Szolcsányi, J., and Mózsik, G. (2006). Capsaicin and glucose absorption and utilization in healthy human subjects. *Eur. J. Pharmacol.* 534 (1), 280–283. doi:10.1016/j.ejphar.2006.01.017
- Dulloo, A. (1993). Ephedrine, xanthines and prostaglandin-inhibitors: Actions and interactions in the stimulation of thermogenesis. *Int. J. Obes. Relat. Metab. Disord.* 17, S35–S40.
- Dulloo, A. G., Geissler, C. A., Horton, T., Collins, A., and Miller, D. S. (1989). Normal caffeine consumption: Influence on thermogenesis and daily energy expenditure in lean and postobese human volunteers. *Am. J. Clin. Nutr.* 49 (1), 44–50. doi:10.1093/ajcn/49.1.44
- Dulloo, A. G., Seydoux, J., Girardier, L., Chantre, P., and Vandermander, J. (2000). Green tea and thermogenesis: Interactions between catechin-polyphenols, caffeine and sympathetic activity. *Int. J. Obes. Relat. Metab. Disord.* 24 (2), 252–258. doi:10.1038/sj.ijo.0801101
- Dutt, H. C., Singh, S., Avula, B., Khan, I. A., and Bedi, Y. S. (2012). Pharmacological review of Caralluma R.Br. with special reference to appetite suppression and anti-obesity. *J. Med. Food* 15 (2), 108–119. doi:10.1089/jmf.2010.1555
- Elliot, W., and Chan, J. (1997). *Fenfluramine and dexfenfluramine withdrawn from market*. Atlanta: AHC Media.
- Eyolfson, D. A., Tikuisis, P., Xu, X., Weseen, G., and Giesbrecht, G. G. (2001). Measurement and prediction of peak shivering intensity in humans. *Eur. J. Appl. Physiology* 84 (1), 100–106. doi:10.1007/s004210000329
- Feng, S., Reuss, L., and Wang, Y. (2016). Potential of natural products in the inhibition of adipogenesis through regulation of PPAR γ expression and/or its transcriptional activity. *Molecules* 21 (10), 1278. doi:10.3390/molecules21101278
- Fernandes, A. B., Alves da Silva, J., Almeida, J., Cui, G., Gerfen, C. R., Costa, R. M., et al. (2020). Postgestive modulation of food seeking depends on vagus-mediated dopamine neuron activity. *Neuron* 106 (5), 778–788. doi:10.1016/j.neuron.2020.03.009
- Ferreira, T., Shuler, J., Guimarães, R. J., and Farah, A. (2019). “CHAPTER 1: introduction to coffee plant and genetics: Production, quality and chemistry,” in *Coffee* (London, United Kingdom: Royal Society of Chemistry).
- Fruhbeck, G., Gómez-Ambrosi, J., Muruzábal, F. J., and Burrell, M. A. (2001). The adipocyte: A model for integration of endocrine and metabolic signaling in energy metabolism regulation. *Am. J. Physiology-Endocrinology Metabolism* 280 (6), E827–E847. doi:10.1152/ajpendo.2001.280.6.E827
- Fu, C., Jiang, Y., Guo, J., and Su, Z. (2016). Natural products with anti-obesity effects and different mechanisms of action. *J. Agric. Food Chem.* 64 (51), 9571–9585. doi:10.1021/acs.jafc.6b04468
- Gadde, K. M., and Atkins, K. D. (2020). The limits and challenges of antiobesity pharmacotherapy. *Expert Opin. Pharmacother.* 21 (11), 1319–1328. doi:10.1080/14656566.2020.1748599
- Gardiner, J. V., Kong, W. M., Ward, H., Murphy, K. G., Dhillon, W. S., and Bloom, S. R. (2005). AAV mediated expression of anti-sense neuropeptide Y cRNA in the arcuate nucleus of rats results in decreased weight gain and food intake. *Biochem. Biophys. Res. Commun.* 327 (4), 1088–1093. doi:10.1016/j.bbrc.2004.12.113
- Geoffroy, P., Ressault, B., Marchioni, E., and Miesch, M. (2011). Synthesis of Hoodigogenin A, aglycone of natural appetite suppressant glycosides extracted from *Hoodia gordonii*. *Steroids* 76 (7), 702–708. doi:10.1016/j.steroids.2011.03.014
- Ghaben, A. L., and Scherer, P. E. (2019). Adipogenesis and metabolic health. *Nat. Rev. Mol. Cell Biol.* 20 (4), 242–258. doi:10.1038/s41580-018-0093-z
- Ginsberg, H. N. (2000). Insulin resistance and cardiovascular disease. *J. Clin. Invest.* 106 (4), 453–458. doi:10.1172/JCI10762
- Godard, M. P., Johnson, B. A., and Richmond, S. R. (2005). Body composition and hormonal adaptations associated with forskolin consumption in overweight and obese men. *Obes. Res.* 13 (8), 1335–1343. doi:10.1038/oby.2005.162
- Gómez, R., Navarro, M., Ferrer, B., Trigo, J. M., Bilbao, A., Del Arco, I., et al. (2002). A peripheral mechanism for CB1 cannabinoid receptor-dependent modulation of feeding. *J. Neurosci.* 22 (21), 9612–9617. doi:10.1523/JNEUROSCI.22-21-09612.2002
- Gómez-Hernández, A., Beneit, N., Díaz-Castroverde, S., and Escibano, Ó. (2016). Differential role of adipose tissues in obesity and related metabolic and vascular complications. *Int. J. Endocrinol.* 2016, 1216783. doi:10.1155/2016/1216783
- González-Abuín, N., Pinet, M., Casanova-Martí, A., Arola, L., Blay, M., and Ardevol, A. (2015). Procyanidins and their healthy protective effects against type 2 diabetes. *Curr. Med. Chem.* 22 (1), 39–50. doi:10.2174/0929867321666140916115519
- Goossens, G. H. (2008). The role of adipose tissue dysfunction in the pathogenesis of obesity-related insulin resistance. *Physiology Behav.* 94 (2), 206–218. doi:10.1016/j.physbeh.2007.10.010
- Goyal, B. R., Goyal, R. K., and Mehta, A. A. (2007). PHCOG rev. Plant review phytopharmacology of *Achyranthes aspera*: A review. *Pharmacogn. Rev.* 1 (1).
- Gray, D. E., Rottinghaus, G. E., Garrett, H. E., Pallardy, S. G., and Rottinghaus, G. E., (2000). Simultaneous determination of the predominant hyperforins and hypercins in *St. John's Wort* (*Hypericum perforatum* L.) by liquid chromatography. *J. AOAC Int.* 83 (4), 944–949. doi:10.1093/jaoac/83.4.944
- Gregoire, F. M., Smas, C. M., and Sul, H. S. (1998). Understanding adipocyte differentiation. *Physiol. Rev.* 78 (3), 783–809. doi:10.1152/physrev.1998.78.3.783
- Grunvald, E., Shah, R., Hernaez, R., Chandar, A. K., Pickett-Blakely, O., Teigen, L. M., et al. (2022). AGA clinical practice guideline on pharmacological interventions for adults with obesity. *Gastroenterology* 163 (5), 1198–1225. doi:10.1053/j.gastro.2022.08.045
- Gupta, A., Gupta, R., and Lal, B. (2001). Effect of trigonella foenum-graecum (fenugreek) seeds on glycaemic control and insulin resistance in type 2 diabetes mellitus: A double blind placebo controlled study. *J. Assoc. Physicians India* 49, 1057–1061.
- Gustafson, B., and Smith, U. (2015). Regulation of white adipogenesis and its relation to ectopic fat accumulation and cardiovascular risk. *Atherosclerosis* 241 (1), 27–35. doi:10.1016/j.atherosclerosis.2015.04.812
- Guzman, J. D. (2014). Natural cinnamic acids, synthetic derivatives and hybrids with antimicrobial activity. *Molecules* 19 (12), 19292–19349. doi:10.3390/molecules191219292
- Ha, Y. W., Na, Y. C., Seo, J. J., Kim, S. N., Linhardt, R. J., and Kim, Y. S. (2006). Qualitative and quantitative determination of ten major saponins in *Platycodon Radix* by high performance liquid chromatography with evaporative light scattering detection and mass spectrometry. *J. Chromatogr. A* 1135 (1), 27–35. doi:10.1016/j.chroma.2006.09.015
- Halbach, H. (1972). Medical aspects of the chewing of khat leaves. *Bull. World Health Organ* 47 (1), 21–29.
- Halford, J. C. G., Wanninayake, S. C. D., and Blundell, J. E. (1998). Behavioral satiety sequence (BSS) for the diagnosis of drug action on food intake. *Pharmacol. Biochem. Behav.* 61 (2), 159–168. doi:10.1016/s0091-3057(98)00032-x
- Halford, J. C., Harrold, J. A., Lawton, C. L., and Blundell, J. E. (2005). Serotonin (5-HT) drugs: Effects on appetite expression and use for the treatment of obesity. *Curr. Drug Targets* 6 (2), 201–213. doi:10.2174/1389450053174550
- Han, J., Yi, J., Liang, F., Jiang, B., Xiao, Y., Gao, S., et al. (2015). X-3, a mangiferin derivative, stimulates AMP-activated protein kinase and reduces hyperglycemia and obesity in db/db mice. *Mol. Cell. Endocrinol.* 405, 63–73. doi:10.1016/j.mce.2015.02.008
- Han, L.-K., Zheng, Y. N., Xu, B. J., Okuda, H., and Kimura, Y. (2002b). Saponins from *Platycodon Radix* ameliorate high fat diet-induced obesity in mice. *J. Nutr.* 132 (8), 2241–2245. doi:10.1093/jn/132.8.2241
- Han, L. K., Kimura, Y., Kawashima, M., Takaku, T., Taniyama, T., Hayashi, T., et al. (2001). Anti-obesity effects in rodents of dietary teasaponin, a lipase inhibitor. *Int. J. Obes. Relat. Metab. Disord.* 25 (10), 1459–1464. doi:10.1038/sj.ijo.0801747
- Han, L. K., Zheng, Y. N., Xu, B. J., Okuda, H., and Kimura, Y. (2002a). Saponins from *platycodon radix* ameliorate high fat diet-induced obesity in mice. *J. Nutr.* 132 (8), 2241–2245. doi:10.1093/jn/132.8.2241
- Hannan, J. M., Ali, L., Rokeya, B., Khaleque, J., Akhter, M., Flatt, P. R., et al. (2007). Soluble dietary fibre fraction of *Trigonella foenum-graecum* (fenugreek) seed improves glucose homeostasis in animal models of type 1 and type 2 diabetes by delaying carbohydrate digestion and absorption, and enhancing insulin action. *Br. J. Nutr.* 97 (3), 514–521. doi:10.1017/S0007114507657869
- Hansen, J. B., and Kristiansen, K. (2006). Regulatory circuits controlling white versus Brown adipocyte differentiation. *Biochem. J.* 398 (2), 153–168. doi:10.1042/BJ20060402
- Hareshbhai, P. H. (2021). Review of herbal plants used in the treatment of skin diseases. *J. Pharmacogn. Phytochemistry* 10 (3), 349–356.
- Hariharan, V., and Rangaswami, S. (1970). Structure of saponins A and B from the seeds of *achyranthes aspera*. *Phytochemistry* 9 (2), 409–414. doi:10.1016/s0031-9422(00)85154-7
- Hariri, M., and Ghasvand, R. (2016). Cinnamon and chronic diseases. *Adv. Exp. Med. Biol.* 929, 1–24. doi:10.1007/978-3-319-41342-6_1
- Harmon, A. W., Patel, Y. M., and Harp, J. B. (2002). Genistein inhibits CCAAT/enhancer-binding protein beta (C/EBPbeta) activity and 3T3-L1 adipogenesis by

- increasing C/EBP homologous protein expression. *Biochem. J.* 367, 203–208. doi:10.1042/BJ20020300
- Harms, M., and Seale, P. (2013). Brown and beige fat: Development, function and therapeutic potential. *Nat. Med.* 19 (10), 1252–1263. doi:10.1038/nm.3361
- Hasani-Ranjbar, S., Jouyandeh, Z., and Abdollahi, M. (2013). A systematic review of anti-obesity medicinal plants - an update. *J. Diabetes Metabolic Disord.* 12, 28. doi:10.1186/2251-6581-12-28
- Haththotuwa, R. N., Wijeyaratne, C. N., and Senarath, U. (2020). "Chapter 1 - worldwide epidemic of obesity," in *Obesity and obstetrics*. Editors T A Mahmood, S Arulkumaran, and F A Chervenak. Second Edition (Amsterdam, Netherlands: Elsevier), 3–8.
- Hesham, A. A., Kok, K. P., and Yvonne, T. F. T. (2011). Herbal delivery system for treatment of obesity administration of encapsulated khat-extracts on body weight of rats. *Obes. Res. Clin. Pract.* 5 (4), e305–e312. doi:10.1016/j.orcp.2011.03.008
- Hondares, E., Rosell, M., Díaz-Delfin, J., Olmos, Y., Monsalve, M., Iglesias, R., et al. (2011). Peroxisome proliferator-activated receptor α (PPAR α) induces PPAR γ coactivator 1 α (PGC-1 α) gene expression and contributes to thermogenic activation of Brown fat: Involvement of PRDM16. *J. Biol. Chem.* 286 (50), 43112–43122. doi:10.1074/jbc.M111.252775
- Hsu, C.-L., and Yen, G.-C. (2007). Effects of capsaicin on induction of apoptosis and inhibition of adipogenesis in 3T3-L1 cells. *J. Agric. Food Chem.* 55 (5), 1730–1736. doi:10.1021/jf062912b
- Huang, C., Zhang, Y., Gong, Z., Sheng, X., Li, Z., Zhang, W., et al. (2006). Berberine inhibits 3T3-L1 adipocyte differentiation through the PPAR γ pathway. *Biochem. Biophys. Res. Commun.* 348 (2), 571–578. doi:10.1016/j.bbrc.2006.07.095
- Huang, L., Zhang, J., Zhu, X., Mi, X., Li, Q., Gao, J., et al. (2021). The phytochemical rhein mediates M(6)a-independent suppression of adipocyte differentiation. *Front. Nutr.* 8, 756803. doi:10.3389/fnut.2021.756803
- Hughes, G. M., Boyland, E. J., Williams, N. J., Mennen, L., Scott, C., Kirkham, T. C., et al. (2008). The effect of Korean pine nut oil (PinnoThin) on food intake, feeding behaviour and appetite: A double-blind placebo-controlled trial. *Lipids health Dis.* 7, 6. doi:10.1186/1476-511x-7-6
- Ikedo, K., and Yamada, T. (2020). UCP1 dependent and independent thermogenesis in Brown and beige adipocytes. *Front. Endocrinol. (Lausanne)* 11, 498. doi:10.3389/fendo.2020.00498
- Ikedo, Y., Murakami, A., and Ohigashi, H. (2008). Ursolic acid: An anti- and pro-inflammatory triterpenoid. *Mol. Nutr. Food Res.* 52 (1), 26–42. doi:10.1002/mnfr.200700389
- Islam, M., and Choi, H. K. (2008). Comparative effects of dietary ginger (Zingiber officinale) and garlic (Allium sativum) investigated in a Type 2 diabetes model of rats. *J. Med. Food* 11 (1), 152–159. doi:10.1089/jmf.2007.634
- Jain, S., and Singh, S. N. (2013). Metabolic effect of short term administration of Hoodia gordonii, an herbal appetite suppressant. *South Afr. J. Bot.* 86, 51–55. doi:10.1016/j.sajb.2013.02.002
- James, W. P. T., Caterson, I. D., Coutinho, W., Finer, N., Van Gaal, L. F., Maggioni, A. P., et al. (2010). Effect of sibutramine on cardiovascular outcomes in overweight and obese subjects. *N. Engl. J. Med.* 363 (10), 905–917. doi:10.1056/NEJMoa1003114
- Jamous, R. M., Abu-Zaitoun, S. Y., Akkawi, R. J., and Ali-Shtayeh, M. S. (2018). Antiobesity and antioxidant potentials of selected Palestinian medicinal plants. *Evidence-based complementary Altern. Med.* 2018, 8426752. doi:10.1155/2018/8426752
- Jang, S.-M., Yee, S. T., Choi, J., Choi, M. S., Do, G. M., Jeon, S. M., et al. (2009). Ursolic acid enhances the cellular immune system and pancreatic β -cell function in streptozotocin-induced diabetic mice fed a high-fat diet. *Int. Immunopharmacol.* 9, 113–119. doi:10.1016/j.intimp.2008.10.013
- Javadi, B., Sahebkar, A., and Emami, S. A. (2013). A survey on saffron in major Islamic traditional medicine books. *Iran. J. Basic Med. Sci.* 16 (1), 1–11.
- Jayaprakasha, G. K., and Rao, L. J. M. (2011). Chemistry, biogenesis, and biological activities of Cinnamomum zeylanicum. *Crit. Rev. Food Sci. Nutr.* 51 (6), 547–562. doi:10.1080/10408391003699550
- Jelsing, J., Vrang, N., Hansen, G., Raun, K., Tang-Christensen, M., and Knudsen, L. B. (2012). Liraglutide: Short-lived effect on gastric emptying -- long lasting effects on body weight. *Diabetes Obes. Metab.* 14 (6), 531–538. doi:10.1111/j.1463-1326.2012.01557.x
- Jeremic, N., Chaturvedi, P., and Tyagi, S. C. (2017). Browning of white fat: Novel insight into factors, mechanisms, and therapeutics. *J. Cell. physiology* 232 (1), 61–68. doi:10.1002/jcp.25450
- Jeukendrup, A. E., and Randell, R. (2011). Fat burners: Nutrition supplements that increase fat metabolism. *Obes. Rev.* 12 (10), 841–851. doi:10.1111/j.1467-789X.2011.00908.x
- Jiang, J., Cai, X., Pan, Y., Du, X., Zhu, H., Yang, X., et al. (2020). Relationship of obesity to adipose tissue insulin resistance. *BMJ Open Diabetes Res. Care* 8 (1), e000741. doi:10.1136/bmjdr-2019-000741
- Jung, S., Ha, Y. J., Shim, E. K., Choi, S. Y., Jin, J. L., Yun-Choi, H. S., et al. (2007). Insulin-mimetic and insulin-sensitizing activities of a pentacyclic triterpenoid insulin receptor activator. *Biochem. J.* 403, 243–250. doi:10.1042/BJ20061123
- Kajimura, S., Seale, P., Tomaru, T., Erdjument-Bromage, H., Cooper, M. P., Ruas, J. L., et al. (2008). Regulation of the Brown and white fat gene programs through a PRDM16/CtBP transcriptional complex. *Genes Dev.* 22 (10), 1397–1409. doi:10.1101/gad.1666108
- Kalyanasundar, B., Perez, C. I., Luna, A., Solorio, J., Moreno, M. G., Elias, D., et al. (2015). D1 and D2 antagonists reverse the effects of appetite suppressants on weight loss, food intake, locomotion, and rebalance spiking inhibition in the rat NAc shell. *J. neurophysiology* 114 (1), 585–607. doi:10.1152/jn.00012.2015
- Kang, C., Lee, H., Jung, E. S., Seyedian, R., Jo, M., Kim, J., et al. (2012). Saffron (Crocus sativus L) increases glucose uptake and insulin sensitivity in muscle cells via multipathway mechanisms. *Food Chem.* 135 (4), 2350–2358. doi:10.1016/j.foodchem.2012.06.092
- Kassaian, N., Azadbakht, L., Forghani, B., and Amini, M. (2009). Effect of fenugreek seeds on blood glucose and lipid profiles in type 2 diabetic patients. *Int. J. Vitam. Nutr. Res.* 79 (1), 34–39. doi:10.1024/0300-9831.79.1.34
- Kawabata, F., Inoue, N., Masamoto, Y., Matsumura, S., Kimura, W., Kadowaki, M., et al. (2009). Non-pungent capsaicin analogs (capsinoids) increase metabolic rate and enhance thermogenesis via gastrointestinal TRPV1 in mice. *Biosci. Biotechnol. Biochem.* 73 (12), 2690–2697. doi:10.1271/bbb.90555
- Kawada, T., Watanabe, T., Takaishi, T., Tanaka, T., and Iwai, K. (1986). Capsaicin-induced beta-adrenergic action on energy metabolism in rats: Influence of capsaicin on oxygen consumption, the respiratory quotient, and substrate utilization. *Proc. Soc. Exp. Biol. Med.* 183, 250–256. doi:10.3181/00379727-183-42414
- Kershaw, E. E., and Flier, J. S. (2004). Adipose tissue as an endocrine organ. *J. Clin. Endocrinol. Metab.* 89 (6), 2548–2556. doi:10.1210/jc.2004-0395
- Khan, J. I., Kennedy, T. J., and Christian, D. R. (2012). "Phenethylamines," in *Basic principles of forensic chemistry*. Editors J. I. Khan, T. J. Kennedy, and D. R. Christian Jr (Totowa, NJ: Humana Press), 157–176.
- Khandouzi, N., Shidfar, F., Rajab, A., Rahideh, T., Hosseini, P., and Mir Taheri, M. (2015). The effects of ginger on fasting blood sugar, hemoglobin a1c, apolipoprotein B, apolipoprotein a-I and malondialdehyde in type 2 diabetic patients. *Iran. J. Pharm. Res. IJPR* 14 (1), 131–140.
- Kim, S. H., and Chung, S. Y. (2010). Antihyperglycemic and antihyperlipidemic action of cinnamomi cassiae (cinnamon bark) extract in C57BL/Ks db/db mice. *Archives Pharmacol. Res.* 33 (2), 325–333. doi:10.1007/s12272-010-0219-0
- Kobayashi, K., Saito, Y., Nakazawa, I., and Yoshizaki, F. (2000). Screening of crude drugs for influence on amylase activity and postprandial blood glucose in mouse plasma. *Biol. Pharm. Bull.* 23 (10), 1250–1253. doi:10.1248/bpb.23.1250
- Komarnitsky, S., Esposito, D., Rathinasabapathy, T., Poulev, A., and Raskin, I. (2013). Effects of pregnane glycosides on food intake depend on stimulation of the melanocortin pathway and BDNF in an animal model. *J. Agric. Food Chem.* 61 (8), 1841–1849. doi:10.1021/jf3033649
- Kumar, A., Sundaram, K., Teng, Y., Mu, J., Sriwastva, M. K., Zhang, L., et al. (2022). Ginger nanoparticles mediated induction of Foxa2 prevents high-fat diet-induced insulin resistance. *Theranostics* 12 (3), 1388–1403. doi:10.7150/thno.62514
- Kuriyan, R., Raj, T., Srinivas, S. K., Vaz, M., Rajendran, R., and Kurpad, A. V. (2007). Effect of Caralluma fimbriata extract on appetite, food intake and anthropometry in adult Indian men and women. *Appetite* 48 (3), 338–344. doi:10.1016/j.appet.2006.09.013
- Kuryłowicz, A., and Puzianowska-Kuźnicka, M. (2020). Induction of adipose tissue browning as a strategy to combat obesity. *Int. J. Mol. Sci.* 21 (17), 6241. doi:10.3390/ijms21176241
- Kwan, H. Y., Wu, J., Su, T., Chao, X. J., Liu, B., Fu, X., et al. (2017). Cinnamon induces browning in subcutaneous adipocytes. *Sci. Rep.* 7 (1), 2447. doi:10.1038/s41598-017-02263-5
- Kwok, K. H., Lam, K. S., and Xu, A. (2016). Heterogeneity of white adipose tissue: Molecular basis and clinical implications. *Exp. Mol. Med.* 48 (3), e215. doi:10.1038/emmm.2016.5
- Kwon, C.-S., Sohn, H. Y., Kim, S. H., Kim, J. H., Son, K. H., Lee, J. S., et al. (2003b). Anti-obesity effect of Dioscorea nipponica Makino with lipase-inhibitory activity in rodents. *Biosci. Biotechnol. Biochem.* 67 (7), 1451–1456. doi:10.1271/bbb.67.1451
- Kwon, C. S., Sohn, H. Y., Kim, S. H., Kim, J. H., Son, K. H., Lee, J. S., et al. (2003a). Anti-obesity effect of Dioscorea nipponica Makino with lipase-inhibitory activity in rodents. *Biosci. Biotechnol. Biochem.* 67 (7), 1451–1456. doi:10.1271/bbb.67.1451
- Latha, B. P. (2011). Therapeutic efficacy of *Achyranthes aspera* saponin extract in high fat diet induced hyperlipidaemia in male wistar rats. *Afr. J. Biotechnol.* 10 (74), 17038–17042.
- Lee, A. G., Kang, S., Im, S., and Pak, Y. K. (2022). Cinnamic acid attenuates peripheral and hypothalamic inflammation in high-fat diet-induced obese mice. *Pharmaceutics* 14 (8), 1675. doi:10.3390/pharmaceutics14081675
- Lee, H. E., Yang, G., Han, S. H., Lee, J. H., and Jang, J. K. (2018). Anti-obesity potential of Glycyrrhiza uralensis and licochalcone A through induction of adipocyte browning. *Biochem. Biophysical Res. Commun.* 503 (3), 2117–2123. doi:10.1016/j.bbrc.2018.07.168

- Lee, J., Li, Y., Li, C., and Li, D. (2011). Natural products and body weight control. *N. Am. J. Med. Sci.* 3 (1), 13–19. doi:10.4297/naajms.2011.313
- Lee, K. J., and Jeong, H. G. (2002). Protective effect of Platycodi radix on carbon tetrachloride-induced hepatotoxicity. *Food Chem. Toxicol.* 40 (4), 517–525. doi:10.1016/s0278-6915(01)00104-1
- Lee, Y. K., Lee, W. S., Hwang, J. T., Kwon, D. Y., Surh, Y. J., and Park, O. J. (2009). Curcumin exerts antidifferentiation effect through AMPKalpha-PPAR-gamma in 3T3-L1 adipocytes and antiproliferatory effect through AMPKalpha-COX-2 in cancer cells. *J. Agric. Food Chem.* 57 (1), 305–310. doi:10.1021/jf802737z
- Lefebvre, P., and Staels, B. (2012). Naturally improving insulin resistance with amorphfrutins. *Proc. Natl. Acad. Sci. U. S. A.* 109 (19), 7136–7137. doi:10.1073/pnas.1204455109
- Leibowitz, S. F., Weiss, G. F., and Suh, J. S. (1990). Medial hypothalamic nuclei mediate serotonin's inhibitory effect on feeding behavior. *Pharmacol. Biochem. Behav.* 37 (4), 735–742. doi:10.1016/0091-3057(90)90556-w
- Lemieux, A. M., Li, B., and al'Absi, M. (2015). Khat use and appetite: An overview and comparison of amphetamine, khat and cathinone. *J. Ethnopharmacol.* 160, 78–85. doi:10.1016/j.jep.2014.11.002
- Li, J., Chen, Q., Zhai, X., Wang, D., Hou, Y., and Tang, M. (2021). Green tea aqueous extract (GTAE) prevents high-fat diet-induced obesity by activating fat browning. *Food Sci. Nutr.* 9 (12), 6548–6558. doi:10.1002/fsn3.2580
- Li, R., Lan, Y., Chen, C., Cao, Y., Huang, Q., Ho, C. T., et al. (2020). Anti-obesity effects of capsaicin and the underlying mechanisms: A review. *Food & Funct.* 11 (9), 7356–7370. doi:10.1039/d0fo01467b
- Lin, J., Della-Fera, M. A., and Baile, C. A. (2005). Green tea polyphenol epigallocatechin gallate inhibits adipogenesis and induces apoptosis in 3T3-L1 adipocytes. *Obes. Res.* 13 (6), 982–990. doi:10.1038/oby.2005.115
- Lin, X., and Li, H. (2021). Obesity: Epidemiology, pathophysiology, and therapeutics. *Front. Endocrinol. (Lausanne)* 12, 706978. doi:10.3389/fendo.2021.706978
- Litosch, I., Hudson, T. H., Mills, I., and Fain, J. N. (1982). Forskolin as an activator of cyclic AMP accumulation and lipolysis in rat adipocytes. *Mol. Pharmacol.* 22 (1), 109–115.
- Liu, C. T., Hse, H., Lii, C. K., Chen, P. S., and Sheen, L. Y. (2005). Effects of garlic oil and diallyl trisulfide on glycemic control in diabetic rats. *Eur. J. Pharmacol.* 516 (2), 165–173. doi:10.1016/j.ejphar.2005.04.031
- Liu, L., Zhang, T., Hu, J., Ma, R., He, B., Wang, M., et al. (2020a). Adiponectin/SIRT1 Axis induces white adipose browning after vertical sleeve gastrectomy of obese rats with type 2 diabetes. *Obes. Surg.* 30 (4), 1392–1403. doi:10.1007/s11695-019-04295-4
- Liu, Q., Zhang, X. L., Tao, R. Y., Niu, Y. J., Chen, X. G., Tian, J. Y., et al. (2011). Rhein, an inhibitor of adipocyte differentiation and adipogenesis. *J. Asian Nat. Prod. Res.* 13 (8), 714–723. doi:10.1080/10286020.2011.586341
- Liu, T.-T., Liu, X. T., Chen, Q. X., and Shi, Y. (2020b). Lipase inhibitors for obesity: A review. *Biomed. Pharmacother.* 128, 110314. doi:10.1016/j.biopha.2020.110314
- Liu, Y., Toubro, S., Astrup, A., and Stock, M. J. (1995). Contribution of beta 3-adrenoceptor activation to ephedrine-induced thermogenesis in humans. *Int. J. Obes. Relat. Metab. Disord.* 19, 678–685.
- Loe, Y. C., Bergeron, N., Rodriguez, N., and Schwarz, J. M. (2001). Gas chromatography/mass spectrometry method to quantify blood hydroxycitrate concentration. *Anal. Biochem.* 292 (1), 148–154. doi:10.1006/abio.2001.5046
- Lu, F. R., Shen, L., Qin, Y., Gao, L., Li, H., and Dai, Y. (2008). Clinical observation on trigonella foenum-graecum L. total saponins in combination with sulfonylureas in the treatment of type 2 diabetes mellitus. *Chin. J. Integr. Med.* 14 (1), 56–60. doi:10.1007/s11655-007-9005-3
- Ludy, M.-J., Moore, G. E., and Mattes, R. D. (2012). The effects of capsaicin and capsiate on energy balance: Critical review and meta-analyses of studies in humans. *Chem. Senses* 37 (2), 103–121. doi:10.1093/chemse/bjr100
- Ludy, M. J., and Mattes, R. D. (2011). The effects of hedonically acceptable red pepper doses on thermogenesis and appetite. *Physiology Behav.* 102 (3–4), 251–258. doi:10.1016/j.physbeh.2010.11.018
- Luo, L., and Liu, M. (2016). Adipose tissue in control of metabolism. *J. Endocrinol.* 231 (3), R77–R99. doi:10.1530/JOE-16-0211
- Ma, S., Benzie, I. F. F., Chu, T. T. W., Fok, B. S. P., Tomlinson, B., and Critchley, L. A. H. (2008). Effect of Panax ginseng supplementation on biomarkers of glucose tolerance, antioxidant status and oxidative stress in type 2 diabetic subjects: Results of a placebo-controlled human intervention trial. *Diabetes, Obes. Metabolism* 10 (11), 1125–1127. doi:10.1111/j.1463-1326.2008.00858.x
- MacLean, D. B., and Luo, L. G. (2004). Increased ATP content/production in the hypothalamus may be a signal for energy-sensing of satiety: Studies of the anorectic mechanism of a plant steroidal glycoside. *Brain Res.* 1020 (1–2), 1–11. doi:10.1016/j.brainres.2004.04.041
- Malapaka, R. R. V., Khoo, S., Zhang, J., Choi, J. H., Zhou, X. E., Xu, Y., et al. (2012). Identification and mechanism of 10-carbon fatty acid as modulating ligand of peroxisome proliferator-activated receptors. *J. Biol. Chem.* 287 (1), 183–195. doi:10.1074/jbc.M111.294785
- Mao, Q. Q., Xu, X. Y., Cao, S. Y., Gan, R. Y., Corke, H., Beta, T., et al. (2019). Bioactive compounds and bioactivities of ginger (zingiber officinale Roscoe). *Foods* 8 (6), 185. doi:10.3390/foods8060185
- Marti, A., Berraondo, B., and Martinez, J. (1999). Leptin: Physiological actions. *J. physiology Biochem.* 55 (1), 43–49.
- Matsuyama, T., Tanaka, Y., Kamimaki, I., Nagao, T., and Tokimitsu, I. (2008). Catechin safely improved higher levels of fatness, blood pressure, and cholesterol in children. *Obes. (Silver Spring, Md.)* 16 (6), 1338–1348. doi:10.1038/oby.2008.60
- Maurer, S., Harms, M., and Boucher, J. (2021). The colorful versatility of adipocytes: white-to-brown transdifferentiation and its therapeutic potential in humans. *FEBS J.* 288 (12), 3628–3646. doi:10.1111/febs.15470
- Maury, J., Issad, T., Perdureau, D., Gouhot, B., Ferré, P., and Girard, J. (1993). Effect of acarbose on glucose homeostasis, lipogenesis and lipogenic enzyme gene expression in adipose tissue of weaned rats. *Diabetologia* 36 (6), 503–509. doi:10.1007/BF02743265
- McLaughlin, J. T., Lomax, R. B., Hall, L., Dockray, G. J., Thompson, D. G., and Warhurst, G. (1998). Fatty acids stimulate cholecystokinin secretion via an acyl chain length-specific, Ca²⁺-dependent mechanism in the enteroendocrine cell line STC-1. *J. Physiol.* 513, 11–18. doi:10.1111/j.1469-7793.1998.011by.x
- Mehta, A., Marso, S. P., and Neeland, I. J. (2017). Liraglutide for weight management: A critical review of the evidence. *Obes. Sci. Pract.* 3 (1), 3–14. doi:10.1002/osp4.84
- Milajerdi, A., Jazayeri, S., Hashemzadeh, N., Shirzadi, E., Derakhshan, Z., Djazayeri, A., et al. (2018). The effect of saffron (crocus sativus L) hydroalcoholic extract on metabolic control in type 2 diabetes mellitus: A triple-blinded randomized clinical trial. *J. Res. Med. Sci.* 23, 16. doi:10.4103/jrms.JRMS_286_17
- Miura, T., Ichiki, H., Hashimoto, I., Iwamoto, N., Kato, M., Kubo, M., et al. (2001). Antidiabetic activity of a xanthone compound, mangiferin. *Phytomedicine* 8, 85–87. doi:10.1078/0944-7113-00009
- Mladenova, S. G., Vasileva, L. V., Savova, M. S., Marchev, A. S., Tews, D., Wabitsch, M., et al. (2021). Anti-adipogenic effect of Alchemilla monticola is mediated via PI3K/AKT signaling inhibition in human adipocytes. *Front. Pharmacol.* 12, 707507. doi:10.3389/fphar.2021.707507
- Mobasser, M., Ostadrahimi, A., Tajaddini, A., Asghari, S., Barati, M., Akbarzadeh, M., et al. (2020a). Effects of saffron supplementation on glycemia and inflammation in patients with type 2 diabetes mellitus: A randomized double-blind, placebo-controlled clinical trial study. *Diabetes Metab. Syndr.* 14 (4), 527–534. doi:10.1016/j.dsx.2020.04.031
- Mobasser, M., Ostadrahimi, A., Tajaddini, A., Asghari, S., Barati, M., Akbarzadeh, M., et al. (2020b). Effects of saffron supplementation on glycemia and inflammation in patients with type 2 diabetes mellitus: A randomized double-blind, placebo-controlled clinical trial study. *Diabetes & Metabolic Syndrome Clin. Res. Rev.* 14 (4), 527–534. doi:10.1016/j.dsx.2020.04.031
- Moshawih, S., Mydin, R. B., Kalakotla, S., and Jarrar, Q. B. (2019). Potential application of resveratrol in nanocarriers against cancer: Overview and future trends. *J. Drug Deliv. Sci. Technol.* 53, 101187. doi:10.1016/j.jddst.2019.101187
- Mukherjee, P. K., Mukherjee, D., Maji, A. K., Rai, S., and Heinrich, M. (2009). The sacred lotus (*Nelumbo nucifera*)—phytochemical and therapeutic profile. *J. Pharm. Pharmacol.* 61 (4), 407–422. doi:10.1211/jpp/61.04.0001
- Mukund, V., Mukund, D., Sharma, V., Mannarapu, M., and Alam, A. (2017). Genistein: Its role in metabolic diseases and cancer. *Crit. Rev. Oncology/Hematology* 119, 13–22. doi:10.1016/j.critrevonc.2017.09.004
- Muoio, D. M., and Newgard, C. B. (2005). Metabolism: A is for adipokine. *Nature* 436 (7049), 337–338. doi:10.1038/436337a
- Nedergaard, J., Bengtsson, T., and Cannon, B. (2007). Unexpected evidence for active Brown adipose tissue in adult humans. *Am. J. Physiol. Endocrinol. Metab.* 293 (2), E444–E452. doi:10.1152/ajpendo.00691.2006
- Nedergaard, J., and Cannon, B. (2014). The browning of white adipose tissue: Some burning issues. *Cell metab.* 20 (3), 396–407. doi:10.1016/j.cmet.2014.07.005
- Nicholls, D. G. (2006). The physiological regulation of uncoupling proteins. *Biochim. Biophys. Acta* 1757 (5–6), 459–466. doi:10.1016/j.bbabi.2006.02.005
- Ohia, S. E., Awe, S. O., LeDay, A. M., Opere, C. A., and Bagchi, D. (2001). Effect of hydroxycitric acid on serotonin release from isolated rat brain cortex. *Res. Commun. Mol. Pathol. Pharmacol.* 109 (3–4), 210–216.
- Ohia, S. E., Opere, C. A., LeDay, A. M., Bagchi, M., Bagchi, D., and Stohs, S. J. (2002). Safety and mechanism of appetite suppression by a novel hydroxycitric acid extract (HCA-SX). *Mol. Cell. Biochem.* 238, 89–103. doi:10.1023/a:1019911205672
- Onakpoya, I. J., Heneghan, C. J., and Aronson, J. K. (2016). Post-marketing withdrawal of anti-obesity medicinal products because of adverse drug reactions: A systematic review. *BMC Med.* 14 (1), 191. doi:10.1186/s12916-016-0735-y
- Ono, K., Tsukamoto-Yasui, M., Hara-Kimura, Y., Inoue, N., Nogusa, Y., Okabe, Y., et al. (2011). Intragastric administration of capsiate, a transient receptor potential channel agonist, triggers thermogenic sympathetic responses. *J. Appl. Physiol.* 110 (3), 789–798. doi:10.1152/japplphysiol.00128.2010

- Ono, Y., Hattori, E., Fukaya, Y., Imai, S., and Ohizumi, Y. (2006a). Anti-obesity effect of *Nelumbo nucifera* leaves extract in mice and rats. *J. Ethnopharmacol.* 106 (2), 238–244. doi:10.1016/j.jep.2005.12.036
- Ono, Y., Hattori, E., Fukaya, Y., Imai, S., and Ohizumi, Y. (2006b). Anti-obesity effect of *Nelumbo nucifera* leaves extract in mice and rats. *J. Ethnopharmacol.* 106 (2), 238–244. doi:10.1016/j.jep.2005.12.036
- Ortweiler, W., Simon, H. U., Splinter, F. K., Peiker, G., Siegert, C., and Traeger, A. (1985). Determination of caffeine and metimazole elimination in pregnancy and after delivery as an *in vivo* method for characterization of various cytochrome p-450 dependent biotransformation reactions. *Biomed. Biochim. Acta* 44, 1189–1199.
- Otton, R., Petrovic, N., Cannon, B., and Nedergaard, J. (2021). On the validity of adipogenic cell lines as model systems for browning processes: In authentic Brown, brite/beige, and white preadipocytes, there is No cell-autonomous thermogenic recruitment by green tea compounds. *Front. Nutr.* 8, 715859. doi:10.3389/fnut.2021.715859
- Ou-Yang, S.-H., Jiang, T., Zhu, L., and Yi, T. (2018). *Dioscorea nipponica* Makino: A systematic review on its ethnobotany, phytochemical and pharmacological profiles. *Chem. Central J.* 12 (1), 57–18. doi:10.1186/s13065-018-0423-4
- Panchal, S., Bliss, E., and Brown, L. (2018). Capsaicin in metabolic syndrome. *Nutrients* 10 (5), 630. doi:10.3390/nu10050630
- Pantelis, C., Hindler, C. G., and Taylor, J. C. (1989). Use and abuse of khat (*Catha edulis*): A review of the distribution, pharmacology, side effects and a description of psychosis attributed to khat chewing. *Psychol. Med.* 19 (3), 657–668. doi:10.1017/s0033291700024259
- Park, M., Sharma, A., and HJ, L. (2019b). Anti-adipogenic effects of delphinidin-3-O- β -glucoside in 3T3-L1 preadipocytes and primary white adipocytes. *Molecules* 24 (10), 1848. doi:10.3390/molecules24101848
- Park, S. J., Park, M., Sharma, A., Kim, K., and Lee, H. J. (2019a). Black ginseng and ginsenoside Rb1 promote browning by inducing UCP1 expression in 3T3-L1 and primary white adipocytes. *Nutrients* 11 (11), 2747. doi:10.3390/nu11112747
- Park, Y.-J., Seo, D. W., Ju, J. Y., and Cha, Y. Y. (2019c). The antiobesity effects of Buginawa in 3T3-L1 preadipocytes and in a mouse model of high-fat diet-induced obesity. *BioMed Res. Int.* 2019, 3101987. doi:10.1155/2019/3101987
- Pasman, W. J., Heimerikx, J., Rubingh, C. M., van den Berg, R., O'Shea, M., Gambelli, L., et al. (2008). The effect of Korean pine nut oil on *in vitro* CCK release, on appetite sensations and on gut hormones in post-menopausal overweight women. *Lipids Health Dis.* 7, 10. doi:10.1186/1476-511X-7-10
- Patel, N. B. (2000). Mechanism of action of cathinone: The active ingredient of khat (*Catha edulis*). *East Afr. Med. J.* 77 (6), 329–332. doi:10.4314/eamj.v77i6.46651
- Perez, C. I., Kalyanasundar, B., Moreno, M. G., and Gutierrez, R. (2019). The triple combination phentermine plus 5-HTP/carbidopa leads to greater weight loss, with fewer psychomotor side effects than each drug alone. *Front. Pharmacol.* 10, 1327. doi:10.3389/fphar.2019.01327
- Periasamy, M., Herrera, J. L., and Reis, F. C. G. (2017). Skeletal muscle thermogenesis and its role in whole body energy metabolism. *Diabetes Metab. J.* 41 (5), 327–336. doi:10.4093/dmj.2017.41.5.327
- Peter Amaladhas, T., Usha, M., and Naveen, S. (2013). Sunlight induced rapid synthesis and kinetics of silver nanoparticles using leaf extract of *Achyranthes aspera* L. and their antimicrobial applications. *Adv. Mater. Lett.* 4 (10), 779–785. doi:10.5185/amlett.2013.2427
- Piantadosi, C. A., and Suliman, H. B. (2006). Mitochondrial transcription factor A induction by redox activation of nuclear respiratory factor 1. *J. Biol. Chem.* 281 (1), 324–333. doi:10.1074/jbc.M508805200
- Picardi, P. K., Calegari, V. C., Prada, P. O., Prada, P. d. O., Moraes, J. C., Araújo, E., et al. (2008). Reduction of hypothalamic protein tyrosine phosphatase improves insulin and leptin resistance in diet-induced obese rats. *Endocrinology* 149 (8), 3870–3880. doi:10.1210/en.2007-1506
- Preuss, H. G., Rao, C. V. S., Garis, R., Bramble, J. D., Ohia, S. E., Bagchi, M., et al. (2004). An overview of the safety and efficacy of a novel, natural(-)-hydroxycitric acid extract (HCA-SX) for weight management. *J. Med.* 35, 33–48.
- Puri, D., Prabhu, K. M., and Murthy, P. S. (2002). Mechanism of action of a hypoglycemic principle isolated from fenugreek seeds. *Indian J. Physiol. Pharmacol.* 46 (4), 457–462.
- Qian, H., Hausman, G. J., Compton, M. M., Azain, M. J., Hartzell, D. L., and Baile, C. A. (1998). Leptin regulation of peroxisome proliferator-activated receptor- γ , tumor necrosis factor, and uncoupling protein-2 expression in adipose tissues. *Biochem. biophysical Res. Commun.* 246 (3), 660–667. doi:10.1006/bbrc.1998.8680
- Qiang, L., Wang, L., Kon, N., Zhao, W., Lee, S., Zhang, Y., et al. (2012). Brown remodeling of white adipose tissue by SirT1-dependent deacetylation of Pparg. *Cell* 150 (3), 620–632. doi:10.1016/j.cell.2012.06.027
- Rani, N., Sharma, S. K., and Vasudeva, N. (2012b). Assessment of antiobesity potential of *Achyranthes aspera* Linn. Seed. *Evid. Based Complement. Altern. Med.* 2012, 715912. doi:10.1155/2012/715912
- Rani, N., Vasudeva, N., and Sharma, S. K. (2012a). Quality assessment and anti-obesity activity of *Stellaria media* (Linn) Vill. *BMC Complementary Altern. Med.* 12 (145), 145. doi:10.1186/1472-6882-12-145
- Ransac, S., Gargouri, Y., Moreau, H., and Verger, R. (1991). Inactivation of pancreatic and gastric lipases by tetrahydrolipstatin and alkyl-dithio-5-(2-nitrobenzoic acid). A kinetic study with 1,2-didecanoyl-sn-glycerol monolayers. *Eur. J. Biochem.* 202 (2), 395–400. doi:10.1111/j.1432-1033.1991.tb16387.x
- Rao, A., Briskey, D., Dos Reis, C., and Mallard, A. R. (2021a). The effect of an orally-dosed Caralluma Fimbriata extract on appetite control and body composition in overweight adults. *Sci. Rep.* 11 (1), 6791–6799. doi:10.1038/s41598-021-86108-2
- Rao, A., Briskey, D., Dos Reis, C., and Mallard, A. R. (2021b). The effect of an orally-dosed Caralluma Fimbriata extract on appetite control and body composition in overweight adults. *Sci. Rep.* 11, 6791. doi:10.1038/s41598-021-86108-2
- Raouf, G. F. A., and Kareem, A. M. Z. A. E. (2020). The golden role of natural products in obesity. *Int. J. Pharma Res. Health Sci.* 8 (6), 3248–3255. doi:10.21276/ijprhs.2020.06.03
- Rayalam, S., Della-Fera, M. A., and Baile, C. A. (2008). Phytochemicals and regulation of the adipocyte life cycle. *J. Nutr. Biochem.* 19 (11), 717–726. doi:10.1016/j.jnutbio.2007.12.007
- Reinbach, H. C., Martinussen, T., and Møller, P. (2010). Effects of hot spices on energy intake, appetite and sensory specific desires in humans. *Food Qual. Prefer.* 21 (6), 655–661. doi:10.1016/j.foodqual.2010.04.003
- Rios, J., Recio, M. C., Giner, R. M., and Máñez, S. (1996). An update review of saffron and its active constituents. *Phytotherapy Res.* 10, 189–193. doi:10.1002/(sici)1099-1573(199605)10:3<189:aid-pt754>3.0.co;2-c
- Robidoux, J., Cao, W., Quan, H., Daniel, K. W., Moukdar, F., Bai, X., et al. (2005). Selective activation of mitogen-activated protein (MAP) kinase kinase 3 and p38 α MAP kinase is essential for cyclic AMP-dependent UCP1 expression in adipocytes. *Mol. Cell Biol.* 25 (13), 5466–5479. doi:10.1128/MCB.25.13.5466-5479.2005
- Rodríguez-Landa, J. F., and Contreras, C. M. (2003). A review of clinical and experimental observations about antidepressant actions and side effects produced by *Hypericum perforatum* extracts. *Phytomedicine* 10 (8), 688–699. doi:10.1078/0944-7113-00340
- Rosenstock, J., Klaff, L. J., Schwartz, S., Northrup, J., Holcombe, J. H., Wilhelm, K., et al. (2010). Effects of exenatide and lifestyle modification on body weight and glucose tolerance in obese subjects with and without pre-diabetes. *Diabetes Care* 33 (6), 1173–1175. doi:10.2337/dc09-1203
- Rossato, M., Granzotto, M., Macchi, V., Porzionato, A., Petrelli, L., Calcagno, A., et al. (2014). Human white adipocytes express the cold receptor TRPM8 which activation induces UCP1 expression, mitochondrial activation and heat production. *Mol. Cell. Endocrinol.* 383 (1–2), 137–146. doi:10.1016/j.mce.2013.12.005
- Rue, E. A., Rush, M. D., and van Breemen, R. B. (2018). Procyanidins: A comprehensive review encompassing structure elucidation via mass spectrometry. *Phytochem. Rev.* 17 (1), 1–16. doi:10.1007/s11101-017-9507-3
- Ruschke, K., Fishbein, L., Dietrich, A., Klötting, N., Tönjes, A., Oberbach, A., et al. (2010). Gene expression of PPAR γ and PGC-1 α in human omental and subcutaneous adipose tissues is related to insulin resistance markers and mediates beneficial effects of physical training. *Eur. J. Endocrinol.* 162 (3), 515–523. doi:10.1530/EJE-09-0767
- Saely, C. H., Geiger, K., and Drexler, H. (2012). Brown versus white adipose tissue: A mini-review. *Gerontology* 58 (1), 15–23. doi:10.1159/000321319
- Saito, M. (2015). Capsaicin and related food ingredients reducing body fat through the activation of TRP and Brown fat thermogenesis. *Adv. Food Nutr. Res.* 76, 1–28. doi:10.1016/bs.afnr.2015.07.002
- Saleh, S., El-Maraghy, N., Reda, E., and Barakat, W. (2014). Modulation of diabetes and dyslipidemia in diabetic insulin-resistant rats by mangiferin: Role of adiponectin and TNF- α . *An. Acad. Bras. Ciências.* 86 (4), 1935–1948. doi:10.1590/0001-3765201420140212
- Sam, S., and Mazzone, T. (2014). Adipose tissue changes in obesity and the impact on metabolic function. *Transl. Res.* 164 (4), 284–292. doi:10.1016/j.trsl.2014.05.008
- Saper, R., Eisenberg, D., and Phillips, R. (2004). Common dietary supplements for weight loss. *Am. Fam. Physician* 70, 1731–1738.
- Sayan, M., and Soumya, M. (2017). The potential role of phytochemicals in regulating human appetite: A novel approach towards diet management 1. *Botanica* 67, 34–39.
- Sbarbati, A. (2014). “Adipose tissue anatomy,” in *Stem cells in aesthetic procedures: Art, science, and clinical techniques*. Editors M. A. Shiffman, A. Di Giuseppe, and F. Bassetto (Berlin, Heidelberg: Springer Berlin Heidelberg), 239–248.
- Schneider, C., Rotschheid, K., and Breitmaier, E. (1993). Vier neue Pregnanglycoside aus *Gongronema latifolium* (Asclepiadaceae). *Liebigs Ann. Chem.* 1993 (10), 1057–1062. doi:10.1002/jlac.1993199301170
- Schwarzschild, M. A., Xu, K., Oztas, E., Petzer, J. P., Castagnoli, K., Castagnoli, N., et al. (2003). Neuroprotection by caffeine and more specific A2A receptor antagonists in animal models of Parkinson's disease. *Neurology* 61 (11), S55–S61. doi:10.1212/01.wnl.0000095214.53646.72

- Seale, P., Conroe, H. M., Estall, J., Kajimura, S., Frontini, A., Ishibashi, J., et al. (2011). Prdm16 determines the thermogenic program of subcutaneous white adipose tissue in mice. *J. Clin. Invest.* 121 (1), 96–105. doi:10.1172/JCI44271
- Sekiya, K., Ohtani, A., and Kusano, S. (2004). Enhancement of insulin sensitivity in adipocytes by ginger. *Biofactors* 22 (1-4), 153–156. doi:10.1002/biof.5520220130
- Semlitsch, T., Stigler, F. L., Jeitler, K., Horvath, K., and Siebenhofer, A. (2019). Management of overweight and obesity in primary care—a systematic overview of international evidence-based guidelines. *Obes. Rev.* 20 (9), 1218–1230. doi:10.1111/obr.12889
- Sepahi, S., Mohajeri, S. A., Hosseini, S. M., Khodaverdi, E., Shoeibi, N., Namdari, M., et al. (2018). Effects of crocin on diabetic maculopathy: A placebo-controlled randomized clinical trial. *Am. J. Ophthalmol.* 190, 89–98. doi:10.1016/j.ajo.2018.03.007
- Sergio, W. (1988). A natural food, the Malabar Tamarind, may be effective in the treatment of obesity. *Med. Hypotheses* 27 (1), 39–40. doi:10.1016/0306-9877(88)90081-3
- Shabalina, I. G., Petrovic, N., de Jong, J. M. A., Kalinovich, A. V., Cannon, B., and Nedergaard, J. (2013). UCP1 in brite/beige adipose tissue mitochondria is functionally thermogenic. *Cell Rep.* 5 (5), 1196–1203. doi:10.1016/j.celrep.2013.10.044
- Sharma, R. (2003). *Medicinal plants of India: An encyclopaedia*. Daryaganj: Daya Publishing House.
- Shukla, Y. J., Pawar, R. S., Ding, Y., Li, X. C., Ferreira, D., and Khan, I. A. (2009). Pregnane glycosides from *Hoodia gordonii*. *Phytochemistry* 70 (5), 675–683. doi:10.1016/j.phytochem.2009.02.006
- Silva, J. E. (2003). The thermogenic effect of thyroid hormone and its clinical implications. *Ann. Intern. Med.* 139 (3), 205–213. doi:10.7326/0003-4819-139-3-200308050-00010
- Smith, C., and Krygsman, A. (2014). *Hoodia gordonii*: To eat, or not to eat. *J. Ethnopharmacol.* 155 (2), 987–991. doi:10.1016/j.jep.2014.06.033
- Smith, M., Ulbricht, C., Kuo, G., and Szapary, P. (2003). Therapeutic applications of fenugreek. *Altern. Med. Rev.* 8 (1), 20–27.
- Snehlata, H. S., and Payal, D. R. (2012). Fenugreek (*trigonella foenum-graecum* L): An overview. *Int. J. Curr. Pharm. Rev. Res.* 2 (4), 169–187.
- Sobenin, I. A., Nedosugova, L. V., Filatova, L. V., Balabolkin, M. I., Gorchakova, T. V., and Orekhov, A. N. (2008). Metabolic effects of time-released garlic powder tablets in type 2 diabetes mellitus: The results of double-blinded placebo-controlled study. *Acta diabetol.* 45 (1), 1–6. doi:10.1007/s00592-007-0011-x
- Spiegelman, B. M. (2013). Banting lecture 2012: Regulation of adipogenesis: Toward new therapeutics for metabolic disease. *Diabetes* 62 (6), 1774–1782. doi:10.2337/db12-1665
- Stohs, S. J., and Badmaev, V. (2016). A review of natural stimulant and non-stimulant thermogenic agents. *Phytother. Res.* 30 (5), 732–740. doi:10.1002/ptr.5583
- Stoner, G. D. (2013). Ginger: Is it ready for prime time? *Cancer Prev. Res.* 6 (4), 257–262. doi:10.1158/1940-6207.CAPR-13-0055
- Sun, N. N., Wu, T. Y., and Chau, C. F. (2016). Natural dietary and herbal products in anti-obesity treatment. *Molecules* 21 (10), 1351. doi:10.3390/molecules21101351
- Sun, Q., He, M., Zhang, M., Zeng, S., Chen, L., Zhou, L., et al. (2020). Ursolic acid: A systematic review of its pharmacology, toxicity and rethink on its pharmacokinetics based on PK-pd model. *Fitoterapia* 147, 104735. doi:10.1016/j.fitote.2020.104735
- Sun, T., Wang, Q., Yu, Z., Zhang, Y., Guo, Y., Chen, K., et al. (2007). Hyrtiosal, a PTP1B inhibitor from the marine sponge *Hyrtios erectus*, shows extensive cellular effects on PI3K/AKT activation, glucose transport, and TGFbeta2/Smad2 signaling. *Chembiochem* 8 (2), 187–193. doi:10.1002/cbic.200600349
- Taj Eldin, I. M., Abdalmutalab, M. M., and Bikir, H. E. (2013). An *in vitro* anticoagulant effect of Fenugreek (*Trigonella foenum-graecum*) in blood samples of normal Sudanese individuals. *Sudan J. Paediatr.* 13 (2), 52–56.
- Tamai, M., Shimada, T., Hiramatsu, N., Hayakawa, K., Okamura, M., Tagawa, Y., et al. (2010). Selective deletion of adipocytes, but not preadipocytes, by TNF-alpha through C/EBP- and PPARgamma-mediated suppression of NF-kappaB. *Lab. Invest.* 90 (9), 1385–1395. doi:10.1038/labinvest.2010.118
- Tamori, Y., Masugi, J., Nishino, N., and Kasuga, M. (2002). Role of peroxisome proliferator-activated receptor-gamma in maintenance of the characteristics of mature 3T3-L1 adipocytes. *Diabetes* 51 (7), 2045–2055. doi:10.2337/diabetes.51.7.2045
- Tan, D. X., Manchester, L. C., Fuentes-Broto, L., Paredes, S. D., and Reiter, R. J. (2011). Significance and application of melatonin in the regulation of Brown adipose tissue metabolism: Relation to human obesity. *Obes. Rev.* 12 (3), 167–188. doi:10.1111/j.1467-789X.2010.00756.x
- Tasić-Kostov, M., Arsić, I., Pavlović, D., Stojanović, S., Najman, S., Naumović, S., et al. (2019). Towards a modern approach to traditional use: *In vitro* and *in vivo* evaluation of *Alchemilla vulgaris* L. Gel wound healing potential. *J. Ethnopharmacol.* 83, 111789. doi:10.1016/j.jep.2019.03.016
- Tellez, L. A., Perez, I. O., Simon, S. A., and Gutierrez, R. (2012). Transitions between sleep and feeding states in rat ventral striatum neurons. *J. neurophysiology* 108 (6), 1739–1751. doi:10.1152/jn.00394.2012
- Thitimuta, S., Pithayanukul, P., Nithitanakool, S., Bavovada, R., Leanpolchareanchai, J., and Saparpakorn, P. (2017). *Camellia sinensis* L. Extract and its potential beneficial effects in antioxidant, anti-inflammatory, anti-hepatotoxic, and anti-tyrosinase activities. *Molecules* 22 (3), 401. doi:10.3390/molecules22030401
- Tian, J. Y., Tao, R. y., Zhang, X. L., Liu, Q., He, Y. B., Su, Y. L., et al. (2015). Effect of *Hypericum perforatum* L. extract on insulin resistance and lipid metabolic disorder in high-fat-diet induced obese mice. *Phytother. Res.* 29 (1), 86–92. doi:10.1002/ptr.5230
- Tokgöz, H. B., and Altan, F. (2020). *Hypericum perforatum* L. A medicinal plant with potential as a curative agent against obesity-associated complications. *Mol. Biol. Rep.* 47 (11), 8679–8686. doi:10.1007/s11033-020-05912-7
- Törrönen, R., Sarkkinen, E., Niskanen, T., Tapola, N., Kilpi, K., and Niskanen, L. (2012). Postprandial glucose, insulin and glucagon-like peptide 1 responses to sucrose ingested with berries in healthy subjects. *Br. J. Nutr.* 107 (10), 1445–1451. doi:10.1017/S0007114511004557
- Tucci, S. A. (2010). Phytochemicals in the control of human appetite and body weight. *Pharm. (Basel)* 3 (3), 748–763. doi:10.3390/ph3030748
- Türküzü, D., and Tek, N. A. (2017). A minireview of effects of green tea on energy expenditure. *Crit. Rev. Food Sci. Nutr.* 57 (2), 254–258. doi:10.1080/10408398.2014.986672
- Van Dam, R. M., Hu, F. B., and Willett, W. C. (2020). Coffee, caffeine, and health. *N. Engl. J. Med.* 383, 369–378. doi:10.1056/NEJMr1816604
- Vermaak, I., Hamman, J. H., and Viljoen, A. M. (2011). *Hoodia gordonii*: An up-to-date review of a commercially important anti-obesity plant. *Planta Med.* 77 (11), 1149–1160. doi:10.1055/s-0030-1250643
- Vernochet, C., Peres, S. B., Davis, K. E., McDonald, M. E., Qiang, L., Wang, H., et al. (2009). C/EBPalpha and the corepressors CtBP1 and CtBP2 regulate repression of select visceral white adipose genes during induction of the Brown phenotype in white adipocytes by peroxisome proliferator-activated receptor gamma agonists. *Mol. Cell. Biol.* 29 (17), 4714–4728. doi:10.1128/MCB.01899-08
- Villarroya, F., Iglesias, R., and Giral, M. (2007). PPARs in the control of uncoupling proteins gene expression. *PPAR Res.* 2007, 74364. doi:10.1155/2007/74364
- Vogler, B. K., Pittler, M. H., and Ernst, E. (1999). The efficacy of ginseng. A systematic review of randomised clinical trials. *Eur. J. Clin. Pharmacol.* 55 (8), 567–575. doi:10.1007/s002280050674
- Vuksan, V., Sievenpiper, J. L., Koo, V. Y., Francis, T., Beljan-Zdravkovic, U., Xu, Z., et al. (2000). American ginseng (*Panax quinquefolius* L) reduces postprandial glycemia in nondiabetic subjects and subjects with type 2 diabetes mellitus. *Arch. Intern. Med.* 160 (7), 1009–1013. doi:10.1001/archinte.160.7.1009
- Vuksan, V., Sung, M. K., Sievenpiper, J. L., Stavro, P. M., Jenkins, A. L., Di Buono, M., et al. (2008). Korean red ginseng (*Panax ginseng*) improves glucose and insulin regulation in well-controlled, type 2 diabetes: Results of a randomized, double-blind, placebo-controlled study of efficacy and safety. *Nutr. Metabolism Cardiovasc. Dis.* 18 (1), 46–56. doi:10.1016/j.numecd.2006.04.003
- Walid, A.-D., Molham, A.-H., and Ahmed, A.-G. (2006). Human khat (*Catha edulis*) chewers have elevated plasma leptin and nonesterified fatty acids. *Nutr. Res.* 26 (12), 632–636. doi:10.1016/j.nutres.2006.09.007
- Wang, L., Teng, R., Rogers, H., Wu, H., and Kopp, J. B., (2013). PPARα and Sirt1 mediate erythropoietin action in increasing metabolic activity and browning of white adipocytes to protect against obesity and metabolic disorders. *Diabetes* 62 (12), 4122–4131. doi:10.2337/db13-0518
- Wang, Q., Zhang, M., Xu, M., Gu, W., Xi, Y., Qi, L., et al. (2015a). Brown adipose tissue activation is inversely related to central obesity and metabolic parameters in adult human. *PLoS One* 10 (4), e0123795. doi:10.1371/journal.pone.0123795
- Wang, S., Wang, X., Ye, Z., Xu, C., Zhang, M., Ruan, B., et al. (2015b). Curcumin promotes browning of white adipose tissue in a norepinephrine-dependent way. *Biochem. Biophysical Res. Commun.* 466 (2), 247–253. doi:10.1016/j.bbrc.2015.09.018
- Wani, S. A., and Kumar, P. (2018). Fenugreek: A review on its nutraceutical properties and utilization in various food products. *J. Saudi Soc. Agric. Sci.* 17 (2), 97–106. doi:10.1016/j.jssas.2016.01.007
- Weidner, C., de Groot, J. C., Prasad, A., Freiwald, A., Quedenau, C., Kliem, M., et al. (2012). Amorphutins are potent antidiabetic dietary natural products. *Proc. Natl. Acad. Sci. U. S. A.* 109 (19), 7257–7262. doi:10.1073/pnas.1116971109
- Weinstein, A. M., Rosca, P., Fattore, L., and London, E. D. (2017). Synthetic cathinone and cannabinoid designer drugs pose a major risk for public health. *Front. Psychiatry* 8, 156. doi:10.3389/fpsy.2017.00156
- Wenthur, C. J., Bennett, M. R., and Lindsley, C. W. (2014). Classics in chemical neuroscience: Fluoxetine (prozac). *ACS Chem. Neurosci.* 5 (1), 14–23. doi:10.1021/cn400186j
- Westerterp-Plantenga, M. S. (2010a). Green tea catechins, caffeine and body-weight regulation. *Physiol. Behav.* 100 (1), 42–46. doi:10.1016/j.physbeh.2010.02.005
- Westerterp-Plantenga, M. S. (2010b). Green tea catechins, caffeine and body-weight regulation. *Physiology Behav.* 100 (1), 42–46. doi:10.1016/j.physbeh.2010.02.005
- WHO (2021). Obesity and overweight. [cited 2022 August]; Available from: <http://www.who.int/mediacentre/factsheets/fs311/en/>.

- WHO (2022). *WHO European regional obesity report 2022*. Copenhagen: WHO.
- Wise, S. D. (1992). Clinical studies with fluoxetine in obesity. *Am. J. Clin. Nutr.* 55 (1), 181S–184S. doi:10.1093/ajcn/55.1.181S
- Wolff, R. L., Pédrone, F., Pasquier, E., and Marpeau, A. M. (2000). General characteristics of *Pinus* spp. seed fatty acid compositions, and importance of delta5-olefinic acids in the taxonomy and phylogeny of the genus. *Lipids* 35 (1), 1–22. doi:10.1007/s11745-000-0489-y
- WonLicochalcone, S.-R. A., Kim, Y. M., Lee, P. H., Ryu, J. H., and Kim, J. W., (2007). Licochalcone A: A lipase inhibitor from the roots of *Glycyrrhiza uralensis*. *Food Res. Int.* 40, 1046–1050. doi:10.1016/j.foodres.2007.05.005
- Wu, Z., Bucher, N. L., and Farmer, S. R. (1996). Induction of peroxisome proliferator-activated receptor gamma during the conversion of 3T3 fibroblasts into adipocytes is mediated by C/EBPbeta, C/EBPdelta, and glucocorticoids. *Mol. Cell Biol.* 16 (8), 4128–4136. doi:10.1128/mcb.16.8.4128
- Wu, Z., Puigserver, P., Andersson, U., Zhang, C., Adelman, G., Mootha, V., et al. (1999b). Mechanisms controlling mitochondrial biogenesis and respiration through the thermogenic coactivator PGC-1. *Cell* 98 (1), 115–124. doi:10.1016/S0092-8674(00)80611-X
- Wu, Z., Rosen, E. D., Brun, R., Hauser, S., Adelman, G., Troy, A. E., et al. (1999a). Cross-regulation of C/EBP alpha and PPAR gamma controls the transcriptional pathway of adipogenesis and insulin sensitivity. *Mol. Cell* 3 (2), 151–158. doi:10.1016/S1097-2765(00)80306-8
- Xie, W., Zhao, Y., and Zhang, Y. (2011). Traditional Chinese medicines in treatment of patients with type 2 diabetes mellitus. *Evid. Based Complement. Altern. Med.* 2011, 726723. doi:10.1155/2011/726723
- Xu, B. J., Han, L. K., Zheng, Y. N., Lee, J. H., and Sung, C. K. (2005). *In vitro* inhibitory effect of triterpenoidal saponins from *Platycodi Radix* on pancreatic lipase. *Archives pharmacol Res.* 28 (2), 180–185. doi:10.1007/BF02977712
- Xu, H., Barnes, G. T., Yang, Q., Tan, G., Yang, D., Chou, C. J., et al. (2003). Chronic inflammation in fat plays a crucial role in the development of obesity-related insulin resistance. *J. Clin. investigation* 112 (12), 1821–1830. doi:10.1172/JCI19451
- Yamashita, Y., Okabe, M., Natsume, M., and Ashida, H. (2013). Cinnamtannin A2, a tetrameric procyanidin, increases GLP-1 and insulin secretion in mice. *Biosci. Biotechnol. Biochem.* 77 (4), 888–891. doi:10.1271/bbb.130095
- Yang, J. Y., Della-Fera, M. A., Hartzell, D. L., Nelson-Dooley, C., Hausman, D. B., and Baile, C. A. (2006). Esculetin induces apoptosis and inhibits adipogenesis in 3T3-L1 cells. *Obes. (Silver Spring)* 14 (10), 1691–1699. doi:10.1038/oby.2006.194
- Yau, W. W., and Yen, P. M. (2020). Thermogenesis in adipose tissue activated by thyroid hormone. *Int. J. Mol. Sci.* 21, 3020. doi:10.3390/ijms21083020
- Ye, J. (2013). Mechanisms of insulin resistance in obesity. *Front. Med.* 7 (1), 14–24. doi:10.1007/s11684-013-0262-6
- Yoneshiro, T., and Saito, M. (2013). Transient receptor potential activated Brown fat thermogenesis as a target of food ingredients for obesity management. *Curr. Opin. Clin. Nutr. Metab. Care* 16, 625–631. doi:10.1097/MCO.0b013e3283653ee1
- Yoshioka, M., Lim, K., Kikuzato, S., Kiyonaga, A., Tanaka, H., Shindo, M., et al. (1995). Effects of red-pepper diet on the energy metabolism in men. *J. Nutr. Sci. Vitaminol. (Tokyo)* 41, 647–656. doi:10.3177/jnsv.41.647
- Zelger, J. L., and Carlini, E. A. (1980). Anorexigenic effects of two amines obtained from *Catha edulis* Forsk. (Khat) in rats. *Pharmacol. Biochem. Behav.* 12 (5), 701–705. doi:10.1016/0091-3057(80)90152-5
- Zhang, K., Yang, X., Zhao, Q., Li, Z., Fu, F., Zhang, H., et al. (2020b). Molecular mechanism of stem cell differentiation into adipocytes and adipocyte differentiation of malignant tumor. *Stem Cells Int.* 2020, 8892300. doi:10.1155/2020/8892300
- Zhang, L., Xie, Q., and Li, X. (2022). Esculetin: A review of its pharmacology and pharmacokinetics. *Phytother. Res.* 36 (1), 279–298. doi:10.1002/ptr.7311
- Zhang, Q., Huang, Y., Li, X., Liu, H., He, B., Wang, B., et al. (2019). Mangiferin improved palmitate-induced-insulin resistance by promoting free fatty acid metabolism in HepG2 and C2C12 cells via PPARα: Mangiferin improved insulin resistance. *J. Diabetes Res.* 2019, 7403978. doi:10.1155/2019/7403978
- Zhang, Y., and Huang, C. (2012). Targeting adipocyte apoptosis: A novel strategy for obesity therapy. *Biochem. biophysical Res. Commun.* 417 (1), 1–4. doi:10.1016/j.bbrc.2011.11.158
- Zhang, Y., Liu, X., Ruan, J., Zhuang, X., Zhang, X., and Li, Z. (2020a). Phytochemicals of garlic: Promising candidates for cancer therapy. *Biomed. Pharmacother.* 123, 109730. doi:10.1016/j.biopha.2019.109730
- Zhang, Z., Zhang, H., Li, e. a. B., Meng, X., Wang, J., Zhang, Y., et al. (2014). Berberine activates thermogenesis in white and Brown adipose tissue. *Nat. Commun.* 5, 5493. doi:10.1038/ncomms6493
- Zwick, R. K., Guerrero-Juarez, C. F., Horsley, V., and Plikus, M. V. (2018). Anatomical, physiological, and functional diversity of adipose tissue. *Cell Metab.* 27 (1), 68–83. doi:10.1016/j.cmet.2017.12.002



OPEN ACCESS

EDITED BY

Ochuko Lucky Erukainure,
University of the Free State, South Africa

REVIEWED BY

Laiba Arshad,
Forman Christian College, Pakistan
Md Afjalus Siraj,
Yale University, United States

*CORRESPONDENCE

Emmanuel Mfotie Njoya,
✉ mfotiefr@yahoo.fr,
✉ enjoya@cut.ac.za
Tshepiso J. Makhafola,
✉ jmakhafola@cut.ac.za

RECEIVED 13 April 2023

ACCEPTED 12 June 2023

PUBLISHED 21 June 2023

CITATION

Mfotie Njoya E, Ndemangou B, Akinyelu J,
Munvera AM, Chukwuma CI, Mkounga P,
Mashele SS, Makhafola TJ and McGaw LJ
(2023), *In vitro* antiproliferative, anti-
inflammatory effects and molecular
docking studies of natural compounds
isolated from *Sarcocephalus pobeguini*
(Hua ex Pobég).
Front. Pharmacol. 14:1205414.
doi: 10.3389/fphar.2023.1205414

COPYRIGHT

© 2023 Mfotie Njoya, Ndemangou,
Akinyelu, Munvera, Chukwuma,
Mkounga, Mashele, Makhafola and
McGaw. This is an open-access article
distributed under the terms of the
[Creative Commons Attribution License](#)
(CC BY). The use, distribution or
reproduction in other forums is
permitted, provided the original author(s)
and the copyright owner(s) are credited
and that the original publication in this
journal is cited, in accordance with
accepted academic practice. No use,
distribution or reproduction is permitted
which does not comply with these terms.

In vitro antiproliferative, anti-inflammatory effects and molecular docking studies of natural compounds isolated from *Sarcocephalus pobeguini* (Hua ex Pobég)

Emmanuel Mfotie Njoya^{1,2,3*}, Brigitte Ndemangou⁴,
Jude Akinyelu⁵, Aristide M. Munvera⁶, Chika. I. Chukwuma¹,
Pierre Mkounga⁶, Samson S. Mashele¹, Tshepiso J. Makhafola^{1*}
and Lyndy J. McGaw²

¹Centre for Quality of Health and Living, Faculty of Health and Environmental Sciences, Central University of Technology, Bloemfontein, South Africa, ²Department of Paraclinical Sciences, Faculty of Veterinary Science, University of Pretoria, Pretoria, South Africa, ³Department of Biochemistry, Faculty of Science, University of Yaoundé I, Yaoundé, Cameroon, ⁴University Institute of Technology of Wood Technology, Mbalmayo, Cameroon, ⁵Department of Biochemistry, Federal University Oye-Ekiti, Oye, Nigeria, ⁶Department of Organic Chemistry, Faculty of Science, University of Yaoundé I, Yaoundé, Cameroon

Background: *Sarcocephalus pobeguini* (Hua ex Pobég) is used in folk medicine to treat oxidative-stress related diseases, thereby warranting the investigation of its anticancer and anti-inflammatory properties. In our previous study, the leaf extract of *S. pobeguini* induced significant cytotoxic effect against several cancerous cells with high selectivity indexes towards non-cancerous cells.

Aim: The current study aims to isolate natural compounds from *S. pobeguini*, and to evaluate their cytotoxicity, selectivity and anti-inflammatory effects as well as searching for potential target proteins of bioactive compounds.

Methods: Natural compounds were isolated from leaf, fruit and bark extracts of *S. pobeguini* and their chemical structures were elucidated using appropriate spectroscopic methods. The antiproliferative effect of isolated compounds was determined on four human cancerous cells (MCF-7, HepG2, Caco-2 and A549 cells) and non-cancerous Vero cells. Additionally, the anti-inflammatory activity of these compounds was determined by evaluating the nitric oxide (NO) production inhibitory potential and the 15-lipoxygenase (15-LOX) inhibitory activity. Furthermore, molecular docking studies were carried out on six putative target proteins found in common signaling pathways of inflammation and cancer.

Results: Hederagenin (**2**), quinovic acid 3-O-[α -D-quinovopyranoside] (**6**) and quinovic acid 3-O-[β -D-quinovopyranoside] (**9**) exhibited significant cytotoxic effect against all cancerous cells, and they induced apoptosis in MCF-7 cells by increasing caspase-3/-7 activity. (**6**) showed the highest efficacy against all cancerous cells with poor selectivity (except for A549 cells) towards non-cancerous Vero cells; while (**2**) showed the highest selectivity warranting its potential safety as a chemotherapeutic agent. Moreover, (**6**) and (**9**)

significantly inhibited NO production in LPS-stimulated RAW 264.7 cells which could mainly be attributed to their high cytotoxic effect. Besides, the mixture naucleatifoline G and naucleofficine D (**1**), hederagenin (**2**) and chletric acid (**3**) were active against 15-LOX as compared to quercetin. Docking results showed that JAK2 and COX-2, with the highest binding scores, are the potential molecular targets involved in the antiproliferative and anti-inflammatory effects of bioactive compounds.

Conclusion: Overall, hederagenin (**2**), which selectively killed cancer cells with additional anti-inflammatory effect, is the most prominent lead compound which may be further investigated as a drug candidate to tackle cancer progression.

KEYWORDS

Sarcocephalus pobeguini, hederagenin, inflammation, cancer, cytotoxicity, selective index, apoptosis, docking score

1 Introduction

Cancer is one of the leading causes of death worldwide, accounting 19.3 million new cancer cases and about 10 million deaths in 2020 (Sung et al., 2021). This chronic disease is characterized by abnormal and uncontrolled proliferation of cancer cells which later invades normal tissues and organs, and eventually spreading throughout the body. Several reports have proven the cross-talk between inflammation and cancer due to the fact that common signaling pathways are modulated in both deleterious ailments (Hibino et al., 2021; Zhao et al., 2021). Regardless to the cancer type, inflammation conditions have been considered as one of the key factors that promotes all stages of tumorigenesis. Inflammation also helps the survival of malignant cells, therefore impeding the immune surveillance or altering the efficacy of chemotherapeutic agents (Mantovani et al., 2008; Peczek et al., 2022). As one of the most important cancer treatment strategies, chemotherapy uses powerful drugs to kill fast-growing cells, but it induces substantial side effects due to the fact that normal cells are also affected (Amjad et al., 2022). To date, great progress has been made for the discovery and development of effective and safe chemotherapeutic agents, however the number of cancer-related deaths increases every day. This situation urgently requires the search of alternative treatments to improve the quality of life of patients. Natural therapies including medicinal plants constitute a reservoir for the discovery of new anticancer lead compounds. Additionally, as above-mentioned, chronic inflammation accelerates cancer progression, and it has been proven that some anti-inflammatory drugs such as aspirin, celecoxib, diclofenac, etc. are being used against cancer (Rayburn et al., 2009; Zappavigna et al., 2020; Lai et al., 2022). As such, controlling inflammation may represent a valid strategy for cancer prevention and therapy. Thus, developing anticancer agents with additional anti-inflammatory effect is the best approach to tackle cancer progression.

Cameroon has a rich biodiversity, with about 8,620 plants species which are used by local population for the treatment of several ailments (Kuate and Efferth, 2010; Ntie-Kang et al., 2013). Among these plants, *Sarcocephalus pobeguini* (Hua ex Pobég) (synonym of *Nauclea pobeguini* (Hua ex Pobég) Merr.) is used as infusion or decoction in the treatment of fever, malaria, stomach-ache, sexual and reproductive dysfunctions, epilepsy, diabetes mellitus, hypertension, infectious diseases and jaundice (Mesia

et al., 2005; Jiofack et al., 2009; Karou et al., 2011; Kuete et al., 2015; Haudecoeur et al., 2018). In a study investigating the cytotoxicity of selected Cameroonian medicinal plants, the bark extract of *S. pobeguini* and its isolated compounds (resveratrol and a glucoside derivative) exhibited antiproliferative potential against multi-factorial drug-resistant cancer cell lines (Kuate et al., 2015). In our previous study, the antiproliferative effect of different plant parts (leaf, fruit, bark and root) extracts of *S. pobeguini* were evaluated on several human cancer cell lines, and leaf extract induced significant cytotoxic effect with high selectivity indexes (Mfotie Njoya et al., 2017). So far, phytochemical investigations carried out on bark and root extracts of *S. pobeguini* have resulted in the isolation and characterization of compounds such as strictosamide, 5-carboxystrictosidine, methylangustoline, 3-O- β -D-fucosyl-quinovic-acid, 3-keto-quinovic-acid; 19-O-methylangustoline, 3-acetoxy-11-oxo-urs-12-ene, p-coumaric acid, citric acid trimethyl ester, resveratrol, resveratrol β -D-glucopyranoside (Karou et al., 2011; Kuete et al., 2015; Yuće et al., 2019). Despite the use of leaves and fruits of *S. pobeguini* in traditional medicine, the isolation of compounds from these plant parts as well as their biological effects have not yet been investigated to the best of our knowledge. Moreover, the use of leaves and fruits for medicinal purposes instead of roots and barks is advantageous for the conservation and sustainable maintenance of medicinal plants. Therefore, the current work aims to find bioactive compounds from leaf and fruit extracts of *S. pobeguini* and to evaluate their efficacy, selectivity and anti-inflammatory effects. In addition, this study has been also extended to the isolation of active constituents from roots of *S. pobeguini* which might also yield to the discovery of new anticancer lead compounds.

2 Materials and methods

2.1 Plant material

Different parts (leaves, fruits, and barks) of *S. pobeguini* were harvested in Ezezan (Nyom II), a neighbouring locality situated at 40 km from Yaoundé (Cameroon). A voucher specimen was prepared and the authentication was done by Mr. Ngansop Eric, a plant taxonomist, after comparison with the specimen number N°32,567 BRF/CAM already available in the library of the National

Herbarium of Cameroon. Our plant material was then registered under the number Letouzey R.12493 (YA).

2.2 Preparation of extracts and isolation of compounds

The powder (907 g) obtained from the air dried and grounded fruits of *S. pobeguinii* was macerated in the mixture of methanol and methylene chloride (1:1) at room temperature for 48 h with occasional stirring, and the crude extract was obtained after filtration with Whatman N°1, followed by evaporation of the solvent to dryness *in vacuo*. The dried extract (76.5 g) was re-dissolved in MeOH and partitioned with ethyl acetate (EtOAc) to yield the EtOAc fraction (10.2 g) and the MeOH residue (54.7 g). The MeOH soluble fraction was then subjected to silica gel column chromatography (CC) eluted with a gradient mixture of *n*-hexane-EtOAc (9:1; 7:3; 6:4; 0:1). The collected sub-fractions were pooled based on their thin layer chromatography (TLC) profiles and yielded six sub-fractions (F1-F6) after evaporation. Sub-fraction F₃ (8 g) was submitted to silica gel CC, and eluted with the mixture of *n*-hexane-EtOAc (2:1) to yield the following compounds: (1) (6 mg) identified as a mixture of nauclealatifoline G and naucleofficine D (Agomuoh et al., 2013); (2) (7 mg) known as hederagenin (Joshi et al., 1999); and (3) (6 mg) characterized as chletric acid (Takahashi and Takani, 1978).

The powder of air-dried leaves of *S. pobeguinii* (1 kg) was extracted in MeOH and heated at 40°C–50°C for 2 h. The methanolic extract was concentrated *in vacuo* to yield a dark greenish mass (66 g) which was partitioned with *n*-hexane. The *n*-hexane soluble part and the methanolic residue were evaporated under pressure to obtain respectively a black residue (26.5 g) and a greenish brown extract (37.3 g). The latter was subjected to silica gel flash chromatography, and eluted respectively with CH₂Cl₂; CH₂Cl₂/MeOH (1:1) and MeOH. The *n*-hexane soluble part and the CH₂Cl₂ fraction were mixed due to their similar TLC profiles, and this mixed fraction was submitted to silica gel CC eluted with the gradient mixture of *n*-hexane and EtOAc (9:1; 3:1; 3:2; 1:1; 1:3) to afford compound (4) (5 mg) identified as taraxerol (Yen et al., 2013) collected in *n*-hexane/EtOAc (3:1); compound (5) (4 mg) known as α -amyrin (3 β -hydroxy-urs-12-en-3-ol) (Viet et al., 2021) collected in *n*-hexane/EtOAc (1:1); and (6) (6 mg) known as quinovic acid 3-O-[α -D-quinovopyranoside] (Mohamed, 1999) collected in *n*-hexane/EtOAc (1:3).

The powder of dried bark of *S. pobeguinii* (1 kg) was extracted in MeOH and heated at 40°C–50°C for 2 h. The crude extract was obtained after filtration with Whatman N°1, followed by evaporation under reduced pressure to obtain a yellow gummy residue (77 g). This methanolic extract was partitioned with *n*-hexane to yield the *n*-hexane fraction (15 g) and a residual MeOH fraction (54 g). The MeOH fraction was then subjected to silica gel CC, and eluted with a gradient of *n*-hexane/EtOAc yielding the following compounds: (7) (4 mg) identified as erythrodiol and (8) (8 mg) known as quinovic acid (Fatima et al., 2002; Aktar et al., 2009) both collected in the *n*-hexane/EtOAc (9:1); then compound (9) (8 mg) characterized as quinovic acid 3-O-[β -D-quinovopyranoside] (Yopez et al., 1991) collected in *n*-hexane/EtOAc (3:1); and finally compound (10) (4 mg) identified as

latifoliamide C (Agomuoh et al., 2013) collected in *n*-hexane/EtOAc (1:9).

2.3 Characterization and structural elucidation of isolated compounds

The chemical constituents of *S. pobeguinii* were purified using open silica gel column chromatography (Merck, [Darmstadt, Germany]). TLC was done on Alu g R; SIL G/UV₂₅₄ silica gel plates (Merck, [Darmstadt, Germany]), and visualization of the spots on TLC plates was achieved either by exposure to iodine vapour, UV light or by spraying sulphuric acid and heating the plate at 75°C. Melting points were recorded on a Buchi B-54 apparatus. ¹H and ¹³C NMR spectra as well as 2D NMR experiments (see Supplementary Material, Supplementary Figures S1–S22) were recorded in CDCl₃, MeOH-*d*₄, DMSO-*d*₆ and pyridine-*d*₅ in a JEOL ECX 500 spectrometer (Akishima, Japan) and on a Bruker ARX 400. Chemical shifts were expressed in part per million (δ) relative to tetramethylsilane as internal standard. The spectroscopy data recorded were compared with data from literature, for the characterization of the chemical structures of isolated compounds which are presented in Figure 1.

2.4 Cell culture

Cancerous cell lines (MCF-7: human breast adenocarcinoma cells; HepG2: human hepatocellular carcinoma cells; Caco-2: human epithelial colorectal adenocarcinoma cells; A549: human epithelial lung adenocarcinoma cells), obtained from the American Type Culture Collection (ATCC) (Rockville, MD, United States of America), were cultured in Dulbecco's Modified Eagle's Medium (DMEM) high glucose (4.5 g/L) containing L-glutamine (4 mM) and sodium-pyruvate (Hyclone™) supplemented with 10% (v/v) fetal bovine serum (FBS) (Capricorn Scientific GmbH, South America), and incubated at 37°C with 5% CO₂ in a humidified environment. African green monkey (Vero) kidney cells (also obtained from ATCC), a non-cancerous cell line, were grown in DMEM high glucose (4.5 g/L) containing L-glutamine (Lonza, Belgium) and supplemented with 5% FBS (Capricorn Scientific GmbH, South America) and 1% gentamicin (Virbac, RSA) in the same environment as cancer cells. The RAW 264.7 murine macrophage cells (obtained from ATCC) were cultured in DMEM high glucose (4.5 g/L) containing L-glutamine (Lonza, Belgium), supplemented with 10% FBS (Capricorn Scientific GmbH, South America) and 1% penicillin/streptomycin/fungizone (PSF) solution, and kept at 37°C in a 5% CO₂ humidified environment.

2.5 Antiproliferation assay

The cancerous and non-cancerous cells were seeded at a density of 10⁴ cells per well in 96-well microtiter plates, and they were incubated overnight at 37°C with 5% CO₂ in a 5% CO₂ humidified environment in order to allow the attachment of cells at the bottom of the plates. Then, the cells were exposed to increasing

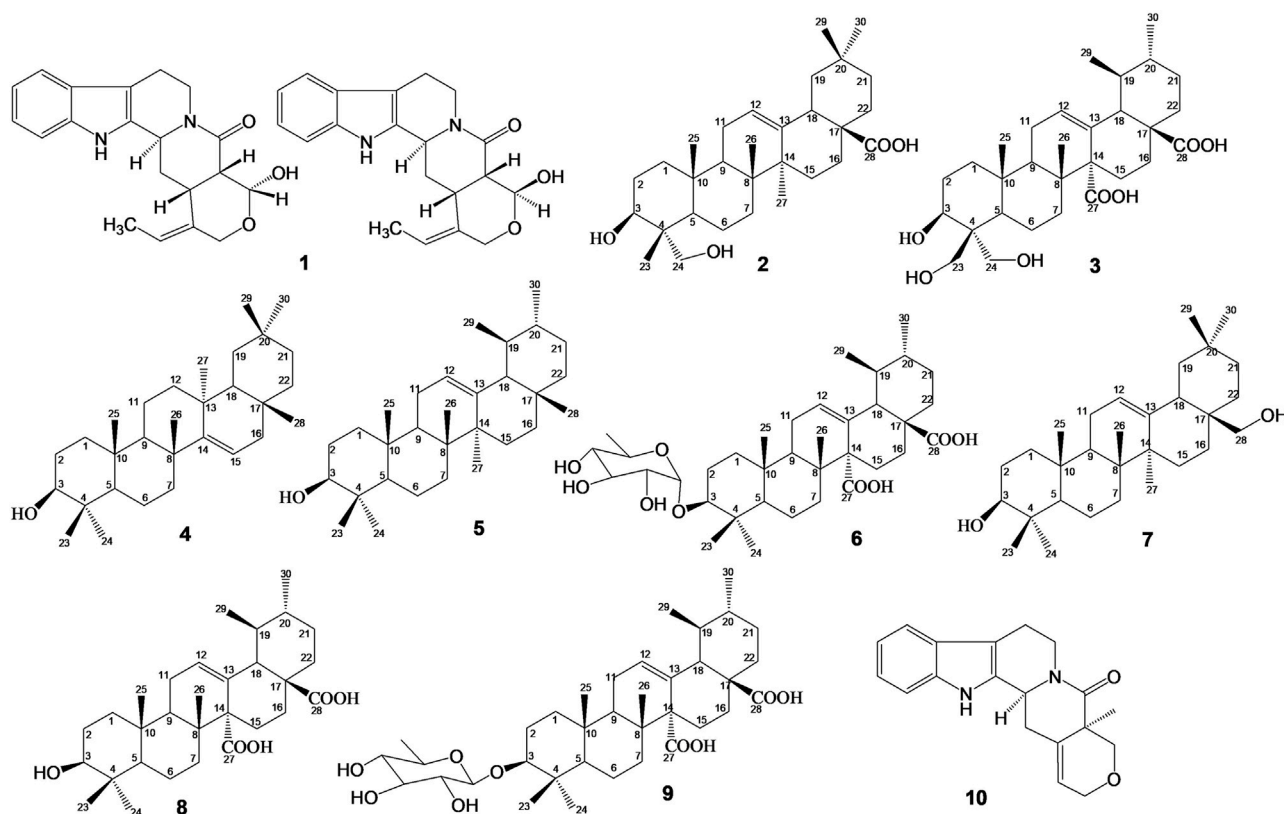


FIGURE 1

Chemical structures of isolated compounds: Mixture of Nauclealatifoline G (C₂₀H₂₂N₂O₃, 338.40 g/mol) and naucleoficine D (C₂₀H₂₂N₂O₃, 338.40 g/mol) (1), hederagenin (C₃₀H₄₈O₄, 472.73 g/mol) (2) and chletic acid (C₃₀H₄₆O₈, 534.69 g/mol) (3) were isolated from fruit extract of *S. pobeguini*. Taraxerol (C₃₀H₅₀O, 426.73 g/mol) (4), α -amyrin (3 β -hydroxy-urs-12-en-3-ol) (C₃₀H₅₀O, 426.73 g/mol) (5) and quinovic acid 3-O- α -D-quinovopyranoside] (C₃₆H₅₆O₉, 632.84 g/mol) (6) were isolated from leaf extract of *S. pobeguini*. Erythrodiol (C₃₀H₅₀O₂, 442.73 g/mol) (7), quinovic acid (C₃₀H₄₆O₅, 486.69 g/mol) (8), quinovic acid 3-O- β -D-quinovopyranoside] (C₃₆H₅₆O₉, 632.84 g/mol) (9) and latifoliamide C (C₁₉H₂₀N₂O₂, 308.38 g/mol) (10) were isolated from bark extract of *S. pobeguini*.

concentrations of compounds (100, 50, 25, 10 and 5 μ g/mL) dissolved in dimethyl sulfoxide (DMSO) and further diluted in fresh culture medium. In this assay, the final concentration of DMSO in the culture medium was 0.5% used as negative control while doxorubicin hydrochloride (Pfizer, United States of America) was used as a positive control. The culture plates were incubated for 48 h at 37°C in a 5% CO₂ humidified environment, after which the culture medium was discarded, and replaced by 200 μ L of fresh culture medium with 30 μ L of 3-(4,5-dimethylthiazol-2-yl)-2,5-diphenyl-2H-tetrazolium bromide (MTT) (5 mg/mL) dissolved in phosphate buffered saline (Mosmann, 1983). After 4 h of incubation, the medium was gently removed, and the formazan crystals were solubilized in 50 μ L of DMSO. The absorbance was measured at 570 nm after shaking for 1 min on a microplate reader (Synergy Multi-Mode Reader, BioTek, Winooski, United States of America).

The cell viability rate was determined at each concentration of the compound as a percentage of cells treated with DMSO at 0.5% used as negative control. The 50% inhibitory concentrations (IC₅₀) were determined by using the non-linear regression graphical analysis of cell viability rate against the logarithm (log₁₀) of compound concentrations with the software GraphPad Prism 6.0

(GraphPad software Inc., United States of America). The selectivity index (Supporting Material) values were calculated for each compound by dividing the IC₅₀ of non-cancerous cells by the IC₅₀ of cancerous cells in the same units (Mfotie Njoya et al., 2018; Mfotie Njoya et al., 2020).

2.6 Caspase-3/-7 luminescence assay

The effect of the most bioactive compounds (2), (6) and (9) were used for the analysis of caspase-3 and caspase-7 activities on MCF-7 cells by using the Caspase-Glo® 3/7 kit (Promega, Germany). In fact, MCF-7 cells were seeded at a density of 10⁴ cells per well on 96-well microtiter plates, and the plates were incubated overnight at 37 °C in a 5% CO₂ humidified environment. Then, the cells were exposed to the active compounds at different concentrations ($\frac{1}{2}$ IC₅₀, IC₅₀ and 2 \times IC₅₀) or DMSO (0.5%) used as negative control, and further incubated for 18 h at 37°C in a 5% CO₂ humidified environment. Thereafter, 100 μ L of Caspase-Glo® 3/7 reagent was added to each well, mixed and incubated in the dark for 1 h at room temperature. The luminescence was then measured on a microplate reader (Synergy Multi-Mode Reader, BioTek, Winooski, United States of

America). The caspase-3/-7 activity was expressed as fold change of cells treated with 0.5% DMSO (control).

2.7 Anti-inflammatory assays

2.7.1 Nitric oxide production inhibitory assay

Nitric oxide (NO) production was evaluated in lipopolysaccharide (LPS)-stimulated RAW 264.7 cells by measuring the influence of tested compounds on the accumulation of nitrite, an indicator of NO in the cell supernatant, which can be detected with Griess reagent (Merck, Darmstadt, Germany). Briefly, the RAW 264.7 cells at their exponential growth phase were seeded at a density of 2×10^4 cells per well in 96 well-microtiter plates, and they were incubated overnight at 37°C in a 5% CO₂ humidified environment to allow attachment. The cells were pre-treated with tested compounds (100 µg/mL) or DMSO 0.5% (negative control) and incubated for 1 h at 37°C in a 5% CO₂ humidified environment. Then, culture medium containing LPS (2 µg/mL) was added to each well and further incubated for 24 h at 37°C in a 5% CO₂ humidified environment. Thereafter, 100 µL of cell supernatant from each well were transferred into a new 96-well microtiter plate and an equal volume of Griess reagent was added according to protocol described by the manufacturer. The microtiter plate was incubated for 10 min in the dark at room temperature, and the absorbance of the mixture was measured at 550 nm on a microplate reader (Synergy Multi-Mode Reader, BioTek, Winooski, United States of America). The quantity of nitrite was determined from a sodium nitrite standard curve, and the percentage of NO production was calculated based on the ability of each tested sample to inhibit nitric oxide production by LPS-stimulated RAW 264.7 cells compared to the control (cells treated with LPS without samples which was considered as 100% NO production). Additionally, the cell viability of treated cells was determined by using the MTT assay as previously described (Mosmann, 1983). The whole experiment was repeated at different concentrations (100, 50, 25, 10 and 5 µg/mL) only for tested compounds that were able to inhibit at 50% of NO production, and the IC₅₀ values was calculated as previously described (Mfotie Njoya et al., 2023).

2.7.2 Soybean 15-LOX inhibitory assay

This assay is based on the formation of the Fe³⁺/xylenol orange (FOX) complex with maximal absorption at 560 nm (Pinto et al., 2007). Forty microliters of 15-LOX (final concentration: 200 UI/mL) from *Glycine max* (Merck, Darmstadt, Germany) was incubated with 20 µL of tested samples (100, 50, 25, 10, and 5 µg/mL) at 25°C for 5 min, with DMSO at 10% (v/v) being used as negative control. Thereafter, 40 µL of linoleic acid (final concentration, 140 µM) prepared in Tris-HCl buffer (50 mM, pH 7.4) was added, and the plates were further incubated at 25°C for 20 min in the dark. The assay was terminated by adding 100 µL of FOX reagent [sulfuric acid (30 mM), xylene orange (100 µM), ferrous II) sulfate (100 µM), dissolved in methanol/water (9:1)], followed by the incubation of the plates at 25°C for 30 min in the dark. Finally, the absorbance was measured at 560 nm on a microplate reader (Epoch, BioTek, Winooski, United States of America). The blanks were made in the same way as tested samples except that the substrate was added

after the FOX reagent. The 15-LOX inhibitory activity was calculated by using the following formula:

$$15 - \text{LOX inhibitory activity (\%)} = 100 - \left[\frac{\text{Abs (sample)} - \text{Abs (blank)}}{\text{Abs (negative control)} - \text{Abs (blank)}} \times 100 \right] \quad (1)$$

Abs: absorbance.

2.8 Statistical analysis

All experiments were performed in triplicate, and the results are presented as mean ± standard deviation (SD) values. The statistical analysis was done with the software GraphPad Prism 6.0 (GraphPad software Inc., United States of America) on which one-way analysis of variance (ANOVA) and Student–Newman–Keuls or Dunnett's tests were used for the comparison of data among tested samples and/or controls. Results were considered significantly different when the *p*-value was greater than 0.05.

2.9 Molecular docking study

The X-ray crystal structures of putative target proteins in complex with inhibitors were retrieved from Protein Data Bank (<https://www.rcsb.org/>, accessed on 14 March 2023): Cyclooxygenase-2: COX-2 (PDB ID: 5KIR); Nuclear factor NF-kappa-B (p65 subunit): NFKB-p65 (PDB ID: 2RAM); Janus kinase 2: JAK2 (PDB ID: 6BBV); Signal transducer and activator of transcription 3: STAT3 (PDB ID: 6TLC); CASPASE-3 (PDB ID: 3DEI), CASPASE-7 (PDB ID: 1SHJ). PyMol v 2.0.7, was used to prepare the proteins for simulation by removing the inhibitors, water molecules, multi-chains and heteroatoms. MarvinSketch was used to draw the chemical structures of the ligands, and the Merck Molecular Force Field (MMFF94) as provided by MarvinSketch was used for energy minimization on the ligands (compounds) (Novichikhina et al., 2020). The energy minimization was carried out to make the ligands more stable near their initial states during molecular docking process. AutoDock Vina v 1.5.6 was used to add hydrogen atoms and Gasteiger charges accordingly to the ligands prior to molecular docking (Trott and Olson, 2010). The active sites of the target proteins were identified using CASTp 2.0 web-based tool (Tian et al., 2018). Further, AutoDock Vina v 1.5.6 was used to create a grid box around the identified active sites of the target proteins. Thereafter, standard precision ligand docking was performed using the same software. The best of nine binding poses based on the docking scores were visualized and captured in BIOVIA Discovery Studio Visualizer 2021 (Mfotie Njoya et al., 2023).

3 Results and discussion

3.1 Cytotoxic effect of isolated compounds and selectivity towards non-cancerous cells

The growth inhibitory effect of natural compounds isolated from leaf, fruits and bark of *Sarcocephalus pobeguini* (Rubiaceae) against four

TABLE 1 Cytotoxic effects (IC₅₀ values) of natural compounds isolated from roots, fruits, bark and leaves of *Sarcocephalus pobeguini* and reference drug (doxorubicin) against cancer cell lines and non-cancerous Vero cells.

Compounds	IC ₅₀ (μg/mL/μM)									
	Vero		MCF-7		HepG2		Caco-2		A549	
	μg/mL	μM	μg/mL	μM	μg/mL	μM	μg/mL	μM	μg/mL	μM
1	85.74 ± 1.64 ^a	126.68 ± 2.42 ^a	77.96 ± 2.79 ^a	115.19 ± 4.51 ^a	63.00 ± 1.29 ^a	93.08 ± 1.91 ^a	>100	>147.75	56.40 ± 3.79 ^a	83.33 ± 5.07 ^a
2	45.54 ± 2.34 ^b	96.34 ± 4.95 ^b	8.92 ± 1.12^b	18.87 ± 2.37^b	24.88 ± 1.75^b	52.63 ± 3.70^b	36.69 ± 2.19^a	77.61 ± 4.63^a	18.96 ± 0.96^b	40.11 ± 2.03^b
3	>100	>187.02	>100	>187.02	80.02 ± 1.71 ^c	149.66 ± 3.20 ^c	>100	>187.02	>100	>187.02
4	>100	>234.34	81.35 ± 1.48 ^a	190.64 ± 3.47 ^c	54.20 ± 1.64 ^d	127.01 ± 3.84 ^d	>100	>234.34	75.63 ± 3.74 ^c	177.23 ± 5.16 ^c
5	>100	>234.34	82.80 ± 1.35 ^a	194.03 ± 3.16 ^c	84.53 ± 1.45 ^c	198.08 ± 3.40 ^e	>100	>234.34	92.70 ± 3.73 ^d	217.23 ± 5.77 ^d
6	6.21 ± 0.56^c	9.81 ± 0.79^c	5.96 ± 1.53^c	9.42 ± 2.41^d	41.94 ± 1.71^e	66.27 ± 2.70^f	7.41 ± 1.68^b	11.71 ± 2.65^b	1.96 ± 0.21^e	3.08 ± 0.33^e
7	84.02 ± 3.27 ^a	189.77 ± 5.68 ^d	>100	>225.87	73.94 ± 4.22 ^c	167.01 ± 6.05 ^c	>100	>225.87	>100	>225.87
8	>100	>205.47	97.96 ± 5.72 ^a	201.28 ± 8.02 ^c	100.00 ± 3.82 ^f	205.47 ± 5.84 ^e	81.60 ± 3.88 ^c	167.66 ± 5.97 ^c	99.46 ± 3.85 ^d	204.36 ± 5.01 ^d
9	47.07 ± 3.66 ^b	74.38 ± 5.78 ^c	51.50 ± 4.93 ^d	81.38 ± 5.96 ^d	47.22 ± 4.09^e	74.62 ± 6.62^f	53.67 ± 4.97 ^d	84.81 ± 5.85 ^a	44.22 ± 2.04^f	69.87 ± 3.96^e
10	65.81 ± 2.29 ^d	213.41 ± 4.12 ^d	32.88 ± 3.78 ^c	106.62 ± 2.25 ^a	54.55 ± 3.51 ^d	176.89 ± 4.35 ^c	63.24 ± 4.04 ^d	205.07 ± 3.10 ^d	44.23 ± 4.59 ^a	143.43 ± 6.61 ^f
Doxorubicin (μM)	4.85 ± 0.51 ^f		1.09 ± 0.06 ^c		0.56 ± 0.05 ^g		4.97 ± 0.74 ^e		0.71 ± 0.05 ^g	

Data are presented as means of triplicate measurements ± standard deviation. Superscript letters a–g represent statistical difference between data obtained, and for each column of the above table, data with same letters are statistically not different while data with different letters are significantly different at $p < 0.05$. IC₅₀: concentration which inhibit 50% of cell growth compared to cells treated with DMSO (0.5%) used as negative control. Mixture of nauclealatifoline G and naucleoofficine D (1), hederagenin (2) and chletric acid (3) were isolated from CH₂Cl₂/MeOH (1:2) fruit extract of *S. pobeguini*. Taraxerol (4), α-amyrin(3β-hydroxy-urs-12-en-3-ol) (5) and quinovic acid 3-O-[α-D-quinovopyranoside] (6) were isolated from methanol leaf extract of *S. pobeguini*. Erythrodiol (7), quinovic acid (8), quinovic acid 3-O-[β-D-quinovopyranoside] (9) and latifoliamide C (10) were isolated from the methanol bark extract of *S. pobeguini*. Bold values mean compounds significantly active in the assay.

cancerous cells (MCF-7, HepG2, Caco-2 and A549) and non-cancerous Vero cells was expressed as percentage of respective cells treated with DMSO (0.5%) used as negative controls. Based on the results obtained for each compound tested at different concentrations, the 50% inhibitory concentrations (IC₅₀) were determined and presented in Table 1. It was observed that hederagenin (2), quinovic acid 3-O-[α-D-quinovopyranoside] (6) and quinovic acid 3-O-[β-D-quinovopyranoside] (9) exhibited significant ($p < 0.05$) antiproliferative effect against all cancerous cells, especially for (6) which showed the highest cytotoxic effect on A549 cells with IC₅₀ of 1.96 μg/mL (3.08 μM). Additionally, (6) was also toxic to the non-cancerous Vero cells with IC₅₀ of 6.21 μg/mL (9.81 μM). By calculating the selectivity indexes (SI) as presented in Table 2, we found that (6), isolated from leaves of *S. pobeguini*, had a poor selectivity ($SI \leq 1$) (except for A549 cells) towards non-cancerous Vero cells where SI was 3.17. Similarly, (9), isolated from bark of *S. pobeguini*, also had poor selectivity ($SI \leq 1$) for all cancer types. On the other hand, (2), isolated from fruits of *S. pobeguini*, was the only compound which had acceptable

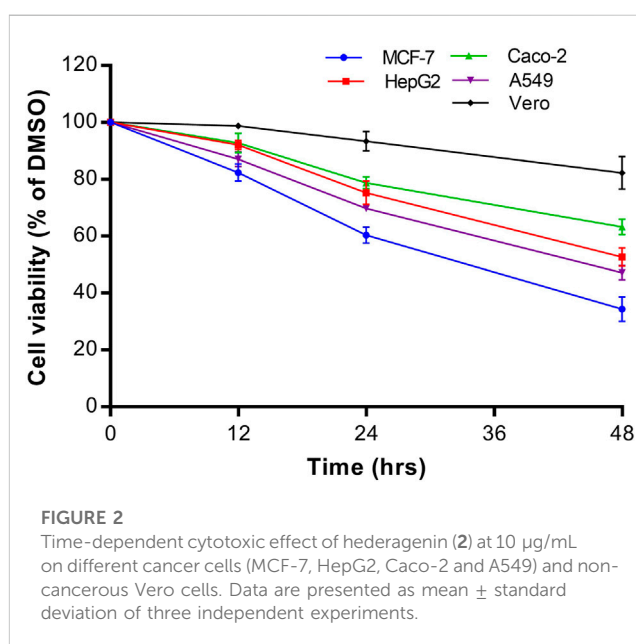
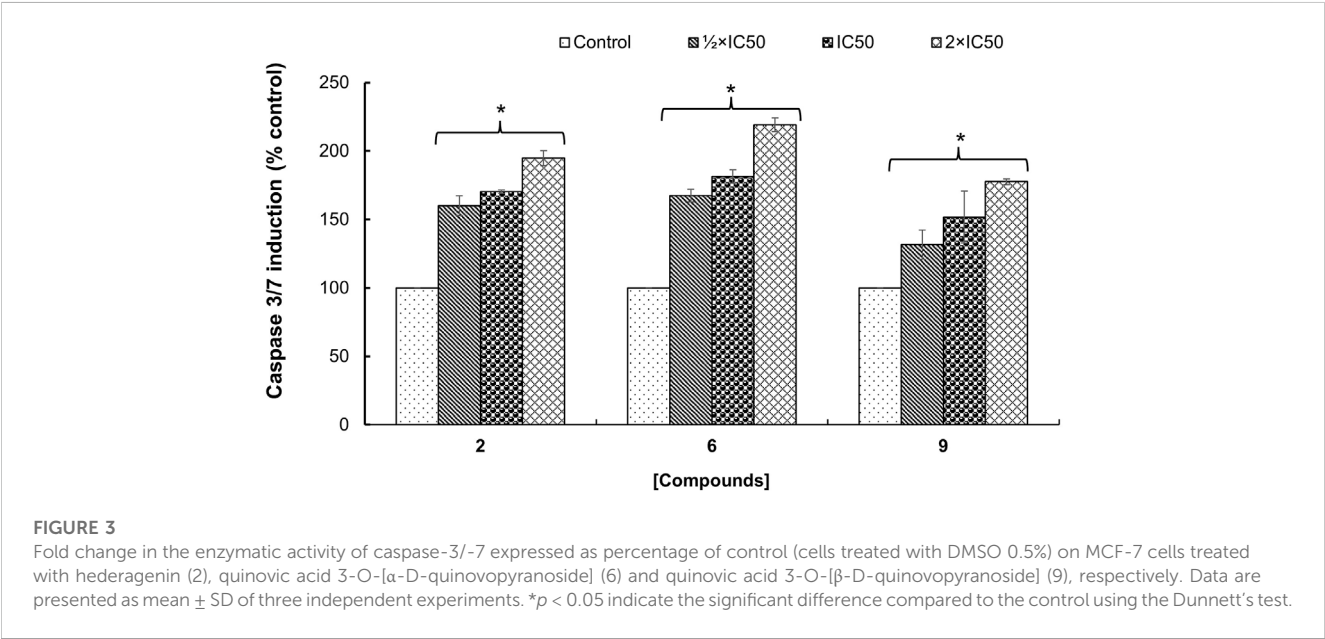


TABLE 2 Selectivity index (SI) values of natural compounds.

Compounds	SI values			
	MCF7	HepG2	Caco-2	A549
1	1.10	1.36	nd	1.52
2	5.11	1.83	1.24	2.40
3	nd	nd	nd	nd
4	nd	nd	nd	nd
5	nd	nd	nd	nd
6	1.04	0.14	0.83	3.17
7	nd	1.13	nd	nd
8	nd	nd	nd	nd
9	0.91	0.99	0.88	1.06
10	2.01	1.20	1.04	1.49
Doxorubicin	4.45	8.66	0.98	6.83

Mixture of naucleatifoline G and naucleofficine D (1), hederagenin (2) and chletric acid (3) were isolated from CH₂Cl₂/MeOH (1:2) fruit extract of *S. pobeguinii*. Taraxerol (4), α-amyrin(3β-hydroxy-urs-12-en-3-ol) (5) and quinovic acid 3-O-[α-D-quinovopyranoside] (6) were isolated from methanol leaf extract of *S. pobeguinii*. Erythrodiol (7), quinovic acid (8), quinovic acid 3-O-[β-D-quinovopyranoside] (9) and latifoliamide C (10) were isolated from the methanol bark extract of *S. pobeguinii*. nd: not determined. Bold values mean compounds with good selectivity index.



selectivity ($1.24 \leq SI \leq 5.11$) for all cancer cells towards non-cancerous Vero cells thereby suggesting that this compound can selectively kill cancer cells at the IC₅₀ without causing harmful effects on non-cancerous cells. Therefore, regarding the fact that hederagenin (2) exhibited good selectivity, this compound was tested at 10 μg/mL on all cancer cells and non-cancerous cells for 12, 24 and 48 h in order to evaluate the time-dependent cytotoxic effect on cell growth. It was observed that (2) induced the growth inhibition of different cancer cells in a time-dependent manner, and the cytotoxic effect was more

pronounced on cancer cells compared to non-cancerous cells (Figure 2). In fact, the MCF-7 cells followed by A549 cells were the most sensitive to the cytotoxic effect of hederagenin (2) which was less toxic to non-cancerous Vero cells. Interestingly, hederagenin, isolated from several plants, has been previously reported to potentially inhibit the proliferation of human lung cancer cells A549 (IC₅₀ values of 26.3 and 39 μM) (Gauthier et al., 2009; Gao et al., 2016). In the current study, hederagenin inhibits A549 growth with an IC₅₀ of 40.11 μM which is comparable to results obtained from previous works.

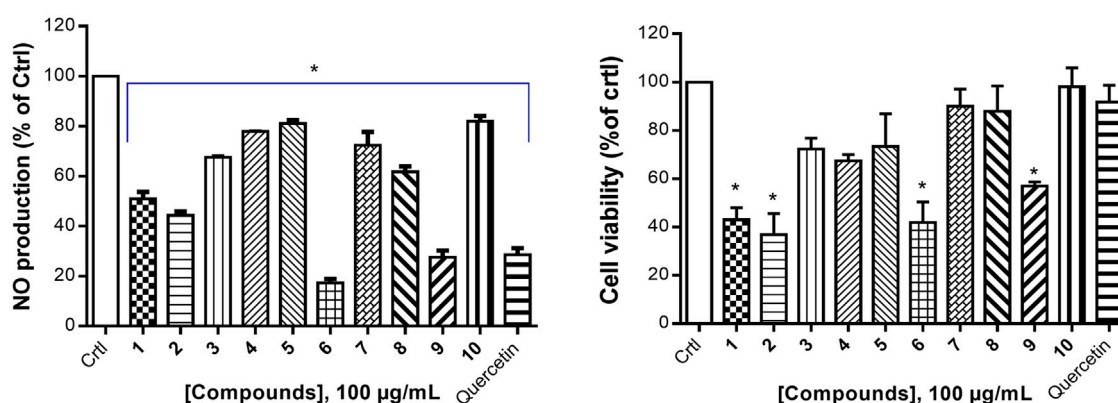


FIGURE 4

Nitric oxide production inhibition by natural compounds in LPS-stimulated RAW 264.7 cells (A) and their respective percentage of cell viability (B). The NO production inhibition was determined based on the efficacy of tested samples to reduce NO release by LPS-stimulated RAW 264.7 cells compared with the negative control (RAW 264.7 cells treated with LPS and DMSO at 0.5% without test samples), which was considered to be 100% of NO production. Quercetin was used as a positive control. Data represent the mean \pm standard deviation of three independent experiments; (*) means a statistical difference ($p < 0.05$) between the tested samples versus the negative control (Ctrl).

TABLE 3 Anti-inflammatory effect (IC_{50} values) of natural compounds isolated from fruits, leaves and bark of *Sarcocephalus pobeguini*.

Compounds	IC_{50} values			
	NO		15-LOX	
	$\mu\text{g/mL}$	μM	$\mu\text{g/mL}$	μM
1	94.92 ± 4.66^a	140.25 ± 5.89^a	11.17 ± 0.96^a	16.51 ± 1.42^a
2	65.13 ± 1.23^b	137.78 ± 2.17^a	13.43 ± 1.59^a	28.20 ± 3.71^b
3	>100	>187.02	22.01 ± 1.39^b	41.17 ± 2.61^c
4	>100	>234.34	>100	>234.34
5	>100	>234.34	>100	>234.34
6	18.17 ± 1.26^c	28.71 ± 1.99^b	>100	>158.02
7	95.63 ± 4.95^a	216.00 ± 6.18^c	65.23 ± 4.45^c	147.33 ± 6.07^d
8	86.02 ± 2.09^d	176.74 ± 4.29^d	34.97 ± 2.68^d	71.86 ± 4.67^e
9	48.96 ± 4.92^e	77.36 ± 5.77^e	74.81 ± 2.19^e	118.22 ± 3.46^f
10	>100	>324.27	78.09 ± 4.13^e	253.22 ± 7.40^g
Quercetin	12.85 ± 1.59^f	42.52 ± 4.99^f	18.72 ± 2.72^b	61.94 ± 4.51^h

Data are presented as means of triplicate measurements \pm standard deviation. Superscript letters a–h represent statistical difference between data obtained, and for each column of the above table, data with same letters are statistically not different while data with different letters are significantly different at $p < 0.05$. IC_{50} : concentration of the tested samples which inhibit 50% of biological effect. Mixture of nauclealatifoline G and naucleofficine D (1), hederagenin (2) and chelonic acid (3) were isolated from $\text{CH}_2\text{Cl}_2/\text{MeOH}$ (1:2) fruit extract of *S. pobeguini*. Taraxerol (4), α -amyrin(3 β -hydroxy-urs-12-en-3-ol) (5) and quinovic acid 3-O- $[\alpha$ -D-quinovopyranoside] (6) were isolated from methanol leaf extract of *S. pobeguini*. Erythrodiol (7), quinovic acid (8), quinovic acid 3-O- $[\beta$ -D-quinovopyranoside] (9) and latifoliamide C (10) were isolated from the methanol bark extract of *S. pobeguini*.

Bold values mean compounds significantly active in the assay.

Additionally, hederagenin was found to be less cytotoxic to human normal skin fibroblasts (WS1) cell lines (IC_{50} of 77 μM) (Gauthier et al., 2009) which also confirms the fact that this compound selectively kills cancer cells with least toxic effect to normal cells. Further, hederagenin, extracted in high quantities from the fruits of *Sapindus saponaria* L., (Sapindaceae), has been reported to be cytotoxic

to different cancer cells, and structural modifications resulted to the development of potent anti-tumour compounds (Rodriguez-Hernandez et al., 2015; Rodriguez-Hernandez et al., 2016). Overall, hederagenin was isolated for the first time from fruits of *S. pobeguini* (Rubiaceae), and our data corroborates its use as a potential candidate for the development of anticancer agents.

TABLE 4 Molecular docking score (kcal/mol) and interacting residues of the most bioactive compounds against six putative target proteins based on the best protein-ligand binding pose.

Compounds	Putative targets	Docking score values (kcal/mol)	Interacting residues
Hederagenin	COX-2	−6.1	B chain: THR94, GLY354, HIS351
	NFκB-p65	−5.7	A chain: ARG236, SER240, PHE239
	STAT3	−5.3	A chain: VAL537,ILE522, ALA505, LEU525,TRP501
	JAK2	−6.8	A chain: SER1025, SER1029, ILE1018, SER1074
	CASPASE-3	−4.3	C chain: LEU168, PHE256, ALA254
	CASPASE-7	−4.4	A chain: ARG87, CYS186
Quinovic acid 3-O-[α-D-quinovopyranoside]	COX-2	−6.7	B chain: LYS468, LYS473, PRO474
	NFκB-p65	−5.2	B chain: ARG236, PRO256, PHE239
	STAT3	5.0	B chain: THR526, LUE525, ALA505
	JAK2	−6.4	A chain: LYS1030, ARG1034, ARG1117
	CASPASE-3	−4.9	C chain: LEU168, PHE246, ALA254
	CASPASE-7	−5.3	A chain: TRP 240, VAL220, HIS144
Quinovic acid 3-O-[β-D-quinovopyranoside]	COX-2	−6.5	B chain: GLN192, PHE580, SER581, SER579, VAL582
	NFκB-p65	−5.0	B chain: ASP53,LYS28, ARG30
	STAT3	5.8	B chain: SER399, LEU260, CYS259, PRO256, ILE258, ALA250, CYS257, ARG325, PRO366
	JAK2	−6.8	A chain: SER1029, SER1025, GLU1012, TYR1021, LEU1026, VAL1025, PRO1013, ILE1018, ILE1074, PHE1019
	CASPASE-3	−5.3	A chain: THR62, THR166, MET61, PHE128, GLY122, C chain: THR166, LEU168
	CASPASE-7	−5.7	A chain: ARG236, SER240, PHE239

3.2 Structure–activity relationship

Three triterpenoids including two saponins isolated from *S. pobequinii* were cytotoxic to cancer cells, and their efficacy varied according to their structural configuration or the presence of some functional groups. When compared to other triterpenoids, the cytotoxic effect of the two bioactive saponins, namely, quinovic acid 3-O-[α-D-quinovopyranoside] (6) and quinovic acid 3-O-[β-D-quinovopyranoside] (9) can be attributed to the presence of a pyranose moiety attached at position C-3. Moreover, the α anomer (6) is highly cytotoxic compared to the β anomer (9) which suggests that the configuration of the glycosidic bond (C-O-sugar bond) has an impact on the cytotoxic effect. According to several reports, the anticancer activity of triterpenoid saponins is strongly linked to the presence of functional carboxylic and hydroxyl groups on the aglycone chain, the stereo-selectivity and the type of sugar molecule attached (Nag et al., 2012; Xu et al., 2013; Elekofehinti et al., 2021; Podolak et al., 2023). In contrast, we observed from our study that despite the presence carboxylic and hydroxyl groups, other triterpenoids (3), (4), (5), (7) and (8) were less cytotoxic or inactive compared to hederagenin (2) which strongly inhibit the growth of several cancer cells. We therefore suggest that the efficacy of hederagenin might be attributed to the asymmetric carbon at

position C-4 which yield a different conformation due to irregular spatial arrangements of chemical groups. This conformation might ease the interaction with molecular targets involved in the activation of cancer cell death pathways. Further, the solubility of hederagenin in culture media may also be responsible for its efficacy on cancer cells.

3.3 Caspase-dependent activation by bioactive compounds

The potential mechanism of action of bioactive compounds on cellular viability was explored by quantifying the caspase-3/-7 activity in MCF-7 cells. It was found that the caspase-3/-7 activity was significantly ($p < 0.05$) induced in a concentration-dependent manner compared to control cells treated with DMSO 0.5% (Figure 3). Additionally, the optimal effect was observed with hederagenin (2) and quinovic acid 3-O-[α-D-quinovopyranoside] (6) tested at $2 \times IC_{50}$ where an induction up to 2-fold change in the activation of caspase-3/-7 activity was recorded. Caspases 3 and 7 are known as “executioners” of apoptosis, and the combined role of both caspases is crucial for the activation of apoptotic pathways

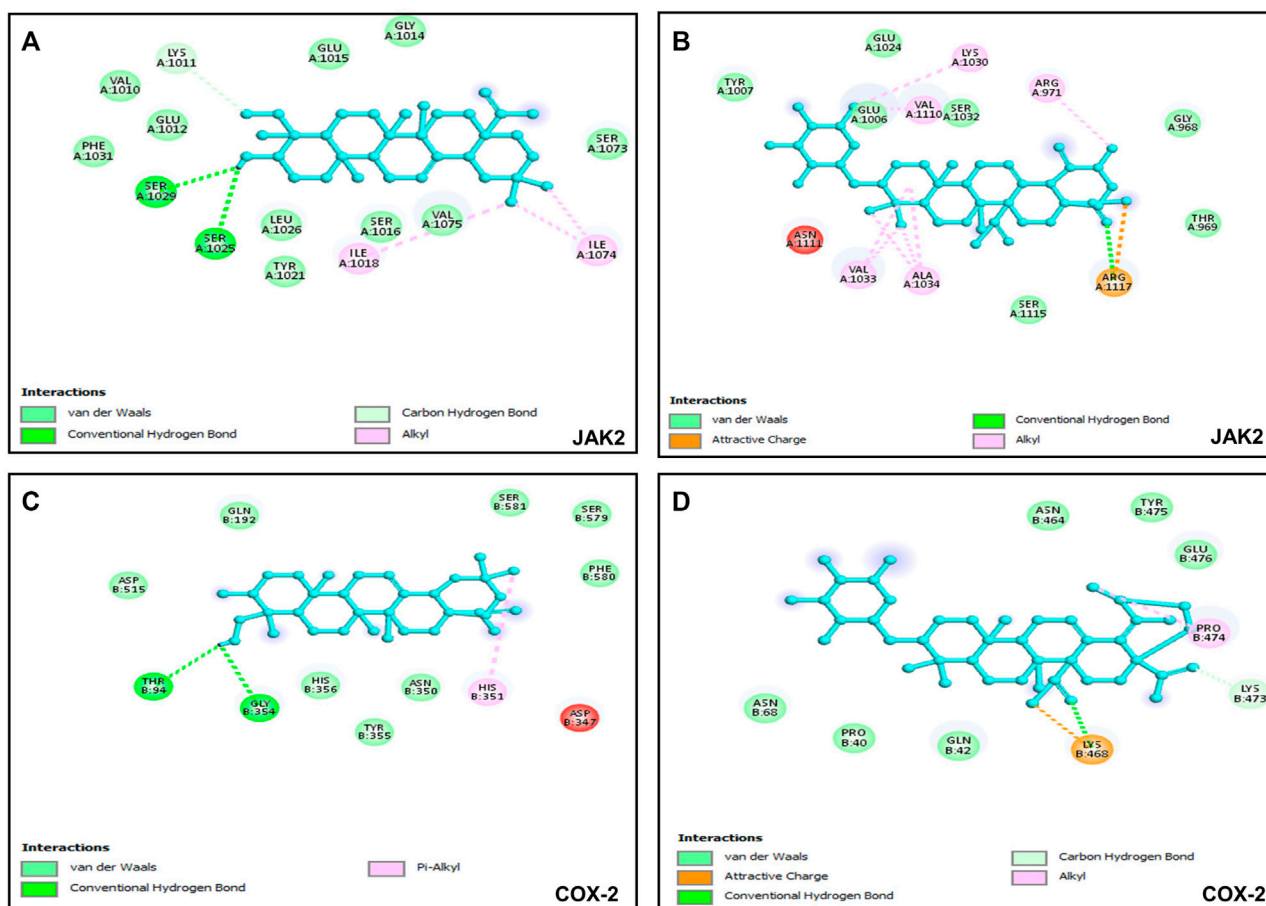


FIGURE 5

Visualization of binding interactions by using BIOVIA Discovery Studio Visualizer 2021 software; (A) protein-ligand interactions between JAK2 and hederagenin (−6.8 kcal/mol); (B) protein-ligand interactions between JAK2 and quinovic acid 3-O-α-D-quinovopyranoside (−6.4 kcal/mol); (C) protein-ligand interactions between COX-2 and hederagenin (−6.1 kcal/mol); (D) protein-ligand interactions between COX-2 and quinovic acid 3-O-α-D-quinovopyranoside (−6.7 kcal/mol).

(Olsson and Zhivotovsky, 2011). In fact, caspase 3 controls DNA fragmentation and morphologic changes of apoptosis, while caspase 7 is more important for the loss of cellular viability (Lakhani et al., 2006). Therefore, the induction of caspase-3/-7 activity after treatment with bioactive compounds implied that the activation of apoptotic pathways is involved in the mechanism of induced cell death in MCF-7 cells.

3.4 Anti-inflammatory effect of isolated compounds

Cancer development is known as a multistep process during which inflammation is one of the factors contributing to the promotion of cell proliferation, invasion, angiogenesis, and metastasis. Moreover, it has been proven that patients on Nonsteroidal anti-inflammatory drugs (NSAIDs) are at reduced risk of cancer development (Singh et al., 2019). One of the possible reasons is that anti-inflammatory drugs might also interfere with signaling pathways modulated in both inflammation and cancer. Therefore, we decided to investigate

the anti-inflammatory effect of compounds isolated from *S. pobeguini* on two experimental models. We found that all compounds (tested at 100 µg/mL) inhibited the NO production in LPS-stimulated RAW 264.7 cells, with the mixture naucleatifoline G and naucleofficine D (1), hederagenin (2), quinovic acid 3-O-α-D-quinovopyranoside (6) and quinovic acid 3-O-β-D-quinovopyranoside (9) being the most active by reducing at least 50% of NO production (Figure 4A). However, the NO production inhibitory effect of compounds (1), (2), (6) and (9) might be attributed to their cytotoxic effect on LPS-stimulated RAW 264.7 cells as it was observed that these compounds significantly ($p < 0.05$) reduced the cell viability (Figure 4B). Besides, by determining the IC_{50} values as presented in Table 3, we found that (6) and (9) strongly inhibits NO production in a concentration-dependent manner with IC_{50} values of 28.71 and 77.36 µM, respectively. On the other hand, we examined the inhibitory effect of isolated compounds on the activity of 15-LOX, an enzyme which regulate the inflammatory responses via the generation of pro-inflammatory mediators known as leukotrienes. It resulted that the mixture of naucleatifoline G and naucleofficine D (1), hederagenin (2) and chletric acid (3)

strongly inhibited the activity of 15-LOX with IC₅₀ values of 16.51, 28.20 and 41.17 μ M, respectively (see Table 3). These compounds were even more active than quercetin, which had an IC₅₀ value of 61.94 μ M. Based on the fact that 15-LOX and NO are among the mediators involved in the progression of various inflammation-related diseases including cancer (Zhao et al., 2021), our study therefore identified compounds which can be considered as potential anticancer agents with additional anti-inflammatory effect for the effective management of both diseases.

3.5 Binding efficacy of bioactive compounds against putative molecular targets

Six putative proteins, namely, COX-2, NF κ B-p65, JAK2, STAT3, CASPASE-3 and CASPASE-7 were chosen for molecular docking based on the fact that they are frequently used as therapeutic targets to regulate inflammatory signaling pathways in cancer treatment (Jha et al., 2022). As presented in Table 4, the docking score (kcal/mol) of the best binding pose was determined for each ligand against the selected proteins. According to these results, hederagenin (2), quinovic acid 3-O-[α -D-quinovopyranoside] (6) and quinovic acid 3-O-[β -D-quinovopyranoside] (9) exhibited activity within the range of -4.3 to -6.8 kcal/mol, where -6.8 kcal/mol was the most effective interaction between JAK2 and (9), and -4.3 kcal/mol was the lowest binding score between CASPASE-3 and (2). Taken individually, each of the three bioactive compounds exhibited the greatest binding efficacy (binding score above -6 kcal/mol) against JAK2 and COX-2 which suggests that these proteins are the potential molecular targets involved in their antiproliferative and anti-inflammatory effects (Figure 5). In addition, STAT3 and NF κ B-p65 also interacted well with bioactive compounds. According to the literature reports, the high activation of JAK2/STAT3 signaling pathway, frequently detected in various tumors, has recently emerged as a new site for the development of novel anti-tumor agents, and these proteins (JAK2 and STAT3) are promising therapeutic targets for the treatment of many solid tumors (Huang et al., 2022; Mengie Ayele et al., 2022). Moreover, NF κ B-p65 is constitutively activated in many human cancers, where it contributes to almost all steps of tumorigenesis including sustained proliferation, cell death resistance, tumor-promoting inflammation, tissue invasion, angiogenesis, and metastasis (Lin et al., 2010). As such, the NF- κ B pathway is an attractive therapeutic target in a broad range of human cancers, as well as in numerous non-malignant diseases. Furthermore, COX-2, an enzyme that catalyzes the first step in the synthesis of prostanoids, is associated with inflammatory diseases and carcinogenesis (Liu et al., 2015). An overexpression of COX-2 is observed in cancers of the pancreas, breast, colorectal, stomach, and lung carcinoma. Therefore, COX-2 is considered as a significant target for the development of new anticancer agents (Mohsin et al., 2022). Among the bioactive compounds investigated, the mechanism of action of hederagenin has been extensively studied in several studies. In fact, hederagenin has been reported to have anti-tumour and anti-inflammatory effects by regulating the NF κ B, PI3K/AKT and JAK2/STAT3/MAPK signalling pathways, and by reducing the expression of pro-inflammatory cytokines or enzyme production, including Tumor Necrosis Factor- α (TNF- α), interleukin 6 (IL-6), NO, prostaglandin E2 (PGE₂), inducible nitric oxide synthase (iNOS) and COX-2 (Zhang et al.,

2012; Lee et al., 2015; Kim et al., 2017; Yu et al., 2020; Shen et al., 2023). Our results indicate the accordance between the molecular docking and the previous studies thereby confirming the efficacy of hederagenin as a prominent lead compound for the management of inflammation and cancer development. Further investigations are required for quinovic acid 3-O-[α -D-quinovopyranoside] and quinovic acid 3-O-[β -D-quinovopyranoside] which modes of action are still not experimentally investigated.

4 Conclusion

This study reported the isolation of ten natural compounds from leaf, fruit and bark of *Sarcocephalus pobeguini*, and described their antiproliferative and anti-inflammatory effects as well as exploration of potential target proteins of bioactive compounds. Hederagenin (2), quinovic acid 3-O-[α -D-quinovopyranoside] (6) and quinovic acid 3-O-[β -D-quinovopyranoside] (9) exhibited antiproliferative effect against all cancerous cells by inducing apoptosis via caspase-3/-7 activation. Among these bioactive compounds, hederagenin, isolated for the first time from the fruits of *S. pobeguini*, selectively kills cancer cells with additional anti-inflammatory potential, and it interacts with JAK2 and COX-2 suggesting these proteins as its potential molecular targets. The molecular docking results were in agreement with previously reported experimental data thereby confirming hederagenin as a prominent drug candidate to tackle cancer progression. Furthermore, apart from hederagenin, nauclealatifoline G and naucleofficine D (1), and chletric acid (3) strongly inhibited the activity of 15-LOX as compared to quercetin, which opens further research direction aiming to investigate experimentally their mode of action on molecular targets of inflammation.

Data availability statement

The original contributions presented in the study are included in the article/Supplementary Material, further inquiries can be directed to the corresponding authors.

Author contributions

EMN conceptualized the study design; EMN, AM, BN, and JA participated in data collection and in conducting the study. AM, PM, and BN analyzed the spectroscopic data. EMN and AM wrote the original draft of the manuscript. EMN and CC contributed to the statistical analysis of data. LM, TM, and SM provided facility and funding to carried out this study. All authors contributed to the article and approved the submitted version.

Funding

This research was funded by the Central University of Technology operational expenses (RES. 10/22/04 awarded to EMN) and the National Research Foundation (NRF), South Africa, through the Incentive Funding for Rated Researchers

(awarded to LM). The APC was funded by the Central University of Technology research expenses (TM).

Acknowledgments

EN is very grateful to the Central University of Technology for the Track1 Postdoctoral fellowship.

Conflicts of interest

The authors declare that the research was conducted in the absence of any commercial or financial relationships that could be construed as a potential conflict of interest.

References

- Agomuo, A. A., Ata, A., Udenigwe, C. C., Aluko, R. E., and Irenus, I. (2013). Novel indole alkaloids from *Nauclea latifolia* and their renin-inhibitory activities. *Chem. Biodivers.* 10 (3), 401–410. doi:10.1002/cbdv.201200023
- Aktar, F., Abul Kaiser, M., Hamidul Kabir, A. N. M., Hasanand, C. M., and Rashid, M. A. (2009). Phytochemical and biological investigations of *Ixora arborea*. *Dhaka Univ. J. Pharm. Sci.* 8 (2), 161–166. doi:10.3329/dujps.v8i2.6031
- Amjad, M. T., Chidharla, A., and Kasi, A. (2022). *Cancer chemotherapy*. StatPearls: Treasure Island FL.
- Elekofehinti, O. O., Iwaloye, O., Olawale, F., and Ariyo, E. O. (2021). Saponins in cancer treatment: Current progress and future prospects. *Pathophysiology* 28 (2), 250–272. doi:10.3390/pathophysiology28020017
- Fatima, N., Taponjdou, L. A., Lontsi, D., Sondengam, B. L., Atta Ur, R., and Choudhary, M. I. (2002). Quinovic acid glycosides from *Mitragyna stipulosa*-first examples of natural inhibitors of snake venom phosphodiesterase I. *Nat. Prod. Lett.* 16 (6), 389–393. doi:10.1080/10575630290033169
- Gao, Y., He, C., Bi, W., Wu, G., and Altman, E. (2016). Bioassay guided fractionation identified hederagenin as a major cytotoxic agent from cyclocarya paliurus leaves. *Planta Med.* 82 (1–2), 171–179. doi:10.1055/s-0035-1557900
- Gauthier, C., Legault, J., Girard-Lalancette, K., Mshvildadze, V., and Pichette, A. (2009). Haemolytic activity, cytotoxicity and membrane cell permeabilization of semi-synthetic and natural lupane- and oleanane-type saponins. *Bioorg. Med. Chem.* 17 (5), 2002–2008. doi:10.1016/j.bmc.2009.01.022
- Haudecoeur, R., Peuchmaur, M., Peres, B., Rome, M., Taiwe, G. S., Boumendjel, A., et al. (2018). Traditional uses, phytochemistry and pharmacological properties of african *Nauclea* species: A review. *J. Ethnopharmacol.* 212, 106–136. doi:10.1016/j.jep.2017.10.011
- Hibino, S., Kawazoe, T., Kasahara, H., Itoh, S., Ishimoto, T., Sakata-Yanagimoto, M., et al. (2021). Inflammation-induced tumorigenesis and metastasis. *Int. J. Mol. Sci.* 22 (11), 5421. doi:10.3390/ijms22115421
- Huang, B., Lang, X., and Li, X. (2022). The role of IL-6/JAK2/STAT3 signaling pathway in cancers. *Front. Oncol.* 12, 1023177. doi:10.3389/fonc.2022.1023177
- Jha, N. K., Arfin, S., Jha, S. K., Kar, R., Dey, A., Gundamaraju, R., et al. (2022). Re-establishing the comprehension of phytomedicine and nanomedicine in inflammation-mediated cancer signaling. *Semin. Cancer Biol.* 86 (2), 1086–1104. doi:10.1016/j.semcancer.2022.02.022
- Jiofack, T., Ayissi, I., Fokunang, C., Guedje, N., and Kemeuze, V. (2009). Ethnobotany and phytomedicine of the upper Nyong valley forest in Cameroon. *Afr. J. Pharm. Pharmacol.* 3 (4), 144–150. doi:10.5897/AJPP.9000140
- Joshi, B. S., Singh, K. L., and Raja, R. (1999). Complete assignments of ¹H and ¹³C NMR spectra of the pentacyclic triterpene hederagenin from *Nigella sativa* Linn. *Magnetic Reson. Chem.* 37, 295–298. doi:10.1002/(sici)1097-458x(199904)37:4<295:aid-mrc457>3.0.co;2-z
- Karou, S. D., Tchacondo, T., Ilboudo, D. P., and Simporé, J. (2011). Sub-saharan rubiaceae: A review of their traditional uses, phytochemistry and biological activities. *Pak. J. Biol. Sci. Pjbs* 14 (3), 149–169. doi:10.3923/pjbs.2011.149.169
- Kim, G. J., Song, D. H., Yoo, H. S., Chung, K. H., Lee, K. J., and An, J. H. (2017). Hederagenin supplementation alleviates the pro-inflammatory and apoptotic response to alcohol in rats. *Nutrients* 9 (1), 41. doi:10.3390/nu9010041
- Kuete, V., and Efferth, T. (2010). Cameroonian medicinal plants: Pharmacology and derived natural products. *Front. Pharmacol.* 1, 123. doi:10.3389/fphar.2010.00123
- Kuete, V., Sandjo, L. P., Mbaveng, A. T., Seukep, J. A., Ngadjui, B. T., and Efferth, T. (2015). Cytotoxicity of selected Cameroonian medicinal plants and *Nauclea pobequinii* towards multi-factorial drug-resistant cancer cells. *BMC Complement. Altern. Med.* 15, 309. doi:10.1186/s12906-015-0841-y
- Lai, H., Liu, Y., Wu, J., Cai, J., Jie, H., Xu, Y., et al. (2022). Targeting cancer-related inflammation with non-steroidal anti-inflammatory drugs: Perspectives in pharmacogenomics. *Front. Pharmacol.* 13, 1078766. doi:10.3389/fphar.2022.1078766
- Lakhani, S. A., Masud, A., Kuida, K., Porter, G. A., Jr., Booth, C. J., Mehal, W. Z., et al. (2006). Caspases 3 and 7: Key mediators of mitochondrial events of apoptosis. *Science* 311 (5762), 847–851. doi:10.1126/science.1115035
- Lee, C. W., Park, S. M., Zhao, R., Lee, C., Chun, W., Son, Y., et al. (2015). Hederagenin, a major component of *Clematis mandshurica* Ruprecht root, attenuates inflammatory responses in RAW 264.7 cells and in mice. *Int. Immunopharmacol.* 29 (2), 528–537. doi:10.1016/j.intimp.2015.10.002
- Lin, Y., Bai, L., Chen, W., and Xu, S. (2010). The NF-kappaB activation pathways, emerging molecular targets for cancer prevention and therapy. *Expert Opin. Ther. targets* 14 (1), 45–55. doi:10.1517/14728220903431069
- Liu, B., Qu, L., and Yan, S. (2015). Cyclooxygenase-2 promotes tumor growth and suppresses tumor immunity. *Cancer Cell. Int.* 15, 106. doi:10.1186/s12935-015-0260-7
- Mantovani, A., Allavena, P., Sica, A., and Balkwill, F. (2008). Cancer-related inflammation. *Nature* 454 (7203), 436–444. doi:10.1038/nature07205
- Mengie Ayele, T., Tilahun Muche, Z., Behaile Teklemariam, A., Bogale Kassie, A., and Chekol Abebe, E. (2022). Role of JAK2/STAT3 signaling pathway in the tumorigenesis, chemotherapy resistance, and treatment of solid tumors: A systemic review. *J. Inflamm. Res.* 15, 1349–1364. doi:10.2147/JIR.S353489
- Mesia, G. K., Tona, G. L., Penge, O., Lusakibanza, M., Nanga, T. M., Cimanga, R. K., et al. (2005). Antimalarial activities and toxicities of three plants used as traditional remedies for malaria in the democratic republic of Congo: *Croton mubango*, *Nauclea pobequinii* and *pyrenacantha staudtii*. *Ann. Trop. Med. Parasitol.* 99 (4), 345–357. doi:10.1179/136485905X36325
- Mfotie Njoya, E., Eloff, J. N., and McGaw, L. J. (2018). *Croton gratissimus* leaf extracts inhibit cancer cell growth by inducing caspase 3/7 activation with additional anti-inflammatory and antioxidant activities. *BMC Complement. Altern. Med.* 18 (1), 305. doi:10.1186/s12906-018-2372-9
- Mfotie Njoya, E., Maza, H. L. D., Mkounga, P., Koert, U., Nkengfack, A. E., and McGaw, L. J. (2020). Selective cytotoxic activity of isolated compounds from *Globimetula dinklagei* and *Phragmanthera capitata* (Loranthaceae). *Z. Naturforsch. C J. Biosci.* 75 (5–6), 135–144. doi:10.1515/znc-2019-0171
- Mfotie Njoya, E., Maza, H. L. D., Swain, S. S., Chukwuma, C. I., Mkounga, P., Nguekeu Mba, Y. M., et al. (2023). Natural compounds isolated from african mistletoes (loranthaceae) exert anti-inflammatory and acetylcholinesterase inhibitory potentials: *In vitro* and *in silico* studies. *Appl. Sci.* 13 (4), 2606. doi:10.3390/app13042606
- Mfotie Njoya, E., Munvera, A. M., Mkounga, P., Nkengfack, A. E., and McGaw, L. J. (2017). Phytochemical analysis with free radical scavenging, nitric oxide inhibition and antiproliferative activity of *Sarcocephalus pobequinii* extracts. *BMC Complement. Altern. Med.* 17 (1), 199. doi:10.1186/s12906-017-1712-5
- Mohamed, M. (1999). Quinovic acid glycosides from *Zygophyllum aegyptium*. *Bull. Pharm. Sci.* 22 (1), 47–53. doi:10.21608/bfsa.1999.66076
- Mohsin, N. U. A., Aslam, S., Ahmad, M., Irfan, M., Al-Hussain, S. A., and Zaki, M. E. A. (2022). Cyclooxygenase-2 (COX-2) as a target of anticancer agents: A review of novel synthesized scaffolds having anticancer and COX-2 inhibitory potentialities. *Pharm. (Basel)* 15 (12), 1471. doi:10.3390/ph15121471

Publisher's note

All claims expressed in this article are solely those of the authors and do not necessarily represent those of their affiliated organizations, or those of the publisher, the editors and the reviewers. Any product that may be evaluated in this article, or claim that may be made by its manufacturer, is not guaranteed or endorsed by the publisher.

Supplementary material

The Supplementary Material for this article can be found online at: <https://www.frontiersin.org/articles/10.3389/fphar.2023.1205414/full#supplementary-material>

- Mosmann, T. (1983). Rapid colorimetric assay for cellular growth and survival: Application to proliferation and cytotoxicity assays. *J. Immunol. methods* 65 (1–2), 55–63. doi:10.1016/0022-1759(83)90303-4
- Nag, S. A., Qin, J. J., Wang, W., Wang, M. H., Wang, H., and Zhang, R. (2012). Ginsenosides as anticancer agents: *In vitro* and *in vivo* activities, structure-activity relationships, and molecular mechanisms of action. *Front. Pharmacol.* 3, 25. doi:10.3389/fphar.2012.00025
- Novichikhina, N., Ilin, I., Tashchilova, A., Sulimov, A., Kutov, D., Ledenyova, I., et al. (2020). Synthesis, docking, and *in vitro* anticoagulant activity assay of hybrid derivatives of pyrrolo[3,2,1-ij]Quinolin-2(1H)-one as new inhibitors of factor xa and factor XIa. *Molecules* 25 (8), 1889. doi:10.3390/molecules25081889
- Ntie-Kang, F., Lifongo, L. L., Mbaze, L. M., Ekwelle, N., Owono Owono, L. C., Megnassan, E., et al. (2013). Cameroonian medicinal plants: A bioactivity versus ethnobotanical survey and chemotaxonomic classification. *BMC Complement. Altern. Med.* 13, 147. doi:10.1186/1472-6882-13-147
- Olsson, M., and Zhivotovsky, B. (2011). Caspases and cancer. *Cell. death Differ.* 18 (9), 1441–1449. doi:10.1038/cdd.2011.30
- Peczek, P., Gajda, M., Rutkowski, K., Fudalej, M., Deptala, A., and Badowska-Kozakiewicz, A. M. (2022). Cancer-associated inflammation: Pathophysiology and clinical significance. *J. Cancer Res. Clin. Oncol.* 149, 2657–2672. doi:10.1007/s00432-022-04399-y
- Pinto, M. C., Tejada, A., Duque, A. L., and Macias, P. (2007). Determination of lipoxygenase activity in plant extracts using a modified ferrous oxidation-xylene orange assay. *J. Agric. food Chem.* 55 (15), 5956–5959. doi:10.1021/jf070537x
- Podolak, I., Grabowska, K., Sobolewska, D., Wrobel-Biedrawa, D., Makowska-Was, J., and Galanty, A. (2023). Saponins as cytotoxic agents: An update (2010–2021). Part II—triterpene saponins. *Phytochem. Rev.* 22, 113–167. doi:10.1007/s11101-022-09830-3
- Rayburn, E. R., Ezell, S. J., and Zhang, R. (2009). Anti-inflammatory agents for cancer therapy. *Mol. Cell. Pharmacol.* 1 (1), 29–43. doi:10.4255/mcpharmacol.09.05
- Rodriguez-Hernandez, D., Demuner, A. J., Barbosa, L. C., Csuk, R., and Heller, L. (2015). Hederagenin as a triterpene template for the development of new antitumor compounds. *Eur. J. Med. Chem.* 105, 57–62. doi:10.1016/j.ejmech.2015.10.006
- Rodriguez-Hernandez, D., Demuner, A. J., Barbosa, L. C., Heller, L., and Csuk, R. (2016). Novel hederagenin-triazolyl derivatives as potential anti-cancer agents. *Eur. J. Med. Chem.* 115, 257–267. doi:10.1016/j.ejmech.2016.03.018
- Shen, Y., Teng, L., Qu, Y., Huang, Y., Peng, Y., Tang, M., et al. (2023). Hederagenin suppresses inflammation and cartilage degradation to ameliorate the progression of osteoarthritis: An *in vivo* and *in vitro* study. *Inflammation* 46 (2), 655–678. doi:10.1007/s10753-022-01763-5
- Singh, N., Baby, D., Rajguru, J. P., Patil, P. B., Thakkannavar, S. S., and Pujari, V. B. (2019). Inflammation and cancer. *Ann. Afr. Med.* 18 (3), 121–126. doi:10.4103/aam.aam_56_18
- Sung, H., Ferlay, J., Siegel, R. L., Laversanne, M., Soerjomataram, I., Jemal, A., et al. (2021). Global cancer statistics 2020: GLOBOCAN estimates of incidence and mortality worldwide for 36 cancers in 185 countries. *CA Cancer J. Clin.* 71 (3), 209–249. doi:10.3322/caac.21660
- Takahashi, K., and Takani, M. (1978). Studies on the constituents of the medicinal plants. XXI. Constituents of the leaves of *Clethra barbinervis* Sieb. et Zucc. (2) and the ¹³C-nuclear magnetic resonance spectra of 19-ALPHA. hydroxyurs-12-en-28-oic acid type of triterpenoids. *Bulletin* 26, 2689–2693. doi:10.1248/cpb.26.2689
- Tian, W., Chen, C., Lei, X., Zhao, J., and Liang, J. (2018). CASTp 3.0: Computed atlas of surface topography of proteins. *Nucleic acids Res.* 46 (1), W363–W7. doi:10.1093/nar/gky473
- Trott, O., and Olson, A. J. (2010). AutoDock Vina: Improving the speed and accuracy of docking with a new scoring function, efficient optimization, and multithreading. *J. Comput. Chem.* 31 (2), 455–461. doi:10.1002/jcc.21334
- Viet, T. D., Xuan, T. D., and Anh, H. (2021). α -Amyrin and β -amyrin isolated from *Celastrus hindsii* leaves and their antioxidant, anti-xanthine oxidase, and anti-tyrosinase potentials. *Molecules* 26 (23), 7248. doi:10.3390/molecules26237248
- Xu, K., Shu, Z., Xu, Q. M., Liu, Y. L., Li, X. R., Wang, Y. L., et al. (2013). Cytotoxic activity of *Pulsatilla chinensis* saponins and their structure-activity relationship. *J. Asian Nat. Prod. Res.* 15 (6), 680–686. doi:10.1080/10286020.2013.790901
- Yen, C. K., Keng, C. W., Hasnah, O., Ibrahim, E., and Mohammad, Z. A. (2013). Chemical constituents and biological activities of *Strobilanthes crispus*. *Rec. Nat. Prod.* 7, 59–64.
- Yepez, A. M., de Ugaz, O. L., Alvarez, C. M., De Feo, V., Aquino, R., De Simone, F., et al. (1991). Quinovic acid glycosides from *Uncaria guianensis*. *Phytochemistry* 30 (5), 1635–1637. doi:10.1016/0031-9422(91)84223-f
- Yu, H., Song, L., Cao, X., Li, W., Zhao, Y., Chen, J., et al. (2020). Hederagenin attenuates cerebral ischaemia/reperfusion injury by regulating MLK3 signalling. *Front. Pharmacol.* 11, 1173. doi:10.3389/fphar.2020.01173
- Yüce, I., Agnani, H., and Morlock, G. E. (2019). New antidiabetic and free-radical scavenging potential of strictosamide in *Sarcocephalus pobequinii* ground bark extract via effect-directed analysis. *ACS Omega* 4 (3), 5038–5043. doi:10.1021/acsomega.8b02462
- Zappavigna, S., Cossu, A. M., Grimaldi, A., Bocchetti, M., Ferraro, G. A., Nicoletti, G. F., et al. (2020). Anti-inflammatory drugs as anticancer agents. *Int. J. Mol. Sci.* 21 (7), 2605. doi:10.3390/ijms21072605
- Zhang, L. J., Cheng, J. J., Liao, C. C., Cheng, H. L., Huang, H. T., Kuo, L. M., et al. (2012). Triterpene acids from *Euscaphis japonica* and assessment of their cytotoxic and anti-NO activities. *Planta Med.* 78 (14), 1584–1590. doi:10.1055/s-0032-1315040
- Zhao, H., Wu, L., Yan, G., Chen, Y., Zhou, M., Wu, Y., et al. (2021). Inflammation and tumor progression: Signaling pathways and targeted intervention. *Signal Transduct. Target Ther.* 6 (1), 263. doi:10.1038/s41392-021-00658-5



OPEN ACCESS

EDITED BY

Aliyu Muhammad,
Ahmadu Bello University, Nigeria

REVIEWED BY

Abdurrahman Pharmacy Yusuf,
Federal University of Technology Minna,
Nigeria
Kang-Hoon Kim,
Monell Chemical Senses Center,
United States

*CORRESPONDENCE

Fuer Lu,
✉ felutjh88@163.com
Fen Yuan,
✉ echo_yf@tjh.tjmu.edu.cn

RECEIVED 25 May 2023

ACCEPTED 26 June 2023

PUBLISHED 04 July 2023

CITATION

Wu W, Xia Q, Guo Y, Wang H, Dong H,
Lu F and Yuan F (2023), Berberine
enhances the function of db/db mice islet
 β cell through GLP-1/GLP-1R/PKA
signaling pathway in intestinal L cell and
islet α cell.
Front. Pharmacol. 14:1228722.
doi: 10.3389/fphar.2023.1228722

COPYRIGHT

© 2023 Wu, Xia, Guo, Wang, Dong, Lu and
Yuan. This is an open-access article
distributed under the terms of the
[Creative Commons Attribution License](https://creativecommons.org/licenses/by/4.0/)
(CC BY). The use, distribution or
reproduction in other forums is
permitted, provided the original author(s)
and the copyright owner(s) are credited
and that the original publication in this
journal is cited, in accordance with
accepted academic practice. No use,
distribution or reproduction is permitted
which does not comply with these terms.

Berberine enhances the function of db/db mice islet β cell through GLP-1/GLP-1R/PKA signaling pathway in intestinal L cell and islet α cell

Wenbin Wu¹, Qingsong Xia¹, Yujin Guo¹, Hongzhan Wang¹,
Hui Dong², Fuer Lu^{2*} and Fen Yuan^{2*}

¹Institution of Integrated Traditional Chinese and Western Medicine, Tongji Hospital, Tongji Medical College, Huazhong University of Science and Technology, Wuhan, Hubei, China, ²Department of Integrated Traditional Chinese and Western Medicine, Tongji Hospital, Tongji Medical College, Huazhong University of Science and Technology, Wuhan, Hubei, China

Background: The evidence on berberine stimulating the secretion of GLP-1 in intestinal L cell has been studied. However, few research has explored its role on generating GLP-1 of islet α cell. Our experiment aims to clarify the mechanism of berberine promoting the secretion of GLP-1 in intestinal L cell and islet α cell, activating GLP-1R and its downstream molecules through endocrine and paracrine ways, thus improving the function of islet β cell and treating T2DM.

Methods: After confirming that berberine can lower blood glucose and improve insulin resistance in db/db mice, the identity maintenance, proliferation and apoptosis of islet cells were detected by immunohistochemistry and immunofluorescence. Then, the activation of berberine on GLP-1/GLP-1R/PKA signaling pathway was evaluated by Elisa, Western blot and PCR. Finally, this mechanism was verified by *in vitro* experiments on Min6 cells, STC-1 cells and aTC1/6 cells.

Results: Berberine ameliorates glucose metabolism in db/db mice. Additionally, it also increases the number and enhances the function of islet β cell. This process is closely related to improve the secretion of intestinal L cell and islet α cell, activate GLP-1R/PKA signaling pathway through autocrine and paracrine, and increase the expression of its related molecule such as GLP-1, GLP-1R, PC1/3, PC2, PKA, Pdx1. *In vitro*, the phenomenon that berberine enhanced the GLP-1/GLP-1R/PKA signal pathway had also been observed, which confirmed the results of animal experiments.

Conclusion: Berberine can maintain the identity and normal function of islet β cell, and its mechanism is related to the activation of GLP-1/GLP-1R/PKA signal pathway in intestinal L cell and islet α cell.

KEYWORDS

berberine, GLP-1, GLP-1r, islet β cell, T2DM

Abbreviations: T2DM, Type 2 diabetes; GTT, Glucose tolerance test; ITT, Insulin tolerance test; HOMA-IR, Homeostatic model assessment of insulin resistance; FBG, Fasting blood glucose; GLP-1, Glucagon-like peptide-1; PA, Palmitic acid; BCA, Bis-creatine; RT-qPCR, Real-time quantitative polymerase chain reaction.

Introduction

Type 2 diabetes (T2DM) has become one of the biggest health crises. Recent data reported by the International Diabetes Federation (IDF) in 2021 have demonstrated that the global prevalence of diabetes was estimated at 10.5% (approximately 537 million people) (Sun H. et al., 2022). Patients with T2DM are usually older than 65 years old, with varying degrees of potential insulin resistance and uncontrolled hyperglycemia (Perreault et al., 2021). T2DM is due to insulin resistance and β cell dysfunction, gradually leading to uncontrollable hyperglycemia (Rizza, 2010). In the T2DM process, the compensatory high insulin secretion state of β cell will lead to the dedifferentiation and transdifferentiation of β cell (Hudish et al., 2019). As the duration of T2DM prolongs, the dysfunction of β cell will also deepen (Sun et al., 2019).

Glucagon-like peptide-1 (GLP-1) is an insulin-promoting hormone and can enhance glucose-dependent insulin secretion, inhibit glucagon secretion and delay gastric emptying. In addition, GLP-1 can also inhibit the identity loss and dysfunction of pancreatic islets β cell (Muller et al., 2019). GLP-1 agonists are widely used in the treatment of T2DM and have significant therapeutic effects on patients with hyperglycemia, insulin resistance, and β cell dysfunction (Lee et al., 2018). In the past, it was recognized that it was produced by intestinal L cell, but now it is found that pancreatic α cell can also secrete GLP-1. Functional supplementation by islet derived GLP-1 when intestinal derived GLP-1 secretion decreases (Marchetti et al., 2012). GLP-1 acts on GLP-1R of pancreatic β cell through endocrine and paracrine ways respectively (Huising, 2020). GLP-1R activates adenylate cyclase (AC) to produce cAMP, which in turn activates protein kinase A (PKA) (Que et al., 2019).

PC1/3 and PC2 are neuroendocrine specific endoproteases belonging to the subtilisin-like serine protease family. They can process peptide hormones into bioactive products (Smeekens et al., 1992). Under their shearing action, proinsulin is converted into insulin and glucagon and secreted into blood. At the same time, PC1/3 has the effect of cutting glucagon to form GLP-1 (Muller et al., 2019). Pdx1 is a major regulator of pancreatic organogenesis, β cell maturation and identity preservation, and also has the function of promoting normal insulin secretion (Ebrahim et al., 2022). Research has found that after high glucose and high fat culture *in vitro*, the expression of Pdx1 in primary pancreatic islets decreases, intervention with liraglutide can significantly increase the secretion of Pdx1, while GLP-1R inhibitors can counteract this effect (Cataldo et al., 2021). The GLP-1/GLP-1R/PKA signaling pathway can maintain the identity of islet β cell and promote insulin secretion by promoting the expression of these molecules.

Berberine is a bioactive component of Huanglian (*Coptis chinensis* Franch.), which has extensive pharmacological effects and is widely used in the treatment of digestive and endocrine system diseases in clinical practice (Song et al., 2020). When studying the mechanism of berberine in the treatment of diabetes, a study has already pointed out that berberine can promote insulin secretion, improve insulin resistance and inhibit pancreatic islet β cell dysfunction (He Q. et al., 2022). Meanwhile, a study has also confirmed that berberine promotes the secretion of GLP-1 by L cell in intestinal tissue, while activating GLP-1R and the phosphorylation of PKA through endocrine pathways (Sun S. et al.,

2022). However, there is relatively little or no research on the protection of pancreatic islet cell identity and promotion of GLP-1 paracrine secretion by berberine. Our study supplements the mechanism by which berberine protects the identity and function of pancreatic islet cells from the perspective of promoting GLP-1 paracrine secretion by islet α cell.

In this experiment, we used *in vivo* and *in vitro* experiments and explored the process of berberine improving the function of islet β cell by stimulating the endocrine and paracrine GLP-1 in intestinal L cell and islet α cell and activating the GLP-1R/PKA signaling pathway.

Materials and methods

Antibodies and reagents

PC2 antibody (D1E1S), t-PKA antibody (D38C6), p-PKA antibody (D45D3), Pdx1 antibody (D59H3), GLP-1R antibody (HA500204) and all secondary antibodies used in Western blot were purchased from Cell Signaling Technology (Beverly, MA, United States); PC1/3 antibody (ab220363) was obtained from Abcam (Cambridge, United Kingdom); Ki67 antibody (A16919) was obtained from Abclonal (Wuhan, China); GLP-1 antibody (55292-1-AP), insulin antibody (66198-1-Ig) and glucagon antibody (15954-1-AP) were bought from Proteintech (Wuhan, China); β -actin antibody (20536-1-AP) was obtained from Santa Cruz Biotechnology (Santa Cruz, CA). Berberine, Palmitic acid (PA), GLP-1 (9-36) amide were purchased from Sigma-Aldrich (MO, United States). Other regular reagents were obtained from Wuhan Gugeshengwu Technology Co., Ltd. unless otherwise specified.

Animal experiment

Male seven-week-old db/db and db/m mice were obtained from Nanjing Biomedical Research Institute of Nanjing University. We kept the animals in the animal experiment center (SPF-grade) of Huazhong University of science and technology ($22^{\circ}\text{C} \pm 2^{\circ}\text{C}$, 12 h light/dark cycles, 40%–60% humidity). Db/m mice were set as the Control group, and db/db mice were randomly divided into Model group, Low group and High group. The Control group and Model group were given distilled water by gavage, while the Low group and High group were given 150 mg/kg and 300 mg/kg berberine by gavage respectively. The experimental protocol is illustrated in Figure 1A. After the experiment, 3% pentobarbital sodium (45 mg/kg, intraperitoneal injection) was used for anesthesia. The separated pancreas and ileum were partially fixed in polyformaldehyde and partially placed in a refrigerator at -80°C . The animal experiment was approved by the Animal Ethics Committee of Tongji Medical College, Huazhong University of Science and Technology (HUST) and its IACUC number is S2095.

Measurement of insulin and GLP-1

Insulin and GLP-1 was quantified by ELISA kits. We drew a standard curve using the gradient dilution of the standard product as

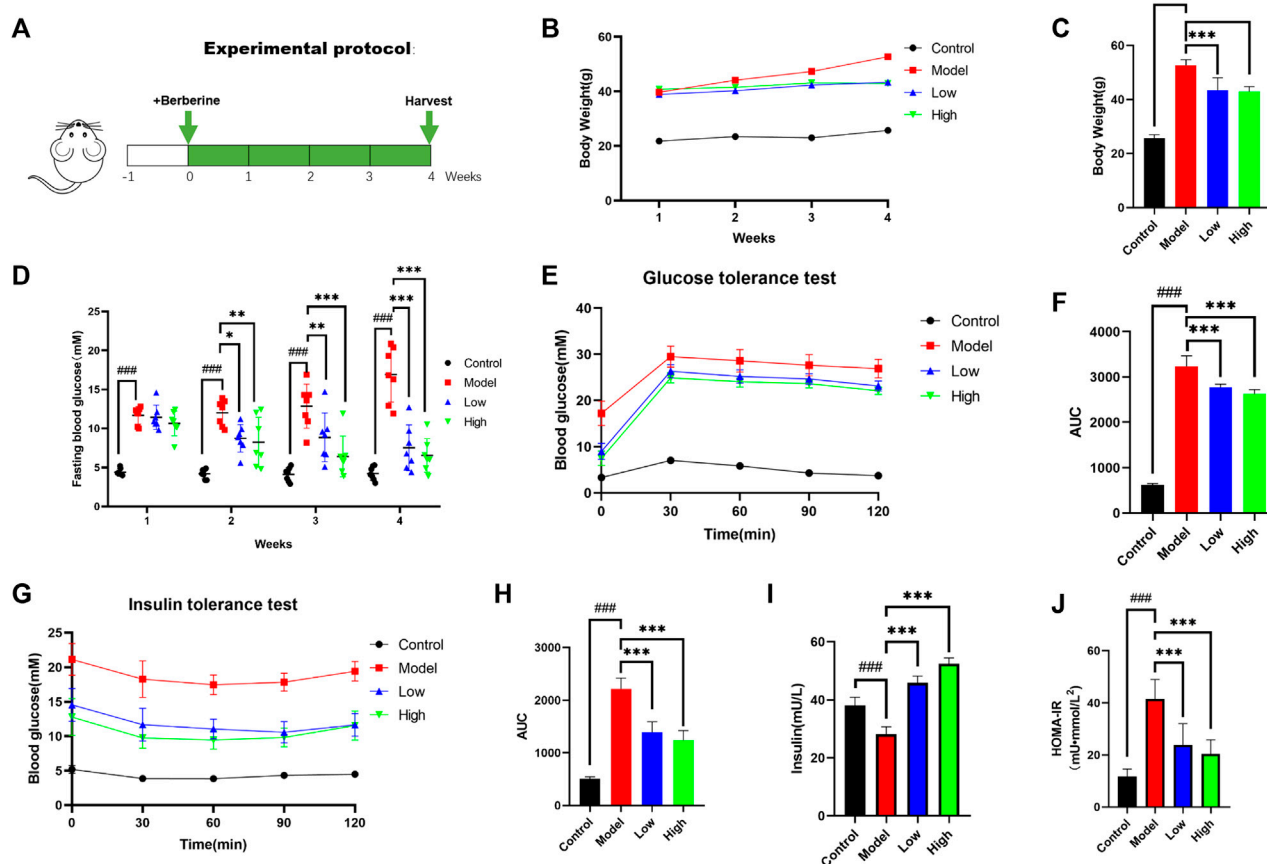


FIGURE 1

Berberine improved T2DM symptoms in db/db mice. (A) Animal experimental protocol. (B) Body weight of mice was recorded weekly ($n = 8$). (C) The bar graph represents the final body weight at the ending of experiment ($n = 8$). (D) Fasting blood glucose of mice was recorded weekly ($n = 7$). (E) For GTT, mice were fasted overnight and intraperitoneally injected with glucose (i.p., 0.75 g/kg), blood glucose was measured at 0, 30, 60, and 120 min after glucose administration ($n = 7$). (F) The bar graph represents average area under the GTT curve ($n = 7$). (G) For ITT, mice were fasted overnight and intraperitoneally injected with insulin (i.p., 1.0 U/kg), blood glucose was measured at 0, 30, 60, and 120 min after insulin administration; the bar graph represents average area under the curve ($n = 7$). (H) The bar graph represents average area under the ITT curve ($n = 7$). (I) Fasting insulin was determined at the ending of experiment ($n = 5$). (J) HOMA-IR index was calculated according to standard formula: $\text{HOMA-IR} = \text{FBG (mM)} \times \text{fasting insulin (mU/L)} / 22.5$ ($n = 8$). All data are presented as means \pm SEM. Compared to control group, $*p < 0.05$, $**p < 0.01$, $***p < 0.001$; Compared to model group, $*p < 0.05$, $**p < 0.01$, $***p < 0.001$.

a template, added the sample, antibody and HRP aggregation reagent, and put it in a 37°C water bath, then washed it five times with a washing solution, we added the chromogenic solution and reacted for 10 min, then detected the absorbance of each hole at a wavelength of 450 nm.

Immunohistochemistry and immunofluorescence staining

For immunohistochemistry, paraffin sections were dewaxed and washed. Then, the slices were placed in the microwave to repair the antigen. After cooling to room temperature, the chips were put into 3% H_2O_2 for 30 min. After washing with PBS, chips were sealed with 10% goat serum for 1 h. The first antibody was added and incubated at 4°C for 14 h and the second antibody was added and incubated for

1 h. DAB is used for color development, and then hematoxylin is used for nuclear staining.

For immunofluorescence, except for the need to block endogenous peroxidase with H_2O_2 , its process did not differ from immunohistochemistry until the primary antibody was incubated. After the primary antibody was incubated for 14 h, the secondary antibody was added and incubated for 1 h. We used DAPI to stain the nucleus.

Cell culture

The mouse pancreatic β -cell line, Min6, was cultured in DMEM high glucose medium containing 10% fetal bovine serum. The mouse intestinal L-cell line, STC-1, was cultured in 1648 medium containing 10% fetal bovine serum. The mouse pancreatic α -cell

TABLE 1 Primers used for RT-qPCR.

Gene	Forward (5'–3')	Reverse (5'–3')
GLP-1R	CTCCGAGCACTGTCCGTCTT	GATAACGAACAGCAGCGGAAC
PC1/3	GTACTGTTGGCTGAAAGGGAAG	CGCTTCTCCACAACATTCACC
PC2	TCTTGACCTACGGCATGATGAG	CACTCCTAGCAGCAGGTTCTCAT
Pdx1	AGCTCGCTGGGATCACTGGA	TGTAAGCACCTCCTGCCCACT
GAPDH	CCTCGTCCCGTAGACAAAATG	TGAGGTCAATGAAGGGGTCGT

line, α TC1/6, was cultured in DMEM high glucose medium containing 15% fetal bovine serum.

PA was used to construct T2DM model in cells, and berberine was used to observe its therapeutic effect. GLP-1 (9-36) amide was a competitive inhibitor of GLP-1R, and was used to observe the effect of berberine on GLP-1/GLP-1R/PKA signal pathway.

After determining the appropriate drug concentration in each cell with cck8, the three drugs were applied to the cell for 24 h. The culture supernatants were collected for GLP-1 assays, and the cells were lysed for protein or mRNA analysis.

Western blot analysis

Proteins were extracted from tissues and cells, and then protein concentrations were quantified using a Bis-creatine (BCA) kit. Samples were electrophoresed (80 V, 0.5 h, then 120 V, 1 h) and transferred to polyvinylidene fluoride membranes (280 mA, 1 kDa/min). Bands were put into blocking buffer for 1 h and incubated in primary antibody for 14 h. After cleaning, the secondary antibody was applied for 1 h. After cleaning, the strips were sent for exposure.

Real-time quantitative polymerase chain reaction (RT-qPCR)

The samples were added into Trizol for cracking, then chloroform was added for centrifugation to obtain the upper liquid phase, and isopropyl alcohol was added for centrifugation to obtain the precipitate. The precipitate was washed with ethanol and then dissolved with DEPC water. After reverse transcription, reagents and sample cDNA were added according to PCR reaction system and performed on LightCycler[®]96 system (Roche Diagnostics, Mannheim, Germany). Sequences of the primers are listed in Table 1.

Statistical analysis

Data are presented as mean \pm SD. All data were tested for normality using Shapiro wilk. When $p < 0.05$, we performed Kruskal–Wallis analysis. When $p > 0.05$, we used one-way ANOVA to compare differences between groups. Statistical analysis was performed using GraphPad Prism software, and $p < 0.05$ was considered statistically significant.

Results

Berberine ameliorates diabetic conditions in db/db mice

As a mature T2DM animal model, db/db mice were used to explore the effect of berberine on their T2DM symptoms. We recorded the weight of mice since the beginning of the experiment and the differences in the last weight of each group. Compared with the Model group, the Low group and the High group had a clear weight loss effect (Figure 1B). We recorded the changes of the fasting blood glucose level of mice every week. We can see that the rate of fasting blood glucose decline in the Low group is slightly slower than that in the High group, but it also maintained at a lower level with the High group at the end of the experiment (Figures 1C, D). After the administration of berberine, we conducted glucose tolerance test (GTT) and insulin tolerance test (ITT). Compared with db/db mice, the Low and High groups treated with berberine had lower blood glucose levels after intraperitoneal injection of glucose and insulin (Figures 1E, G). At the same time, the area under the curve (AUC) of GTT and ITT in these two groups was also lower (Figures 1F, H). In order to evaluate the effect of berberine on insulin secretion, we measured the serum insulin level at fasting. It can be found that compared with the Model group, the Low group and High group secreted more insulin after berberine treatment (Figure 1I), and calculated homeostatic model assessment of insulin resistance (HOMA-IR) index according to the following formula: $\text{HOMA-IR} = \text{FBG (mM)} \times \text{Fasting insulin (mU/L)} / 22.5$ (Figure 1J). These data suggested that berberine ameliorates diabetic conditions in db/db mice.

Effect of berberine on islet cells of db/db mice

We used H&E staining method to observe the shape of mouse islets (Figure 2A). After comparing the shape, quantity and area of islets, that there was no significant difference in these indicators between groups (Figure 2B). We used glucagon and insulin to label α cell and β cell for co-staining, and found that the ratio of α cell to β cell in Model group increased observably, while the two groups treated with berberine improved this trend (Figure 2C, D). Then we used Tunel fluorescence staining to detect the apoptosis signal in islet cells and immunofluorescence staining for the value-added related antigen Ki67 (Figures 2E, F). However, the expression of value-added and apoptosis-related signals between the groups was

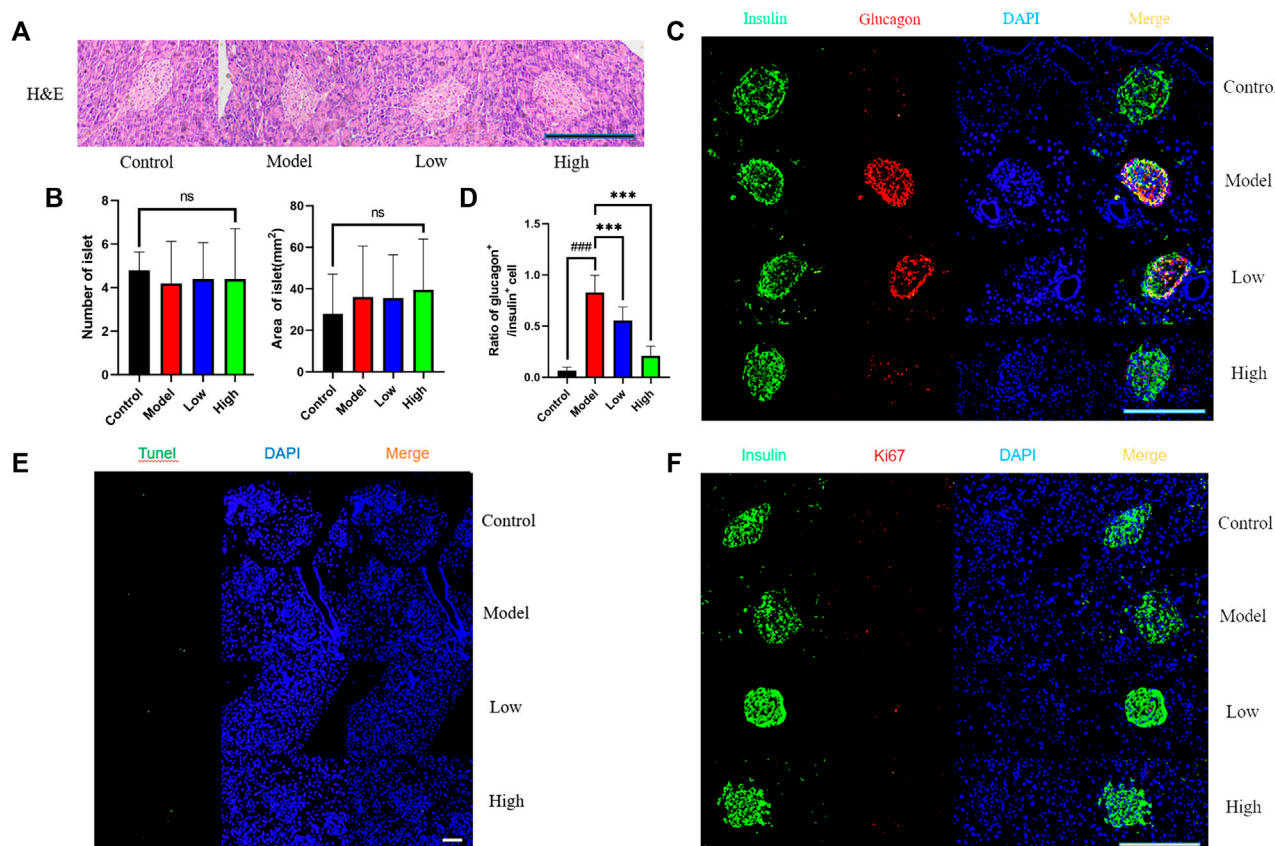


FIGURE 2

Effect of berberine on islet cells of db/db rats. (A) Representative H&E staining in different groups of pancreas. Scale bar, 400 μ m. (B) Representative figure of islet number and islet area in different groups ($n = 5$). (C) Immunofluorescence images showing the glucagon (red) and insulin (green) expression in different groups of pancreas. DAPI staining indicates the nuclei (blue). Scale bar, 400 μ m. (D) Representative figure of the ratio of glucagon⁺ cells to insulin⁺ cells in ($n = 3$). (E) Representative figures of TUNEL (green) immunofluorescence staining in different groups of pancreas. DAPI staining indicates the nuclei (blue). Scale bar, 400 μ m. (F) Immunofluorescence images showing the Ki67 (red) and insulin (green) expression in different groups of pancreas. DAPI staining indicates the nuclei (blue). Scale bar, 400 μ m. All data are presented as means \pm SEM. Compared to model group, * $p < 0.05$, ** $p < 0.01$, *** $p < 0.001$. ### $p < 0.01$, ### $p < 0.001$; Compared to control group, # $p < 0.05$, ## $p < 0.01$, ### $p < 0.001$.

very little, and there was no significant difference. These data indicate that berberine had no significant effect on the morphology, quantity and proliferation apoptosis of islet cells, but it inhibited db/db mice β cell transformation a cell process. Therefore, we had further studied the signal pathway that maintains the identity of β cell and inhibits β cell dysfunction.

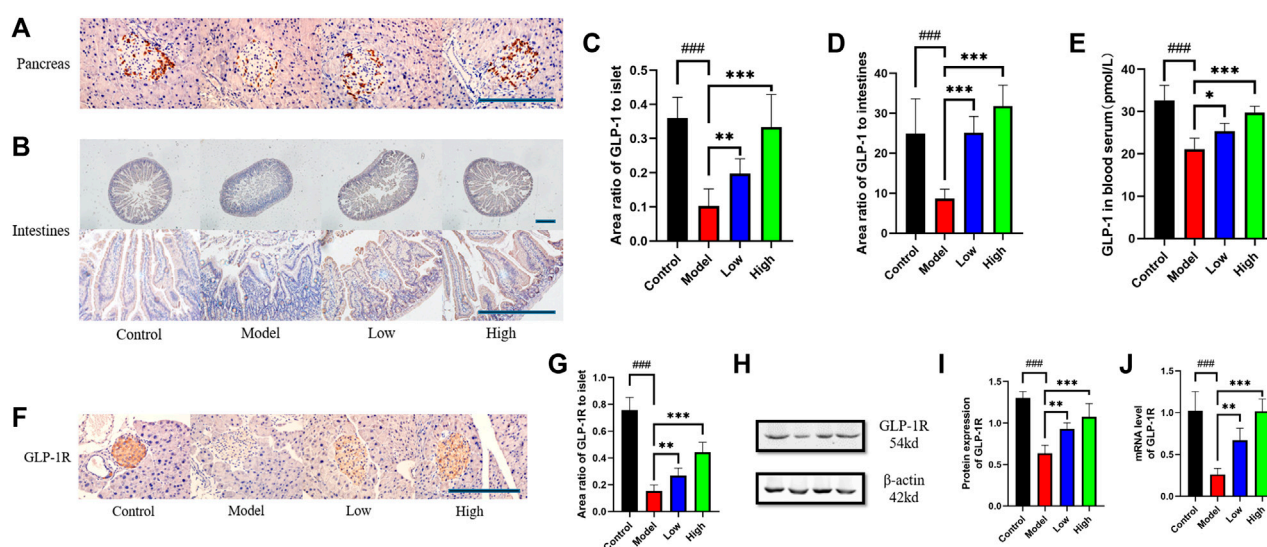
Berberine increased the expression of GLP-1 and GLP-1R

The expression level of GLP-1 in pancreas and intestine was measured by immunohistochemistry. The pancreas was photographed under $\times 400$ microscope and the intestine was photographed under $\times 100$ and $\times 400$ microscope respectively (Figures 3A, B). Through statistical analysis of GLP-1 positive area, it can be seen that the expression of GLP-1 in the pancreas and intestine of the Model group decreased compared with that of the Control group, while the Low and High groups given berberine reversed this trend (Figures 3C, D). In addition to GLP-1 in tissues,

we used ELISA to detect the level of GLP-1 in serum, and its trend was also consistent with that of GLP-1 in pancreas and intestine (Figure 3E). We observed GLP-1R in the pancreas under $\times 400$ microscope by immunohistochemistry, and found that berberine reversed the downward trend of GLP-1R expression in the Model group (Figures 3F, G). For the expression of GLP-1R in the intestine, we used Western blot to detect its protein content and PCR to detect its transcription level (Figure 3H). Statistics showed that berberine increased the expression of GLP-1R in db/db mice at the protein content and mRNA level (Figures 3I, J). These data indicated that berberine can activate the intestinal—islet GLP-1/GLP-1R/PKA signaling pathway.

Berberine increased the expression of PKA, PC1/3, PC2, and Pdx1

In the pancreas, we observed PC1/3 and PC2 under $\times 400$ microscope by immunohistochemical method (Figures



4A, B). Statistics showed that PC1/3 and PC2 in Model group was significantly lower than that in Control group, and then increased after berberine treatment (Figures 4C, D). We observed the expression level of Pdx1 by immunofluorescence method and found that it increased after berberine treatment (Figures 4E, F). In the intestine, we detected the protein levels of PC1/3 and PKA by Western blot (Figure 4G), and found that the expression of PC1/3 and the phosphorylation level of PKA increased after the treatment of berberine (Figures 4H, I). At the same time, we detected the mRNA levels of PC1/3, PC2 and Pdx1. The treatment of berberine promoted the transcription of these molecules in the intestine (Figures 4J–L). These data indicated that the status of β cell in pancreas and intestine is maintained and the molecular expression level of β cell dysfunction is increased after treatment.

Berberine activated GLP-1/GLP-1R/PKA signaling pathway in Min6 cell

Min6 cell is a cell line established in insulinoma obtained by targeted expression in transgenic mice, and retains the physiological characteristics of normal β cell. We used the method of CCK8 to determine the concentration of PA, berberine and GLP-1 (9-36) amide in Min6 cell (Figure 5A). Then, protein content of GLP-1R, PKA, PC1/3, PC2 and Pdx1 in four groups of cells was detected using Western blot (Figure 5B). After statistics, we found that the expression of these proteins decreased after PA modeling, and increased after adding

berberine, while after giving GLP-1R inhibitor, this trend of berberine was inhibited (Figures 5C–G). We measured mRNA levels of GLP-1R, PC1/3, PC2 and Pdx1 in cells by PCR, and the trend was also consistent with the trend of their protein expression (Figures 5H–K). These data indicated that berberine activated the GLP-1/GLP-1R/PKA signaling pathway in Min6 cell.

Berberine activated GLP-1/GLP-1R/PKA signaling pathway in STC-1 cell

STC-1 cell has many characteristics of natural intestinal endocrine cells, and can express and secrete many intestinal hormones such as GLP-1 (McCarthy et al., 2015). We used the method of CCK8 to determine the concentration of PA, berberine and GLP-1 (9-36) amide in STC-1 cells (Figure 6A). STC-1 is a cell line that can secrete GLP-1. We extracted the culture medium after cell culture for ELISA detection. We can see that the secretion of GLP-1 increases after adding berberine (Figure 6B). We used Western blot to detect the protein contents of GLP-1R, PKA, PC1/3 and PC2 in STC-1 cells (Figure 6C). After statistics, we found that proteins increased after the addition of berberine, but after the administration of GLP-1R inhibitor, this trend of berberine was inhibited (Figures 6D–G). We detected GLP-1R, PC1/3, PC2 and Pdx1 in cells by PCR, and found that their mRNA expression level increased after berberine administration (Figures 6H–K). These data indicated that berberine activated GLP-1/GLP-1R/PKA signaling pathway in STC-1 cell.

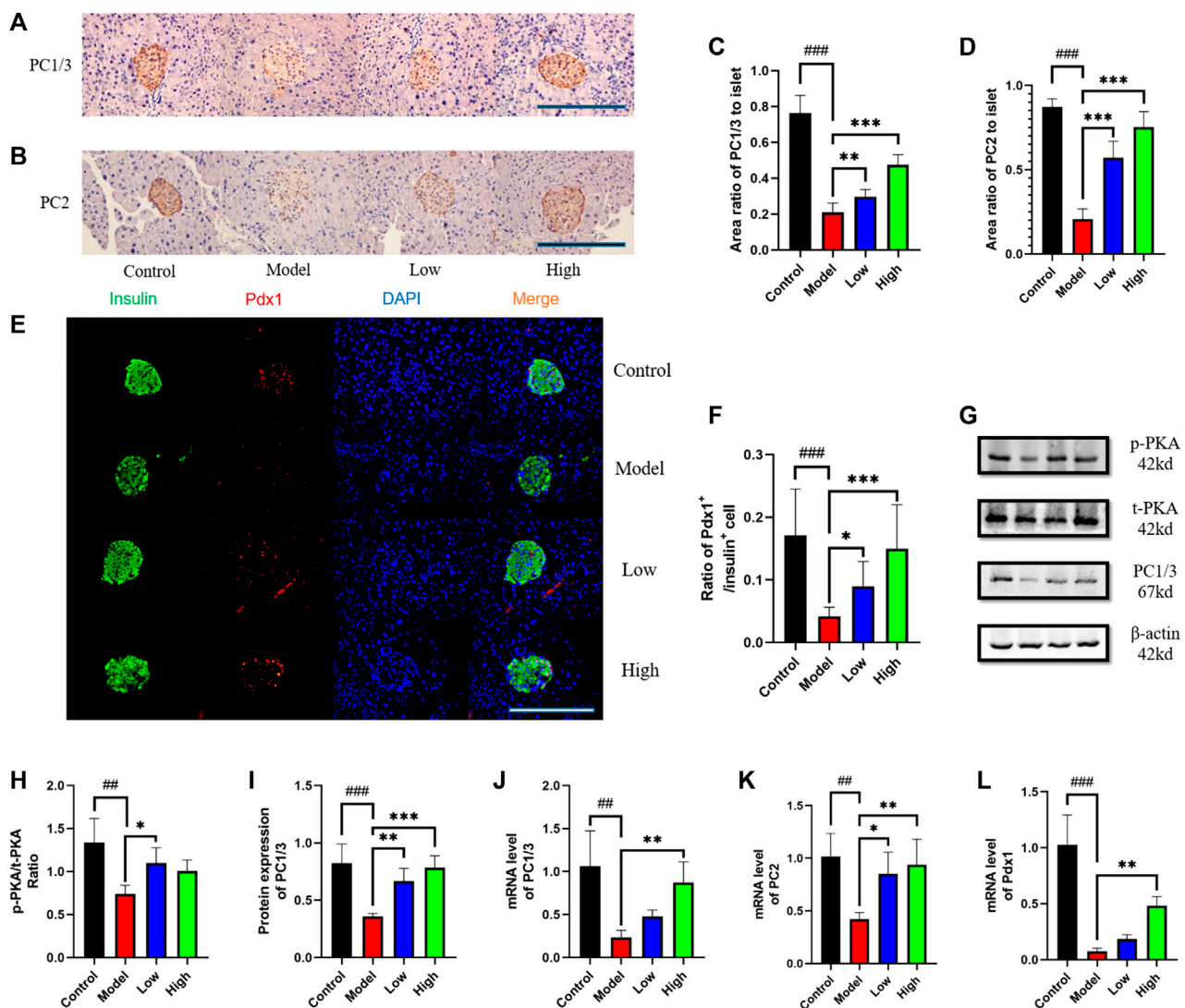


FIGURE 4

Berberine increased the expression of PKA, PC1/3, PC2, and Pdx1. (A) Representative immunohistochemical figures of PC1/3 in pancreas. Scale bar, 400 μ m. (B) Representative immunohistochemical figures of PC1/3 in pancreas. Scale bar, 400 μ m. (C) Representative figure of PC1/3 area in pancreas ($n = 3$). (D) Representative figure of PC2 area in pancreas ($n = 3$). (E) Immunofluorescence images showing the Pdx1 (red) and insulin (green) expression in different groups of pancreas. DAPI staining indicates the nuclei (blue). Scale bar, 400 μ m. (F) Representative figure of the ratio of Pdx1⁺ cells to insulin⁺ cells in different groups of pancreas ($n = 3$). (G) Representative western blots for immunoprecipitation of PKA and PC1/3 in intestine. (H) The quantification of PKA immunoprecipitation in intestine ($n = 4$). (I) The quantification of PC1/3 immunoprecipitation in intestine ($n = 4$). (J) The mRNA levels of PC1/3 in intestine of different groups ($n = 4$). (K) The mRNA levels of PC2 in intestine of different groups ($n = 4$). (L) The mRNA levels of Pdx1 in intestine of different groups ($n = 4$). All data are presented as means \pm SEM. Compared to control group, $\#p < 0.05$, $\#\#p < 0.01$, $\#\#\#p < 0.001$; Compared to model group, $*p < 0.05$, $**p < 0.01$, $***p < 0.001$.

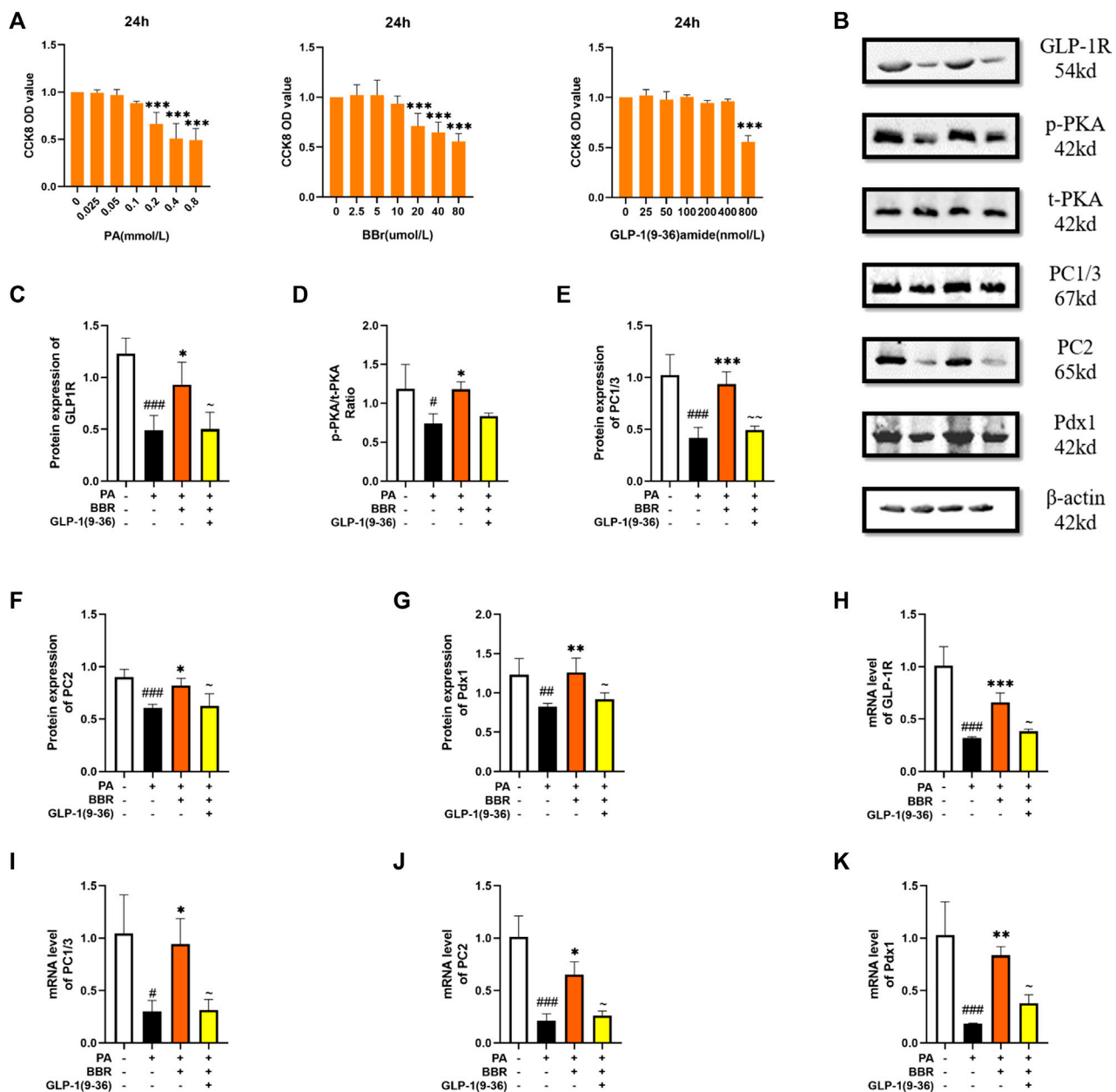
Berberine activated GLP-1/GLP-1R/PKA signaling pathway in α TC1/6 cell

α TC1/6 cell has the physiological characteristics of islet α cell (Suga et al., 2019). We used the method of CCK8 to determine the concentration of PA, BBR and GLP-1 (9-36) amide in α TC1/6 cell (Figure 7A). We extracted the culture medium after cell culture for ELISA detection, and we can see that the secretion of GLP-1 increases after adding berberine (Figure 7B). We detected the protein contents of GLP-1R, PKA, and Pdx1 by Western blot method (Figure 7C). After statistics, we found that the expression level of these proteins increased after adding berberine, but after giving GLP-1R inhibitor, this trend of

berberine was inhibited (Figures 7D–F). We also detected PC1/3 and PC2, but they were too low to be detected. We detected GLP-1R and Pdx1 in cells by PCR, and the trend was also consistent with the trend of their protein expression (Figures 7G, H). These data indicated that berberine activated GLP-1/GLP-1R/PKA signaling pathway in α TC1/6 cell.

Discussion

In animal experiments, we verified the therapeutic effect of berberine on T2DM and the function improvement of islet β cell.



Subsequently, we examined molecules of the GLP-1/GLP-1R/PKA signaling pathway in pancreatic and intestinal tissues and found that their expression was increased. Although previous studies on berberine promoting GLP-1 have been performed, they are limited to the impact on intestinal L cell. In our experiment, we took the function of a cell into consideration and observed the effect of berberine on pancreatic islet a cell, which made the evidence more convinced.

We focused on the effect of berberine on the islet cells of db/db mice. In our immunofluorescence experiment with insulin labeled β cell and glucagon labeled α cell, we found that after berberine treatment, the ratio of β cell to α cell increased. From this, we can conclude that berberine mainly affects the number and function of β cell to treat T2DM. The study indicates that the process is due to the transdifferentiation between islet cells, and the intestine-islet

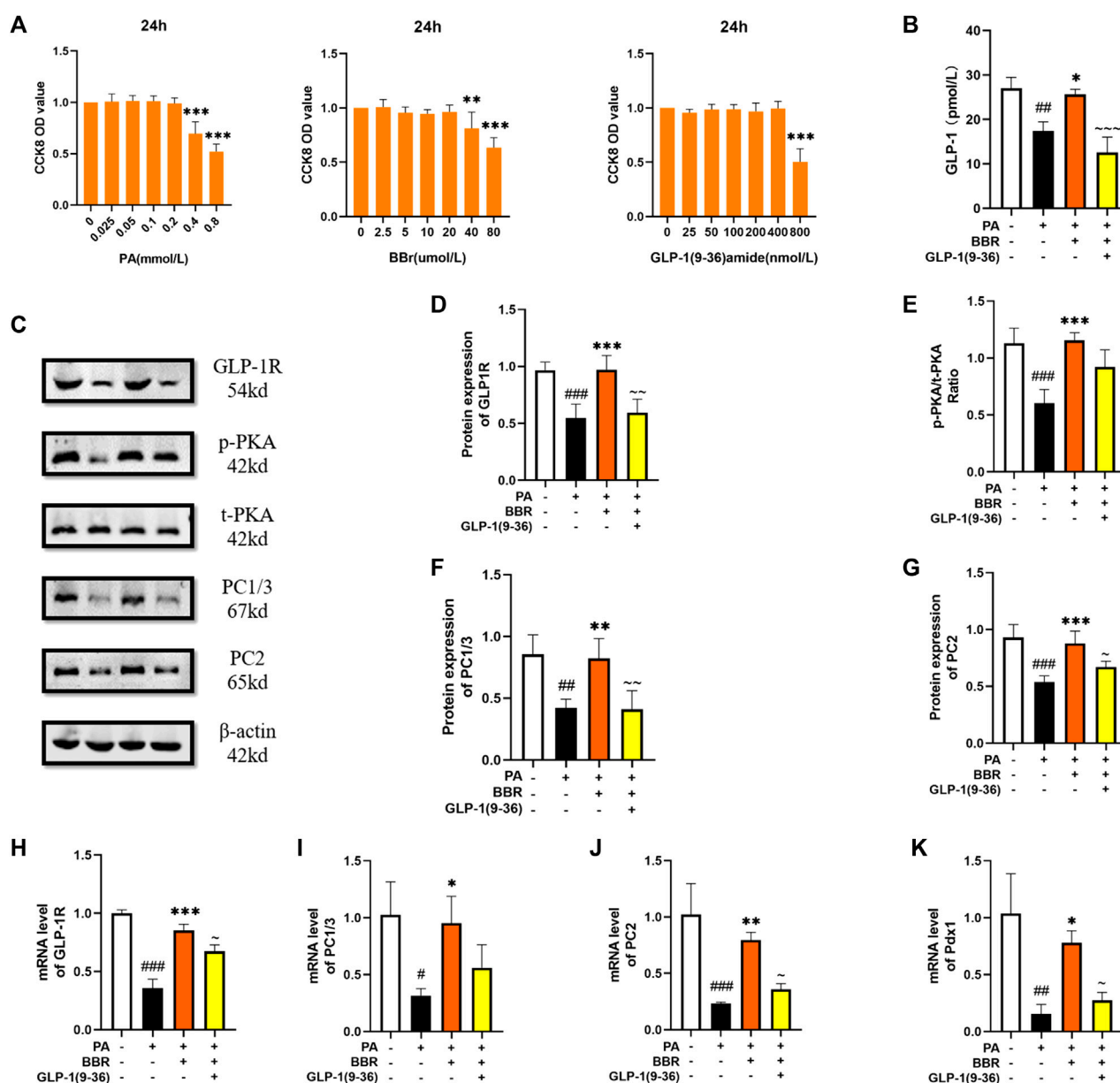


FIGURE 6

Berberine activated GLP-1/GLP-1R/PA signaling pathway in STC-1 cells. (A) The cck8 representative figures of PA, BBR and GLP-1 (9-36) amide ($n = 3$). (B) Representative figure of GLP-1 in cell ($n = 3$). (C) Representative western blots for immunoprecipitation of GLP-1R, PKA, PC1/3 and PC2 in STC-1. (D) The quantification of GLP-1R immunoprecipitation in STC-1 ($n = 4$). (E) The quantification of PKA immunoprecipitation in STC-1 ($n = 4$). (F) The quantification of PC1/3 immunoprecipitation in STC-1 ($n = 4$). (G) The quantification of PC2 immunoprecipitation in STC-1 ($n = 4$). (H) The mRNA levels of GLP-1R in STC-1 of different groups ($n = 3$). (I) The mRNA levels of PC1/3 in STC-1 of different groups ($n = 3$). (J) The mRNA levels of PC2 in STC-1 of different groups ($n = 3$). (K) The mRNA levels of Pdx1 in STC-1 of different groups ($n = 3$). All data are presented as means \pm SEM. Compared to control group, # $p < 0.05$, ## $p < 0.01$, ### $p < 0.001$; Compared to model group, * $p < 0.05$, ** $p < 0.01$, *** $p < 0.001$; Compared to BBR group, ~ $p < 0.05$, ~~ $p < 0.01$, ~~~ $p < 0.001$.

GLP-1/GLP-1R/PA signal pathway is one of the important pathways to produce this process (Baggio and Drucker, 2007; Mayendraraj et al., 2022).

GLP-1 is one of the hormones responsible for the incretin effect, and exerts a wide variety of actions such as potentiation of glucose-stimulated insulin secretion, reduction of appetite, delay of gastric emptying and inhibit β cell dysfunction (Rondas et al., 2013).

However, with the progress of research, it is found that GLP-1 is produced jointly by intestinal L cell and islet α cell, and acts cooperatively through endocrine and paracrine pathways, GLP-1 produced by islet α cell can act on islet β cell faster with paracrine effect (Vilsbøll, 2009; Villalba et al., 2020). With the treatment of berberine, like other studies, we have found an increase in GLP-1 secretion from intestinal L cell (Yu et al., 2015; Wang et al., 2021),

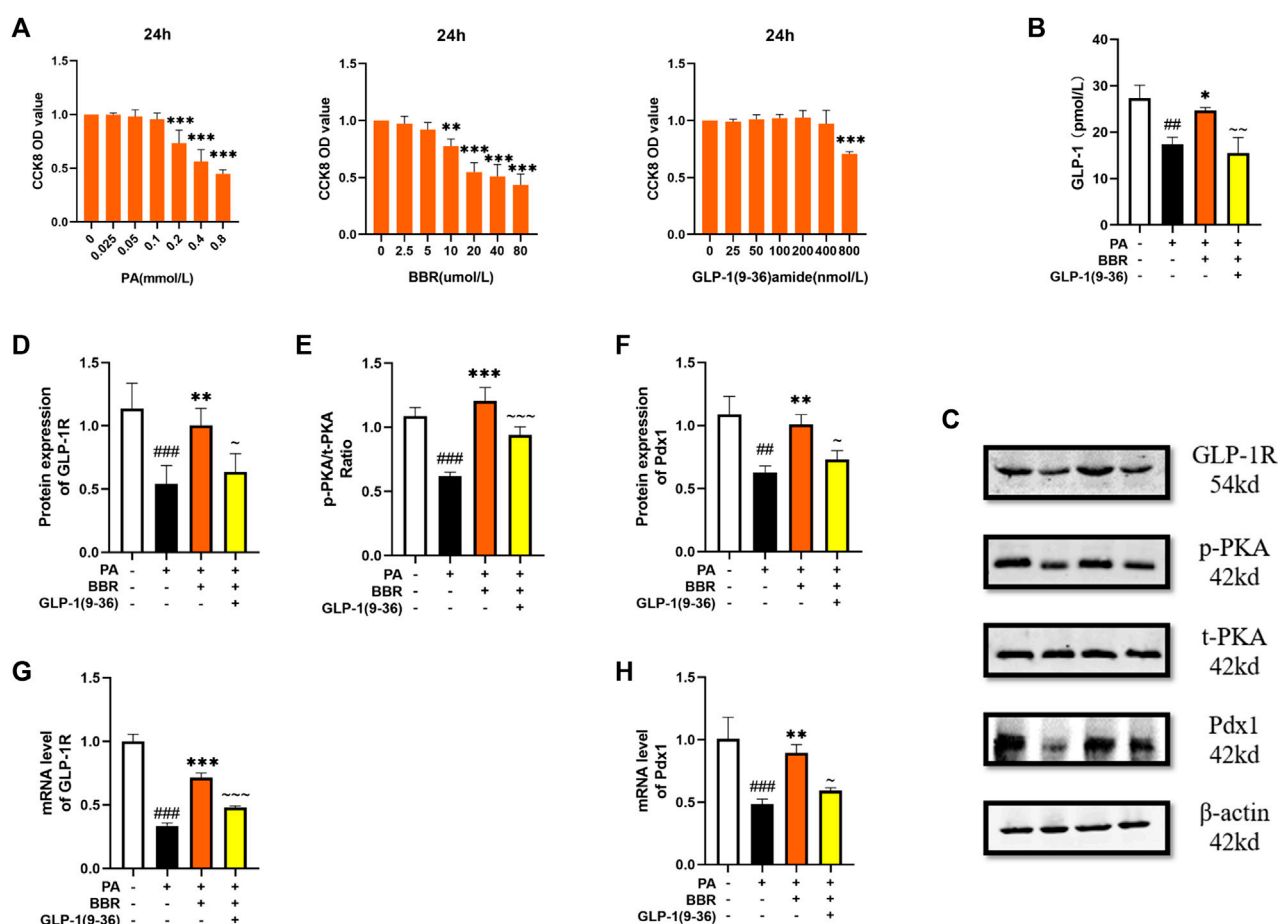


FIGURE 7

Berberine activated αGLP-1/GLP-1R/PA signaling pathway in αTC1/6 cells. (A) The cck8 representative figures of PA, BBR and GLP-1 (9-36) amide ($n = 3$). (B) Representative figure of GLP-1 in cell ($n = 3$). (C) Representative western blots for immunoprecipitation of GLP-1R, PKA and Pdx1 in αTC1/6. (D) The quantification of GLP-1R immunoprecipitation in αTC1/6 ($n = 4$). (E) The quantification of PKA immunoprecipitation in αTC1/6 ($n = 4$). (F) The quantification of Pdx1 immunoprecipitation in αTC1/6 ($n = 4$). (G) The mRNA levels of GLP-1R in αTC1/6 of different groups ($n = 3$). (H) The mRNA levels of Pdx1 in αTC1/6 of different groups ($n = 3$). All data are presented as means \pm SEM. Compared to control group, # $p < 0.05$, ## $p < 0.01$, ### $p < 0.001$; Compared to model group, * $p < 0.05$, ** $p < 0.01$, *** $p < 0.001$; Compared to BBR group, ~ $p < 0.05$, ~~ $p < 0.01$, ~~~ $p < 0.001$.

but in addition, we have also noticed a significant increase in GLP-1 secretion in the pancreatic islets, which has been ignored in previous studies. From this, we can prove that berberine not only activates GLP-1R of islet β cell through the secretion of intestinal L cell, but also promotes the function of GLP-1 secretion of islet α cell.

PC1/3 and PC2, as the important proteases of β cell, play an important role in the process of transforming proinsulin into insulin (Lafferty et al., 2021). Islet specific transcription factor Pdx1 has the function of maintaining islets β cell identity, inhibiting the transformation of β cell to α cell and promoting the secretion of insulin by β cell (Ebrahim et al., 2022). We detected the expression levels of these molecules in intestinal and pancreatic tissues, and the results showed an increase in expression in both tissues. This also indicates that berberine activates the GLP-1/GLP-1R/PA signaling pathway in intestinal and pancreatic tissues, which synergistically improves the function of pancreatic β cell.

In order to have a further study about the effect of berberine on GLP-1/GLP-1R/PA signaling pathway, we

performed experiment *in vitro*. Min6 cell, a kind of islet β cell line, has been used as a model for glucose metabolism *in vitro* (Wang and Hu, 2021). In our experiment, berberine stimulation increased the expression of related molecules in the GLP-1/GLP-1R/PA signaling pathway in MIN6 cells. STC-1 cell is an intestinal L cell line and often used in GLP-1 related research as a cell secreting GLP-1 (Wei et al., 2020). After we administered berberine stimulation, we found an increase in GLP-1 secretion by STC-1 cells, as well as an increase in the expression of molecules such as GLP-1R, PC1/3, PC2, and Pdx1. However, the administration of GLP-1R antagonists inhibited this phenomenon, demonstrating the role of berberine in activating the GLP-1/GLP-1R/PA signaling pathway in STC-1 cell.

We investigated the effect of berberine stimulation on the GLP-1/GLP-1R/PA signaling pathway in αTC1/6 cell. With the discovery of the endocrine function of islet α cell in recent years, some people began to use it in some experiments (He Y. et al., 2022). As a secretory cell of GLP-1, it was stimulated by berberine

and showed the same phenomenon of increased GLP-1 secretion as STC-1 cell, as well as increased expression of GLP-1R, p-PKA, Pdx1 and other related molecules. But the difference is that we did not observe a significant increase in PC1/3 and PC2 in it. A study has shown that mature α cell only express low levels of PC1/3 (Kilimnik et al., 2010), and GLP-1R agonists increase α cell PC1/3 expression through a β cell GLP-1R dependent manner (Garibay et al., 2018; Saikia et al., 2021). From this, we speculate that the significant increase in PC1/3 and PC2 that could not be detected may due to we only studied the effect of berberine alone on α TC1/6 cell. These results indicate that berberine can not only act on intestinal cells, but also promote the secretion of GLP-1 by pancreatic islet cells. The combined action of paracrine and endocrine produced GLP-1 on the GLP-1R of β cell activates its downstream signaling pathway.

Intestine-islet GLP-1/GLP-1R/PKA signaling pathway plays an important role in maintaining the identity and function of β cell. Although, there are some of studies related to the treatment of T2DM by berberine in activating this signaling pathway in intestine cell, it is few study about the paracrine effect of GLP-1 in a cell (Sandoval and D'Alessio, 2015). We consider that islet α cell is also indispensable in the process of islet function improvement. According to our research, it has been proved for the first time that berberine can improve T2DM by promoting the synergistic effect of intestinal-islet GLP-1/GLP-1R/PKA signal pathway. At the same time, we also carried out cell experiments to more clearly demonstrate that berberine promotes GLP-1 secretion and GLP-1R and its downstream molecules expression.

Conclusion

In conclusion, we confirmed *in vivo* that berberine has the effect of treating T2DM and enhancing the function of islet β cell, and then showed that this effect is produced by activating the GLP-1/GLP-1R/PKA signal pathway in the intestine and islet. Then we verified the effect of berberine on GLP-1/GLP-1R/PKA signal pathway in related cells through *in vitro* experiments. This experiment more comprehensively revealed the mechanism of berberine acting on GLP-1/GLP-1R/PKA signal pathway, and also showed that islet α cell probably play an important role in the treatment of T2DM, providing some ideas for the follow-up study of islet function.

References

- Baggio, L. L., and Drucker, D. J. (2007). Biology of incretins: GLP-1 and GIP. *Gastroenterology* 132 (6), 2131–2157. doi:10.1053/j.gastro.2007.03.054
- Cataldo, L. R., Vishnu, N., Singh, T., Bertonnier-Brouty, L., Bsharat, S., Luan, C., et al. (2021). The MafA-target gene PPP1R1A regulates GLP1R-mediated amplification of glucose-stimulated insulin secretion in β -cells. *Metabolism* 118, 154734. doi:10.1016/j.metabol.2021.154734
- Ebrahim, N., Shakirova, K., and Dashinimaev, E. (2022). PDX1 is the cornerstone of pancreatic β -cell functions and identity. *Front. Mol. Biosci.* 9, 1091757. doi:10.3389/fmolb.2022.1091757
- Garibay, D., Lou, J., Lee, S. A., Zaborska, K. E., Weissman, M. H., Sloma, E., et al. (2018). β cell GLP-1R signaling alters α cell proglucagon processing after vertical sleeve gastrectomy in mice. *Cell. Rep.* 23 (4), 967–973. doi:10.1016/j.celrep.2018.03.120
- He, Q., Chen, B., Wang, G., Zhou, D., Zeng, H., Li, X., et al. (2022). Co-crystal of rosiglitazone with berberine ameliorates hyperglycemia and insulin resistance through the PI3K/AKT/TXNIP pathway *in vivo* and *in vitro*. *Front. Pharmacol.* 13, 842879. doi:10.3389/fphar.2022.842879
- He, Y., Fu, Q., Sun, M., Qian, Y., Liang, Y., Zhang, J., et al. (2022). Phosphoproteome reveals molecular mechanisms of aberrant rhythm in neurotransmitter-mediated islet hormone secretion in diabetic mice. *Clin. Transl. Med.* 12 (6), e890. doi:10.1002/ctm2.890
- Hudish, L. I., Reusch, J. E., and Sussel, L. (2019). β Cell dysfunction during progression of metabolic syndrome to type 2 diabetes. *J. Clin. Invest.* 129 (10), 4001–4008. doi:10.1172/JCI129188
- Huising, M. O. (2020). Paracrine regulation of insulin secretion. *Diabetologia* 63 (10), 2057–2063. doi:10.1007/s00125-020-05213-5

Data availability statement

The original contributions presented in the study are included in the article/supplementary material, further inquiries can be directed to the corresponding authors.

Ethics statement

The animal study was reviewed and approved by the Animal Ethics Committee of Tongji Medical College, Huazhong University of Science and Technology (HUST).

Author contributions

In the experiment, WW completed the main operation of the experiment, QX, YG, and HW participated in the experiment and provided technical guidance for the experiment, HD and FL provided guidance for the experimental scheme, and FY provided financial support and detailed arrangement for the experimental plan. All authors contributed to the article and approved the submitted version.

Funding

Supported by grants from the National Natural Science Foundation of China (No. 82004358).

Conflict of interest

The authors declare that the research was conducted in the absence of any commercial or financial relationships that could be construed as a potential conflict of interest.

Publisher's note

All claims expressed in this article are solely those of the authors and do not necessarily represent those of their affiliated organizations, or those of the publisher, the editors and the reviewers. Any product that may be evaluated in this article, or claim that may be made by its manufacturer, is not guaranteed or endorsed by the publisher.

- Kilimnik, G., Kim, A., Steiner, D. F., Friedman, T. C., and Hara, M. (2010). Intraislet production of GLP-1 by activation of prohormone convertase 1/3 in pancreatic α -cells in mouse models of β -cell regeneration. *Islets* 2 (3), 149–155. doi:10.4161/isl.2.3.11396
- Lafferty, R. A., O'Harte, F. P. M., Irwin, N., Gault, V. A., and Flatt, P. R. (2021). Proglucagon-derived peptides as therapeutics. *Front. Endocrinol. (Lausanne)* 12, 689678. doi:10.3389/fendo.2021.689678
- Lee, Y. S., Lee, C., Choung, J. S., Jung, H. S., and Jun, H. S. (2018). Glucagon-like peptide 1 increases β -cell regeneration by promoting α -to β -cell transdifferentiation. *Diabetes* 67 (12), 2601–2614. doi:10.2337/db18-0155
- Marchetti, P., Lupi, R., Bugliani, M., Kirkpatrick, C. L., Sebastiani, G., Grieco, F. A., et al. (2012). A local glucagon-like peptide 1 (GLP-1) system in human pancreatic islets. *Diabetologia* 55 (12), 3262–3272. doi:10.1007/s00125-012-2716-9
- Mayendraraj, A., Rosenkilde, M. M., and Gasbjerg, L. S. (2022). GLP-1 and GIP receptor signaling in beta cells - a review of receptor interactions and co-stimulation. *Peptides* 151, 170749. doi:10.1016/j.peptides.2022.170749
- McCarthy, T., Green, B. D., Calderwood, D., Gillespie, A., Cryan, J. F., and Giblin, L. (2015). "STC-1 cells," in *The impact of food bioactives on health: In vitro and ex vivo models*. Editors K. Verhoeckx, P. Cotter, I. López-Expósito, C. Kleiveland, T. Lea, A. Mackie, et al. (Cham: Springer), 211–220.
- Muller, T. D., Finan, B., Bloom, S. R., D'Alessio, D., Drucker, D. J., Flatt, P. R., et al. (2019). Glucagon-like peptide 1 (GLP-1). *Mol. Metab.* 30, 72–130. doi:10.1016/j.molmet.2019.09.010
- Perreault, L., Skyler, J. S., and Rosenstock, J. (2021). Novel therapies with precision mechanisms for type 2 diabetes mellitus. *Nat. Rev. Endocrinol.* 17 (6), 364–377. doi:10.1038/s41574-021-00489-y
- Que, Q., Guo, X., Zhan, L., Chen, S., Zhang, Z., Ni, X., et al. (2019). The GLP-1 agonist, liraglutide, ameliorates inflammation through the activation of the PKA/CREB pathway in a rat model of knee osteoarthritis. *J. Inflamm. (Lond)* 16, 13. doi:10.1186/s12950-019-0218-y
- Rizza, R. A. (2010). Pathogenesis of fasting and postprandial hyperglycemia in type 2 diabetes: Implications for therapy. *Diabetes* 59 (11), 2697–2707. doi:10.2337/db10-1032
- Rondas, D., D'Hertog, W., Overbergh, L., and Mathieu, C. (2013). Glucagon-like peptide-1: Modulator of β -cell dysfunction and death. *Diabetes Obes. Metab.* 15 (3), 185–192. doi:10.1111/dom.12165
- Saikia, M., Holter, M. M., Donahue, L. R., Lee, I. S., Zheng, Q. C., Wise, J. L., et al. (2021). GLP-1 receptor signaling increases PCSK1 and β cell features in human α cells. *JCI Insight* 6 (3), e141851. doi:10.1172/jci.insight.141851
- Sandoval, D. A., and D'Alessio, D. A. (2015). Physiology of proglucagon peptides: Role of glucagon and GLP-1 in health and disease. *Physiol. Rev.* 95 (2), 513–548. doi:10.1152/physrev.00013.2014
- Smekens, S. P., Montag, A. G., Thomas, G., Albiges-Rizo, C., Carroll, R., Benig, M., et al. (1992). Proinsulin processing by the subtilisin-related proprotein convertases furin, PC2, and PC3. *Proc. Natl. Acad. Sci. U. S. A.* 89 (18), 8822–8826. doi:10.1073/pnas.89.18.8822
- Song, D., Hao, J., and Fan, D. (2020). Biological properties and clinical applications of berberine. *Front. Med.* 14 (5), 564–582. doi:10.1007/s11684-019-0724-6
- Suga, T., Kikuchi, O., Kobayashi, M., Matsui, S., Yokota-Hashimoto, H., Wada, E., et al. (2019). SGLT1 in pancreatic α cells regulates glucagon secretion in mice, possibly explaining the distinct effects of SGLT2 inhibitors on plasma glucagon levels. *Mol. Metab.* 19, 1–12. doi:10.1016/j.molmet.2018.10.009
- Sun, H., Saeedi, P., Karuranga, S., Pinkepank, M., Ogurtsova, K., Duncan, B. B., et al. (2022). IDF Diabetes Atlas: Global, regional and country-level diabetes prevalence estimates for 2021 and projections for 2045. *Diabetes Res. Clin. Pract.* 183, 109119. doi:10.1016/j.diabres.2021.109119
- Sun, J., Ni, Q., Xie, J., Xu, M., Zhang, J., Kuang, J., et al. (2019). β -Cell dedifferentiation in patients with T2D with adequate glucose control and nondiabetic chronic pancreatitis. *J. Clin. Endocrinol. Metab.* 104 (1), 83–94. doi:10.1210/je.2018-00968
- Sun, S., Yang, Y., Xiong, R., Ni, Y., Ma, X., Hou, M., et al. (2022). Oral berberine ameliorates high-fat diet-induced obesity by activating TAS2Rs in tuft and endocrine cells in the gut. *Life Sci.* 311, 121141. doi:10.1016/j.lfs.2022.121141
- Villalba, A., Rodriguez-Fernandez, S., Perna-Barrull, D., Ampudia, R. M., Gomez-Muñoz, L., Pujol-Autonell, I., et al. (2020). Repurposed analog of GLP-1 ameliorates hyperglycemia in type 1 diabetic mice through pancreatic cell reprogramming. *Front. Endocrinol. (Lausanne)* 11, 258. doi:10.3389/fendo.2020.00258
- Vilsbøll, T. (2009). The effects of glucagon-like peptide-1 on the beta cell. *Diabetes Obes. Metab.* 11 (3), 11–18. doi:10.1111/j.1463-1326.2009.01073.x
- Wang, J., Wei, L. R., Liu, Y. L., Ding, C. Z., Guo, F., Wang, J., et al. (2021). Berberine activates the β -catenin/TCF4 signaling pathway by down-regulating miR-106b to promote GLP-1 production by intestinal L cells. *Eur. J. Pharmacol.* 911, 174482. doi:10.1016/j.ejphar.2021.174482
- Wang, R., and Hu, W. (2021). Asprosin promotes β -cell apoptosis by inhibiting the autophagy of β -cell via AMPK-mTOR pathway. *J. Cell. Physiol.* 236 (1), 215–221. doi:10.1002/jcp.29835
- Wei, R., Cui, X., Feng, J., Gu, L., Lang, S., Wei, T., et al. (2020). Dapagliflozin promotes beta cell regeneration by inducing pancreatic endocrine cell phenotype conversion in type 2 diabetic mice. *Metabolism* 111, 154324. doi:10.1016/j.metabol.2020.154324
- Yu, Y., Hao, G., Zhang, Q., Hua, W., Wang, M., Zhou, W., et al. (2015). Berberine induces GLP-1 secretion through activation of bitter taste receptor pathways. *Biochem. Pharmacol.* 97 (2), 173–177. doi:10.1016/j.bcp.2015.07.012



OPEN ACCESS

EDITED BY

Ochuko Lucky Erukainure,
University of the Free State, South Africa

REVIEWED BY

Prabhakar Semwal,
Graphic Era University, India
Mithun Rudrapal,
Vignan's Foundation for Science,
Technology and Research, India

*CORRESPONDENCE

Oluwafemi Adeleke Ojo,
✉ oluwafemi.ojo@bowen.edu.ng

RECEIVED 06 June 2023

ACCEPTED 29 June 2023

PUBLISHED 20 July 2023

CITATION

Ojo OA, Ogunlakin AD, Gyebi GA, Ayokunle DI, Odugbemi AI, Babatunde DE, Ajayi-Odoko OA, Iyobhebhe M, Ezea SC, Akintayo CO, Ayeleso A, Ojo AB and Ojo OO (2023), GC-MS chemical profiling, antioxidant, anti-diabetic, and anti-inflammatory activities of ethyl acetate fraction of *Spilanthes filicaulis* (Schumach. and Thonn.) C.D. Adams leaves: experimental and computational studies. *Front. Pharmacol.* 14:1235810. doi: 10.3389/fphar.2023.1235810

COPYRIGHT

© 2023 Ojo, Ogunlakin, Gyebi, Ayokunle, Odugbemi, Babatunde, Ajayi-Odoko, Iyobhebhe, Ezea, Akintayo, Ayeleso, Ojo and Ojo. This is an open-access article distributed under the terms of the [Creative Commons Attribution License \(CC BY\)](https://creativecommons.org/licenses/by/4.0/). The use, distribution or reproduction in other forums is permitted, provided the original author(s) and the copyright owner(s) are credited and that the original publication in this journal is cited, in accordance with accepted academic practice. No use, distribution or reproduction is permitted which does not comply with these terms.

GC-MS chemical profiling, antioxidant, anti-diabetic, and anti-inflammatory activities of ethyl acetate fraction of *Spilanthes filicaulis* (Schumach. and Thonn.) C.D. Adams leaves: experimental and computational studies

Oluwafemi Adeleke Ojo^{1*}, Akingbolabo Daniel Ogunlakin¹, Gideon Ampoma Gyebi², Damilare IyinKristi Ayokunle³, Adeshina Isaiah Odugbemi¹, Dare Ezekiel Babatunde⁴, Omolola Adenike Ajayi-Odoko⁵, Matthew Iyobhebhe⁶, Samson Chukwuemeka Ezea⁷, Christopher Oloruntoba Akintayo⁸, Ademola Ayeleso^{1,9}, Adebola Busola Ojo¹⁰ and Omolara Olajumoke Ojo¹⁰

¹Phytomedicine, Molecular Toxicology, and Computational Biochemistry Research Laboratory (PMTCB-RL), Department of Biochemistry, Bowen University, Iwo, Nigeria, ²Department of Biochemistry, Bingham University, Karu, Nigeria, ³Department of Pure and Applied Biology, Bowen University, Iwo, Nigeria, ⁴Department of Anatomy, Bowen University, Iwo, Nigeria, ⁵Department of Microbiology, Bowen University, Iwo, Nigeria, ⁶Department of Biochemistry, Landmark University, Omu-Aran, Nigeria, ⁷Department of Pharmacognosy and Environmental Medicine, University of Nigeria, Nsukka, Nigeria, ⁸Department of Physiology, Afe Babalola University, Ado-Ekiti, Nigeria, ⁹Department of Life and Consumer Sciences, School of Agriculture and Life Sciences, University of South Africa, Roodepoort, South Africa, ¹⁰Department of Biochemistry, Ekiti State University, Ado-Ekiti, Nigeria

Introduction: This study aimed to investigate the chemical profile of GC-MS, antioxidant, anti-diabetic, and anti-inflammatory activities of the ethyl acetate fraction of *Spilanthes filicaulis* leaves (EFSFL) via experimental and computational studies.

Methods: After inducing oxidative damage with FeSO₄, we treated the tissues with different concentrations of EFSFL. An *in-vitro* analysis of EFSFL was carried out to determine its potential for antioxidant, anti-diabetic, and anti-inflammatory activities. We also measured the levels of CAT, SOD, GSH, and MDA.

Results and discussion: EFSFL exhibited anti-inflammatory properties through membrane stabilizing properties (IC₅₀ = 572.79 µg/ml), proteinase inhibition (IC₅₀ = 319.90 µg/ml), and inhibition of protein denaturation (IC₅₀ = 409.88 µg/ml). Furthermore, EFSFL inhibited α-amylase (IC₅₀ = 169.77 µg/ml), α-glucosidase (IC₅₀ = 293.12 µg/ml) and DPP-IV (IC₅₀ = 380.94 µg/ml) activities, respectively. Our results indicated that induction of tissue damage reduced the levels of GSH, SOD, and CAT activities, and increased MDA levels. However, EFSFL treatment restores these levels to near normal. GC-MS profiling shows that EFSFL contains 13 compounds, with piperine being the most abundant. *In silico* interaction of the phytoconstituents using molecular and ensembled-based docking revealed

strong binding tendencies of two hit compounds to DPP IV (alpha-caryophyllene and piperine with a binding affinity of -7.8 and -7.8 Kcal/mol), α -glucosidase (alpha-caryophyllene and piperine with a binding affinity of -9.6 and -8.9 Kcal/mol), and to α -amylase (piperine and Benzocycloheptano[2,3,4-*l*]isoquinoline, 4,5,6,6a-tetrahydro-1,9-dihydroxy-2,10-dimethoxy-5-methyl with a binding affinity of -7.8 and -7.9 Kcal/mol), respectively. These compounds also presented druggable properties with favorable ADMET. Conclusively, the antioxidant, antidiabetic, and anti-inflammatory activities of EFSFL could be due to the presence of secondary metabolites.

KEYWORDS

Spilanthes filicaulis, antioxidant, antidiabetic, anti-inflammatory, GC-MS profiling, molecular docking and dynamic simulations

1 Introduction

Researchers have explored various plants based on World Health Organization (WHO) authorization (World Health Organization, 1999). Researchers are using plants and their extracts to treat disorders such as diabetes and inflammation-related diseases (Andlib et al., 2023). Diabetes-related conditions rank among the top ten killer diseases in the world (Rendra et al., 2019). The symptoms of diabetes mellitus (DM) are caused by cellular dysfunction resulting from an imbalance between the antioxidant defense system and oxidative stress (Rendra et al., 2019). This reactive oxygen species (ROS) bonds with available proteins in a reactive process known as glycation. Diabetes is an elevation of blood glucose concentrations in the body (Cole and Florez, 2020). It is a form of the disease, that is, known to manifest when there is a perpetual and continuous increase in concentration, and it manifests in three major ways: first, this condition occurs when the pancreas is dysfunctional or even destroyed, and this state of condition is referred to as an “insulin-dependent condition” (Bellary et al., 2021). Because the beta cells present in the islets of Langerhans in the pancreas produce insulin. Second, this condition is also manifested when the body’s system is not responding to the insulin produced by the pancreas or when not enough insulin is produced to combat the increased concentration of glucose in the system (McIntyre et al., 2019; Bellary et al., 2021). This state of the disease has been linked to an increase in fat deposits over time due to people who lack exercise and those who have decided to live a sedentary lifestyle. This disease state is called insulin resistance, and it is the most common type of this disease condition because it occurs from childhood to adulthood (Bellary et al., 2021). Third, gestational diabetes, which is frequent among women, manifests itself in pregnant women when their glucose concentration in the system increases during pregnancy (McIntyre et al., 2019). The causative agent of this condition is free radicals, which initiate different manifestations of this disease, such as cardiomyopathy, nephropathy, neuropathy, and retinopathy. This disease condition has received a lot of interest in recent times, and several therapeutic means have been adopted by researchers to deal with it, such as the manufacture of antidiabetic drugs, including metformin (Ojo et al., 2022). But over the years, the drugs produced have not been able to fully manage the complications that arise from oxidative stress. The focus has now been on the use of organic therapies such as plants (Ojo et al., 2022). Furthermore, it has been identified that plants

possess certain bioactive compounds, making them a powerful force in combating various diseases, including diabetes. These compounds, also known as phytochemicals, are known to also increase defense mechanism functions in the system, such as catalase (CAT), superoxide dismutase (SOD), and reduced glutathione (GSH), as well as suppress malondialdehyde (MDA) activities (Truong and Jeong, 2021). In the tropical and subtropical parts of the world, including Africa, America, Borneo, India, Sri Lanka, and Asia, *Spilanthes filicaulis* is also known as Creeping Spot Flower or African Cress (Tiwari et al., 2011). It is an annual plant that creeps and has prostrate stems that root from the nodes. They used seeds for reproduction. Their leaves are oval and alternating. On a short, somewhat hairy petiole, they tightly affixed the blade to the stem. The inflorescence is made up of short axillary peduncles with ovoid flower heads. They have blooms with golden rays and discs (Akoachere et al., 2015). In Babungo, northern Cameroon, the entire *S. filicaulis* plant is used to treat malaria, gastritis, toothaches, and stomachaches (Simbo, 2010). Additionally, the whole plant is used to cure chest discomfort, dermatitis, guinea worms, stomach problems, headaches, coughing, and toothaches. Additionally, it is used topically as a local anesthetic and as an enema to treat side discomfort (Ndenecho, 2009; Elufioye et al., 2019). This study aims to determine the antioxidant, antidiabetic, and anti-inflammatory properties of the ethyl acetate fraction of *S. filicaulis* leaves via experimental and computational studies.

2 Materials and methods

2.1 Chemicals and reagents

In this study, analytical grade solvents and reagents were used. Pancreatic α -amylase and α -glucosidase were obtained from Central Research Lab. Ltd, Ilorin. All chemicals used were of analytical grade.

2.2 Plant material and preparation of ethyl acetate fractions of *Spilanthes filicaulis* leaf

We obtained the leaves of *S. filicaulis* from Bowen University’s farmlands and identified them with the herbarium number BUH035. We cleaned the leaves to remove dirt and dust particles

and left them to air dry for 2 weeks. Once dry, we processed them into a powdery form. Then, 30 g of powder was dissolved with an appropriate amount of methanol and water, and the mixture was allowed to macerate for 72 h. The resulting extract (MESFL) was filtered, concentrated, and stored at -20°C for further analysis. Subsequently, 20 g of MESFL was fractionated exhaustively with ethyl acetate to obtain the ethyl acetate fraction (EFSFL). We concentrated the ethyl acetate fraction using a rotary evaporator and stored the concentrate for further analysis.

2.3 *In vitro* antioxidant

2.3.1 2,2-Diphenyl-1-picrylhydrazyl (DPPH) scavenging ability

We followed the procedure outlined by Ojo et al. (2022) to evaluate the ability of the extracts to scavenge DPPH radicals. For the comparative analysis, ascorbic acid served as the reference standard. The percentage of DPPH inhibition was determined by employing the following formula:

$$\% \text{DPPH} = \frac{\text{Abs}_{\text{control}} - \text{Abs}_{\text{sample}}}{\text{Abs}_{\text{control}}} \times 100$$

2.3.2 Ferric reducing antioxidant power (FRAP) potential

The standard procedures of (Ojo et al., 2022; Ahmad et al., 2023) with a slight modification were used to measure the ability of EFSFL to reduce ferric ions. We measured the absorbance at 593 nm and we reported the outcome as $\mu\text{mol Fe (II)}/\text{g}$ of the powder's dry weight using the FeSO_4 standard curve for calculation.

2.4 *In vitro* antidiabetic properties

2.4.1 α -amylase inhibitory potential

This study followed the standard protocol (Ahmad et al., 2023) to determine the α -amylase inhibitory potential of EFSFL. To begin, we made a fresh preparation of enzyme, comprising 5 units per milliliter, in pH 6.7 ice-cold PBS with a concentration of 20 mM and including 6.7 mM NaCl. Then, 250 μL of the enzyme was combined with inhibitors (acarbose or EFSFL) at varying concentrations (excluding a blank sample), and the mixture was incubated at 37°C for 20 min. We subsequently added a starch solution with a concentration of 0.5% (w/v), and the mixture was incubated for an additional 15 min at 37°C . Immediately after the DNS reagent was added, the mixture was mixed and placed in a water bath at 100°C for 10 min. Finally, the absorbance was read at 540 nm.

2.4.2 α -glucosidase inhibitory potential

The effect of EFSFL on intestinal α -glucosidase activity was evaluated using a technique described by (Bouslamti et al., 2023), which quantified the glucose generated by sucrose breakdown. To perform the assay, 100 μL of sucrose (50 mM), 1000 μL of phosphate buffer (50 mM; pH = 7.5), and 100 μL of α -glucosidase enzyme solution were prepared as the test solution

(10 I.U.). Control (distilled water), positive control (acarbose), or EFSFL were all added to this mixture at varying concentrations. We read the absorbance of the ultimate solution at 500 nm.

2.4.3 Dipeptidyl peptidase-IV (DPP-IV) activity

We carried out the inhibition of DPP-IV activity in 96-well ELISA plates. Evogliptin was used as the standard inhibitor. In each well, 30 μL of Tris-HCl buffer solution, 100 μL of enzyme DPP-IV, 100 μL of various concentrations (15.625, 31.25, 62.5, 125, 250, 500, and 1000 $\mu\text{g}/\text{mL}$) of the fraction or standard, and 50 μL gly-pro-pnitroanilide as the substrate, were added. After adding the mixture, they incubated it for 30 min at 37°C , and then the absorbance was read by microplate readers at 405 nm (Bharti et al., 2012).

We calculated %inhibition using the formula:

$$\% \text{ Inhibition} = \frac{\text{DPP - IV activity (with fraction)}}{\text{DPP - IV activity (without fraction)}} \times 100$$

2.5 Anti-inflammatory *in vitro* assays

2.5.1 Human red blood cell (HRBC; RBC) membrane stability test

We conducted the procedure for the HRBC membrane stabilization assay following established protocols (Hogan et al., 2023). In summary, 2 ml reaction mixtures were prepared by combining varying amounts of EFSFL or a standard diclofenac drug with a 10% suspension of red blood cells. We kept these mixtures for 30 min at a temperature of 56°C . Afterward, they were subjected to centrifugation at a speed of 2500 revolutions per minute (rpm) for 5 min. The resulting liquid above the sediment, known as the supernatant, was read for its absorbance at a wavelength of 560 nm.

2.5.2 Protein denaturation inhibition

We carried out this assay to measure the inhibition of protein denaturation by following the procedure described by Hogan et al. (2023). The test sample included different concentrations of EFSFL and/or standard diclofenac, with a 10 μL 1% solution of bovine serum albumin. This mixture was heated to a temperature of 55°C for 30 min and left to cool. The turbidity of the samples was measured at a wavelength of 660 nm, and the extent to which the protein denaturation was prevented was calculated as the percentage of inhibition.

2.5.3 Proteinase inhibitory assay

The proteinase inhibitory assay was carried out using the approach outlined in (Hogan et al., 2023). The procedure involved incubating 1 mL of the extract with a reaction mixture containing 2 ml of Tris-HCl buffer and 0.06 mg trypsin at 37°C for 5 min. Then, 0.8% (w/v) casein was added to the reaction mixture and allowed to incubate for 20 min. The reaction was stopped by adding 2 ml of 70% perchloric acid, and the resulting supernatant was measured for absorbance at 210 nm after centrifugation.

2.6 Ex-vivo studies

2.6.1 Rat experiments and organ harvesting

The study utilized healthy male Wistar rats, weighing between 200 and 250 g each, obtained from the Anatomy Department at Bowen University in Iwo, Nigeria. Before being put to death using ketamine, the rats underwent an overnight fasting period. The livers were then extracted and blended in a 50 mM phosphate buffer solution containing 1% Triton X-100. For *ex-vivo* research purposes, we collected the supernatants in plain tubes after centrifugation at 15,000 rpm and 40°C. The study was approved under a specific identification number (BUAC/BCH/2023/0001A), and the protocols approved by Bowen University's institutional animal ethics committee were followed when caring for the rats.

2.6.2 Induction of liver damage

The protocol defined by Ojo et al. (2022) was employed to induce liver injury *ex vivo* in experimental rats. To perform this, the organ supernatant, which had different concentrations of EFSFL (varying between 31.25 µg/ml to 1000 µg/mL), was mixed with 200 µL. We added 100 µL of a solution containing 0.1 mM FeSO₄. We then placed the resulting mixture in a 37°C environment for 30 min to allow for biochemical analysis. In the normal control, only the organ supernatant was used in the reaction mixture, while the negative control comprises the tissue supernatant and FeSO₄.

2.7 Ex vivo analysis

2.7.1 Catalase (CAT) activity

We assessed the CAT activity assay of EFSFL with slight modifications to the method described by Ojo et al. (2022). Tissue samples containing different concentrations of EFSFL were mixed with 780 µl of 50 mM phosphate buffer, followed by the addition of 300 µl of 2 M H₂O₂. For 3 minutes, we read the absorbance at 240 nm at 1-min intervals.

2.7.2 Superoxide dismutase

We used the method provided in (Ajiboye et al., 2019) to determine SOD activity. To summarize, we mixed 170 µl of diethylenetriaminepentaacetic acid and 15 µl of the incubated sample in a test tube. Then, we added 15 µl of 6-hydroxydopamine to the solution and gently shook it. Finally, we measured the solution at 492 nm for 3 min with a 1-min interval.

2.7.3 Reduced glutathione level

Based on the protocol depicted in (Ajiboye et al., 2019), the tissue lysates, with a volume of 600 µl, were treated to remove proteins by adding 600 µl of a solution containing 10% TCA. After 10 min of centrifuging the mixture at 3500 rpm, 500 µl of the sample was transferred to a new test tube. Next, 100 µl of Ellman reagent was added to the sample, and the mixture was allowed to incubate at a temperature of 25°C for 5 min. We subsequently measured the absorbance of the solution at a wavelength of 415 nm.

2.7.4 Lipid peroxidation level

The ability of EFSFL to inhibit lipid peroxidation by following the method outlined in reference (McIntyre et al., 2019) They carried out the process by taking 100 µl of tissue lysates that contained varying concentrations of EFSFL. We added 1000 µl of 0.25% thiobarbituric acid, 100 µl of 8.1% SDS, and 375 µl of 20% acetic acid to it. We boiled the mixture at 95°C for an hour in a water bath. After cooling it to room temperature, they measured its absorbance at 532 nm.

2.8 Molecular docking studies of GCMS identified compounds against α-amylase, dipeptidyl peptidase IV (DPP IV), and α-glucosidase

2.8.1 Protein structure preparation

The retrieval of protein structures was from the Protein Data Bank (<http://www.rcsb.org>) for the deposited three-dimensional structures of human dipeptidyl peptidase IV (DPP IV) complexed with evogliptin (PDBID: 5Y7K), human pancreatic α-amylase (HPA) complexed with acarbose (PDBID: 1B2Y), and human α-glucosidase complexed with acarbose (HG) (PDB ID: 3TOP). The existing ligands and water molecules were removed from all the crystal structures while missing hydrogen atoms were added using MGL-AutoDock Tools (ADT, v1.5.6) (Morris et al., 2009).

2.8.2 Ligand preparation

The retrieval of Structure Data Format (SDF) of acarbose (reference inhibitors) and 13 phytocompounds identified by GC-MS analyses of EFSFL were downloaded from the PubChem database (www.pubchem.ncbi.nlm.nih.gov) before their conversion to PDB chemical format using Open Babel (O'Boyle et al., 2011). Non-polar hydrogen molecules were merged with the carbons, while the polar hydrogen charges of the Gasteiger-type were assigned to atoms. Furthermore, ligand molecules were converted to dockable PDBQT format with the help of AutoDock Tools.

2.8.3 Validation of molecular docking protocol

The virtual screening docking protocol was validated by aligning the docked poses of the native ligands (acarbose and evogliptin) with the extracted co-crystallized ligand from both proteins, which had the lowest binding affinity from the initial docking. We calculated the RMSD using Discovery Studio Visualizer, BIOVIA, 2020.

2.8.4 Molecular docking of phytochemicals with the targeted active site

The active site targeted molecular docking with the reference inhibitors and the GC-MS identified compounds against DPP IV, HPA, and HG was performed using AutoDock Vina in PyRx 0.8 (Trott and Olson, 2010). For the docking analysis, the ligands were imported, and energy minimization was accomplished using Open Babel (O'Boyle et al., 2011) incorporated into PyRx 0.8. The Universal Force Field (UFF) and conjugate gradient descent were employed as the energy minimization parameter and optimization algorithm, respectively. Although other parameters were left at their

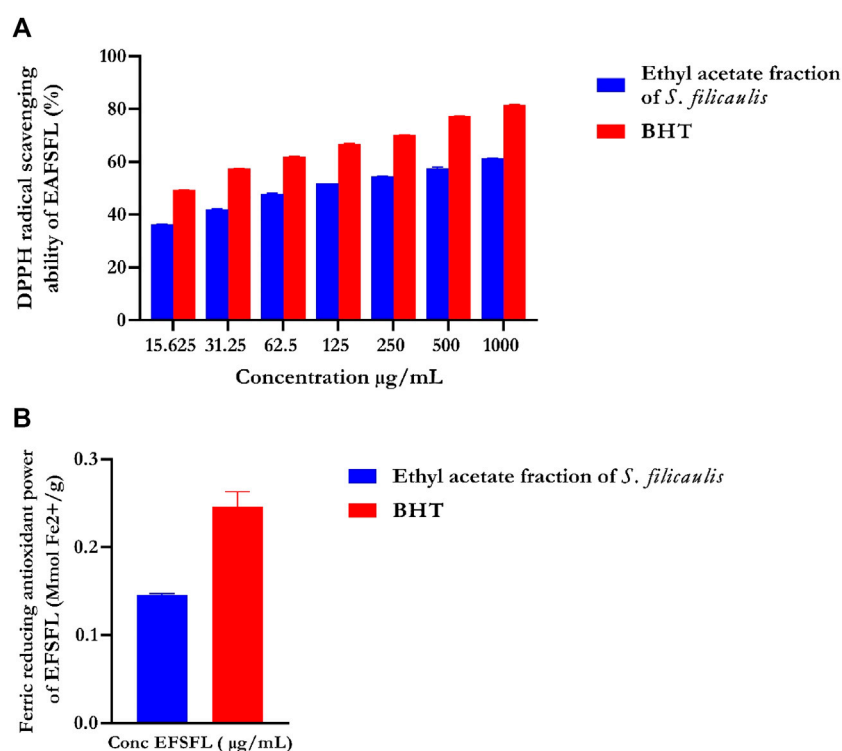


FIGURE 1

In vitro antioxidant activities of ethyl acetate fraction of *S. filicaulis* leaf. (A) DPPH radical scavenging ability and (B) ferric reducing antioxidant power. Legends: Data are represented as mean \pm SD ($n = 3$). EFSFL: ethyl acetate fraction of *S. filicaulis*; BHT: butylated hydroxytoluene.

TABLE 1 IC_{50} values of ethyl acetate fraction of *S. filicaulis* leaves against DPPH, FRAP, α -amylase, α -glucosidase, membrane stabilization, protein denaturation, and proteinase inhibition.

Activity	Plant extract/Standard	IC_{50} ($\mu\text{g/mL}$)
DPPH	EFSFL	274.32
	BHT	16.11
α -amylase	EFSFL	169.77
	Acarbose	121.79
α -glucosidase	EFSFL	293.12
	Acarbose	189.75
Dipeptidyl peptidase-IV	EFSFL	380.94
	Evogliptin	211.35
Membrane stabilization	EFSFL	572.79
	Diclofenac	3.74
Protein denaturation	EFSFL	409.88
	Diclofenac	58.90
Proteinase inhibition	EFSFL	319.90
	Diclofenac	154.66

EFSFL, ethyl acetate fraction of *S. filicaulis*

default values, the binding site coordinates of the target enzymes are shown in [Supplementary Table S1](#), and the molecular interactions were viewed using Discovery Studio Visualizer version 16.

2.8.5 Molecular dynamics

For ensemble-based docking, the DPP IV, HPA, and HG apoenzymes were subjected to a 50 ns simulation of molecular dynamics. The MD trajectory obtained was also used in cluster analysis. GROMACS 2019.2 and GROMOS96 43a1 forcefield (Lee et al., 2016; Lee et al., 2017; Lee et al., 2020) were used for the analysis. We generated protein and ligand topology files using the Charmm GUI (Lee et al., 2016; Lee et al., 2020). The solvation system, periodic boundary conditions, physiological conditions, minimization of the systems, and equilibration in a constant number of atoms, constant pressure, and constant temperature (NPT) used in the simulation are similar to those in our previous report (Gyebi et al., 2021; Ogunyemi et al., 2021; Ogunlakin et al., 2023; Ogunyemi et al., 2023). Velocity rescales and Parrinello-Rahman barostat were used to maintain the temperature and pressure at 310 K and 1 atm, respectively. We used a 2-femtosecond time step with a leap-frog integrator. Each system underwent a 100 ns simulation, with snapshots taken every 0.1 nanosecond and totaling 1000 frames for each system. From the MDs trajectories, the RMSD and RMSF were computed and presented as [Supplementary Material](#).

2.8.6 Molecular dynamic trajectory clustering of unattached proteins

A representative conformation that was obtained from the generated cluster from the clustering of the 500 ns MD trajectories of the unbound enzymes was employed for

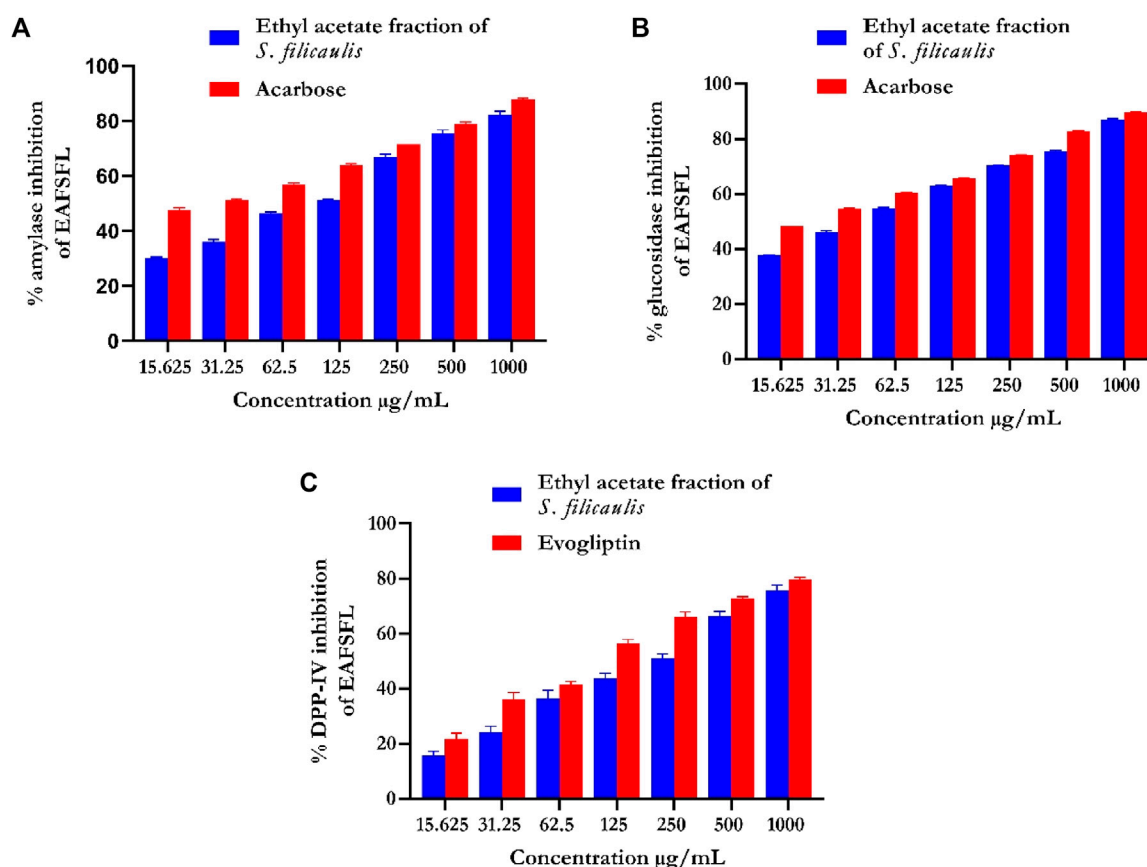


FIGURE 2

In vitro antidiabetic activities of ethyl acetate fraction of *S. filicaulis* leaf. (A) α-amylase inhibition, (B) α-glucosidase inhibition, and (C) dipeptidyl peptidase-4 (DPP-4) inhibition. The bar chart illustrates the percentage of proteinase activity inhibition. The data from three separate assays are presented as mean ± SD.

ensemble-docking studies. We performed the MD simulation trajectory clustering using TTClust V 4.9.0 (Lee et al., 2020). The systems were automatically clustered using the Python TTClust package, which uses the elbow approach to establish the ideal number of clusters before generating a representative frame for each cluster.

2.8.7 Ensembled-based docking of the GCMS identified phytochemicals to different conformations of the enzymes

Using the AutoDock Vina program (Trott and Olson, 2010), the phytocompounds identified by GCMS were docked to the various representative conformers of DPP IV (4), HPA (2), and HG (4). The average binding affinities of the phytochemicals to each of the proteins were computed from the binding affinities of the phytochemicals to each of the conformations of the enzymes. The average binding energies of the compounds for the two targets were calculated and then their affinities were scored. The Discovery Studio Visualizer, BIOVIA 2020, was used to see how the lead chemicals interacted with one another on a molecular level.

2.8.8 Physicochemical properties and ADMET in silico study

The top two phytochemicals of each protein were then analyzed for ADMET filtering and drug-likeness using a variety of descriptors. SwissADME was used for the drug-likeness analysis using Lipinski filtering methods (<http://www.swissadme.ch/index.php>) on the webserver, while the anticipated toxicity, distribution, metabolism, and absorption (ADME/tox) study was analyzed with the SuperPred webserver (<http://lmmd.ecust.edu.cn/admetzar1/predict/>). The SDF file and the canonical SMILES of the compounds were downloaded from the PubChem database or copied from ChemDraw to calculate the ADMET properties using default parameters.

2.9 Statistical analysis

The data was analyzed with software called GraphPad Prism version 9.0.1. We reported descriptive statistics as mean ± SD. GraphPad was used to analyze the results, which are presented as graphs. To compare the means, a statistical method known as one-way ANOVA was followed by Tukey's *post hoc* test with a significance level of $p < 0.05$.

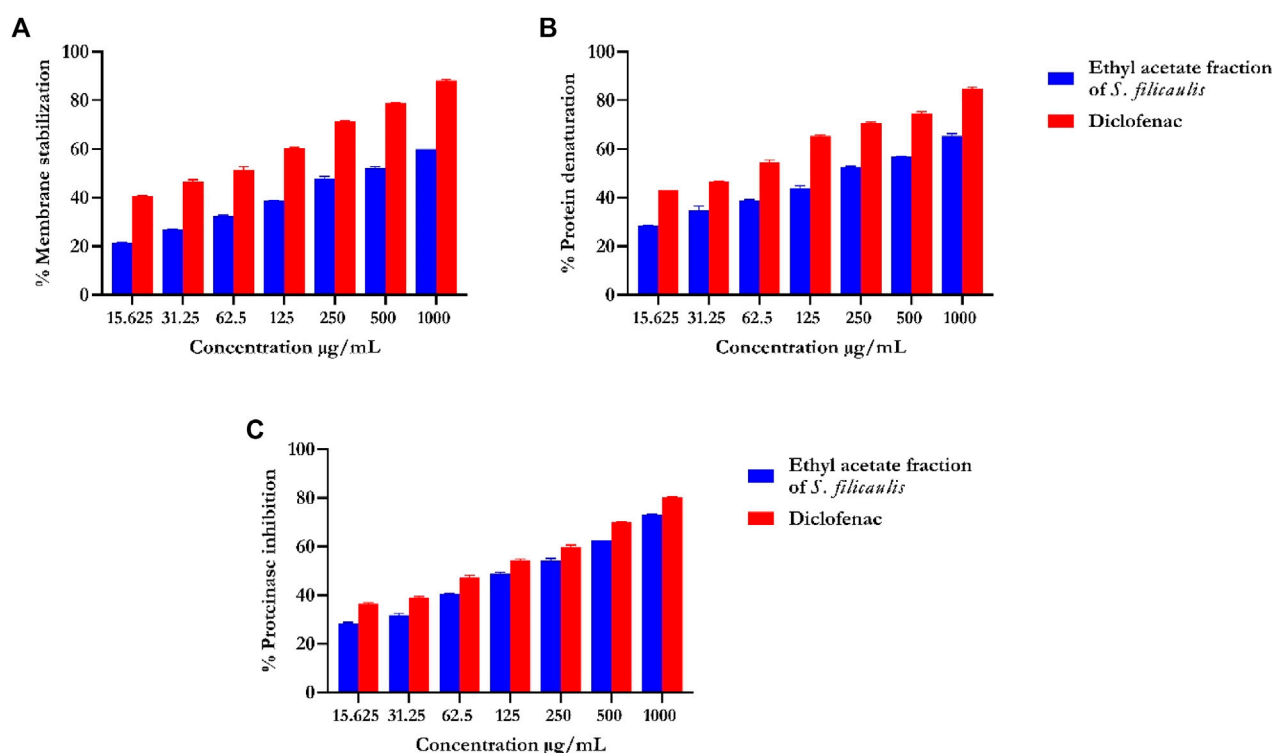


FIGURE 3

In vitro inflammatory activities of ethyl acetate fraction of *S. filicaulis* leaf. (A) Membrane stabilization, (B) inhibition of protein denaturation, and (C) proteinase inhibitory activity by Legend: The bar chart illustrates the percentage of proteinase activity inhibition. The data from three separate assays are presented as mean \pm SD (n = 3).

3 Results

3.1 1,1-Diphenyl-2-picrylhydrazyl (DPPH) quenching ability

DPPH, an unvarying radical, is commonly utilized to assess the effectiveness of antioxidants derived from plant sources. Figure 1A illustrates the percentage inhibition of DPPH scavenging ability by EFSFL at different concentrations. EFSFL exhibited a significant ability to counteract the DPPH radical, with an IC_{50} value of 46.40 ± 5.31 μ g/mL. Comparatively, the IC_{50} value of butylated hydroxytoluene (BHT), was 15.76 ± 0.58 μ g/mL, as indicated in Table 1.

3.2 Ferric reducing antioxidant power (FRAP) of EFSFL

The FRAP assay was used to assess the ferric-reducing potential of EFSFL. The results demonstrated increased FRAP activities at the highest concentration studied, 1000 μ g/mL. Standard butylated hydroxytoluene (BHT) showed the highest reducing property compared to MESFL (Figure 1B).

3.3 *In vitro* anti-diabetic studies

3.3.1 Evaluation of α -amylase inhibition

EFSFL efficiently blocked α -amylase in a concentration-dependent manner and had an IC_{50} value of 307.02 ± 4.25 μ g/mL compared with those of the standard (Figure 2A; Table 1). Acarbose revealed an 87.94% inhibitory property of α -amylase (IC_{50} 121.79 ± 2.26 μ g/mL) (Figure 2A; Table 1).

3.3.2 Evaluation of α -glucosidase inhibition

EFSFL efficiently inhibited α -glucosidase at all concentrations tested and an IC_{50} value of 215.51 ± 0.47 μ g/mL (Figure 2B; Table 1). Acarbose revealed an 89.68% inhibitory property of α -glucosidase (IC_{50} 189.79 ± 0.67 μ g/mL) (Figure 2B; Table 1).

3.3.3 Evaluation of DPP-IV inhibitory activity of ethyl acetate fraction of *S. filicaulis* leaf

Figure 2C shows the DPP-IV inhibitory activity of EFSFL. With an IC_{50} value of 380.94 μ g/mL (Table 1), EFSFL inhibited DPP-IV in a concentration-dependent manner. The EFSFL DPP-IV inhibitory activity, however, was less potent than that of the standard DPP-IV inhibitor, evogliptin (IC_{50} = 211.35 μ g/mL).

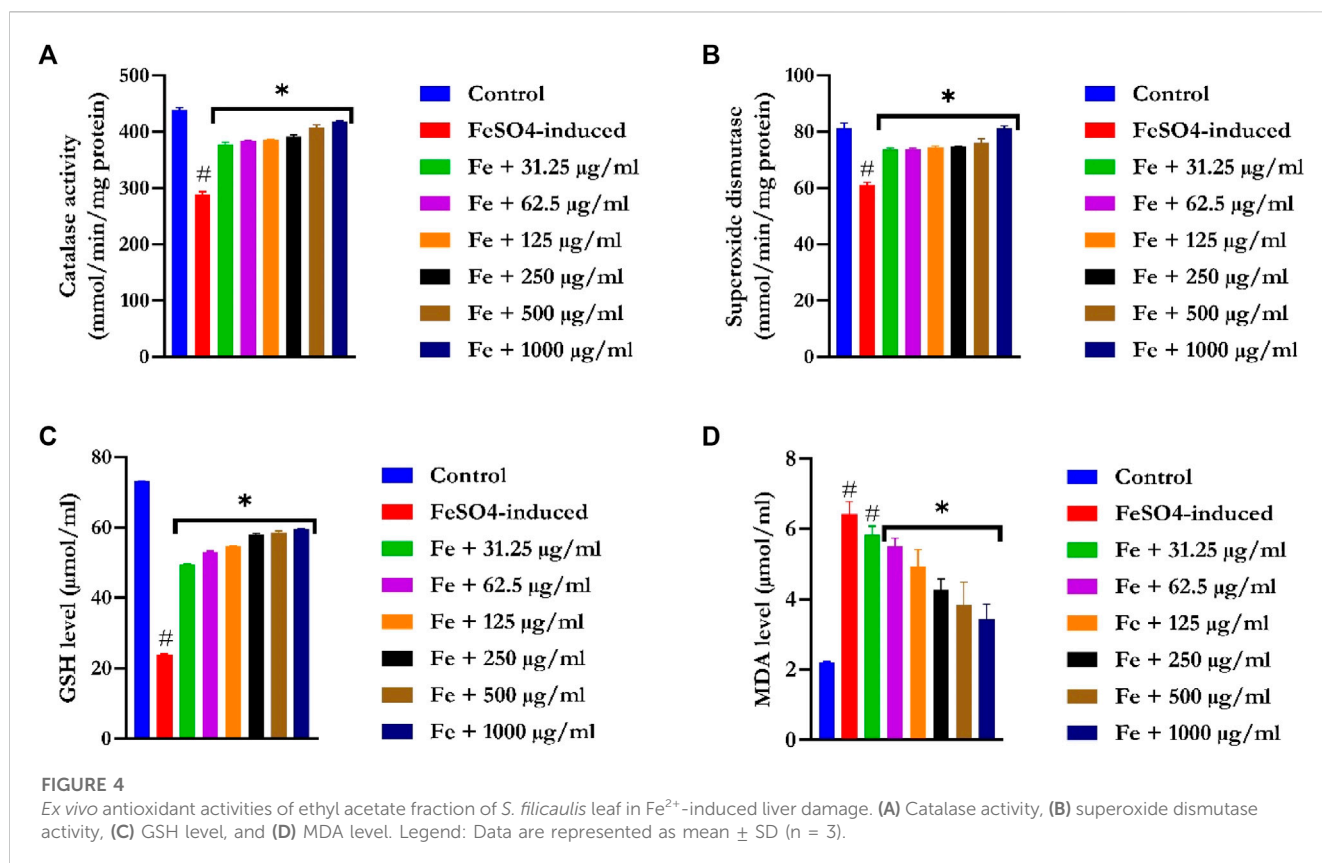


TABLE 2 GC-MS predicted compounds of ethyl acetate fraction of *S. filicaulis* leaves with their molecular weight, formula, and peak area (%).

S/N	R.T	Compound	Molecular formula	Molecular weight	Area (%)
1	11.142	Cycloheptasiloxane, tetradecamethyl-	$\text{C}_{14}\text{H}_{42}\text{O}_7\text{Si}_7$	519.08	3.96
2	12.247	Benzocycloheptano[2,3,4-I,j]isoquinoline, 4,5,6,6a-tetrahydro-1,9-dihydroxy-2,10-dimethoxy-5-methyl-	$\text{C}_{20}\text{H}_{23}\text{NO}_4$	314.40	0.09
3	12.472	Erucic acid	$\text{C}_{22}\text{H}_{42}\text{O}_2$	338.60	0.82
4	12.994	Spilanthol	$\text{C}_{14}\text{H}_{23}\text{NO}$	221.34	0.80
5	13.159	Octadec-9-enoic acid	$\text{C}_{18}\text{H}_{34}\text{O}_2$	282.50	0.38
6	13.243	Petroselaidic acid	$\text{C}_{18}\text{H}_{34}\text{O}_2$	282.50	0.17
7	13.486	α -caryophyllene	$\text{C}_{15}\text{H}_{24}$	204.35	0.58
8	14.071	Oleic Acid	$\text{C}_{18}\text{H}_{34}\text{O}_2$	282.50	3.96
9	14.680	2-Methyl-Z,Z-3,13-octadecadienol	$\text{C}_{19}\text{H}_{36}\text{O}$	280.50	3.72
10	15.098	cis-9-Hexadecenoic acid	$\text{C}_{16}\text{H}_{30}\text{O}_2$	254.41	0.89
11	15.312	Pinene	$\text{C}_{10}\text{H}_{16}$	136.23	0.57
12	16.776	Piperine	$\text{C}_{17}\text{H}_{19}\text{NO}_3$	284.34	16.45
13	17.078	Ocimene	$\text{C}_{10}\text{H}_{16}$	136.23	10.73

TABLE 3 Binding energies of GCMS phytoconstituents identified from ethyl acetate fraction of *S. flicaulis* leaves against human dipeptidyl peptidase IV (DPP IV), α -amylase and α -glucosidase.

S/No	Compound	Binding energy (Kcal/mol)		
		DPP IV	HG	HPA
S1	Acarbose_1b2y (E = 376.73)		−10.6	−8.3
S2	Evogliptin (E = 415.60)	−7.8		
1	alpha-caryophyllene (E = 1912.23)	−7.8	−9.6	−7.4
2	Piperine (E = 356.64)	−7.8	−8.9	−7.8
3	Petroselaidic_acid (E = 84.42)	−7.5	−8.8	−5.3
4	Pinene (E = 661.52)	−5.8	−6.6	−5.5
5	2-Methyl-Z,3, 13-octadecadienol (E = 123.57)	−4.9	−6.4	−5.9
6	Octadec-9-enoic_acid (E = 69.17)	−4.7	−6.2	−5.6
7	Spilanthol (E = 103.48)	−4.9	−6.1	−6
8	Erucic_acid (E = 99.56)	−5.7	−6.1	−5.4
9	Cycloheptasiloxane, tetradecamethyl	−5.6	−6.1	−5.2
10	Ocimene (E = 113.15)	−5	−6.1	−5.1
11	Benzocycloheptano[2,3,4-I,j]isoquinoline, 4,5,6,6a-tetrahydro-1,9-di hydroxy-2,10-dimethoxy-5-methyl (BCQDM)	−5.7	−6	−7.9
12	cis-9-Hexadecenoic_acid (E = 85.30)	−5.2	−5.9	−5.6
13	Oleic_Acid (E = 81.73)	−4.5	−5.7	−5.5

3.4 In vitro anti-inflammatory analysis

3.4.1 Human red blood cell (RBC; HRBC) membrane stabilization test

Our data revealed that the EFSFL demonstrated HRBC membrane stabilization potential ($IC_{50} = 319.85 \pm 4.54 \mu\text{g/mL}$) in a concentration-dependent manner. The standard drug, diclofenac, showed 89.68% membrane stabilization potential ($IC_{50} = 3.63 \pm 1.32 \mu\text{g/mL}$) (Figure 3A; Table 1).

3.4.2 Inhibition of protein denaturation

Our analysis also revealed concentration-dependent increases in the inhibition of protein denaturation ($IC_{50} = 72.75 \pm 11.06 \mu\text{g/mL}$) by EFSFL. The standard drug, diclofenac, also exhibited protein denaturation inhibition ($IC_{50} = 59.13 \pm 12.40 \mu\text{g/mL}$) (Figure 3B; Table 1).

3.4.3 Proteinase inhibitory assay

Our analysis revealed that EFSFL exhibited significant proteinase inhibitory activities ($IC_{50} = 296.08 \pm 11.47 \mu\text{g/mL}$). The standard drug, diclofenac, also exhibited proteinase inhibitory activities ($IC_{50} = 154.62 \pm 4.29 \mu\text{g/mL}$) (Figure 3C; Table 1).

3.5 Ex vitro antioxidant analysis

3.5.1 Evaluation of catalase activity

Figure 4A showed a significant ($p < 0.05$) reduction in CAT activities in the liver tissues of FeSO_4 -induced animals. Treatment with EFSFL concentration-dependently ($p < 0.05$) increased the

activity in a significant manner, with the most pronounced activity found in the 1000 $\mu\text{g/mL}$ treated group.

3.5.2 Evaluation of superoxide dismutase activity

SOD activities were significantly ($p < 0.05$) reduced in the liver tissues of FeSO_4 -induced animals (Figure 4B). Treatment with EFSFL dose-dependently ($p < 0.05$) elevated SOD activity in a manner close to that of the normal group.

3.5.3 Evaluation of reduced glutathione

GSH levels were drastically ($p < 0.05$) decreased in the liver tissues of FeSO_4 -induced animals (Figure 4C). In contrast, EFSFL-treated groups significantly ($p < 0.05$) increased the levels of GSH in a manner close to the normal group, with the most pronounced effect found in the 1000 $\mu\text{g/mL}$ treated group.

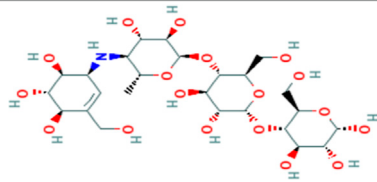
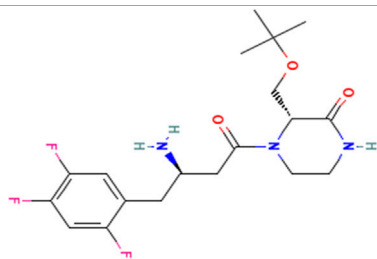
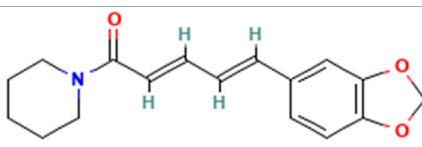
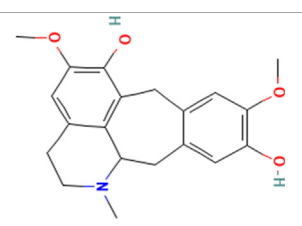
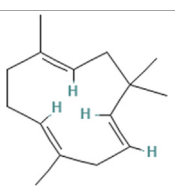
3.5.4 Determination of malondialdehyde level

The MDA level was notably increased in the liver tissues of FeSO_4 -induced animals (Figure 4D). In contrast, EFSFL-treated groups significantly ($p < 0.05$) reduced the level of malondialdehyde to near normal, with the most striking effect found in the 1000 $\mu\text{g/mL}$ treated group.

3.6 GC-MS analysis

EFSFL underwent GC-MS analysis to determine its phytoconstituents. By contrasting the GC-MS spectra with a

TABLE 4 Top two ranked compounds from the molecular docking of the GCMS-identified phytoconstituents from ethyl acetate fractions of *S. filicaulis* leaves against human dipeptidyl peptidase IV (DPP IV), α -amylase and α -glucosidase.

S/No	Name	Structure
	Acarbose	
1	Evogliptin	
1	Piperine	
2	Benzocycloheptano[2,3,4-I,j]isoquinoline, 4,5,6,6a-tetrahydro-1,9-dihydroxy-2,10-dimethoxy-5-methyl (BCQDM)	
3	α -caryophyllene	

reference library (NIST), 13 compounds were identified and are listed in Table 2. The two most abundant compounds in EFSFL were piperine (16.45%) and ocimene (10.73%). Cycloheptasiloxane, tetradecamethyl- (3.96%) oleic acid (3.96%), and 2-Methyl-Z,Z-3,13-octadecadienol (3.72%) were found in small amounts, whereas Benzocycloheptano[2,3,4-I,j]isoquinoline, 4,5,6,6a-tetrahydro-1,9-dihydroxy-2,10-dimethoxy-5-methyl- (−0.09%), erucic acid (0.82%), spilanthal (0.80%), octadec-9-enoic acid (0.38%), petroselaidic acid (0.17%), α -caryophyllene (0.58%), 2-methyl-Z,Z-3,13-octadecadienol (0.89%), and cis-9-Hexadecenoic acid (0.57%) were present in minute amounts. The GC-MS chromatograms of the phytocompounds are displayed in the Supplementary Material (Supplementary Material S1).

3.7 Molecular docking studies

3.7.1 Docking protocol validation

The protocol to be used was validated to predict the precision, reliability, and accuracy of the docking protocol (Ogunyemi et al., 2023) before the docking of the GCMS-identified compounds to the target proteins. The generated docked poses of the reference compounds having the least energetic conformation were superimposed on the native ligand that was co-crystallized. After the superimposition, the root-mean-square deviation (RMSD) was computed. The RMSD, or acarbose complexed with 5y7K and 3top, was 3.5651 and 0.4341 Å respectively. The low RMSD shows that the docking protocol was suitable for the docking of phytochemicals (Supplementary Figure S2).

TABLE 5 Interaction of amino acid residues of dipeptidyl peptidase IV, α -amylase, and α -glucosidase with the top two GCMS-identified phytoconstituents from ethyl acetate fraction of *S. filicaulis* leaves.

Compounds	Protein		Hydrogen bonds (Bond distance (Å))		Hydrophobic interaction (Bond distance (Å))
		Numbers	Interacting residues	Numbers	Interacting residues
Evogliptin	DPP IV	8	His126 Glu206 Arg125 Glu205 Ans10	3	Phe357 Tyr666 Tyr662
alpha-caryophyllene		1	Ser209	1	Phe357
Piperine		2	Tyr662 Tyr547	3	Tyr666 Arg358 Arg356
Acarbose	HPA	18	Trp59 (2) Gln63 Tyr62 Thr163 Arg195 Asp197 Lys200 (2) Glu233 Asp300 Gly30 His299 Glu233 Ile235 (2) Glu240 Gly306 His305	1	Trp59
Piperine		0		3	Tyr62 Gln63 Trp59 Ala198
Benzocycloheptano [2,3,4-I,j] isoquinoline, 4,5,6,6a- tetrahydro-1,9-di			Asp197 Glu233 Arg195 Ala198 His305	2	Asp300 Tyr62
hydroxy-2,10- dimethoxy-5- methyl (BCQDM)					
Acarbose	HG	14	Arg1582 Arg1510 Asp1526 Tyr1167 Met1421 Asp1157 Lys1460 Gln1561 Thr1528 Trp1355 Asp1279 His1584 Asp1317 Asp1555	3	Tyr1251 Phe1559 Phe1560
Piperine		2	Lys1460 Arg1510	5	Phe1427 Trp1369 Ile1280 Trp1355 Tyr1251
alpha-caryophyllene		0		2	Phe1560 Trp1355

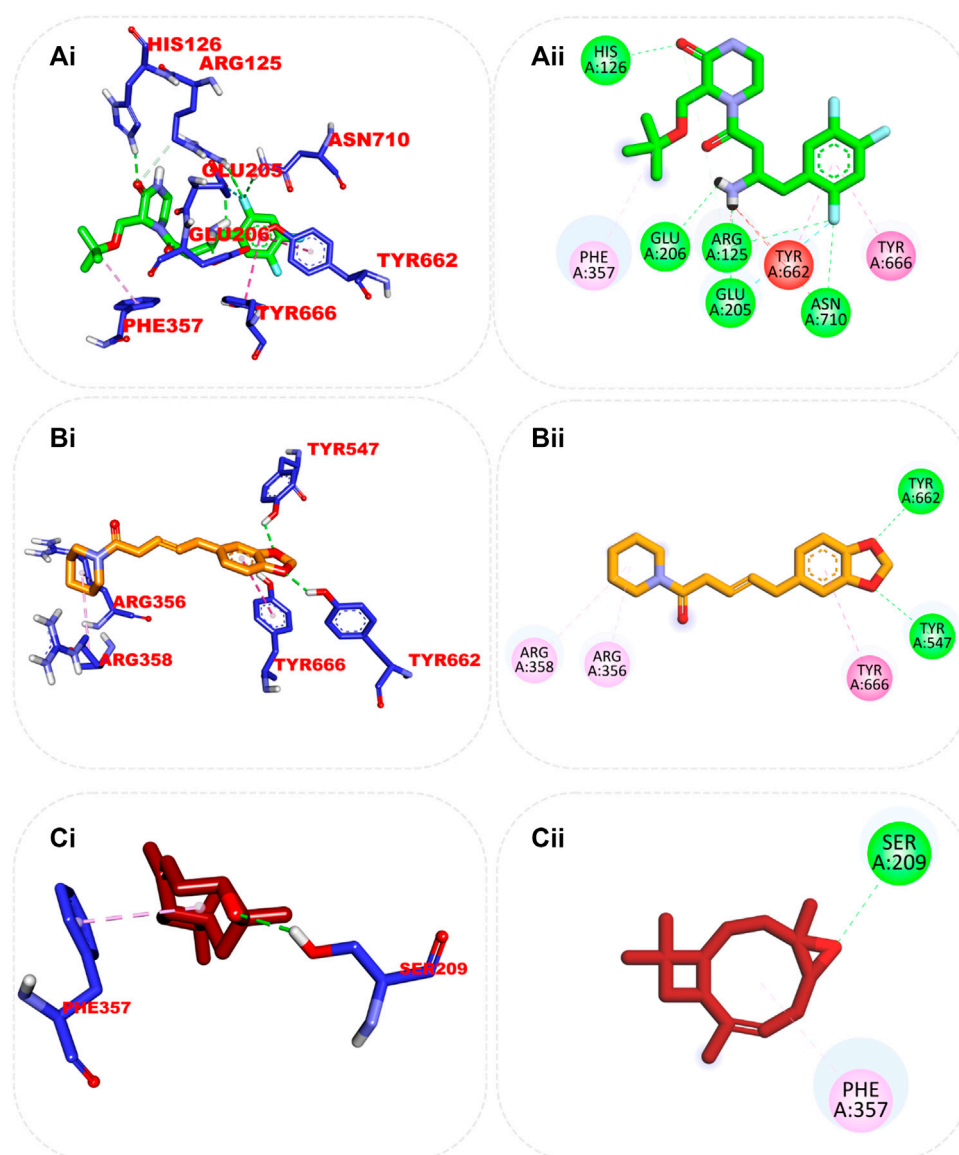


FIGURE 5

Top ranked secondary metabolites and reference blocker (acarbose) from the docking analysis of GCMS phytochemicals from ethyl acetate fraction of *S. filicaulis* leaves in a human's active site dipeptidyl peptidase IV. The ligands are displayed as sticks and distinguished by their colors (Ai) 3D interaction of evogliptin (reference inhibitor) is presented in green, (Aii) 2D interaction of evogliptin, (Bi) 3D interaction of alpha-caryophyllene is presented in gold (Bii) 2D interaction of alpha-caryophyllene, and (Ci) 3D interaction of piperine is shown in red (Cii) 2D interaction of piperine.

3.7.2 Molecular docking of identified compounds against human dipeptidyl peptidase IV, α -amylase, and α -glucosidase

Table 3 shows the docking affinities of the 13 GCMS-identified phytochemicals from EFSFL and the reference molecule (acarbose) against DPP IV, HPA, and HG. Based on the lowest binding energies, binding poses, and interactions in the catalytic site, the top two ranked phytochemicals for each enzyme were selected for interactive analysis (Table 4). The two top docked phytochemicals to the DPP IV are alpha-caryophyllene and piperine, with binding affinity values of -7.8 and -7.8 Kcal/mol, respectively, compared to the

reference inhibitor (evogliptin) (-7.8 Kcal/mol). Alpha-caryophyllene and piperine were the top-ranked phytochemicals for HG, with binding affinities of -9.6 and -8.9 Kcal/mol, respectively, compared to the reference inhibitor (acarbose), which had a binding affinity of 10.6 Kcal/mol. For HPA, the top-ranked phytochemicals were piperine and benzocycloheptano[2,3,4-I,j]isoquinoline, 4,5,6,6a-tetrahydro-1,9-dihydroxy-2,10-dimethoxy-5-methyl, with binding affinities of -7.8 and -7.9 Kcal/mol, compared to acarbose, which had a binding affinity of -8.3 Kcal/mol. The results from the initial docking studies showed that alpha-caryophyllene and piperine had high multi-target binding tendencies (Table 4).

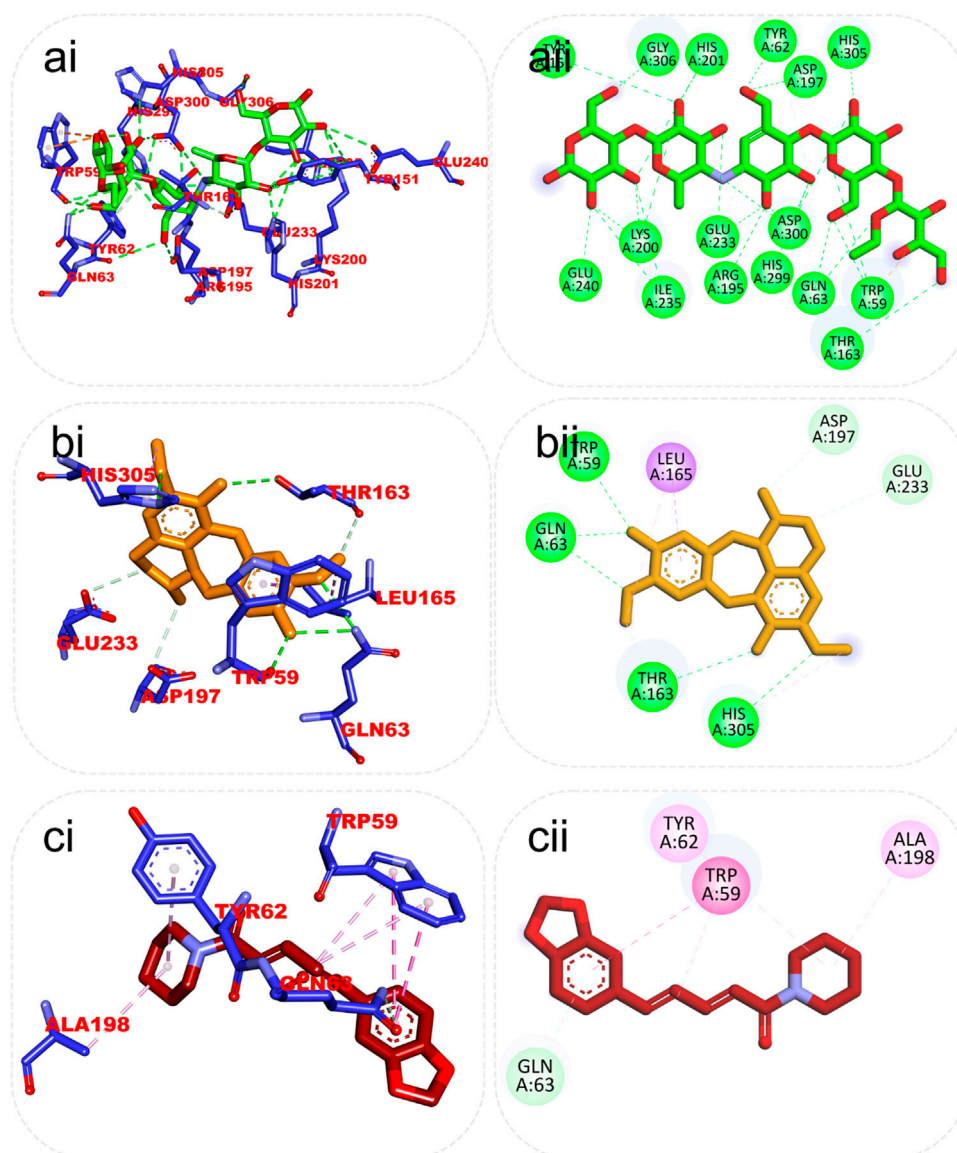


FIGURE 6

Top ranked secondary metabolites and reference inhibitor (acarbose) from the docking analysis of GCMS phytochemicals from ethyl acetate fraction of *S. filicaulis* leaves found to interact with the active site of human α -amylase. The ligands are displayed as sticks and distinguished by their colors (Ai) 3D interaction of acarbose is shown in green, (Aii) 2D interaction of acarbose, (Bi) 3D interaction of Benzocycloheptano[2,3,4-l]isoquinoline, 4,5,6,6a-tetrahydro-1,9-dihydroxy-2,10-dimethoxy-5-methyl is shown in gold, (Bii) 2D interaction of Benzocycloheptano[2,3,4-l]isoquinoline, 4,5,6,6a-tetrahydro-1,9-dihydroxy-2,10-dimethoxy-5-methyl, and (Ci) 3D interaction of piperine is shown in red, (Cii) 2D interaction of piperine.

3.7.3 Amino acid interaction of top docked compounds with human dipeptidyl peptidase IV (DPP IV), α -amylase, and α -glucosidase

The interaction of the reference compound and two top-docked phytochemicals with amino acids of the catalytic residues of DPP IV, HPA, and HG is represented in Table 5. The interaction of respective ligand groups with residues of the enzymes was majorly hydrophobic, with a few H-bonds below (less than 3.40 Å). Top-docked compounds were oriented in the active site of DPP IV and interacted with the amino acid to which we docked the reference compound. The interaction

between α -caryophyllene and DPP IV was stabilized by a hydrogen bond with Ser209 and a hydrophobic contact with Phe357, while piperine formed two hydrogen bonds with Tyr662 and Tyr547 and pi-alkyl hydrophobic Tyr666, Arg358, and Arg356 (Figure 5).

Although the orientation of acarbose in the binding site of HPA was stretched into the five subsites, the top docked phytocompounds piperine and 4-hydroxy-3-methylacetophenone were docked into the -3 and -1 subsets of the α -amylase. Piperine did not establish hydrogen bonds like the reference compounds, but it did interact with the catalytic

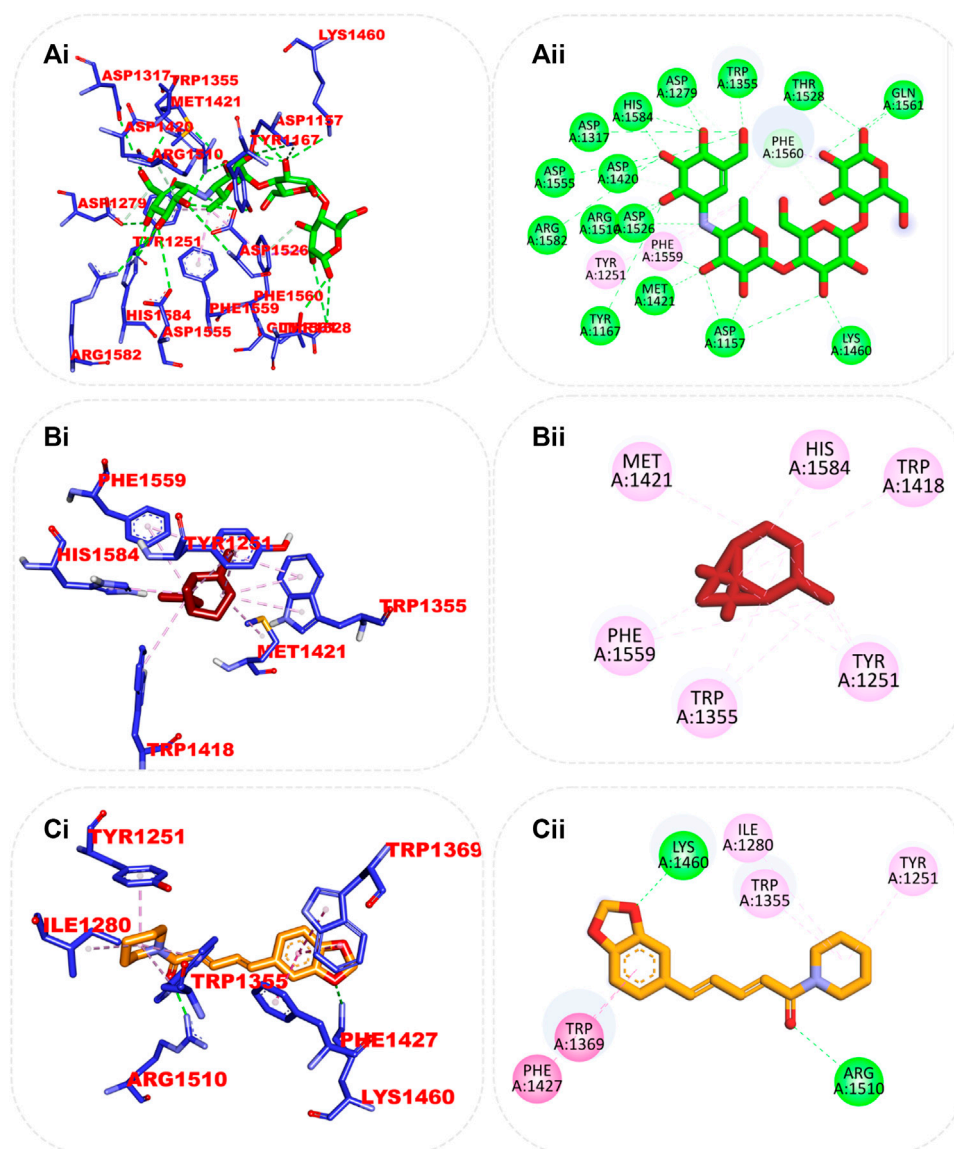


FIGURE 7

Top ranked secondary metabolites and reference inhibitor (acarbose) from the docking analysis of GCMS phytochemicals from ethyl acetate fraction of *S. filicaulis* leaves in the active site of human α -glucosidase. The ligands are displayed as sticks and distinguished by their colors (Ai) 3D interaction of acarbose is shown in green, (Aii) 2D interaction of acarbose, (Bi) 3D interaction of alpha-caryophyllene is presented in red, (Bii) 3D interaction of alpha-caryophyllene, and (Ci) 3D interaction of piperine is presented in gold, (Cii) 2D interaction of piperine.

residues at the hydrophobic gate of α -amylase, which are Trp-59, Tyr62, and His299. BCQDM made several hydrogen bonds with the catalytic residues, including Asp197, Glu233, Arg195, Ala198, and His305; a pi-sigma contact with Leu165; and carbon hydrogen contacts with Asp197 and Glu233 (Figure 6). The piperine formed one hydrogen bond with Lys1460 and Arg1510, pi-pi stacking, and pi-pi-T-shaped stacking with Phe1427 and Trp1369 of HG. The 1-piperoyl moiety made pi-alkyl contact with Trp1355 and alkyl contact with Ile1280 and Tyr1251. While the bond between alpha-caryophyllene and HG with pi-alkyl contact with Phe1560 and Trp1355 (Figure 7).

3.7.4 Cluster analysis and ensemble-based docking of GCMS-identified phytoconstituents from ethyl acetate fraction of *S. filicaulis* leaves with conformers of dipeptidyl peptidase IV, α -amylase, and α -glucosidase enzyme

From the trajectories obtained from the MDS analysis of the dipeptidyl peptidase IV, α -amylase, and α -glucosidase enzymes, the RMSD and RMSF plots were calculated to measure the extent of fluctuation during the simulation period (Supplementary Figures S3, S4). We obtained 1000 conformers of the 1000 frames from the MD simulation trajectories using TTclust to provide 4, 2, and 4 clusters for dipeptidyl peptidase, α -amylase, and α -glucosidase, respectively.

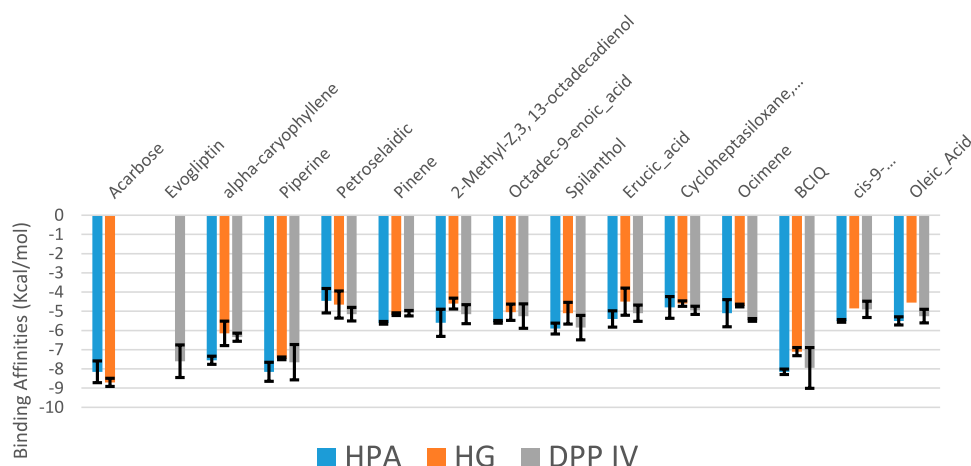


FIGURE 8

Average binding energies of the acarbose, evogliptin, and GCMS-identified phytoconstituents against representative conformation obtained from the clustering analysis of the MD simulation trajectories of DPP IV, α -amylase and α -glucosidase enzyme. Clusters counts for HPA (2), HG (4) and DPP IV (4)

The [Supplementary Material](#) shows the dimensions of the cluster, which are the number of individual frames that make up the clusters, the number of frames of the representative conformation, and the spread, which is the average distance among the conformations that make up the cluster. From these clusters, representative conformations were selected. An ensemble docking was performed by docking the phytochemicals to the representative structures of the various conformers. We calculated the mean and standard deviation for each enzyme of the phytochemical docking scores with minimal energy for each conformation (Figure 8). The results of the ensemble-based docking analysis further confirmed piperine as the phytochemical with the highest binding affinities to DPP IV (-7.65 ± 0.92 Kcal/mol), α -amylase (-8.15 ± 0.50 Kcal/mol), and α -glucosidase (-7.45 ± 0.468 Kcal/mol), while benzocycloheptano[2,3,4-I,j]isoquinoline, 4,5,6,6a-tetrahydro-1,9-dihydroxy-2,10-dimethoxy-5-methyl was the second top docked phytochemical to DPP IV (-7.95 ± 1.06 Kcal/mol), α -amylase (-8.14 ± 0.05 Kcal/mol), and α -glucosidase (-7.1 ± 0.14 Kcal/mol) respectively. The representative cluster with the lowest binding affinities to the best-docked phytochemicals was selected for interactive analysis and is presented in Figure 9.

3.7.5 Top-docked steroidal saponins' drug-likeness and pharmacokinetic characteristics

Predictive drug-likeness and ADMET (absorption, distribution, metabolism, excretion, and toxicity) filtering studies were conducted on the two hit compounds that were obtained from the ensemble-based docking analysis. The results are shown in [Supplementary Tables S2, S3](#). The two top-docked phytochemicals, piperine and BCQDM, fulfilled the requirement for the four filters (Lipinski, Veber, Ghose, and Egan), hence they are predicted to have favorable druggable properties.

Piperine and BCQDM were further subjected to predictive ADMET analysis. The substantial gastrointestinal absorption of piperine and BCQDM suggests high bioavailability. Both piperine and BCQDM demonstrated the ability to cross the blood-brain

barrier, which is a crucial characteristic of medications used for neurotherapeutic purposes ([Supplementary Table S2](#)). Piperine and BCQDM were predicted to be negative substrates of the p-glycoprotein with very high plasma protein binding tendencies. A variety of molecular cytochrome P450 descriptors were employed to investigate the effects of lead metabolites on the biotransformation of drugs in the liver. It was concluded that these descriptors would not be inhibited by piperine and BCQDM. Lead compounds were neither mutagenic, carcinogenic, nor likely to cause skin sensitivity, according to the prediction analysis. The projected LD_{50} , half-life, and clearance rate of the lead phytochemicals fell within an acceptable range ([Supplementary Table S2; Figure 10](#)).

4 Discussion

The use of plant extracts is gaining attention in combating various diseases and ailments, and this is because of the vast phytochemicals present in them that help in mopping up the free radicals present in the systems of the body (Ojo et al., 2020). Oxidative stress arises because unpaired electrons in the system react with proteins and enzymes in a process called glycation (Ahmad et al., 2023). We expect this disease to have a double-digit prevalence in the coming years. It is therefore of great importance that the disease be managed properly to suppress its coming prevalence (Ajiboye et al., 2020). Phytochemicals (phenolics and flavonoids) are known constituents of plant tissues, and they are the main antioxidant driver in plants, which makes them very potent in combating oxidative stress-related diseases. It is no news that year in and year out, researchers have continued to link both phenolics and flavonoids to their antioxidant potential (Kosakowska et al., 2021). We screened the extract of the plant for potential phytochemicals, and we show the resulting outcomes in Table 2.

This research, for the first time, makes use of the leaf part of the *S. filicaulis* plant in a diabetic study, and according to the result of the

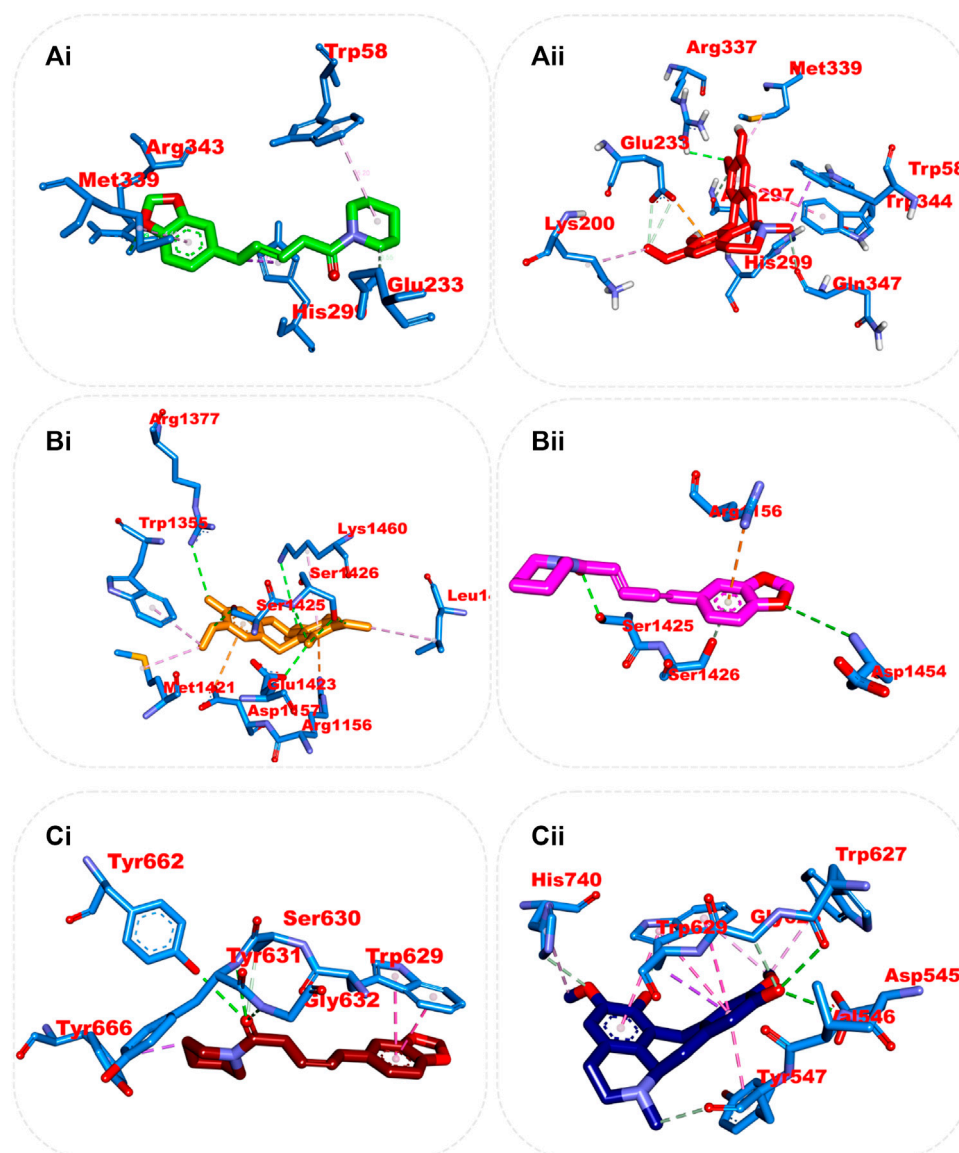


FIGURE 9

Amino acid interaction of two top docked phytochemicals (piperine and BCQDM) obtained from the ensemble-based docking studies with the representative conformation of (Ai) α -amylase with piperine, (Aii) α -amylase with BCQDM, (Bi) α -glucosidase with piperine, (Bii) α -glucosidase with BCQDM, and (Ci) DPP IV with the lowest binding affinity with piperine, (Cii) DPP IV and BCQDM.

in vitro analysis, DPPH scavenging radicals are well-known for their extraordinary scavenging ability, and from our fraction, it was observed that there was an elevated degree of DPPH quenching potential. This implies that EFSFL may contain beneficial antioxidants capable of removing free radicals from the system. FRAP analysis also signifies the potential of EFSFL to combat ROS, thus reducing the chances of oxidative stress. Our findings support earlier research that suggested plants with reducing and DPPH scavenging abilities do so because they can donate hydrogen to free radicals (Ajiboye et al., 2020; Ojo et al., 2020; Ojo et al., 2022; Ahmad et al., 2023).

In this study, we carried out the inhibition of α -amylase and α -glucosidase by EFSFL. The results analyzed showed that the plant extract expressed the inhibitory activity of these enzymes.

α -Amylase reduces the elevated level of glucose in the blood after eating by reducing the rate at which starch is converted to sugar. α -Glucosidase inhibitory potential was also increased in the extract, which shows that the plant has the potential to combat hyperglycemia (Kartini et al., 2023). They prevent the digestion of carbohydrates, and they are competitive inhibitors. Also, prevent the conversion of carbohydrates to glucose. According to the findings of this study, EFSFL was shown to possess chelating radical scavenging activities, such that as the concentration increases, the ion chelating ability also increases and the aqueous extract could chelate Fe^{2+} in a concentration-dependent manner. We could attribute this chelating ability to the existence of phytochemicals with antioxidant properties in the extract. According to (Sarkar et al., 2012; Ojo et al., 2022),

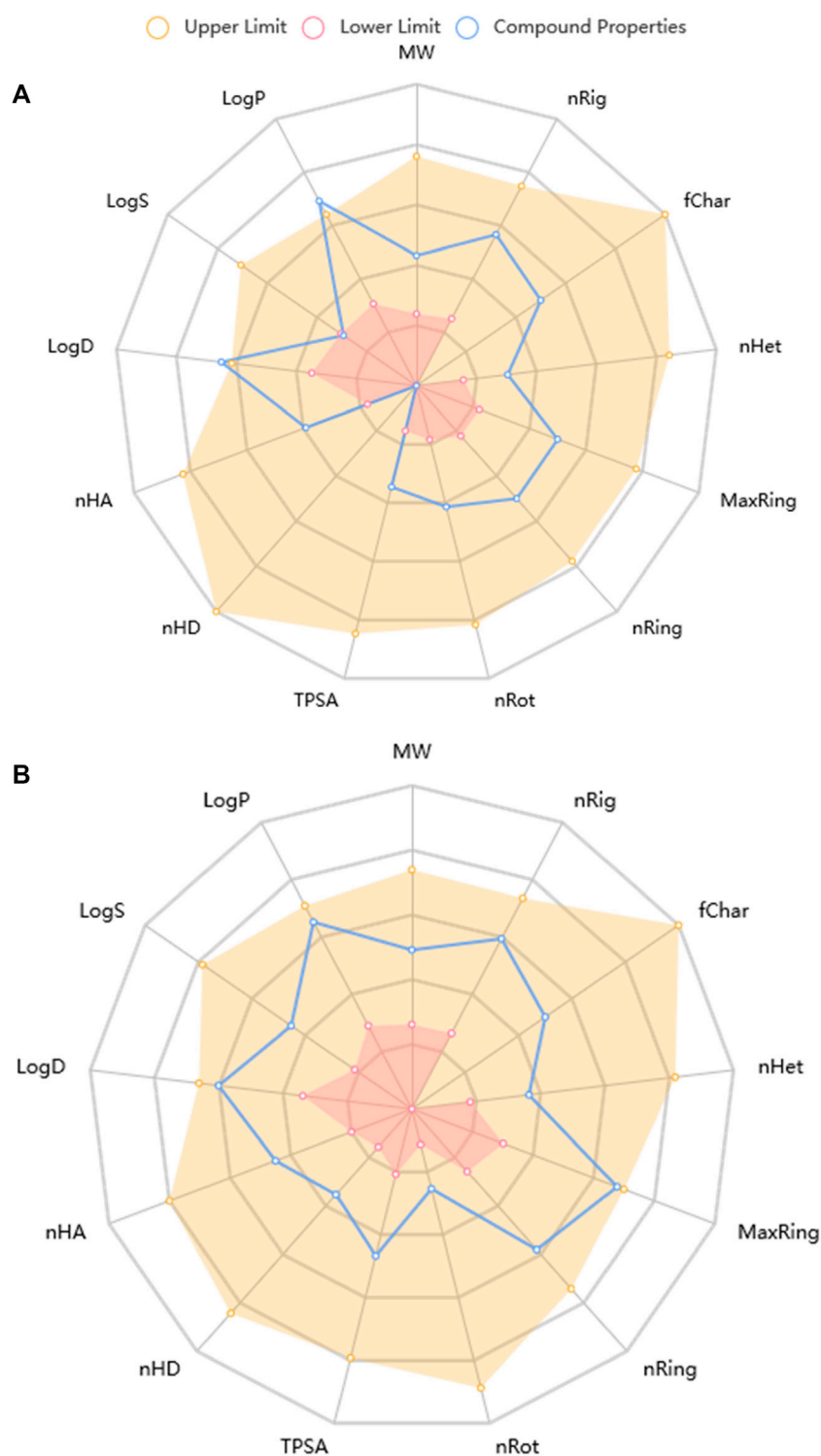


FIGURE 10

Physicochemical Property of top docked phytochemicals (A) Piperine and (B) Benzocycloheptano[2,3,4-l,j]isoquinoline, 4,5,6,6a-tetrahydro-1,9-dihydroxy-2,10-dimethoxy-5-methyl.

iron encourages the process of creating reactive oxygen species (ROS), which can stimulate the peroxidation of lipids. When iron II (Fe^{2+}) reacts with H_2O_2 through the Fenton reaction, it generates an extremely reactive hydroxyl radical. This radical

has detrimental effects on protein, lipid, and nucleic acid processes. As a result, EFSFL Fe^{2+} -chelating activity might be useful in managing or preventing disorders like neurological disorders.

DPP-IV inhibitors are a novel way to manage type 2 diabetes. The pre-meal insulin secretion stimulant glucagon-like peptide-1 (GLP-1) and the glucose-dependent insulintropic peptide (GIP) are both improved by DPP-IV inhibitors (Borde et al., 2016). DPP-IV inhibition has become an appealing treatment option because various DPP-IV inhibitors consistently lowered blood glucose, primarily postprandially, and this is connected with increases in active circulating glucagon-like peptide-1 (GLP-1) (Green et al., 2006). DPP-IV inhibitors increase GLP-1 and GIP, decreasing glucagon release, which boosts insulin secretion and decreases gastric emptying (Pathak and Brideman, 2010). Several studies have shown the anti-diabetic properties of medicinal plant extracts, but this is the first to indicate that the ethyl acetate fraction of *S. filicaulis* exhibits strong DPP-IV inhibitory activity. EFSFL showed concentration-dependent inhibition (the percentage of inhibition increases as the concentration increases) activity against DPP-IV in our study, with IC_{50} values of 380.94 μ g/mL. On the other hand, standard evogliptin exhibited strong action against DPP-IV with IC_{50} values of 211.35 μ g/mL. The inhibitory action of EFSFL was comparable to that of the synthetic DPP-IV inhibitor evogliptin. Thus, based on the findings, it is possible to conclude that EFSFL can be an excellent source of indigenously developed DPP-IV inhibitors. The action of EFSFL demonstrated its capacity to prevent incretin from being degraded by DPP-IV into metabolites devoid of insulin-releasing activity.

A molecular docking study of *S. filicaulis* leaf extract showed inhibitory activity on DPP-IV. The results of *in silico* analysis showed that there were two top compounds of ethyl acetate fraction of *S. filicaulis* leaf may serve as DPP inhibitors, that is, alpha-caryophyllene, and piperine. Their binding affinity values were favorable. The top two compounds, alpha-caryophyllene, and piperine, showed a low value in binding free energy. It means that the binding between ligand and molecule target is easy, which causes strong DPP-IV inhibitory activity. The low binding free energy means that these compounds can inhibit DPP-IV activity. We predicted a stronger biological activity for the compound with a higher binding value since it can bind both ligand and molecule targets. This shows comparable interactions and potency with evogliptin.

EFSFL demonstrated that the extract has the capability of stabilizing the membranes of lysosomes and hindering inflammation in tissues (Cigremis et al., 2009). The extract's ability to inhibit proteinases enhances its ability to inhibit tissue inflammation (Yazdanparast et al., 2008). The increased MDA level in the untreated tissue indicates lipid peroxidation, which is linked to catalase function depletion in the untreated tissue, which means there is a suppression of antioxidant potential. EFSFL treatment improved CAT, SOD activities, and GSH while decreasing MDA levels, indicating a protective effect against oxidative damage produced by ferric-induced oxidation. Previous reports on the use of plants as antioxidants in managing oxidative-related diseases found similar results (Han et al., 2013; Salekzamani et al., 2019; Yue et al., 2020; Tekin and Seven, 2022).

In this research work, the GCMS-identified phytochemicals were docked against DPP IV, HPA, and HG using both molecular docking and ensemble-based docking protocols. The result from the initial docking analysis identified alpha-caryophyllene, piperine, and benzocycloheptano[2,3,4-I,j]

isoquinoline, 4,5,6,6a-tetrahydro-1,9-dihydroxy-2,10-dimethoxy-5-methyl as the top docked phytochemicals to the three target proteins. The ensemble-based molecular docking approach in which the phytochemicals were docked to different conformational structures of the targeted proteins that were clustered from the MD simulation trajectory afforded a more in-depth analysis (Amaro et al., 2018) that further confirmed piperine and benzocycloheptano[2,3,4-I,j]isoquinoline, 4,5,6,6a-tetrahydro-1,9-dihydroxy-2,10-dimethoxy-5-methyl as the top docked phytochemicals. We found these compounds to be strongly bound to the catalytic residues of the enzymes. The DPP IV top-docked compounds interacted with residues in the S1 hydrophobic pocket and some residues (Tyr662, Tyr666, Val711, Asn710, Val656, Ser630, and Trp659) of the pocket and S2 pocket. Among such residues is Phe357 in the S2 extensive subsite, which has been reported to play a vital role in the inhibitory activities of evogliptin (Lee et al., 2017). This interaction corresponds to that of sitagliptin (Kim et al., 2005). Also, Asp197 of HPA has been reported to be mainly responsible for the cleavage of the glycosidic bonds in polysaccharides (Zhang et al., 2009; Taha et al., 2019). reported the role of Asp197 as a catalytic nucleophile in hydrolytic reactions and its interaction with known inhibitors. The results from the predictive physiochemical and drug-likeness analysis over several filtering tools revealed piperine and benzocycloheptano [2,3,4-I,j]isoquinoline, 4,5,6,6a-tetrahydro-1,9-dihydroxy-2,10-dimethoxy-5-methyl have druggable drug properties, while 13-octadecenal did not pass the filtering analysis (Daina et al., 2017). Favorable Veber and Lipinski characteristics suggest good penetration, retention, and bioavailability via the mouth (Lipinski, 2000; Veber et al., 2002). The hERG channel plays a vital role in cardiac cells in that the compounds that block the hERG channel during the repolarization and termination stages of an action potential may be responsible for cardiotoxicity. The main phytochemicals did not show signs of being hERG channel blockers, implying that they may not produce cardiotoxicity via the hERG channel (Raschi et al., 2008; Kratz et al., 2017). Both phytochemicals were not substrates for P-gp. Permeability glycoprotein (P-gp) is expressed in the proximal tubular cells of the kidney, liver cells, intestinal epithelium, and capillary endothelial cells comprising the blood-brain barrier and blood-testis barrier, where it pumps xenobiotics back into the urine-conducting ducts, intestinal lumen, bile ducts, and capillaries, respectively (Lin and Yamazaki, 2003). Using a good deal of cytochrome P₄₅₀ descriptors, we also looked into the influence of lead compounds on phase I drug absorption and utilization. The findings showed that the various cytochrome P₄₅₀ had lower inhibitory potential. Suggesting that they might not significantly affect the absorption and utilization of phase I drugs (Kratz et al., 2017). Both phytochemicals were predicted to be within the classified LD₅₀ value (Zhu et al., 2009; Djoumbou Feunang et al., 2016) and did not display mutagenicity or carcinogenicity (Xu et al., 2012).

5 Conclusion

This study revealed that EFSFL possesses a significant amount of secondary metabolites, which are likely responsible for its antioxidant, antidiabetic, and anti-inflammatory effects. The

bioactive constituents identified through GC-MS were found to have antioxidant, anti-inflammatory, and antidiabetic properties, which further supported the results. The study showed that α -caryophyllene, piperine, and benzocycloheptano[2,3,4-I,j] isoquinoline, 4,5,6,6a-tetrahydro-1,9-di hydroxy-2,10-dimethoxy-5-methyl (BCQDM) can inhibit the activities of dipeptidyl peptidase IV, α -amylase, and α -glucosidase. It is recommended that additional investigations of the toxicity effects of EFSFL in nonhuman subjects should be done before their medicinal application.

Data availability statement

Data are available on reasonable request from the corresponding author.

Ethics statement

The animal study was reviewed and approved by the Bowen University Animal Ehtics Committee.

Author contributions

OAo, Conceptualization and designed the study. OAo, ADO, GAG, DIA, AIO, DEB, OAA-O, MI, SCE, COA, AA, ABO, and OOO, conducted and investigated the study. OAo, ADO, GAG, DIA, AIO, DEB, OAA-O, MI, SCE, COA, AA, ABO, and OOO, analyzed and curated the data. OAo, DIA, GAG, OAA-O, ABO, and MI, wrote the manuscript draft. OAo, GAG, DIA, OAA-O, AA, ABO, and OOO, helped with technical editing and critical revision of the manuscript. All authors read and approved the final version of the manuscript.

References

- Ahmad, S., Alrouji, M., Alhajlah, S., Alomeir, O., Pandey, R. P., Ashraf, M. S., et al. (2023). Secondary metabolite profiling, antioxidant, antidiabetic and neuroprotective activity of *Cestrum nocturnum* (night scented-jasmine): Use of *in vitro* and *in silico* approach in determining the potential bioactive compound. *Plants* 12 (6), 1206. doi:10.3390/plants12061206
- Ajiboye, B. O., Ojo, O. A., Oyinloye, B. E., Okesola, M. A., Oluwatosin, A., Boligon, A. A., et al. (2020). Investigation of the *in vitro* antioxidant potential of polyphenolic-rich extract of *Artocarpus heterophyllus* lam stem bark and its antidiabetic activity in streptozotocin-induced diabetic rats. *J. Evidence-Based Integr. Med.* 25, 2515690X20916123. doi:10.1177/2515690X20916123
- Ajiboye, B. O., Oyinloye, B. E., Agboinghale, P. E., and Ojo, O. A. (2019). *Cnidioscolus aconitifolius* (Mill) IM Johnst leaf extract prevents oxidative hepatic injury and improves muscle glucose uptake *ex vivo*. *J. food Biochem.* 43 (12), e13065. doi:10.1111/jfbc.13065
- Akoachere, J. F. T. K., Suylika, Y., Mbah, A. J., Ayimele, A. G., Assob, J. C. N., Fodouop, S. P. C., et al. (2015). *In vitro* antimicrobial activity of agents from *Spilanthes filicaulis* and *Laportea ovalifolia* against some drug resistant bacteria. *Br. J. Pharm. Res.* 6, 76–87. doi:10.9734/bjpr/2015/15582
- Amaro, R. E., Baudry, J., Chodera, J., Demir, Ö., McCammon, J. A., Miao, Y., et al. (2018). Ensemble docking in drug discovery. *Biophysical J.* 114 (10), 2271–2278. doi:10.1016/j.bpj.2018.02.038
- Andlib, N., Sajad, M., Kumar, R., and Thakur, S. C. (2023). Abnormalities in sex hormones and sexual dysfunction in males with diabetes mellitus: A mechanistic insight. *Acta Histochem.* 125 (1), 151974. doi:10.1016/j.acthis.2022.151974
- Bellary, S., Kyrou, I., Brown, J. E., and Bailey, C. J. (2021). Type 2 diabetes mellitus in older adults: Clinical considerations and management. *Nat. Rev. Endocrinol.* 17 (9), 534–548. doi:10.1038/s41574-021-00512-2
- Bharti, S. K., Sharma, N. K., Kumar, A., Jaiswal, S. K., Krishnan, S., Gupta, A. K., et al. (2012). Dipeptidyl peptidase IV inhibitory activity of seed extract of *Castanospermum australe* and molecular docking of their alkaloids. *Topclass J. Herb. Med.* 1, 29–35.
- Borde, M. K., Mohanty, I. R., Suman, R. K., and Deshmukh, Y. (2016). Dipeptidyl peptidase-IV inhibitory activities of medicinal plants: *Terminalia arjuna*, *Commiphora mukul*, *Gymnema sylvestre*, *Morinda citrifolia*, *Embolia officinalis*. *Asian J. Pharm. Clin. Res.* 9 (3), 180–182.
- Bouslamti, M., Loukili, E. H., Elrherabi, A., El Moussaoui, A., Chebaibi, M., Bencheikh, N., et al. (2023). Phenolic profile, inhibition of α -amylase and α -glucosidase enzymes, and antioxidant properties of *Solanum elaeagnifolium* cav. (Solanaceae): *In vitro* and *in silico* investigations. *Processes* 11 (5), 1384. doi:10.3390/pr11051384
- Cigremis, Y., Turel, H., Adiguzel, K., Akgoz, M., Kart, A., Karaman, M., et al. (2009). The effects of acute acetaminophen toxicity on hepatic mRNA expression of SOD, CAT, GSH-Px, and levels of peroxynitrite, nitric oxide, reduced glutathione, and malondialdehyde in rabbit. *Mol. Cell. Biochem.* 323, 31–38. doi:10.1007/s11010-008-9961-8
- Cole, J. B., and Florez, J. C. (2020). Genetics of diabetes mellitus and diabetes complications. *Nat. Rev. Nephrol.* 16 (7), 377–390. doi:10.1038/s41581-020-0278-5
- Daina, A., Michielin, O., and Zoete, V. (2017). SwissADME: A free web tool to evaluate pharmacokinetics, drug-likeness and medicinal chemistry friendliness of small molecules. *Sci. Rep.* 7 (1), 42717. doi:10.1038/srep42717

Funding

This research was funded by Bowen University via Bowen University Research Grant (BURG) (Grant No: BURG/2023/006) for 2022-2023.

Acknowledgments

OAo acknowledges Bowen University, Iwo, Nigeria for Bowen University Research Grant (BURG/2023/006) and for paying the article processing charge (APC).

Conflict of interest

The authors declare that the research was conducted in the absence of any commercial or financial relationships that could be construed as a potential conflict of interest.

Publisher's note

All claims expressed in this article are solely those of the authors and do not necessarily represent those of their affiliated organizations, or those of the publisher, the editors and the reviewers. Any product that may be evaluated in this article, or claim that may be made by its manufacturer, is not guaranteed or endorsed by the publisher.

Supplementary material

The Supplementary Material for this article can be found online at: <https://www.frontiersin.org/articles/10.3389/fphar.2023.1235810/full#supplementary-material>

- Djombou Feunang, Y., Eisner, R., Knox, C., Chepelev, L., Hastings, J., Owen, G., et al. (2016). ClassyFire: Automated chemical classification with a comprehensive, computable taxonomy. *J. cheminformatics* 8, 61–20. doi:10.1186/s13321-016-0174-y
- Elufioye, T. O., Unachukwu, C. C., and Oyedele, A. O. (2019). Anticholinesterase and antioxidant activities of spilanthus filiculis whole plant extracts for the management of alzheimer's disease. *Curr. Enzyme Inhib.* 15 (2), 103–113. doi:10.2174/1573408015666190730113405
- Green, B. D., Flatt, P. R., and Bailey, C. J. (2006). Inhibition of dipeptidylpeptidase IV activity as a therapy of type 2 diabetes. *Expert Opin. Emerg. Drugs* 11, 525–539. doi:10.1517/14728214.11.3.525
- Gyebi, G. A., Ogunyemi, O. M., Ibrahim, I. M., Afolabi, S. O., and Adebayo, J. O. (2021). Dual targeting of cytokine storm and viral replication in COVID-19 by plant-derived steroidal pregnanes: An *in silico* perspective. *Comput. Biol. Med.* 134, 104406. doi:10.1016/j.compbiomed.2021.104406
- Han, Z. H., Ye, J. M., and Wang, G. F. (2013). Evaluation of *in vivo* antioxidant activity of Hericium erinaceus polysaccharides. *Int. J. Biol. Macromol.* 52, 66–71. doi:10.1016/j.ijbiomac.2012.09.009
- Hogan, I. A., Kuo, Y. C., Abubakar, A. N., Lawal, B., Agboola, A. R., Lukman, H. Y., et al. (2023). Attenuation of hyperglycemia-associated dyslipidemic, oxidative, cognitive, and inflammatory crises via modulation of neuronal ChEs/NF- κ B/COX-2/NOx, and hepatorenal functional deficits by the Trianax procumbens extract. *Biomed. Pharmacother.* 158, 114114. doi:10.1016/j.biopha.2022.114114
- Kartini, S., Juariah, S., Mardhiyani, D., Bakar, M. F. A., Bakar, F. I. A., and Endrini, S. (2023). Phytochemical properties, antioxidant activity and α -amylase inhibitory of curcuma caesia. *J. Adv. Res. Appl. Sci. Eng. Technol.* 30 (1), 255–263. doi:10.37934/araset.30.1.255263
- Kim, D., Wang, L., Beconi, M., Eiermann, G. J., Fisher, M. H., He, H., et al. (2005). 2 R)-4-Oxo-4-[3-(trifluoromethyl)-5, 6-dihydro [1, 2, 4] triazolo [4, 3-a] pyrazin-7 (8 H)-yl]-1-(2, 4, 5-trifluorophenyl) butan-2-amine: A potent, orally active dipeptidyl peptidase IV inhibitor for the treatment of type 2 diabetes. *J. Med. Chem.* 48 (1), 141–151. doi:10.1021/jm0493156
- Kosakowska, O., Weglarz, Z., Pióro-Jabrucka, E., Przybył, J. L., Kraśniewska, K., Gniewosz, M., et al. (2021). Antioxidant and antibacterial activity of essential oils and hydroethanolic extracts of Greek oregano (*O. vulgare* L. subsp. hirtum (Link) Ietswaart) and common oregano (*O. vulgare* L. subsp. vulgare). *Molecules* 26 (4), 988. doi:10.3390/molecules26040988
- Kratz, J. M., Grienke, U., Scheel, O., Mann, S. A., and Rollinger, J. M. (2017). Natural products modulating the hERG channel: Heartaches and hope. *Nat. Product. Rep.* 34 (8), 957–980. doi:10.1039/c7np00014f
- Lee, H. K., Kim, M. K., Kim, H. D., Kim, H. J., Kim, J. W., Lee, J. O., et al. (2017). Unique binding mode of evogliptin with human dipeptidyl peptidase IV. *Biochem. Biophysical Res. Commun.* 494 (3–4), 452–459. doi:10.1016/j.bbrc.2017.10.101
- Lee, J., Cheng, X., Swails, J. M., Yeom, M. S., Eastman, P. K., Lemkul, J. A., et al. (2016). CHARMM-GUI input generator for NAMD, GROMACS, AMBER, OpenMM, and CHARMM/OpenMM simulations using the CHARMM36 additive force field. *J. Chem. theory Comput.* 12 (1), 405–413. doi:10.1021/acs.jctc.5b00935
- Lee, J., Hitzberger, M., Rieger, M., Kern, N. R., Zacharias, M., and Im, W. (2020). CHARMM-GUI supports the Amber force fields. *J. Chem. Phys.* 153 (3), 035103. doi:10.1063/1.5012280
- Lin, J. Y., and Yamazaki, M. (2003). Role of P-glycoprotein in pharmacokinetics. *Clin. Pharmacokinet.* 42, 59–98. doi:10.2165/00003088-200342010-00003
- Lipinski, C. A. (2000). Drug-like properties and the causes of poor solubility and poor permeability. *J. Pharmacol. Toxicol. methods* 44 (1), 235–249. doi:10.1016/s1056-8719(00)00107-6
- McIntyre, H. D., Catalano, P., Zhang, C., Desoye, G., Mathiesen, E. R., and Damm, P. (2019). Gestational diabetes mellitus. *Nat. Rev. Dis. Prim.* 5 (1), 47. doi:10.1038/s41572-019-0098-8
- Morris, G. M., Huey, R., Lindstrom, W., Sanner, M. F., Belew, R. K., Goodsell, D. S., et al. (2009). AutoDock4 and AutoDockTools4: Automated docking with selective receptor flexibility. *J. Comput. Chem.* 30 (16), 2785–2791. doi:10.1002/jcc.21256
- Ndenecho, E. N. (2009). Herbalism and resources for the development of ethnopharmacology in Mount Cameroon region. *Afr. J. Pharm. Pharmacol.* 3 (3), 78–86.
- O'Boyle, N., Hutchison, G. R., and James, B. M. (2011). Open Babel: An open chemical toolbox. *J. Cheminf* 3 (1), 33. doi:10.1186/1758-2946-3-33
- Ogunlakin, A. D., Sonibare, M. A., Yeye, O. E., Gyebi, G. A., Ayokunle, D. I., Arigbede, O. E., et al. (2023). Isolation and characterization of novel hydroxyflavone from kigelia africana (lam) benth. Fruit ethyl acetate fraction against CHO 1 and HeLa cancer cell lines: *In vitro* and *in silico* studies. *J. Mol. Struct.* 1282, 135180. doi:10.1016/j.molstruc.2023.135180
- Ogunyemi, O. M., Gyebi, G. A., Ibrahim, I. M., Esan, A. M., Olaiya, C. O., Soliman, M. M., et al. (2023). Identification of promising multi-targeting inhibitors of obesity from Vernonia amygdalina through computational analysis. *Mol. Divers.* 27 (1), 1–25. doi:10.1007/s11030-022-10397-6
- Ogunyemi, O. M., Gyebi, G. A., Ibrahim, I. M., Olaiya, C. O., Ocheje, J. O., Fabusiwa, M. M., et al. (2021). Dietary stigmastane-type saponins as promising dual-target directed inhibitors of SARS-CoV-2 proteases: A structure-based screening. *RSC Adv.* 11 (53), 33380–33398. doi:10.1039/d1ra05976a
- Ojo, A. B., Gyebi, G., Alabi, O., Iyobhebe, M., Nwonuma, C. O., Ojo, O. A., et al. (2022). Syzygium aromaticum (L) Merr. and L.M.Perry mitigates iron-mediated oxidative brain injury via *in vitro*, *ex vivo*, and *in silico* approaches. *J. Mol. Struct.* 1268C, 133675. doi:10.1016/j.molstruc.2022.133675
- Ojo, O. A., Osukoya, O. A., Ekakitie, L. I., Ajiboye, B. O., Oyinloye, B. E., Agboinghale, P. E., et al. (2020). Gongronema latifolium leaf extract modulates hyperglycaemia, inhibits redox imbalance and inflammation in alloxan-induced diabetic nephropathy. *J. diabetes and metabolic Disord.* 19, 469–481. doi:10.1007/s40200-020-00533-0
- Pathak, R., and Brideman, M. B. (2010). Dipeptidyl peptidase-4 (DPP-4) inhibitors in the management of diabetes. *Pharm. Ther.* 35 (9), 509–513.
- Raschi, E., Vasina, V., Poluzzi, E., and De Ponti, F. (2008). The hERG K⁺ channel: Target and antitarget strategies in drug development. *Pharmacol. Res.* 57 (3), 181–195. doi:10.1016/j.phrs.2008.01.009
- Rendra, E., Riabov, V., Mossel, D. M., Sevastyanova, T., Harmsen, M. C., and Kzhyshkowska, J. (2019). Reactive oxygen species (ROS) in macrophage activation and function in diabetes. *Immunobiology* 224 (2), 242–253. doi:10.1016/j.imbio.2018.11.010
- Salekzamani, S., Ebrahimi-Mameghani, M., and Rezaadeh, K. (2019). The antioxidant activity of artichoke (cynara scolymus): A systematic review and meta-analysis of animal studies. *Phytotherapy Res.* 33 (1), 55–71. doi:10.1002/ptr.6213
- Sarkar, R., Hazra, B., and Mandal, N. (2012). Hepatoprotective potential of Caesalpinia crista against iron-overload-induced liver toxicity in mice. *Evidence-Based Complementary Altern. Med.* 2012, 896341. doi:10.1155/2012/896341
- Simbo, D. J. (2010). An ethnobotanical survey of medicinal plants in Babungu, Northwest Region, Cameroon. *J. Ethnobiol. Ethnomedicine* 6, 8–7. doi:10.1186/1746-4269-6-8
- Taha, M., Noreen, T., Imran, S., Nawaz, F., Chigurupati, S., Selvaraj, M., et al. (2019). Synthesis, α -amylase inhibition and molecular docking study of bisindolylmethane sulfonamide derivatives. *Med. Chem. Res.* 28, 2010–2022. doi:10.1007/s00044-019-02431-4
- Tekin, S., and Seven, E. (2022). Assessment of serum catalase, reduced glutathione, and superoxide dismutase activities and malondialdehyde levels in keratoconus patients. *Eye* 36 (10), 2062–2066. doi:10.1038/s41433-021-01753-1
- Tiwari, K. L., Jadhav, S. K., and Joshi, V. (2011). An updated review on medicinal herb genus Spilanthes. *Zhong xi yi jie he xue bao = J. Chin. Integr. Med.* 9 (11), 1170–1178. doi:10.3736/jcim201111103
- Trott, O., and Olson, A. J. (2010). AutoDock Vina: Improving the speed and accuracy of docking with a new scoring function, efficient optimization, and multithreading. *J. Comput. Chem.* 31 (2), 455–461. doi:10.1002/jcc.21334
- Truong, V. L., and Jeong, W. S. (2021). Cellular defensive mechanisms of tea polyphenols: Structure-activity relationship. *Int. J. Mol. Sci.* 22 (17), 9109. doi:10.3390/ijms22179109
- Veber, D. F., Johnson, S. R., Cheng, H. Y., Smith, B. R., Ward, K. W., and Kopple, K. D. (2002). Molecular properties that influence the oral bioavailability of drug candidates. *J. Med. Chem.* 45 (12), 2615–2623. doi:10.1021/jm020017n
- World Health Organization (1999). *WHO monographs on selected medicinal plants*. World Health Organization.
- Xu, C., Cheng, F., Chen, L., Du, Z., Li, W., Liu, G., et al. (2012). *In silico* prediction of chemical Ames mutagenicity. *J. Chem. Inf. Model.* 52 (11), 2840–2847. doi:10.1021/ci300400a
- Yazdanparast, R., Bahramikia, S., and Ardestani, A. (2008). Nasturtium officinale reduces oxidative stress and enhances antioxidant capacity in hypercholesterolaemic rats. *Chemico-Biological Interact.* 172 (3), 176–184. doi:10.1016/j.cbi.2008.01.006
- Yue, S., Xue, N., Li, H., Huang, B., Chen, Z., and Wang, X. (2020). Hepatoprotective effect of apigenin against liver injury via the non-canonical NF- κ B pathway *in vivo* and *in vitro*. *Inflammation* 43, 1634–1648. doi:10.1007/s10753-020-01238-5
- Zhang, R., Li, C., Williams, L. K., Rempel, B. P., Brayer, G. D., and Withers, S. G. (2009). Directed "in situ" inhibitor elongation as a strategy to structurally characterize the covalent glycosyl-enzyme intermediate of human pancreatic α -amylase. *Biochemistry* 48 (45), 10752–10764. doi:10.1021/bi901400p
- Zhu, H., Martin, T. M., Ye, L., Sedykh, A., Young, D. M., and Tropsha, A. (2009). Quantitative structure-activity relationship modeling of rat acute toxicity by oral exposure. *Chem. Res. Toxicol.* 22 (12), 1913–1921. doi:10.1021/tx900189p



OPEN ACCESS

EDITED BY

Mansour Sobeh,
Mohammed VI Polytechnic University,
Morocco

REVIEWED BY

Sultan Ayesh Mohammed Saghir,
Al Hussein Bin Talal University, Jordan
Oluwafemi Adeleke Ojo,
Bowen University, Nigeria
Rogers Mwakalukwa,
Muhimbili University of Health and Allied
Sciences, Tanzania

*CORRESPONDENCE

Motlalepula G. Matsabisa,
✉ matsabisamg@ufs.ac.za

RECEIVED 12 May 2023

ACCEPTED 27 July 2023

PUBLISHED 07 August 2023

CITATION

Salau VF, Erukainure OL, Olofinisan KA,
Schoeman RLS and Matsabisa MG (2023),
Lippia javanica (Burm. F.) Herbal Tea:
Modulation of Hepatoprotective Effects
in Chang Liver Cells via Mitigation of
Redox Imbalance and Modulation of
Perturbed Metabolic Activities.
Front. Pharmacol. 14:1221769.
doi: 10.3389/fphar.2023.1221769

COPYRIGHT

© 2023 Salau, Erukainure, Olofinisan,
Schoeman and Matsabisa. This is an
open-access article distributed under the
terms of the [Creative Commons
Attribution License \(CC BY\)](https://creativecommons.org/licenses/by/4.0/). The use,
distribution or reproduction in other
forums is permitted, provided the original
author(s) and the copyright owner(s) are
credited and that the original publication
in this journal is cited, in accordance with
accepted academic practice. No use,
distribution or reproduction is permitted
which does not comply with these terms.

Lippia javanica (Burm. F.) Herbal Tea: Modulation of Hepatoprotective Effects in Chang Liver Cells via Mitigation of Redox Imbalance and Modulation of Perturbed Metabolic Activities

Veronica F. Salau¹, Ochuko L. Erukainure², Kolawole A. Olofinisan³,
Recardia L. S. Schoeman¹ and Motlalepula G. Matsabisa^{1*}

¹Department of Pharmacology, University of the Free State, Bloemfontein, South Africa, ²Department of Biochemistry, University of KwaZulu-Natal, Durban, South Africa, ³Laser Research Centre, Faculty of Health Sciences, University of Johannesburg, Doornfontein, South Africa

Introduction: Hepatic oxidative injury is one of the pathological mechanisms that significantly contributes to the development of several liver diseases. In the present study, the hepatoprotective effect of *Lippia javanica* herbal tea was investigated in Fe²⁺-mediated hepatic oxidative injury.

Methods: Using an *in vitro* experimental approach, hepatic oxidative injury was induced by co-incubating 7 mM FeSO₄ with Chang liver cells that have been pre-incubated with or without different concentrations (15–240 µg/mL) of *L. javanica* infusion. Gallic acid and ascorbic acid served as the standard antioxidants.

Results: The infusion displayed a reducing antioxidant activity in ferric-reducing antioxidant power (FRAP) assay and a potent scavenging activity on 2,2-diphenyl-2-picrylhydrazyl (DPPH) radical. Pretreatment with *L. javanica* infusion significantly elevated the levels of reduced glutathione and non-protein thiol, and the activities of superoxide dismutase (SOD) and catalase, with concomitant decrease in hepatic malondialdehyde levels, acetylcholinesterase, glucose-6-phosphatase, fructose-1,6-bisphosphatase, glycogen phosphorylase and lipase activities. The infusion showed the presence of phytoconstituents such as phenolic compounds, tannins, phenolic glycosides and terpenoids when subjected to liquid chromatography–mass spectrometry analysis. Molecular docking revealed a strong binding affinity of dihydroquercetin and obacunone with both SOD and catalase compared to other phytoconstituents.

Conclusion: These results portray a potent antioxidant and hepatoprotective effect of *L. javanica*, which may support the local usage of the herbal tea as a prospective therapeutic agent for oxidative stress-related liver diseases.

KEYWORDS

oxidative stress, hepatotoxicity, gluconeogenesis, antioxidants, cholinergic enzyme

Introduction

About two million cases of global mortality are attributed to liver diseases, with liver cirrhosis and liver cancer being the most common causes of these deaths (Asrani et al., 2019). Besides increased risks of mortality, chronic liver diseases cause several extrahepatic morbidities which contribute notably to low quality of life. Thus, liver diseases, though underestimated, pose a high economic burden which is a major concern (Stepanova et al., 2017; Asrani et al., 2019).

Regardless of the cause, most chronic liver diseases are typified by oxidative stress (Cichoż-Lach and Michalak, 2014). Excessive reactive oxygen species (ROS) cause disturbances in redox homeostasis which results in oxidative stress, a major pathological mechanism involved in the development and progression of several liver diseases. Oxidative stress induces dire alterations in liver proteins, lipids and DNA components as well as impair pathways involved in normal biological functions of the liver (Li et al., 2014; Li et al., 2015). The liver is the main organ usually attacked by ROS, as the parenchymal cells, hepatic stellate cells, Kupffer cells and endothelial cells of the liver are all vulnerable to oxidative injury, causing damages to each cell types (Cichoż-Lach and Michalak, 2014). Several risk factors including drugs, alcohol, irradiation and environmental pollutants such as heavy metals may mediate hepatic oxidative stress. Damages induced by oxidative stress significantly contribute to impairment of gene expression and progression of liver diseases as well as apoptosis and necrosis (Cichoż-Lach and Michalak, 2014; Li et al., 2015).

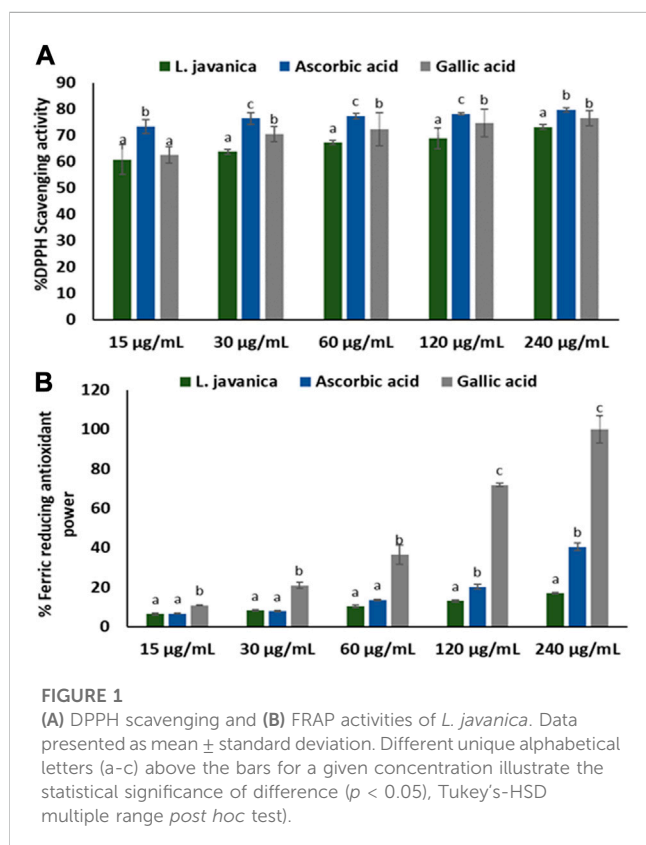
Severe disturbances in hepatic glucose and lipid metabolism homeostasis have been recognized as some of the major

mechanisms involved in liver diseases such as liver cirrhosis, liver steatosis and fatty liver, with oxidative stress being a key contributor (Mikszewicz et al., 2012; Ding et al., 2018). Excess cellular levels of glucose and lipids can serve as substrates for the generation of glucotoxic and lipotoxic species, respectively, which can cause damage to biomolecules, induce metabolic stress and eventual cell death (Mota et al., 2016; Chen et al., 2020). Additionally, altered cholinergic enzyme activities have been implicated in the pathogenesis of liver diseases and studies have reported oxidative stress as facilitator of cholinergic dysfunction (Garcia-Ayllon et al., 2012; Erukainure et al., 2021a). These corroborates the use of antioxidants as therapies for targeting oxidative stress in the management of liver diseases (Upadhyay et al., 2022).

Several medicinal plants, including herbal infusions have been globally used over the decades for the treatment of several chronic liver diseases due to their availability, curative effects and minute adverse effects. These therapeutic characteristics have been ascribed to the phytochemical components of the plants (Hong et al., 2015; Chukwuma et al., 2019). Studies have indicated that medicinal plants and their phytochemicals exhibit their hepatoprotective effects in several ways including mitigation of oxidative stress, blockage of fibrogenesis and suppression of tumorigenesis (Dhiman et al., 2012; Hong et al., 2015).

Lippia javanica (Burm.f.) (Family: Verbenaceae) is a multi-stemmed, woody, drought-resistant shrub that is naturally distributed in central, eastern and southern Africa including South Africa, Malawi, Botswana, Kenya, Zambia, Angola, Zanzibar, Tanzania and Mozambique, as well as tropical Indian sub-continent (Germishuizen et al., 2006; Shahriar et al., 2014). In South Africa, it is widely distributed in different provinces which include KwaZulu-Natal, Gauteng, Free State, Limpopo, Eastern Cape and Northwest. It is known as one of the aromatic indigenous shrubs in South Africa. The common names of *L. javanica* include fever tree, wild sage, wild tea and lemon bush. The Xhosa community of South Africa call it *inzinzinba* while the Zulus call it *umwazi* (Maroyi, 2017). Traditionally, *L. javanica* has been used from time immemorial as herbal tea or as either root or leave decoction to treat fever, malaria, cough, cold, chest pain, asthma, bronchitis, and diarrhea. The Zulus in South Africa use the herbal tonic as an immune booster. In Zimbabwe and South Africa, the burnt whole plant or leaves are used as mosquito repellent (Lukwa et al., 2009; Maroyi, 2017). The reported pharmacological activities of the plant include antioxidant, antimalarial, antidiabetic, anticancer, antiviral and antimicrobial activities (Fouché et al., 2008; Mujovo et al., 2008; Shikanga et al., 2010; Maroyi, 2017). The neuroprotective effect of its herbal tea infusion on lead-induced brain oxidative damage in Wistar rats was also reported by Suleman et al. (2022). Despite its numerous documented medicinal properties, there is limited information on the effect of *L. javanica* on liver diseases.

The purpose of the present study was to investigate the potential hepatoprotective effect of *L. javanica* tea infusion on iron-induced oxidative hepatic injury in Chang liver cells by assessing its effect on oxidative stress, cholinergic dysfunction, altered carbohydrate metabolism and lipase activities.



Materials and methods

Plant material

Plant collection and verification

Lippia javanica (Burm.f.) Spreng leaves were collected from Langenhoven Park, Bloemfontein, Free State Province, South Africa (GPS Coordinates: 29°05'32.2"S 26°09'25.6"E) by Prof. M.G. Matsabisa. The plant sample was deposited at the Geo Potts Herbarium, University of the Free State, Bloemfontein 9,300, South, where it was identified, authenticated and assigned a voucher specimen number (BLFU/MGM005).

Plant infusion preparation

After air-drying at room temperature, the *L. javanica* leaves were pulverized into powder. Extraction was done by boiling 50 g of the leave powder in 500 mL of distilled water for 10 min. The mixture was allowed to cool and then filtered into a pre-weighed glass beaker using a Whatman filter (Whatman, England). The extract was concentrated in a water bath at 50°C. The dry plant infusion was scrapped and transferred into a glass vial and stored at −20°C.

The infusion was re-constituted in distilled water by preparing a stock solution of 1 mg/mL from which various working concentrations ranging from 15 to 240 µg/mL were prepared for different assays. Similarly, the same working concentrations were prepared for two antioxidant standards, ascorbic acid and gallic acid from a stock solution of 1 mg/mL.

Phytochemical characterization and quantification

Total phenolic content

The total phenolic content of the infusion was determined using the Folin-Ciocalteu’s phenol reagent as described by McDonald et al. (2001). In brief, 40 µL of 240 µg/mL plant extract was incubated in the dark with 200 µL of 10% Folin Ciocalteau reagent and 160 µL of 0.7 M Na₂CO₃ for 30 min at room temperature. The absorbance of the triplicates were measured at 765 nm, using a Multiskan ascent plate reader (Thermo scientific, S.A). The total phenolic content was estimated from a gallic acid standard curve and results were expressed as gallic acid equivalents (GAE) in milligrams per gram of dry weight.

Total flavonoid content

The total flavonoid content of the infusion was estimated by utilizing the aluminum chloride colorimetric method described by Chang et al. (2002), with slight modification. Briefly, 100 µL of the infusion (240 µg/mL) was added to a mixture of 100 µL of methanol, 10 µL of aluminum chloride, 10 µL of 1 mol/L potassium chloride and 200 µL of distilled water. The mixture was allowed to stand for 30 min at room temperature. The absorbance of the independent triplicates were measured at 415 nm and the total flavonoid content was estimated from a quercetin calibration standard curve. The results were expresses as quercetin equivalent (QE) in milligrams per gram of dry weight.

TABLE 1 IC₅₀ values of DPPH and FRAP activities of *L. javanica* herbal leaves.

Activities	<i>L. javanica</i>	Ascorbic acid	Gallic acid
DPPH	1.22	0.01	0.61
FRAP	>1,000	975.73	63.81

Values are expressed as µg/ml. DPPH: 2,2-diphenyl-1-picrylhydrazyl, FRAP: ferric reducing antioxidant power.

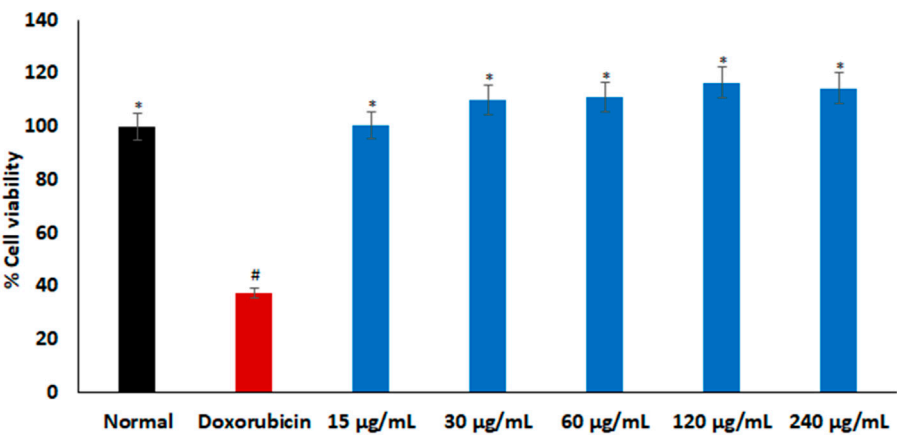


FIGURE 2 Cytotoxic effect of *L. javanica* on Chang liver cells. Value = mean ± SD; n = 3. *Statistically significant compared to doxorubicin group; #statistically significant compared to the normal control cell (p < 0.05, Dunnett’s multiple range post hoc test).

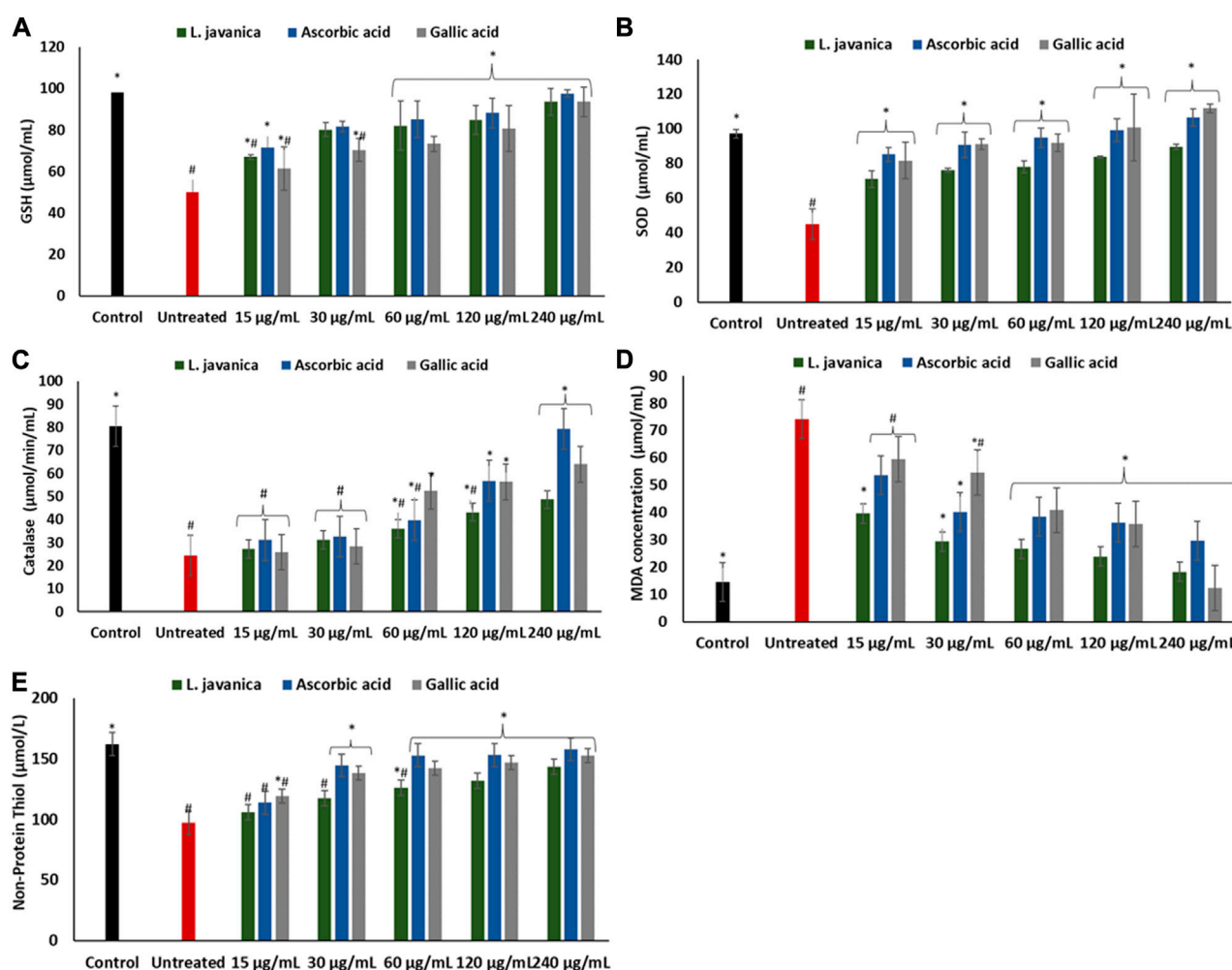


FIGURE 3

Effect of *L. javanica* on (A) GSH level (B) SOD activity, (C) catalase activity, (D) MDA level, and (E) non-protein thiol level in oxidative hepatic injury. Value = mean \pm SD; $n = 3$. *Statistically significant compared to untreated hepatic cells; #statistically significant compared to the control cells ($p < 0.05$, Dunnett's range post hoc test). GSH = Reduced glutathione, SOD = superoxide dismutase, MDA = Malondialdehyde.

Liquid chromatography-mass spectrometry (LC-MS) analysis of *L. javanica*

The pharmacologically active chemical constituents present in the *L. javanica* infusion were characterized via direct-loop injection into Shimadzu LC/MS-2020 Single Quadrupole Liquid Chromatograph Mass Spectrometer (LCMS) equipped with an electrospray ionization (ESI) source. The analysis data acquisition duration was set at 50 min at a low-pressure gradient, while the LC photodiode array (PDA) sampling frequency was kept at 1.5625 Hz. The oven temperature range was maintained between 40°C–50°C, and the pump flow rate was kept at 300 μ L/min. The mobile phase solvent system contained 0.1% formic acid in water (phase A) and methanol: acetonitrile (1:1) (phase B). Scanning was done at positive and negative polarities with other operating parameters which include, Start Time: 0.0 min; End Time: 50.0 min; Event Time: 0.25 s; Cell Temperature: 40°C; Threshold: 0; Start Wavelength: 220 nm; End Wavelength: 400 nm; Detector Voltage: +0.00 kV; Scan Speed: 5,000 u/s; Start and End m/z: 100.0 and 1,000.0,

respectively. The compounds were identified by direct comparison of the generated spectra containing the relative abundance and the m/z fragmentation patterns with those in the m/z cloud database at <https://www.mzcloud.org/>.

In vitro antioxidant activities of the infusion

2,2-Diphenyl-1-picrylhydrazyl (DPPH) scavenging activity

The free radical (DPPH) scavenging activity of the infusion was determined by using a previously established protocol (Changlian et al., 2000). In brief, 50 μ L of 0.3 mM DPPH in methanol was mixed with 100 μ L of different concentrations (15–240 μ g/mL) of the infusions or the standards ascorbic acid and gallic acid in a 96-well plate. The plate with the samples was incubated in the dark at room temperature for 30 min. The absorbance was measured against a blank solution at 517 nm, and the percentage scavenging activity was calculated.

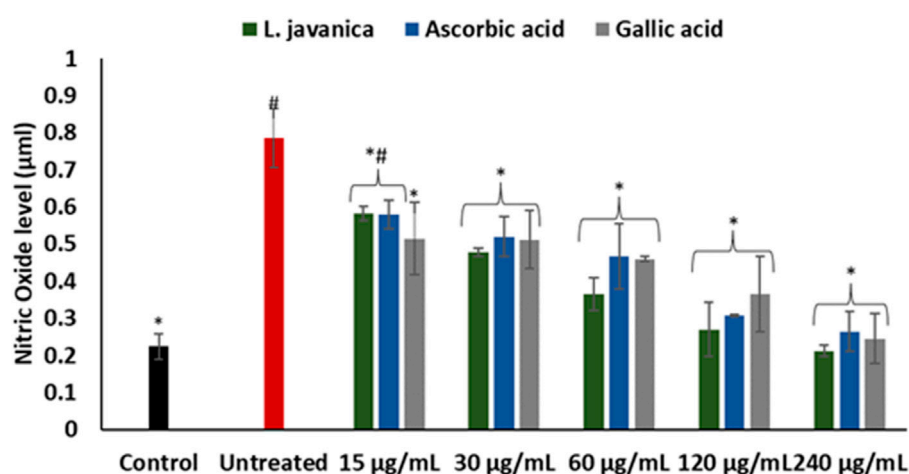


FIGURE 4

Effect of *L. javanica* on nitric oxide level in oxidative hepatic injury. Value = mean \pm SD; $n = 3$. *Statistically significant compared to untreated hepatic cells; #statistically significant compared to the control cells ($p < 0.05$, Dunnett's multiple range *post hoc* test).

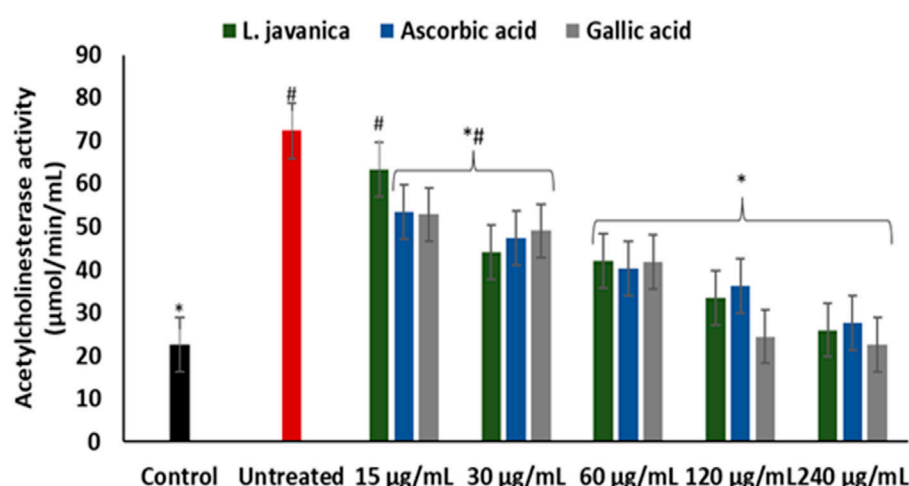


FIGURE 5

Effect of *L. javanica* on acetylcholinesterase activity in oxidative hepatic injury. Value = mean \pm SD; $n = 3$. *Statistically significant compared to untreated hepatic cells; #statistically significant compared to the control cells ($p < 0.05$, Dunnett's multiple range *post hoc* test).

Ferric reducing antioxidant power (FRAP)

The ferric-reducing capacity of the infusion was determined by the potassium ferricyanide method according to Benzie and Strain (1996) with slight modifications. 20 μ L of different concentrations (15–240 μ g/mL) of the herbal infusion was incubated with 20 μ L of 0.2 M sodium phosphate buffer (pH 6.6) and 20 μ L of 1% potassium ferricyanide at 50°C for 30 min. 10% trichloroacetic acid (20 μ L) was then added to the reaction mixture to acidify it. An aliquot of the acidified sample was added to 20 μ L of distilled water and 20 μ L of 10% FeCl₃. The absorbance was read at 700 nm. The results were expressed as a percentage of the absorbance of the sample to the absorbance of gallic acid.

Cell lines

Chang liver cells (ATCC® CCL-13™) were procured from the American Type Culture Collection (ATCC®), Manassas, Virginia, United States.

Cytotoxicity screening

Chang liver cells were seeded in a 96-well plate (Nunc, Thermofischer Scientific) at a cell density of 10,000 cells/well (100 μ L/well) and left to attach overnight at 37°C in humidified atmosphere with a 5% CO₂ concentration. The cells were then treated with various concentrations of *L. javanica* (15–240 μ g/mL) and incubated for 48 h at 37°C.

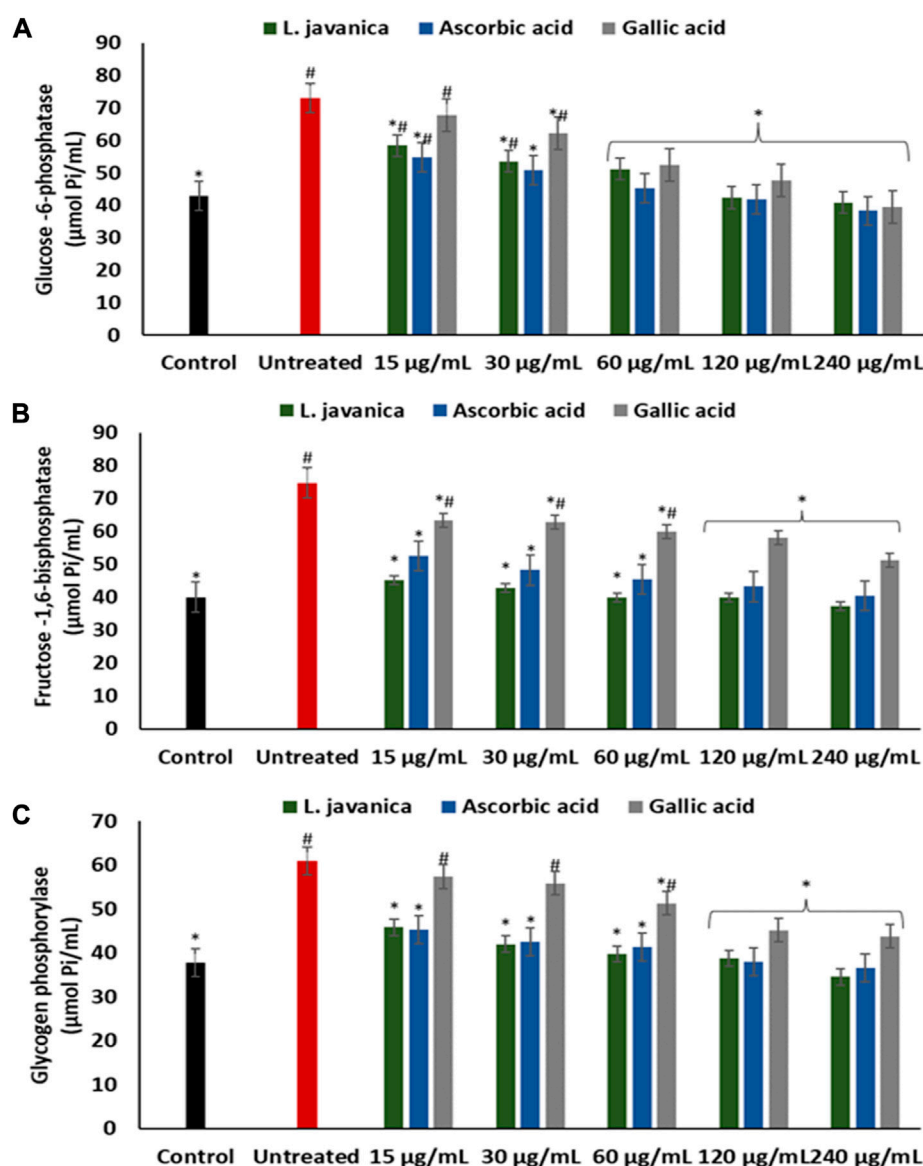


FIGURE 6

Effect of *L. javanica* on (A) Glucose 6 phosphatase, (B) Fructose 1,6 bisphosphatase and (C) Glycogen phosphorylase activities in oxidative hepatic injury. Value = mean \pm SD; $n = 3$. *Statistically significant compared to untreated hepatic cells; #statistically significant compared to the control cells ($p < 0.05$, Dunnett's multiple range post hoc test).

Doxorubicin (3 $\mu\text{g/mL}$) was used as a positive control. Dimethylsulfoxide (DMSO) (0.5%) was used as a vehicle control. The cytotoxicity of the cells were evaluated using MTT [3-(4,5-dimethylthiazol-2-yl)-2,5-diphenyltetrazolium bromide. After treatment, the spent media was aspirated and replaced with 0.5 mg/mL MTT solution (100 μL /well) dissolved in fresh media followed by an incubation at 37°C for 2 h. After the incubation, the MTT solution was removed and 100 μL of dimethylsulfoxide was added. Subsequently, the absorbance was read at 550 nm using the Multiskan GO spectrophotometer (Thermo Scientific). The results were expressed as mean \pm SD the percentage cell viability of biological repeats.

Induction of oxidative stress in Chang liver cells

Oxidative stress was induced in Chang liver cells using a modified method from a previous protocol (Chukwuma et al., 2019). Briefly, the cells were seeded into 6-well plates (TPP®, Merck) at 160,000 cells/well (2 mL/well) and left to attach overnight at 37°C. After attachment, the cells were incubated with various concentrations of *L. javanica* extract or the standards, ascorbic acid and gallic acid (15–240 $\mu\text{g/mL}$) at 37°C for 25 min. Thereafter, 600 μL of 7 mM iron sulphate (FeSO_4) was added to each well and the cells further incubated for 30 min at 37°C. Positive controls and negative controls were included and comprised of untreated cells with and without the addition of FeSO_4 . After incubation, the treatment was removed, and the cells washed twice

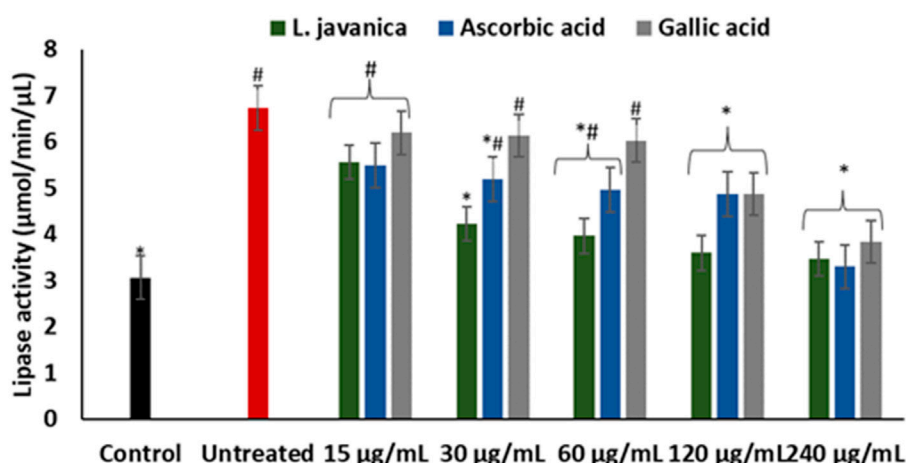


FIGURE 7

Effect of *L. javanica* on lipase activity in oxidative hepatic injury. Value = mean \pm SD; $n = 3$. *Statistically significant compared to untreated hepatic cells; #statistically significant compared to the control cells ($p < 0.05$, Dunnett's multiple range *post hoc* test).

TABLE 2 Liquid Chromatography Mass Spectrometry (LC-MS) identified chemical compounds of *L. javanica*.

Retention time (min.)	Area/Height	Phytoconstituents (suspected)	[M + H] ⁺ -m/z
6.111	15.713	4-Aminophenol	133.10
8.114	20.322	Dihydoroseoside	387.10
10.325	21.875	[1-(3,4-Dihydroxy-5-methoxyphenyl)-7-(3,4-dihydroxyphenyl) heptan-3-yl] acetate	403.05
10.928	13.971	Corilagin	277.10
11.891	17.901	Radicicol	321.10
12.684	19.806	Coniferin	365.10
13.303	14.885	Obacunone	409.20
16.671	16.316	3-Ethyl-4-hydroxy-1-phenylquinolin-2(1H)-one	266.20

with PBS (1 mL/well). The PBS was aspirated and the cells were dissociated using 200 μ L of trypsin/EDTA and incubated at 37°C until the cells were completely dissociated. The trypsin was neutralized using 700 μ L of complete media (DMEM with 10% FBS). The cell suspension was collected in 1.5 mL microcentrifuge tubes respectively and centrifuged at 17,000 $\times g$ for 12 min using the Hettich® MIKRO 120 centrifuge. The supernatant collected and stored at -80°C until further use.

Determination of oxidative stress biomarkers

Oxidative stress biomarkers were determined in the cell by analyzing the level of reduced glutathione (GSH), activities of superoxide dismutase (SOD) and catalase, as well as and malondialdehyde (MDA) level.

Reduced glutathione (GSH) level

GSH levels were determined in the hepatic cells by utilizing Ellman's spectrophotometric method (Ellman, 1959) with slight modification. Briefly, 0.2 mL of the cell's supernatant was mixed with 0.6 mL of trichloroacetic acid (10%) and centrifuged for 5 min at 1,000 $\times g$. 0.2 mL aliquot of the supernatant (deproteinized

solution) and 0.05 mL of Ellman's reagent were placed in a 96 well microplate and incubated for 10 min at room temperature. Absorbance was read at 415 nm, and GSH protein level was estimated from a glutathione standard curve.

Superoxide dismutase (SOD) activity

The SOD activity in the cells were determined by utilizing a modified procedure of Kakkar et al. (1984). Briefly, a 96- well microplate containing the supernatant (15 μ L), 100 μ M diethylenetriaminepentaacetic acid (DETAPAC; 170 μ L) and 15 μ L of 1.6 mM hydroxydopamine (6-HD) was gently swirled before the absorbance was immediately measured at 492 nm thrice at 1 min interval.

Catalase activity

The hepatic catalase activity was measured in the supernatant by adopting the method of Hadwan and Abed (2016). Briefly, 100 μ L of the supernatant was added to 1,000 μ L of 0.065 μ M H₂O₂ and incubated for 2 min at 37°C. 100 μ L of 32.4 mM ammonium molybdate was used to terminate the reaction and the absorbance was read at 347 nm against the blank containing only H₂O₂.

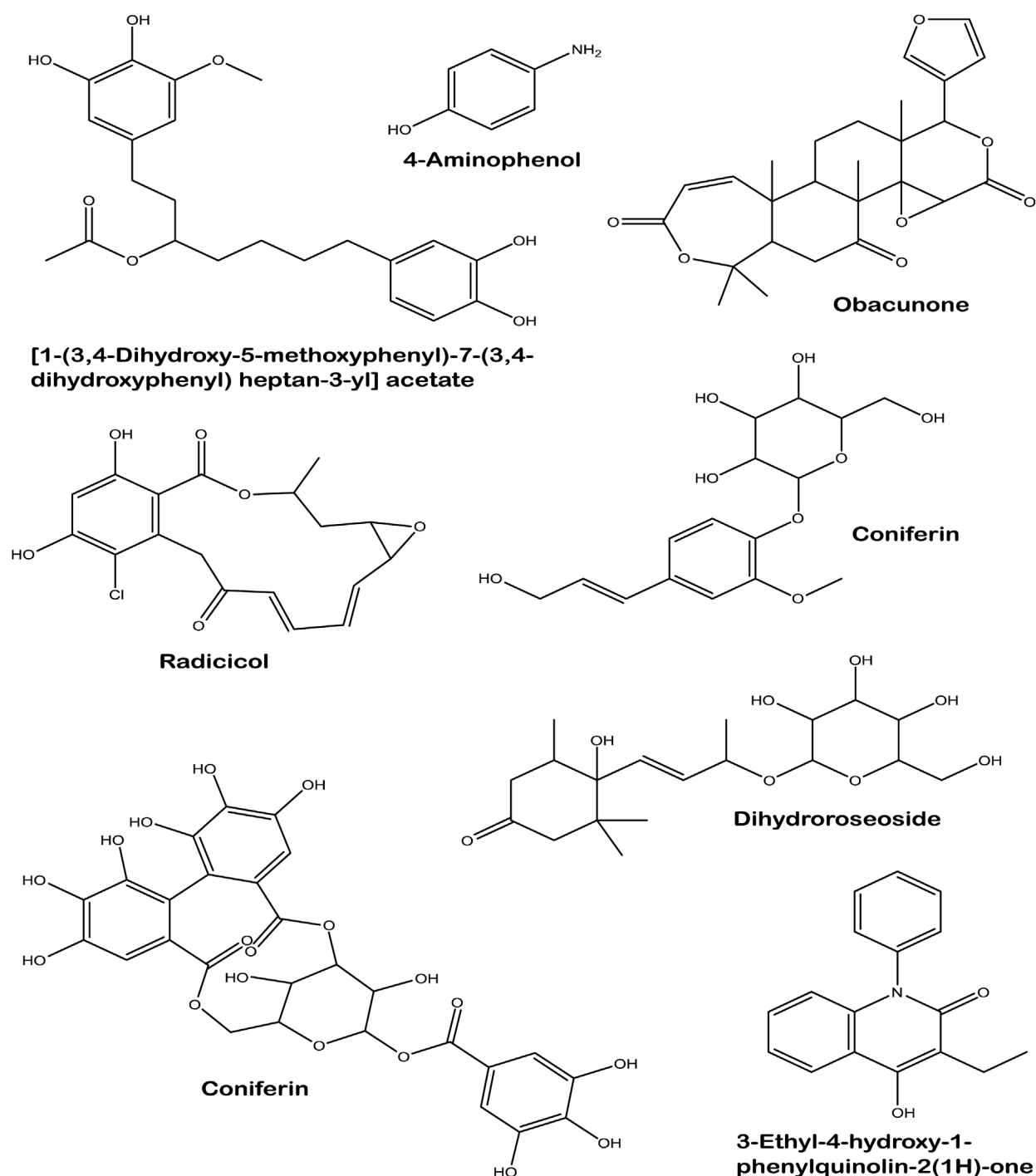


FIGURE 8
Structures of identified compounds in *L. javanica* infusion.

Malondialdehyde (MDA) levels

Lipid peroxidation levels were determined by analyzing for MDA concentration according to previous method (Chowdhury and Soulsby, 2002). Briefly, 100 μ L of the cell's supernatant was added to a mixture containing 100 μ L of 8.1% sodium dodecyl sulfate solution, 375 μ L of 20% pure acetic acid and 1,000 μ L of 0.25% thiobarbituric acid. The reaction mixture boiled for 1 h in water bath, and the absorbance was read at 532 nm after cooling, to estimate MDA levels.

Determination of non-protein thiol (NPSH) content

Hepatic non-protein thiol level was estimated spectrophotometrically using Ellman's method (Ellman, 1959). Briefly, a mixture of 300 μ L of cell supernatant and the same volume of 10% trichloroacetic acid were centrifuged at $1,000 \times g$ for 5 min. 50 μ L of the resulting supernatant, 150 μ L of Ellman's reagent and 50 μ L of 0.1 M phosphate buffer were mixed and incubated for 10 min at 37°C. The absorbance was read at

TABLE 3 Binding energies (Kcal/mol) of the phytochemical constituents of *L. javanica* with antioxidant enzymes.

Phytoconstituents	Catalase	Superoxide dismutase
4-Aminophenol	−5.2	−3.7
Dihydoroseoside	−10.5	−7.1
[1-(3,4-Dihydroxy-5-methoxyphenyl)-7-(3,4-dihydroxyphenyl) heptan-3-yl] acetate	−3.6	−2.4
Corilagin	−2.0	−1.7
Radicicol	−5.7	−7.2
Coniferin	−2.0	−1.7
Obacunone	−11.7	−9.8
3-Ethyl-4-hydroxy-1-phenylquinolin-2(1H)-one	−8.7	−6.6
Gallic acid	−7.1	−6.7
Ascorbic acid	−4.8	−5.3

412 nm and non-protein thiol content were calculate from standard curve of cysteine.

Determination of nitric oxide (NO) level

Hepatic nitric oxide level was determined based on Greiss method according to Tsikas (2005). Briefly a solution made up of 100 μ L of the cell supernatant and equal volume of Greiss reagent in a 96 well-plate was incubated in the dark for 30 min at room at 25°C, using the same volume of distilled water as the blank. After incubation, absorbance of the solution was measured at 548 nm.

Determination of acetylcholinesterase activity

Acetylcholinesterase activity was determined in the hepatic cells by employing a previously established method (Ellman et al., 1961). Briefly, a solution containing 100 μ L of the supernatant was added to 50 μ L of 3.3 mM Ellman's reagent (pH 7.0) and 250 μ L of 0.1 M phosphate buffer (pH 8) was incubated for 20 min at 25°C. 50 μ L of 0.05 M acetylcholine iodide was then added. The absorbance was immediately measured at 412 nm at 3 min intervals.

Determination of glucogenic enzymes activities

Glucose 6-phosphatase activity

Glucose 6-phosphatase activity was estimated in the hepatic cells according to a modified method of Balogun and Ashafa (2017). Briefly, 200 μ L of the cell supernatant, 100 μ L of 0.1 M glucose 6-phosphate, 200 μ L of 5 mM KCl, and 1.3 mL of 0.1 M Tris-HCl buffer mixture was incubated at 37°C for 20 min. An addition of 1,000 μ L 10% trichloroacetic acid was used to terminate the reaction, after which it was allowed to stand on ice for 10 min before centrifuging for 10 min at 5,000 g. 250 μ L aliquot of the supernatant was placed in a 96-well plate and the absorbance was read at 340 nm.

Fructose-1-6-bisphosphatase activity

Fructose-1-6-bisphosphatase activity of the cells were determined according to a modified method by Balogun and Ashafa (2017). Briefly, 100 μ L of the cell supernatant was transferred to tube containing 0.05 M 100 μ L of fructose (0.05 M), 100 μ L of potassium chloride (0.1 M), 250 μ L of magnesium chloride (0.1 M), 1.2 mL of Tris-HCl buffer (0.1 M,

pH 7.0) and 250 μ L of Ethylenediaminetetraacetic acid (1 mM) and incubated for 15 min at 37°C. 10% trichloroacetic acid was used to halt the reaction and further centrifuged for 10 min at 5,000 g (4°C). Thereafter, 50 μ L of 1.25% ammonium molybdate and 9% ascorbic acid was included in the reaction, it was allowed to stand for 20 min at room temperature. The absorbance was read at 680 nm.

Glycogen phosphorylase activity

The glycogen phosphorylase activity of cells were evaluated based on the procedure of Balogun and Ashafa (2017). Briefly, 200 μ L of the cell supernatant, 100 μ L solution of 64 mM glucose-1-phosphate and 100 μ L 4% glycogen were mixed and incubated for 10 min at 30°C. 20% ammonium molybdate in concentrated sulfuric acid was used to terminate the reaction. Thereafter, Elon reducer and distilled water was added to the mixture and further incubated for 45 min at 30°C. The absorbance was measured at 340 nm.

Determination of lipase activity

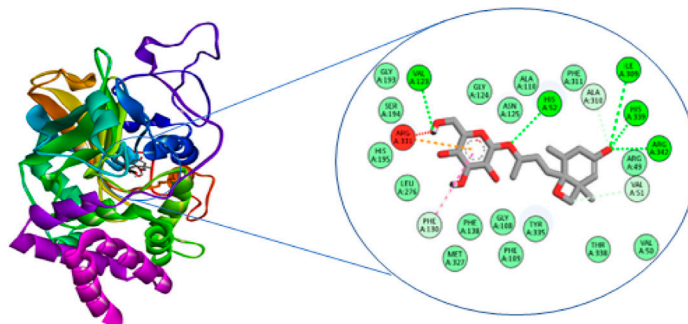
Hepatic lipase activity in the cells was estimated according to a previous method with slight modifications (Kim et al., 2010). Briefly, 200 μ L of the cell supernatant was added 390 μ L of Tris buffer (pH 7.0) and incubated at 37°C for 15 min 100 μ L of p-nitrophenyl butyrate in dimethylformamide (p-NPB) was then added to the mixture before incubating for another 15 min. The absorbance was measured at 405 nm at 1 min interval. Lipase activity of the hepatic cells was expressed as the rate of reaction ($\Delta A/\text{min}$).

Molecular docking

This computer analysis was employed to determine the binding affinities of the phytochemicals of *L. javanica* infusion with catalase and SOD antioxidant enzymes. The x-ray diffraction structure of the respective proteins (1F4J and 2C9V) with 2.40 Å and 1.07 Å resolutions were retrieved from the Protein Data Bank (<https://www.rcsb.org/>). Non-proteins and water molecules co-crystallized with the proteins were removed using the Dock prep tool algorithm of the Chimera software (V.1.16). Next, the automated program also added hydrogen atoms and gasteiger charges, as described according to Wang et al. (2006). Subsequently, the 3D structure of the LC-MS identified chemical compounds in the *L. javanica* infusion were similarly downloaded from the Zinc database (<https://zinc15>).

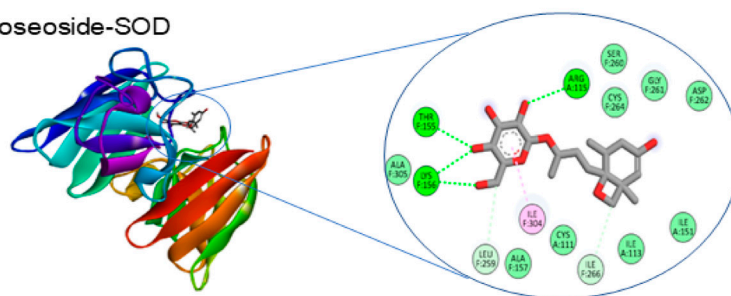
Dihydroroseoside-CAT

A



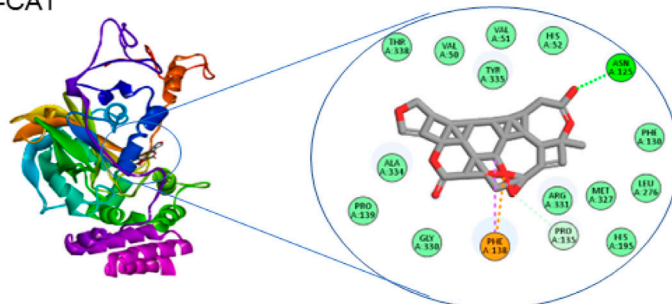
Dihydroroseoside-SOD

B



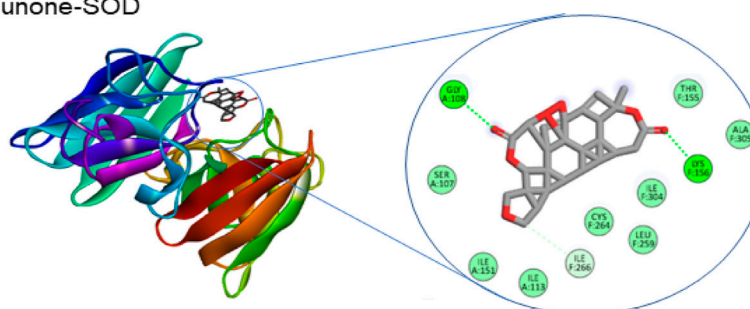
Obacunone-CAT

C



Obacunone-SOD

D



van der waals
 Conventional Hydrogen Bond
 Carbon Hydrogen Bond
 Unfavourable Donor-Donor

Interactions

Pi-Cation
 Pi-Alkyl
 Pi-Pi Stacked
 Pi-Sigma

FIGURE 9

The 3D and 2D images of the molecular interaction of dihydroroseoside with the amino active site of (A) catalase and (B) SOD; and 3D and 2D images of the molecular interaction of obacunone with active sites of (C) catalase, and (D) SOD. SOD = superoxide dismutase.

docking.org/substances/home/) and prepared using the previous software employed for the antioxidant enzymes. The catalytic pocket of the proteins were determined using the algorithm of

the CASTp online server (<http://cast.engr.uic.edu/>) before molecular docking was carried out within a search volume covering X, Y, and Z dimension of $13 \times 13 \times 13$ for SOD and

18 × 16 × 14 for catalase. Then, the calculated binding energies of the most stable ligand-protein complexes were recorded, and the 2D images of the various interactions involved were visualized using with BIOVIA Discovery Studio application.

Statistical analysis

The experiments were carried out in triplicate ($n = 3$) and results were presented as mean ± SD. Analysis of data was achieved by utilizing SPSS (Windows V25) and statistically significant difference between test groups was established at $p < 0.05$ using a one-way analysis of variance (ANOVA), followed by the use of Dunnett and Tukey's HSD multiple range Post-hoc tests for comparison of experimental mean values.

Results

The infusion extract of *L. javanica* revealed a total phenolic content of 25.95 ± 0.74 mg GAE/g and a total flavonoid content of 73.57 ± 2.12 mg QE/g of dry weight of extract. The extract showed a higher amount of flavonoid than phenolics.

As indicated in Figure 1A, *L. javanica* infusion significantly ($p < 0.05$) scavenged DPPH free radical at increasing concentrations, with a low IC_{50} value of $1.22 \mu\text{g/mL}$ (Table 1) and compared favorably with the standards, ascorbic acid (IC_{50} : values of $0.11 \mu\text{g/mL}$) and gallic acid (IC_{50} : values of $0.61 \mu\text{g/mL}$). However, the infusion only exhibited slight increase in Fe^{3+} reducing activity (Figure 1B) with IC_{50} value of $>1,000 \mu\text{g/mL}$ as compared to ascorbic acid at 120 and 240 $\mu\text{g/mL}$ doses (IC_{50} : values of 975.73 $\mu\text{g/mL}$) and gallic acid at all tested concentrations (IC_{50} : values of 63.81 $\mu\text{g/mL}$).

As portrayed in Figure 2, there was no significant difference in % cell viability between the cells treated with *L. javanica* infusion and the normal Chang liver cells. Treatment with doxorubicin significantly ($p < 0.05$) reduced the cell viability when compared to the normal control.

As depicted in Figures 3A–E, the induction of oxidative injury in Chang liver cells using ferrous sulphate led to significant ($p < 0.05$) depletion in the levels of GSH and NPSH, activities of SOD and catalase, with a concurrent increase in MDA level when compared with the normal control. Pretreatment of the cells with *L. javanica* significantly ($p < 0.05$) reversed these levels and activities and compared favorably with the two standard antioxidants, ascorbic acid and gallic acid. However, there was no significant difference in the catalase activity and NPSH level of the untreated cells and *L. javanica*-treated cells at lower concentrations.

Induction of oxidative stress led to a significant ($p < 0.05$) elevation in hepatic nitric oxide (NO) level (Figure 4). Pretreatment of cells with *L. javanica* infusion led to remarkable lower levels of NO in a dose-dependent trend. The infusion presented a better effect on NO level than both ascorbic acid and gallic acid.

There was a significant ($p < 0.05$) elevation in acetylcholinesterase activity on incubation of Chang liver cells with $FeSO_4$ (Figure 5). Except at the lowest dose, pretreatment with *L. javanica* infusion led to a significant ($p < 0.05$) dose-dependent suppression of acetylcholinesterase activity and was competitive with those of the standards, ascorbic acid and gallic acid.

Induction of oxidative injury caused significant ($p < 0.05$) elevation of glucose-6-phosphatase, fructose-1,6-bisphosphatase and glycogen phosphorylase activities as depicted in Figures 6A–C. Pretreatment with *L. javanica* led to significant suppression of the enzyme's activities in a dose-dependent trend to levels indistinguishable from the normal control.

As presented in Figure 7, induction of hepatic oxidative injury significantly ($p < 0.05$) elevated the activity of lipase. Incubation of the cells with *L. javanica* significantly ($p < 0.05$) depleted the activity of the enzyme which outperformed the activities of ascorbic acid and gallic acid.

LC-MS analysis of *L. javanica* infusion revealed the presence of phenolic compound such as amino phenol; tannins such as corilagin; phenolic glycosides such as coniferin and dihydroroseoside and terpenoids such as obacunone and radicol. [1-(3,4-Dihydroxy-5-methoxyphenyl)-7-(3,4-dihydroxyphenyl) heptan-3-yl] acetate and 3-Ethyl-4-hydroxy-1-phenylquinolin-2(1H)-one were also identified in the infusion (Table 2; Figure 8).

Table 3 shows the free binding energies of the molecular docking of the phytoconstituents of *L. javanica* and antioxidant standards (ascorbic acid and gallic acid) with catalase and SOD, which indicates that dihydroroseoside and obacunone had the highest binding affinity. Figure 8 gives a representation of 3D and 2D images of the molecular interaction of the active site of catalase with dihydroroseoside (Figure 9A), SOD with dihydroroseoside (Figure 9B) and catalase with obacunone (Figure 9C), and SOD with obacunone (Figure 9D). The compounds molecular interacted with the amino acid residues of the binding pocket of the proteins via hydrogen bonds (H-bond), carbon hydrogen bonds, and vanda Waal forces. Dihydroroseoside shared multiple H-bond with both catalase and SOD, while obacunone shared a single and double H-bond with catalase and SOD, respectively.

Discussion

Oxidative hepatic injury is a culprit in the pathological mechanisms that leads to the initiation and development of various liver diseases. Liver diseases have been reported to contribute significantly to socio-economic burden, low quality of life and mortality (Li et al., 2015; Asrani et al., 2019). Medicinal plants constitute a variety of secondary metabolites with inherent antioxidant properties that has been widely reported for the prevention and treatment of hepatic oxidative injury and numerous liver diseases (Stickel and Schuppan, 2007; Chukwuma et al., 2019). In this study, the protective effect of *L. javanica* herbal tea was investigated in iron-induced oxidative hepatic cells injury.

When surplus ROS are generated in the body, they deplete antioxidant levels, leading to a failure to counteract ROS deleterious activities which then result in cellular injury (Pham-Huy et al., 2008). Medicinal plants, including herbal teas are well noted for their rich antioxidant competence, which are ascribed to the presence of prominent phytoconstituents such as phenolics, terpenes, flavonoids, tannins, glycosides, alkaloids and saponins (Mathivha et al., 2020). The antioxidant capacity of these plant constituents are attributed to their ability to act as reducing agents, metal ion chelators, quenchers of singlet oxygen and free radical scavengers (Bendary et al., 2013; Salau et al., 2021). The potent DPPH

scavenging activity of *L. javanica* infusion (Figure 1A), coupled with its ability to reduce Fe^{3+} to Fe^{2+} (Figure 1B) indicate the antioxidant pharmacological property of this plant. This can be linked to the high phenolic and flavonoid contents of the plant as well as the presence of LC-MS identified bioactive compounds which include terpenoids, tannins, phenols and glycosides (Figure 8; Table 2). These results corroborates with the previous study of Osunsanmi et al. (2019) who reported that the crude extract of *L. javanica*'s leaves are embedded with varieties of phytochemicals that are a source of natural antioxidants for treating and managing oxidative stress related diseases.

To further buttress the antioxidant and other possible pharmacological potential of *L. javanica* as attributed to its phytoconstituents, its effect on iron induced oxidative hepatic injury were assessed. The liver is an organ that is constantly exposed to oxidative attack due to its critical and numerous physiological roles in the body that also involves generation of ROS as by-products and involvement in ROS-generation reactions (Li et al., 2015; Conde de la Rosa et al., 2022). This includes the liver being the major site of iron storage which makes it a major target for iron toxicity (Pietrangelo, 2016). The ability of iron to exist in dual forms: Fe^{2+} and Fe^{3+} , presents it as a major cofactor in many enzymatic redox reactions as well as a potent prooxidant (Erukainure et al., 2017). Thus, hepatic iron overload and/or iron toxicity leads to the generation of reactive oxygen species and reactive nitrogen species, which are responsible for lipid, protein and nucleic acid peroxidation and proinflammation that ultimately contributes the promotion of hepatic oxidative injury and numerous liver diseases (Videla et al., 2003; Milic et al., 2016). The suppressed levels of GSH and NPSH, SOD and catalase activities and increased levels of MDA and NO on induction of hepatic injury (Figures 3A–E; Figure 4) indicate an occurrence of oxidative stress and proinflammation. This corroborates previous study on Fe^{2+} induced oxidative injury in Chang liver cells (Chukwuma et al., 2019). Treatment with the *L. javanica* infusion demonstrated an antioxidant and anti-proinflammatory effect by significantly elevating the levels of GSH and NSPH, SOD and catalase activities and suppressing MDA and NO levels. Thus, indicating a protective effect of *L. javanica* on oxidative hepatic injury. The strong molecular interaction formed between the LC-MS identified phytoconstituents of *L. javanica* and the amino residue active sites of catalase and SOD (Figure 9; Table 3) further indicates the antioxidant potency of the infusion. These properties may be attributed to the synergistic activities of the identified phytochemical constituents.

Cholinergic dysfunction typified by elevated cholinesterase activities has been reported as one of the instigators of hepatotoxicity as it incites hepatic cells inflammation (Erukainure et al., 2021b). Altered acetylcholinesterase level has been reported as a useful biomarker for liver disease (García-Ayllón et al., 2006). Studies have linked oxidative stress and proinflammation to a rise in acetylcholinesterase activities (Bondok et al., 2013; Rodríguez-Fuentes et al., 2015). In the present study, the elevated activity of hepatic acetylcholinesterase (Figure 5) on induction of hepatic injury conforms with oxidative stress occurrence (Figure 3) and increased NO level (Figure 4). Cholinesterase inhibitors are targets for protecting against and treating liver diseases (Steinebrunner et al., 2014). The depleted activity of acetylcholinesterase on

treatment with *L. javanica* infusion insinuates a protective effect of the herbal tea against cholinergic dysfunction in oxidative hepatic injury.

The liver plays a pivotal function in the maintenance of glucose homeostasis and metabolism. Perturbations in hepatic glucose level is implicated in development of several liver diseases (Ding et al., 2018; Zhang et al., 2019). Oxidative stress contributes to disturbances in carbohydrate metabolism, which can lead to perturbed energy metabolism (Yazdi et al., 2019). Increased activities of enzymes involved in hepatic gluconeogenesis and glycogenolysis leads to the generation of excess glucose. Glucose toxicity characterised by hepatic glucose accumulation promotes hepatic oxidative stress which results in severe liver oxidative injury and eventual hepatic cell death (Chandrasekaran et al., 2012; Mota et al., 2016). Reports have shown the protective property of various plant-based antioxidants in scavenging free radical and the improvement of liver carbohydrate metabolism (Yazdi et al., 2019; Erukainure et al., 2021a; Olofinson et al., 2022). This is in accordance with the ability of *L. javanica* herbal infusion to significantly reduce the activities of glucose-6-phosphatase, fructose-1,6-bisphosphatase and glycogen phosphorylase in oxidative hepatic injury (Figures 6A–C), suggesting a hepatoprotective and hepatic metabolic function-improving potential of the herbal tea infusion.

The damaging effect of oxidative stress in the development of liver diseases cannot be overemphasized. ROS can induce lipid peroxidation by attacking the polyunsaturated fatty acids of lipid membrane and impair cellular functions (Barrera, 2012). Increased level of lipase activity in the liver has been reported in hepatotoxicity due to its catalyzed excessive breakdown of triglycerides, which causes accumulation of hepatic free fatty acids (Erukainure et al., 2021a). Thus, oxidative attack of vulnerable fatty acids progresses oxidative injury. Cytotoxic products generated from hepatic lipid peroxidation such as malondialdehyde (MDA) have been implicated in hepatic fibrogenesis (Koruk et al., 2004). The elevation of lipase activity on induction of oxidative injury (Figure 7) with concomitant increased MDA level (Figure 3D) may indicate progressive oxidative hepatic injury and development of liver disease. The ability of *L. javanica* infusion to significantly suppress hepatic lipase activity may further suggest the protective effect of the herbal infusion against oxidative hepatic injury.

Phytopharmaceuticals play a key role in medical practice for various diseases treatment and management. However, in addition to their therapeutic properties, many medicinal herbs may contain potential toxic properties that may cause more harm to human health (Lombardi et al., 2017). Cytotoxicity studies is thus a crucial step in determining the safety and therapeutic properties of plants and plant-derived compounds for oral pharmacological agent development (Beseni et al., 2022). The cell viability effect of *L. javanica* infusion (Figure 2) portrays a non-cytotoxic effect on liver cells. Thus, implying the safety of the *L. javanica* herbal tea on hepatic cells.

Conclusion

Results from this study demonstrated that *L. javanica* conferred hepatoprotection against oxidative hepatic injury by mitigating

oxidative stress and cholinergic dysfunction as well as improved impaired glucogenic and lipase enzymes activities. These biological activities may be attributed to the synergistic effect of the identified phytoconstituents. Thus, these results may support the ingestion of *L. javanica* herbal tea as potential curative agent for liver diseases. Further *in vivo* and molecular studies are required to unravel the mechanisms by which *L. javanica* brings about its hepatoprotective effect in hepatic oxidative injury. The limitation of the present study is the non-use of commercial standard for the LC-MS analysis. We therefore propose the use commercially available standards for future characterization of *L. javanica* phytoconstituents.

Data availability statement

The original contributions presented in the study are included in the article/Supplementary material, further inquiries can be directed to the corresponding author.

Author contributions

VS: conceptualization; data curation; investigation; methodology; writing-original draft. OE: formal analysis; methodology; writing-review and editing. KO: data curation; methodology; writing-review and editing. RS: methodology; writing-review and editing. MM: resources; supervision; writing-

review and editing. All authors contributed to the article and approved the submitted version.

Acknowledgments

VS acknowledges University of the Free State, Bloemfontein, South Africa for Postdoctoral Fellowship Grant (2022162164). MM acknowledges the funding support from the IK-based Technology Innovations at the Department of Science and Innovation.

Conflict of interest

The authors declare that the research was conducted in the absence of any commercial or financial relationships that could be construed as a potential conflict of interest.

Publisher's note

All claims expressed in this article are solely those of the authors and do not necessarily represent those of their affiliated organizations, or those of the publisher, the editors and the reviewers. Any product that may be evaluated in this article, or claim that may be made by its manufacturer, is not guaranteed or endorsed by the publisher.

References

- Asrani, S. K., Devarbhavi, H., Eaton, J., and Kamath, P. S. (2019). Burden of liver diseases in the world. *J. hepatology* 70, 151–171. doi:10.1016/j.jhep.2018.09.014
- Balogun, F., and Ashafa, A. (2017). Aqueous root extracts of *Dicoma anomala* (Sond) extenuates postprandial hyperglycaemia *in vitro* and its modulation on the activities of carbohydrate-metabolizing enzymes in streptozotocin-induced diabetic Wistar rats. *South Afr. J. Bot.* 112, 102–111. doi:10.1016/j.sajb.2017.05.014
- Barrera, G. 2012. *Oxidative stress and lipid peroxidation products in cancer progression and therapy*. China, International Scholarly Research Notices,
- Bendary, E., Francis, R., Ali, H., Sarwat, M., and el Hady, S. (2013). Antioxidant and structure-activity relationships (SARs) of some phenolic and anilines compounds. *Ann. Agric. Sci.* 58, 173–181. doi:10.1016/j.aas.2013.07.002
- Benzie, I. F., and Strain, J. J. (1996). The ferric reducing ability of plasma (FRAP) as a measure of "antioxidant power": The FRAP assay. *Anal. Biochem.* 239, 70–76. doi:10.1006/abio.1996.0292
- Beseni, B. K., Olofinson, K. A., Salau, V. F., Erukainure, O. L., and Islam, M. S. (2022). Rhus longipes (Engl) infusions improve glucose metabolism and mitigate oxidative biomarkers in ferrous sulfate-induced renal injury. *Asian Pac. J. Trop. Biomed.* 12, 453. doi:10.4103/2221-1691.360561
- Bondok, R. S., Ahmed, M. A., Soliman, N. B. E., el-Shokry, M. H., Ali, R. M., Fahmy, H. F., et al. (2013). The effect of cholinesterase inhibition on liver dysfunction in experimental acute liver failure. *Egypt. J. Crit. Care Med.* 1, 51–59. doi:10.1016/j.ejccm.2013.05.002
- Chandrasekaran, K., Swaminathan, K., Mathan Kumar, S., Clemens, D. L., and Dey, A. (2012). *In vitro* evidence for chronic alcohol and high glucose mediated increased oxidative stress and hepatotoxicity. *Alcohol. Clin. Exp. Res.* 36, 1004–1012. doi:10.1111/j.1530-0277.2011.01697.x
- Chang, C.-C., Yang, M.-H., Wen, H.-M., and Chern, J.-C. (2002). Estimation of total flavonoid content in propolis by two complementary colorimetric methods. *J. food drug analysis* 10. doi:10.38212/2224-6614.2748
- Changlian, P., Shaowei, C., Zhifang, L., and Guizhu, L. (2000). Detection of antioxidative capacity in plants by scavenging organic free radical DPPH. *Sheng wu hua xue yu Sheng wu wu li jin Zhan* 27, 658–661.
- Chen, Z., Tian, R., She, Z., Cai, J., and Li, H. (2020). Role of oxidative stress in the pathogenesis of nonalcoholic fatty liver disease. *Free Radic. Biol. Med.* 152, 116–141. doi:10.1016/j.freeradbiomed.2020.02.025
- Chowdhury, P., and Soulsby, M. (2002). Lipid peroxidation in rat brain is increased by simulated weightlessness and decreased by a soy-protein diet. *Ann. Clin. Laboratory Sci.* 32, 188–192.
- Chukwuma, C. I., Matsabisa, M. G., Rautenbach, F., Rademan, S., Oyedemi, S. O., Chaudhary, S. K., et al. (2019). Evaluation of the nutritional composition of *Myrothamnus flabellifolius* (Welw) herbal tea and its protective effect against oxidative hepatic cell injury. *J. food Biochem.* 43, e13026. doi:10.1111/jfbc.13026
- Cichoż-Lach, H., and Michalak, A. (2014). Oxidative stress as a crucial factor in liver diseases. *World J. gastroenterology WJG* 20, 8082–8091. doi:10.3748/wjg.v20.i25.8082
- Conde De la Rosa, L., Goicoechea, L., Torres, S., Garcia-Ruiz, C., and Fernandez-Checa, J. C. (2022). Role of oxidative stress in liver disorders. *Livers* 2, 283–314. doi:10.3390/livers2040023
- Dhiman, A., Nanda, A., and Ahmad, S. (2012). A recent update in research on the antihepatotoxic potential of medicinal plants. *Zhong xi yi jie he xue bao= J. Chin. Integr. Med.* 10, 117–127. doi:10.3736/jcim20120201
- Ding, H.-R., Wang, J.-L., Ren, H.-Z., and Shi, X.-L. 2018. Lipometabolism and glycometabolism in liver diseases. *BioMed Res. Int.*, 2018, 1287127, doi:10.1155/2018/1287127
- Ellman, G. L., Courtney, K. D., Andres, V., JR, and Featherstone, R. M. (1961). A new and rapid colorimetric determination of acetylcholinesterase activity. *Biochem. Pharmacol.* 7, 88–95. doi:10.1016/0006-2952(61)90145-9
- Ellman, G. L. (1959). Tissue sulfhydryl groups. *Archives Biochem. biophysics* 82, 70–77. doi:10.1016/0003-9861(59)90090-6
- Erukainure, O. L., Matsabisa, M. G., Salau, V. F., Oyedemi, S. O., Oyenih, O. R., Ibeji, C. U., et al. (2021a). Cannabis sativa L (var Indica) exhibits hepatoprotective effects by modulating hepatic lipid profile and mitigating gluconeogenesis and cholinergic dysfunction in oxidative hepatic injury. *Front. Pharmacol* 12, 705402. doi:10.3389/fphar.2021.705402
- Erukainure, O. L., Mopuri, R., Oyebo, O. A., Koorbanally, N. A., and Islam, M. S. (2017). *Dacryodes edulis* enhances antioxidant activities, suppresses DNA fragmentation in oxidative pancreatic and hepatic injuries; and inhibits carbohydrate digestive enzymes linked to type 2 diabetes. *Biomed. Pharmacother.* 96, 37–47. doi:10.1016/j.biopha.2017.09.106
- Erukainure, O. L., Sanni, O., Salau, V. F., Koorbanally, N. A., and Islam, M. S. (2021b). *Cola nitida* (kola nuts) attenuates hepatic injury in type 2 diabetes by improving

- antioxidant and cholinergic dysfunctions and dysregulated lipid metabolism. *Endocr. Metabolic Immune Disorders-Drug Targets (Formerly Curr. Drug Targets-Immune, Endocr. Metabolic Disord.)* 21, 688–699. doi:10.2174/1871530320666200628030138
- Fouché, G., Cragg, G., Pillay, P., Kolesnikova, N., Maharaj, V., and Senabe, J. (2008). *In vitro* anticancer screening of South African plants. *J. Ethnopharmacol.* 119, 455–461. doi:10.1016/j.jep.2008.07.005
- García-Ayllón, M.-S., Millán, C., Serra-Basante, C., Bataller, R., and Sáez-Valero, J. (2012). Readthrough acetylcholinesterase is increased in human liver cirrhosis. *PLoS One* 7, e45598. doi:10.1371/journal.pone.0044598
- García-Ayllón, M. S., Silveyra, M. X., Candela, A., Compañ, A., Clària, J., Jover, R., et al. (2006). Changes in liver and plasma acetylcholinesterase in rats with cirrhosis induced by bile duct ligation. *Hepatology* 43, 444–453. doi:10.1002/hep.21071
- Germishuizen, G., Meyer, N., Steenkamp, Y., and Keith, M. (2006). *A checklist of South African plants. Southern african botanical diversity network report No. 41*. Pretoria: SABONET.
- Hadwan, M. H., and Abed, H. N. (2016). Data supporting the spectrophotometric method for the estimation of catalase activity. *Data brief* 6, 194–199. doi:10.1016/j.dib.2015.12.012
- Hong, M., Li, S., Tan, H. Y., Wang, N., Tsao, S.-W., and Feng, Y. (2015). Current status of herbal medicines in chronic liver disease therapy: The biological effects, molecular targets and future prospects. *Int. J. Mol. Sci.* 16, 28705–28745. doi:10.3390/ijms161226126
- Kakkar, P., Das, B., and Viswanathan, P. (1984). A modified spectrophotometric assay of superoxide dismutase. *Indian J. Biochem. Biophys.* 21, 130–132.
- Kim, Y. S., Lee, Y. M., Kim, H., Kim, J., Jang, D. S., Kim, J. H., et al. (2010). Anti-obesity effect of morus bombycis root extract: Anti-lipase activity and lipolytic effect. *J. Ethnopharmacol.* 130, 621–624. doi:10.1016/j.jep.2010.05.053
- Koruk, M., Taysi, S., Savas, M. C., Yilmaz, O., Akcay, F., and Karakok, M. (2004). Oxidative stress and enzymatic antioxidant status in patients with nonalcoholic steatohepatitis. *Ann. Clin. Laboratory Sci.* 34, 57–62.
- Li, A.-N., Li, S., Zhang, Y.-J., Xu, X.-R., Chen, Y.-M., and Li, H.-B. (2014). Resources and biological activities of natural polyphenols. *Nutrients* 6, 6020–6047. doi:10.3390/nu6126020
- Li, S., Tan, H.-Y., Wang, N., Zhang, Z.-J., Lao, L., Wong, C.-W., et al. (2015). The role of oxidative stress and antioxidants in liver diseases. *Int. J. Mol. Sci.* 16, 26087–26124. doi:10.3390/ijms161125942
- Lombardi, V. R., Carrera, I., and Cacabelos, R. (2017). *In vitro screening for cytotoxic activity of herbal extracts*. Germany, Evidence-Based Complementary and Alternative Medicine.
- Lukwa, N., Molgaard, P., Furu, P., and Bogh, C. (2009). *Lippia javanica* (burm F) Spreng: Its general constituents and bioactivity on mosquitoes. *Trop. Biomed.* 26, 85–91.
- Maroyi, A. (2017). *Lippia javanica* (burm F) Spreng: Traditional and commercial uses and phytochemical and pharmacological significance in the african and indian subcontinent. *Evidence-based complementary Altern. Med.*, 2017, 1. doi:10.1155/2017/6746071
- Mathivha, P. L., Msagati, T. A., Thibane, V. S., and Mudau, F. N. (2020). *Herbal medicine in India: Indigenous knowledge, practice, innovation and its value*, 281–301. Phytochemical analysis of herbal teas and their potential health, and food safety benefits: A review
- Mcdonald, S., Prenzler, P. D., Antolovich, M., and Robards, K. (2001). Phenolic content and antioxidant activity of olive extracts. *Food Chem.* 73, 73–84. doi:10.1016/s0308-8146(00)00288-0
- Mikszowicz, V., Lucero, D., Zago, V., Cacciagliú, L., Lopez, G., Gonzalez Ballerga, E., et al. (2012). Hepatic lipase activity is increased in non-alcoholic fatty liver disease beyond insulin resistance. *Diabetes/metabolism Res. Rev.* 28, 535–541. doi:10.1002/dmrr.2312
- Milic, S., Mikolasevic, I., Orlic, L., Devic, E., Starcevic-Cizmarevic, N., Stimac, D., et al. (2016). The role of iron and iron overload in chronic liver disease. *Med. Sci. Monit. Int. Med. J. Exp. Clin. Res.* 22, 2144–2151. doi:10.12659/msm.896494
- Mota, M., Banini, B. A., Cazanave, S. C., and Sanyal, A. J. (2016). Molecular mechanisms of lipotoxicity and glucotoxicity in nonalcoholic fatty liver disease. *Metabolism* 65, 1049–1061. doi:10.1016/j.metabol.2016.02.014
- Mujovo, S. F., Hussein, A. A., Meyer, J. M., Fourie, B., Muthivhi, T., and Lall, N. (2008). Bioactive compounds from *Lippia javanica* and *Hoslundia opposita*. *Nat. Prod. Res.* 22, 1047–1054. doi:10.1080/14786410802250037
- Olofinson, K. A., Erukainure, O. L., Brian, B. K., and Islam, M. S. (2022). *Harpephyllum caffrum* stimulates glucose uptake, abates redox imbalance and modulates purinergic and glucogenic enzyme activities in oxidative hepatic injury. *Asian Pac. J. Trop. Biomed.* 12, 9. doi:10.4103/2221-1691.333209
- Osunsami, F. O., Zharare, G. E., and Opoku, A. R. (2019). Phytochemical constituents and antioxidant potential of crude extracts from *Lippia Javanica* (Burm. f.) Spreng Leaves *Pharmacogn. J.* 11, 803–807. doi:10.5530/pj.2019.11.128
- Pham-Huy, L. A., He, H., and Pham-Huy, C. (2008). Free radicals, antioxidants in disease and health. *Int. J. Biomed. Sci. IJBS* 4, 89–96.
- Pietrangolo, A. (2016). Iron and the liver. *Liver Int.* 36, 116–123. doi:10.1111/liv.13020
- Rodríguez-Fuentes, G., Rubio-Escalante, F. J., Noreña-Barroso, E., Escalante-Herrera, K. S., and Schlenk, D. (2015). Impacts of oxidative stress on acetylcholinesterase transcription, and activity in embryos of zebrafish (*Danio rerio*) following Chlorpyrifos exposure. *Comp. Biochem. Physiology Part C Toxicol. Pharmacol.* 172, 19–25. doi:10.1016/j.cbpc.2015.04.003
- Salau, V. F., Erukainure, O. L., Koorbanally, N. A., and Islam, M. S. (2021). Ferulic acid promotes muscle glucose uptake and modulate dysregulated redox balance and metabolic pathways in ferric-induced pancreatic oxidative injury. *J. Food Biochem.* 46, e13641. doi:10.1111/jfbc.13641
- Shahriar, M., Chowdhury, A., Rahman, M., Uddin, M., Al-Amin, M., Rahman, M., et al. (2014). Scientific validation of medicinal plants used by a folk medicinal practitioner of Chuadanga district, Bangladesh. *World J. Pharm. Pharm. Sci. (WJPPS)* 3, 13–24.
- Shikanga, E., Combrinck, S., and Regnier, T. (2010). South African *Lippia* herbal infusions: Total phenolic content, antioxidant and antibacterial activities. *South Afr. J. Bot.* 76, 567–571. doi:10.1016/j.sajb.2010.04.010
- Steinebrunner, N., Mogler, C., Vittas, S., Hoyler, B., Sandig, C., Stremmel, W., et al. (2014). Pharmacologic cholinesterase inhibition improves survival in acetaminophen-induced acute liver failure in the mouse. *BMC Gastroenterol.* 14, 148–8. doi:10.1186/1471-230X-14-148
- Stepanova, M., De Avila, L., Afendy, M., Younossi, I., Pham, H., Cable, R., et al. (2017). Direct and indirect economic burden of chronic liver disease in the United States. *Clin. Gastroenterology Hepatology* 15, 759–766. e5. doi:10.1016/j.cgh.2016.07.020
- Stickel, F., and Schuppan, D. (2007). Herbal medicine in the treatment of liver diseases. *Dig. liver Dis.* 39, 293–304. doi:10.1016/j.dld.2006.11.004
- Suleman, Z., Engwa, G. A., Shauli, M., Musarurwa, H. T., Katuruza, N. A., and Sewani-Rusike, C. R. (2022). Neuroprotective effects of *Lippia javanica* (Burm. F) Spreng. Herbal tea infusion on Lead-induced oxidative brain damage in Wistar rats. *BMC Complementary Med. Ther.* 22, 4–10. doi:10.1186/s12906-021-03471-3
- Tsikak, D. (2005). Methods of quantitative analysis of the nitric oxide metabolites nitrite and nitrate in human biological fluids. *Free Radic. Res.* 39, 797–815. doi:10.1080/10715760500053651
- Upadhyay, J., Tiwari, N., Durgapal, S., and Farzaei, M. H. (2022). *Antioxidants and liver diseases. Antioxidants effects in health*. Germany: Elsevier.
- Videla, L. A., Fernández, V., Tapia, G., and Varela, P. (2003). Oxidative stress-mediated hepatotoxicity of iron and copper: Role of kupffer cells. *Biometals* 16, 103–111. doi:10.1023/a:1020707811707
- Wang, J., Wang, W., Kollman, P. A., and Case, D. A. (2006). Automatic atom type and bond type perception in molecular mechanical calculations. *J. Mol. Graph. Model.* 25, 247–260. doi:10.1016/j.jmgm.2005.12.005
- Yazdi, H. B., Hojati, V., Shiravi, A., Hosseini, S., Vaezi, G., and Hadjzadeh, M. A. R. (2019). Liver dysfunction and oxidative stress in streptozotocin-induced diabetic rats: Protective role of artemisia turanica. *J. pharmacopuncture* 22, 109–114. doi:10.3831/KPI.2019.22.014
- Zhang, X., Yang, S., Chen, J., and Su, Z. (2019). Unraveling the regulation of hepatic gluconeogenesis. *Front. Endocrinol.* 9, 802. doi:10.3389/fendo.2018.00802



OPEN ACCESS

EDITED BY

Aliyu Muhammad,
Ahmadu Bello University, Nigeria

REVIEWED BY

Babangida Sanusi,
Ahmadu Bello University, Nigeria
Munaf Hashim Zalala,
University of Baghdad, Iraq
Gilead Forcados,
National Veterinary Research Institute
(NVRI), Nigeria

*CORRESPONDENCE

Jinyue Sun,
✉ moon_s731@hotmail.com
Xinhua Song,
✉ 892442572@qq.com
Wenlong Sun,
✉ 512649113@qq.com

[†]These authors have contributed equally
to this work and share first authorship

RECEIVED 06 July 2023

ACCEPTED 25 September 2023

PUBLISHED 06 October 2023

CITATION

Xin M, Wang H, Wang M, Yang B, Liang S,
Xu X, Dong L, Cai T, Huang Y, Wang Q,
Wang C, Cui Y, Xu Z, Sun W, Song X and
Sun J (2023), Attenuating effect of
Polygala tenuifolia Willd. seed oil on
progression of MAFLD.
Front. Pharmacol. 14:1253715.
doi: 10.3389/fphar.2023.1253715

COPYRIGHT

© 2023 Xin, Wang, Wang, Yang, Liang, Xu,
Dong, Cai, Huang, Wang, Wang, Cui, Xu,
Sun, Song and Sun. This is an open-
access article distributed under the terms
of the [Creative Commons Attribution
License \(CC BY\)](https://creativecommons.org/licenses/by/4.0/). The use, distribution or
reproduction in other forums is
permitted, provided the original author(s)
and the copyright owner(s) are credited
and that the original publication in this
journal is cited, in accordance with
accepted academic practice. No use,
distribution or reproduction is permitted
which does not comply with these terms.

Attenuating effect of *Polygala tenuifolia* Willd. seed oil on progression of MAFLD

Meiling Xin^{1†}, Hanlin Wang^{1†}, Meng Wang^{1†}, Bendong Yang¹,
Shufei Liang¹, Xiaoxue Xu¹, Ling Dong¹, Tianqi Cai¹, Yuhong Huang²,
Qing Wang³, Chao Wang¹, Yuting Cui¹, Zhengbao Xu¹,
Wenlong Sun^{1,4*}, Xinhua Song^{1,4*} and Jinyue Sun^{3,4*}

¹School of Life Sciences and Medicine, Shandong University of Technology, Zibo, Shandong, China, ²College of Life Sciences, Yangtze University, Jingzhou, Hubei, China, ³Key Laboratory of Novel Food Resources Processing, Key Laboratory of Agro-Products Processing Technology of Shandong Province, Ministry of Agriculture and Rural Affairs, Institute of Agro-Food Science and Technology, Shandong Academy of Agricultural Sciences, Jinan, China, ⁴Shandong Qingyujiaxing Biotechnology Co., Ltd., Zibo, Shandong, China

Introduction: Metabolic-associated fatty liver disease (MAFLD) is a common chronic metabolic disease that seriously threatens human health. The pharmacological activity of unsaturated fatty acid-rich vegetable oil interventions in the treatment of MAFLD has been demonstrated. This study evaluated the pharmacological activity of *Polygala tenuifolia* Willd, which contains high levels of 2-acetyl-1,3-diacyl-sn-glycerols (sn-2-acTAGs).

Methods: In this study, a mouse model was established by feeding a high-fat diet (HFD, 31% lard oil diet), and the treatment group was fed a *P. tenuifolia* seed oil (PWSO) treatment diet (17% lard oil and 14% PWSO diet). The pharmacological activity and mechanism of PWSO were investigated by total cho-lesterol (TC) measurement, triglyceride (TG) measurement and histopathological observation, and the sterol regulatory element-binding protein-1 (SREBP1), SREBP2 and NF-κB signaling pathways were evaluated by immunofluorescence and Western blot analyses.

Results: PWSO attenuated the increases in plasma TC and TG levels. Furthermore, PWSO reduced the hepatic levels of TC and TG, ameliorating hepatic lipid accumulation. PWSO treatment effectively improves the level of hepatic inflammation, such as reducing IL-6 levels and TNF-α level.

Discussion: PWSO treatment inactivated SREBP1 and SREBP2, which are involved in lipogenesis, to attenuate hepatic lipid accumulation and mitigate the inflammatory response induced via the NF-κB signaling pathway. This study demonstrated that PWSO can be used as a relatively potent dietary supplement to inhibit the occurrence and development of MAFLD.

KEYWORDS

metabolic-associated fatty liver disease, *Polygala tenuifolia* Willd., seed oil, SREBPs, NF-κB signaling pathway

Abbreviations: sn-2-acTAGs, 2-acetyl-1,3-diacyl-sn-glycerols; ACC, acetyl-CoA carboxylase; ALT, alanine aminotransferase; AST, aspartate aminotransferase; FASN, fatty acid synthase; GC, gas chromatography; H&E, hematoxylin and eosin; HDL-C, high-density lipoprotein cholesterol; HFD group, high-fat diet group; LDL-C, low-density lipoprotein cholesterol; MAFLD, metabolic-associated fatty liver disease; NAFLD, non-alcoholic fatty liver disease; NC group, normal control group; PWSO, *P. tenuifolia* seed oil; *P. tenuifolia*, *Polygala tenuifolia* Willd.; PW group, PWSO treatment group; SREBP1, sterol regulatory element-binding protein-1; TC, total cholesterol; TCM, traditional Chinese medicine; TG, triglyceride.

1 Introduction

Metabolic-associated fatty liver disease (MAFLD), also called non-alcoholic fatty liver disease (NAFLD), is a disorder of excessive lipid deposition in hepatocytes caused by factors other than alcohol and other definite factors, and the indicative test result is a hepatic triglyceride (TG) content exceeding 5% after alcohol-free testing (Stefan et al., 2019; Eslam et al., 2020). Many metabolic disorders exist, including hyperglycemia, type 2 diabetes, insulin impedance, dyslipidemia, and adipokine abnormalities, all of which have a significant association with the pathogenesis of MAFLD (Anstee et al., 2013).

MAFLD and its symptoms can be effectively treated with a healthy diet and weight loss, with effects such as a decline in inflammation and improvement in fibrosis (Romero-Gomez et al., 2017). However, many people's lifestyles and habits do not allow them to maintain an adequate exercise program and healthy diet. As a result, drug intervention is used to ameliorate or prevent MAFLD. Due to the complex mechanism of MAFLD and the fact that Western medicine typically has a single therapeutic target, emphasis on prevention and treatment by traditional Chinese medicine (TCM), which has more complex components, is increasing. Moreover, TCM treatment and prevention methods are widely accepted by the public as safer and more effective than other methods (Gao et al., 2020). TCM with the same origin as medicine and food is characterized by few toxic side effects and high patient compliance. Studies have shown that these TCM practices have had a positive impact on the development of MAFLD, and they are considered an approach for the treatment and prevention of MAFLD (Liu et al., 2014). Numerous researchers have reported that many vegetable and animal oils rich in unsaturated fatty acids might be beneficial for the prevention of lipid metabolism disorders and MAFLD (Henkel et al., 2018; Yang et al., 2019). Recently, vegetable and animal oils rich in 2-acetyl-1,3-diacyl-sn-glycerols (sn-2-acTAGs) were reported, and the high content of sn-2-acTAGs was considered one factor responsible for its pharmacological effects (Smith et al., 2018). However, the effects of oils containing high levels of sn-2-acTAGs on MAFLD were not evaluated.

Polygala tenuifolia Willd. is a traditional Chinese medicine that consists mainly of triterpene saponins, sanguinarides and oligosaccharides (Zhao et al., 2020). The main medicinal component of *P. tenuifolia* is the root or the whole herb, which has pharmacological activities such as antidepressant, cholesterol-lowering, anti-inflammatory and anticancer activities (Son et al., 2022). Research has also shown that *P. tenuifolia* and its functional components have a variety of neuroprotective effects, such as the ability to treat and prevent Alzheimer's disease, neuroinflammatory diseases, and depression (Wang et al., 2017; Yao et al., 2020; Jee et al., 2021). The high level of sn-2-acTAGs in *P. tenuifolia* seed oil (PWSO) might contribute to the pharmacological effects, but the pharmacological activity and potential mechanism of PWSO on MAFLD remain unclear.

In this study, we explored the fatty acid composition of PWSO by gas chromatography (GC) and determined its pharmacological activity on MAFLD in an established mouse model, wherein it inhibited lipid accumulation and liver inflammation by attenuating the activation of the SREBP and NF- κ B signaling pathways. We suggest that PWSO may be a potential agent for treating and preventing MAFLD symptoms.

2 Materials and methods

2.1 Reagents

Seeds of *P. tenuifolia* (Chinese name: Yuan Zhi) were purchased from Xuxin Pharmaceutical Sale (Anhui, China). Commercial kits, including the total cholesterol (TC, A111-1-1), triglyceride (TG, A110-1-1), low-density lipoprotein cholesterol (LDL-C, A113-1-1), high-density lipoprotein cholesterol (HDL-C, A112-1-1), alanine aminotransferase (ALT, C009-2-1), and aspartate aminotransferase (AST, C011-2-1) kits, were purchased from Nanjing Jiancheng Bioengineering Institute (Nanjing, China). The fatty acid standards were purchased from Sigma (United States). Anti- β -actin (K101527P), anti-LAMB1 (K006070P), anti-sterol regulatory element-binding protein 1 (SREBP1, K106528P), anti-fatty acid synthase (FASN, K001685P), anti-acetyl-CoA carboxylase (ACC, 16087-1-AP), anti-3-hydroxy-3-methylglutaryl-CoA reductase (HMGCR, K002888P), anti-IL-6 (K001738P), anti-TNF- α (SEKM-0034), anti-SREBP2 (K106821P), and anti-NF- κ B (80979-1-RR) antibodies were purchased from Solarbio (Beijing, China).

2.2 Preparation of PWSO

According to previous study (Smith et al., 2018), the dried seeds of *P. tenuifolia* were cold pressed to obtain the crude oil extract (the pressing pressure was 40–50 MPa, and the pressing temperature was approximately 60°C). Then, the raw *P. tenuifolia* extract was degummed with hot water, deacidified with alkaline solution, and decolorized with white clay for the following experiments. The composition of PWSO has been fully verified in our previous study (Smith et al., 2018), including TLC, GC, MALDI-TOF MS and ^{13}C NMR analyses.

2.3 Animal experiments

All animal experimental procedures were approved by the Animal Ethics Committee of Shandong University of Technology (the approval date is 17-11-2021, and the approval certification number of the study is YLX20211101). The protocols followed the Guidelines for the Care and Use of Laboratory Animals of Shandong University of Technology. Male Kunming mice (6 weeks old, 18–20 g) were acquired from the Shandong Laboratory Animal Center (Jinan, China) (approval number SCXK 2020-0005) and were housed under standard laboratory conditions with 55%–65% humidity, 25°C \pm 3°C, and a 12-h light/dark cycle. All mice were randomly divided into three groups: the normal control group (NC group; $n = 8$), the high-fat diet group (HFD group; $n = 8$), and the PWSO treatment group (PW group; $n = 8$). The mice in the NC group remained on the standard diet throughout the whole experimental period. The mice in the HFD group remained on the HFD throughout the whole experimental period. The PW group was fed a HFD (31% lard oil diet), and after 4 weeks, the mice in the PW group were switched to a PWSO treatment diet (17% lard oil and 14% PWSO diet) for 8 weeks. The whole experiment lasted for 12 weeks. Detailed dietary information can be obtained from Table 1.

TABLE 1 Details of the HFD and PWSO diet.

Ingredient	HFD		PWSO diet	
	gm	kcal	gm	kcal
Casein, 80 Mesh	200	800	200	800
L-Cystine	3	12	3	12
Cholesterol	12	0	12	0
PWSO	0	0	111	999
Lard Oil	245	2,205	134	1205.8
Maltodextrin 10	123	500	123	500
Sucrose	68.8	275.2	68.8	275.2
Cellulose, BW200	50	0	50	0
Soybean Oil	25	225	25	225
Mineral Mix, S10026	10	0	10	0
Dicalcium Phosphate	13	0	13	0
Calcium Carbonate	5.5	0	5.5	0
Potassium Citrate, 1 H ₂ O	16.5	0	16.5	0
Vitamin Mix, V10001	10	40	10	40
Vitamin Mix, V10001	2	0	2	0
FD&C Blue Dye	0.05	0	0.05	0
Total	785.85	4,057	785.85	4,057

2.4 Biochemical measurements

Body weight and food intake were recorded weekly throughout the experimental period. The mice were sacrificed after 12 weeks of feeding following intraperitoneal injection of pentobarbital sodium (30 mg/kg) for anesthesia. The mice were killed by CO₂ inhalation; enucleation was then performed, and blood was collected (0.8–1.2 ml per mouse) and then centrifuged (5 min, 4°C, 3,000 rpm) to obtain plasma. The levels of TC, TG, LDL-C and HDL-C were determined with a microplate reader (Gen 5, BioTek, United States).

2.5 Histological observations

Liver tissues from each mouse were collected and fixed with 4% paraformaldehyde for 24 h. Then, the liver tissue specimens were embedded in paraffin and cut into 3-μm-thick sections. Finally, the obtained sections were dyed with hematoxylin and eosin (H&E) and Sirius red for pathological analysis.

2.6 Western blot analysis

We evaluated the effects of PWSO on important indicators (such as SREBPs, ACC, FASN, HMGCR and NF-κB) of nuclear and cytoplasmic activity by Western blot analysis. Liver tissue homogenate was obtained by supplementing RIPA lysis buffer with 1% PMSF (Beyotime, China). The protein concentration

was measured using a BCA kit (Beyotime, China). Liver tissue samples were separated using 12% SDS–PAGE and transferred onto PVDF membranes. Then, the membranes were incubated with 5% non-fat milk for approximately 2 h for blocking. Subsequently, the membranes were incubated overnight at 4°C with primary antibodies, including anti-SREBP1 (1:1000, Solarbio, China), anti-ACC (1:1000, Solarbio, China), anti-FASN (1:1000, Solarbio, China), anti-SREBP2 (1:1000, Solarbio, China), anti-HMGCR (1:1000, Solarbio, China), and anti-NF-κB (1:1000, Solarbio, China) antibodies in skim milk powder TBST solution. The membranes were washed three times with TBST and then incubated with the appropriate secondary antibody (1:3500, Solarbio, China) at room temperature for 2 h. The membranes were washed again for development observation. Three samples were selected for analysis.

Protein bands were visualized by using an ECL Plus kit (Beyotime, China), and the band densities were quantified by ImageJ software. β-Actin or LAMB1 was used as a reference, and all protein expression levels were standardized to these band intensities.

2.7 Immunofluorescence analysis

We evaluated the effects of PWSO on important indicators (such as SREBP1, IL-6, TNF-α and NF-κB) of nuclear and cytoplasmic activity by immunofluorescence analysis. According to previous study (Yang et al., 2021), the liver slice samples were first fixed with 4% paraformaldehyde for 15 min. The fixed samples were blocked with 2% BSA for 30 min and then incubated with primary antibodies (anti-SREBP1, anti-IL-6, anti-TNF-α and anti-NF-κB, 1:200) overnight at 4°C. Next, the sections were washed and incubated with a FITC-labeled secondary antibody (goat anti-rabbit IgG, 1:500) for 2 h. After the samples were stained with DAPI, a fluorescence microscope was used to acquire images. Three samples were selected for analysis.

2.8 Statistical analysis

GraphPad Prism version 8.0.0 was used for graphing. SPSS Statistics V22.0 was used for data analysis. Differences between the groups were analyzed using one-way analysis of variance (ANOVA) and *post hoc* Tukey's tests. In the *in vitro* and *in vivo* experiments, the data are presented as the means ± standard errors. The significance of differences is denoted as follows: **p* < 0.05; ***p* < 0.01; ****p* < 0.001.

3 Results

3.1 Effects of PWSO on serum lipids in mice fed a HFD

After feeding for 12 weeks, relative to the NC group, a clear increase (*p* < 0.001) in body weight was observed in the HFD group (Figure 1A). However, taking the HFD group as the reference, PWSO treatment did not have a significant impact on the weight of mice. Taking the food intake of the NC group as the reference, the food intake of the HFD group

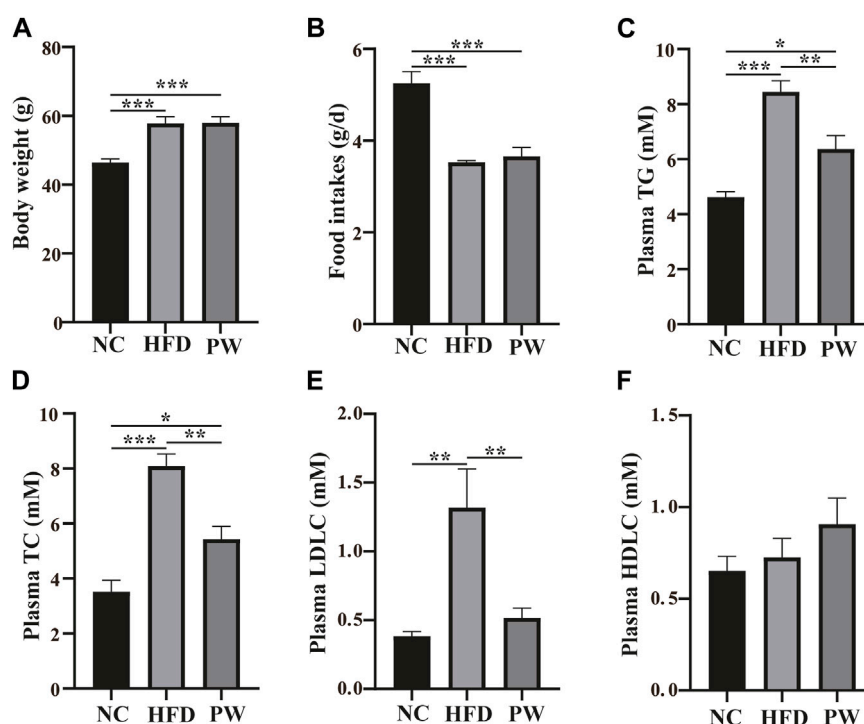


FIGURE 1

The effect of PWSO on blood lipids in mice with MAFLD. (A): Body weight; (B): Food intake; (C) Plasma TG; (D): Plasma TC; (E): Plasma LDL-C; (F): Plasma HDL-C. Statistics: * $p < 0.05$, ** $p < 0.01$, *** $p < 0.001$. NC, normal control group; HFD, high-fat diet group; PW, PWSO treatment group. MAFLD, metabolic-associated fatty liver disease; TG, triglyceride; TC, total cholesterol; HDL-C, high-density lipoprotein cholesterol; LDL-C, low-density lipoprotein cholesterol.

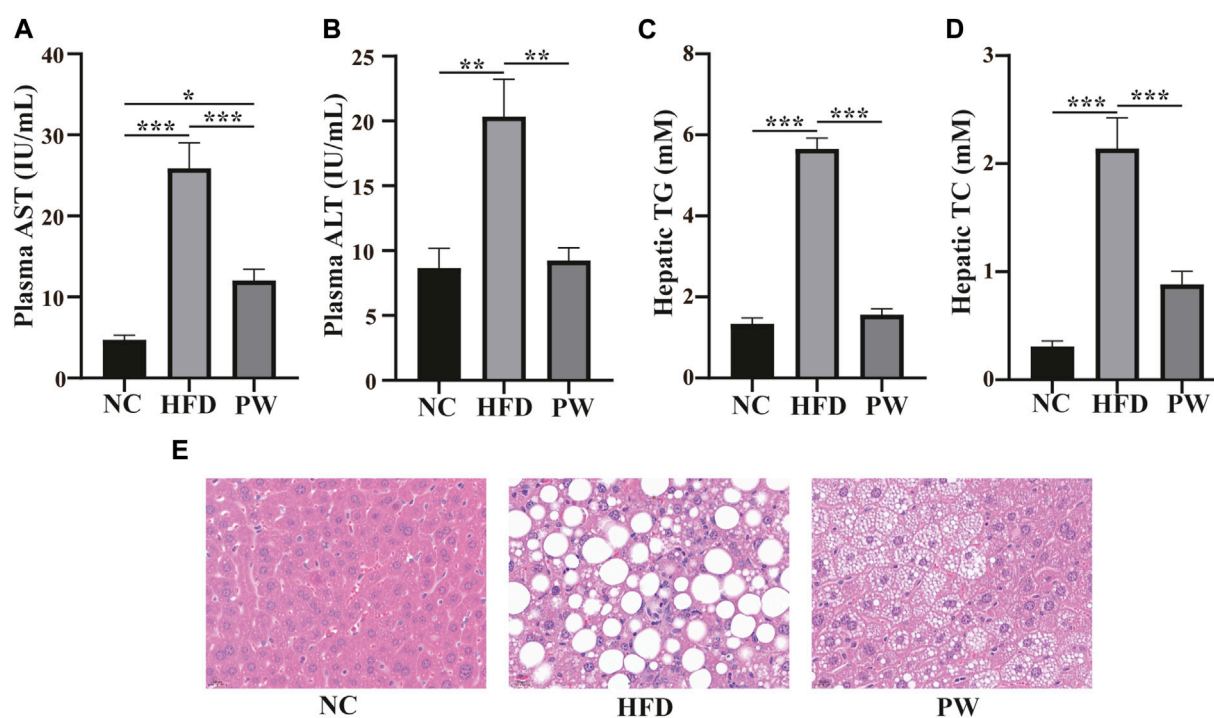


FIGURE 2

The effect of PWSO on lipids in mice with MAFLD. (A): AST; (B): ALT; (C): Hepatic TG; (D): Hepatic TC; (E): micrographs of hepatic H&E staining; scale bar = 20 μ m for H&E staining. Statistics: * $p < 0.05$, ** $p < 0.01$, *** $p < 0.001$. NC, normal control group; HFD, high-fat diet group; PW, PWSO treatment group. TC, total cholesterol; TG, triglyceride; ALT, plasma alanine aminotransferase; AST, aspartate aminotransferase; H&E, hematoxylin and eosin.

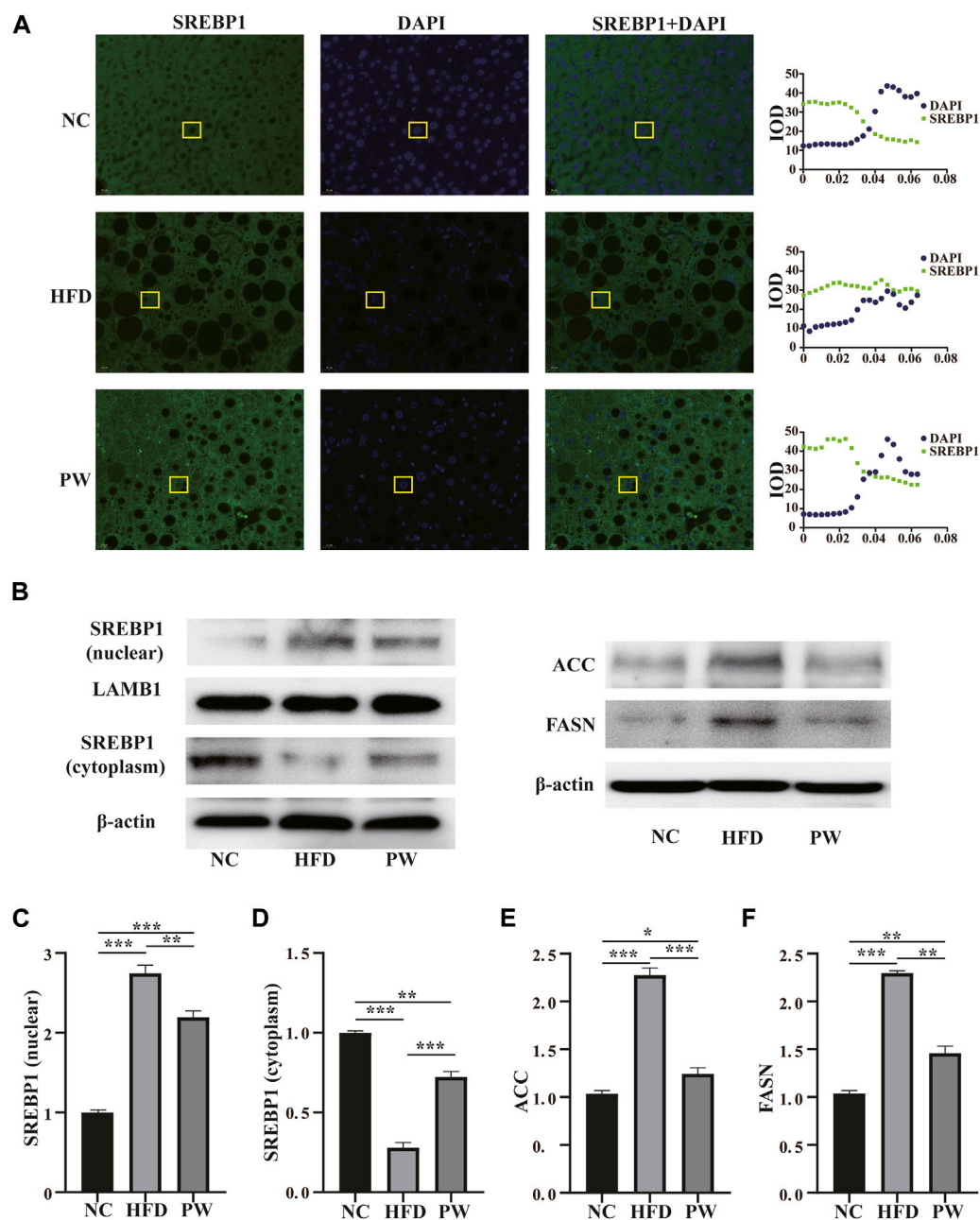


FIGURE 3

The effect of PWSO on lipogenesis. (A): Immunofluorescence staining for SREBP1 in liver tissue (original magnification, $\times 200$); (B): Expression of SREBP1, ACC and FASN; (C): SREBP1 level in the nucleus; (D): SREBP level in the cytoplasm; (E): ACC level; (F): FASN level. Statistics: * $p < 0.05$, ** $p < 0.01$, *** $p < 0.001$. NC, normal control group; HFD, high-fat diet group; PW, PWSO treatment group. FASN, fatty acid synthase; ACC, acetyl-CoA carboxylase; SREBPs, sterol regulatory element-binding proteins.

decreased ($p < 0.001$) due to the higher energy content in the HFD (Figure 1B). Taking the food intake of the HFD group as the reference, PWSO treatment did not increase food intake. Furthermore, taking the biochemical indicators of the NC group as the reference, there was a significant increasing trend in the plasma levels of TC, TG, and LDL-C ($p < 0.001$, $p < 0.001$, and $p < 0.01$, respectively) in the HFD group (Figures 1C–F). Moreover, PWSO treatment significantly reduced the levels of TC, TG, and LDL-C ($p < 0.01$, $p < 0.01$, and $p < 0.01$, respectively; Figures 1C–E). Regarding the plasma HDL-C level, the NC group, HFD group, and PW group showed consistency (Figure 1F).

3.2 Effects of PWSO on serum ALT and AST levels and hepatic lipids in mice fed a HFD

After feeding for 12 weeks, the levels of serum AST and ALT in the HFD group were significantly higher ($p < 0.001$ and $p < 0.01$, respectively) than those in the NC group. However, a reduction in AST and ALT levels ($p < 0.001$ and $p < 0.01$, respectively; Figures 2A, B) was observed with PWSO treatment. Moreover, the liver TC and TG levels were significantly increased ($p < 0.001$ and $p < 0.001$, respectively) in the HFD group and were significantly decreased in

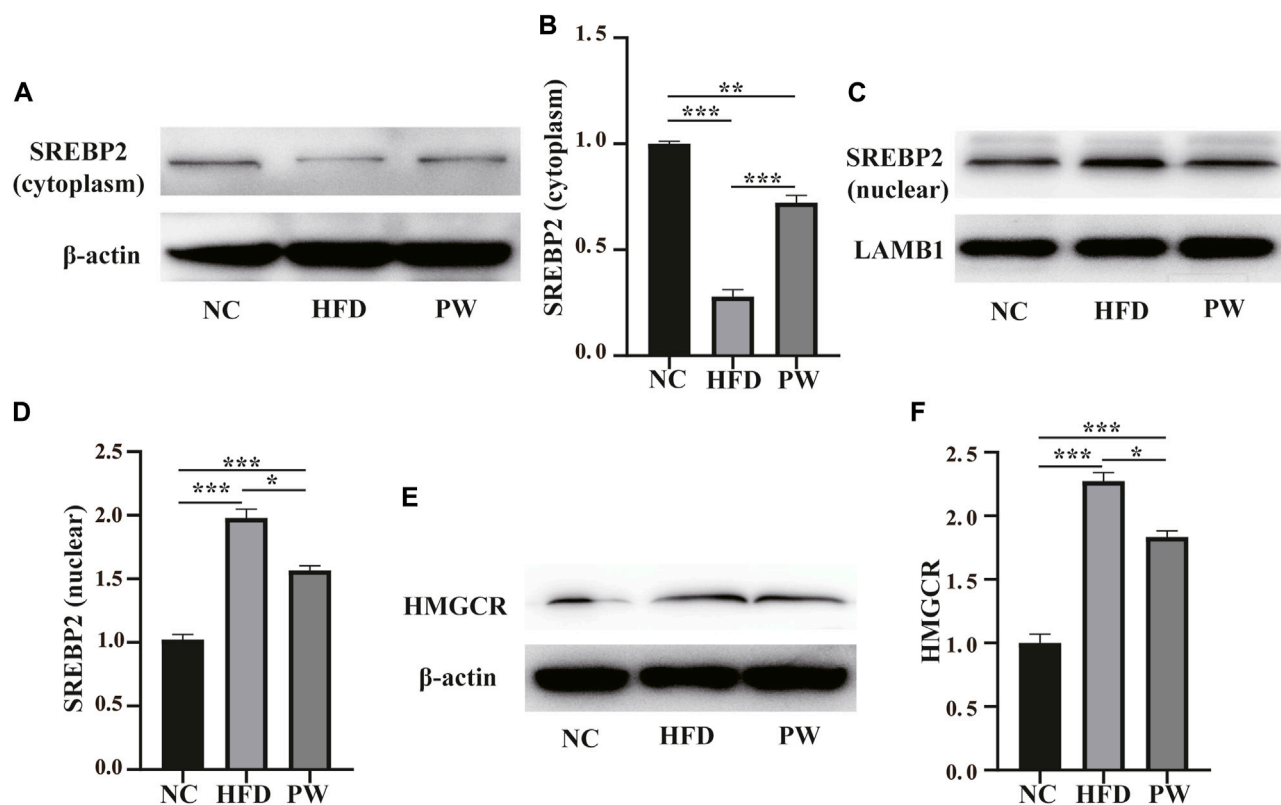


FIGURE 4

The effect of PWSO on lipogenesis. (A,B): SREBP2 level in the cytoplasm; (C,D): SREBP2 level in the nucleus; (E,F): Expression of HMGCR. Statistics:

* $p < 0.05$, ** $p < 0.01$, *** $p < 0.001$. NC, normal control group; HFD, high-fat diet group; PW, PWSO treatment group. SREBPs, sterol regulatory element-binding proteins; HMGCR, 3-hydroxy-3-methylglutaryl-CoA reductase.

the PW group ($p < 0.01$ and $p < 0.01$, respectively; Figures 2C, D). Robust lipid accumulation in hepatocytes was observed in the HFD group, indicating that HFD-fed mice develop MAFLD (Figure 2E). Moreover, PWSO treatment clearly ameliorated hepatic lipid accumulation. The range of visible lipid droplets was decreased, and the structure of hepatic cells was improved by PWSO treatment (Figure 2E).

3.3 Effects of PWSO on SREBP expression and localization and the related signaling pathways in mice fed a HFD

The immunofluorescence staining results showed that the PW group had increased SREBP1 levels in the cytoplasm (Figure 3A). Moreover, the Western blot analysis showed that the HFD group had a significant increase ($p < 0.001$) in the SREBP1 level in the nucleus when compared to that in the NC group. PWSO treatment significantly decreased ($p < 0.01$) the level of SREBP1 in the nucleus compared with that in the HFD group (Figures 3B, C). However, the HFD group had a significant decrease ($p < 0.001$) in the SREBP1 level in the cytoplasm compared with that in the NC group. Furthermore, PWSO treatment significantly increased ($p < 0.001$) the level of SREBP1 in the cytoplasm (Figures 3B, D). There was a significant increasing trend ($p < 0.001$) in ACC expression observed in the HFD group compared with the NC group, and this

trend was reversed ($p < 0.001$) after PWSO treatment (Figures 3B, E). Furthermore, the expression of FASN was significantly increased in the HFD group compared with the NC group ($p < 0.001$). PWSO treatment significantly decreased the expression of FASN (Figures 3B, F).

Western blot analysis showed a clear decreasing trend ($p < 0.001$) in the level of cytoplasmic SREBP2 in the HFD group compared to the NC group. PWSO reversed the HFD-induced decrease in cytoplasmic SREBP2 levels ($p < 0.001$) (Figures 4A, B). Moreover, a clear increasing trend ($p < 0.001$) in the level of nuclear SREBP2 was observed in the HFD group in comparison to the NC group. PWSO significantly prevented the decrease in nuclear SREBP2 levels caused by a HFD ($p < 0.001$) (Figures 4C, D). Western blot analysis showed a clear increasing trend ($p < 0.001$) in the level of HMGCR in the HFD group relative to the NC group. Moreover, in comparison with the HFD group, PWSO treatment significantly reduced the level of HMGCR (Figures 4E, F).

3.4 Effects of PWSO on fibrosis and the inflammatory response in mice fed a HFD

Sirius red staining and immunofluorescence staining showed that the HFD group exhibited severe fibrosis ($p < 0.001$) in comparison to that in the NC group. However, fibrosis was

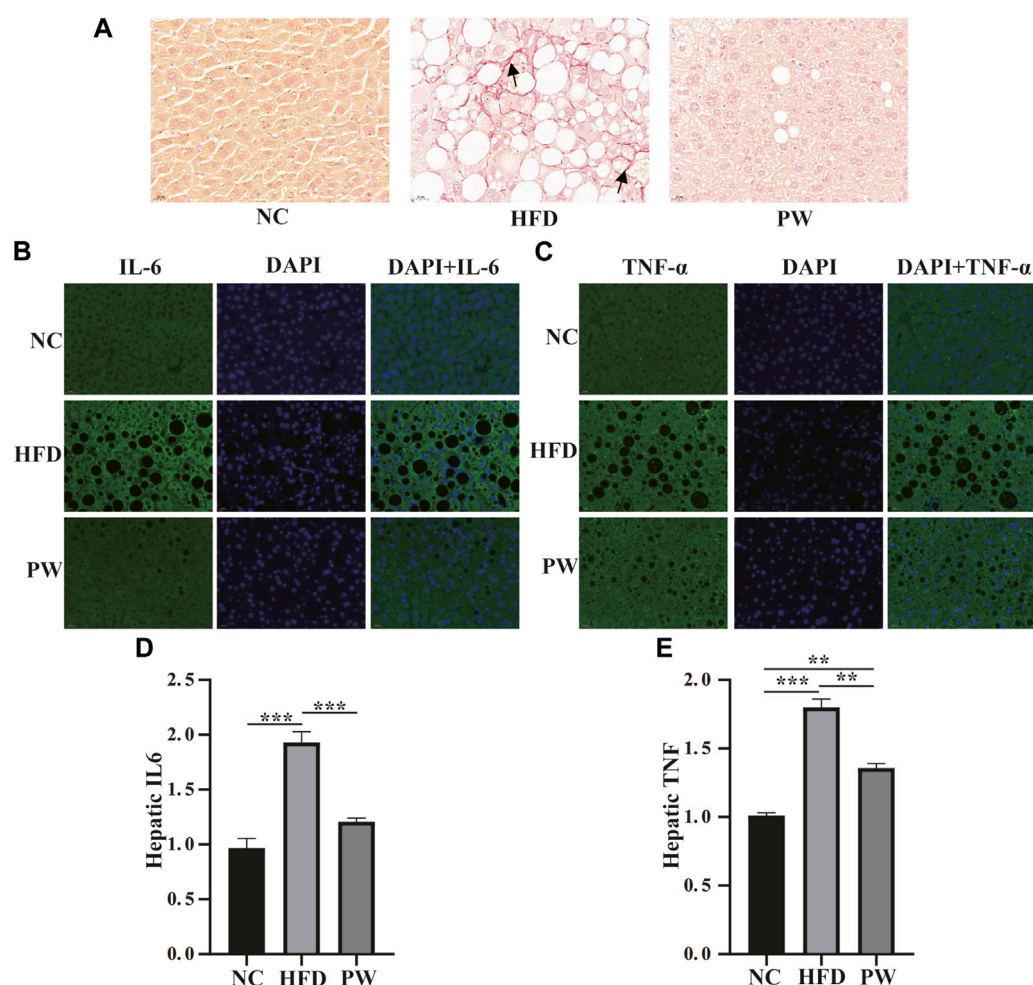


FIGURE 5

The effect of PWSO on the inflammatory response. (A): Micrographs of hepatic H&E staining; scale bar = 20 μ m for H&E staining. (B): Immunofluorescence staining for IL-6 in liver tissue (original magnification, $\times 200$); (C): Immunofluorescence staining for TNF- α in liver tissue (original magnification, $\times 200$); (D): Hepatic IL-6; (E): Hepatic TNF- α . Statistics: * $p < 0.05$, ** $p < 0.01$, *** $p < 0.001$. NC, normal control group; HFD, high-fat diet group; PW, PWSO treatment group. H&E, hematoxylin and eosin.

significantly attenuated by PWSO treatment ($p < 0.001$) (Figures 5A–C). Furthermore, after HFD feeding, the PWSO diet and standard diet were administered for 8 weeks, and the IL-6 and TNF- α levels were found to be elevated. Significant increases in hepatic IL-6 and TNF levels ($p < 0.001$ and $p < 0.001$, respectively) were observed in the HFD group compared with the NC group (Figures 5D, E). However, PWSO treatment significantly decreased the levels of IL-6 and TNF ($p < 0.001$ and $p < 0.01$, respectively; Figures 5D, E).

3.5 Effects of PWSO on the NF- κ B level

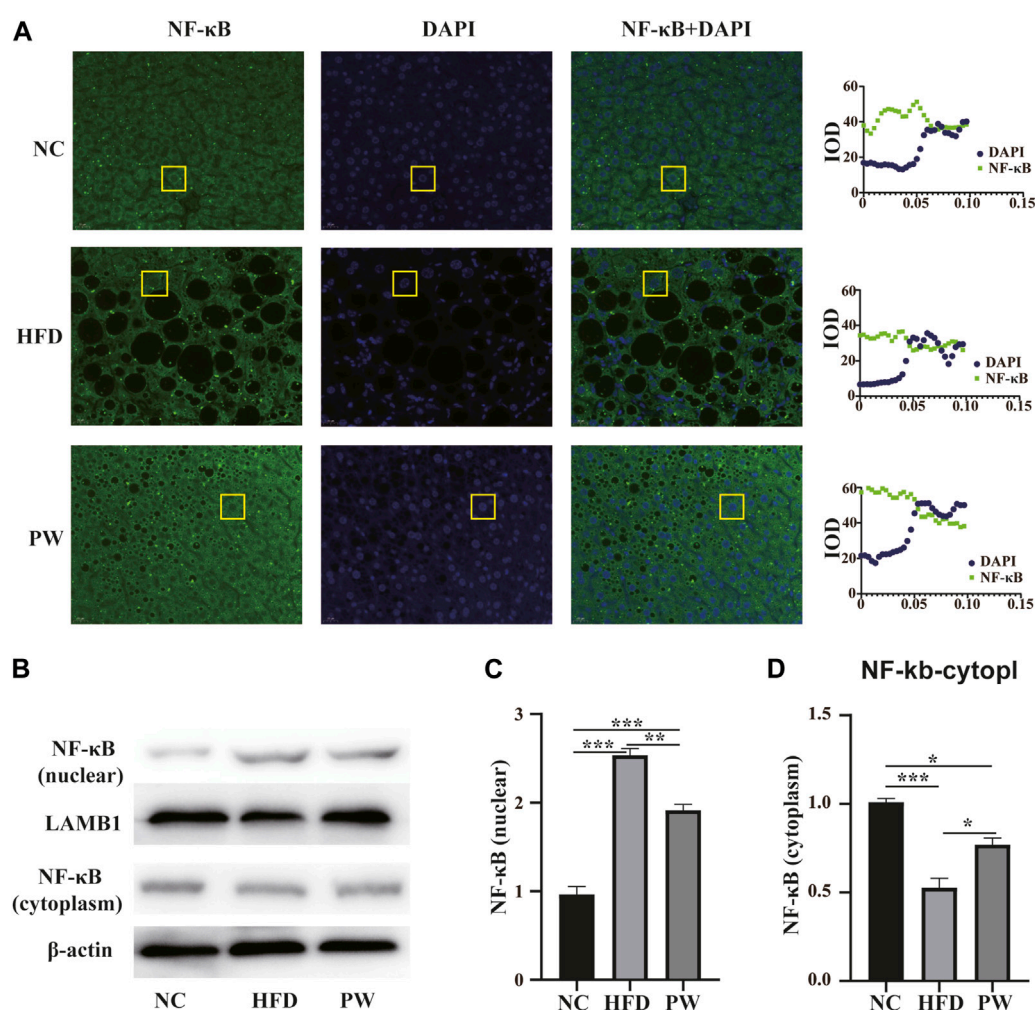
Immunofluorescence analysis revealed that PWSO increased the NF- κ B level in the cytoplasm and decreased the NF- κ B level in the nucleus (Figure 6A). In addition, Western blot analysis showed a significant increase ($p < 0.001$) in the level of nuclear NF- κ B in the HFD group compared with the NC group (Figure 6B). The nuclear NF- κ B level was significantly decreased in the PW group compared

with the HFD group ($p < 0.01$) (Figure 6C). However, a significant decrease ($p < 0.001$) in the level of cytoplasmic NF- κ B was observed in the HFD group. Moreover, compared to the HFD group, the PW group showed a clear increasing trend ($p < 0.05$) in the level of cytoplasmic NF- κ B (Figure 6D).

4 Discussion

The pharmacological activity and use of PWSO, which is characterized by high levels of sn-2-acTAGs (Smith et al., 2018), remain to be solved. In our research, the effects of PWSO on MAFLD were examined. Our results showed that treatment with PWSO attenuated the increases in TC and TG levels in MAFLD, thereby ameliorating hepatic lipid accumulation and the inflammatory response. This health benefit was associated with inactivation of SREBPs and inhibition of the NF- κ B signaling pathway.

Currently, a multiple hit hypothesis for the pathogenesis of MAFLD is accepted. Genetic susceptibility, epigenetics, hepatic lipid

**FIGURE 6**

The effect of PWSO on the NF-κB signaling pathway. (A): Immunofluorescence staining for SREBP1 in liver tissue (original magnification, x200); (B): Expression of NF-κB in the nucleus and cytoplasm; (C): NF-κB level in the nucleus; (D): NF-κB level in the cytoplasm. Statistics: * $p < 0.05$, ** $p < 0.01$, *** $p < 0.001$. NC, normal control group; HFD, high-fat diet group; PW, PWSO treatment group.

metabolism, insulin sensitivity, lipid peroxidation, and inflammatory responses contribute to the occurrence and development of MAFLD (Friedman et al., 2018; Valenti and Baselli, 2018; Sanyal, 2019; Zhou et al., 2020). Among these contributors, hepatic lipid accumulation is considered the initial cause of MAFLD, and an effective reduction in hepatic lipid accumulation plays an important role in the regression of MAFLD. Inhibiting hepatic lipid synthesis is a main strategy to ameliorate hepatic lipid accumulation. SREBPs are cholesterol sensors in the endoplasmic reticulum that regulate sterol homeostasis through certain feedback mechanisms (DeBose-Boyd and Ye, 2018). Typically, SREBPs exist in a complex in the cytoplasm and are then activated in the Golgi when they receive a biochemical signal (DeBose-Boyd et al., 1999). Active SREBPs enter the nucleus to bind to SREBPs in promoters, which then initiates the expression of genes related to lipogenesis (Athaniyar et al., 1998). Therefore, changes in SREBP levels in the cytoplasm and nucleus are important for the activation of the SREBP signaling pathway. The experiments demonstrated that the levels of SREBPs in the nucleus in the PW

group were lower than those in the HFD group. Compared with levels in the HFD group, the levels of SREBPs in the cytoplasm were significantly increased in the PW group. It is obvious that PWSO may inhibit the activation of SREBPs and regulate the synthesis of lipogenesis-related enzymes.

In concrete terms, SREBPs are present as three isoforms in mammals: SREBP1c, SREBP1a, and SREBP2 (Brown and Goldstein, 1999). A large amount of SREBP1c is expressed in the liver and mainly regulates the expression of FASN and ACC (Guo et al., 2014; DeBose-Boyd and Ye, 2018). FASN, which is well recognized as a rate-limiting enzyme, plays a vital role in fatty acid synthesis and contributes to the production of TG in the liver. ACC catalyzes the carboxylation of acetyl-CoA to form malonyl-CoA and is an important regulator in the first step of fatty acid synthesis. Our results indicated that PWSO can inactivate SREBP1 and decrease the expression of FASN and ACC, inhibiting the synthesis of TG in the liver (Zhu et al., 2019). Moreover, this result is also the critical cause of the reduction in the plasma TG level. SREBP2 is primarily responsible for sterol metabolism and homeostasis. HMGCR

catalyzes the *de novo* synthesis of cholesterol and is directly regulated by SREBP2 (Ren et al., 2017). Its activation has a strong effect on the production of cholesterol. Our results suggested that PWSO can inhibit the activation of SREBP2 and then reduce the expression of HMGCR. Lipid accumulation, a critical event in the development of MAFLD, was decreased by treatment with PWSO.

With hepatic lipid accumulation, lipid peroxidation occurs and initiates inflammation, which leads to cytokine expression and fibrosis in the liver (Welty et al., 2016; Wang et al., 2021). Thus, managing the hepatic inflammatory response is critical for controlling the occurrence and development of MAFLD. NF- κ B is responsible for the cellular responses to free radicals and lipid peroxidation (Liu et al., 2017; Poma, 2020). When hepatic cells are damaged by lipid peroxidation, I κ B- α is in turn activated and phosphorylated, releasing NF- κ B (P65) from the NF- κ B/I κ B- α complex in the cytoplasm. The p65/RelA dimer undergoes rapid nuclear translocation and binds to NF- κ B response elements in target genes via the p65 subunit, thereby initiating the expression of target genes such as TNF- α and IL-6, which eventually leads to tissue inflammation and even causes fibrosis in the liver (Liu et al., 2017). Thus, importantly, the ratio of cytoplasmic to nuclear NF- κ B indicates activation of the NF- κ B signaling pathway. Our results showed that the concentration of nuclear NF- κ B (p65) was higher in the HFD group than in the NC group, and PWSO treatment successfully mitigated the increase in NF- κ Bp65 levels in the nucleus caused by a HFD. Moreover, the increases in TNF- α and IL-6 expression after activation of the NF- κ B signaling pathway were significantly ameliorated by PWSO treatment. These results indicated that PWSO can partially inhibit the inflammatory response in the liver, which efficiently prevents the development of MAFLD.

The high sn-2-acTAG content and unsaturated fatty acid content of PWSO may have beneficial effects compared to other vegetable oils. Unsaturated fatty acids, especially omega-3 and omega-6 unsaturated fatty acids, are generally considered safer than saturated fatty acids (Scorletti and Byrne, 2018). The high content of unsaturated fatty acids in PWSO may also be the main reason for its pharmacological activity. The present study investigated the protective effects of PWSO against MAFLD, but the association between the structure and function of PWSO needs further examination.

It is important to further the use of PWSO as an edible oil. In our study, the mice did not exhibit any discomfort, abnormal mental state, or diarrhea after PWSO administration. These observations provide an important research direction for verifying the safety of PWSO, but further comprehensive toxicological experiments need to be performed.

5 Conclusion

PWSO attenuates hepatic lipid accumulation by regulating the activation of SREBPs and the related signaling pathways, inhibits liver inflammation by mitigating the activation of the NF- κ B signaling pathway, and ultimately has pharmacological activity in MAFLD. Our study provides not only support for the popularization and use of PWSO but also new perspectives on utilizing the pharmacological activities of plant oils in MAFLD.

Data availability statement

The original contributions presented in the study are included in the article/Supplementary Material, further inquiries can be directed to the corresponding authors.

Ethics statement

The animal study was approved by the Animal Ethics Committee of Shandong University of Technology (the approval date is 17/11/2021, and the approval certification number of the study is YLX20211101). The study was conducted in accordance with the local legislation and institutional requirements.

Author contributions

MX: Writing—original draft, Writing—review and editing, Investigation, Visualization. HW: Data curation, Writing—review and editing. MW: Funding acquisition, Methodology, Writing—review and editing. BY: Data curation, Writing—review and editing. SL: Data curation, Writing—review and editing. XX: Data curation, Writing—review and editing. LD: Data curation, Writing—review and editing. TC: Data curation, Writing—review and editing. YH: Data curation, Writing—review and editing. QW: Visualization, Writing—review and editing. CW: Visualization, Writing—review and editing. YC: Visualization, Writing—review and editing. ZX: Funding acquisition, Methodology, Writing—review and editing. WS: Funding acquisition, Supervision, Writing—review and editing. XS: Funding acquisition, Supervision, Writing—review and editing. JS: Funding acquisition, Supervision, Writing—review and editing. All authors contributed to the article and approved the submitted version.

Funding

This work was supported by the Taishan Scholar's Program of Shandong to JS, the University Youth Innovation Team of Shandong Province (2022KJ229), China Post doctoral Science Foundation (2023T160729 and 2023M733918), the Natural Science Foundation of Shandong Province (ZR2023MH263, ZR2022MH306, and ZR2020QB004), and the National Natural Science Foundation of China (82104112), the Innovation Ability Improvement Project of Science and Technology SMEs in Shandong Province (2022TSGC2245), Zhangdian School-City Integrated Development Project (2021PT0001).

Conflict of interest

Authors WS, XS, and JS were employed by Shandong Qingyujiangxing Biotechnology Co., Ltd.

The remaining authors declare that the research was conducted in the absence of any commercial or financial relationships that could be construed as a potential conflict of interest.

Publisher's note

All claims expressed in this article are solely those of the authors and do not necessarily represent those of their affiliated

organizations, or those of the publisher, the editors and the reviewers. Any product that may be evaluated in this article, or claim that may be made by its manufacturer, is not guaranteed or endorsed by the publisher.

References

- Anstee, Q. M., Targher, G., and Day, C. P. (2013). Progression of NAFLD to diabetes mellitus, cardiovascular disease or cirrhosis. *Nat. Rev. Gastroenterol. Hepatol.* 10 (6), 330–344. doi:10.1038/nrgastro.2013.41
- Athanikar, J. N., and Osborne, T. F. (1998). Specificity in cholesterol regulation of gene expression by coevolution of sterol regulatory DNA element and its binding protein. *Proc. Natl. Acad. Sci. U. S. A.* 95 (9), 4935–4940. doi:10.1073/pnas.95.9.4935
- Brown, M. S., and Goldstein, J. L. (1999). A proteolytic pathway that controls the cholesterol content of membranes, cells, and blood. *Proc. Natl. Acad. Sci. U. S. A.* 96 (20), 11041–11048. doi:10.1073/pnas.96.20.11041
- DeBose-Boyd, R. A., Brown, M. S., Li, W. P., Nohturfft, A., Goldstein, J. L., and Espenshade, P. J. (1999). Transport-dependent proteolysis of SREBP: Relocation of site-1 protease from Golgi to ER obviates the need for SREBP transport to Golgi. *Cell* 97 (7), 703–712. doi:10.1016/s0092-8674(00)81668-2
- DeBose-Boyd, R. A., and Ye, J. (2018). SREBPs in lipid metabolism, insulin signaling, and beyond. *Trends Biochem. Sci.* 43 (5), 358–368. doi:10.1016/j.tibs.2018.01.005
- Eslam, M., Newsome, P. N., Sarin, S. K., Anstee, Q. M., Targher, G., and Romero-Gomez, M., (2020). A new definition for metabolic dysfunction-associated fatty liver disease: An international expert consensus statement. *J. Hepatol.* 73 (1), 202–209. doi:10.1016/j.jhep.2020.03.039
- Friedman, S. L., Neuschwander-Tetri, B. A., Rinella, M., and Sanyal, A. J. (2018). Mechanisms of NAFLD development and therapeutic strategies. *Nat. Med.* 24 (7), 908–922. doi:10.1038/s41591-018-0104-9
- Gao, Y., Zhang, W., Zeng, L. Q., Bai, H., Li, J., and Zhou, J., (2020). Exercise and dietary intervention ameliorate high-fat diet-induced NAFLD and liver aging by inducing lipophagy. *Redox Biol.* 36, 101635. doi:10.1016/j.redox.2020.101635
- Guo, D., Bell, E. H., Mischel, P., and Chakravarti, A. (2014). Targeting SREBP-1-driven lipid metabolism to treat cancer. *Curr. Pharm. Des.* 20 (15), 2619–2626. doi:10.2174/13816128113199990486
- Henkel, J., Alfine, E., Sain, J., Johrens, K., Weber, D., and Castro, J. P., (2018). Soybean oil-derived poly-unsaturated fatty acids enhance liver damage in NAFLD induced by dietary cholesterol. *Nutrients* 10 (9), 1326. doi:10.3390/nu10091326
- Jee, W., Lee, S. H., Ko, H. M., Jung, J. H., Chung, W. S., and Jang, H. J. (2021). Anti-obesity effect of polygalin C isolated from *Polygala japonica* houtt. Via suppression of the adipogenic and lipogenic factors in 3T3-L1 adipocytes. *Int. J. Mol. Sci.* 22 (19), 10405. doi:10.3390/ijms221910405
- Liu, J., Zhang, H., Ji, B., Cai, S., Wang, R., and Zhou, F., (2014). A diet formula of *Puerariae radix*, *Lycium barbarum*, *Crataegus pinnatifida*, and *Polygonati rhizoma* alleviates insulin resistance and hepatic steatosis in CD-1 mice and HepG2 cells. *Food Funct.* 5 (5), 1038–1049. doi:10.1039/c3fo60524h
- Liu, T., Zhang, L., Joo, D., and Sun, S. C. (2017). NF- κ B signaling in inflammation. *Signal Transduct. Target Ther.* 2, 17023. doi:10.1038/sigtrans.2017.23
- Poma, P. (2020). NF- κ B and disease. *Int. J. Mol. Sci.* 21 (23), 9181. doi:10.3390/ijms21239181
- Ren, R., Gong, J., Zhao, Y., Zhuang, X., Ye, Y., and Lin, W. (2017). Sulfated polysaccharides from *Enteromorpha prolifera* suppress SREBP-2 and HMG-CoA reductase expression and attenuate non-alcoholic fatty liver disease induced by a high-fat diet. *Food Funct.* 8 (5), 1899–1904. doi:10.1039/c7fo00103g
- Romero-Gomez, M., Zelber-Sagi, S., and Trenell, M. (2017). Treatment of NAFLD with diet, physical activity and exercise. *J. Hepatol.* 67 (4), 829–846. doi:10.1016/j.jhep.2017.05.016
- Sanyal, A. J. (2019). Past, present and future perspectives in nonalcoholic fatty liver disease. *Nat. Rev. Gastroenterol. Hepatol.* 16 (6), 377–386. doi:10.1038/s41575-019-0144-8
- Scorletti, E., and Byrne, C. D. (2018). Omega-3 fatty acids and non-alcoholic fatty liver disease: Evidence of efficacy and mechanism of action. *Mol. Asp. Med.* 64, 135–146. doi:10.1016/j.mam.2018.03.001
- Smith, M. A., Zhang, H., Burton, I. W., Liu, C., Cheng, A. W., and Sun, J. Y. (2018). 2-Acetyl-1,3-Diacyl-sn-Glycerols with unusual acyl composition in seed oils of the genus *Polygala*. *Eur. J. Lipid Sci. Technol.* 120 (8). doi:10.1002/ejlt.201800069
- Son, S. R., Yoon, Y. S., Hong, J. P., Kim, J. M., Lee, K. T., and Jang, D. S. (2022). Chemical constituents of the roots of *Polygala tenuifolia* and their anti-inflammatory effects. *Plants (Basel)* 11 (23), 3307. doi:10.3390/plants11233307
- Stefan, N., Haring, H. U., and Cusi, K. (2019). Non-alcoholic fatty liver disease: Causes, diagnosis, cardiometabolic consequences, and treatment strategies. *Lancet Diabetes Endocrinol.* 7 (4), 313–324. doi:10.1016/S2213-8587(18)30154-2
- Valenti, L. V. C., and Baselli, G. A. (2018). Genetics of nonalcoholic fatty liver disease: A 2018 update. *Curr. Pharm. Des.* 24 (38), 4566–4573. doi:10.2174/1381612825666190119113836
- Wang, C. C., Yen, J. H., Cheng, Y. C., Lin, C. Y., Hsieh, C. T., and Gau, R. J., (2017). *Polygala tenuifolia* extract inhibits lipid accumulation in 3T3-L1 adipocytes and high-fat diet-induced obese mouse model and affects hepatic transcriptome and gut microbiota profiles. *Food Nutr. Res.* 61 (1), 1379861. doi:10.1080/16546628.2017.1379861
- Wang, H., Mehal, W., Nagy, L. E., and Rotman, Y. (2021). Immunological mechanisms and therapeutic targets of fatty liver diseases. *Cell Mol. Immunol.* 18 (1), 73–91. doi:10.1038/s41423-020-00579-3
- Welty, F. K., Alfaddagh, A., and Elajami, T. K. (2016). Targeting inflammation in metabolic syndrome. *Transl. Res.* 167 (1), 257–280. doi:10.1016/j.trsl.2015.06.017
- Yang, B., Sun, J., Liang, S., Wu, P., Lv, R., and He, Y., (2021). Prediction of srebp-1 as a key target of qing Gan san against MAFLD in rats via RNA-sequencing profile analysis. *Front. Pharmacol.* 12, 680081. doi:10.3389/fphar.2021.680081
- Yang, J., Fernandez-Galilea, M., Martinez-Fernandez, L., Gonzalez-Muniesa, P., Perez-Chavez, A., and Martinez, J. A., (2019). Oxidative stress and non-alcoholic fatty liver disease: Effects of omega-3 fatty acid supplementation. *Nutrients* 11 (4), 872. doi:10.3390/nu11040872
- Yao, Z., Li, Y., Wang, Z., Lan, Y., Zeng, T., and Gong, H., (2020). Research on anti-hepatocellular carcinoma activity and mechanism of *Polygala fallax* Hemsl. *J. Ethnopharmacol.* 260, 113062. doi:10.1016/j.jep.2020.113062
- Zhao, X., Cui, Y., Wu, P., Zhao, P., Zhou, Q., and Zhang, Z., (2020). *Polygalae radix*: A review of its traditional uses, phytochemistry, pharmacology, toxicology, and pharmacokinetics. *Fitoterapia* 147, 104759. doi:10.1016/j.fitote.2020.104759
- Zhou, J., Zhou, F., Wang, W., Zhang, X. J., Ji, Y. X., and Zhang, P., (2020). Epidemiological features of NAFLD from 1999 to 2018 in China. *Hepatology* 71 (5), 1851–1864. doi:10.1002/hep.31150
- Zhu, L., Du, W., Liu, Y., Cheng, M., Wang, X., and Zhang, C., (2019). Prolonged high-glucose exposure decreased SREBP-1/FASN/ACC in Schwann cells of diabetic mice via blocking PI3K/Akt pathway. *J. Cell Biochem.* 120 (4), 5777–5789. doi:10.1002/jcb.27864



OPEN ACCESS

EDITED BY

Aliyu Muhammad,
Ahmadu Bello University, Nigeria

REVIEWED BY

Mosebolatan Adegbola,
Federal Polytechnic Ede, Nigeria
Kolawole Ayodapo Olofinan,
University of Johannesburg, South Africa

*CORRESPONDENCE

A. J. Salemcity,
✉ asalemcity@unimed.edu.ng

RECEIVED 30 May 2023

ACCEPTED 30 October 2023

PUBLISHED 14 November 2023

CITATION

Salemcity AJ, Olanlokun JO,
Olowofolahan AO, Olojo FO,
Adegoke AM and Olorunsogo OO (2023),
Reversal of mitochondrial permeability
transition pore and pancreas
degeneration by chloroform fraction of
Ocimum gratissimum (L.) leaf extract in
type 2 diabetic rat model.
Front. Pharmacol. 14:1231826.
doi: 10.3389/fphar.2023.1231826

COPYRIGHT

© 2023 Salemcity, Olanlokun,
Olowofolahan, Olojo, Adegoke and
Olorunsogo. This is an open-access
article distributed under the terms of the
[Creative Commons Attribution License](#)
(CC BY). The use, distribution or
reproduction in other forums is
permitted, provided the original author(s)
and the copyright owner(s) are credited
and that the original publication in this
journal is cited, in accordance with
accepted academic practice. No use,
distribution or reproduction is permitted
which does not comply with these terms.

Reversal of mitochondrial permeability transition pore and pancreas degeneration by chloroform fraction of *Ocimum gratissimum* (L.) leaf extract in type 2 diabetic rat model

A. J. Salemcity^{1,2*}, John Oludele Olanlokun²,
A. O. Olowofolahan², F. O. Olojo², Ayodeji Mathias Adegoke^{2,3}
and O. O. Olorunsogo²

¹Department of Biochemistry, University of Medical Sciences, Ondo, Nigeria, ²Department of Biochemistry, Faculty of Basic Medical Sciences, College of Medicine, University of Ibadan, Ibadan, Nigeria, ³Department of Pharmacology, Faculty of Health Sciences, University of the Free State, Bloemfontein, South Africa

Introduction: Unmanaged Diabetes Mellitus (DM) usually results to tissue wastage because of mitochondrial dysfunction. Adverse effects of some drugs used in the management of DM necessitates the search for alternative therapy from plant origin with less or no side effects. *Ocimum gratissimum* (L.) (OG) has been folklorically used in the management of DM. However, the mechanism used by this plant is not fully understood. This study was designed to investigate the effects of chloroform fraction of OG leaf (CFOG) in the reversal of tissue wastage in DM via inhibition of mitochondrial-mediated cell death in streptozotocin (STZ)-induced diabetic male Wistar rats.

Methods: Air-dried OG leaves were extracted with methanol and partitioned successively between *n*-hexane, chloroform, ethylacetate and methanol to obtain their fractions while CFOG was further used because of its activity. Diabetes was induced in fifteen male Wistar rats, previously fed with high fat diet (28 days), via a single intraperitoneal administration of STZ (35 mg/kg). Diabetes was confirmed after 72 h. Another five fed rats were used as the normal control, treated with corn oil (group 1). The diabetic animals were grouped (*n* = 5) and treated for 28 days as follows: group 2 (diabetic control: DC) received corn oil (10 mL/kg), groups 3 and 4 were administered 400 mg/kg CFOG and 5 mg/kg glibenclamide, respectively. Body weight and Fasting Blood Glucose (FBG) were determined while Homeostasis Model Assessment of Insulin Resistance (HOMA-IR) and beta cell (HOMA-β), and pancreatic tissue regenerating potential by CFOG were assessed. Activity-guided purification and characterization of the most active principle in CFOG was done using chromatographic and NMR techniques. The animals were sacrificed after 28 days, blood samples were collected and serum was obtained. Liver mitochondria were isolated and mitochondrial permeability transition (mPT) was investigated by spectrophotometry.

Results: CFOG reversed diabetic-induced mPT pore opening, inhibited ATPase activity and lipid peroxidation. CFOG reduced HOMA-IR but enhanced HOMA-β and caused regeneration of pancreatic cells relative to DC. Lupanol was a major metabolite of CFOG.

Discussion: Normoglycemic effect of CFOG, coupled with reversal of mPT, reduced HOMA-IR and improved HOMA- β showed the probable antidiabetic mechanism and tissue regenerating potentials of OG.

KEYWORDS

Ocimum gratissimum (L.), mitochondrial permeability transition pore, diabetes mellitus, glucose homeostasis, mitochondrial dysfunction

1 Introduction

Diabetes mellitus (DM) is a metabolic derangement typified by perturbation of intermediary metabolism. Preliminary symptoms are polyuria, polydipsia, polyphagia and weight loss (Ekaiko et al., 2016). Glycosuria and ketonuria are other symptoms commonly found in children, although it could also be observed in adults. The DM has been a worrisome global health concern attributable to its attendant complications, high degree of morbidity and death (Beaglehole and Yach, 2003; Yach et al., 2004; American Diabetes Association, 2012). Long term effect of untreated DM is associated with complications which can either be microvascular or macrovascular. The former is linked to damage of the small blood vessels resulting to retinopathy, neuropathy, nephropathy, amelia-phocomelia, coma and even death. The latter is associated with disorders of large vasculatures such as atherosclerosis and cardiomyopathy (Ubaid et al., 2019). About 463 million people was reported to be living with the disease in 2019. Its prevalence in Nigeria has increased to over 6 million adults (IDF, 2019; Ugwu et al., 2020).

There are two types of DM namely, type 1 (T1DM) and 2 (T2DM). The T1DM is a disease characterised by autoimmune-dependent beta cell wreckage and lack of insulin. It is otherwise referred to as insulin dependent DM. On the other hand, T2DM is related to insulin resistance ensuing from insensitivity of the receptor to insulin in the skeletal muscle and other peripheral tissues alongside partial β -cell obliteration. It is also known as insulin non-dependent DM. Hyperglycemia, which causes several organ impairment, is a general clinical feature of DM (Feldman, et al., 2019). The T2DM accounts for about 90% of disease incidence reported (Nguyen et al., 2020).

At present, hypoglycemia drugs are employed in monitoring T2DM and these agents sometimes elicit adverse effects such as faintness, pain, dejection, sustained hypoglycemia, headache (sulphonylureas), diarrhea, vomiting, palpitation, skin rash (biguanides), oedema and cardiac arrest (thiazolidinediones) (Ganesan et al., 2020). As a result of the adverse effects associated with the use of the orthodox medicine, search for alternative with little or no side effect is necessary.

Ocimum gratissimum (OG) is a candidate plant which its role in the management of diabetes mellitus is being explored. *Ocimum gratissimum* belongs to Lamiaceae family, and it is widely scattered all through Africa (including Nigeria), India and some parts of south eastern Asia (Ayissi and Nyadedzor, 2003). In Nigeria, Yoruba, Hausa and Igbo tribes refer to it as “Efinrin Nla”, “Dai doya” and “Nchuawu” (mosquito repellent), respectively. India and Brazil call it *Vana Tulsi* and *alfavaca*, correspondingly (Effraim et al., 2000).

The plant develops to roughly 1–3 m in altitude. The dark-brown stems bear leaves which are slim and egg-shaped maturing

between 5 and 13 cm in height and width of 3–9 cm. These leaves usually green in colour, possess strong aromatic fragrance similar to sweet scent of camphor. The plant grows well in lake shores, costal bush lands and in sub-montane regions (Kamboj, 2000; Alvarenga et al., 2008).

The medicinal values of the plant reside in its phytometabolites, which elicit definite physiological actions that enable it to be potent in treating malaria, dysentery, pile and lowering of blood glucose forklorically (Danziel, 1996). It has been established that phytometabolites have disease-preventing or -ameliorating capabilities and they are efficient in tackling or precluding diseases due to their antioxidant potential (Farombi, 2000).

Phytochemical investigations showed that methanol extract of OG has abundant tannins, steroids, terpenoids, flavonoids, resin, terpenoid, saponin and cardiac glycosides; and as well possesses an excellent antioxidant propensity (Afolabi et al., 2007; Okoye and Madumelu, 2013). Its leaves possess volatile essential oil which comprises majorly about 31%–66% thymol, and eugenol. It also has xanthenes, terpene and lactone (Ezekwesili et al., 2004; Mohammed et al., 2007).

Experimental evidence using rats showed that its leaves extract could prevent diarrhea. It was also discovered that the methanol extract showed hepatoprotective ability in male albino rats (Salemcity et al., 2014). The OG leaf extract was also shown to have the capability to abrogate alloxan-stimulated DM in rats (Ekaiko et al., 2016). This botanical drug possesses some qualities with high beneficial health relevance. These range from prevention of convulsions and seizures, reduction of high blood glucose, relaxation of intestinal muscles and anti-nociceptive use, antidotes for cough, antibronchitis and anticonjunctivitis.

Research has shown that unmanaged DM can activate the mitochondrial permeability transition (mPT) pore, leading to the release of pro-apoptotic factors such as cytochrome c into the cytosol (Daniel et al., 2018). When this pore opening is activated by some disease states and other pathological conditions, it enables the free passage of macromolecules into the mitochondria. This is preceded by factors such as calcium overload, reactive oxygen species (ROS), cytotoxic compounds, oncoproteins, DNA damage, and certain chemotherapeutic agents (such as anthracycline-doxorubicin, sunitinib, and alkylating agent-cisplatin) (Gorini et al., 2018). The mPT is accompanied by processes such as mitochondrial swelling, membrane rupture, and the release of apoptotic proteins (Wang and Youle, 2009; Olanlokun et al., 2017; Oyeboode et al., 2017).

While most normoglycemic effects of *O. gratissimum* has been monitored using the leaf extract only, there is paucity of information on the purification of active principle in the most potent fraction and the probable mechanism of such metabolite to prevent tissue wastage via the modulation of the mitochondrial permeability

TABLE 1 Composition of High fat diet.

Ingredients	Diet (g/kg)
Powdered Normal Pellet Diet	365
Lard	310
Casein	250
Cholesterol	10
Vitamin-mineral mix	60
DL-methionine	3
Yeast powder	1
NaCl	1

(Srinivasan et al., 2005).

transition pore opening. Therefore, this study aims to investigate the mechanism by which *O. gratissimum* leaf prevents hyperglycemia-induced cell death and tissue wastage in a diabetic rat model induced by streptozotocin and a high-fat diet.

2 Materials and methods

2.1 Experimental animals and treatment

Male Wistar rats each weighing between 80 and 100 g were acquired from the Veterinary Medicine Animal Holding, Department of Veterinary, University of Ibadan, Nigeria. They were conditioned for 2 weeks in Department of Biochemistry Animal Care Unit in the same institution. Water and rat chow were given *ad libitum* to the animals in a conducive environmental situations of temperature and 12-hour bright/gloom phase.

2.2 Induction of type 2 diabetes mellitus

Srinivasan et al. (2005) showed that T2DM could be induced in rat model by placing them on high fat diet (HFD) for 2 weeks and thereafter administered STZ. The HFD composition was presented in Table 1. Fifty rats in this study were exposed to HFD for 28 days after which a single dose STZ (35 mg/kg) dissolved in cold citrate (0.1M) buffer adjusted to pH 4.5, was administered intraperitoneally to induce diabetes mellitus (Detaile et al., 2005). After 3 days the rats underwent an overnight fast and their blood glucose was determined using glucometer (On-Call Plus[®]). Animals having blood glucose status >250 mg/dL were confirmed diabetic and ascertained suitable for further experiment. Thirty-one rats were discovered to have blood glucose level of 250 mg/dL and above. The success rate was 60%. However, ten out of the thirty-one diabetic rats died before the commencement of the treatment, with only twenty-one diabetic rats left for the experiment.

2.3 Grouping of animals

The normal control (fed normally with rat chow) and diabetic rats were grouped (n = 7) and treated orally once daily as follows:

Group1: Normal Control (NC) (Received corn oil)

Group 2: Diabetic control (Administered corn oil)

Group 3: Diabetic + CFOG (400 mg/kg using corn oil as vehicle)

Group 4: Diabetic + Glibenclamide (5 mg/kg using corn oil as vehicle)

Key: CFOG: Chloroform fraction of *O. gratissimum* leaf extract

2.4 Ethical approval

Approval for this research was obtained from Animal Care and Use Research Ethics Committee with reference number UI-ACUREC/19/0065.

2.5 Preparation of *Ocimum gratissimum* (L.) extract and fractions

2.5.1 Chemicals

All chemicals used were analytical grade and purchased from Sigma.

2.5.2 Source of plant material

Ocimum gratissimum (L.) was procured from “Oja-Bodija” market, Ibadan, Oyo State, Nigeria and validated in the Department of Pharmacognosy, University of Ibadan, Nigeria (Voucher specimen number: DPUI No 1504).

2.5.3 Preparation of plant materials

The leaves of *O. gratissimum* (L) were air-dried at room temperature between 28–30°C for four (4) weeks and pulverized to a smooth mill with a clean grinder. The powdered leaves were kept at room temperature in a clean jar.

2.5.4 Extraction and partitioning of the plant extract

Cold extraction was performed using absolute methanol in a ratio of 1:10 (w/v). The jar containing the powdered leaves and methanol was allowed to stand for 72 h. The extract was then filtered through sterile Whatman No. 1 filter paper. The green-coloured extract was concentrated using a rotary evaporator under reduced pressure. The resulting crude concentrate was further concentrated in a water bath at 37°C to obtain a solvent-free methanol extract. The final crude extract obtained, weighed 450 g from an initial dried plant sample weighing 750 g. The percentage yield of the extract was 60%. The column of the Vacuum Liquid Chromatography (VLC) was packed with silica gel for Thin Layer Chromatography (TLC) under pressure with *n*-hexane. 10 g sample of the methanol extract of *O. gratissimum* (L) was adsorbed with 10 g of the TLC gel and allowed to dry. The adsorbed sample was loaded on the VLC column and washed with *n*-hexane until exhaustion. Further to this, the column was washed with chloroform, then ethylacetate and finally with methanol successively. The fractions were concentrated using rotary evaporator and were further rendered solvent-free in a water bath. The solvent-free fractions were kept in the fridge until used.

$$\text{Percentage Yield} = \frac{\text{Weight of crude extract}}{\text{Weight of pulverised sample}} \times 100$$

2.6 Sample collection

The rats were sacrificed by cervical dislocation, the blood sample was collected into anticoagulant-free tube and centrifuged at 3,500 rpm for 5 minutes to obtain the serum. The abdominal cavity was opened up and the pancreas was excised into 10% formalin for histological studies.

2.7 Isolation of mitochondria from the rat liver

Reduced ionic strength mitochondria were separated using method designed by [Younes and Schneider \(1984\)](#), and [Johnson and Lardy \(1967\)](#). The rats were sacrificed by cervical dislocation and the abdominal cavity was opened up and liver samples were removed into ice-cold beaker. The blood stain was rinsed from the liver with isolation buffer that contains 0.21M mannitol, 0.079M sucrose, 0.005M HEPES-KOH and 0.001M EGTA (pH 7.4, Sigma). The samples were weighed and chopped into small pieces using a pair of scissors. This was then homogenized using Teflon and homogenizer (DELFLEX[®]) in a 10% suspension in isolation buffer. The entire process was carried out at 4°C to ensure viability of the mitochondrial membrane. The homogenate was subjected to five differential centrifugation steps in a cold centrifuge MSE. The first two-5 minutes each was used to separate the nuclear debris as the pellet at 2,300 rpm. The supernatant was then discarded, and the pellet containing the mitochondria was resuspended in a wash buffer (0.21M mannitol, 0.079M sucrose, 0.005M HEPES-KOH, pH 7.4, and 0.5% BSA, Sigma). The re-suspended mitochondria were centrifuged twice for 10 min at 12,000 rpm to wash away any artifacts. The pellet was re-suspended in suspension buffer (0.21M mannitol, 0.079M sucrose, 0.005M HEPES-KOH, pH 7.4, Sigma) and kept on ice for immediate use.

2.8 Determination of mitochondrial protein

Mitochondrial protein concentration was determined according to the method of [Lowry et al \(1951\)](#) using Bovine Serum Albumin as standard. Mitochondria (10 µL) were suspended in 990 µL of distil water in test tubes in triplicate. Then, 3 mL mixture of 100:1:1 of 2 g Na₂CO₃, 0.1M NaOH and 1% CuSO₄.5H₂O respectively, was added to the protein suspension, thoroughly mixed and left standing for 10 min. Thereafter, 300 µL of 2N Folin-Ciocalteu diluted in four-fold was added into the mixture, followed by energetic shaking and incubation for 30 min. At the expiration of the time, absorbance was determined spectrophotometrically at 750 nm.

2.9 The procedure and method for mPT determination

The mitochondria were first investigated to determine their suitability for this experiment. Isolated mitochondria protein (0.4 mg/mL) from normal control group were pre-incubated

with 8 µM rotenone for 3.5 min. Subsequently, 5 mM succinate was added to energize the reaction and change in absorbance was read using UV-752 spectrophotometer at 540 nm for 12 min at 30 s interval. Similarly, assessment of the inductive effect of calcium was carried out as follows: mitochondria of the same protein concentration (0.4 mg/mL) were pre-incubated with 8 µM rotenone for 3 min, followed by the addition of exogenous 3 µM calcium. Thirty seconds later, 5 µM succinate was added and the absorbance was measured. The reversal of the calcium-induced opening was assessed by pre-incubating the same mitochondria protein with 8 µM rotenone and 4 mM spermine. Exogenous calcium was then added immediately after 3 min pre-incubation; succinate was added after 30 s and absorbance was read. Corresponding mitochondria protein from the treatment groups were investigated for permeability transition under similar condition without addition of exogenous calcium.

2.10 Assessment of mitochondrial ATPase activity

Isotonic solution (0.25M sucrose) was used to isolate mitochondria of viable integrity from rat liver in this experiment. The isolation followed the same process with that of mPT ([Section 2.6](#)) except for the buffer employed.

Mitochondrial ATPase activity was determined as described by [Lardy and Wellman \(1953\)](#) with minor modification. Each test tube (in triplicate) contained 25 mM sucrose, 65 mM Tris-HCl (pH 7.4) and 0.5 mM KCl in 1 mL final reaction volume. The ATP (1 mM) was added to the set of tubes labelled ATP only, uncoupler, zero time, test groups and control with the exception of the tube labelled mitochondria only. These were incubated at 27 °C in a shaking water bath. Mitochondria (0.4 mg/mL protein) from the test groups were dispensed into labelled tubes other than mitochondria only, uncoupler and zero time tubes which contained mitochondria isolated from the normal control group. While uncoupler (25 µM, 2, 4-dinitrophenol) was added to the uncoupler tubes instantly after mitochondria were added, 1 mL of 10% sodium dodecylsulphate (SDS) was immediately added to the zero-time test tubes. The suspensions were incubated for 30 min and the reaction was terminated by adding 1 mL SDS except in the zero time test tube which had been stopped before. One ml suspension was withdrawn from each test tube and diluted with 4 mL distilled water. Thereafter, 1 mL of 1.25% ammonium molybdate (prepared in 6.5% H₂SO₄) and 1 mL of 9% ascorbic acid newly prepared were added successively and the absorbance was read at λ_{660 nm} in a UV-752 spectrophotometer. Ammonium molybdate (1 mM) was also treated as the sample and used as the standard from which the absorbance of the unknown could be extrapolated. Inorganic phosphate released was quantified using a phosphate standard curve.

2.11 Determination of DNA fragmentation

Liver samples (0.25 g) from each rat were weighed and homogenized with 5 mL TET (5 mM Tris-hydroxymethyl-

aminomethane, 20 mM EDTA and 2 mL of Triton X-100, adjusted to pH 8.0, Sigma) buffer and spinned using ultracentrifuge at 27,000 rpm for one-third hour. Supernatant was removed and the pellet was reconstituted to concentration of 1:1 (v/v) using TE (5 mM Tris-HCl and 20 mM EDTA pH 8.0) buffer. Exactly 0.5 mL of the supernatant and reconstituted pellet were withdrawn and 1.5 mL of 9 mM diphenyl amine solution (prepared in amber bottle because of photosensitivity) was added to each mixture. The mixture in each test tube was allowed to incubate at physiologic temperature for 16 h to 1 day for colour development to be observed and absorbance taken at 620 nm via UV-752 spectrophotometer.

$$\text{Percentage DNA fragmentation} = \frac{A}{A + B} \times 100$$

Where A is the absorbance of supernatant; B is the absorbance of the pellet.

2.12 Estimation of lipid peroxidation

A modified TBARS (thiobarbituric acid reactive substances) method was used for determining the level of peroxidation in mitochondrial membrane lipids (Ruberto et al., 2000). For this assay, exactly 2 mL of a 10% mitochondrial suspension was dispensed into a test tube and diluted with distilled water to a final volume of 4 mL. The mixture was allowed to stand at room temperature for 30 min. Subsequently, 6 mL of 20% acetic acid and 6,000 μ L of 0.75% TBA in 1.1% SDS were added to the tube. The resulting solution was then subjected to steam heating for 60 min. After cooling, 5 mL of butanol was added to the solution, leading to the formation of organic and aqueous layers. The malondialdehyde (MDA), a product of lipid peroxidation, was selectively extracted into the butanol phase. The mixture was centrifuged at 3,000 rpm, resulting in a clear demarcation between the butanol and aqueous phases.

The butanol phase, containing the extracted MDA, was measured spectrophotometrically at a wavelength of 532 nm to quantify the level of peroxidation in the mitochondrial membrane.

2.13 Antioxidant assays

2.13.1 Determination of catalase activity

It was examined as described by Claiborne (1985) protocol. This procedure is dependent on the reducing absorbance seen at wavelength 240 nm upon the action of the enzyme on H₂O₂. The extinction coefficient of 0.0436/mM/cm was used (Noble and Gibson, 1970). The dilution was carried out on the samples in 1:50. The reaction mixtures 2 mL H₂O₂ solution (19 mM) and 2.5 mL phosphate buffer (0.05 M pH 7.4). One and a half ml of the assay mixture was added into 3 mL of dichromate acetic acid reagent at 60 s periodically and then read using UV 752 spectrophotometer.

$$\text{Catalase activity} = \frac{\Delta A_{240} / \text{min} \times \text{reaction volume} \times \text{dilution factor}}{0.0436 \times \text{sample volume} \times \text{mg protein/ml}}$$

The unit is μ mole H₂O₂/min/mg protein.

2.13.2 Assessment of reduced glutathione (GSH) level

Concentration of GSH was investigated via the protocol of Beutler et al. (1963). Precipitating solution (4% sulphosalicylic acid prepared with solution containing 4 g of sodium chloride in final volume of 100 mL) and sample were in a mixture of 0.2 mL each, thoroughly mixed and centrifuged at 4,000 rpm. Subsequently, 0.25 mL of the supernatant and 0.75 mL of Ellman's reagent (1 mM) were added. The absorbance readings were taken at 412 nm via spectrophotometer (UV-752).

2.13.3 Assessment of glutathione S- transferase activity

GST activity was estimated in accordance to Habig et al. (1974) method. The reduction in absorbance was read using UV-752 spectrophotometer at wavelength 340 nm, 30 s interval for 4 min. GST activity was calculated as unit per mg protein based on a molar extinction coefficient of 9.6×10^3 L/mol/cm. One unit of GST was defined as the amount of enzyme that catalyzes the conjugation of 1 nmol of GSH-CDNB per minute.

2.14 Isolation and purification of active metabolites using preparative thin layer chromatography

To further purify the chloroform fraction of *O. gratissimum* leaf extract, a graded solvent system was employed using vacuum liquid chromatography, resulting in the isolation of the methanol/chloroform subfraction (1:1; v/v). Preparative thin layer chromatography plates were utilized for the analysis. Various solvent systems were employed to facilitate the elution of the samples on the plate.

To identify specific phytochemicals, chromogenic agents were applied to the separated metabolites on the plate, which was subsequently visualized under UV light (both at 254 nm and 366 nm). The samples dissolved in suitable solvents, were carefully spotted on the plate using capillary tubes. After drying, the plate was gently positioned in a chromatographic jar containing the appropriate solvent system. The jar was sealed, allowing the samples to migrate with the mobile phase. The experiment was concluded when the solvent front reached a point about 1 cm before reaching the top of the plate. The plate was then removed, air-dried, and examined under the UV light. Later, the spots on the plate were separately scraped, dissolved in the appropriate solvent and spun in the centrifuge to sediment the gel. Dissolved isolated metabolites were aspirated from the centrifuge tubes and concentrated to dryness. The samples were subjected to analysis using a nuclear magnetic resonance system (Bruker Avance^{III} 400 MHz).

2.15 Assessment of serum insulin concentration

Calibrators and samples (25 μ L each) were added into the right micro-wells along with 100 μ L enzyme conjugate 1X deposited in each well and shaken in a shaker at normal environmental temperature for 2 h to allow for incubation to occur. It was washed repeatedly six rounds with washing buffer 1X solution and the left-over reaction content was disposed off by inversion of the microplate. Afterwards, wash solution

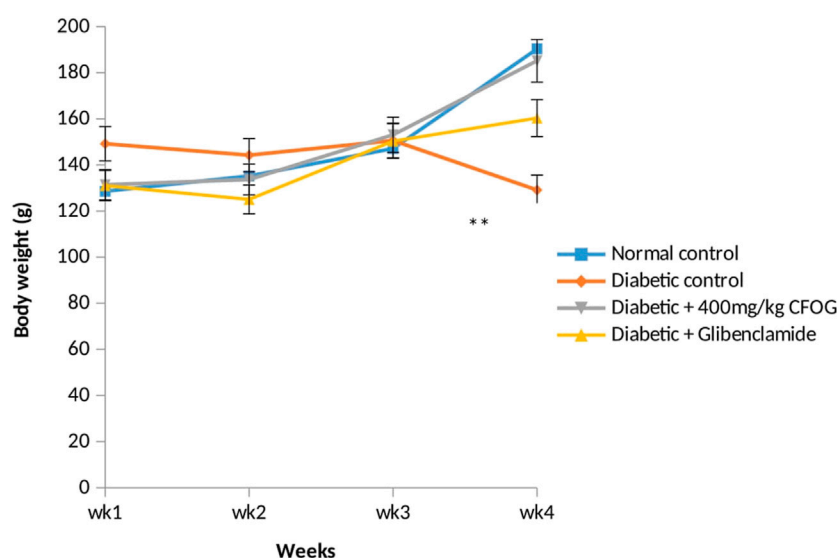


FIGURE 1

The assessment of body weight of normal and STZ-induced diabetic rats Key: CFOG: Chloroform fraction of *O. gratissim* um.

(WS) (350 μ L) was introduced and later removed using absorbent material. The removal of WS was performed in five successive intervals. Incubation at room temperature was allowed to proceed for 15 min after addition of substrate, TMB (200 μ L) to the wells. The reaction was thereafter halted with “stop solution” (50 μ L) and thoroughly mixed using shaker for just 5 s. Spectrometry method via microplate reader was then employed to take the optical density reading at λ 450 nm not later than duration of half-an hour.

2.16 Homeostasis model assessment of insulin resistance and beta cell function

These were calculated using the relationship between serum insulin and blood glucose level (Matthews et al., 1985).

$$\text{HOMA} - \text{IR} = \frac{\text{Insulin} (\mu\text{U/ml}) \times \text{Glucose} (\text{mg/dl})}{405}$$

$$\text{HOMA} - \beta = \frac{360 \times \text{Insulin} (\mu\text{U/ml})}{\text{Glucose} (\text{mg/dl}) - 63}$$

2.17 Hemoxilyn and eosin procedure for pancreatic architecture

Wax was removed using xylene for about 15 min and passed through absolute, 95% and 70% alcohol successively. This would be followed by rinsing the section in water and staining with Harris hematoxylin for 300s. Before differentiating quickly in 1% acid alcohol, it was dipped in water again. After this, it was put under running tap for 10 min and counterstained with 1% Eosin stain for 180s, then rinsed with water. It was dried in rising grades of alcohol and cleared in xylene subsequent to mounting in DPX (Avwioro, 2010).

2.18 Statistical analysis

Statistical analysis was carried out using Graph pad prism (version 8.0) for one-way ANOVA and Turkey's multiple comparison test was used to compare the mean among the groups. Level of significance was set at $p < 0.05$. All the results were expressed as mean \pm standard deviation (SD). Representative profiles of absorbance of mitochondria were used for the mitochondrial permeability transition pore opening assays. Each assay was repeated three times (in each case) and representative of similar kinetic assay for the mPT in each group was used.

3 Results

3.1 Effect of the chloroform fraction of *O. gratissimum* (L) leaf extract on body weight, glycemic index and mito-protective biomarkers in STZ-triggered diabetic rats

3.1.1 Effect of chloroform fraction of OG on body weight on STZ-induced diabetic rats

Body weight is one of the indices for tissue wastage which is common in individuals with unmanaged diabetes mellitus. Figure 1 illustrates the body mass of non-diabetic and CFOG-treated diabetic rats for a period of 28 days. It was noticed that no significant difference among the glibenclamide-, CFOG-treated animals and control. In contrast, sharp decline was observed in the diabetic untreated group when compared to control.

3.1.2 Evaluation of insulin and glucose levels in CFOG-treated diabetic rats

Table 2 depicts the effect of CFOG on concentrations of glucose and insulin in STZ-stimulated diabetic rats. There was significant difference in the insulin level in untreated diabetic group relative to

TABLE 2 Effect of chloroform fraction of *Ocimum gratissimum* (L.) leaf extract on insulin and blood glucose concentrations in STZ- and HFD-induced diabetic rats.

Groups	Insulin concentration (μU/ml)	Blood glucose level (mg/dL)
Normal Control	1.41 ± 0.01 [#]	106.74 ± 5 [#]
Diabetic Control	1.74 ± 0.01 [*]	492.3 ± 10 [*]
Diabetic +400 mg/kg CFOG	1.42 ± 0.03 [#]	169.92 ± 7 [#]
Diabetic +5 mg/kg Glibenclamide	1.42 ± 0.03 [#]	181.08 ± 11 [#]

Key: * test groups compared to Normal control; # other groups relative to Diabetic control.
CFOG: chloroform fraction of *ocimum gratissimum* leaf extract.

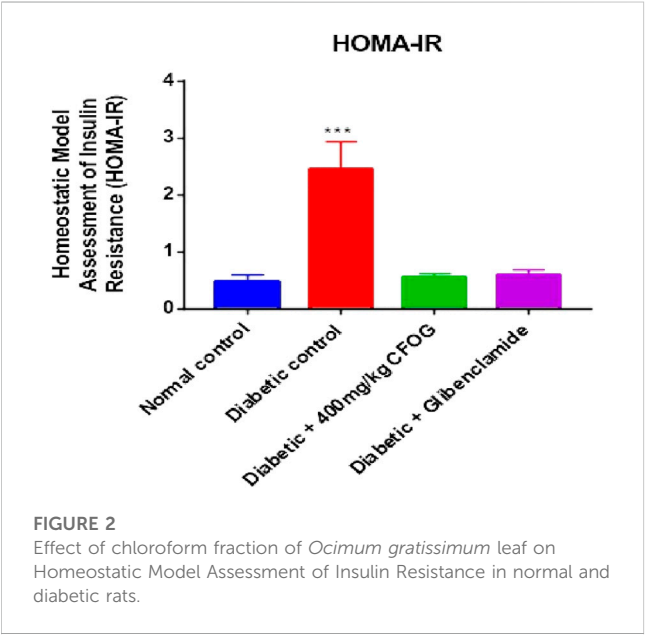


FIGURE 2
Effect of chloroform fraction of *Ocimum gratissimum* leaf on Homeostatic Model Assessment of Insulin Resistance in normal and diabetic rats.

control. Whereas, no significant statistical change was observed in the remaining test groups compared to control. Moreover, a significant increase was observed in glucose concentration in the untreated, glibenclamide-treated and 400 mg/kg CFOG groups relative to control. However, in comparison with the diabetic control, there was obvious reduction in blood glucose level in CFOG-treated and glibenclamide groups.

3.2 Investigation of chloroform fraction of *O. gratissimum* (L) effect on homeostasis model assessments of insulin resistance and pancreatic beta cell function

Homeostasis model assessment is typically used in type 2 diabetes mellitus as index to measure the sensitivity of the insulin to its receptor and as well as viability and availability of beta cells that are responsible for synthesizing insulin. Figure 2 illustrates the influence of CF of *O. gratissimum* (L) leaf on insulin resistance status in STZ-induced diabetic rats. There was significant elevation of this parameter in the diabetic control relative to normal control. Conversely, no significant difference exists between the remaining treated groups compared to normal control.

A highly significant reduction of β -cell function was observed in the untreated group in comparison with normal control. However, there

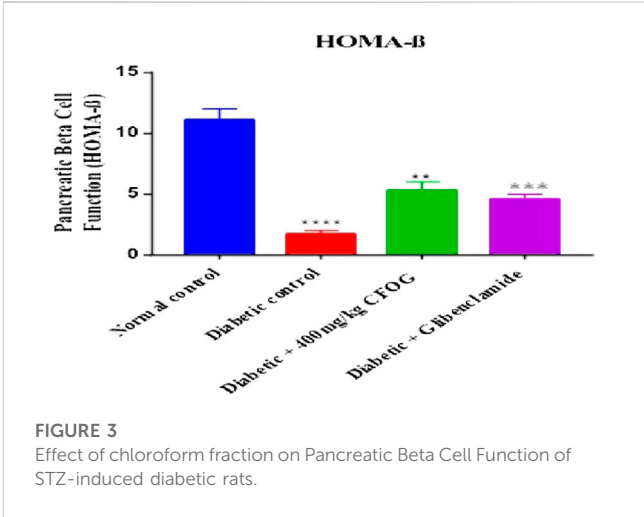


FIGURE 3
Effect of chloroform fraction on Pancreatic Beta Cell Function of STZ-induced diabetic rats.

was drastic increase in beta cell status in the CFOG and glibenclamide treated groups compared to the untreated diabetic control (Figure 3).

3.3 Effect of chloroform fraction of OG on mPT in STZ-induced diabetic rats

The status of mPT pore of the normal rats is crucial to knowing whether the pore opening in diabetic untreated rats was actually due to the administered diabetogenic agent (STZ) or not. Therefore, it is necessary to investigate the mitochondria intactness of normal control rats (non-diabetic). Figure 4 presents the evaluation of calcium induction and spermine inhibition of mPT in normal control rats. The results showed that large amplitude swelling was observed when intact mitochondria were challenged with exogenous calcium (6.3 folds), the triggering agent. However, spermine (standard inhibitor) subsequently reversed calcium-induced opening by 82%.

Furthermore, a significant pore induction (8.5 folds) was discovered in STZ-induced diabetic rats (Figure 5). However, CFOG and glibenclamide were able to preclude the pore opening observed in STZ-induced diabetic rats by 90% and 72% successively.

3.4 Assessment of the impact of CFOG on mLPO in STZ-stimulated diabetic rats

One of the diabetogenic mechanisms of STZ is generation of free radicals which could lead to lipid peroxidation measured as

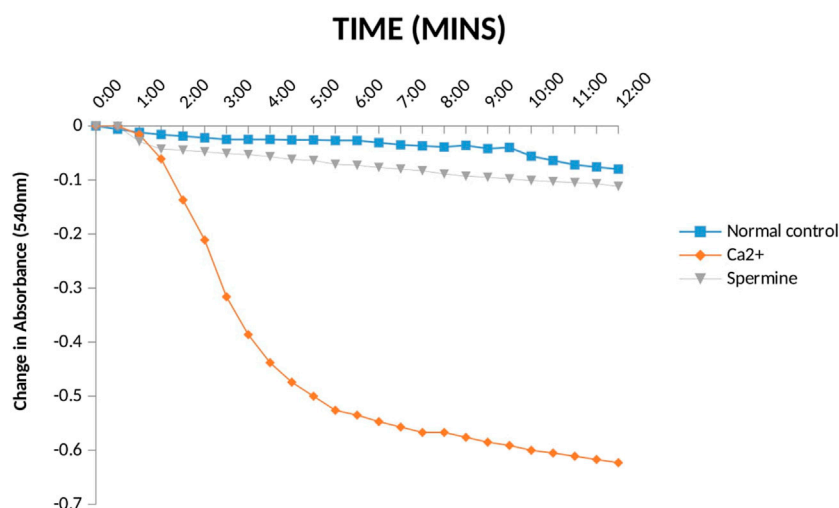


FIGURE 4

Effect Ca²⁺ and spermine on Mitochondrial Membrane Permeability Transition pore for normal control rats.

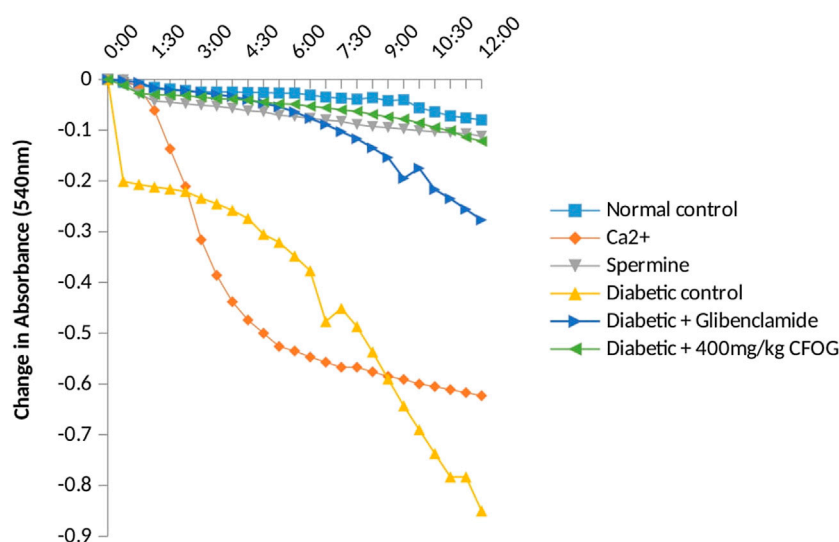


FIGURE 5

Assessment of effect of chloroform fraction of OG leaf on type 2 diabetic rat liver.

malondialdehyde (MDA) in this study. The impact of CFOG on lipid peroxidation in STZ-induced diabetic rats was displayed in Figure 6. It was observed that only the diabetic control showed highly significant difference in MDA level relative to normal control. In contrast, MDA produced in other groups were similar to normal control group.

3.5 Investigation of the CFOG leaf effect on mATPase activity in diabetic rats

Table 3 represents the effect of CFOG on mitochondrial ATPase function in STZ-triggered diabetic rats. Diabetic control was observed to display highly significant difference in the enzyme

activity compared to normal rats. However, 400 mg/kg CFOG and 5 mg/kg glibenclamide drastically reduced the enzyme activity relative to diabetic control.

3.6 Examination of the influence of CFOG on DNA fragmentation in diabetic rats model

Figure 7 is an illustration of modulation of chromosomal DNA segmentation by CFOG in STZ-induced diabetic rats. Significantly high DNA fragmentation was observed in the diabetic control relative to normal control. Conversely, there was no significant difference in test groups, 400 mg/kg CFOG and 5 mg/kg glibenclamide in comparison with normal control.

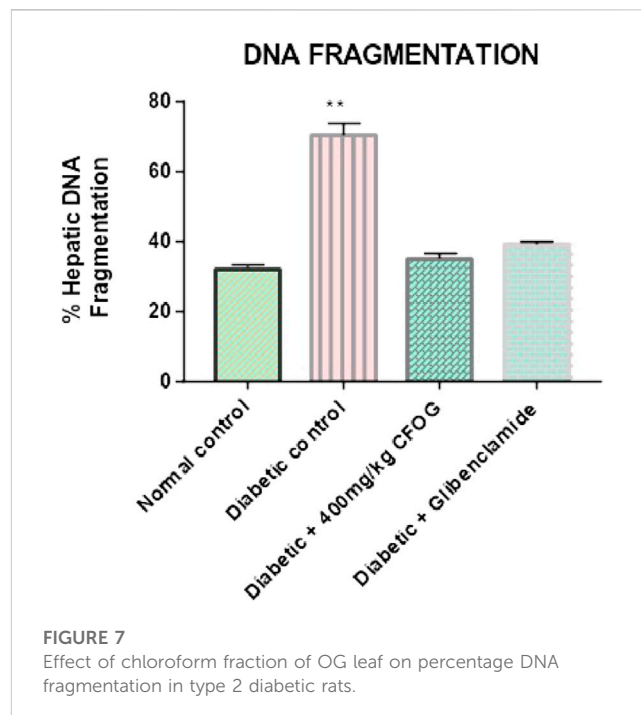
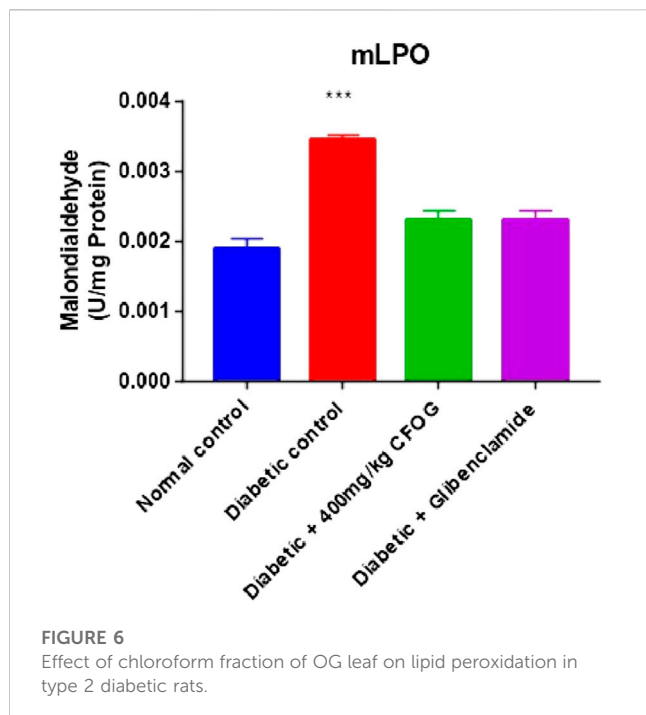


TABLE 3 Assessment of the Effect of Chloroform Fraction of OG on mATPase Activity in STZ-induced Diabetic Rats.

Groups	micromole Pi/min/mg protein
Normal Control	0.018 ± 0.0 ^{##}
Diabetic Control	3.4 ± 0.0 ^{**}
Diabetic + 400 mg/kg CFOG	0.42 ± 0.0 ^{*#}
Diabetic + 5 mg/kg Glibenclamide	0.62 ± 0.0 ^{*#}
UCP	5.8 ± 0.0 ^{****#}

UCP: uncoupler.

*Means comparison of the test group with normal control.

#Means comparison other groups with diabetic control group.

mATPase: mitochondrial ATPase.

CFOG: chloroform fraction of *ocimum gratissimum* leaf extract.

3.7 Histological examination of pancreatic architecture of STZ-Induced diabetic rats treated with chloroform fraction of OG

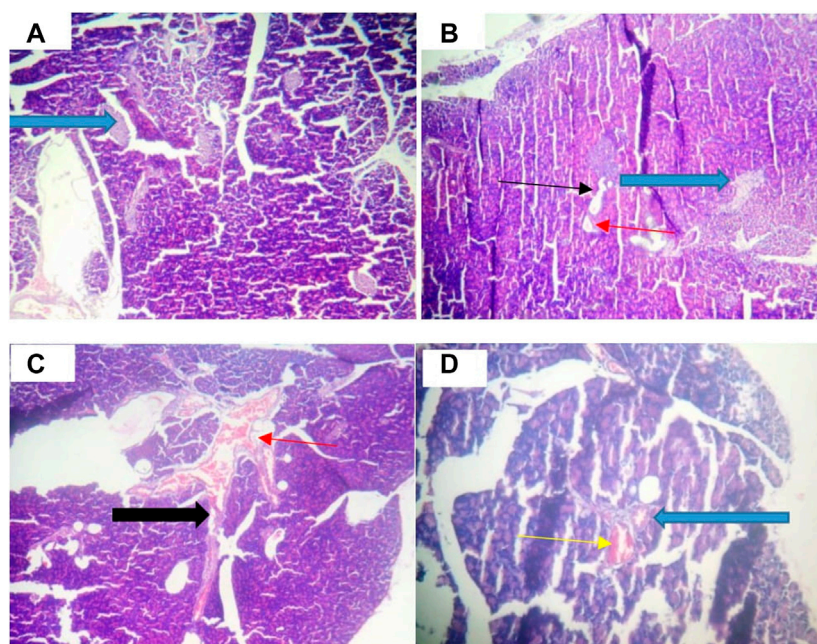
Figure 8A shows that the pancreatic architecture was normal with exocrine acini (blue arrow) abundant and standard. The inter- and intra-lobular ducts were intact. Figure 8B depicts normal pancreas structure. Interlobular duct shows necrosis (black slender arrow) and haemorrhagic abrasion (red arrow). Figure 8C illustrates that exocrine acini filled with zymogen but the intralobular duct (black arrow) looked swelling and hyperemia (red) were noticed. In Figure 8D, undistorted exocrine acini (blue arrow), but intralobular distension and congestion (yellow arrow) were observed.

Figure 9A illustrates that abundant number of islets was normally distributed within the parenchyma cells. Figure 9B shows that some islets of Langerhans appear atrophic (white

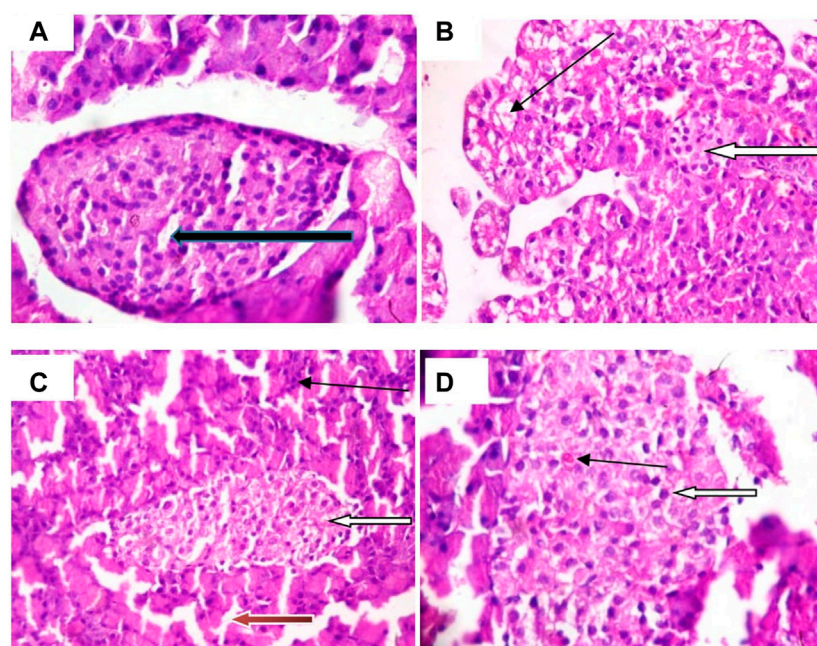
arrow). The results in Figures 9C,D indicate normal islets of Langerhans (white arrow) consisting of round to oval collections of endocrine cells. Conversely, treatment with CFOG shows that it possesses phytochemicals that can repair damage islet cells.

3.8 Antioxidants status of STZ-induced diabetic rats treated with chloroform fraction of OG

GSH level, glutathione-S-transferase and catalase activities were displayed in Figure 10. The results showed that similar trends of significant decline were observed in the antioxidant status of diabetic control relative to normal control. Whereas, in the group treated with 400 mg/kg CFOG, there was no significant difference observed in the antioxidant enzymes activities and GSH level in comparison with the normal control.

**FIGURE 8**

Pancreatic histology of STZ-induced diabetic rats treated with chloroform fraction of *Ocimum gratissimum* (X400).

**FIGURE 9**

Photomicrograph of Islet cell of type 2 diabetic rats treated with chloroform fraction of *Ocimum gratissimum* leaf (X400).

3.9 Purified bioactive compound from chloroform fraction of OG

Figure 11 shows the structural elucidation of the bioactive principle which could be responsible for anti-diabetic agent. Lupanol was characterized from *O. gratissimum* leaf extract.

4 Discussion

Mitochondria are very vital organelles to the existence and survival of the cells as they are useful for energy production and other biochemical processes. Because of these salient roles, they are highly gated to prevent ‘intruders’ that could hamper their efficient

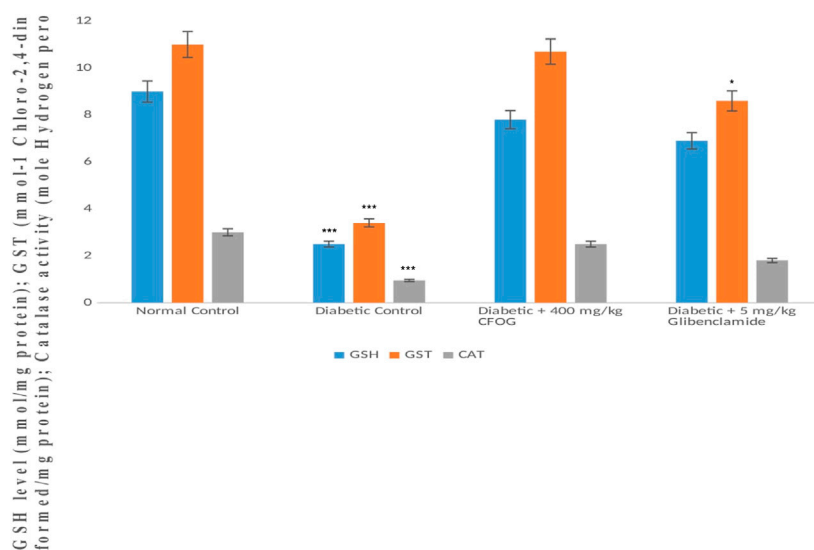


FIGURE 10

Assessment of the effect of CFOG on GSH level, GST and CAT activities in type 2 diabetic rats. *Means comparison of the test group with normal control.

functioning. Any condition that could lead to compromising the integrity of the two tight mitochondrial barriers would eventually collapse the organelles and the whole cell. The mitochondria breakdown could result from membrane potential dissipation and oxidative stress among others.

From the results above (Figure 4), the observed constancy of absorbances in the mitochondria suspension without triggering agent (calcium) and large amplitude pore opening in the suspension challenged with calcium in separate experiments depict that the membrane integrity has not been compromised. Subsequent reversal of the calcium-induced opening by spermine (a potent pore inhibitor), in another experiment over a period of 12 min at 30 s interval, in the presence of rotenone and succinate, further substantiates that the mitochondria were intact, not uncoupled and suitable for further use. This experiment is very important because the integrity of the mitochondrial membrane is crucial for ATP synthesis. In other words, mitochondria with lost membrane integrity cannot synthesize energy.

Diabetes mellitus is a derangement in carbohydrates, lipid and proteins metabolism. This pathophysiological condition is associated with inflammation, loss of integrity of beta cell mitochondria, elevated blood insulin and glucose, increased and overexpressed apoptosis. In the results obtained from the impact of CFOG on STZ-induced diabetic rats, normoweighted condition (Figure 1) was discovered in rats treated with the CFOG and this might have stemmed from its ability to attenuate tissue wastage related to DM due to the presence of phytochemicals that aid proper maintenance of macromolecules metabolism in the biological system. Glucose and insulin levels were also normalized by the administration of CFOG to diabetic rats (Table 2). This indicates that its bioactive metabolites could have played abrogating roles in normalizing the insulin and blood sugar status in the rats. Diets containing necessary antioxidants have been shown to demonstrate good anti-diabetic efficacy (Bacanli et al., 2016). Genistein, an isoflavone, significantly reduced glucose intolerance in diabetic rats (Lee, 2006). Tannin was reported to exhibit an anti-nutrient activity by inhibiting α -glucosidase, thus impeding or slowing down the

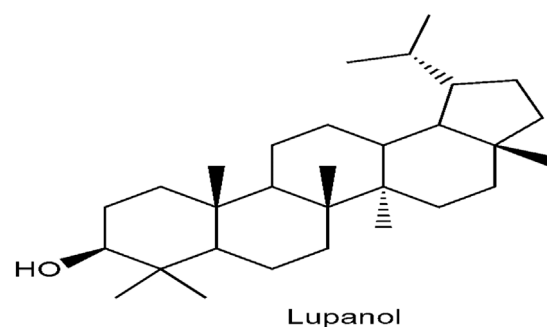


FIGURE 11

Characterisation of lupanol from *Ocimum gratissimum* (L.) leaf extract.

absorption rate of glucose across the intestinal epithelial cell. Nutritive soy isoflavones drastically enhanced insulin biosynthesis thereby ameliorating excessive blood sugar and as well mitigated diabetic complication such as cataracts. Anti-hyperglycemic effect of low dose quercetin and quinic acid has been well documented (Arya, et al., 2014). *Beta vulgaris* was reported to lower blood glucose (Bolkent, et al., 2009). Similarly, complete abrogation of insulin resistance and considerable improvement in beta cell biomass were shown in Figures 3, 4 respectively. This depicts that CFOG could inhibit desensitization of insulin and probably its receptor too. Myriads of phytoactive molecules known to exhibit antioxidant potentials play crucial role in enhancing alertness and response of insulin in a condition of elevated glycemia (Bacanlia et al., 2019). Procyanidin from blueberry was also shown to reduce insulin resistance by mimicking this protein and also increase sensitivity through correction of the perturbed circulation of lipids and carbohydrate in the system (Yamashita et al., 2012).

Permeabilization of mitochondrial inner barrier to molecules of greater than 1.5 kDa, which leads to cell demise, is prominent in

diseases associated with tissue wastage. STZ had 8.5folds pore induction and there was subsequent reversal of this, by 400 mg/kg CFOG (90%) as shown in Figure 5. This may suggest the ability of the fraction to maintain the viability of the rat liver mitochondria and as well block the triggering of pore formation associated with apoptosis. It is also coupled with obliteration of lipid peroxides (Figure 6) and prevention of the activation of ATPase activity (Table 3). Absence of mDNA fragmentation (Figure 7) in the diabetic rats treated with CFOG is an evidence that cell death did not occur. Similarly, histological examination of pancreas showed intact exocrine acini, normal and abundant (Fan et al., 2017; Baburina et al., 2019) islets in the diabetic rats administered CFOG as opposed to severely damaged pancreatic architecture in the diabetic control rat (Figures 8, 9). The presence of the phytochemicals in this solvent fraction could be liable for the anti-apoptotic properties observed in this experiment. Research substantiated that polyphenols boost mitochondria biogenesis and prevent mitochondrial insult (Park, et al., 2012). They also promote viability and survival of cells in conditions such as aging, neurodegenerative diseases and diabetes mellitus (Lionaki et al., 2015).

Moreover, our antioxidant results showed increase in the enzymes activities such as GST (phase II detoxifying enzyme), and CAT in the CFOG treated group as against the diabetic control rats (Figure 10). The similar elevation was also observed in non-enzymic endogenous antioxidant, GSH in the group administered 400 mg/kg CFOG (Figure 10). This may be owing to the availability of phytochemicals in the extract. Many researches have implicated oxidative stress in the pathogenesis of diabetes mellitus stemming from excess blood glucose and lipids (Dembinska-Kiec et al., 2008). It has been reported that in DM and its attendant complications such atherosclerosis and cardiovascular disorder, there is an obvious reduction in the plasma levels of vitamins C and E, zeaxanthin, beta-carotene and lycopene, showing that overwhelming free radicals and oxidative stress are culprits in precipitating these diseases (Cheng et al., 2014; Girones-Vilaplana et al., 2014).

Vegetables and fruits which are usually rich in these phytonutrients are mostly recommended by the medical practitioners for the management of DM in order to ward off pro-oxidants generated in the course of the disease and to block its complications (Braun and Venter, 2008). Polyphenols are severally reported to profoundly prevent the onset of chronic ailments which are associated with oxidative imbalance in the cell. Due to the presence of phenolics, mulberry fruit was discovered to possess neuro-preserving and antidiabetic potency (Wang et al., 2013).

In this study, lupanol (Figure 11), a penta triterpene, was discovered to be present in *O. gratissimum* leaf using NMR technique. Terpenes have been implicated to possess anti-diabetic effect (Jovanovic et al., 2021). Research showed that 23, 28-dihydroxyl lupan-20 (29) ene 3 β caffeat obtained from *Sorbus decora* which is structurally close to lupanol, was discovered to improve glucose uptake in C2C12 skeletal muscle cell line. *Momordica charantia* contains two terpenes such as 3 β , 25-dihydroxyl-7 β , 25- trimethoxy cucurbita-5, 23- (E)-diene and 3 β , 25-dihydroxyl-7 β , 25- trimethoxy cucurbita-5, 23- (E)-dien-19-al. These bioactive agents exhibit their functions as insulin sensitizers which could help reduce insensitivity of insulin to its receptor (Panigrahy et al., 2020).

Furthermore, corosolic acid isolated from *Lagerstroemia speciosa* acts as α -glucosidase inhibitor, while lupeol obtained

from mango leaf significantly scavenge ROS and thus reduced oxidative stress in albino mice (Panigrahy et al., 2020).

5 Conclusion

It could be inferred from the above data that chloroform fraction of *O. gratissimum* (L) leaf extract prevents programmed cell death as evident in its ability to inhibit pore-opening, ATPase activity and lipid peroxidation in STZ-induced diabetic rats which could lead to tissue wastage experienced in diabetes mellitus. It could also be suggested that chloroform fraction probably contains bioactive principles which was able to scavenge free radicals generated in STZ-induced diabetic rats as observed in the antioxidant status of the extract-treated rats. The leaf fraction was also able to lower blood glucose, homeostasis model assessment of insulin resistance and enhance homeostasis model assessment of pancreatic beta cell. This shows the plant fraction has inherent metabolites which could act as insulin sensitizer and secretagogues. The presence of lupanol may be one of the bioactive compounds responsible for anti-diabetic activity of *O. gratissimum* leaf.

Data availability statement

The original contributions presented in the study are included in the article/supplementary material, further inquiries can be directed to the corresponding author.

Ethics statement

The animal study was approved by Animal Care and Use Research Ethics Committee, University of Ibadan, Oyo State, Nigeria. Reference number UI-ACUREC/19/0065. The study was conducted in accordance with the local legislation and institutional requirements.

Author contributions

AS conceptualized the research, data collection and analysis; JO monitored the design and manuscript correction; AO contributed to the design of methods; AA helped in proofreading of the manuscript, FO helped with laboratory work, OO monitored the overall process of the research. All authors contributed to the article and approved the submitted version.

Funding

The research was sponsored by the individual authors.

Conflict of interest

The authors declare that the research was conducted in the absence of any commercial or financial relationships that could be construed as a potential conflict of interest.

Publisher's note

All claims expressed in this article are solely those of the authors and do not necessarily represent those of their affiliated

References

- Afolabi, C., Akinmoladun, E. O., Ibukun, E. A., Obuotor, E., and Farombi, E. O. (2007). Phytochemical metabolite and antioxidant activity of extract from the leaves of *O. gratissimum*. *Scientific Research and Essay*, 2(5), 163–166.
- Alvarenga, P., Gonçalves, A. P., Fernandes, R. M., de Varennes, A., Vallini, G., Duarte, E. C., et al. (2008). Evaluation of composts and liming materials in the phytostabilization of a mine soil using perennial ryegrass. *Sci. Total Environ.* 406, 43–56. doi:10.1016/j.scitotenv.2008.07.061
- American Diabetes Association (2012). Diagnosis and classification of diabetes mellitus. *Diabetes care* 35 (1), 564–S71. doi:10.2337/dc12-s064
- Arya, A., Al-Obaidi, M. M., Shalud, N., Noordin, M. I., Looi, C. Y., Wong, W. F., et al. (2014). Synergistic effect of quercetin and quinic acid by alleviating structural degeneration in the liver, kidney and pancreas tissues of STZ-induced diabetic rats: a mechanistic study. *Food Chem. Toxicol.* 71, 183–196. doi:10.1016/j.fct.2014.06.010
- Avwioro, O. (2010). *Histochemistry and tissue principle and techniques*. Lagos, Nigeria: Claverianum press.
- Ayissi, N. K., and Nyadedzor, C. (2003). Comparative *in vitro* effects of AZT and extracts of *Ocimum gratissimum*, *Ficus polita*, *Clausena anisata*, *Alchorne cordifolia*, and *Elaeophorbia drupifera* against HIV-1 and HIV-3 infections. *Antivir. Res.* 58, 25–33. doi:10.1016/s0166-3542(02)00166-3
- Baburina, Y., Krestinin, R., Odinkova, L., Sotnikova, L., Kriglov, A., and Krestina, O. (2019). Astaxanthin inhibits mitochondrial permeability transition pore opening in rat heart mitochondria. *Antioxidants (Basel)* 8 (12), 576. doi:10.3390/antiox8120576
- Bacanli, M., Göky, H. G., Basaran, N., An, N., and Basaran, A. A. (2016). Beneficial effects of commonly used phytochemicals in diabetes mellitus. *Acta Pharmaceutica Scientia* 54 (1), 9–20.
- Bacanlia, M., Dilsiza, S., Basarana, N., and Basaran, A. A. (2019). *Effects of phytochemicals against diabetes*. Ankara, Turkey: Elsevier Inc.
- Beaglehole, R., and Yach, D. (2003). Globalisation and the prevention and control of non-communicable disease: the neglected chronic disease of adults. *Lancet* 362, 1763–1764. doi:10.1016/S0140-6736(03)14335-8
- Beutler, E., Duron, O., and Kelly, B. M. (1963). Improved method for the determination of blood glutathione. *J. Laboratory Clin. Med.* 61, 882–888.
- Bolkent, Ş., Yanardağ, R., Tabakoğlu-Oğuz, A., and Özsoy-Saçan, Ö. (2009). Effects of chard (*Beta vulgaris L.*) extract on pancreatic B cells in streptozotocin-diabetic rats: a morphological and biochemical study. *J. Ethnopharmacol.* 14, 15–22.
- Cheng, D. M., Pogrebnyak, N., Kuhn, P., Krueger, C., Johnson, W., and Raskin, I. (2014). Development and phytochemical characterization of high polyphenol red lettuce with anti-diabetic properties. *PLoS ONE* 9, e91571. doi:10.1371/journal.pone.0091571
- Claiborne, A. (1985). "Catalase activity," in *Handbook of methods for oxygen free radical research*. Editor R. A. Greenwald (Boca Raton, FL: CRC Press Inc).
- Daniel, O. O., Adeoye, A. O., Ojowu, J., and Olorunsogo, O. O. (2018). Inhibition of liver mitochondrial membrane permeability transition pore opening by quercetin and vitamin E in streptozotocin-induced diabetic rats. *Biochem. Biophysical Res. Commun.* 504 (2), 460–469. doi:10.1016/j.bbrc.2018.08.114
- Danzel, A. (1996). *The useful plants of West Africa*. London: Crown Agents.
- Dembinska-Kiee, A., Mykkanen, O., Klee-Wilk, B., and Mykkanen, H. (2008). Antioxidant phytochemicals against type 2 diabetes. *Br. J. Nutr.* 991, S109S117. doi:10.1017/S000711450896579X
- Detaile, D., Guigas, B., Chauvin, C., Batandier, C., Fontaine, E., Wiernsperger, N., et al. (2005). Metformin prevents high-glucose-induced endothelial cell death through a mitochondrial permeability transition-dependent process. *Diabetes* 54 (7), 2179–2187. doi:10.2337/diabetes.54.7.2179
- Effraim, I. D., Salami, H. A., and Osewa, T. S. (2000). The effect of aqueous leaf extract of *Ocimum gratissimum* on haematological and biochemical parameters in rabbits. *Afr. J. Biomed. Res.* 3, 175–179.
- Ekaike, M., Ndulaka, J., Ogbonna, C., and Asiegbu, E. (2016). AntiAnti-diabetic effect of *Ocimum gratissimum* on blood glucose level in alloxan induced diabetic rats. *J. Pharm. Biol. Sci.* 11 (2), 12–14. doi:10.9790/3008-1102031214
- Ezekwesili, C. N., Obiora, K. A., and Ugwu, O. P. (2004). Evaluation of anti-diarrheal property of crude aqueous extract of *Ocimum gratissimum* L. (Labiatae) in rats. *Biochemstri* 16 (2), 122–131.
- Fan, C. D., Sun, J. Y., Fu, X. T., Hou, Y. J., Li, Y., Yang, M. F., et al. (2017). Astaxanthin attenuates homocysteine-induced cardiotoxicity *in vitro* and *in vivo* by inhibiting mitochondrial dysfunction and oxidative damage. *Front. Physiology* 8 (1048), 1041–1110. doi:10.3389/fphys.2017.01041
- Farombi, E. (2000). Influence of Amodiaquine treatment on microsomal lipid peroxidation and antioxidant defense systems of rats. *Pharmacol. Toxicol.* 87 (6), 249–254. doi:10.1034/j.1600-0773.2000.pto870601.x
- Feldman, E. L., Callaghan, B. C., Pop-Busui, R., Zochodne, D. W., Wright, D. E., Bennett, D. L., et al. (2019). Diabetic neuropathy. *Nat. Rev. Dis. Prim.* 5 (41), 41–10. doi:10.1038/s41572-019-0092-1
- Ganesan, K., Rana, M. B. M., and Sultan, S. (2020). *Oral hypoglycemic medications*. *StatPearls*. Treasure Island (FL: Publishing.
- Girones-Vilaplana, A., Mena, P., Moreno, D., and Garcia-Viguera, C. (2014). Evaluation of sensorial, phytochemical and biological properties of new isotonic beverages enriched with lemon and berries during shelf life. *J. Sci. Food Agric.* 94, 1090–1100. doi:10.1002/jsfa.6370
- Gorini, S., Antonella, D. A., Berrino, L., Malara, N., Rosano, G., and Ferraro, E. (2018). Chemotherapeutic drugs and mitochondrial dysfunction: focus on doxorubicin, trastuzumab and sunitinib. *Oxidative Med. Cell Longev.* 7582730. doi:10.1155/2018/7582730
- Habig, W., Pabst, M., and Jakoby, W. (1974). Glutathione S-transferases. *J. Biol. Chem.* 249, 7130–7139. doi:10.1016/s0021-9258(19)42083-8
- IDF (2019). *IDF diabetes atlas*. United Kingdom: International Diabetes Federation.
- Johnson, D., and Lardy, H. (1967). Isolation of liver or kidney mitochondria. *Methods Enzym.* 10, 94–96. doi:10.1016/0076-6879(67)10018-9
- Jovanovic, J. A., Mihailovic, M., Uskokovic, A., Grdovic, N., Dinic, S., and Vidakovic, M. (2021). The effects of major mushroom bioactive compounds on mechanisms that control blood glucose level. *J. Fungi* 7 (7), 58. doi:10.3390/jof7010058
- Kamboj, V. P. (2000). Herbal medicine, general articles. *Curr. Sci.* 18, 55–39.
- Lardy, H. A., and Wellman, H. (1953). The catalyst effects of 2, 4-dinitrophenol on adenosine triphosphatase hydrolysis by cell particles and soluble enzymes. *Journal of Biological Chemistry* 201, 357–370. doi:10.1016/S0021-9258(18)71378-1
- Lee, J. S. (2006). Effects of soy protein and genistein on blood glucose, antioxidant enzyme activities and lipid profile in streptozotocin-induced diabetic rats. *Life Sciences* 79, 1578–1584. doi:10.1016/j.lfs.2006.06.030
- Lionaki, E., Markaki, M., Palikaras, K., and Tavernarakis, N. (2015). Mitochondria, autophagy and age-associated neurodegenerative diseases: new insights into a complex interplay. *Biochimica Biophysica. Acta* 1847, 1412–1423. doi:10.1016/j.bbacom.2015.04.010
- Lowry, O. H., Rosebrough, M. J., Farr, A. L., and Randal, R. J. (1951). Protein measurement with the folin phenol reagent. *J. Biol. Chem.* 193, 265–275. doi:10.1016/s0021-9258(19)52451-6
- Matthews, D., Hosker, J., Rudenski, A., Naylor, B., Treacher, D., and Turner, R. C. (1985). Homeostasis model assessment: insulin resistance and beta-cell function from fasting plasma glucose and insulin concentrations in man. *Diabetologia* 28, 412–419. doi:10.1007/BF00280883
- Mohammed, A., Tanko, Y., Okasha, M. A., Magaji, R. A., and Yaro, A. H. (2007). Effects of aqueous leaves extract of *Ocimum gratissimum* on blood glucose levels of streptozotocin-induced diabetic Wistar rats. *African Journal of Biotechnology* 6 (18), 2087–2090. doi:10.5897/AJB2007.000-2323
- Nguyen, A. T., Akhter, R., Garde, S., Scott, C., Twigg, S. M., Colagiuri, S., et al. (2020). The association of periodontal disease with the complications of diabetes mellitus, a systematic review. *Diabetes Res. Clin. Pract.* 165 (23), 108244. doi:10.1016/j.diabres.2020.108244
- Noble, R. W., and Gibson, Q. H. (1970). The reaction of ferrous horseradish peroxidase with hydrogen peroxide. *J. Biol. Chem.* 245, 2409–2413. doi:10.1016/s0021-9258(18)63167-9
- Okoye, E. L., and Madumelu, C. B. (2013). Phytochemical constituent of leaves of *Ocimum gratissimum* and production of mosquito coil. *Global Research Journal of Science* 2, 62–66.
- Olanlokun, O. J., Oyebo, T. O., and Olorunsogo, O. (2017). Effects of vacuum liquid chromatography (chloroform) fraction of the stem bark of *Alstonia boonei* on mitochondrial membrane permeability transition pore. *J. Basic Clin. Pharm.* 8 (4), 221–225.

- Oyebode, T. O., Adebusi, O., Akintimehin, S., and Olorunsogo, O. O. (2017). Modulation of cytochrome C release and opening of mitochondrial permeability transition pore by *Calliandra portoricensis* (Benth) root bark methanol extract. *Eur. J. Med. Plants* 20 (1), 1–14. doi:10.9734/ejmp/2017/35211
- Panigrahy, S., Bhatt, R., and Kumar, A. (2020). Targeting type II diabetes with plant terpenes: the new and promising antidiabetic therapeutics. *Biologia* 2020 (1), 241–254. doi:10.2478/s11756-020-00575-y
- Park, S., Ahmad, F., Philp, A., Baar, K., Williams, T., Luo, H., et al. (2012). Resveratrol ameliorates aging-related metabolic phenotypes by inhibiting cAMP phosphodiesterase. *Cell* 148, 421–433. doi:10.1016/j.cell.2012.01.017
- Ruberto, G., Baratta, M. T., Deans, S. G., and Dorman, H. J. (2000). Antioxidant and antimicrobial activity of *Foeniculum vulgare* and *Crithmum maritimum* essential oils. *Planta Medica* 66, 687–693. doi:10.1055/s-2000-9773
- Salemcity, A. J., Nwaneri-Chidozie, V. O., Oladimeji, O., Ekpa, E., Olugbemi, B. T., and Ukwedeh, E. O. (2014). Effect of methanol extract of *Ocimum gratissimum* leaves on lipid peroxidation and lipid profile status in CCl₄-induced hepatotoxicity in albino rats. *Eur. J. Biomed. Pharm. Sci.* 1 (1), 21–27.
- Srinivasan, K., Viswannd, B., Asrat, L., Kaul, C. L., and Ramarao, P. (2005). Combination of high-fat diet-fed and low-dose streptozotocin-treated rat: a model for type 2 diabetes and pharmacological screening. *Pharmacol. Res.* 52, 313–320. doi:10.1016/j.phrs.2005.05.004
- Ubaid, M., Arif, M., Usmani, A., Anayatullah, Khan, N., Dash, P. P., et al. (2019). An insight to diabetes mellitus and its complications. *Adv. Clin. Endocrinol. Metabolism* 2 (1), 37–46.
- Ugwu, E., Young, E., and Nkpozi, M. (2020). Diabetes care Knowledge and practice among primary care physicians in Southeast Nigeria: a cross-sectional study. *BMC Fam. Pract.* 21 (128), 1–11. doi:10.1186/s12875-020-01202-0
- Wang, C., and Youle, R. J. (2009). The role of mitochondria in Apoptosis. *BMB Rep.* 43, 11–22. doi:10.5483/bmbrep.2008.41.1.011
- Wang, Y., Xiang, L., Wang, C., Tang, C., and He, X. (2013). Antidiabetic and antioxidant effects and phytochemicals of Mulberry Fruit (*Morus alba* L.) polyphenol enhanced extract. *PLoS ONE* 8 (7), e71144. doi:10.1371/journal.pone.0071144
- Yach, D., Hawkes, C., Gould, C., and Hofman, K. (2004). The global burden of chronic diseases: overcoming impediments to prevention and control. *JAMA* 291, 2616–2622. doi:10.1001/jama.291.21.2616
- Yamashita, Y., Okabe, M., Natsume, M., and Ashida, H. (2012). Prevention mechanisms of glucose intolerance and obesity by cacao liquor procyanidin extract in high-fat diet-fed C57BL/6 mice. *Archives Biochem. Biophysics* 527, 95–104. doi:10.1016/j.abb.2012.03.018
- Younes, A., and Schneider, J. M. (1984). Effects of bepridil on Ca²⁺ uptake by cardiac mitochondria. *Biochem. Pharmacol.* 33 (8), 1363–1366. doi:10.1016/0006-2952(84)90193-x

Frontiers in Pharmacology

Explores the interactions between chemicals and living beings

The most cited journal in its field, which advances access to pharmacological discoveries to prevent and treat human disease.

Discover the latest Research Topics

[See more →](#)

Frontiers

Avenue du Tribunal-Fédéral 34
1005 Lausanne, Switzerland
frontiersin.org

Contact us

+41 (0)21 510 17 00
frontiersin.org/about/contact

